THE USE OF ISOTOPE HYDROLOGY TO CHARACTERIZE AND ASSESS WATER RESOURCES IN SOUTH(ERN) AFRICA

Tamiru Abiye

Report to the
Water Research Commission

by

School of Geosciences, University of the Witwatersrand

Contributors:
Balt Verhagen
Carl Freese
Chris Harris
Craig Orchard
Eddy van Wyk
Gideon Tredoux
Jennifer Pickles
Julius Kollongei
Liang Xiao
Mannie Levin
Michael Butler
Roger Diamond
Seraphine Grellier
Siep Talma
Simon Lorentz
Tamiru Abiye
Vincent Chaplot
Yongxin Xu

WRC Report No TT 570/13

November 2013

Obtainable from

Water Research Commission
Private Bag X03
Gezina, 0031

orders@wrc.org.za or download from www.wrc.org.za

The publication of this report emanates from a project entitled *The use of isotope hydrology to characterize and assess water resources in South(ern) Africa* (WRC Project No. K5/1907)

THE USE OF ISOTOPE HYDROLOGY TO CHARACTERIZE AND ASSESS WATER RESOURCES IN SOUTH (ERN) AFRICA

Environmental isotopes are routinely employed world-wide in the study of groundwater and surface water, as they provide unique information on transport and interconnectivity of water resources and reservoirs. The term environmental isotope embraces the measurement of isotope ratios of the elements making up the water molecule and of substances dissolved in water that could give rise to hydrogen and oxygen. These are subject to environmental processes and undergo changes, for example during evaporation. Water in specific environments, thus, obtains isotopic labels that are transported and can be traced along the flow pathway. The sustainable development and management of groundwater resources requires an accurate assessment of their occurrence, availability, sustainability and vulnerability to deterioration.

Environmental isotope studies have been shown to provide important information useful in the effective management of water resources in different parts of the World. The overall contribution of this project will be to raise awareness of environmental isotope hydrology as a useful tool in the assessment of water resources at different spatial scale both at local and catchment level.

Generally, the project focuses on previously executed studies as well as newly undertaken investigations which will advance the understanding of the selected individual studies. Where further information has been gathered since the original investigation, interpretations on the capability of isotopes in water resource assessment have been re-interpreted. In particular, the involvement of students in this endeavour exposed them to the analytical disciplines, approaches and methodology of isotope hydrology as well as to the concepts, models and feel involved in the interpretation and integration of the isotope data.

The main objectives of the project were:

- To identify past studies and to undertake new studies suitable for demonstrating the contribution of isotope hydrology to an enhanced under-standing of the systems studied
- Through re-assessment of isotope data to re-interpret former conclusions and identify data gaps, where new study areas are identified, to gather all necessary isotope, hydro geochemical and hydrogeological data, and produce the required conceptual and numerical framework highlighting the role of isotopes
- To gather all necessary isotope, hydro geochemical, hydrogeological and geological data, and produce the required conceptual and numerical framework highlighting the role of isotopes
- Develop course material on the discipline of isotope hydrology.

This project has involved a complex work programme with the participation of many individuals and institutions executing different studies. The main method focuses on identifying completed and on-going isotope related project in different institutions. In some cases new isotope application projects have been identified. In the pre-project phase, a team of researchers were brought together in the light of individual interest, activity, potential contribution to the aims of the project such as existing or previous studies, knowledge of potential study areas etc. The team has identified nine existing and two new projects that form this report.

Table of Contents

Acknowledgements

The authors wish to thank the Water Research Commission for funding this project and the following Steering Committee members:

Shafick Adams	Water Research Commission
Stephan Woodborne	CSIR
Eddy van Wyk	Department of Water Affairs now Golder
Adam West	University of Cape Town
Henk Coetzee	Council for Geoscience
Gideon Steyl	University of the Free State

Accompanying CD

1. Isotope Hydrology References
2. Isotope Hydrology Teaching Material
3. MSExcel Box Model and Guidelines

TASK LEADERS

1. **Prof. Balt Verhagen**, *School of Geosciences, University of the Witwatersrand, Johannesburg. Email: balt.verhagen@wits.ac.za*
2. **Mr. AS Talma,** *P.O. Box 72906, Lynnwood Ridge, 0040, 138 Genl Louis Botha Avenue, Lynnwood Ridge, Pretoria, Email: siep.talma@gmail.com*
3. **Dr. Mannie Levin,** *P. O. Box 1731, Faerie Glen, 0043, Waterpoort Street 986C, Faerie Glen, Pretoria, Email: Mannie.levin@af.aurecongroup.co.za*
4. **Mr. Michael Butler**, *iThemba LABS, Environmental isotope group, Private Bag 11, Wits 2050, Johannesburg. Email: butler@tlabs.ac.za*
5. **Prof. Chris Harris,** University of Cape Town, Dept of Geological Sciences, Rondebosch, Cape Town, Email: chris.harris@uct.ac.za
6. **Prof. Tamiru A. Abiye**, *School of Geosciences, University of the Witwatersrand, Johannesburg. Email: tamiru.abiye@wits.ac.za*
7. **Prof. Yongxin Xu**, *University of the Western Cape, Groundwater Group, Dept. of Earth Sciences, Cape Town, Email: yxu@uwc.ac.za*
8. **Prof. Simon Lorentz**, *University of KwaZulu-Natal, School of Bioresources Engineering and Environmental Hydrology, Scottsville P O Box X01, Pietermaritzburg. Email: lorentz@ukzn.ac.za*

APPLICATION OF ISOTOPE TECHNIQUES TO TRACE LOCATION OF LEAKAGE FROM DAMS AND RESERVOIRS

M Levin and B Th Verhagen

EXECUTIVE SUMMARY

Dams and reservoirs are vital to the sustainability of a large part of the world's population for water supply, irrigation, flood protection and hydropower. The two biggest concerns regarding dam leakage are safety or economic impact. Dam leakages have led to disasters is cases where dam walls collapsed. Dam leakage can cause a big reduction in hydroelectricity output during the dry season. Their ability to function properly for a long time is, therefore, crucial to the wellbeing of these population segments. Very large investments are, therefore, necessary each year for increasing the efficiency of dam and reservoir operations and thereby improving socio-economic development. Among other problems, funds are largely used for engineering and construction to mitigate these problems.

Conventional techniques enhanced by tracer techniques have been used successfully in Africa and South America to detect leakage problems. These techniques are not familiar to organizations responsible for dam construction and management, resulting in repair work being undertaken using only conventional geological and hydrogeological data only. Tracer techniques, accurate data may produce useful and sometimes unique data rapidly resulting in significant savings. The main objective of this project is to introduce the utilization of environmental isotopes in dam leakage studies in Southern Africa in order to raise the awareness of the dam engineering fraternity to this best practice technique in dam leakage studies. Dam safety must be considered throughout the life cycle of the dam.

The Osplaas Dam site was identified and constructed for the Hex Valley Irrigation Board as an off-channel reservoir for winter storage of irrigation water. The dam is located on the left bank tributary of the Hex River about 10 km northeast of De Doorns. Filling of the dam by pumping started in September 2007. In the beginning of 2008 discharging groundwater into the Spoornet Tunnel, located about 1 km northwest of the dam was linked to the dam by Railway staff. However, in the correspondence it is mentioned that the leakage in the tunnel has received attention before the Osplaas Dam had been constructed.

The investigations of the possible connection between the Osplaas Dam and the groundwater flow in the railway tunnel was done using stable isotope technique supported by chemical analysis. The chemical results of samples taken at the dam, boreholes and tunnel indicate no link between the dam water and the water seepage at the tunnel. The 2011 stable isotope data confirm the conclusion from the 2008 study that there is no link between the dam water and water seepage at the tunnel. The structural evidence found during the geotechnical drilling does not link the dam with the tunnel. A radon emanation survey of the structural features was done to confirm if they are open and if connect to the dam site. The radon emanation study confirms the stable isotope investigation that no direct connection exists between the dam and the tunnel. The increase in seepage after the dam was filled may possibly be due to additional head the dam water body placed on the groundwater.

INTRODUCTION

Dams and reservoirs are vital to the sustainability of a large part of the world's population for water supply, irrigation, flood protection and hydropower. The two biggest concerns regarding dam leakage are safety or economic impact. Dam leakages have led to disasters is cases where dam walls collapsed. Dam leakage can cause a big reduction in hydroelectricity output during the dry season. Their ability to function properly for a long time is therefore crucial to the wellbeing of these population segments. Very large investments are therefore necessary each year for increasing the efficiency of dam and reservoir operations and thereby improving socio-economic development. Among other problems, funds are largely used for engineering and construction to mitigate these problems.

Conventional techniques enhanced by tracer techniques have been used successfully in Africa and South America to detect leakage problems. Such tracers can either be added to the water, such as environmentally friendly tracers and dyes, or so-called environmental isotopic tracers, the concentrations of which in water being established by environmental processes. This study deals with environmental isotopic tracers. These techniques are not familiar to organizations responsible for dam construction and management, resulting in repair work being undertaken using only conventional geological and hydrogeological data only. Tracer techniques, accurate data may produce useful and sometimes unique data rapidly resulting in significant savings.

OBJECTIVES

The main objective of this project is to introduce the utilization of environmental isotopes in dam leakage studies in Southern Africa in order to raise the awareness of the dam engineering fraternity to this best practice technique in dam leakage studies. Dam safety must be considered throughout the life cycle of the dam. It begins at the site exploration and selection stage, continues through design and construction, and then the entire operational life of the structure, and even during decommissioning. However, one of the main impediments to effective integration of nuclear techniques in dam safety and sustainability is the lack of knowledge and understanding for their role among end users. The role of nuclear isotope techniques in dam management is to generate information to help end-users make decisions that will guide, optimize and protect investments in dam safety and sustainability. It is estimated that less than 5% of end-users in the dam sector are aware of the existence and potential of isotope hydrology in dam management.

The infiltration and leakage of reservoir water can take place along different pathways. Hence each case has to be approached and analyzed individually in such a way that most adequate techniques are applied as per the particular geological and hydraulic setting. The main objective of this study is to use environmental isotope techniques to link any leakage to the reservoir structure. However, in this study the techniques are used to investigate connection between the proposed leakage and the reservoir.

METHODOLOGY

Conventional techniques

Isotope techniques are always used in association with conventional techniques and support, confirm or add valuable new information on which to make important technical decisions (Plata et al., 2002). The conventional techniques are those applied by geologists, engineering geologists, geochemists and geohydrologists. The techniques include the following:

- Geology (new mapping or verify existing maps, faults, shears, grabens, contacts, etc.)
- Remote Sensing (Satellite imaginary, airborne spectral, magnetic and radiometric surveys)
- Ground Geophysics (Magnetics, electro-magnetics, gravity etc.)
- Engineering Geology (Soil profile and properties, weathering, perched water tables, evaporites etc.)
- Structural Geology (Tensional and compressional structures verify and neotectonics)

Water losses frequently appear below the dam foundation as well as at the abutments. Water can escape from the reservoir either as leakage or as seepage. Leakage can be described as concentrated water losses derived from structural or construction deficiencies such as found at contact surfaces between dam body and the terrain, lack or deficient isolation of alluvial materials, activation of perched levels when flooded by reservoir water etc. In this case the water usually flows through concentrated pathways and emerges downstream forming springs. Plata & Araguás (2002) discuss principles, techniques used in numerous case studies to locate leakages in dams.

On the other hand, the presence of limited seepage through and under embankment dam is a natural and expected process which is evaluated by investigating the permeability of the geological formations in the vicinity of the dam. In the case of an earth dam, the limited flow of water through the cross section is considered as a positive feature, permitting the development of pore pressures within their mass. Hence seepage can be described as spread infiltration produced at the reservoir bottom through permeable or partially permeable granular materials. The escaping water either can be incorporated into downstream aquifers without appearing at the surface or can emerge as diffuse discharge over a wide area downstream.

To develop a structural or foundation failure the following conditions must occur:

- There must be a well-defined flow path
- There must be an unprotected exit, allowing the transport of material
- The material along the flow path may be eroded, to a grain size capable of being transported to the exit point.
- Geohydrology (Aquifers and occurrence, water levels and flow direction and gradient, hydraulic properties, chemistry, isotope data)
- Artificial Tracing (Colour tracers such as Fluorescein or Rhodamine)

The chemical and physical properties of the water are first option to establish any link between leakage and the dam. Isotope tracer and related techniques applied to dam leakage and related investigations rely mostly on the interpretation of natural variations of physical and chemical properties of environmental isotope tracers occurring in water and the geological environment. Most of the applications are based on natural tracers, and only in the final stages of the investigations, artificial radioactive tracers are used (Levin, 2010). Artificial radioisotopes are produced and applied under strict regulatory requirements and the amounts used are also small, with insignificant risk to the environment.

Chemical composition of water

As a general rule, chemical analyses of major ions of the representative points in the study area are recommended to be performed at the initial stages of the investigation. The selection of the water points to be sampled for chemical analyses can be made on the basis of EC values measured in the field. The EC measurements will allow classification of the different points into groups with the same chemical quality, so that the number of samples collected for complete chemical analysis can be drastically reduced.

The chemical composition of water can provide information on its origin, allowing differentiation between reservoir and aquifer water. It can allow identification and evaluation of mixtures of both kinds of water.

ENVIRONMENTAL ISOTOPES

The environmental isotope species that can be employed in dam leakage are the non-radioactive (or 'stable') isotopes ^{18}O and ^{2}H and the radioactive isotope ^{3}H (IAEA, 2000). These label the water molecule itself, and their concentrations are not influenced or altered by chemical reactions. They assist in:

- determining the origins and ages of different water bodies;
- provide an estimate of the degree of mixing;
- determine the location and proportion of water recharge; and
- indicating the velocity of groundwater flow.

Oxygen –18 (18O) and Deuterium (2H)

Oxygen–18 (^{18}O) together with deuterium (^{2}H) are present in water in isotopic abundances of about $^{18}O/^{16}O = 0.2\%$ and $^{2}H/^{1}H = 0.015\%$ with respect to the common, lighter isotopes ^{16}O and ^{1}H respectively. In various combinations, these isotopes constitute water molecules, principally of masses 18, 19 and 20. In phase processes such as evaporation and condensation, the different vapour pressures of these molecules cause small changes in the isotopic abundances, the heavier isotopes tending to concentrate in the denser phase. These small changes can be expected as a fractional deviation from a standard called SMOW (Standard Mean Ocean Water), defined as:

$$\delta = [(R_s/R_r) - 1] \times 1\,000\ (‰)$$

where R_s and R_r are the ratios of the abundances of the rare (heavier) isotope to the more abundant (light) isotope for the sample and reference standard, respectively.

Stable isotope variations result from isotope fractionation which occurs during physical and chemical processes. Examples of physical processes which could lead to isotopic fractionation are evaporation of water or condensation of vapour. During evaporation, the residual liquid is enriched in the heavier isotope molecule because the lighter molecules move rapidly and hence has a greater tendency to escape from the liquid phase – there is a difference in the volatility between the two molecular species. These physical processes change the δ values from those in the original precipitation. The δ values can therefore be diagnostic of water from different origins, such as rain-water, direct recharged groundwater, or surface water from dams.

Tritium (^{3}H)

Environmental tritium ^{3}H is a very useful tracer of water and is widely used in hydrological studies. Tritium (^{3}H) is a radioactive isotope and decays through low energy beta ray emission. It has a half-life of 12.43 years. Tritium is produced in nature by cosmic ray interaction with the upper atmosphere, and readily oxidized to water, in which it is a conservative tracer. Rain-water in South Africa contains natural tritium at concentrations of about 3 Tritium Units (TU). It is possible to identify the recharge period of recent groundwater by comparing its tritium content with those of present-day rainfall. Measurable tritium in boreholes would indicate recharge, while zero tritium would indicate slow or no recharge of that aquifer. Tritium is therefore essential in studies of aquifer dynamics.

OSPLAAS DAM

Introduction

The Osplaas Dam site was identified and constructed for the Hex Valley Irrigation Board as an off-channel reservoir for winter storage of irrigation water. The dam is located on the left bank tributary of the Hex River about 10 km northeast of De Doorns as shown on Map 1. The dam wall is located at an elevation of 600 masl as shown on the 1:50 000 topographic map 3319BC De Doorns in Map 2.

Filling of the dam by pumping started in September 2007. In the beginning of 2008 discharging groundwater into the Spoornet Tunnel, located about 1 km northwest of the dam was linked to the dam by Railway staff. The Tunnel is located at an elevation of 560 masl or about 40 lower than the dam. Correspondence at the time indicates that the first inspections regarding possible linkage of the leakage to the dam in the tunnel, took place during January 2008. However, in the correspondence it is mentioned that

the leakage in the tunnel has received attention before the Osplaas Dam had been constructed.

On 31 January 2008 the site was visited by Railway staff and members of the Irrigation Board (owner) and Water Users Association to investigate the seepage of water into the Railway tunnel. It could not be concluded with certainty whether the leakage derived from the dam but the designing engineers would be consulted. On 4 February 2008 the engineer and Irrigation board visited the site and again concluded that the dam may contribute to the leakage. Monitoring the levels would be continued and the situation reviewed.

Geology

The area of investigation is underlain by rocks of the Ceres Sub-group of the Bokkeveld Group. These rocks consist of bedded sandstone and alternating shale horizons. The regional dip of the strata is about 30° to the southeast, and locally there are variations in the dip angle combined with intra-formational folding. A feature of the site is a very prominent sandstone outcrop, 15 m high and dipping vertically, on the right flank about 50 m upstream of the dam. Nearby, in the right abutment on the axis of the dam, the sandstone horizon is horizontally bedded. The outcrop is the southern limb of a small monoclinal fold with its axis east-west. The structure may have been created by a thrust fault. The feature was not exposed on the left flank. Exposures of weathered shale are observed on the upstream west flank below the railway line and have been exploited for road surfacing material.

Upstream of the proposed dam site, the basin is covered by silty, sandy gravelly colluvium, whilst the riverbed and its banks consist of clayey, silty, sandy, gravelly alluvium with sandstone river cobbles and boulders. Downstream, a flat area adjacent to the right river bank has been covered by silty sand with transported river cobbles and boulders.

Geological Investigations

The dam's (foundation) conditions were investigated by coring of six (6) diamond drilled boreholes located along the proposed dam axis and spillway crest (Ninham Shand, 2005). Cores recovered from the boreholes indicated that, underlying a relatively thin layer of overburden is competent, hard to very hard sandstone. The sandstone is thinly to thickly bedded with well developed, very closely to widely spaced vertical to sub vertical jointing, and is often highly fractured. At shallower depths (less than 10 m) joints are generally wide with clay filling, whilst at greater depths these tend to narrow or are tight. The highly fractured nature of the rock suggested that curtain grouting for a dam foundation would be required.

There is evidence of a shear zone and possible fault trending northwest-southeast along the river channel running under the proposed dam axis. This structure is not recent and almost certainly associated with ancient tectonic processes The depth of overburden and underlying highly weathered rock on the abutments is limited to between 0,5 m to 1 m. In the central valley, up to 5 m of overburden (alluvium and colluvium) or highly weathered material overlies competent rock.

Present Leakage Investigations

The Osplaas Dam site was visited on 2nd April 2011 to familiarise ourselves with the locality and layout of the site. Water samples were taken at the dam site, the outlet and the borehole close to the dam as shown in Map 3. Only one further borehole was available near the N1 Highway and a sample was collected at the South Portal of Spoornet Tunnel as shown on Map 4.

Sample Nr.	OS1	OS2	OS3	OS4	OS5	Class I	Class II
Ca	9.10	70.00	17.00	38.00	120.00	150	300
Mg	3.80	31.00	7.80	80.00	70.00	70	100
Na	14.00	110.00	30.00	320.00	230.00	200	400
K	0.87	1.7	1.00	3.90	3.50	50	100
Mn	<0.06	0.17	0.06	0.23	<0.06	0.1	1
Fe	<0.25	<0.25	<0.25	11.00	<0.25	0.2	2
F	<0.3	3.50	0.65	2.40	2.80	1	1.5
NH4 as N	<0.05	0.16	<0.05	0.49	0.17		
NO3 as N	<0.4	<0.4	<0.4	<0.4	<0.4	10	20
Si	<0.05	7.6	1.4	0.38	7.9	-	-
Cl	22.00	170.00	40.00	440.00	240.00	200	600
SO_4	24.00	170.00	62.00	180.00	370.00	400	600
TDS mg/l	212.00	660.00	220.00	1196.00	1384.00	1000	2400
M-Alk($CaCO_3$)	26.00	140.00	36.00	130.00	210.00	-	-
pH	7.50	7.30	7.40	7.90	8.10	5.0 - 9.5	4.0 - 10.0
EC mS/m	15.00	100.00	30.00	160.00	120.00	150	370

Notes
Yellow = Class I
Tan = Class II
Exceeds Class II Standards
na- not analysed
<n = below detection limit of analytical technique

Table 1: Chemistry of the samples collected at the Osplaas Dam.

Chemistry

Present investigation: The samples taken for chemical analysis were submitted to SGS Environmental Services in Johannesburg, a SANS accredited analytical laboratory.

The results are shown in Table 1 there they are compared to the standards of *SANS 241:2006 Edition 6.1* for drinking water. It is clear from the chemistry that the groundwater in the boreholes and in the Tunnel show high Fluoride values compared to the surface water from the dam and outlet. The other parameters also confirm that the groundwater differs significantly from the surface (dam) water.

In order to verify the conclusion that the surface and groundwater quality differ, the chemical character of the samples was compared using the Piper diagram. The results indicated in Fig. 1 show that the dam and tunnel samples do not have the same chemical character.

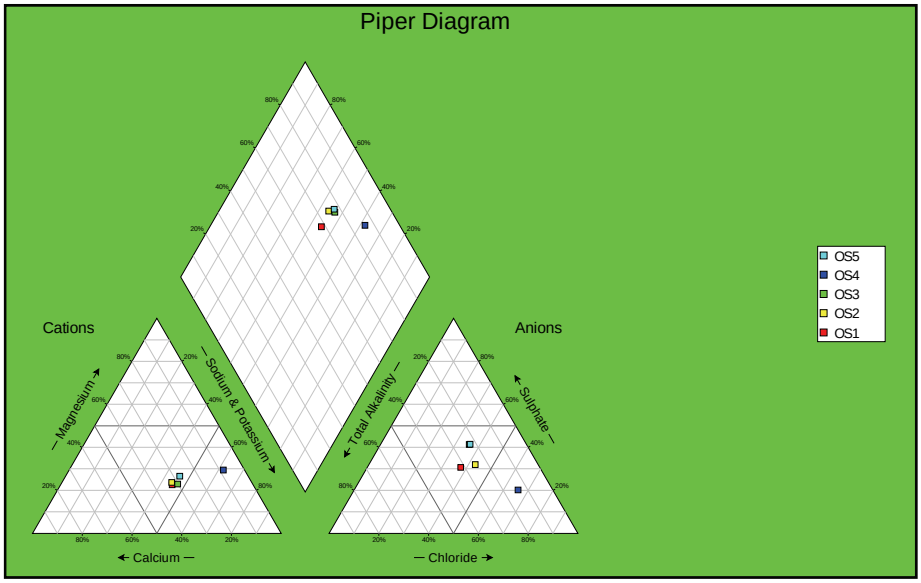

Figure 1: Piper diagram of the Osplaas Dam samples.

Previous investigation: Chemical results of samples taken in January and in April 2008 are available to compare with the present results. The results of samples analysed in 2008 by the CSIR Stellenbosch also show a difference in parameters between surface and tunnel water. However, only a few parameters were analysed as shown in Table 2 where the dam samples results are compared and in Table 3 where tunnel samples are compared. The results indicate similar values for 2008 and 2011 and there is a significant difference in the water quality of the dam and the tunnel. This confirms the present results and no dilution of the tunnel water are noticed since the dam started to fill.

	Feb-08	Apr-08	Mar-11
K	1.6	2.1	0.87
NO3	0	0	0
F	0	0	0
Fe	0	0	0
Mn	0	0	0
EC	11.7	15.5	15
TDS	75	99	212

Table 2: Comparing dam chemistry results

	Feb-08	Apr-08	Mar-11
K	8.3	8.1	3.5
NO3	0.08	0.05	0
F	0.2	0.3	2.8
Fe	0	0	0
Mn	0	0	0
EC	285	265	120
TDS	1824	1696	1384

Table 3: Comparing tunnel chemistry results

Environmental Isotope data

Present investigations: In order to evaluate the physical properties of the water molecules in the dam, groundwater and tunnel water the samples taken for eenvironmental isotope analysis where submitted to iThemba LABS (Gauteng) which is an IAEA accredited isotope laboratory. The results are shown in Table 4.

Laboratory Number	Sample ID	δD (‰)	$\delta^{18}O$ (‰)	Tritium (T.U.)	
STEL 016	OS1	-13.6	-2.07	0.9	±0.2
STEL 017	OS2	-26.5	-4.98	0.3	±0.2
STEL 018	OS3	-15.6	-2.66	0.7	±0.2
STEL 019	OS4	-32.8	-5.77	0.3	±0.2
STEL 020	OS5	-29.6	-5.07	0.5	±0.2

Table 4: Results of the Osplaas samples isotope analyses collected in 2011.

Stable isotopes ^{2}H and ^{18}O

The stable isotope results are shown in Table 4 and the data is plotted on a $\delta^{2}H$ - $\delta^{18}O$ diagram in Fig 1. The Global Meteoric Water Line (GMWL), which characterises precipitation with slope s = 8, is shown for comparison. Samples OS2, OS4 represent groundwater and plot close to the GMWL e.g. rainfall. OS1 and OS3 are dam water which is seen to deviate from the GMWL and lie on an evaporation trend with s = 5.4. The tunnel sample falls between the groundwater sample points with no evaporation trend. The dam sample shows greater evaporation enrichment than the water at the outlet. This may be the result of taking the sample close to the shore. OS2 is the borehole close to the dam yet its sample does not show any admixture of dam water

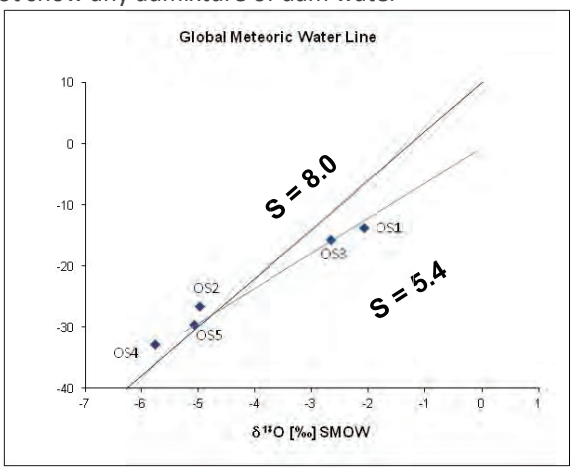

Figure 2: Stable isotope results plotted on the $\delta^{2}H$ - $\delta^{18}O$ diagram

Radioactive Isotope tritium

The tritium results are also shown in Table 4. The groundwater samples OS2, OS4 and OS5 show measurably lower tritium in groundwater than in dam water (OS1 and OS3) due to radioactive decay with longer residence time in the ground. . The dam samples should reflect recent rainfall runoff.

Previous investigations: Water samples taken during March 2008 at the Osplaas Dam and railway tunnel were submitted to Prof Chris Harris, Department of Geological Sciences, University of Cape Town for isotope analysis.

Sample	$\delta^{2}H$ ‰	$\delta^{18}O$ ‰
Osplaasdam Touws	-25.7	-2.79
Osplaasdam De Doorns	-18,7	-2.86
Train Tunnel Touws	-40.7	-6.41
Train Tunnel De Doorns	-38.2	-6.52

Table 5: Results of the isotope analysis March 2008

The March 2008 stable isotope results are plotted on a $\delta^{2}H$ - $\delta^{18}O$ diagram in Fig. 2. The Global Meteoric Water Line (GMWL), which characterises precipitation, is shown for comparison.

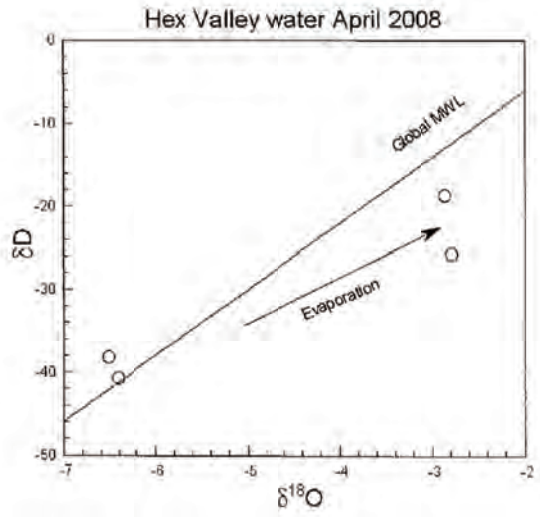

Figure 3: March 2008 stable isotope results plotted on the $\delta^{2}H$ - $\delta^{18}O$ diagram (Harris, 2008).

This study came to the following conclusions:

- The water in the tunnel and the dam are completely unrelated.
- The travel time of water from the dam to the tunnel might be of the order of months. In the time taken for the water to travel from the dam to the tunnel, the isotope composition of the dam could have changed by evaporation.

- The groundwater $\delta^{2}H$ and $\delta^{18}O$ values in the area are actually more negative than measured in the tunnel samples. The tunnel samples could contain a component of dam water similar to the measured value.
- Increased influx of water into the tunnel is due to the additional hydraulic head, and it will take some time for actual dam water to reach the tunnel.
- A radon survey is recommended to locate the structures and confirm no connection.

Map 1: Locality of the Osplaas Dam and Railway Tunnel

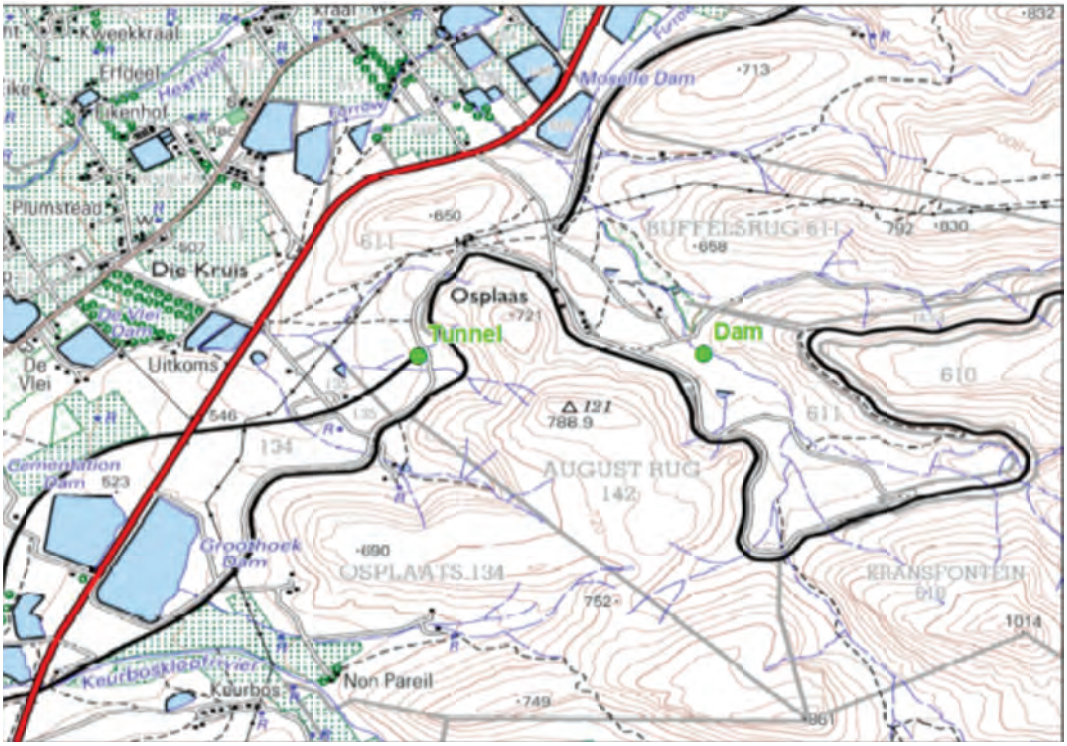

Map 2: Topography of the Osplaas Site area.

Map 3: Locality of the Sample localities close to the Dam (Wall indicated in Blue)

Map 4: Locality of samples taken at Osplaas Dam

Map 5: Locality of a linear structure cutting through the tunnel at the point of seepage.

Map 6: Locality of the structural features identified at the Osplaas Dam Site.

RADON EMANATION STUDY

Based on the results of the chemical and isotope study it was recommended to apply the radon emanation technique to investigate the geological structures present between the dam and the tunnel that may link the two water sources. The technique is capable of locating the area of emission along a structural fault zone by measuring the emanation of radon through the rock structure.

Theoretical background

The radon emanation technique is based on the emission of an α-particle by the radioactive isotope Radium (^{226}Ra) to produce the gas Radon (^{222}Ra). The radium is naturally produced during the decay of uranium (^{238}U). Uranium is present in most rock types in minerals such as zircon, mica, apatite etc.

Radon, being a noble gas, has the ability to migrate from its source without chemical interference. The radon gas emanates from the mineral surfaces into the rock pores or dissolves in the water phase where present. Radon (^{222}Ra) is radioactive with a half-life of 3.8 days. Due to its half-life it is present in groundwater for up to 15 days. This unique combination of features underlies the interest in radon gas as a geophysical tracer.

The technique of field radon-emanometry requires that radon gas escapes from a source and finally emerges at the surface to be detected by some method. It is desirable at this stage to briefly consider the mechanisms whereby radon escapes from the crystals in which it was formed. Andrews and Wood (1972) investigated the problems of radon release from rocks, and found that four mechanisms could be postulated:

a) Recoil directly into the fluid phase, of radon atoms following radium decay at or near the surface of the particle.
b) Diffusion of radon from within the crystal lattices of the mineral phases of the rock particle into the fluid phase.
c) Recoil of radon atoms following radium decay within the particle, into crystal mosaic boundaries, dislocation planes, and grain boundaries, followed by comparatively rapid diffusion along such imperfections to the particle surface.
d) Release of radon by any of the above mechanisms into relatively porous secondary phases in complex rock matrices (for example, into the cementing material in sandstones, followed by its rapid diffusion to the surface, possibly from deep within the rock fragment).

Andrews and Wood (1972) also showed experimentally that radon is released mainly according to the third mechanism, and that crystal imperfections therefore play a vital role. This means that the fraction of the radon released to ground water and soil air will depend largely on the physical nature of the rock and associated fluid phases, rather than on the uranium concentration in the rock. It, therefore, follows that increased concentration can be expected from fractured, faulted and porous rock zones.

A number of detection methods has been developed and tested over the years. Detection is based on either measuring the radio-activity or the energy release by the radon. The radioactivity makes radon easy to measure in small concentration; however, the short half-life means that integrated measurements must be carried out within a few days.

The most widely used method in aerial surface radon surveys is the nuclear tracks (“track etch”) method due to its simplicity and due to the fact that it is an integrating method. The method was developed and utilised for uranium exploration. The method is applied mainly in soils covering the rock formations from which the radon is assumed to migrate. The distribution (diffusion) pattern depends on the structures in the underlying rock and therefore the areas of higher radon concentration correspond with fractures, faults or other more permeable zones as shown in Fig. 3. Knowledge of the underlying geology is essential for interpretation of results.

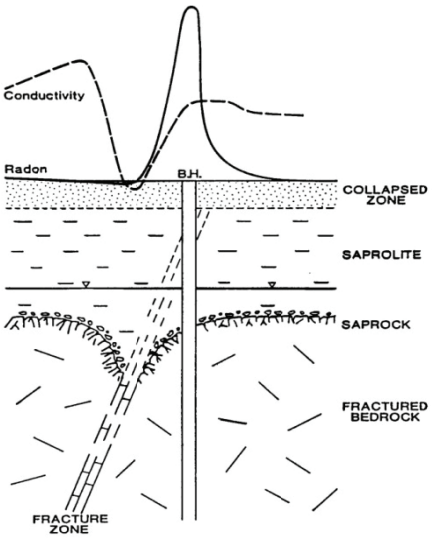

Figure 4: Radon Technique Illustrated

It is expected that the homogeneity of the soil, which is better than that of the underlying rocks, acts as a local homogenizing transport medium for the radon and thus simplifies the interpretation of the results. For ground water exploration radon is exclusively used in soil covered areas as mapping of exposed rock in areas without soil cover would be sufficient for fault detection. Best results can be expected placing the monitors at a depth of at least 50 cm.

Fieldwork

On 23 February 2011 radon monitors were placed in three profile lines were selected, as shown in Figure 4. The lines were selected to intersect the potential east west structures that were identified on the satellite imaginary map of the area. The objective was to establish if there are structural connections between the dam and the railway tunnel. Line 1 was 290 m, Line 2 was 250 m and Line 3 is 280 m in length. The radon monitors were placed in the shallow holes about 500 mm deep and 5m apart. The monitors were placed on the 23rd of February 2012 sequentially starting at line 1 and ending at the end of line 3. The monitors were left for two weeks until the 12th March 2012 when they were retrieved in the same sequence as placed in order to expose all the monitors for the same period. A few monitors were dug out or disturbed by animals as reflected in the graphs in Fig. 5.

Figure 5: Radon Monitor Profile lines.

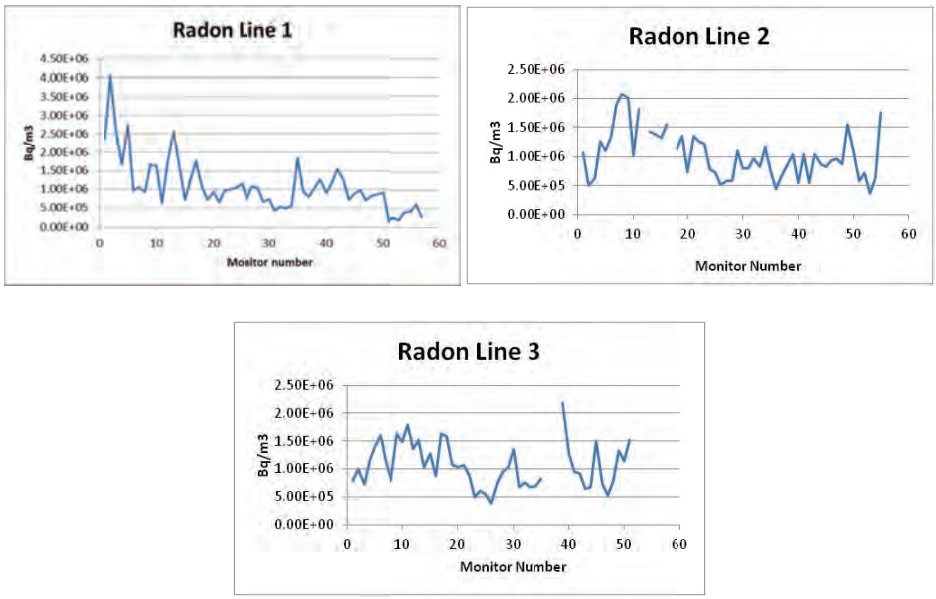

Figure 6: Radon concentration (Bq/m^3) graphs.

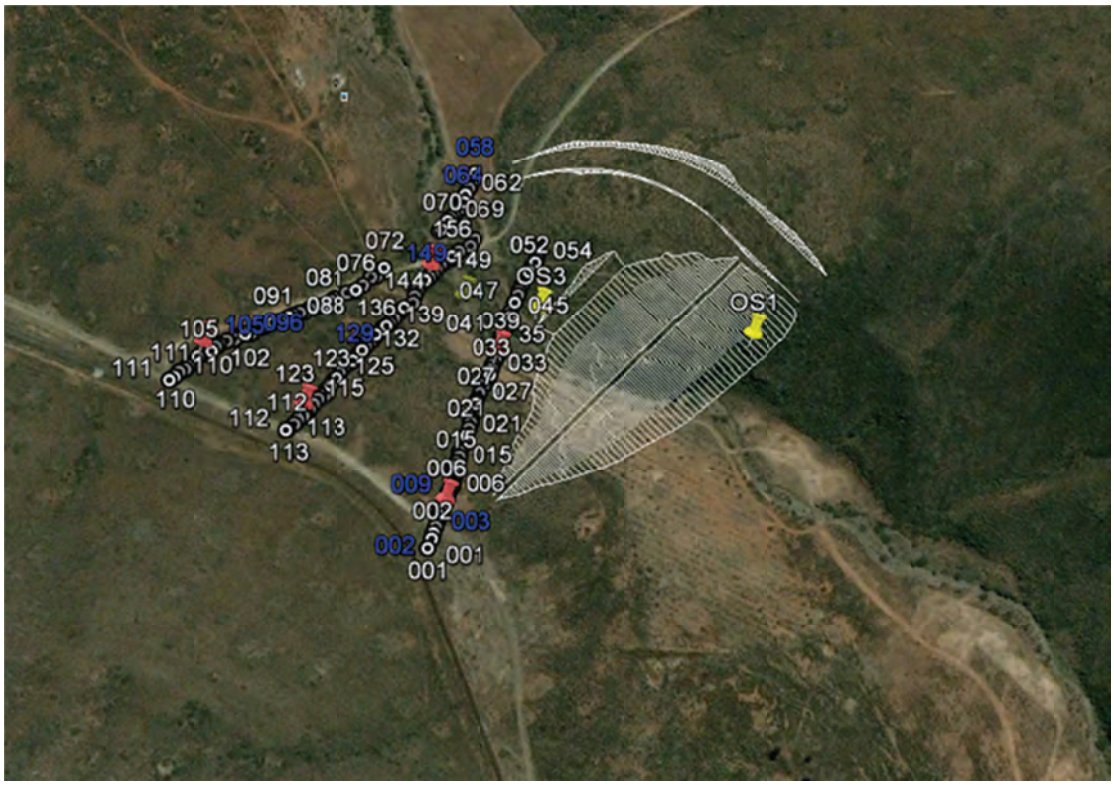

Figure 7: Profile lines showing the red icons.

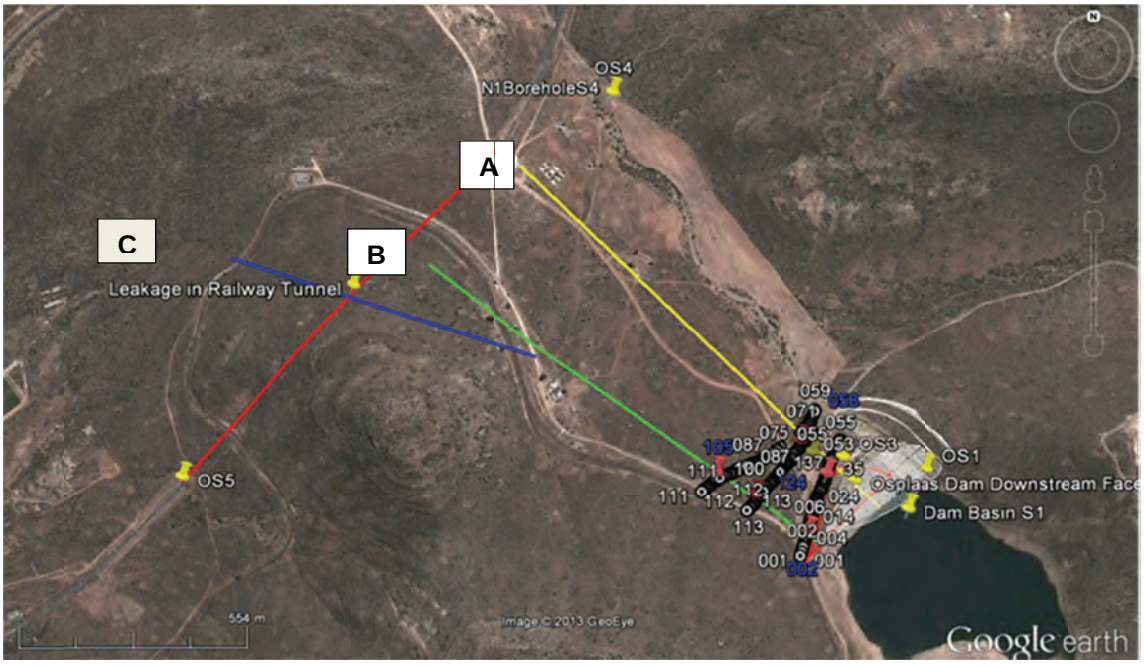

Figure 8: Structures indicated by the radon emanation results

All the monitors retrieved were submitted to the Parc RGM laboratory in Pretoria for processing and measurement. The radon concentration is expressed as radioactivity in Bq/m^3 (Becquerels per m^3). The radon values were plotted against the traverse distance for each profile and the graphs are shown in Fig. 5. The radon concentration above the 1.5 Bq/m^3 level were selected and the localities are shown in Table 6.

The anomalous localities are now showed in blue on the profile lines and the most southern anomaly localities are marked with a red icon as shown in Fig. 6. When the red icons are connected we find two structural lines A and B stretching in a north westerly direction as shown in Fig. 7. This direction was found in the core drilling done for the foundation studies. However, the lines do not pass through the tunnel area. The structure identified on satellite imaginary at the tunnel C on Fig. 7, may intersect the structures. This means that when the dam fills there may be some pressure on the groundwater body that could increase flow into the tunnel. As concluded from the stable isotope investigation there is no direct link between the dam water and the tunnel water. As concluded from the stable isotope investigation there is – at present - no direct link between the dam water and the tunnel water. Continuous monitoring may in the future indicate an impact of the dam on the nearest borehole

Line 1	Line 2	Line 3
2	105	116
3	104	117
4	103	120
5	101	121
9	96	122
10	64	124
12	58	128
13		129
14		149
17		155
35		
42		

Table 6: The localities on the monitoring lines for radon values greater than 1.5 Bq/m^3.

DISCUSSION OF THE RESULTS

The results of samples taken in 2008 were very similar to that taken in 2011. The borehole OS2 close to the dam does not show any impact of dam water on the quality or isotope content. It can further be concluded that after three years the tunnel water still does not show mixing with the dam water. The only possible explanation considered why the tunnel seepage increased after the dam filled in 2008 is the additional head the dam water body placed on the groundwater.

The tunnel did experience seepage before construction according to the correspondence received. A close look at the satellite imagery map of the area indicates a definite geological structure cutting through the tunnel exactly at the leakage area as shown on Map 5. According to the Geotechnical report (Ninham Shand, 2005) evidence was found of a shear and a possible fault zone trending northwest-southeast along the river channel running under the proposed dam axis. This possible fault zone is shown on Map 6 as Structure A while the one cutting through the tunnel is shown as Structure B. There is no evidence that Structure B is linked to the Osplaas Dam. In order to confirm these structures it was recommended that a radon emanation survey (Levin, 2000) be conducted across these structural features to confirm if they are open and if both are connect to the dam site.

Such a radon survey was done in 2012 and the localities at which radon concentration lies above the 1.5 Bq/m^3 level were selected. The anomalous localities were shown on the profile lines and the most southern anomaly localities are marked with a red icon. Connecting these red icons showed two structural lines A and B stretching in a north westerly direction. This direction was found in the core drilling done for the foundation studies. However, the lines do not pass through the tunnel area. The structure identified on satellite imaginary passing through the tunnel leakage area does seems to intersect the other structures and it is concluded that when the dam fills there may be some pressure on the groundwater body that could increase flow into the tunnel.

CONCLUSIONS

The following conclusions are made:

- The chemical results of samples taken at the dam, boreholes and tunnel indicate no link between the dam water and the water seepage at the tunnel.
- The 2011 stable isotope data confirm the conclusion from the 2008 study that there is no
- Link between the dam water and water seepage at the tunnel.
- The structural evidence found during the geotechnical drilling does not link the dam with the tunnel.
- A structure was identified on satellite imagery cutting through the tunnel and appears to produce the seepage but is not linked to the dam site.
- The increase in seepage after the dam was filled may possibly be due to additional head the dam water body placed on the groundwater.
- A radon emanation survey of the structural features should confirm if they are open and if connect to the dam site.
- The radon technique illustrated the emanation of radon gas along the profiles at Osplaas.
- The radon profiles confirmed the existence of a geological fault structures as shown on the satellite imaginary map of the area.
- The radon confirmed the fault direction identified in the drill core during foundation studies.
- Connecting the high radon points show lineaments in the northwest direction not intersecting the tunnel.
- The radon emanation study confirms the stable isotope investigation that no direct connection exists between the dam and the tunnel.
- There may be some intersection between the tunnel structure and the radon structures that could put some pressure on the groundwater body during filling.

ACKNOWLEDGEMENTS

The following people contributed to the success of this project:

- The Water Research Commission for funding the project and ensuring the best scientific results being achieved.
- The Water and Waste Management Units of Aurecon (Pty) Ltd for supporting this project by financial support.
- The University of Stellenbosch for financial and academic support.
- The Hex Valley Irrigation Board for supporting the project financing and providing staff and equipment to assist with fieldwork.

REFERENCES

AFRA Team (2000) *Investigation into Leakage at the Roodekopjes Dam*. End of Mission Report to the IAEA, Vienna.

Harris, C. (2008) Water Samples submitted for O and H isotope analyses March 2008. Report to the Hex Valley Water Users Association.

IAEA (2000). *IHP-V Technical Documents in Hydrology No. 39, Volumes I to VI*

Levin M (2000). *The Radon Emanation Technique as a Tool in Groundwater Exploration*. Borehole Water Journal, Vol 46, 2000.

Levin M (2010) *Isotope Hydrology in Dam Studies Related to Dam Safety and Sustainability.* SANCOLD Symposium, CSIR, Pretoria. 12 – 13 October 2010.

Ninham Shand Consulting Services (2005) *Drilling and Materials Investigation for Osplaas Dam.* HexVallei Besproeiingsraad, May 2005

Plata Bedmar A. Araguás Araguás, L. (2002) *Detection and prevention of leaks from dams.* AA Balkema Publishers.

Levin, M. (2000) *The Radon Emanation Technique as a Tool in Groundwater Exploration* Borehole Water Journal, Vol 46, 2000.

Andrews, J.N., Wood, D.F. (1972) *Mechanism of radon release in rock matrices and entry into groundwaters.* Institute of Mining and Metall. Trans 81, B198-B209.

SOUTH AFRICAN CASE STUDY

The African Regional Co-operative Agreement for research, development and training related to nuclear science and technology (AFRA) was initiated during the late 1990s under the umbrella of the International Atomic Energy Agency (IAEA). AFRA has a membership of 25 countries and has been carrying out co-operative projects in various fields of nuclear science and technology for socio-economic development. Projects to date have covered themes in the fields of radiation safety, human health, and agriculture and radiation technology. Specialised teams have been established to respond at request and on "*when needed basis*" to regional needs in these fields.

The South African counterpart and coordinator for AFRA is the National Atomic Energy Corporation of SA (NECSA). On request from the IAEA and AFRA, specialist teams were selected during 1998 for the investigation of dam safety and dam leakage problems in AFRA member countries. Two teams, one for French speaking and one for English speaking countries were selected. Several case studies on dam leakage were undertaken in Africa by the AFRA teams. During July 2000 fieldwork was conducted to evaluate leakage at

Roodekopjes Dam (AFRA Team, 2000). The results of that work are reported in an end of mission report to the IAEA dated August 2000.

During dam construction, between the period 1979 to 1984, the decision was taken to raise the full supply level (FSL) by 3.5 m from RL 1003m to 1006.5 m in order to increase the yield of the system. The raising involved a re-design of the embankment section and a lengthening of the embankment by some 600m on the right flank. During the re-design of the embankment, no additional geological investigations were undertaken owing mainly to construction time restraints. A change in design engineers took place and they assessed that the weathered granite bedrock was highly impermeable and that the alluvial channel material does not exist as a zone of high permeability.

The present seepage problem evaluated by the team on the right flank has arisen since impounding and is indirectly related to the raising of the dam. It is regarded to be related to the alluvial material in the paleao-channel. Based on the limited data obtained, it was concluded that:

- Using temperature readings the dam was shown to contribute to downstream shallow groundwater.
- The increased EC values at four of the pressure release boreholes indicate the leakage of the dam water.
- Stable isotope data has provided useful information in tracing seepages from the dam.
- Low levels of anthropogenic tritium in the dam water, originating from NECSA, provide evidence confirming the stable isotope and chemical information.

REFERENCES

Levin M, Venter I S, Sellick C, Van Schalkwyk M and Pirow P. (2000) *Africa Expert Team on Dam Leakage and Dam Safety: Investigation into Leakage at the Roodekopjes Dam - End of Mission Report.*

APPLICATION OF ISOTOPE TECHNIQUES TO TRACE POLLUTION IN MONITORING BOREHOLES OF WASTE DISPOSAL SITES

M Levin and B Th Verhagen

EXECUTIVE SUMMARY

In many areas in the Republic of South Africa groundwater is the only source for domestic water supply. It is therefore to the utmost importance to protect these resources from pollution. One of the worst sources of pollution is waste disposal sites. This is especially true of the waste disposal sites not selected or not managed and monitored scientifically. The movement of pollution still need to be detected and monitored to be able to mitigate against impact on the environment. It is therefore necessary to know the dynamics of the underlying aquifer.

Anomalously high levels of artificial tritium have been discovered in leachates from waste sites in the Republic of South Africa and elsewhere, however, the origin of this artificial tritium has not yet been firmly established but in leachate it constitutes a unique tracer. Contrasts between tritium in rain and leachate of up to 4 and more orders of magnitude has been recorded and can be used to trace and identify sensitively tritium-containing spillages or leakages. In this case the source of the tracer is unique (the leachate) and is indisputable. Tritium can be used to establish the recharge and dynamics of monitoring boreholes. Low or zero tritium level in groundwater would indicate slow or no recharge while rain level of tritium would indicate ongoing recharge.

The stable isotopes Oxygen-18 and Deuterium have the capability to indicate if it is groundwater or was it exposed on surface to evaporation. Evaporation effects in the landfill itself may additionally label leachate or may indicate unrelated water occurrences can be identified with stable isotope analysis. Bulk water supply from surface water exposed to evaporation display stable isotope values different to groundwater and can be used for tracing the source of water seepage. The stable isotope values combined with chemical analysis provide an undisputable confirmation of the source.

At the Boitshepi Waste Site the tritium results clearly showed the extent of the pollution in the boreholes and leachate. This is confirmed by the stable isotope and chemical results. The tritium results show the pollution in the leachate which flows outside the waste site boundary into the environment. It was shown that the tritium isotope technique at this site has an order of magnitude greater capability in tracing pollution than the chemical parameters. Once mitigation measures are installed the tritium levels will indicate the success of the pollution management program.

At the Rooikraal site the focus was on tracing the source of the surface water seepage that originated ten years ago at the site. It was thought that the seepage is impacting on the leachate generation. The stable isotope and chemical results of the surface water are exactly similar to that of the Randwater sample collected from the reticulation system. The leakage was further investigated and found that it is leakage at a Bulk Storage Reservoir not far north of the site. If isotope technology was used to trace the source of the surface water seepage when it originated a large amount of money could be saved by repairing the leak and not spent on constructing a channel around the site.

INTRODUCTION

In many areas in the Republic of South Africa groundwater is the only source for domestic water supply. It is therefore to the utmost importance to protect these resources from pollution. One of the worst sources of pollution is waste disposal sites. This is especially true of the waste disposal sites not selected or not managed and monitored scientifically. Numerous waste sites just originated by dumping waste in quarries with no idea that pollution is now placed almost in the underlying aquifer as it was closer to the water table than when placed on surface. This is why the landfill concept makes more sense. However we still have water seeping into the waste and conveying pollutants into the underlying aquifer.

Managing water seepage and collecting leachate is required to reduce the potential impact of the site on the groundwater. The movement of pollution still need to be detected and monitored to be able to mitigate against impact on the environment. It is therefore necessary to know the dynamics of the underlying aquifer.

Anomalously high levels of artificial tritium have been discovered in leachates from waste sites in the Republic of South Africa and elsewhere and indications are that this may be ubiquitous in such sites (Levin & Verhagen, 1997; Verhagen et al., 1998). Simultaneous with these discoveries in South Africa, rather high levels of artificial tritium were reported in leachate from English landfill sites (Robinson & Gronow, 1995).

The potential of these tritium levels for tracing pollutants in water was soon recognized. The origin of this artificial tritium has not yet been firmly established but in leachate it constitutes a unique tracer.

Established background tritium values for rain and recently recharged rainwater in the southern Hemisphere are still low. We can utilize the contrasts of up to 4 orders of magnitude to trace and identify sensitively tritium-containing spillages or leakages. In this case the source of the tracer is unique (the leachate) and is indisputable.

The contrast between environmental and artificial tritium can therefore be used also to evaluate the usefulness of the monitoring boreholes and detect any leakage from the leachate system to the monitoring boreholes and into the environment in general.

The stable isotopes Oxygen-18 and Deuterium have the capability to indicate if it is groundwater or was it exposed on surface to evaporation. Evaporation effects in the landfill itself may additionally label leachate or may indicate unrelated water occurrences can be identified with stable isotope analysis (Levin et al., 1991; Verhagen et al., 1991; Levin & Verhagen, 1997). Bulk water supply from surface water exposed to evaporation display stable isotope values different to groundwater and can be used for tracing the source of water seepage. The stable isotope values combined with chemical analysis provide an undisputable confirmation of the source.

OBJECTIVES

This study develops and evaluates in particular the use of environmental isotope hydrology in assessing groundwater vulnerability to waste disposal. The original project objectives were:

- The main objective is to expose the potential of isotope techniques in the detection, tracing and managing pollution related to waste disposal sites in South Africa.
- Engineers, scientists and Municipal officials need to understand that applying these techniques can assist them to manage and control pollution impact at waste disposal sites.
- It must be understood that isotope techniques is applicable from site selection to site closure.
- To highlight the main objective feasibility studies were done to proof and confirm the positive outcomes of previous studies.
- To trust that these techniques will be included in future NEMA regulations for waste disposal in South Africa.

METHODOLOGY

Background

The environmental isotopes species that can be employed in monitoring of landfill sites are the non-radioactive (or "stable") isotopes ^{18}O and ^{2}H and the radioactive isotopes ^{3}H. These isotopes label the water molecule itself and their concentrations are not influenced or altered by chemical reactions.

Although isotope techniques cannot "find" groundwater it is able to:

- Determine the origins and ages of different water bodies;
- Provide an estimate of the degree of mixing;
- Determine the location and proportion of water recharge; and
- Indicate the velocity of groundwater flow.

Oxygen –18 (^{18}O) and Deuterium (^{2}H)

Oxygen–18 (^{18}O) together with deuterium (^{2}H) are present in water in isotopic abundances of about $^{18}O/^{16}O$ = 0.2% and $^{2}H/^{1}H$ = 0.015% with respect to the common, lighter isotopes ^{16}O and ^{1}H respectively. In various combinations, these isotopes constitute water molecules, principally of masses 18, 19 and 20. In phase processes such as evaporation and condensation, the different vapour pressures of these molecules cause small changes in the isotopic abundances, the heavier isotopes tending to concentrate in the denser phase. These small changes can be expected as a fractional deviation from a standard called SMOW (Standard Mean Ocean Water), defined as:

$$\delta = [(R_s/R_r) - 1] \times 1000 \text{ (‰)}$$

where R_s and R_r are the ratios of the abundances of the rare (heavier) isotope to the more abundant (light) isotope for the sample and reference standard, respectively.

Physical processes such as evaporation can change these δ values from that in the original precipitation. The δ values can therefore be diagnostic of water from different origins such as rainwater, direct recharged groundwater or evaporation ponds or evaporated leachate.

Tritium

Environmental tritium is a very useful tracer of water and widely used in hydrological studies (IAEA 1983; Verhagen et al. 1991). Tritium is produced in nature by cosmic ray interaction with the upper atmosphere, and readily oxidised to water in which it is a conservative tracer as it is part of the water molecule. Depending on geographical location, rain water contains natural tritium at concentrations of up to some 5 TU (1 TU = $[^{3}H]/[^{1}H] = 10^{-18}$). Tritium is radioactive and decays through low-energy beta ray emission with a half-life of 12.43 years. Its radioactivity can only be measured in the laboratory.

Minimum detectable values are about 5 TU by direct (screening) counting; following isotope enrichment, 0.2 TU can routinely be attained. The useful range of measurement of environmental tritium in geohydrological applications spans four to five half-lives and it is therefore measurable only in, and can act as an indicator or, recently recharged ground water.

Thermonuclear weapons testing in the latter 50s and early 60s increased tritium concentrations in rainfall by up to three orders of magnitude in the northern hemisphere and about one order in the southern hemisphere. This tritium "pulse" could be traced through hydrological systems such as ground water. At present, the widespread use of artificial tritium in e.g. Europe maintains tritium in rainfall at about one order of magnitude above the natural value. In Southern Africa, where the use of artificial tritium is much less common, tritium in rainfall has returned to close to natural values. Ground water usually has lower values, depending on residence times or recharge rates. Any water labelled with artificial tritium can therefore readily be detected and traced in the Southern African environment.

Tritium in Groundwater

The presence of tritium in ground water in amounts similar to that in present day rainfall of the area would be an indication of rapid and active percolation. Provided it is well protected against direct inflow from surface a borehole yielding water with present day rainfall values of tritium can therefore be considered an excellent monitoring borehole. It would rapidly respond to leakages and spillages of leachate which might already be visible after the first rainfall following the incident. Such boreholes should be sampled at about two or three monthly intervals.

Low but measurable tritium in ground water points to longer residence times for ground water, due to the delay in the unsaturated zone or low recharge/storage ratio in the unsaturated zone. Monitoring boreholes displaying such values may for a number of years show very little change. However, once pollution is detected in such a borehole it is certain that, even if the source is stopped, the levels of pollution will be maintained for a number of years until it dissipates.

Such boreholes are not considered good monitoring boreholes and frequent sampling is not recommended. A six monthly or annual sampling frequency is recommended depending on the measured base line tritium level. The absence of tritium in ground water sampled from a monitoring borehole indicates very low recharge and ground water residence times well in excess of 50 years. Such boreholes cannot be considered good for early detection pollution monitoring and frequent sampling would be meaningless.

As tritium labels the water molecule itself, its concentration in e.g. ground water is, to a good approximation unaffected by processes in the sub-surface. It is therefore a conservative tracer. Sampling and handling water for tritium analysis is straightforward and requires no special precautions as compared to e.g. sampling for chemistry or dissolved gases. For direct counting a 50 ml sample suffices. For low level detection following isotope enrichment, a litre of water sample is usually required.

Monitoring

All the municipalities are required to permit their waste disposal sites according to NEMA and have monitoring programs for the monitoring boreholes around their landfill sites. The use of the environmental isotope techniques has been included in the Draft Minimum Requirements (DWA, 2005) but this has not yet been published and accepted as a requirement for landfill site monitoring.

Municipalities award monitoring tenders for chemical and biological analysis but are not aware of the usefulness of environmental isotopes - and specifically tritium - data in interpreting the effectiveness of their waste management system.

In most cases due to budget constraints the minimum monitoring takes place and they have no indication of pollution taking place. The best approach is to sample the monitoring boreholes at the waste disposal sites for both chemical and environmental isotopes at least once to establish the character of the isotope results compared to the chemical data. The environmental isotope results are overlain over the present and previous monitoring data to establish leachate leakage, movement of polluted and evaporated pond water.

The Emfuleni Local Municipality required monitoring three of their waste disposal sites and agreed that isotope techniques could be applied to detect and trace any pollution on the sites during the first set of samples of the three year biannual monitoring program. Sampling for monitoring is done at the end of the wet season at end of March and at end of dry season at the end of September. Based on the results obtained during the first monitoring event using chemical and environmental isotopes a management and mitigation plan can be recommended and implemented. Of the three sites the site with serious pollution detected that required mitigation was the Boitshepe Site on which this project focus.

The results of the mitigation and management plan should show in the future monitoring results and if necessary the isotope techniques can be used to confirm improvement.

In another study the Ekurhuleni Metropolitan Municipality requested an investigation to trace the source and possible connection between the surface and leachate at the Rooikraal Landfill Site located on the border between Boksburg and Brakpan in Gauteng.

The concern is that the surface water entering the site has an impact on the volume of leachate flowing into the leachate pond. Previous studies did not trace the source and the application of environmental isotopes was recommended and applied to solve the problem.

SITE INVESTIGATIONS

BOITSHEPE WASTE DISPOSAL SITE

This site is located between the townships of Boipatong and Tshepiso in the Umfeleni Local Municipality. Sampling took place on 8 July 2010. Five boreholes were available for sampling and a leachate sample was collected where it emerges and flows into the regional drainage area. The locality of the boreholes and leachate issue are shown in Fig. 1.

The results of the chemical analysis are shown in Table 1. Only boreholes BH3 and BH4 are not polluted. BH3 is upstream from the landfill area. In order to investigate the chemical character of the boreholes the data were plotted on the Piper diagram shown in Fig. 2. From the Piper diagram is clear that only BH3 is not impacted as it falls in the recharge calcium bicarbonate field. All the polluted boreholes have high salinity similar to the leachate. BH4A is highly polluted as it lies downstream of the landfill site.

The results of borehole BH4 are isotopically least enriched and plots on the GMWL. They probably represent rainwater or local shallow groundwater (no evaporation). BH1, BHB3 and the leachate plot close to the GMWL and appear related. They are significantly enriched with respect to an average rain and could reflect evaporation under saturated moisture conditions inside the landfill mass Sample BH3 shows evaporation under lower moisture conditions whilst BH4A may also reflect some hydrogen isotope exchange within the landfill.

Figure 1: The locality of the boreholes and leachate sampling point at Boitshepe Landfill site with tritium values in TU. Arrows show inferred leachate migration.

Sample Nr.	BH1	BH3	BHB3	BH4	BH4A	Leachate	Class I	Class II
Ca	79.96	29.34	92.18	21.93	178.67	45.80	150	300
Mg	12.50	12.50	94.95	12.50	140.01	57.84	70	100
Na	231,18	11.81	177.02	11.17	525.61	347.82	200	400
K	25.37	6.541	180.78	3.39	126.96	196.82	50	100
Mn mg/l	2.10	1.91	0.241	0.156	91.83	5.76	0.1	1
Total Cr mg/l	<0.002	<0.002	<0.002	<0.002	<0.002	<0.002		
Cu mg/l	0.026	0.023	0.032	0.026	0.179	0.086		
Ni mg/l	0.011	0.01	0.014	0.11	0.593	0.068		
Zn mg/l	0.016	<0.004	0.047	0.016	4.173	0.123		
Co mg/l	0.002	<0.002	<0.002	0.002	0.97	0.034		
Cd mg/l	<0.001	<0.001	<0.001	<0.001	<0.001	<0.001		
Pb mg/l	0.02	0.02	0.03	0.02	0.08	0.02		
Fe mg/l	0.644	0.007	0.011	<0.006	0.06	0.10	0.2	2
F	<0.183	<0.183	0.31	<0.183	1.13	0.65	1	1.5
NH4 as N	3.99	0.90	0.33	0.14	44.77	44.79		
NO2 as N	<0.005	0.37	<0.005	0.34	0.25	0.51		
NO3 as N	<0.057	0.69	<0.057	1.84	1.36	1.49	10	20
Total Hardness	106	125	621	106	1023	353		-
Al	0.664	<0.006	<0.006	<0.006	2.242	<0.006	-	-
PO4 as P	<0.025	<0.025	<0.025	<0.025	<0.025	<0.025	-	-
Cl	652.00	19.90	505.80	62.70	1703.70	908.00	200	600
SO_4	<0.132	<0.132	241.48	<0.132	431.04	82.12	400	600
TDS mg/l	1195.00	161.00	1511.00	148.00	3117.00	1805.00	1000	2400
M-Alk($CaCO_3$)	167.10	132.90	364.70	54.10	15.90	275.10	-	-
pH	7.35	7.71	7.71	6.96	4.52	7.62	5.0 - 9.5	4.0 - 10.0
EC mS/m	291.90	30.97	269.00	31.50	683.00	358.30	150	370

Notes
Yellow = Class I
Tan = Class II
exceeds maximum allowable drinking water standard
na- not analysed
0 = below detection limit of analytical technique

Table 1: Chemical analyses of samples from Boitshepe landfill site in July 2010

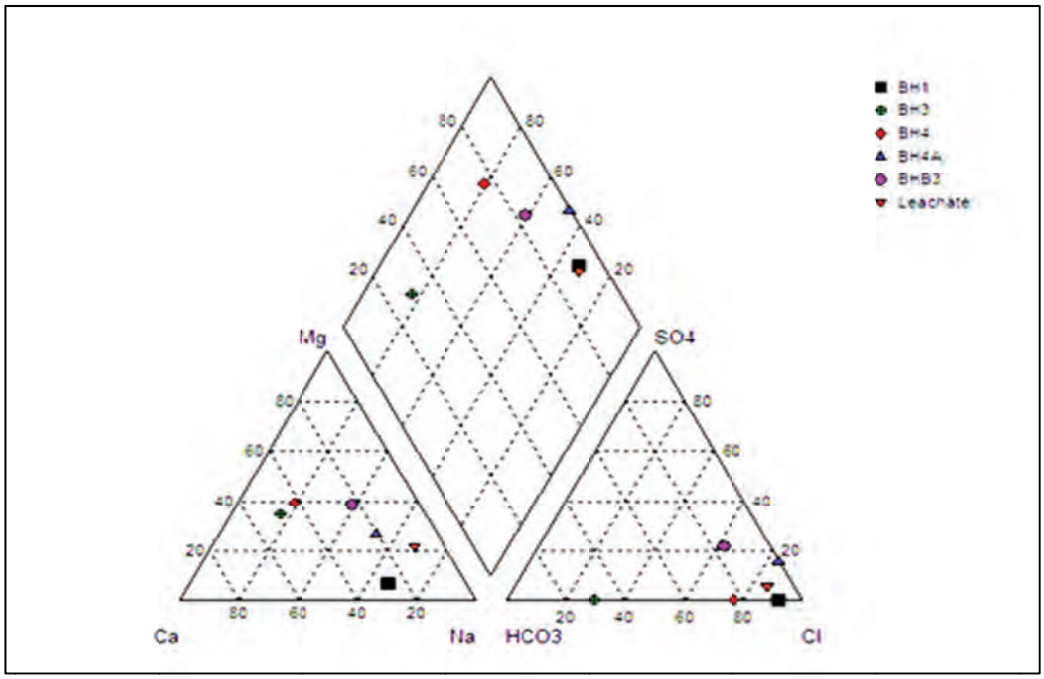

Figure 2: Boitshepi Piper diagram.

The stable isotope data (Table 2) is plotted on the $\delta^{2}H$ vs. $\delta^{18}O$ graph relative to the Global Meteoric Waterline (GMWL) in Fig. 3.

Laboratory Number	Sample Identification	δ D (‰)	δ ^{18}O (‰)	Tritium (T.U.)	
WITS 174	Boitshepi BH1	-11.5	-2.67	136.4	±3.6
WITS 175	Boitshepi BH3	-8.8	-1.73	3.2	±0.3
WITS 176	Boitshepi BH4	-23.6	-4.17	2.5	±0.3
WITS 177	Boitshepi BH4A	-5.0	-2.43	390.9	±9.1
WITS 178	Boitshepi BHB3	-13.0	-2.74	288.5	±7.0
WITS 179	Boitshepi Leachate	-11.4	-2.61	787.1	±26.8

Table 2: Environmental isotope data for Boitshepi Waste Disposal Site

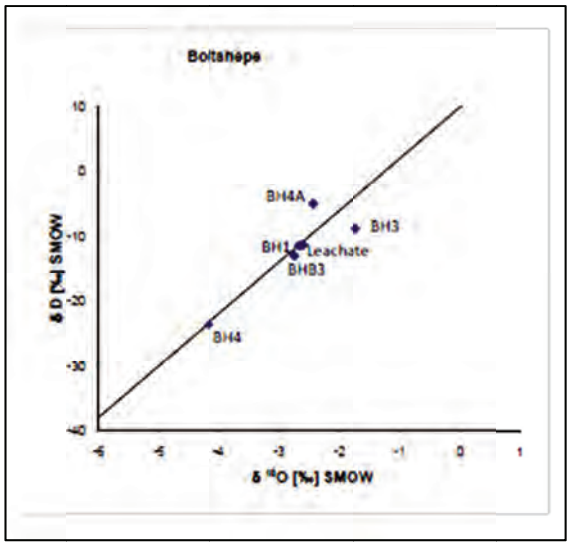

Figure 3: Stable isotope data detail for Boitshepi relative to the Global Meteoric Water Line.

From the results it is clear that the leachate contains anomalous tritium of 787.1 TU. Boreholes BH1, BH4A and BHB3 also have abnormal high tritium values. The source of these anomalous values can only be the leachate. The tritium in the leachate is therefore an excellent tracer not affected or impacted by the chemical properties of the water. This confirms the stable isotope and chemical conclusions regarding impacted boreholes. It is concluded that these boreholes are polluted and that Boitshepi Landfill has presently a serious pollution problem that requires mitigation. Mitigation of the leachate will immediately require containment of the leachate that is currently flowing into the environment at surface. This will require a detail investigation of the underlying geology, design outlay and operation of the site.

DISCUSSION OF RESULTS

Borehole BH3 is upstream and not impacted by the landfill and can be considered background information. All the other boreholes except BH4 which is blocked show pollution related to the leachate. This is confirmed by the stable isotope results. The tritium results show the pollution in the boreholes and in the leachate which flows outside the waste site boundary into the environment. The following calculations show the power of the tritium technique:

BH3 Background Chloride 19.9 mg/l Leachate Chloride 908.0 mg/l. 908/19.9= 45.63 =10^1
BH3 Background Tritium 3.2 TU Leachate Tritium 787.1 TU. 787.1/3.2=245.97=10^2

This indicates that Tritium has an order of magnitude greater capability in tracing pollution than the chemical parameters. More detail investigation of the underlying geology and the borehole geology is required to establish the extent of the pollution plume. The source of the leachate must be investigated and contained inside the landfill site as mitigation to prevent further pollution of the downstream water sources. Further mitigation requires that surface runoff must be controlled around the site to ensure no runoff seeps through the landfill material or flow into the leachate pond. Once mitigation measures are installed the tritium levels will indicate the success of the pollution management program.

ROOIKRAAL WASTE DISPOSAL SITE

The Rooikraal Landfill Site is located next to Barry Marais Road on the border between Boksburg and Brakpan in the Ekurhuleni Metropolitan Municipality shown on Figure 4. The site was visited on the 17th of January 2012 to get an overview of the layout, topography and surface drainage system. There were no water flowing in the natural drainage channel but clean water was flowing out at a point about 140m from the centre of the drainage channel.

The regional geology around the site consists of the Black Reef Quartzite Formation and dolomite of the Malmani Subgroup of the Transvaal Sequence which are partly the younger sediments of the Karoo Sequence. These rocks have been intruded by a post Karoo dolerite sill. The site is underlain by dolerite between 10 and 30 m thick. The dolerite thins out to the south (10m) where dolomite is closer to surface. According to MIE (2004) hydrogeological report, there are no faults and/or fracture systems in the area. They further confirm that the groundwater occurs in at least two distinct aquifer systems beneath the site:

- Perched aquifers in relatively impervious horizons of residual clayey sands derived from weathered dolerite; and
- Deeper, semi-confined to confined weathered and/or fractured zone aquifers within the dolerite and dolomite rocks.

Water levels recorded on the site vary between 1 and 8.5 m below ground level. The presence of perched aquifers and seasonal trends in the water levels confirm that storm water seeps into the subsoil to bedrock and migrates along the gradient in a southerly direction.

Samples were collected on the 17th January 2012 at the available boreholes and of the leachate flowing out of the landfill towards the collection pond. Borehole RBH4 is located in the same area and was sampled. It was decided to sample a borehole downstream out of the site area and Borehole BH6. Samples of Randwater were collected at the kitchen of the offices for comparison reason. The samples collected for chemical analysis were submitted to Clean Stream Scientific Services in Pretoria. The results of the chemical analyses are presented in Table 3.
The inorganic results were compared to the SABS drinking water standards (SANS 241:2006, edition 6.1). Water is classified according to their suitability for human consumption in:

- Class I: Recommended operational limit.
- Class 2: The maximum allowable concentration for short term use only.

The results show that the surface water sampled compared very well with the chemistry of Randwater. The possibility therefore exists that the surface water flow sampled originates from a leak in the Randwater

Figure 4: The locality of the boreholes and leachate sampling point at the Rooikraal Landfill site

reticulation system. The groundwater sampled in BH06 is also of good quality with no parameters above the limits. The water sampled at RWS3, RBH4 and the leachate all have parameters above the Class II limits for drinking water. It is concluded that the leachate from the landfill is impacted on the groundwater in these boreholes.

The regional geology around the site consists of the Black Reef Quartzite Formation and dolomite of the Malmani Subgroup of the Transvaal Sequence which are partly the younger sediments of the Karoo Sequence. These rocks have been intruded by a post Karoo dolerite sill. The site is underlain by dolerite between 10 and 30 m thick. The dolerite thins out to the south (10m) where dolomite is closer to surface. According to MIE (2004) hydrogeological report, there are no faults and/or fracture systems in the area. They further confirm that the groundwater occurs in at least two distinct aquifer systems beneath the site:

- Perched aquifers in relatively impervious horizons of residual clayey sands derived from weathered dolerite; and
- Deeper, semi-confined to confined weathered and/or fractured zone aquifers within the dolerite and dolomite rocks.

Water levels recorded on the site vary between 1 and 8.5 m below ground level. The presence of perched aquifers and seasonal trends in the water levels confirm that storm water seeps into the subsoil to bedrock and migrates along the gradient in a southerly direction.

Samples were collected on the 17th January 2012 at the available boreholes and of the leachate flowing out of the landfill towards the collection pond. Borehole RBH4 is located in the same area and was sampled. It was decided to sample a borehole downstream out of the site area and Borehole BH6. Samples of Randwater were collected at the kitchen of the offices for comparison reason. The samples collected for chemical analysis were submitted to Clean Stream Scientific Services in Pretoria. The results of the chemical analyses are presented in Table 3.

The inorganic results were compared to the SABS drinking water standards (SANS 241:2006, edition 6.1). Water is classified according to their suitability for human consumption in:

- Class I: Recommended operational limit.
- Class 2: The maximum allowable concentration for short term use only.

The chemical results were plotted on the piper diagram to compare the chemical character of the samples. The piper diagram is shown in Fig. 5 and samples from Surface water, Randwater and BH06 all group and plot in the Calcium-Magnesium-Carbonate field expected for rain water and freshly recharged groundwater and surface water. The fact that the Surface water and Randwater samples plot exactly on the same spot confirms that the Surface water could re-presents leakage from the Randwater reticulation system.

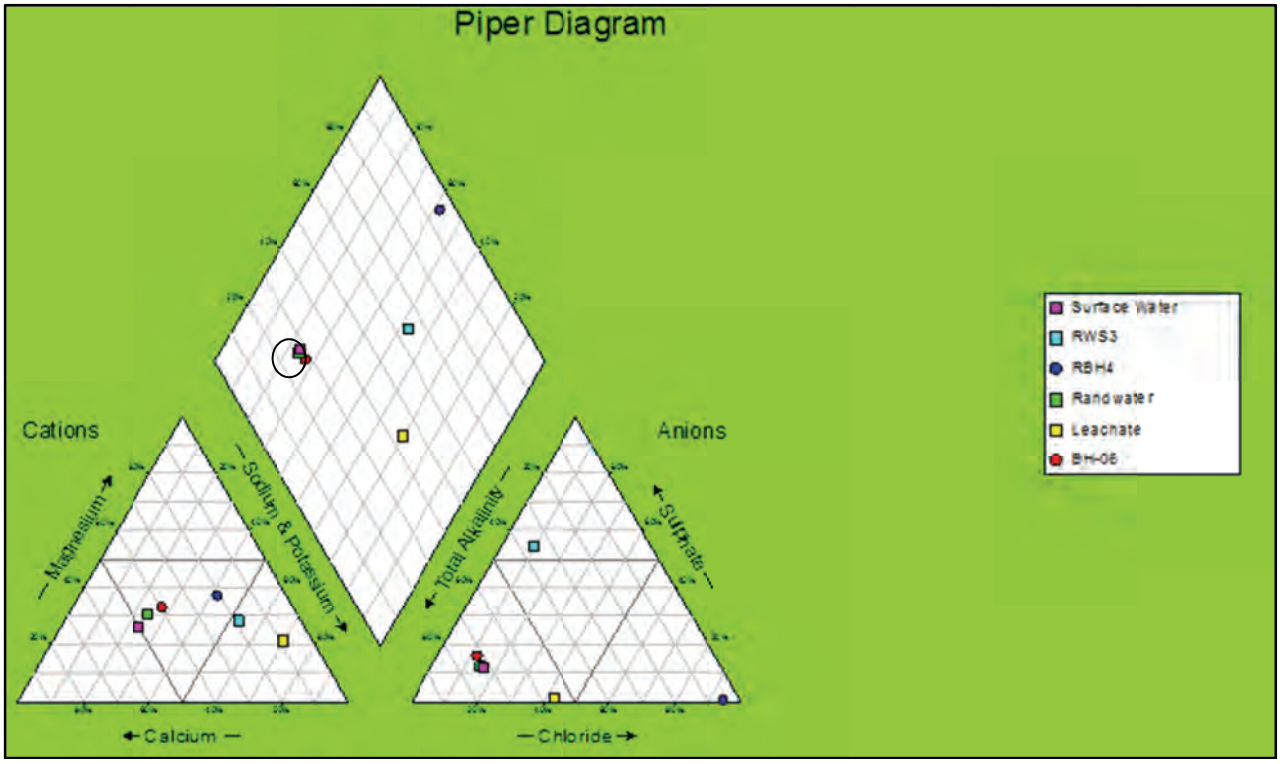

Figure 5: Piper diagram for the Rooikraal Landfill samples taken January 2012.

Sample Nr.	Randwater	Surface Water	RWS3	BH06	RBH4	Leachate	Class I	Class II
Ca	14.92	17.56	110.92	27.51	108.40	157.20	150	300
Mg	6.10	5.48	100.05	13.86	117.76	223.83	70	100
Na	7.77	7.85	357.32	21.78	252.23	1222.51	200	400
K	2,581	3.11	1.474	0.522	1.351	336.198	50	100
Mn mg/l	<0.001	<0.001	<0.001	<0.001	0.64	2.778	0.1	1
Total Cr mg/l	<0.002	<0.002	<0.002	<0.002	<0.002	<0.002		
Cu mg/l	0.006	<0.001	0.01	<0.001	<0.001	0.037		
Ni mg/l	<0.003	<0.003	<0.003	<0.003	<0.003	0.128		
Zn mg/l	<0.004	<0.004	<0.004	<0.004	<0.004	0.034		
Co mg/l	<0.002	<0.002	<0.002	<0.002	<0.002	0.054		
Cd mg/l	<0.001	<0.001	<0.001	<0.001	0.001	0.001		
Pb mg/l	<0.001	<0.001	<0.001	<0.001	<0.001	0.021		
Fe mg/l	<0.006	<0.006	<0.006	<0.006	<0.006	2.069	0.2	2
F	0.201	0.222	0.63	0.2	0.199	1.147	1	1.5
NH4 as N	0.80	0.03	<0.015	<0.015	0.34	1.05		
NO3 as N	0.47	0.64	0.17	0.47	0.08	0.06	10	20
Total Hardness	62	66	689	126	756	1314		-
Al	<0.006	<0.006	<0.006	<0.006	<0.006	<0.006	-	-
PO4 as P	0.05	0.028	0.112	<0.025	<0.025	1.088	-	-
Cl	8.30	9.00	102.40	14.90	808.20	1427.20	200	600
SO_4	10.08	10.23	751.39	27,73	5.52	48.1	400	600
TDS mg/l	88.00	93.00	1731.00	186.00	1329.00	4992.00	1000	2400
M-Alk(CaCO3)	63.80	65.50	512.80	132.90	59.80	2627.40	-	-
pH	8.18	8.05	8.03	7.09	7.44	8.08	5.0 - 9.5	4.0 - 10.0
EC mS/m	20.29	21.97	277.70	41.90	296.70	944.00	150	370
Notes								
Yellow = Class I								
Tan = Class II								
Exceeds maximum allowable drinking water standard								

Table 3: Chemical analyses of samples from Rooikraal landfill site in January 2012

The samples were submitted to iTemba LABS in Johannesburg and the results are presented in Table 4. The data is plotted on the $\delta^{18}O$ vs. $\delta^{2}H$ graph relative to the Global Meteoric Waterline (GMWL) shown in Fig. 6. The GMWL represent the global rainfall data. Groundwater normally plot along this line as it is mainly rainfall that enters the ground profile without any evaporation taking place.

Laboratory Number	Sample Identification	δ D (‰)	$\delta^{18}O$ (‰)	Tritium (T.U.)
AFR 520	RBH4	-5.6	-2.51	
AFR 521	Surface Water	-13.0	-2.49	
AFR 522	Leachate	-	-1.62	781.0 ±17.6
AFR 523	BH6	-14.7	-2.66	
AFR 524	Randwater	-12.2	-2.40	
AFR 525	RWS3	-16.4	-3.32	

Table 4: The isotope results for Rooikraal samples January 2012

The results of Randwater, Surface water and borehole BH6 group together as shown in Fig. 6. Borehole RWS3 plot as expected on the GMWL as expected from groundwater. Unfortunately the Leachate $\delta^{18}O$ could not be measured as it might have indicated a connection to RBH4 which shows slightly heavier isotope values then the rest. It is concluded that some correlation exist between the Randwater, Surface water and borehole BH6.

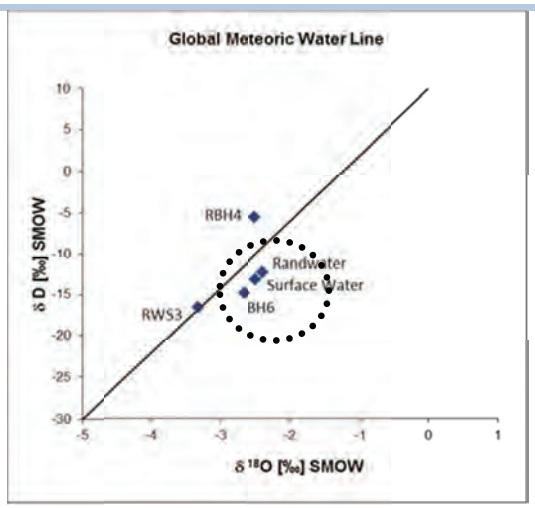

Figure 6: Stable Isotope data relative to the Global Meteoric Water Line

A tritium sample was collected at the leachate stream. The result of the tritium analysis is shown in Table 4. Rainwater results at present in Gauteng normally vary a lot between 2 and 3 TU. From the results it is clear that the Leachate contains anomalous tritium of 781.0 TU. It is expected that RBH4 and all sources impacted by the Leachate will show increased tritium.

DISCUSSION OF RESULTS

Ten years ago when the surface water seepage started a concrete channel was constructed to divert the flow of the seepage around the waste site to limit the impact on the leachate.

The stable isotope results of the surface water are similar to that of the Randwater sample collected from the reticulation system. The chemical results confirm that the surface water has the same chemical character than the Randwater. The leakage was further investigated and found that it is leakage at a Bulk Storage Reservoir not far north of the site. If isotope technology was used to trace the source of the surface water seepage when it originated a large amount of money could be saved by repairing the leak and not spent on constructing a channel around the site. It was recommended that tritium samples be taken at all the boreholes to confirm the impact of the leachate pollution of the groundwater and determine the extent of the pollution plume.

CONCLUSION

At the Boitshepi Waste Site the tritium results clearly showed the extent of the pollution in the boreholes and leachate. This is confirmed by the stable isotope and chemical results. The tritium results show the pollution in the leachate which flows outside the waste site boundary into the environment. It is shown that the tritium isotope technique at this site has an order of magnitude greater capability in tracing pollution than the chemical parameters. More detail investigation of the underlying geology and the borehole geology is required to establish the extent of the pollution plume. Further mitigation requires that surface runoff must be controlled around the site to ensure no runoff seeps through the landfill material or flow into the leachate pond. Once mitigation measures are installed the tritium levels will indicate the success of the pollution management program.

At the Rooikraal site the focus was on tracing the source of the surface water seepage that originated ten years ago at the site. It was thought that the seepage is impacting on the leachate generation. The stable isotope and chemical results of the surface water are exactly similar to that of the Randwater sample collected from the reticulation system. The leakage was further investigated and found that it is leakage at a Bulk Storage Reservoir not far north of the site. If isotope technology was used to trace the source of the surface water seepage when it originated a large amount of money could be saved by repairing the leak and not spent on constructing a channel around the site.

ACKNOWLEDGEMENTS

The following people contributed to the success of this project:

- The Water Research Commission for funding the project and ensuring the best scientific results being achieved.
- The Water and Waste Management Units of Aurecon (Pty) Ltd for supporting this project by making available projects in the field.
- The Emfuleni Local Municipality for giving permission that the data can be used for this WRC research project.
  The Ekurhuleni Metropolitan Municipality for giving permission for the Rooikraal investigation data to be used for this WRC research project

REFERENCES

Levin M., Walton, D., Verhagen, B. Th. (1990/91). *Environmental isotope, hydrological and hydrogeochemical studies of ground water pollution associated with waste disposal.* Joint Water Research Commission project of the AEC and the Schonland Research Centre, Wits. Water Research Commission Project K5/311.

Verhagen B, Th, Levin M, Walton, D. (1991). *Environmental isotopes and hydrochemistry identify pollution sources in waste disposal study. Proceedings Biennial Groundwater Convention Midrand , 20-23 August.*

Levin, M., Verhagen, B. Th. (1997). *The use of environmental isotopes in pollution studies.* Conference on Geology for Engineering, *Urban Planning and the Environment, 13-14 November, Eskom Centre. Midrand.*

Verhagen, B. Th., Levin, M., Fourie, A. (1998) *High level tritium in leachate from landfill sites in the Republic of South Africa with emphasis on its distribution and value as an environmental tracer.* WISA '98, Water Institute of Southern Africa, Biennial Conference, 4-7 May, Baxter Theatre Centre, Cape Town.

Levin, M., Verhagen, B. Th. (1997). *A unique approach to evaluate the utility of landfill monitoring boreholes*. Geotechnics for Developing Africa, Wardle, Blight and Fourie (eds) 1999 Balkema, Rotterdam.

Masakhe Isizwe Engineers (MIE) (2004) *Long-term Development and Operational Plan for the Existing Rooikraal Landfill Site*. Report MIE2232/B0109 dated August 2004.

SANS 241:2006 (Edition 6.1) South African National Standard – *Drinking Water*

DWA (2005) *Minimum Requirements for Water Monitoring at Waste Management Facilities*. Draft document addresses the monitoring of water quality at and around waste disposal facilities.

Robinson, H. D., Gronow, J. R. (1995). *Tritium levels in leachate from domestic wastes in landfill sites*. In: Procs Sardinia 95. *Fifth International Landfill Symposium CISA, Cagliari, Italy.*

Since 1990 when the first WRC project was initiated to evaluate the use of environmental isotopes in pollution studies, several waste disposal and landfill sites were investigated and here we display a few of them.

Water Research Project No 311/1/01

This was the first research project to investigate groundwater pollution associated with waste disposal using an environmental isotope approach. In order to test the various isotope methodologies in various geological environments, five areas were studied on a site specific basis;

1. Olifantsfontein/Clayville -Midrand - Karoo outliers within dolomite (infilling of old clay quarries).
2. Linbro Park - Sandton - Weathered granites (infilling of borrow pit/landfill).
3. Waterval - North western suburbs of Johannesburg - Diorite gneisses and granite (landfill) and
4. Bloemfontein - North - Dolerite (landfill)
5. South - Siltstones and sandstones (landfill)

These sites were chosen specifically in relation to a) their geological environment, b) the type of waste disposal that was being practised and c) the availability of monitoring boreholes for adequate data collection and historic information.

The first recording of anomalous tritium of 23.2 TU was found in the water draining from the Waterfall landfill which has been closed for 20 years. Then The Bloemfontein North and South sites produced values of 26.5 and 40.1 TU respectively. It was thought that the tritium originated from medical radiation material used at the University Research Hospital. It was concluded that the environmental isotope is a powerful tool that can be used to trace and manage pollution. Various recommendations for further studies were made.

Verhagen B Th, Levin M, Walton D G and Butler M J (1996) *Investigation of groundwater pollution associated with waste disposal: Development of an environmental isotope approach.* WRC Project No 311/1/01, January 1996.

Bellville South Landfill Site

In the mid 1990 the Department of Water Affairs and Forestry wanted to close the Bellville South Landfill Site because of pollution detected during a CSIR investigation involving geophysics, drilling and chemical sampling. It was then recommended in 1994 that stable isotope study should be done of the groundwater in all the monitoring boreholes. The stable isotope results showed evaporated water in the groundwater next to the sewerage ponds. This corresponded with the chemical pollution such as nitrates. Enquiries lead to the information that a spillage from the ponds occurred and that upgrading of the ponds is considered. The DWA withdrew their request for closure and saved the Bellville Municipality lot of money exploring for a new site. Now only after 15 years they consider closing the site.

Levin M and Verhagen B Th (1997) *The use of environmental isotopes in pollution studies*. SAIEG Conference, *Geology for Engineering, Urban Planning and the Environment*. Eskom Conference Centre, Midrand, Gauteng, 12 – 14 November 1997.

Bulbul Landfill Site

The Bulbul Landfill Site is located on the southwestern side of Durban west of the Old International Airport. In 1997 a landslip occurred at the landfill and leachate end in the Mlazi River and leachate ponded in the disturbed waste dump. Samples were selected at all monitoring boreholes, the leachate up and downstream in the river. The undiluted leachate measured 76000 TU while the diluted leachate measured between 12000 and 15000 TU. The 100m wide Mlazi River measured upstream 3 TU and downstream 11 TU. Of the 19 monitoring boreholes only two showed 4 and 6 TU and the rest all 0.0 TU. These boreholes were drilled into Dwyka Tillite Formation of the Karoo Supergroup that have very low hydraulic properties. The monitoring boreholes therefore are not recharged and were sampled with no results. Spending on sampling and monitoring could have been avoided if the isotope techniques were employed at the site selection stage. The Tritium in the leachate concentrated at least two orders of magnitude more than the chemical parameters which again highlight the power of artificial Tritium in waste site pollution tracing.

Holfontein Hazardous Waste Disposal Site

During October 1996 the DWA requested an evaluation of the Holfontein Hazardous Waste disposal site. Up to that date no isotope analysis were applied to monitoring the boreholes at the site. Samples were collected at and around the Holfontein site which include the five monitoring boreholes on the site. The leachate showed 448 TU and the monitoring borehole close to the leachate pond showed 31.3 TU. Of the other four boreholes two the tritium showed dynamic recharge while the other two showed little recharge. The tritium results were confirmed by the chemistry showing higher salinity in the dynamic boreholes and

background chemistry in the two low recharge boreholes. Without any information from any initial monitoring reports it was possible to come to important conclusions regarding the pollution potential of the site. Follow-up investigation were done by the site management to control and manage the risk of pollution. The power of using environmental isotopes at waste disposal sites has been demonstrated by this investigation.

Faure Landfill Site

The Faure Landfill Site has been a formal but non-permitted waste disposal site for 20 years and in 2000 a geohydrological investigation was done in order to apply for closure permitting. The landfill is underlain by a sand aquifer in the Witzand Formation and below that the underlying Malmesbury Group Sediments. The geophysical electromagnetic technique survey outlined a plume in the sand aquifer to the south-east. The isotope data conservatively identified and confirmed the pollution plume to the southeast. Tritium values in the 5 boreholes outlining the plume varied between 125 TU and 250 TU with the background tritium in the background boreholes between 1.2 and 4 TU. One borehole in the Malmesbury showed 0 TU and is therefore a non-dynamic not recharged borehole. Based on the results recommendations was made to mitigate against infiltration and to make provision for measures to monitor, control and restrict the movement of the plume. This investigation again proofed the power and value of isotope techniques to indicate beyond doubt the pollution plume and groundwater dynamics.

Marie Louise Landfill Site

In 2008 it was decided to expand the Marie Louise Waste Disposal Site, located in Roodepoort, by empty and backfill the pond in the old quarry that form part of the site. Various options would be considered but first and important information needed was the connection between the pond and the groundwater aquifer underlying the site. Samples were taken at the pond and three existing monitoring boreholes. Unfortunately the two downstream boreholes did not exist anymore and no information exists about them. The pond showed a tritium level of 212 TU with the borehole next to an incline shaft south of the site showed 1170 TU. This borehole is possibly connected to a contact zone feeding leachate as that part of the landfill dated back about ten years. The low tritium in the other two boreholes confirms that no direct connection exist between the pond and the upstream boreholes. This does not exclude connection with downstream boreholes that could not be sampled. This data supplied the data required to plan a lined retention pond to replace the existing pond which will be backfilled. The results confirms the previous findings at waste disposal sites that leachate accumulate high levels of tritium which can be used as an indisputable tracer for monitoring pollution movement on the site.

OXYGEN AND HYDROGEN ISOTOPES RECORD OF CAPE TOWN RAINFALL AND ITS APPLICATION TO RECHARGE STUDIES OF TABLE MOUNTAIN GROUNDWATER

Chris Harris and Roger Diamond

ABSTRACT

Table Mountain rises over 1000m from the surrounding city of Cape Town at sea level and is made up of Table Mountain Group quartzite unconformably overlying Malmesbury Group metasediments and intrusive Cape Granite. The lower half of the mountain is covered extensively by soil and scree of TMG boulders. Many springs issue from the mountain slopes, mostly below 300m elevation, with flow volumes from non-perennial to over 20L/s. Fifteen of these springs were sampled biannually over 2010 - 2012 and along with cumulative monthly rainfall samples from UCT (137m a.m.s.l.) and Table Mountain (1074m a.m.s.l.) were analysed for O and H isotopes.

Results from both rain and springs show significant interannual variation in the mean isotope values and the pattern of change in the springs mimics that of the rainfall, indicating a short residence time of groundwater in the aquifer. An altitude effect of 0.55‰ δD and 0.085‰ $\delta^{18}O$ per 100m was calculated, falling at the lower end of the spectrum of measured altitude effects internationally. Application of the altitude effect reveals the average elevation of spring recharge to be 330m a.m.s.l. A conceptual model is proposed where springs are fed by the scree aquifers and flow within the scree is layered; the upper layers have short residence time, allowed rainfall to be discharged within the same season as recharge occurred, which accounts for the seasonal flow of some springs; the lower layers have longer residence times and account for the non-perennial springs with higher and more steady flow rates.

INTRODUCTION

The aim of this project, as originally proposed, was to compare the variation in O and H isotope composition of rainfall samples collected each month since 1996 at the University of Cape Town (UCT), with that of natural spring water issuing from the slopes at the base of Table Mountain. A pilot study indicated that such data may allow the rate and amount of recharge to be estimated. It was also intended to apply this approach (comparison of the variation of ambient rainfall and groundwater isotope composition over time) to other parts of the Cape Fold Belt. Over the last 3 years, the project researcher's PhD thesis involved a general investigation into the composition of rainfall, springs and groundwater across the Cape Fold Belt; only the Table Mountain spring data are reported and discussed here (see Annex 1 for the data).

STUDY AREA

The springs that were sampled for this project are located on the northern and eastern sides of Table Mountain, as shown in Fig. 1.

The basement geology is either the Neoproterozoic Malmesbury Group, a low-grade sequence of metamorphosed pelitic rocks (Belcher & Kisters, 2003) with poor outcrop and poor permeability, or the Cambrian Cape Granite, which has marginally better outcrop and potentially minor groundwater flow through fractures and portions of the weathered profile (Scheepers and Armstrong, 2002).

Overlying these is the Table Mountain Group of the Cape Supergroup, a Palaeozoic sedimentary sequence that dominates the geology of the Western Cape. The Table Mountain Group is particularly arenaceous and due to light metamorphism during the Permo-Triassic Cape Orogeny (Tankard, 2009), the arenaceous units are quartzite dominated and have no significant primary porosity remaining. Secondary porosity through fractures, however, is extensive and allows groundwater flow through the more quartzitic units (Blake et al., 2010).

Various younger unconsolidated to semi-consolidated materials also occur, namely scree aprons or alluvial fans on the slopes of the mountains and surficial sands and calcarenite on the lowlands or at the coast (Roberts, et al., 2006). The climate in Cape Town is Mediterranean, having cold, wet winters and warm, dry summers. Temperatures average 13°C in winter to 21°C in summer. Rainfall is much more complex, as the complex topography of the Table Mountain range results in drastic changes in rainfall over very short distances. The average annual rainfall amounts for Cape Town vary from 450mm/a at the Cape Town

International Airport on the Cape Flats to 1600mm/a at Kirstenbosch, on the eastern flanks of Table Mountain, a mere 15km apart (SAWB, 1996). The rainfall at UCT, based on 16 years record, and at the Upper Cableway Station on top of Table Mountain, based on an incomplete 2 year record, appear to be similar, at around 1300mm/a.

There are numerous springs that release water from the slopes of Table Mountain. The springs that have been studied in this work were selected on several criteria, including the volume of flow, knowledge of their whereabouts, ease of access and limited geographical extent. Springs occur all around Table Mountain, including the western and southern flanks, but the most famous and highest flow springs are closest to the high and steep parts of the mountain, being the Newlands side on the east and the city centre side to the north.

The selection of springs includes most of the perennial and high volume springs, specifically Albion spring, with a flow rate of around 10L/s and the Stadsfontein with a flow of around 20 L/s. Understanding the springs in the City Bowl area is complicated by the years of development and interference with the various springs. For example, the "field of springs" area off Upper Orange Street in Oranjezicht has a central collection chamber where water from several springs within a kilometre or so, including the Stadsfontein, is piped together. Private off-takes, leaks and other uses (e.g. for the Cape Town Stadium) of these springs make accurate measurements difficult. Most of the springs sit on the lower slopes of the mountain, at elevations lower than 300m, but the Lily Pond, a low flow, yet perennial drip, is at 950m, just below the final cliffs on Table Mountain and almost directly below the TMC rainfall collector about 125m above.

SAMPLING AND ANALYTICAL METHODS

Monthly rain water samples at UCT were collected in a standard rain gauge and transferred at 8 am each morning (assuming that rainfall occurred), to a larger screw-top glass container. At the end of each month, a sample was taken from the integrated rainfall sample for that month and analysed. The monthly samples include all rain from 8 am on the last day of the previous month to 8 am on the last day of the month. For the rain samples on Table Mountain, samples were collected monthly.

All samples were analysed as soon as possible after collection. For oxygen, the CO_2 equilibration method of Socki et al. (1992) employing disposable pre-evacuated 7 ml glass vials was used. For hydrogen, 2 mg of water contained in a microcapilliary tube was dropped into a Pyrex tube containing a few grains of Indiana Zn (Schimmelman and DeNiro 1993). The tube was attached to the vacuum line, frozen in liquid nitrogen, evacuated and then sealed using a torch. Once a large enough batch of samples had been prepared they were placed in a furnace at 450°C to reduce the water to H_2.

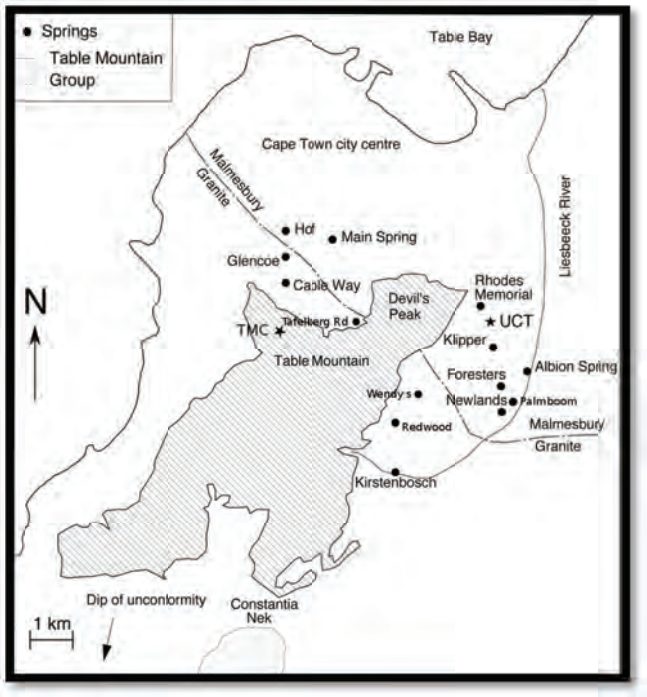

Figure 1: Location of sample sites, including springs (dots) and the two rainfall collection stations (stars); UCT is University of Cape Town and TMC is Table Mountain Cableway. The Lily Pond seep is almost directly beneath the TMC site. The simplified geology is shown, including the contact between the intrusive Cape Granite and the Malmesbury Group (from Geological Survey, 1984).

Isotope ratios of CO_2 and H_2 were measured using a Delta XP mass spectrometer, and the fractionation factor between CO_2 and water at 25°C was assumed to be 1.0412 (Coplen, 1993). Data are reported in the familiar δ notation where $\delta = (R_{sample}/R_{standard} - 1)*1000$, and $R = {}^{18}O/{}^{16}O$ or D/H. The long-term average difference between duplicates of our internal water standards (CTMP3, and CTMP2010) over the course of this research was 1.4 ‰ for hydrogen and 0.10‰ for oxygen. This suggests that the errors are of the order of 1.0 ‰ for δD and 0.05 ‰ for $\delta^{18}O$. The standards V-SMOW and SLAP (and calibrated secondary standards) were analysed to determine the degree of compression of raw data and the equations of Coplen et al. (1993) were used to convert raw data to the SMOW scale. Our internal water standards were run with each batch of samples and used to correct for drift in the reference gases. Evian bottled water (δD -73 ‰, $\delta^{18}O$ -10.11 ‰; Spangenberg and Vennemann, 2008) was analysed routinely with each batch of samples as an additional analytical check.

RAINFALL

Rainfall has been collected at two sites: on the roof of the Geological Sciences building at UCT at 137 m a.m.s.l. and on the roof of the Upper Cableway Station on Table Mountain at 1074 m a.m.s.l. The former site has the benefit of having many years of continuous rainfall collection (from 1996 onwards) and has had very few problems, except the occasional overflow of the rain gauge during an extremely heavy winter rainfall event. The effect of this is that some rainfall is not collected and could potentially alter the integrated isotopic value for that month, and that the exact rainfall amount is not known, which in turn affects the calculation of weighted means. However, it is expected that these few errors will account for minimal overall error in the calculation of weighted means and meteoric water lines.

At the Upper Cableway Station site, several issues unfortunately led to loss of data. Both operator error and equipment failure, largely due to the intense winds that occur on this part of the mountain, resulted in the rainfall amount not being recorded or the rain sample being missed or lost. Nonetheless, a reasonable record of rainfall over 2010-11 and into 2012 was collected on Table Mountain.

The data for both UCT and Table Mountain are shown in Fig. 2 along with the weighted means for these datasets. The weighted means were calculated by weighting the isotopic values with the rainfall amounts for each month. This gives low rainfall months a low weighting. Months with lower rainfall are more likely to have unusual isotope values, as the rainfall is made up of fewer, or even one, events, in which case unusual events are more likely to have their signals preserved, as well as the fact that summer thunderstorms typically produce rainfall of unusual isotopic composition. Evaporation effects are also likely to be larger on the low rainfall samples. Weighting removes much of this 'noise' from the mean.

The UCT meteoric water line calculated by Harris et al. (2010) has been plotted on Figure 2, with the equation $\delta D = 6.4\delta^{18}O + 8.66$, based on 12 years of rain data from UCT (1996-2008). It can be seen that both the UCT 2010-12 and the TMC 2010-12 means fall on the UCT-MWL, which further confirms the validity of this line.

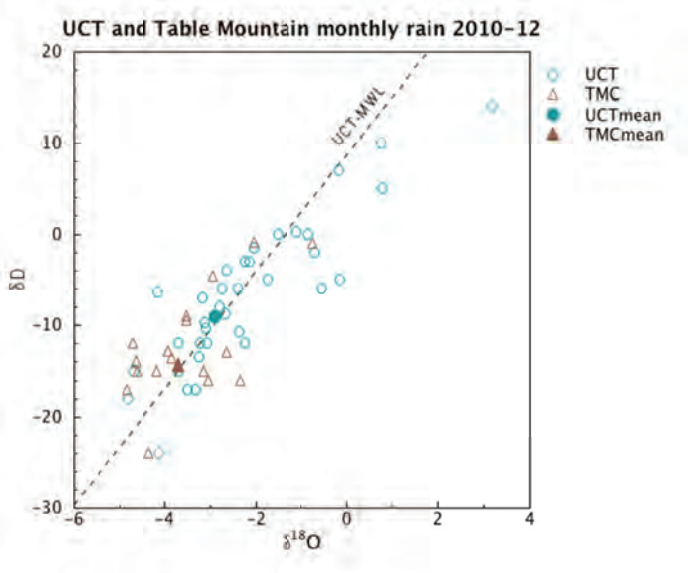

Figure 2: Cumulative monthly rainfall isotope values for TMC and UCT for 2010-12 and their means, weighted by monthly rainfall amounts. The UCT-Meteoric Water Line is that of Harris et al (2010) and therefore uses none of the data displayed on this graph, yet there is clearly an excellent fit between the line, $\delta D = 6.4\delta^{18}O + 8.66$, and the more recent data. A small evaporation shift, to the right of the line, can be seen in the isotopically higher UCT samples, from summer months.

SPRINGS

Fifteen springs have been sampled in the Cape Town area over the 2010-2012 period. An attempt was made to sample each spring twice per year, approximately 6 months apart, straddling the winter rains, however, the fact that a few of the springs are non-perennial and certain access problems meant not all 15 were sampled each time.

The results of the spring sampling are shown in Table 1 and in Fig. 3. Although all the data forms a single large cluster, when grouped according to date, it is clear that there are sub-clusters for each sampling run. There is a varying, but significant temporal shift between the sampling runs, which average 6 months apart. In order to graphically simplify this movement, the means for all springs sampled in a year have been calculated and plotted, and shown in Fig. 3.

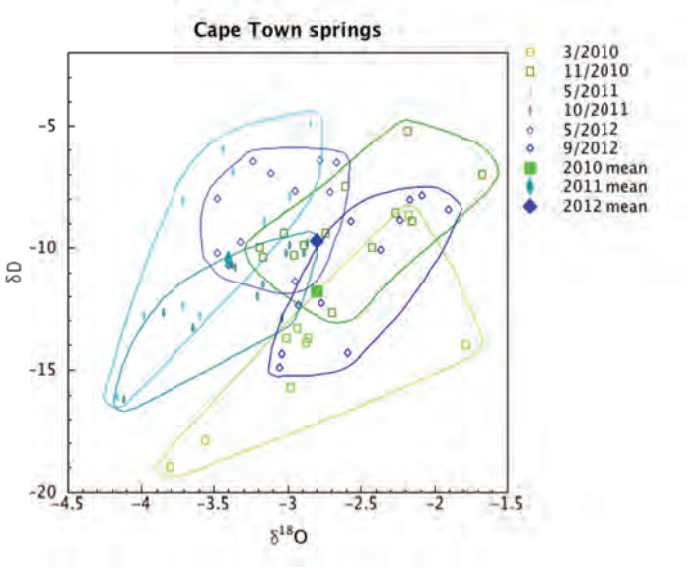

Figure 3: Data for the springs sampled around Cape Town during 2010-2012. Circled clusters are for each sampling run, the dates being shown in the legend, with annual means also shown. It is clear that the isotopic values for spring water vary significantly with time.

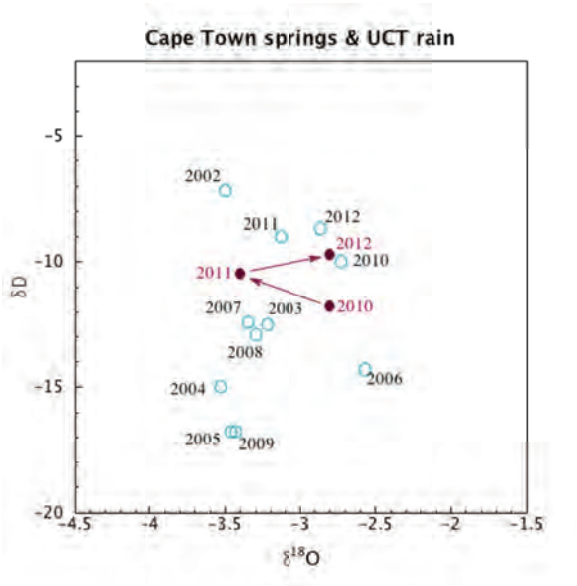

Figure 4: Comparison of the shifts in weighted annual means for UCT rainfall (circles) and average Cape Town springs (dots with arrows). The great similarity in annual shifts for rainfall and springs over 2010-2012 can be seen

COMPARISON BETWEEN SPRING AND RAIN WATER

Weighted mean annual rain water isotope values are different from year to year, sometimes showing very small changes between years, other times much larger. The scale of these changes is broadly similar to those for the spring water and this can be seen on Fig. 5, where both rain and spring water means have been plotted. What is particularly noticeable is that the shifts over 2010-2012 for the spring water appear to be similar to the shifts in the rain water values for the same period. This would suggest that the springs discharge is very recent rain water.

It is Important to bear in mind is that some of the springs have a fairly steady flow rate over the years and therefore must have substantial aquifers that dampen the seasonality of rainfall. A proposed model must therefore account for the discharge of recent (months old) rainwater as well as the steady flow rate over longer periods. In order to accommodate these criteria, a layered aquifer is proposed, that allows recent rainfall to flow on top of older groundwater. A schematic diagram of this proposed model is shown in Fig. 6

Table 1. The $\delta^{18}O$ and δD values of springs sampled during this project

Month/Year	2010/03	2010/03	2010/11	2010/11	2011/05	2011/05	2011/10	2011/10	2012/05	2012/05	2012/09	2012/09
SPRING	δD ‰	$\delta^{18}O$ ‰	δD ‰	$\delta^{18}O$ ‰	δD ‰	$\delta^{18}O$ ‰	δD ‰	$\delta^{18}O$ ‰	δD ‰	$\delta^{18}O$ ‰	δD ‰	$\delta^{18}O$ ‰
Cannon			-9.9	-2.89								
Redwood			-10.3	-2.96			-10.8	-3.36	-8.0	-3.48	-9.6	
Wendy's			-9.4	-2.74			-10.7	-3.38	-9.8	-3.32	-9.1	
Kirstenbosch	-13.7	-3.01	-9.4	-3.03	-12.4	-3.71	-12.9	-3.04	-10.2	-3.48	-10.1	-2.37
Kommetjie	-13.9	-2.88	-8.9	-2.16	-8.9	-3.16	-10.2	-2.89	-6.5	-3.24	-8.5	-1.91
Newlands	-13.3	-2.94	-7.5	-2.61	-6.9	-3.37	-10.2	-3.01	-6.5	-2.67	-7.9	-2.09
Palmboom	-13.7	-2.86	-10.0	-2.43	-4.9	-2.85	-9.9	-2.99	-7.7	-2.95	-8.9	-2.24
Princess Anne							-12.0	-3.21			-8.9	-2.57
Albion	-8.7	-2.18	-7.0	-1.67	-7.9	-2.99	-9.8	-2.87	-7.7	-2.71	-8.1	-2.17
CT Main	-15.7	-2.98	-12.7	-2.70	-12.8	-3.99	-13.3	-3.64	-10.7	-3.40	-12.3	-2.77
Cableway	-19.0	-3.81	-10.4	-3.17					-12.5		-14.9	-3.06
Glencoe	-17.9	-3.56	-10.0	-3.19	-16.1	-4.17	-16.2	-4.12		-3.74	-14.4	-3.04
Leeuwenhof	-14.0	-1.78	-5.2	-2.19	-8.1	-3.71	-11.5	-3.17	-6.4	-2.78	-14.3	-2.59
Tafelberg Road			-8.6	-2.27	-6.0	-3.44	-12.7	-3.85	-6.9	-3.12	-12.4	-2.93
Lily Pond					-12.8	-3.60			-11.4	-2.95		

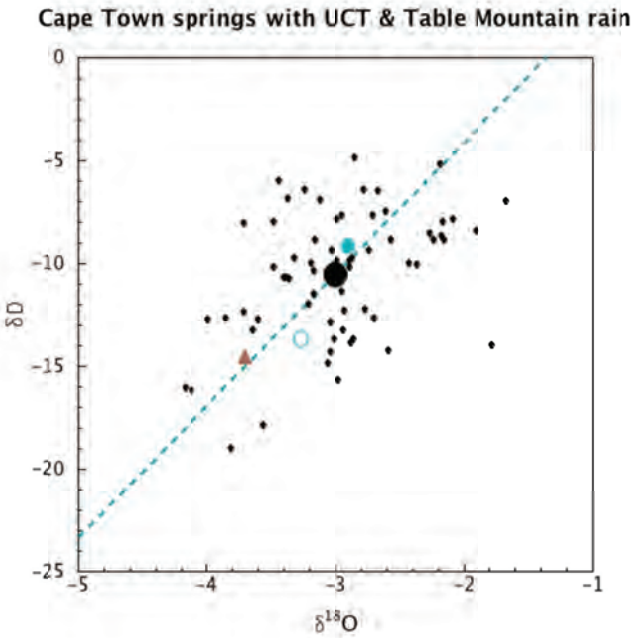

Figure 5: Spring water data (small black dots) and mean (large black circle), weighted mean rain water data for Table Mountain 2010-2012 (triangle), UCT 2010-2012 (solid blue circle) and UCT 2003-2012 (open blue circle), and the UCT-MWL (see Fig. 2).

ALTITUDE EFFECT

The two rainfall stations, UCT and TMC, are located at 137m and 1074mamsl, giving an altitude difference of 937m. The mean isotope values for each station over the 2010-2012 period, using monthly isotope values weighted by rainfall amount are shown in Table 2. The differences are 5.2‰ for δD and 0.8‰ for $\delta^{18}O$, which works out to an altitude gradient of approximately 0.55‰ δD per 100m and 0.085‰ $\delta^{18}O$ per 100m. This altitude effect is at the low end of the spectrum, compared to altitude effects reported by other workers, some of which range up to 4‰ and 0.5‰ (Clark & Fritz, 1997; Poage & Chamberlain, 2001). A possible explanation for this low altitude effect gradient is the small size of Table Mountain and the turbulent effect it has on the winter frontal systems that deliver most of Cape Town's rain. It is well known that rainfall on the lee side of Table Mountain is higher than on the windward side, which is contrary to the orographic effect that mountain ranges have on rainfall. In the case of Table Mountain, the mountain triggers increased rainfall as the weather system moves onto the mountain and this reaches a peak as the weather system leaves the mountain on the eastern side, because of the very small distance across the mountain. It is possible that the isotope behaviour is similarly affected by this. Turbulence in the lee of Table Mountain could cause a local depression in temperature and bring conditions that are higher up in the cloud, to lower elevations, thereby suppressing the altitude effect.

Previous work (Diamond & Harris, 1997) showed a poor correlation between altitude and isotope ratio, but this was based on a snapshot sample from a single storm event.

It therefore seems the altitude effect on Table Mountain is not as clear as that reported in the literature.

The recorded altitude effect is useful in interpreting the likely recharge area for the Cape Town springs. As can be seen in Figure 5, the UCT and TMC rainfall means straddle the mean for all spring discharge. This suggests that the spring recharge areas, as an average, are at higher elevation than UCT, but because the spring mean is much closer to the UCT value than the TMC value, the recharge area is probably still at relatively lower altitude. Quantifying this by simple interpolation between the UCT and TMC elevations, the average elevation for spring water recharge comes to 330m a.m.s.l.

At this elevation on the mountain, the bedrock is generally obscured by scree. This calculation therefore supports the layered discharge model and further suggests that the Cape Town springs exploit the scree apron aquifers that form a skirt around the base of the mountain.

Station	δD ‰	$\delta^{18}O$ ‰
UCT 2010-2012	-9.2‰	-2.90‰
Table Mountain Cableway 2010-2012	-14.4‰	-3.70‰

Table 2: Mean rainfall isotope values for the two rain collection stations over 2010-2012.

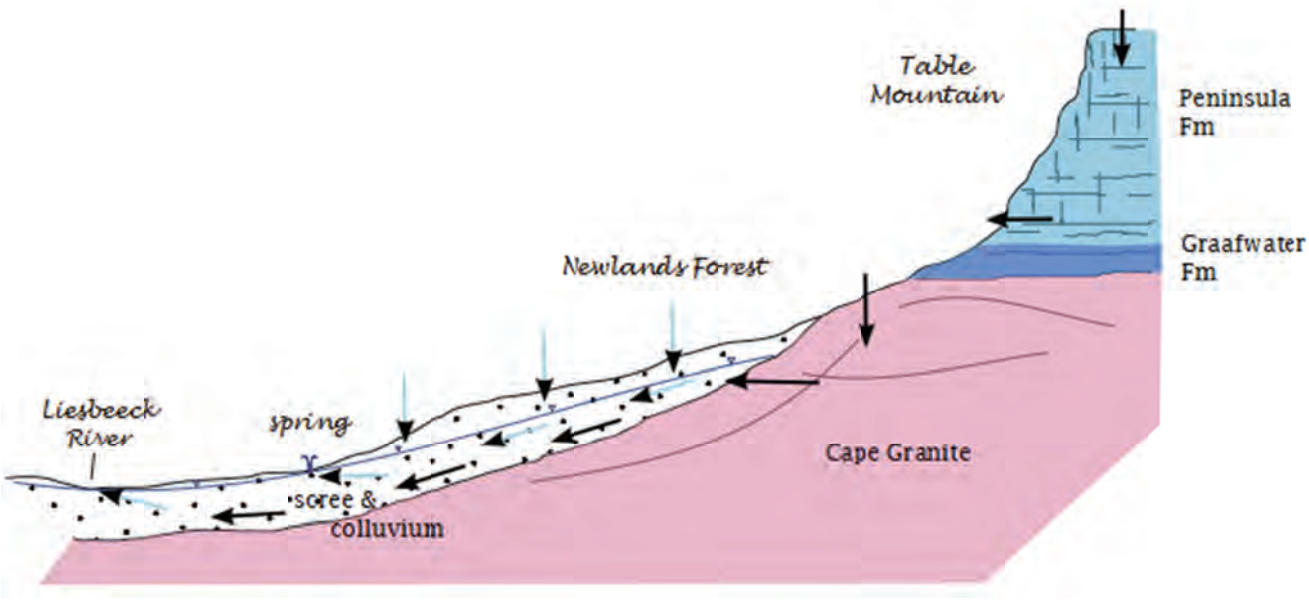

Figure 6: Conceptual model of groundwater flow around Table Mountain, showing a layered aquifer in the scree material, allowing recent recharge to discharge to springs on an annual basis and deeper flow to maintain the spring discharge over a multi-year period, smoothing seasonal variations in rainfall. Diagram is not to scale.

REFERENCES

Belcher, R.W., Kisters, A.F. (2003). Lithostratigraphic correlations in the western branch of the Pan-African Saldania Belt, South Africa: the Malmesbury Group revisited. *South African Journal of Geology, 106, 327-342.*

Blake, D., Mlisa, A., Hartnady, C. (2010). Large scale quantification of aquifer storage and volumes from the Peninsula and Skurweberg Formations in the southwestern Cape. Water SA, 36, 177-184.

Clark, I.D., Fritz, P. (1997). Environmental Isotopes in Hydrogeology. CRC press.

Diamond, R.E., Harris, C. (1997). Oxygen and hydrogen isotope composition of Western Cape meteoric water. *South African Journal Science, 93, 371-374.*

Geological Survey (1984) Map 1:50000 Geological Series. 3318CD Cape Town. Department of Mineral and Energy Affairs. Republic of South Africa.

Harris, C., Burgers, C., Miller, J., Rawoot, F. (2010). O- and H-isotope record of Cape Town Rainfall from 1996 to 2008, and its application to recharge studies of Table Mountain Groundwater, South Africa. *South African Journal of Geology, 113, p33-56.*

Poage, M.A., Chamberlain, C.P. (2001). Empirical relationships between elevation and the stable isotope composition of precipitation and surface water: considerations for studies of palaeoelevation change. *American Journal of Science, 301, 1-15.*

Roberts, D.L., Botha, G.A., Maud, R.R., Pether, J. (2006). Coastal Cenozoic Deposits, In: Geology of South Africa, Johnson, M.R., Anhaeusser, Thomas, R.J. (eds), Geological Society of South Africa, Johannesburg and Council for Geoscience, Pretoria, 605-628.

SAWB (South African Weather Bureau) (1996). The weather and climate of the extreme south-western Cape. Department of Environmental Affairs and Tourism, South Africa.

Scheepers, R., Armstrong, R. (2002). New U-Pb SHRIMP zircon ages of the Cape Granite Suite: implications for magmatic evolution of the Saldania Belt. *South African Journal of Geology, 105, 241-256.*

Schimmelmann, A., DeNiro, M.J. (1993). Preparation of organic and water hydrogen for stable isotope analysis: effects due to reaction vessels and zinc. *Analytical Chemistry, 65, 789-792*

Socki, R.A., Karlsson, H.R., Gibson Jr, E.K. (1992). Extraction technique for the determination of oxygen-18 in water using pre-evacuated glass vials. *Analytical Chemistry, 64, 829-831.*

Spangenberg, J.E. Vennemann, T.W. (2008). The stable hydrogen and oxygen isotope variation of water stored in polyethylene terephthalate (PET) bottles. *Rapid Communications in Mass Spectrometry 22, 672–676.*

Tankard, A., Weksink, H., Aukes, P., Newton, R., Stettler, E. (2009). Tectonic evolution of the Cape and Karoo basins. *Marine & Petroleum Geology, 26, 1379-1412.*

Annex 1. Results for the samples so far gathered and analysed.

Sample Identification	δD ‰	$\delta^{18}O$‰
UNIVERSITY OF CAPE TOWN RAINFALL		
UCT rain Jan 2009 3mm	-3	-0.30
UCT rain Feb 2009 14mm	-4	-0.28
UCT rain Mar 2009 5mm	7	2.03
UCT rain Apr 2009 72mm	-5	-1.88
UCT rain May 2009 220mm	-10	-3.25
UCT rain Jun 2009 393mm	-13	-2.71
UCT rain July 2009 220mm	-23	-4.53
UCT rain Aug 2009 393mm	-23	-4.50
UCT rain Sep 2009 169mm	-8	-2.21
UCT rain Oct 2009 76mm	-17	-3.16
UCT rain Nov 2009 185mm	-32	-5.09
UCT rain Dec 2009 16mm	-1	-0.56
UCT rain Jan 2010 9mm	10	0.75
UCT rain Feb 2010 12mm	-6	-0.54
UCT rain Mar 2010 7mm	0	-0.83
UCT rain Apr 2010 44mm	-12	-2.25
UCT rain May 2010 277mm	-8	-2.78
UCT rain Jun 2010 222mm	-17	-3.31
UCT rain Jul 2010 166mm	-15	-3.69
UCT rain Aug 2010 121mm	-5	-1.74
UCT rain Sep 2010 100mm	-3	-2.24
UCT rain Oct 2010 102mm	-3	-2.15
UCT rain Nov 2010 73mm	-6	-2.39
UCT rain Dec 2010 17mm	-40	-5.06
UCT rain Jan 2011 16mm	-5	-0.15
UCT rain Feb 2011 3mm	14	3.19
UCT rain March 2011 16mm	-24	-4.12
UCT rain April 2011 111mm	-6	-2.73
UCT rain May 2011 145mm	-12	-3.69
UCT rain June 2011 191mm	-18	-4.82
UCT rain July 2011 49mm	-15	-4.68
UCT rain Aug 2011 209mm	-4	-2.63
UCT rain Sept 2011 141mm	0	-1.51
UCT rain Oct 2011 41 mm	-17	-3.48
UCT rain Nov 2011 72mm	-12	-3.21
UCT rain Dec 2011 62mm		-2.05
UCT rain Jan 2012 46mm	5	0.78
UCT rain Feb 2012 21 mm	-2	-0.68
UCT rain March 2012 69 mm	-12	-3.07
UCT rain April 2012 133mm		-3.12
UCT rain May 2012 143mm		-3.08
UCT rain June 2012 >226mm	-6	
UCT rain July 2012 >293mm	-9	
UCT rain Aug 2012 214mm		-3.25
UCT rain Sep 2012 172mm		-2.36
TABLE MOUNTAIN UPPER CABLEWAY RAINFALL		
TM rain May 2010	-15	-3.14
TM rain June 2010	-24	-4.35
TM rain Oct 2010	-16	-3.04
TM rain Nov 2010	-13	-2.65
TM rain Dec 2010	-16	-2.35
TM rain Jan 2011	-1	-0.75
TMUCWS Apr 2011	-15	-4.61
TMUCWS May 2011	-15	-4.17
TMUCWS June 2011	-17	-4.85

Sample Identification	δD ‰	$\delta^{18}O$‰
TMUCWS July 2011	-12	-4.71
TMUCWS Aug 2011	-14	-4.64
TMUCWS Sep 2011	-9	-3.51
UCWS Oct 2011	-14	-3.84
UCWS Nov 2011		-4.52
UCWS Dec 2011	-10	-3.51
UCWS Jan 2012	-5	-2.93
UCWS Feb 2012	-1	-2.05
UCWS Mar 2012	-13	-3.91
RIVERNDALE FARM RAINFALL		
Riverndale rain Jun 2010	-34	-7.58
Riverndale rain Jul 2010	-47	-9.76
Riverndale rain Aug 2010	-2	-2.90
Riverndale rain Sep 2010	-3	-0.79
Riverndale rain Oct 2010	-22	-5.11
Riverndale rain Nov 2010	6	-1.37
Riverndale rain Dec 2010	-12	-1.63
Riverndale rain Jan 2011	11	-0.47
Riverndale rain Feb 2011	3	-0.39
Riverndale March 2011	2	-0.87
Riverndale April 2011	-4	-3.35
Riverndale May 2011	-23	-5.41
Riverndale June 2011	-5	-3.12
Riverndale July 2011	-7	-4.70
Riverndale Aug 2011	-4	-9.60
Riverndale Sep 2011	-1	3.03
Riverndale Oct 2011	-4	-16.73
Riverndale Nov 2011	-4	-16.63
Riverndale Dec 2011	-1	-1
Riverndale Jan 2012	3	-1
Riverndale Feb 2012	20	2
Riverndale Mar 2012	-11	-3
Riverndale Apr 2012	-17	-4
ROBINSON PASS RAINFALL		
Robinson Pass rain Jun 2010	-6	-0.32
Robinson Pass rain Jul 2010	-33	-6.08
Robinson Pass rain Aug 2010	-23	-5.55
Robinson Pass rain Sep 2010	-6	-2.22
Robinson Pass rain Oct 2010	-34	-5.86
Robinson Pass rain Nov 2010	-10	-2.14
Robinson Pass July 2011	-22	-6.68
GOUKAMMA RIVER RAINFALL		
Goukamma rain Jun 2010	-17	-3.30
Goukamma rain Jul 2010	-47	-7.53
Goukamma rain Aug 2010	-14	-3.43
Goukamma rain Sep 2010	1	-0.87
Goukamma rain Oct 2010	-12	-3.13
Goukamma rain Nov 2010	-2	-0.46
Goukamma rain Dec 2010	-33	-4.69
Goukamma Jan 2011	8	-0.64
Goukamma Feb 2011	4	-1.06
Goukamma March 2011	0	-2.15
Goukamma April 2011	7	-1.96
Goukamma May 2011	-35	-6.48
Goukamma June 2011	-15	-4.41
Goukamma July 2011	-9	-4.76
Goukamma Aug 2011	-24	-5.26

Sample Identification	δD ‰	$\delta^{18}O$‰
Goukamma Sep 2011	-11	-2.90
Goukamma Oct 2011	-4	-2.48
Goukamma Nov 2011	-7	-3.70
Goukamma Dec 2011	1	-1.79
Goukamma Jan 2012	3	-0.97
Goukamma Feb 2012	6	-1.75
Goukamma Mar 2012	-10	-3.07
Goukamma Apr 2012	-10	-3.17
Goukamma May 2012	-2	-2.47
Goukamma June 2012	-12	-3.47
LENTELUS FARM RAINFALL		
Lentelus June 2010	-42	-7.80
Lentelus July 2010	-63	-10.04
Lentelus Aug 2010	-18	-4.32
Lentelus Oct 2010	-17	-5.04
Lentelus Nov 2010	-12	-3.18
Lentelus Jan 2011	-14	-2.86
Lentelus Feb 2011	-6	-1.96
Lentelus March 2011	-21	-4.43
Lentelus April 2011	3	-2.59
Lentelus May 2011	-53	-9.23
Lentelus June 2011	-33	-7.15
Lentelus July 2011	-28	-7.22
Lentelus Aug 2011	-7	-44.67
Lentelus Sep 2011	-2	-5.82
Lentelus Oct 2011	-1	3.23
Lentelus Nov 2011	0	-0.30
Lentelus Dec 2011	-24	-3.73
Lentelus Jan 2012	0	-0.57
Lentelus Feb 2012	2	-1.42
Lentelus Mar 2012	-16	-4.33
KAMMANASSIE RAINFALL		
Kammanassie June 2010	-59	-9.94
Kammanassie July 2010	-73	-11.77
Kammanassie Aug 2010	-19	-4.90
Kammanassie Sept 2010	-5	-2.30
Kammanassie Oct 2010	-22	-5.55
Kammanassie Nov 2010	-26	-5.15
Kammanassie April 2011	-18	-5.66
Kammanassie May 2011	-35	-7.05
Kammanassie June 2011	-23	-5.86
Kammanassie July 2011	-22	-6.34
Kammanassie Sep 2011	-10	
BLESBERG RAINFALL		
Blesberg June 2010	-40	-7.17
Blesberg July 2010	-30	-5.34
Blesberg Aug 2010	-30	-5.72
Blesberg Sept 2010	-20	-4.91
Blesberg Oct 2010	-33	-7.06
Blesberg Nov 2010	-25	-5.19
Blesberg Dec 2010	-51	-8.26
Blesberg Jan 2011	-44	-7.62
Blesberg Feb 2011	-21	-4.20
Blesberg March 2011	-19	-4.99
Blesberg April 2011	-22	-6.14
Blesberg Aug 2011	-40	
Blesberg Sep 2011	-22	

Sample Identification	δD ‰	$\delta^{18}O$‰
Blesberg Oct 2011	-27	
Blesberg Feb 2012	-14	
Blesberg Apr 2012	-27	
Blesberg May 2012	-15	
Blesberg June 2012	-27	
GAMKABERG STORE RAINFALL		
Gamka store Jan 2011		0.56
Gamka store Feb 2011	-8	-1.41
Gamka store Mar 2011	14	0.86
Gamka Store April 2011	-23	-3.72
Gamka Store May 2011	-30	-6.08
Gamka Store June 2011	-26	-6.24
Gamka Store July 2011	-16	-4.73
Gamka Store Aug 2011	-13	-2.54
Gamka store Nov 2011	-15	-2.57
Gamka store Dec 2011	0	0.56
Gamka store Jan 2012	1	0.05
Gamka store Mar 2012	-9	-0.58
Gamka store Apr 2012	-8	-2.46
Gamka store May 2012	-6	-2.31
Gamka store June 2012	-10	-2.41
BAKENSKOP RAINFALL		
Bakenskop June 2010	-14	0.72
Bakenskop July 2010	-53	-8.97
Bakenskop August 2010	-22	-5.39
Bakenskop September 2010	-17	-3.95
Bakenskop October 2010	-38	-7.08
Bakenskop November 2010	-17	-3.88
Bakenskop April 2011	-31	-7.16
Bakenskop May 2011	-39	-8.21
Bakenskop June 2011	-34	-6.58
Bakenskop July 2011	-29	-7.79
Bakenskop Aug 2011	-21	-4.97
Bakenskop Sept 2011	-6	-3.53
Bakenskop Oct 2011	-38	-6.38
Bakenskop Nov 2011	-12	-4.92
Bakenskop Dec 2011	-18	-3.37
TWEESPRUIT RAINFALL		
De Doorns June 2011	-27	-4.20
Tweespruit Aug 2011	-6	-2.71
Tweespruit Nov 2011	-2	-1.50
Tweespruit Dec 2011	11	2.43
Tweespruit Jan 2012	1	-0.20
Tweespruit June 2012	-23	-3.19
MATROOSBERG RAINFALL		
Erfdeel May 2010	-24	-5.43
Erfdeel Jan 2011	-45	-7.97
Erfdeel Feb 2011	-42	-7.91
Erfdeel Mar 2011	-32	-4.67
Erfdeel Apr 2011	-42	-7.98
Erfdeel May 2011	-53	-9.28
Erfdeel Jun 2011	-44	-8.19
Erfdeel Jul 2011	-44	-8.07
Erfdeel Aug 2011	-43	-7.97
Erfdeel Sep 2011	-45	-8.22
Erfdeel Oct 2011	-31	-5.90

Sample Identification	δD ‰	$\delta^{18}O$‰
Erfdeel Nov 2011	-31	-6.02
Erfdeel Dec 2011	-42	-7.41
Erfdeel Jan 2012	-27	-5.30
WOLFKOP RAINFALL		
Wolfkop May 2010	-12	-2.57
Wolfkop June 2010	-26	-4.77
Wolfkop July 2010	-15	-3.82
Wolfkop August 2010	-2	-1.55
Wolfkop September 2010	-24	-4.21
Wolfkop October 2010	-1	-1.60
Wolfkop November 2010	2	-0.56
Wolfkop December 2010	-48	-7.12
Wolfkop Feb 2011	-15	-3.13
Wolfkop Mar 2011	-41	-4.13
Wolfkop Apr 2011	-11	-4.07
Wolfkop May 2011	-16	-4.10
Wolfkop June 2011	-15	-4.00
Wolfkop July 2011	-30	-6.06
Wolfkop Aug 2011	-15	-4.17
Wolfkop Sep 2011	4	-1.54
Wolfkop Oct 2011	-12	-3.06
Wolfkop Nov 2011	-40	-7.94
Wolfkop Dec 2011	-1	-2.11
Wolfkop Mar 2012	-31	-5.49
Wolfkop Apr 2012	-10	-3.16
Wolfkop May 2012	11	-1.12
Wolfkop Jun 2012	-16	-4.40
Wolfkop July 2012	-5	-2.65
Wolfkop Aug 2012	-9	-3.51
TWAKTUIN RAINFALL		
Twaktuin May 2010	-13	-3.41
Twaktuin June 2010	-19	-2.54
Twaktuin July 2010	7	0.41
Twaktuin August 2010	-3	-1.73
Twaktuin September 2010	-21	-3.42
Twaktuin October 2010	24	4.09
Twaktuin December 2010	-74	-10.45
Twaktuin May 2011	-18	-4.97
Twaktuin June 2011	-18	-4.94
Twaktuin July 2011	4	-0.19
Twaktuin Aug 2011	4	-0.35
Twaktuin Sep 2011	39	7.74
Twaktuin Apr 2012	12	2.15
Twaktuin May 2012	-4	-2.86
Twaktuin June 2012	-16	-4.88
Twaktuin July 2012	-3	-2.73
Twaktuin Aug 2012	-15	-3.88
UITKYK PASS RAINFALL		
Uitkyk rain Aug 2010	-17	-3.53
Uitkyk rain Sept 2010	-18	0.97
Uitkyk rain Oct 2010	-1	3.43
Uitkyk rain Nov 2010	-17	-3.12
Uitkyk rain Dec 2010	-56	-9.14
Uitkyk rain Jan 2011	-39	-7.72
Uitkyk March 2011	-29	-5.35
Uitkyk Apr 2011	-23	-5.79
Uitkyk May 2011	-22	-5.46

Sample Identification	δD ‰	$\delta^{18}O$‰
Uitkyk June 2011	-25	-5.85
Uitkyk July 2011	-24	-5.85
Uitkyk Aug 2011	-20	-5.21
Uitkyk Oct 2011	-30	-5.13
Uitkyk Nov 2011	-23	-4.94
Uitkyk Dec 2011	-8	-4.17
Uitkyk Mar 2012	-33	-5.57
Uitkyk Apr 2012	-16	-4.05
Uitkyk May 2012	-1	-1.82
Uitkyk July 2012	-18	-4.37
Uitkyk Aug 2012	-20	-5.14
CAPE TOWN SPRING WATER SAMPLES		
Albion spring March 2010	-9	-2.18
CT Main spring March 2010	-16	-2.98
Cableway spring March 2010	-19	-3.81
Glencoe spring March 2010	-18	-3.56
Leeuwenhof spring March 2010	-14	-1.78
Kirstenbosch spring March 2010	-14	-3.01
Kommetjie spring SAB March 2010	-14	-2.88
Palmboom spring March 2010	-14	-2.86
Newlands spring March 2010	-14	-2.94
Kirstenbosch spring May 2011	-13	-3.71
Newlands spring May 2011	-7	-3.37
Kommetjie spring May 2011	-9	-3.16
Palmboom spring May 2011	-5	-2.85
Albion spring May 2011	-8	-2.99
Cape Town Main spring May 2011	-13	-3.99
Glencoe spring May 2011	-16	-4.17
Hof spring May 2011	-8	-3.71
Tafelberg Road spring May 2011	-6	-3.44
Redwood Jan 2011	-10	-3.23
Cannon Jan 2011	-10	-3.56
Wendy's Jan 2011	-9	-4.18
Redwood Jan 2011	-10.8	-3.36
Wendy's Jan 2011	-10.7	-3.38
Kirstenbosch Oct 2011	-12.9	-3.04
Kommetjie Oct 2011	-10.2	-2.89
Newlands Oct 2011	-10.2	-3.01
Palmboom Oct 2011	-9.9	-2.99
Princess Anne Oct 2011	-12.0	-3.21
Albion Oct 2011	-9.8	-2.87
CT Main Oct 2011	-13.3	-3.64
Cableway Oct 2011	No water	
Glencoe Oct 2011	-16.2	-4.12
Leeuwenhof Oct 2011	-11.5	-3.17
Tafelberg Road Oct 2011	-12.7	-3.85
Redwood May 2012	-8	-3.48
Wendy's May 2012	-10	-3.32
Kirstenbosch May 2012	-10	-3.48
Kommetjie May 2012	-6	-3.24
Newlands May 2012	-7	-2.67
Palmboom May 2012	-8	-2.95
Princess Anne May 2012		
Albion May 2012	-8	-2.71
CT Main May 2012	-11	-3.40
Cableway May 2012		
Glencoe May 2012	-13	-3.74
Leeuwenhof May 2012	-6	-2.78
Tafelberg Road May 2012	-7	-3.12

Sample Identification	δD ‰	$\delta^{18}O$‰
Redwood Sept 2012		
Wendy's Sept 2012		
Kirstenbosch Sept 2012	-10	-2.37
Kommetjie Sept 2012	-8	-1.91
Newlands Sept 2012	-8	-2.09
Palmboom Sept 2012	-9	-2.24
Princess Anne Sept 2012	-9	-2.57
Albion Sept 2012	-8	-2.17
CT Main Sept 2012	-12	-2.77
Cableway Sept 2012	-15	-3.06
Glencoe Sept 2012	-14	-3.04
Leeuwenhof Sept 2012	-14	-2.59
Tafelberg Road Sept 2012	-12	-2.93
HOT SPRING WATER SAMPLES		
The Baths May 2010	-22	-4.63
Laingsburg spring Sep 2010	-29	-4.67
The Baths hot spring May 2010	-20	-4.98
Toorwater	-39	-7.11
Calitzdorp	-39	-7.02
Laingsburg	-16	-0.27
Warmwaterberg	-38	-6.78
Brandvlei	-32	-5.79
Goudini	-24	-4.80
Caledon	-24	-4.84
Laingsburg spring Sep 2011	-34	-5.24
Laingsburg spring Sep 2012	-36	-4.82
RIVER WATER SAMPLES		
Groothoekkloof 01 Feb 2010	-14	
Groothoekkloof 02 Feb 2010	-37	-7.59
Groothoekkloof 03 Feb 2010	-35	-7.09
Groothoekkloof 04 Feb 2010	-26	-5.44
Groothoekkloof 05 Feb 2010	-30	-6.27
Groothoekkloof 06 Feb 2010	-34	-6.89
Groothoekkloof 07 Feb 2010	-34	7.97
Groothoekkloof 08 Feb 2010	-31	-5.54
Groothoekkloof 09 Feb 2010	-34	-5.56
Groothoekkloof 10 Feb 2010	-34	16.06
Groothoekkloof 01 Feb 2011	-21	-3.12
Groothoekkloof 02 Feb 2011	-31	-6.10
Groothoekkloof 03 Feb 2011	-28	
Groothoekkloof 04 Feb 2011	-31	-5.62
Groothoekkloof 05 Feb 2011	-22	-5.07
Groothoekkloof 06 Feb 2011	-24	-5.93
Groothoekkloof 08 Feb 2011	-36	-6.18
Groothoekkloof 09 Feb 2011	-34	-5.68
Duiwelskloof 01 Mar 2011	-14	-3.74
Duiwelskloof 02 Mar 2011	-16	-3.91
Duiwelskloof 03 Mar 2011	-11	-3.74
Duiwelskloof 04 Mar 2011	-15	0.60
Duiwelskloof 05 Mar 2011	-21	-3.89
Duiwelskloof 06 Mar 2011	-2	-2.69
Volstruiskloof 01 Mar 2011	-21	-4.54
Volstruiskloof 02 Mar 2011	-11	-3.75
Volstruiskloof 03 Mar 2011	-9	-2.40
Volstruiskloof 04 Mar 2011	-11	-3.35
Witels 1	-27	-4.70
Witels 2	-30	-5.39
Witels 3	-29	-5.35

Sample Identification	δD ‰	$\delta^{18}O$‰
Witels 4	-23	-4.13
Witels 5	-23	-4.50
Witels 6	-28	-5.28
Witels 7	-30	-5.74
Witels 8	-20	-3.12
Witels 9	-27	-5.02
Witels 10	-27	-5.48
Witels 11	-29	-5.61
Witels 12	-23	-4.46
Witels 13	-26	-5.27
Witels 14	-25	-5.32
Witels 15	-27	-5.17
Witels 16	-23	-4.84
Witels 17	-26	-5.27
Witels 18	-24	-5.18
Witels 19	-26	-5.42
Meulkloof 1 Mar 2012	-7	-3.39
Meulkloof 2 Mar 2012	-8	-2.95
Meulkloof 3 Mar 2012	-11	-3.31
Meulkloof 4 Mar 2012	-8	-3.10
Meulkloof 5 Mar 2012	-8	-3.30
Groothoekkloof Jan 2012 1	-28	-5.15
Groothoekkloof Jan 2012 2	-32	-5.73
Groothoekkloof Jan 2012 3	-30	-5.28
Groothoekkloof Jan 2012 4	-24	-5.29
Groothoekkloof Jan 2012 5	-30	-5.70
Groothoekkloof Jan 2012 6	-26	-5.17
Groothoekkloof Jan 2012 7	-29	-5.22
Groothoekkloof Jan 2012 8	-32	-5.62
GroothoekklooF Jan 2012 9	-30	-5.48
Groothoekkloof Jan 2012 10	-31	-5.14
Groothoekkloof Jan 2012 11	-30	-5.33
Groothoekkloof Jan 2012 12	-30	-5.43
MISCELLANEOUS SAMPLES		
DAGEOS CIB3 day 1	-39	
DAGEOS CIB3 day 6	-39	
DAGEOS CIB3 day 11	-40	
DAGEOS CIB3 day 16	-39	
Cederberg Tafelberg hail 01-01-2011	-52	-7.38
Cederberg Spout drip 01-01-2011	-29	-5.68
TM Lily Pond Feb 2011	-12	-2.92
Cederberg Spout drip 16-01-2011	-30	-4.87
Tulbagh stream Feb 2011	-27	-5.29
Tulbagh cold spring Feb 2011	-26	-5.74
Tulbagh warm spring Feb 2011	-29	-5.89
TM Lily Pond drip Feb 2011	-13	-3.60
Towerkop water cave Sep 2010	-25	-4.56
Skull Cave drip Mar 2011	-40	-6.83
Seweweekspoortpiek Cave drip Mar 2011	-32	-6.86
Cederberg Spout drip Mar 2011	-30	-5.20
Goudini cool spring Feb 2011	-20	-4.20
Waaihoek 01	-61	-11.56
Waaihoek 02	-38	-9.11
Waaihoek 03	-31	-9.16
Waaihoek 04	-20	-7.16
Waaihoek 05	-38	-8.69
Waaihoek 06	-34	-8.46

TOWARDS A MANAGEMENT MODEL FOR THE EXPLOITATION OF GROUNDWATER FROM THE TAAIBOSCH KAROO GRABEN, LIMPOPO PROVINCE

MJ Butler and B Th Verhagen

ABSTRACT

Previous work included environmental isotope and hydrochemical studies to assess a conceptual model developed earlier on which a major, regional rural groundwater supply from a basalt aquifer was to be based. Mean residence time and porosity figures indicated that recharge, and therefore sustainable extraction, could be as low as 10% of the model estimates. Chemical and isotope data also questioned model predictions of balancing drainage along a major fault line. These results, suggesting upwelling groundwater, prompted a major re-investigation of the area, involving further exploratory drilling and geophysics. A deeper sandstone aquifer, previously thought to be unproductive, was found to produce high yields of excellent quality groundwater and constituting a potentially major regional resource.

The current study attempted to more firmly establish the basic geohydrologic parameters of the two aquifers, their inter-relationships and to generate an integrated exploitation management concept and model for the Tshipise sandstone in order to maintain the exceptional quality of the sandstone groundwater.

Boreholes were drilled in the north-western portion of the current study area, south of the fault, as very little is known about the sandstone in this area. The δD $-\delta^{18}O$ values for these samples cluster fairly closely, independent of sampling depth and lithology, with a deuterium excess of ~ +3‰. They are significantly less depleted than the values obtained earlier for sandstone water samples. The few radiocarbon values show variable ages for the basalt. Relatively large EC values (>700 µS/cm) are much higher than associated thus far with water in the sandstone. It is possible that in the area of recent drilling, sandstone transmissivities are much lower than observed elsewhere and that the effect of the overlying basalt is more dominant here. These preliminary results underline the importance of assessing the aquifer conditions in various areas in order to arrive at a realistic integrated overall conceptual hydrogeological model.

Agriculture development in the north-eastern portion of the study area appears to be growing at an alarming rate. Satellite images from 2000 and 2008 illustrate this dramatic expansion, with complaints of illegal water use, as well as the interference with monitoring boreholes. Of major concern is the effect of agricultural practices which may contaminate this valuable resource. It is assumed that the uncontrolled extraction is occurring mainly from the sandstone aquifer which would enhance drawdown from the overlying, more mineralised basalt with its often high nitrate concentrations. The infiltration and return flow of irrigation water, or irrigation reflux, may result in substantial increases in the salinity load of the ground water as a result of evaporation.

A comprehensive database was developed with all available data for the study area, from the initial IAEA study initiated in 1998, the WRC study on nitrates in 2003, up to and including the recent drilling programme. This data has been revisited in the current study and contouring of all the data on a regional scale has been performed. These clearly illustrate the relationship between the rural villages and the higher E.C. values. This is also evident in the contoured maps of Na, SO_4, Cl as well as NO_3-N. Contours of the tritium concentrations illustrate the potential of the Terveen Lineament, which may be a tension fault cutting across the NW-SE trending dyke swarm, as a source of recharge to both the basalt and sandstone aquifers. A similar pattern is seen in the carbon-14 contour map. In all the isotope contour maps, the influence of the fault line along the Blouberg in the south, the Tshipise regional fault in the north and the Terveen lineament are clearly discernible. This confirms the model, developed earlier, of localised recharge to especially the sandstone through the southern fault zone and partial (diffuse) discharge along the Tshipise fault.

All available data from previously drilled boreholes, as well as the newly drilled boreholes from the current study were collated with elevation and depth to the base of the basalt to establish the regional range of aquifer parameters for this highly heterogeneous aquifer. It illustrates the sandstone erosional surface had considerable topography, with gradients up to some 2% before the deposition of the basalt. The sandstone comes to near-outcrop in the south-west of the area, and to the north-east within the Louisiana dyke swarm. Through the centre of the study area, a deep NW-SE trending valley is filled with basalt. Although a number of boreholes were drilled many tens of metres into the

sandstone, none has penetrated this formation. The thickness of the sandstone will therefore remain a matter for conjecture, unless assessed in strategically placed boreholes.

Abstraction from three high yielding boreholes, drilled into the sandstone aquifer on the farm Kromhoek, started in order to provide water to the town of Alldays. Abstraction rates for the boreholes were calculated at 15 L/s, 7 L/s and 8.5 L/s respectively, with a combined total abstraction of 2635.2 m^3 over a 24 hour period. Uncontrolled extraction from the agricultural development 12 kilometres to the north-east of Kromhoek is occurring mainly from the sandstone aquifer. This would therefore have major implications on the amounts of ground water calculated for safe abstraction from the Kromhoek well field.

An ongoing programme of monitoring water levels observed a general slow declining trend in ground water levels throughout the Limpopo Province, which is considered part of a natural longer term cycle between major recharge. However, this trend was severely intensified once ground water abstraction commenced from the Kromhoek wellfield. The subsequent rate of decline was initially 0.58 m/month, ten times the natural rate, with a drop of 4 metres in the first 7 months. Should this dramatic decline continue, it is not sure how long the abstraction will be able to continue before the boreholes fail. It is also impossible to sample the present exploitation. Chemical and isotope analyses would be an important component of the monitoring process, as well as abstraction figures which have not been possible to obtain.

PREVIOUS WORK

An investigation conducted in the 1980s into the feasibility of a ground water supply to 26 villages in the Taaibosch area near Alldays in Limpopo Province (Fayazi and Orpen 1989) resulted in a hydrological model proposing that groundwater, recharged to a plain of some 600 km^2 in extent, drains northwards towards the regional Tshipise fault zone in the north, which would act as a sink and also drain ground water westwards towards an ephemeral surface drainage (see Fig. 1). The regional supply from the basalt was therefore designed to be drawn from the fault zone, with an abstraction potential estimated at some $1x10^6$ m^3 per annum per km fault strike.

Isotope and hydrochemical variations, as well as structures later revealed by geophysics (Fig. 2) (Verhagen et al., 2002) largely ruled out this concept.

Optimistic recharge figures based on isotope-derived MRT values amounted to 10% of those arrived at during the original investigation. The variability of isotopic and hydro-chemical parameters in numerous samples taken along the strike of the fault began to cast doubt on the concept of a continuous regional drainage zone. Down-the-hole video observations demonstrated the highly anisotropic nature of the void space in the basalt.

The area is characterised by a featureless plain underlain by Clarens sandstones capped by superficial Lebombo basalt up to more than 200 m in thickness (Fig. 3). Groundwater exploitation, mainly for localised village supply and some irrigation farming, was traditionally restricted to the basalt, as the underlying Karoo sandstone, encountered mainly in test drilling of up-thrown blocks along the fault zone, was found to be poorly yielding and not regarded as a worthwhile target for further exploration. Phreatic water levels lie mainly in the basalt.

The isotope and hydrochemical investigation focused initially on the Tshipise fault zone revealed greater complexity of the fault structure than initially believed (Fig. 4). Numerous samples taken from along the fault zone itself and elsewhere presented a pattern of high radiocarbon values, generally in the range of 80-100 pMC, with accompanying tritium mostly in the range 0-1 TU (Fig. 5). Exponential model plots (Maloszewski and Zuber 1996; Verhagen et al. 1991) of atmospheric ^{14}C (Gonfiantini et al., 1998) and rainfall ^{3}H (Verhagen unpub.) data revealed three categories: 1) a substantial number generally conforming to the model, in spite of the heterogeneity of the basalt aquifer; 2) a category, at low ^{3}H values that lies above the model curves, ascribed to phreatophyte root activity transporting recent (high ^{14}C) CO_2 to the saturated zone and 3) ^{14}C values <80 pMC accompanied by ^{3}H values > 0.5 TU, ascribed to mixtures with older water.

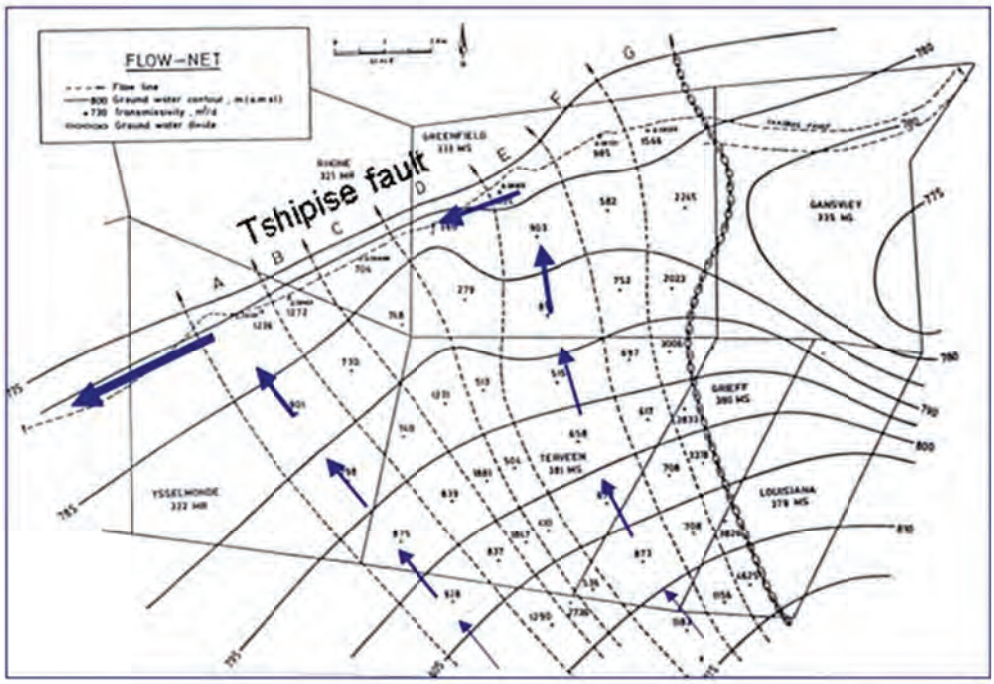

Figure 1: The original groundwater flow model, showing iso-piezometric contours (after: Fayazi and Orpen 1989), interpreted N-W flow in the basalt and balancing drainage along fault zone.

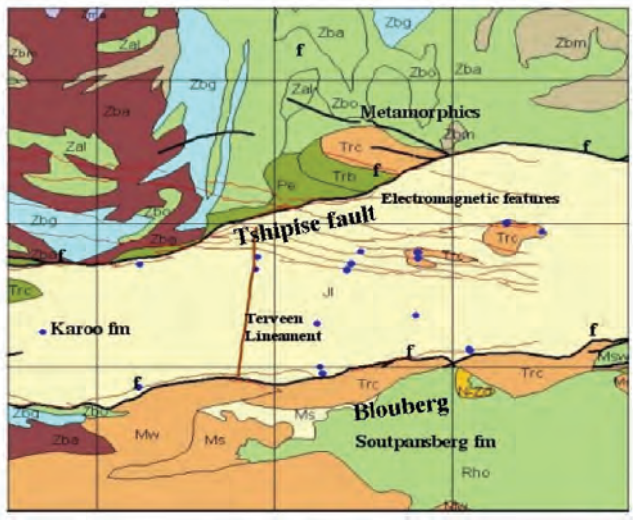

Figure 2: Geological map (Brandl 2002) of the area showing the Karoo graben between older sediments in the south and metamorphics in the north. Electromagnetic features observed during this study were identified as dykes compartmentalising the Karoo

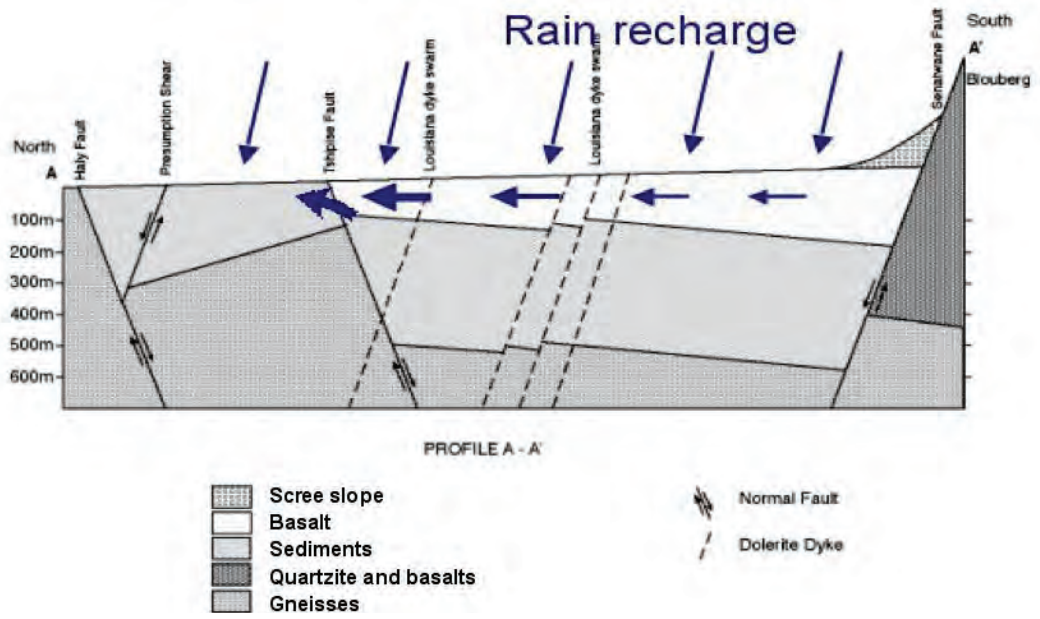

Figure 3: Schematic geological section (after Brandl 2002) showing downthrown Karoo block and original conceptual groundwater model of flow through the shallow basalt aquifer (see Fig. 1)

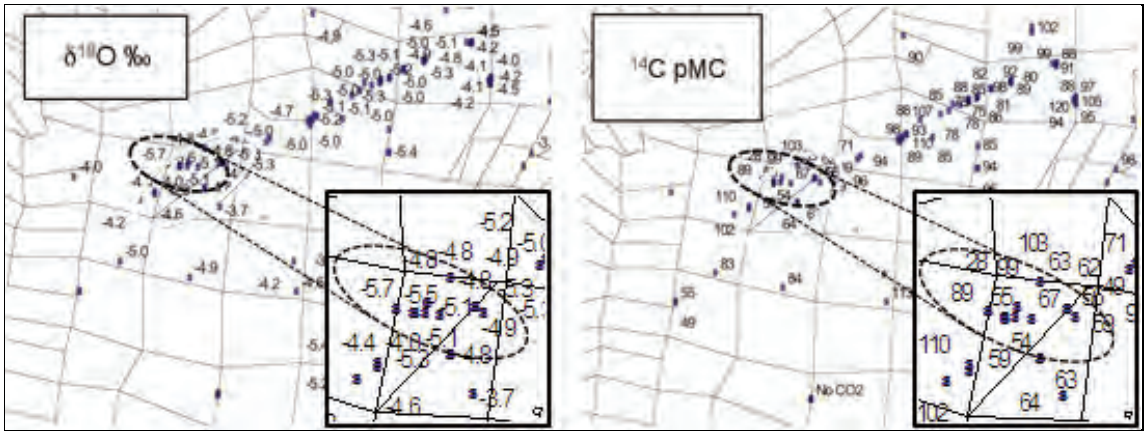

Figure 4: Geographic spread of $\delta^{18}O$ and ^{14}C values. The linear cluster of sampling points follows the Tshipise fault line. The areas containing exceptionally low values of both parameters (shown magnified in insets in the SW of the fault zone are ringed

Monthly composite and single major event rain water samples collected from the three collection stations over three years show a spread of $\delta^{18}O$ from –11‰ to –1‰ with a regression of $\delta^{2}H = 8.1\ \delta^{18}O + 14$ (Fig. 6), while groundwater stable isotope values cluster in a fairly narrow range of $\delta^{18}O$ ~ -4 to -6 ‰, with a regression slope of ~ 5.5 ‰, indicating that recharge conditions to the basalt are fairly uniform, with a degree of surface ponding. Although groundwater stable isotope values in the region do not show a major spread, smaller variations along the fault, e.g. in ^{14}C and $\delta^{18}O$ (Fig. 4), and variable hydrochemistry, suggest that the concept of consistent, regional drainage along the fault, as postulated in the initial model, could not be sustained.

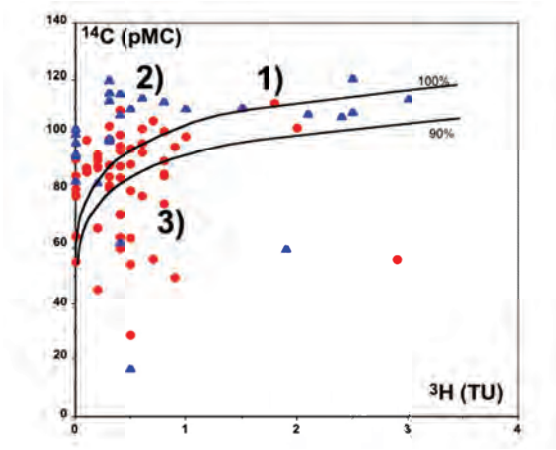

Figure 5: Scattergram of radiocarbon against tritium values for two sampling episodes (red circles and blue triangles) with exponential model plots for different initial values in % atmospheric of ^{14}C (pMC).

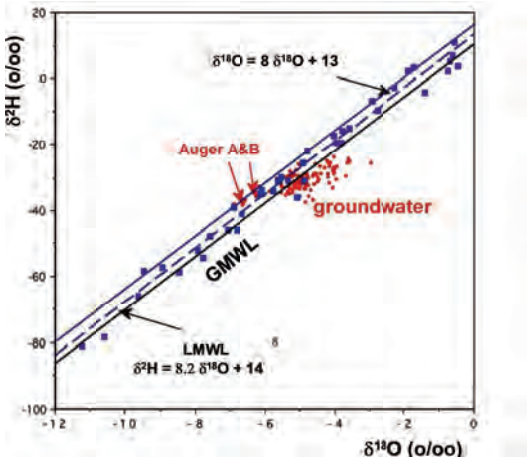

Figure 6: $\delta^{2}H$- $\delta^{18}O$ diagram. Notice the close clustering of groundwater values (red dots) with evaporative trend as against the much wider spread of rainfall values (blue squares) over a period of three years. Also shown are results from water extracted from a wetland at the foot of the Blouberg

Groundwater quality is highly variable in the area with many cases of high nitrate values, which appear to have both anthropogenic and natural sources (Verhagen et al., 2004). The Piper diagram below roughly groups the various lithologies with the water types. Ground water associated with the basalt is predominantly Mg-Ca-HCO_3 type, but also falls in the Mg-Na-Ca-HCO_3 and Na-Mg-HCO_3 types. Generally these groups have high radiocarbon values (>70 pMC) and nitrate ranges from close to zero up to 100 mg/l NO_3-N.

The ground water associated with sandstone falls almost entirely in the Na-HCO_3 type. This water type is almost entirely associated with low radiocarbon values (<60 pMC), and close to zero nitrate values.

In the SW section of the Tshipise fault on the farm Fonteine du Champ, borehole samples gave lower radiocarbon values than seen in the basalt aquifer in the rest of the area. These samples were also associated with more negative stable isotope values, which resemble the values found to the south and samples taken from augered holes at the foot of the Blouberg. This suggested local upwelling of deeper, older groundwater along the fault, with characteristics of groundwater possibly recharged along the scree slopes and fault zone to the south. Upward flow was observed in a borehole along the fault (E. van Wyk, pers. comm.)

A revised model (Fig. 9) postulates major N-W flow through the underlying sandstone, regulating the regional piezometry observed mainly in the basalt aquifer, with local upwelling along faults and fractures into the overlying basalt.

Deeper drilling showed that wherever the sandstone is intersected under basalt, its primary porosity and permeability is preserved, and possibly increased through leaching by circulating groundwater (Fig. 10). Water was always struck just below the basalt/sandstone contact, and yields increased with depth.

Radiocarbon values range from 55 pMC to 24 pMC with vanishing tritium. Especially the lower radiocarbon (higher residence time) samples have lower stable isotope values, with $\delta^{18}O$ < -5.5 ‰ without the evaporative imprint that is characteristic for the basalt. These values trend towards those ascribed to infiltration of mountain run-off and confirm, along with the chemistry and borehole data, the different characteristics of the effective separation of the two main aquifers. This postulated mechanism implies that recharge to the sandstone aquifer is highly episodic and will occur only during major rainfall events that generate significant mountain runoff.

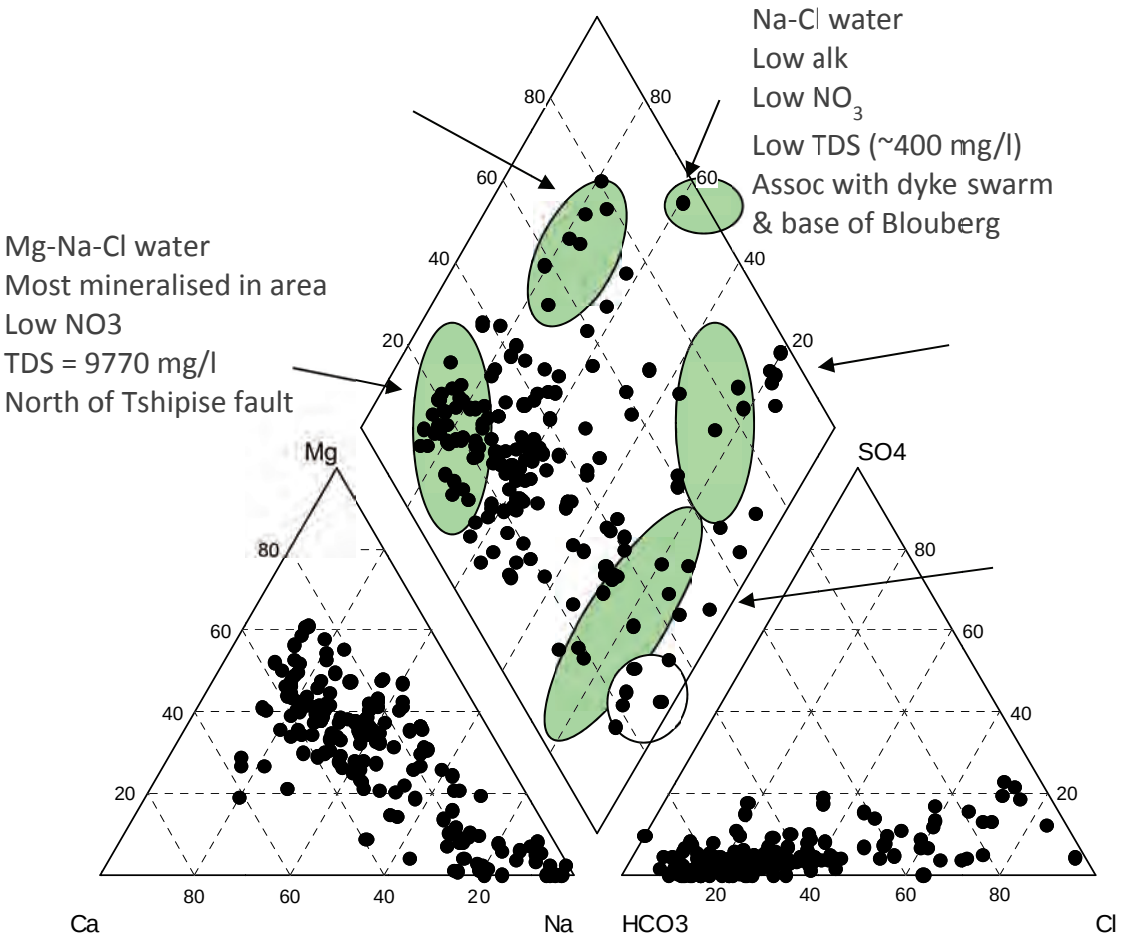

Figure 7: Composite Piper diagram of major ion analyses. The principal and distinct categories are the Lebombo basalt, mainly Mg-Ca-HCO_3 dominant with variable mineralisation and NO_3^- and the Clarens sandstone, Na-HCO_3 dominant, low mineralisation and low NO_3^-

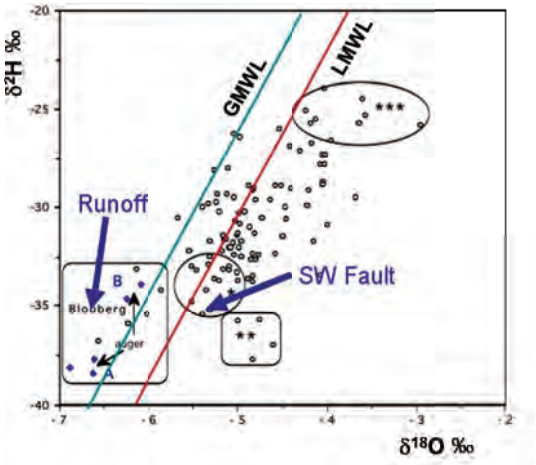

Figure 8: δ^2H- $\delta^{18}O$ diagram (detail of Fig. 5) showing groundwater values with various geographical categories ringed. Note values including the SW fault zone (cf. Fig. 4) and from samples obtained by hand auger from a wetland at the foot of the Blouberg ("Runoff" box), taken to represent mountain runoff

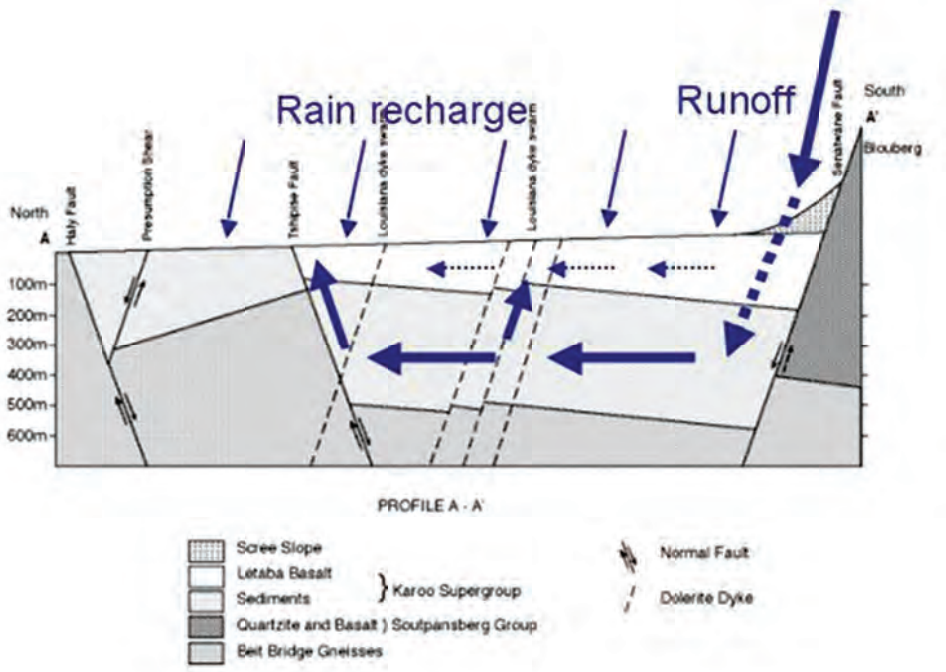

Figure 9: Updated conceptual groundwater flow model, based on isotopic, chemical and geophysical data. Major recharge to sandstone is postulated to derive from mountain run-off infiltrating along scree slopes and the graben along the southern bounding fault zone

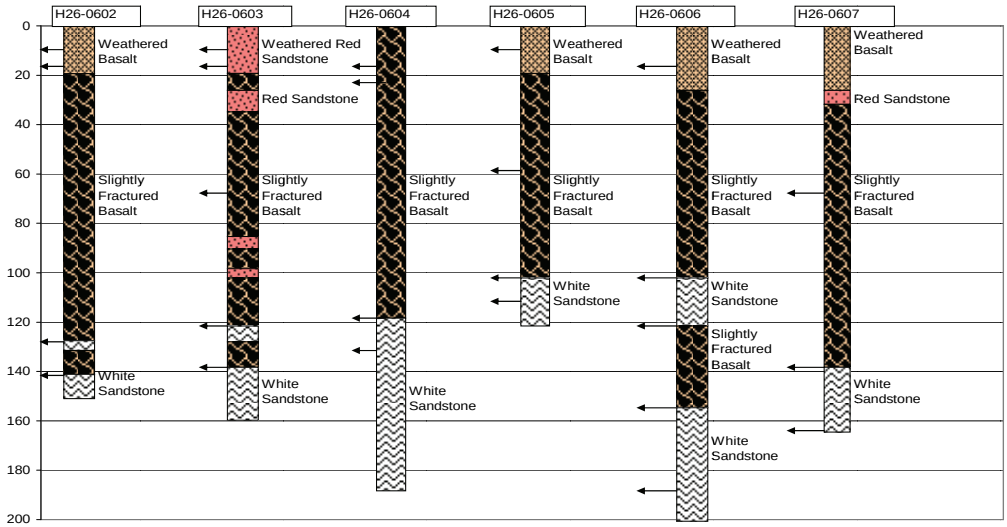

Figure 10: Logs of exploration boreholes drilled to examine the Tshipise sandstone aquifer. Major water strikes were invariably encountered at the contact and deeper in the sandstone profile (Du Toit et al. 2007)

CURRENT STUDY

Initially, the main goal of the current study was to more firmly establish the basic geohydrologic parameters of the two aquifers and their inter-relationships and to generate an integrated exploitation management concept and model for the Tshipise sandstone. The management model would have to deal with maintaining the exceptional quality of the sandstone groundwater that could be compromised by uncontrolled exploitation. An effective recharge rate would have to be arrived at to assess long-term sustainable exploitation rates. As there is no aquitard separating the two aquifers, the distinct differences in groundwater chemistry and isotopic values could be maintained only by the positive pressure in the sandstone. In some areas, the basalt and sandstone may have to be developed in parallel and conjunctive exploitation with blending of water to reasonable potable standards. In all these developments, environmental isotope data will undoubtedly play a crucial role. Already, exploitation of the system is increasing with uncontrolled drilling for large-scale irrigation. A properly designed regional groundwater exploitation strategy is therefore of the utmost urgency.

Although sandstone residence times in the sandstones are higher than for the basalt, when coupled to the high apparent storage significant turnover rates are indicated. The chemistry further suggests that the sandstone is recharged mainly through preferential pathways, along faults and fracture zones, rather than diffuse recharge which could only occur through the basalt. Of note too are the high tested yields (up to 40 L/s) for as yet modest penetration of the aquifer, showing that the sandstone, in addition to its general reliability as an aquifer, could locally support high extraction rates.

As no drilling has been done to assess the thickness of the sandstone, nor the persistence of its favourable aquiferous properties at greater depths, a "Proposal to the Department of Water Affairs and Environment for additional drilling and test pumping of boreholes in the Taaibosch graben area, north of Blouberg in the district of Bochum, Limpopo Province", was approved by the DWAE drilling committee on the 31st of March 2010. This proposal suggested further drilling in the north-western portion of the current study area, south of the fault, as very little is known about the sandstone in this area. Boreholes had already been drilled on the farms Louisenthal and Pax Intrantibus, as well as the southern portions of Fonteine du Champ (Fig. 11). From the available information it appears that the majority of these boreholes end in the basalt. It was therefore proposed that these existing boreholes be used as observation holes, and new boreholes be drilled into the sandstone, cased through the basalt.

Further to the east, the N-S trending "Terveen lineament" (Fig. 12), the exact nature of which has not yet been investigated, is manifested by a depression constituting the most prominent drainage line running from the foot of the Blouberg to the Tshipise fault. It was proposed that an existing borehole drilled on the lineament should be resurrected to get a better understanding of the basalt-sandstone contact in this area.

In addition to the DWAE study on the farm Kromhoek (du Toit et al, 2007) it was proposed that the boreholes be re-tested, as the capacity of the pump was too small to deliver the required drawdown, and at the same time, sample for hydrochemistry and the full suite of environmental isotope analyses.

SITE INVESTIGATION

An initial visit to the proposed drilling sites was undertaken on the 8th of April 2010, together with DWAE staff. The sites of the three boreholes to be drilled were inspected by the DWAE drilling inspector. A proposed borehole, to be drilled on the farm De Vrede along the north-south trending Terveen Lineament, was postponed due to flooding in the area. It was however found that a borehole (H26-0631) had been drilled recently alongside the proposed site. It is therefore possible that no further drilling would be required here.

The second site visited was on the farm Louisenthal, where it was proposed that an existing basalt borehole be used as an observation well, and a new borehole into the sandstones be drilled alongside, approximately 20 metres away. The existing borehole is equipped, and has been since 2003. This borehole provides water to two tanks, which are filled usually twice a day.

The third site visited was on the farm Pax Intrantibus. It was proposed that an existing sandstone borehole be cased. This would mean the borehole would have to be reamed to a depth of 165 metres before casing could be installed. However, it was later decided by the DWAE drilling inspector that a new borehole would have to be drilled instead of using the existing sandstone borehole. A further borehole would then be drilled alongside this borehole to act as an observation well. A second visit to the site was arranged for the 21st of April, together with DWAE staff to obtain permission to drill on the farms Pax Intrantibus and Louisenthal. This went ahead without any problems.

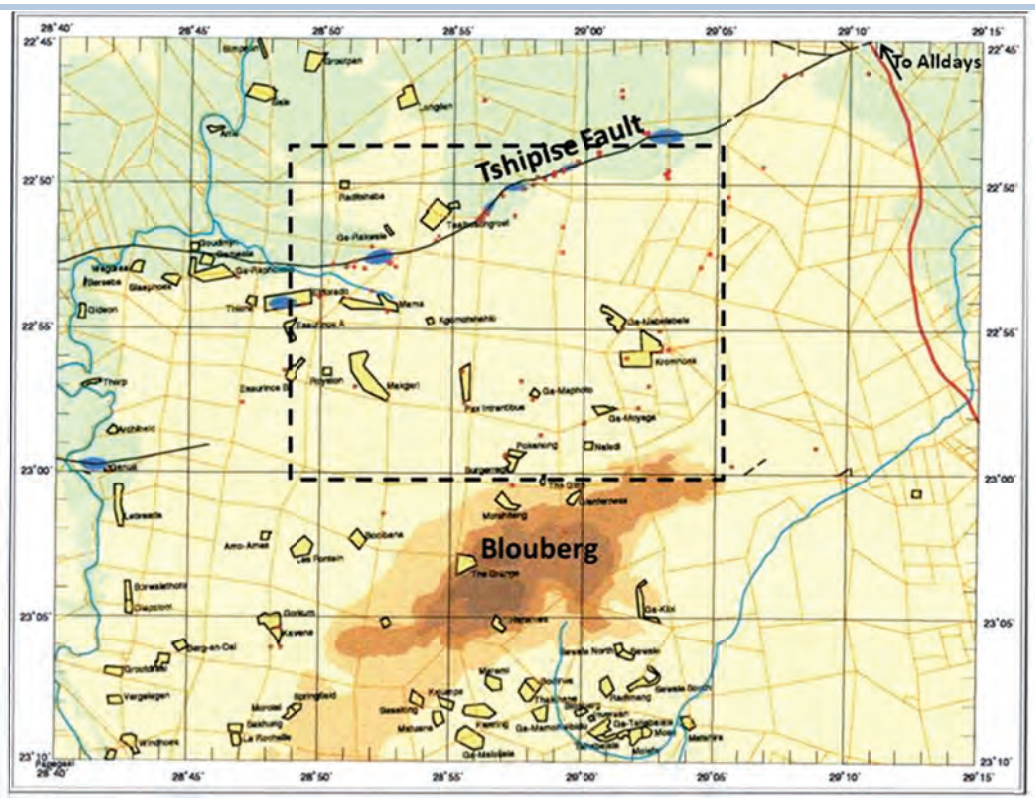

Figure 11: Location of ongoing study area between the Blouberg Mountains in the south and the Tshipise Fault in the north. Also shown is area depicted in detail in Figure 12.

Figure 12: Location of the existing and recently drilled boreholes on the farms Louisenthal, Pax Intrantibus, Fonteine du Champ and Kromhoek, as well as the position of the Terveen lineament.

A Preliminary Source Development application, together with a proposal, was submitted to DWAE, which was forwarded to GPM Consultants in Polokwane. Borehole numbers H26-0742 to H26-0744 were assigned for the three boreholes by GPM Consultants.

DRILLING PROGRESS

Drilling of the sandstone borehole on the farm Pax Intrantibus, H26-0742 (Fig. 12), commenced on the 18th of May. This borehole was drilled approximately 10 metres south of borehole H26-0515. A water strike of ~2.5 l/s was intersected in the basalts at a depth of 169 metres (Fig. 13). The EC was measured at 728 µS/cm, pH 8.27 and temperature was 27.4˚C. Samples were taken for chemistry, as well as the full suite of environmental isotopes. The results of which are shown in Table 1 and Fig. 4. A further 4 metres of basalt was drilled before the basalt/sandstone contact was encountered. No increase in the water yield was observed at the contact of the sandstone. The rest level at this stage was 44 metres. The borehole drilling was stopped at this point, and reaming of the hole to accommodate the casing took place. Steel casing was installed, and bentonite and concrete used to seal off the basalt water. A further 30 metres was drilled into the sandstone, intersecting several water strikes between 176 and 184 metres, totalling 6 l/s, similar to the existing borehole which had a strike of ~5 l/s at around 180 metres. Unfortunately it was not possible to sample the water intercepted in the sandstone.

The observation borehole, H26-0743 (Fig. 12), was drilled 20 metres from this hole to a depth of 120 metres (Fig. 13), as was suggested by the DWAE drilling supervisor, as the proposed depth of 60 metres may be too shallow with a water level of 44 metres. No significant water strikes were encountered, and the borehole was reamed and casing installed to a depth of 20 metres.

The drilling of the sandstone borehole on the farm Louisenthal (H26-0744), alongside Makgari Village (Fig. 12), commenced on the 28th of June. The basalt was found to be significantly more fractured than in the previous two boreholes. The first water strike of ~1.3l/s was intercepted at a depth of 43 metres in a sandstone layer within the basalts, and a second strike of ~3.7l/s at the base of the basalts at a depth of 72 metres (Fig. 13). The borehole was reamed and cased to a depth of 78 metres, 6 metres into the sandstone, in order to seal off the strike at the base of the basalts. The final depth of the borehole is 204 metres, with a water strikes in the sandstone at 87 metres of ~5 l/s and at 197 metres of ~3l/s. Field measurements taken prior to the installation of the casing, but after the borehole had been drilled to a depth of 168 metres, gave an EC of 738 µS/cm, pH of 8.31 and a temperature of 26.6˚C. At the final depth of 204 metres, the EC measurement was 711 µS/cm, pH 8.18 and temperature 27.4˚C. Samples were taken for the full suite of environmental isotopes (Table 1 and Fig. 14) and for chemistry in both cases. The existing equipped borehole, which is to be used as an observation hole, and is drilled into the basalts, gave an E.C. reading of 771 µS/cm, and a temperature of 27.7˚C.

The proposed borehole, to be drilled along the Terveen Lineament on the farm De Vrede, has been put on hold as, during the duration of the drilling exercise, the area was too swampy from late seasonal rainfall. An attempt was also made to sample the three production boreholes on the farm Kromhoek, which are currently supplying the town of Alldays. These boreholes are being pumped 24 hours/day at 15, 11.5 and 9 l/s.

RESULTS

Only a limited number of samples could be taken during the drilling exercise to date. The isotope data on these samples are presented in Table 1.

The $\delta D - \delta^{18}O$ values for these samples cluster fairly closely (Fig. 14) independent of sampling depth and lithology, with a deuterium excess of ~ +3‰. They are significantly less depleted than the values obtained earlier for sandstone water samples from the Kromhoek area.

The few radiocarbon values show both variable ages for the basalt and expected age increase with depth. On the other hand, the relatively large EC values (>700 µS/cm) are much higher than associated thus far with water in the sandstone. It is possible that in the area of recent drilling, sandstone transmissivities are much lower than observed elsewhere and that the effect of the overlying basalt is more dominant here.

Even these preliminary results underline the importance of assessing the aquifer conditions in various areas in order to arrive at a realistic integrated overall conceptual hydrogeological model.

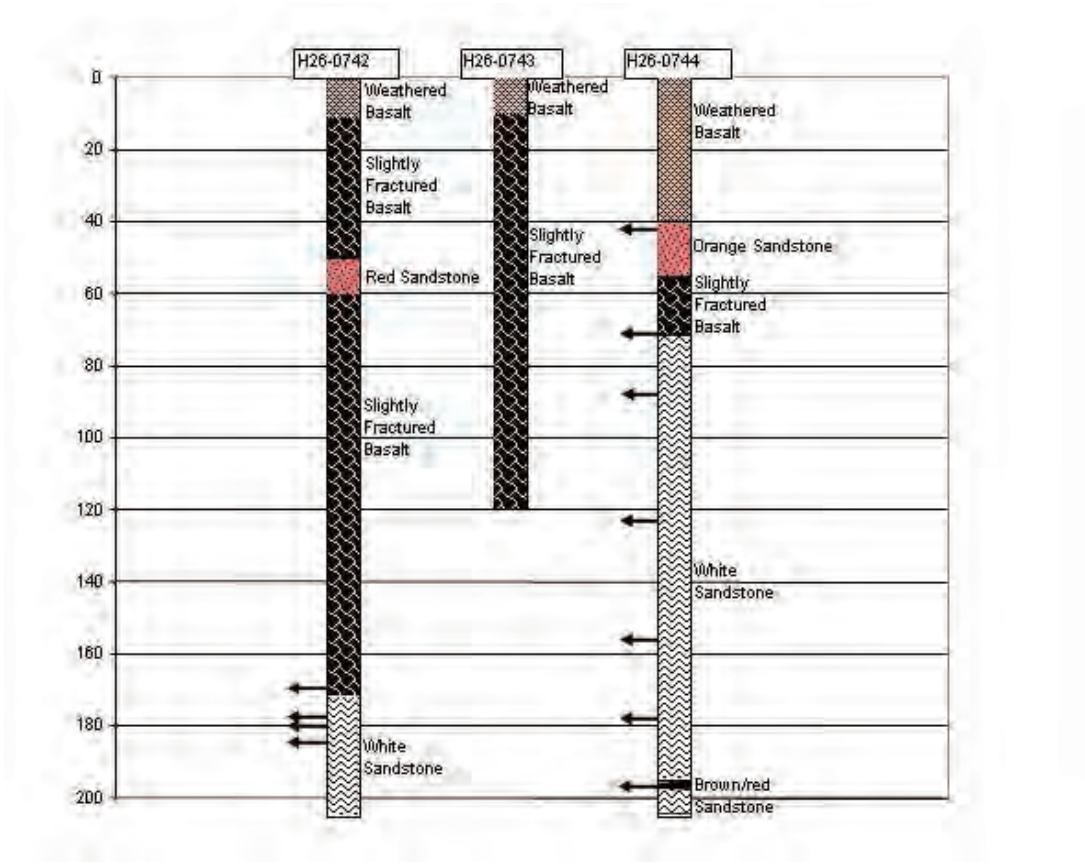

Figure 13: Logs of the sandstone (H26-0742) and monitoring boreholes (H26-0743) drilled on the farm Pax Intrantibus, and the sandstone borehole (H26-0744) drilled on the farm Louisenthal.

		Deuterium	Oxygen-18	Carbon-13	Tritium		Radiocarbon	
Field Name	Date	δD‰ SMOW	δ^{18}O‰ SMOW	^{13}C PDB	TU	±	^{14}C pMC	±
H26-0742 Pax Intrantibus 1st strike	2010/05/21	-29.1	-4.37	-9.70	0.0	0.2	43.3	1.6
H26-0744 Louisiana 1st and 2nd strike	2010/07/02	-33.5	-4.47	-10.99	0.0	0.2	74.5	1.9
H26-0744 Louisiana EOH 204m	2010/07/14	-32.1	-4.11	-10.74	0.2	0.2	56.3	1.8
H26-0121 Louisiana	2010/07/14	-34.8	-4.52		0.2	0.2		
H26-0744 Louisiana 177m	2010/07/13	-31.1	-4.34		0.0	0.2		
H26-0744 Louisiana 190m	2010/07/13	-30.8	-4.06		0.0	0.2		

Table 1. Environmental isotope analyses for samples obtained during drilling exercise

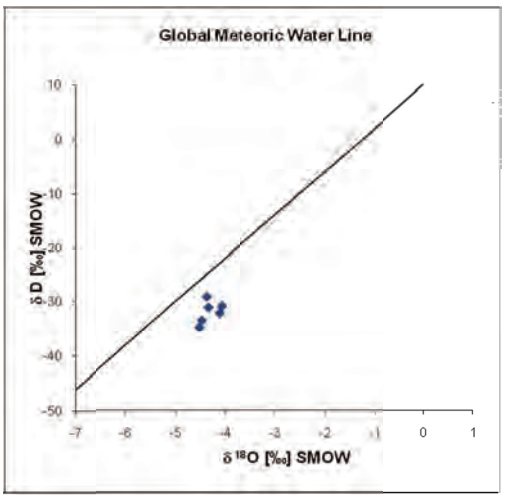

Figure 14: δ D - δ 18O plot of samples obtained during drilling exercise.

INFORMATION GATHERING

The potential significance of the ground water resource in the sandstones underlying the basalt aquifer has been recognised and is being exploited. Three boreholes, drilled into the sandstones through the basalts, on the farm Kromhoek (du Toit et al., 2007) produced high yields of exceptional quality ground water, which now provide water to the town of Alldays. The water is pumped into a high storage tank and from there to Alldays (Fig. 15).

The boreholes are however, completely sealed off and secured in pump houses, and little is known of the current pumping schedules or abstraction volumes. The Department of Water Affairs is said to be monitoring the water levels in the area, but this information has, as yet, not been obtained from the relevant personnel.

It is also not certain whether hydrochemistry monitoring data would be available, as it does not appear that the individual boreholes can be sampled. Water Affairs are not aware of any sampling taking place.

Agriculture development in the north-eastern portion of the study area, about 20 km south of Alldays (Fig. 16), appears to be growing at an alarming rate. The Department of Water Affairs has satellite images from 2000 and 2008, illustrating the dramatic expansion, but it has not been possible to acquire copies. There have been complaints of illegal water use, and the expansion has apparently started to interfere with monitoring boreholes in the area.

Figure 15: Production borehole and storage tank

The illegal water use has been reported to the Compliance Monitoring and Enforcement (CME) Directorate in Polokwane by Willem du Toit the Deputy Director at Department of Water Affairs, Polokwane, but at this stage there has been no feedback.

Of major concern in the area is the effect of agricultural practises on the quality of the ground water. Pollutants such as phosphates, herbicides, pesticides, nitrates and bacteria may contaminate this valuable resource. It is assumed that the uncontrolled extraction is occurring mainly from the sandstone aquifer which would enhance drawdown from the overlying, more mineralised basalt with its often high nitrate concentrations.

These developments pose a threat to the excellent quality of the ground water in the underlying aquifer. Furthermore, the infiltration and return flow of irrigation water, or irrigation reflux, may result in substantial increases in the salinity load of the ground water as a result of evaporation.

It is of utmost urgency that, 1) information becomes available on the existing overall groundwater extraction from the area, both for potable water supply and for irrigation 2) hydrochemical monitoring data is made available and on-going monitoring is assured 3) Some form of control is established over further expansion of irrigation demand of the resource 4. Recognition is given to its long-term regional potential as a potable water supply.

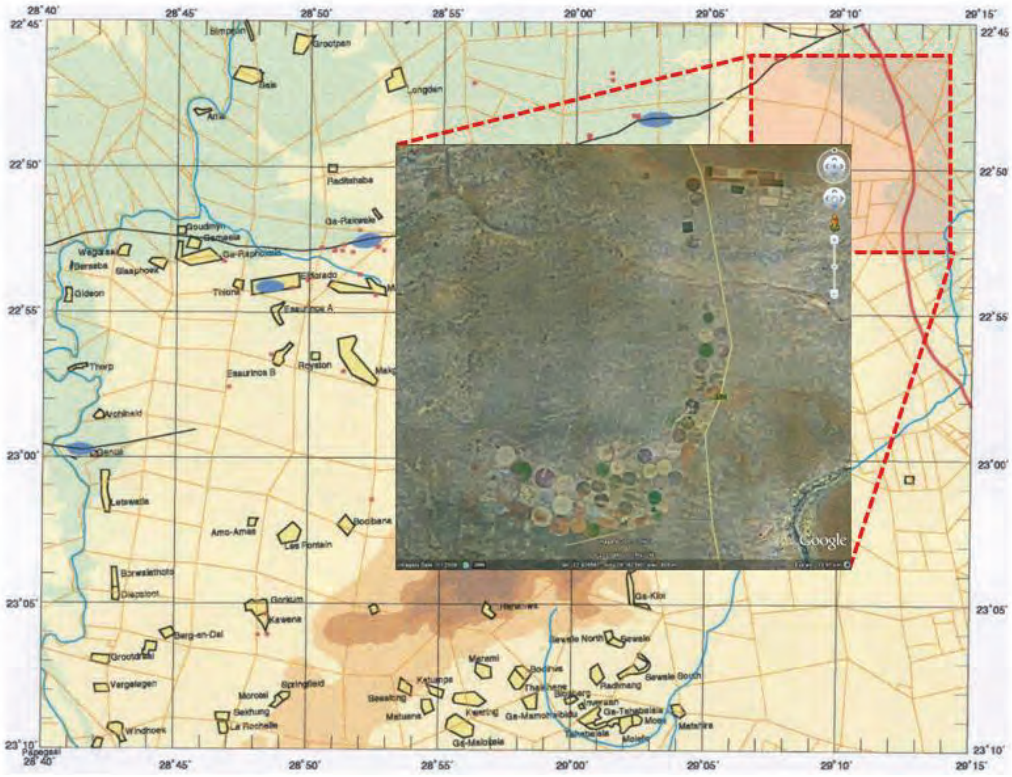

Figure 16: Map illustrating location of agricultural expansion using pivot irrigation (source: Google Earth) westwards into the main body of the (known) aquifer.

COMPREHENSIVE DATA BASE

A database, in Excel format, has been developed with all available data for the study area (Table 2). This includes data from the initial IAEA study which was initiated in 1998, the WRC study on nitrates in 2003, up to and including the recent drilling programme. This data has been revisited in the current study and, with the aid of Surfer, contouring of all the data on a regional scale has been performed.

UPDATED AREAL PLOTS

Fig. 17 illustrates the EC values throughout the study area. What is immediately obvious is the relationship between the rural villages (yellow blocks) with the higher EC values. This is also evident in the contoured maps of Na, SO_4, Cl as well as NO_3-N (Figs. 18 to 21). It should be pointed out that the data pertain almost exclusively to samples taken from boreholes nominally tapping he basalt aquifer. Although most of the high nitrate values in the area are associated with the rural villages, there is a number of boreholes with nitrate values above the WHO limit for safe drinking water which do not appear to be related to any anthropogenic sources.

Contours of the tritium concentrations (Fig. 22) illustrate higher values through the centre of the study area, from the Blouberg Mountains - the main source of run-off - in the south, northwards along and west of the Terveen Lineament to the Tshipise Fault, and in a north-westerly direction. This demonstrates the potential of the Terveen Lineament, which may be a tension fault cutting across the NW-SE trending dyke swarm, as a source of recharge to both the basalt and sandstone aquifers. A similar pattern is seen in the carbon-14 contour map (Fig. 23).

Fig. 24 shows the contour map of $\delta\ ^{18}O$ values. More negative values are shown near the Blouberg in the south and then again at certain points along the Tshipise fault. The distribution pattern of measured parameters shown in these contour maps is of necessity influenced by the distribution of the sampling points. However, in all the isotope contour maps, the influence of the fault line along the Blouberg in the south, the Tshipise regional fault in the north and the Terveen lineament are clearly discernible.

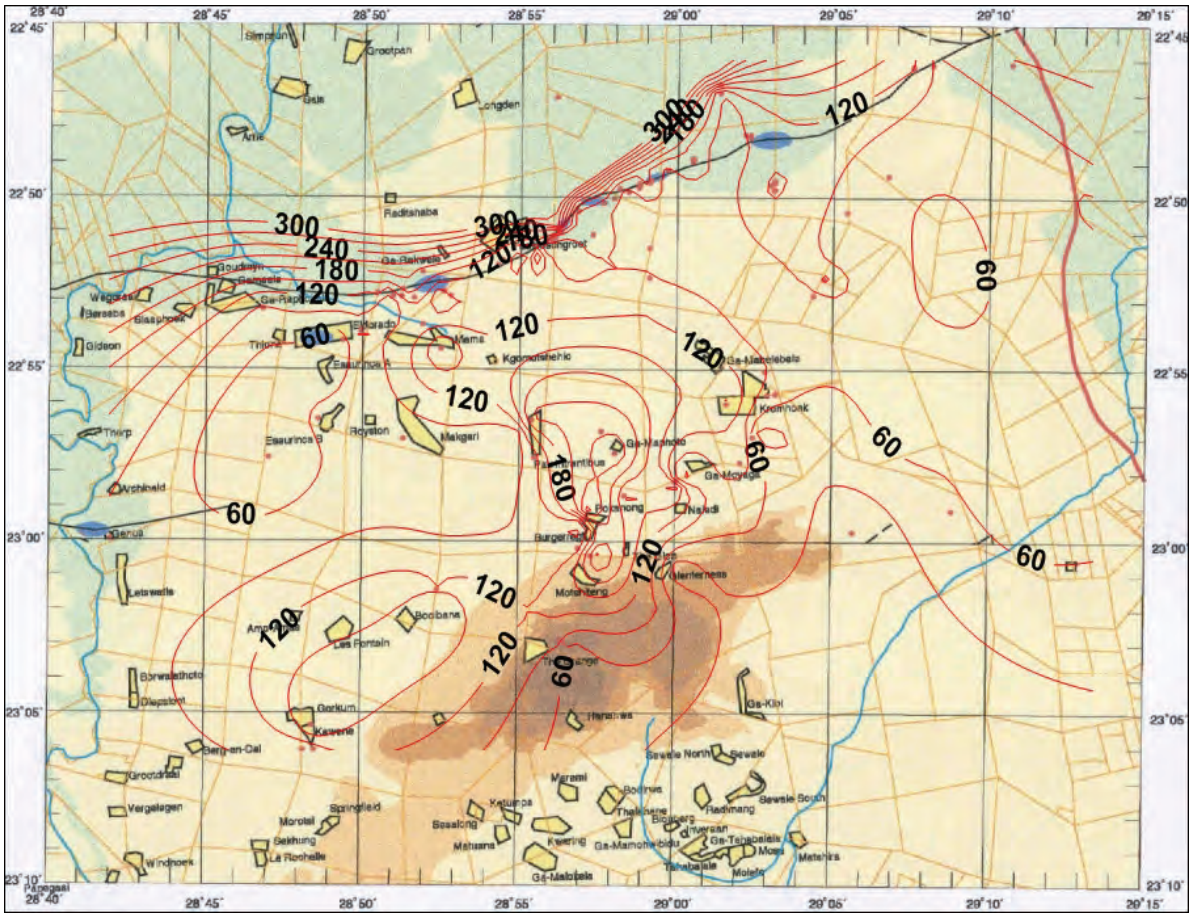

Figure 17: Map with contours of E.C. values (mS/m) for all data.

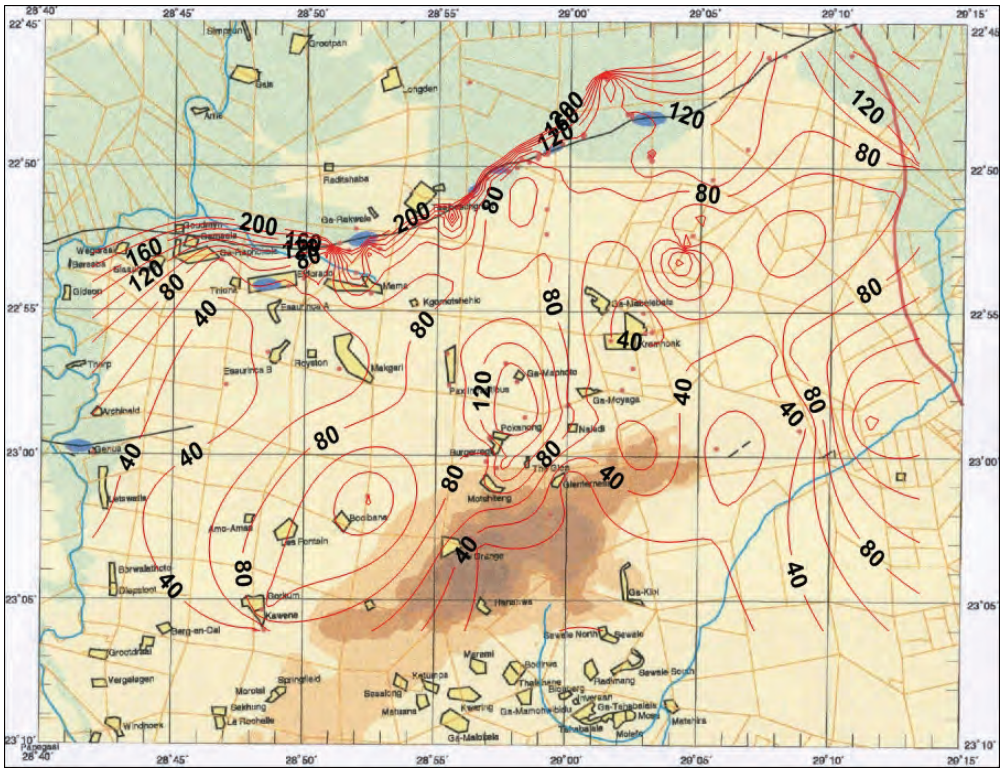

Figure 18: Map with contours of Na values (mg/l) for all data.

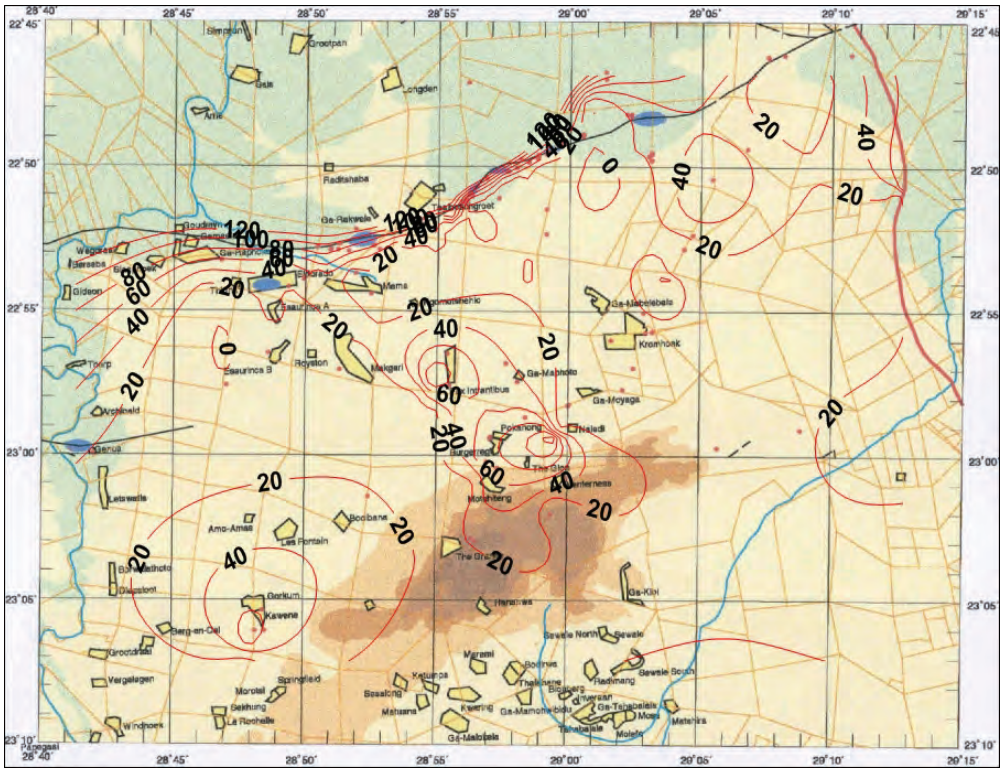

Figure 19: Map with contours of SO_4 values (mg/l) for all data.

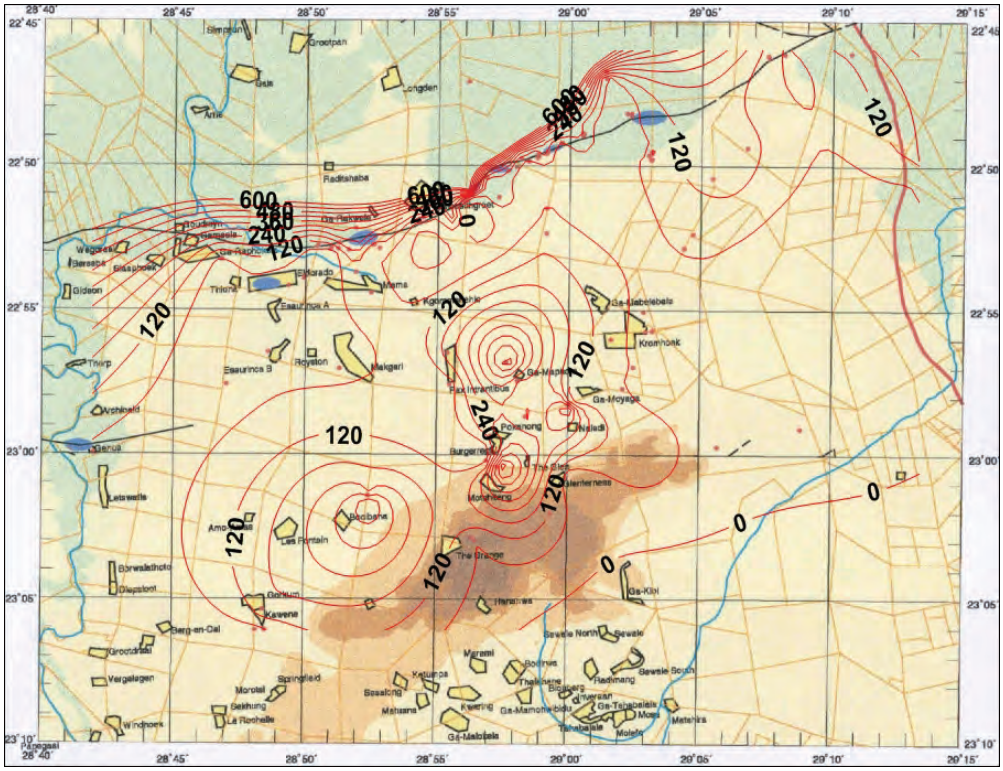

Figure 20: Map with contours of Cl values (mg/l) for all data.

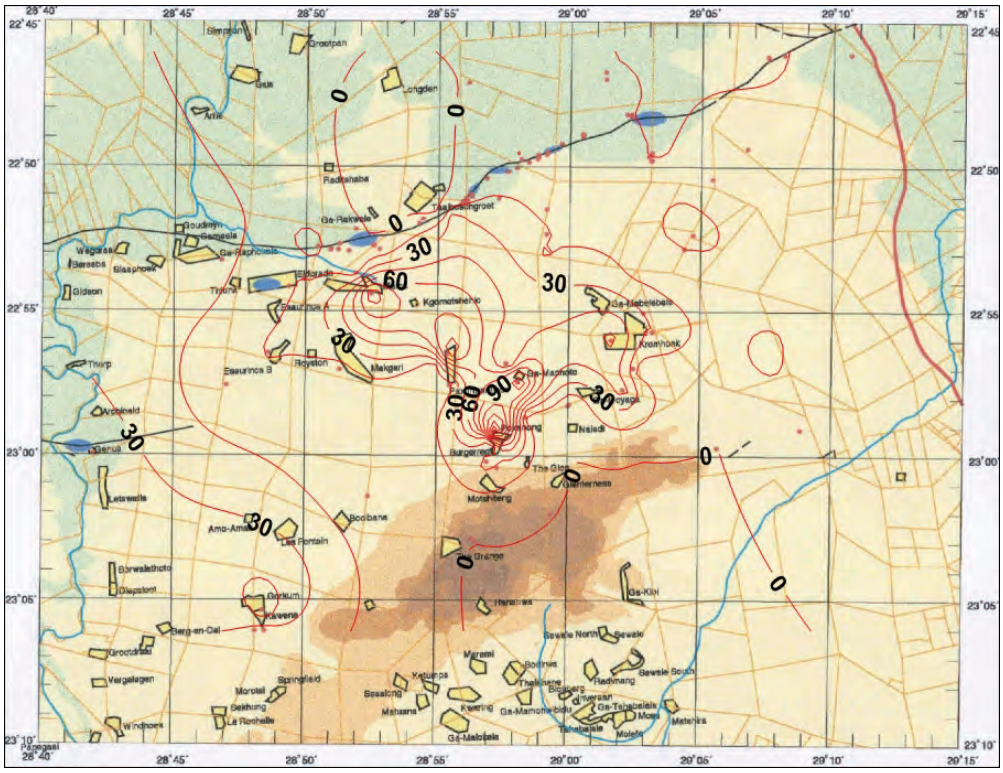

Figure 21: Map with contours of NO_3-N values (mg/l) for all data.

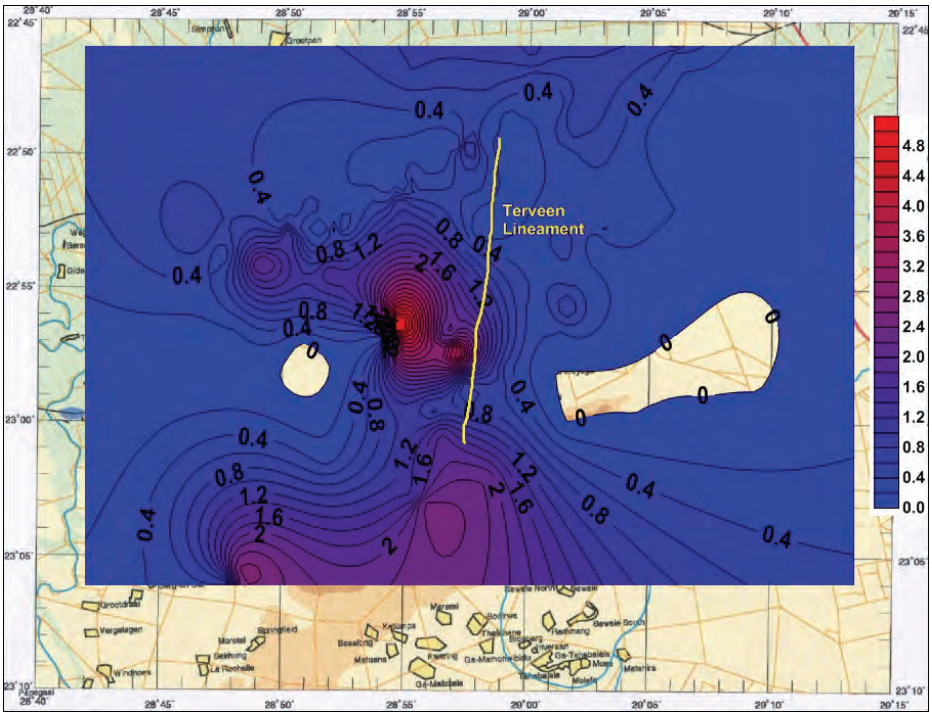

Figure 22: Map with contours of tritium values (T.U.) for all data.

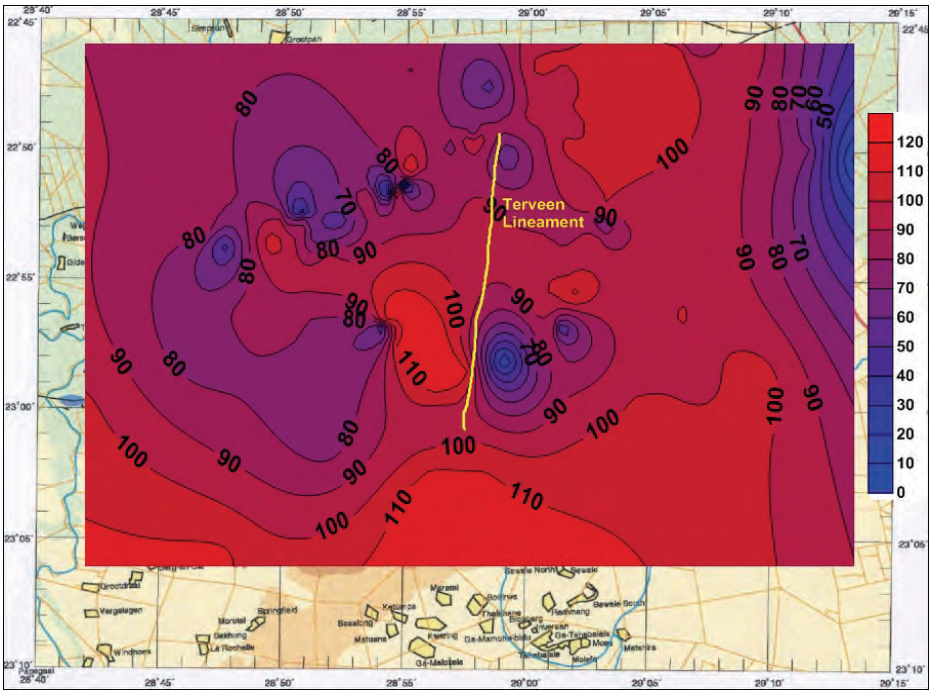

Figure 23: Map with contours of radiocarbon values (pMC) for all data.

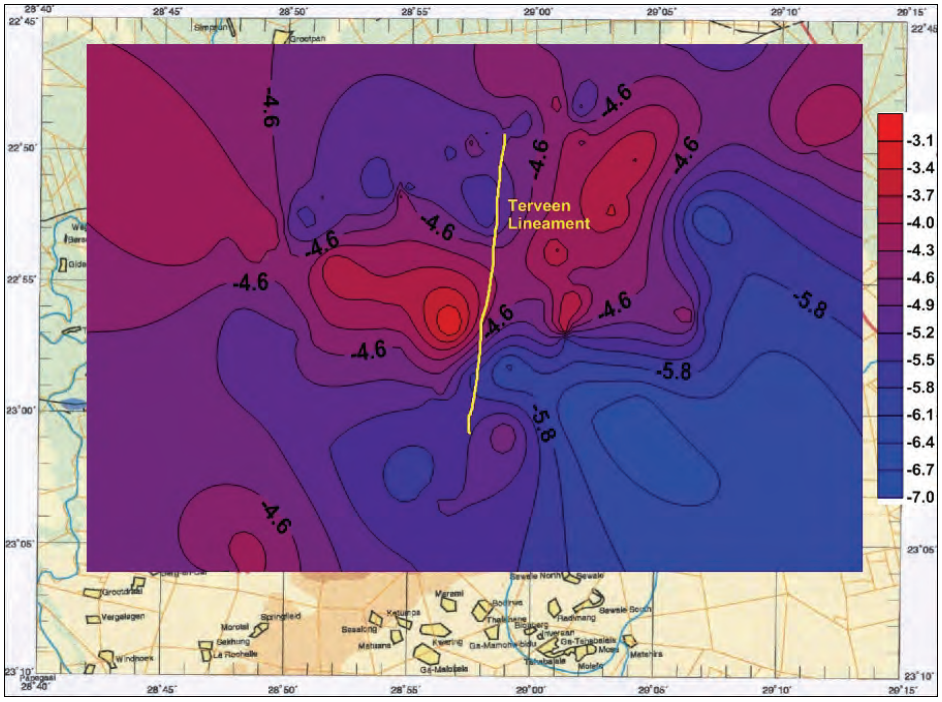

Figure 24: Map with contours of $\delta^{18}O$ values (‰) for all data.

This confirms the model, developed earlier, of localised recharge to especially the sandstone through the southern fault zone and partial (diffuse) discharge along the Tshipise fault. The probability that the Terveen lineament could contribute significantly to the sandstone aquifer water balance has been strengthened by these updated contour diagrams.

OUTLINE OF BOCHUM NITRATE STUDY

Recently, a final account has been presented on the follow-up Phase 2 of the Taaibosch nitrate study in the Bochum area in an MSc (Wits) dissertation by S.C. Mutheiwana entitled: A multi-tracer study of the origins, systematics and hydrological linkages of high

nitrate concentrations in ground water in Bochum District, Limpopo Province (2011).The study established that, as in Taaibosch (Verhagen et al. 2004a,b), a high proportion (53%) of boreholes sampled gave nitrate concentrations exceeding the generally accepted potable limit, as well as some exceedingly high values > 100 mg/l NO_3-N. Nitrate concentrations do not appear to be influenced either by the aquifer environment, or major ion development. In the Taaibosch study (Verhagen et al., 2004a, b) several cases of high nitrate concentration in the basalt aquifer were found well away from human settlements and cattle concentrations.

It was found additionally that many high nitrate concentrations (> 10 mg/l NO_3-N) were observed only for $Si(OH)_4$ (expressed as Si) values > 25 mg/l see Fig. 25. This provided an important clue to the model of natural development of high(er) NO_3 concentrations in groundwater through the following steps. The decay of discarded functional (fine, annual) root material mobilises reduced nitrogen. Fluctuations in groundwater level could subsequently produce oxic conditions enabling mineralisation to NO_3^-. The concomitant production of CO_2 from the organic material reduces the pH of groundwater.

Feldspar dissolution recommences in the aquifer thus mobilising dissolved Si (Verhagen et al., 2004a, b). The model proposes an indirect positive association involving many local rate-determining factors, rather than a strict correlation between NO_3^- and Si. One of the motivations for the Bochum study was to establish whether similar processes would/could operate in a geological environment other than basalt. The comparative plot for Bochum in Fig. 25(a) and (b) shows a similar trend of higher NO_3 values associated with the Si concentration range of 30-40 mg/l, suggesting a similar mechanism of NO_3 production in the two areas.

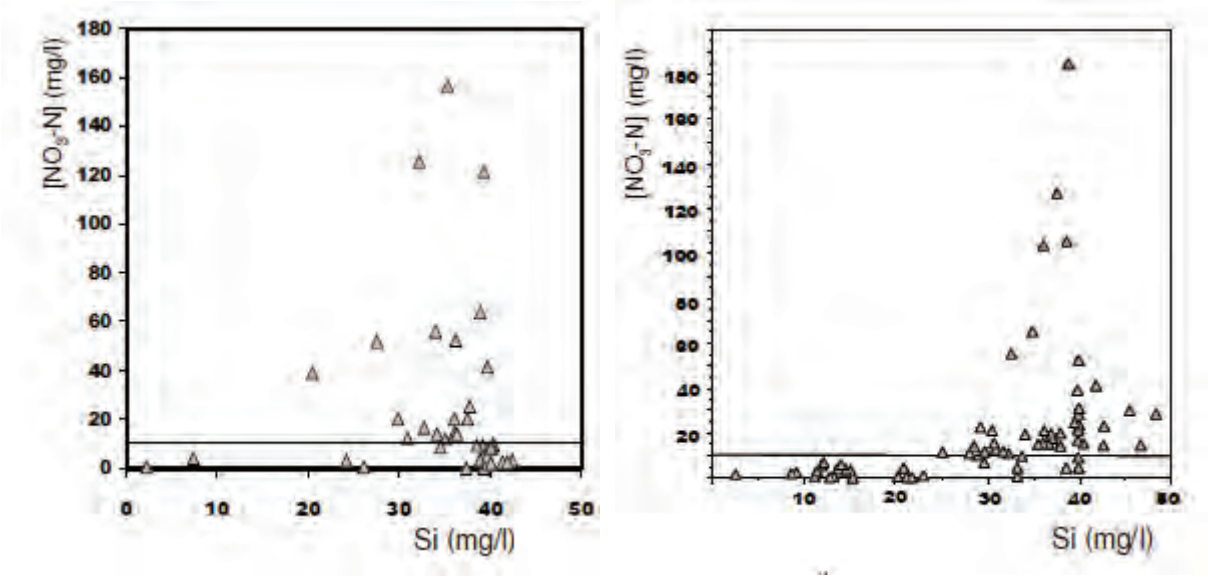

Figure 25: 2D plots of (a) NO_3- concentration against Si concentration for Bochum (Phase 2); (b) plot of NO_3- against Si for Taaibosch (Phase I).

In the original Phase 1 study, it was speculated (Verhagen et al. 2004a, b) that the Karoo basalt, with mainly macropore porosity overlying sandstone, provided the enabling environment for this process.

In comparing the results from the Bochum study with those obtained at Taaibosch, Mutheiwana (2011) observed the following:

1. The category of high 14C/low 3H ("forbidden") values that was ascribed to the transport of recent biogenic carbon to the water table by phreatophyte roots at Taaibosch is much less prominent in Bochum (Fig. 25).
2. The category of 14C/ 3H values that plots well below the exponential model curves fitted to the Taaibosch data set, interpreted as a mixture of distinct water types (basalt/sandstone), is totally absent at Bochum with its different geology.
3. There is a similar striking number of cases showing a concurrence between high NO3 and high dissolved silicon concentrations such as observed at Taaibosch (Fig. 24). This feature therefore appears not to be unique to the basalt aquifer.
4. The significant inverse correlation between δ15N and dissolved oxygen (Fig. 26), taken as a measure of de-nitrification at Bochum, was not observed at Taaibosch. Lower DOC values at the latter may be the controlling factor.

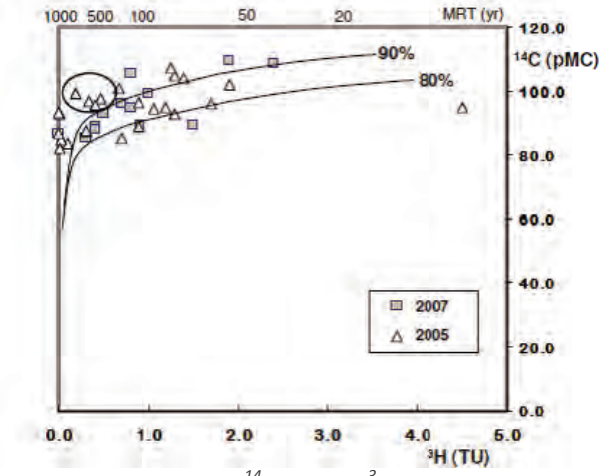

Figure 26: 2D plot of ^{14}C against ^{3}H for both sampling periods. Also shown are plots of expected exponential model values for different initial ^{14}C values and estimated mean residence time as shown along the top of the diagram

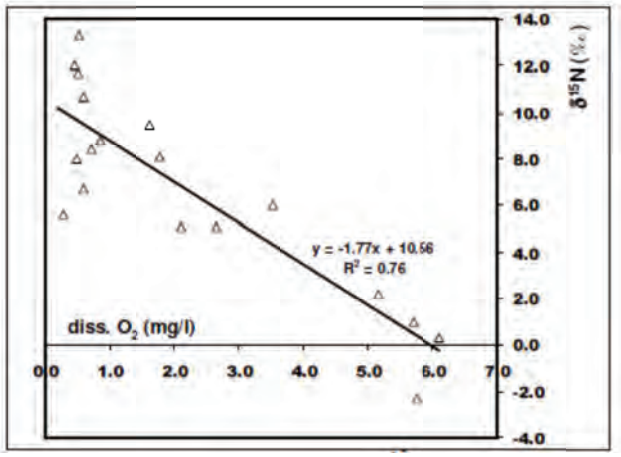

Figure 27: The relationship between $\delta^{15}N$ and dissolved oxygen concentrations for the 2005 sample set

No meaningful relationship of $\delta^{15}N$ with any other measured parameter was found except for the significant inverse relationship between nitrate $\delta^{15}N$ values and dissolved oxygen levels in individual ground water samples (Fig. 27). It should be pointed out that dissolved oxygen measurements were conducted at the well head. Samples for nitrogen isotope analysis were immediately frozen and only thawed shortly before analysis. The relationship suggests a process of de-nitrification under increasingly anoxic conditions of dissolved nitrate, itself formed by mineralisation under oxic conditions. The latter may to a considerable extent be responsible for the high nitrate $\delta^{15}N$ values observed.

The points with dissolved oxygen below 1.0 mg/l are all from boreholes at relatively densely inhabited villages. The large range of $\delta^{15}N$ values in this group appears to be independent of dissolved oxygen content and may suggest the presence of variable concentrations of organic solutes, or dissolved organic carbon (DOC), in the groundwater. This is a potability factor possibly overlooked up to now and may require further investigation. No such apparent denitrification had been observed at Taaibosch.

Mutheiwana (2011) concludes from the extension of the Taaibosch nitrate study in Bochum that both anthropogenic and natural processes of nitrate formation lead to the phenomenon of high NO_3 concentrations co-inciding with high values Si values in both areas. The direct ingress of nitogenous material through surface pollution does not involve the liberation of CO_2 leading to furher decomposition of feldspars and the liberation of dissolved Si. Higher ground water nutrient levels might enhance the intermediary step of root decay. Further research is required to investigate these processes. As the (hydro)geology of the two areas is quite different, it is concluded that, contrary to earlier impessions, it is likely that this phenomenon may be found in groundwater in a variety of aquifers, possibly excluding aquifers with very low or absent feldspar component. It may be a useful parameter for nitrate investigations in other (hydro) geological environments

BASALT AQUIFER THICKNESS

In order to establish the regional range of aquifer parameters for the highly heterogeneous basalt aquifer, it is essential to understand the variability of the basalt aquifer thickness. To this end, all available data from previous Department of Water Affairs boreholes, as well as the newly drilled boreholes from the current study were collated with elevation and depth to the base of the basalt. This data is illustrated in Figs. 28 to 31.

Figs. 28 and 29 illustrate the surface topography of the area. The gentle slope from the base of the Blouberg in a north-westerly direction is clearly shown. The slight rise in the north-east of the area can be related to the Louisiana dyke swarm

The depth to the base of the basalt and the Tshipise sandstone contact is illustrated in Figures 30 and 31. It is clear that sandstone erosional surface had considerable topography, with gradients up to some 2% before the deposition of the basalt. The sandstone comes to near-outcrop in the south-west of the area, and to the north-east within the Louisiana dyke swarm. Further east, the sandstone is seen to outcrop on the farm Langjan. Through the centre of the study area, a deep NW-SE trending valley is filled with basalt.

The basalt in the region of the Melpomene borehole, located on the western side of the study area, is only 25 metres thick. It was realised very early that,

although this borehole is drilled into the sandstone to a depth of 340 meters, its chemistry is unlike any other sandstone borehole, and plots on a Piper diagram in the Mg-Ca-HCO_3 quadrant, generally associated with basalt boreholes (Fig. 32). This is most likely the case due to the thin basalt cover and an exceptionally fluctuating piezometric level within the sandstone.

It should be pointed out that although a number of boreholes were drilled many tens of metres into the sandstone, none has penetrated this formation. Even Melpomene borehole at 340 m depth did not fully penetrate the sandstone. The thickness of the sandstone will therefore remain a matter for conjecture, unless a considerable number of strategically placed boreholes are sunk.

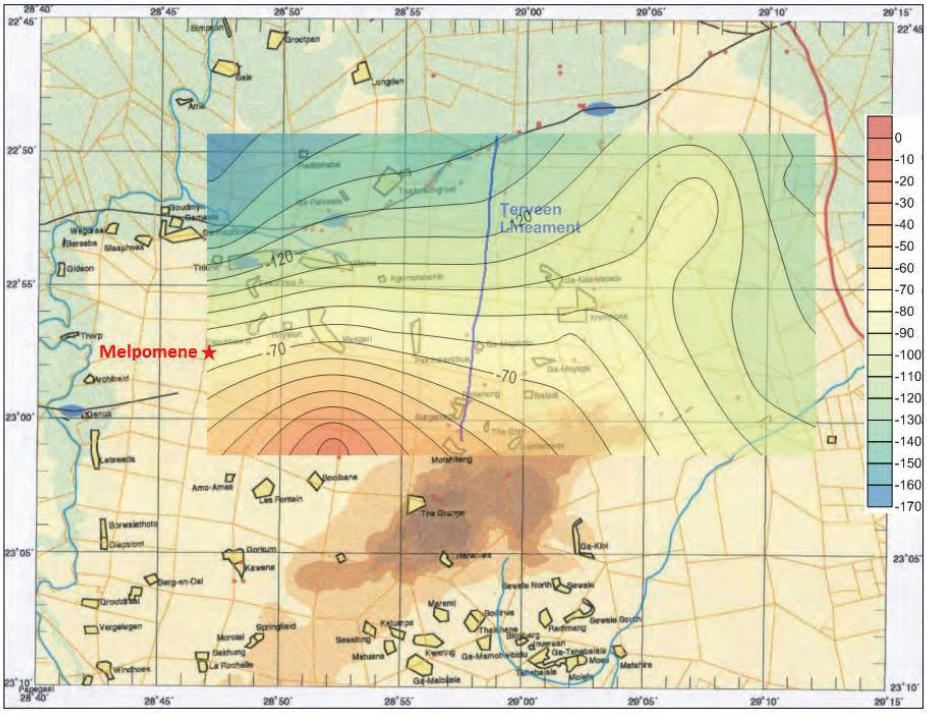

Figure 28: Map with contours of the surface topography.

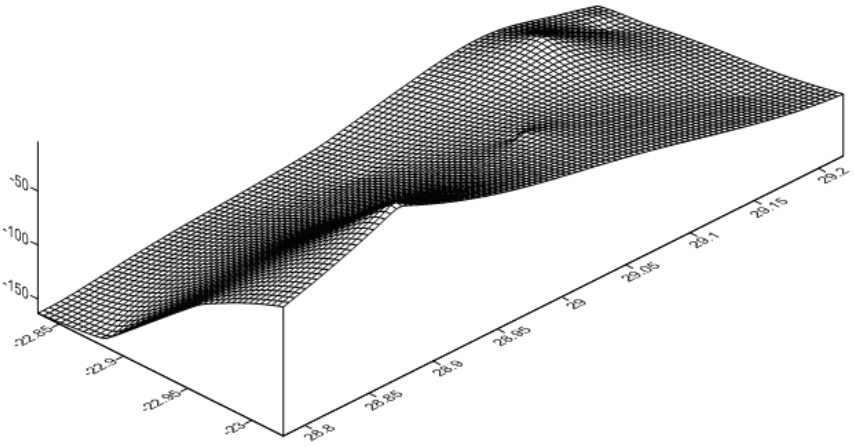

Figure 29: 3D wireframe of the surface topography

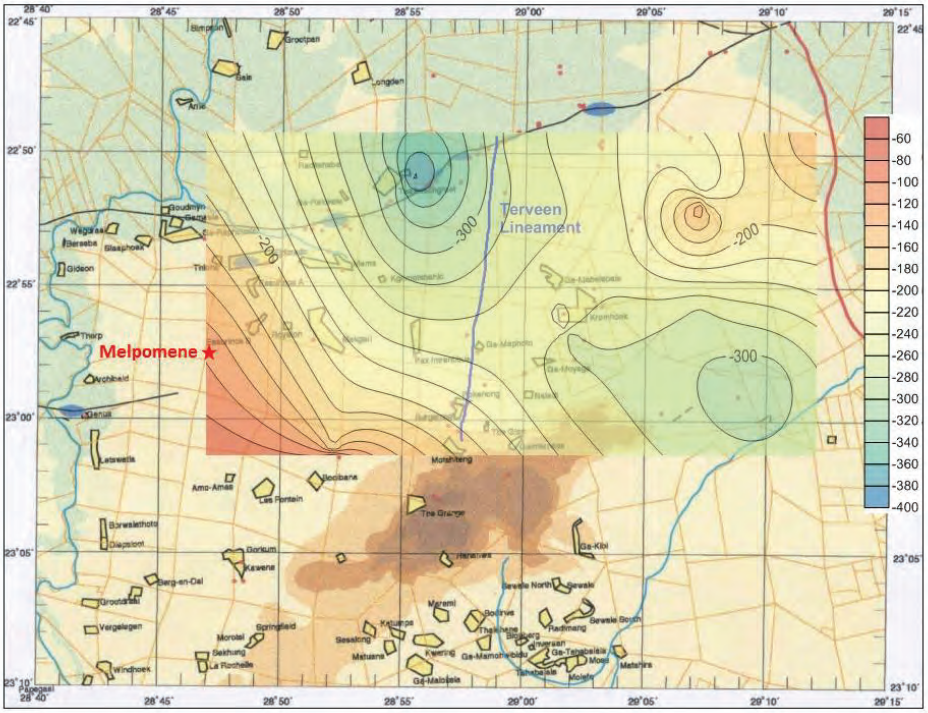

Figure 30: Map with contours illustrating depth to basalt/sandstone contact

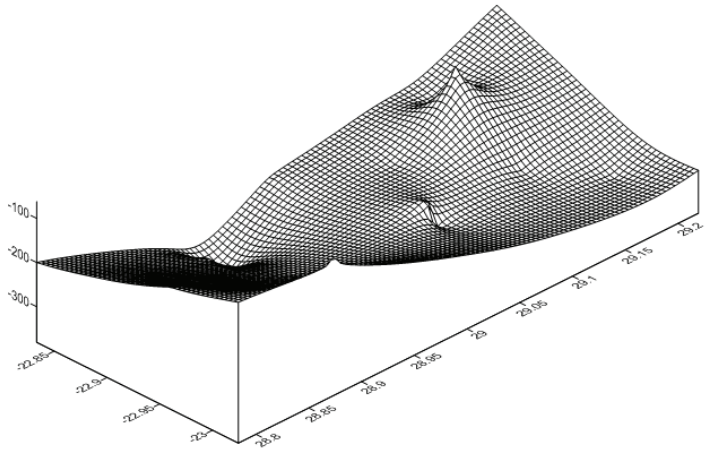

Figure 31: 3D Wireframe of depth to base of the basalt

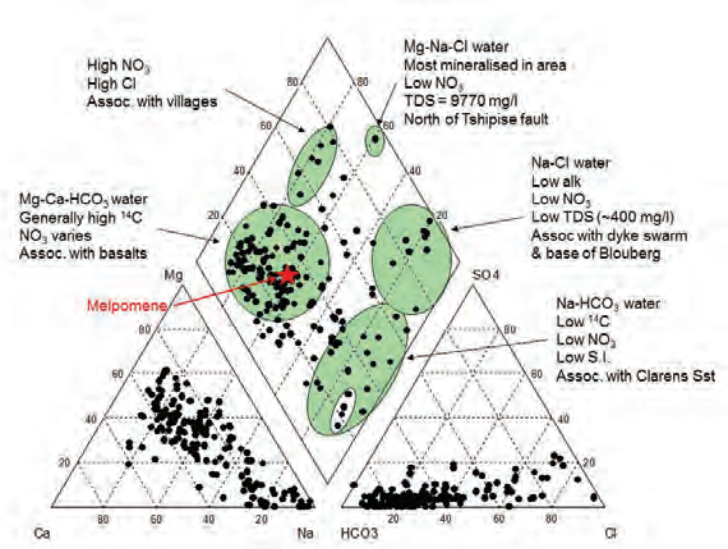

Figure 32: Piper diagram illustrating the categories for the basalt and Clarens sandstone, with the Melpomene borehole indicated.

KROMHOEK WELLFIELD

Boreholes drilled into the underlying sandstone aquifer on the farm Kromhoek produced high yields of exceptional quality ground water. During October 2010, abstraction from three of these boreholes started in order to provide water to the town of Alldays. Two boreholes (H26-0608 and H26-0457)(Fig. 33) are sodium bicarbonate water and are of an excellent quality, while the third borehole (H26-0602) is calcium-magnesium-bicarbonate water, with significantly higher electrical conductivity and nitrates, although still considered fit for human consumption (du Toit et al., 2007). It was assumed that the basalts had not been completely sealed off in this borehole. The borehole water was therefore mixed to supply a water quality that is suitable for human consumption.

Step and constant rate tests were conducted on the three boreholes H26-0457, H26-0602, and H26-0608 (du Toit et al., 2007). Recommended abstraction rates for the boreholes were calculated at 15 L/s, 7 L/s and 8.5 L/s respectively, with a combined total abstraction of 2635.2 m^3 over a 24 hour period. Further recommendations were made to sample the production boreholes on a bi-annual basis to monitor changes in the water quality which would allow remedial action, such as a reduction in the recommended safe yields of the boreholes.

One of the main assumptions made when calculating the abstraction rates was that there were no other production boreholes in the same aquifer. It has been previously reported that there is substantial agricultural development 12 kilometres to the north-east of Kromhoek. It is assumed that the uncontrolled extraction in the area is occurring mainly from the sandstone aquifer. This would therefore have major implications on the amounts of ground water calculated for safe abstraction from the Kromhoek well field.

Currently the Limpopo Region Sub-Directorate: Water Resources Information of the Department of Water Affairs is involved in an ongoing programme of monitoring water levels and water quality at various stations in Limpopo. What has been observed is a general slow declining trend in ground water levels throughout the Limpopo Province (Verster, 2012). This is considered part of a natural longer term cycle between major recharge events such as those in 1958, 1976, 1996 and 2000. This trend was observed at the monitoring boreholes H26-0442 and H26-0604 on the farm Kromhoek (Figs. 34a and 34b), with a decline of about 3.5 m in 60 months, or 0.058 m/month.

However, this trend was severely intensified once ground water abstraction commenced in October 2010. The subsequent rate of decline was initially 0.58 m/month, ten times the previous rate, with a drop of 4 metres in the first 7 months. This has since decreased, but is still declining steadily. It has become impossible to sample the present exploitation to Alldays for either isotopes or chemistry. Chemical analyses would be an important component of the monitoring process. However, at this stage, it does appear as if these analyses are being carried out, and if so, the data is not easily available. A further problem is that apparently no abstraction figures are available or are impossible to obtain. Should this dramatic decline continue, it is not sure how long the abstraction will be able to continue before the boreholes fail.

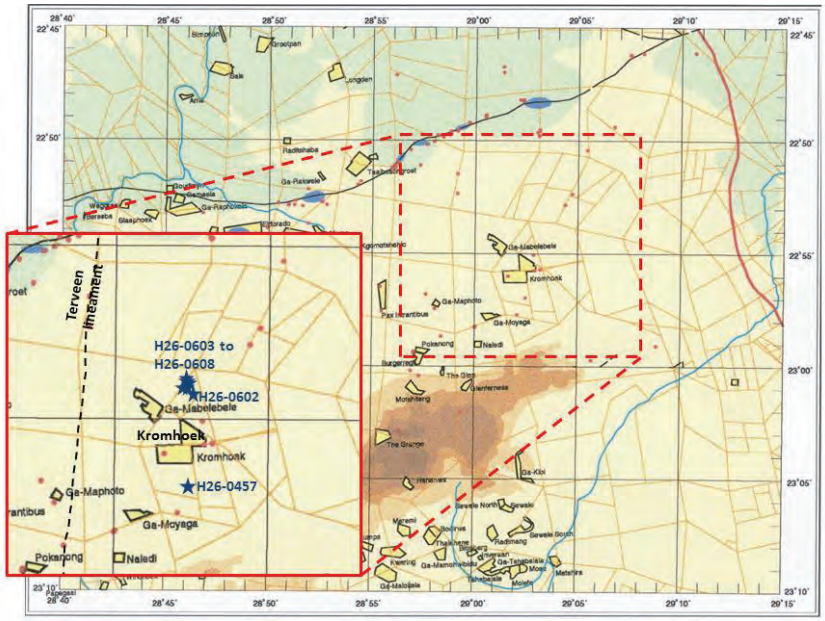

Figure 33: Location of boreholes on the farm Kromhoek being pumped for the Alldays groundwater supply scheme.

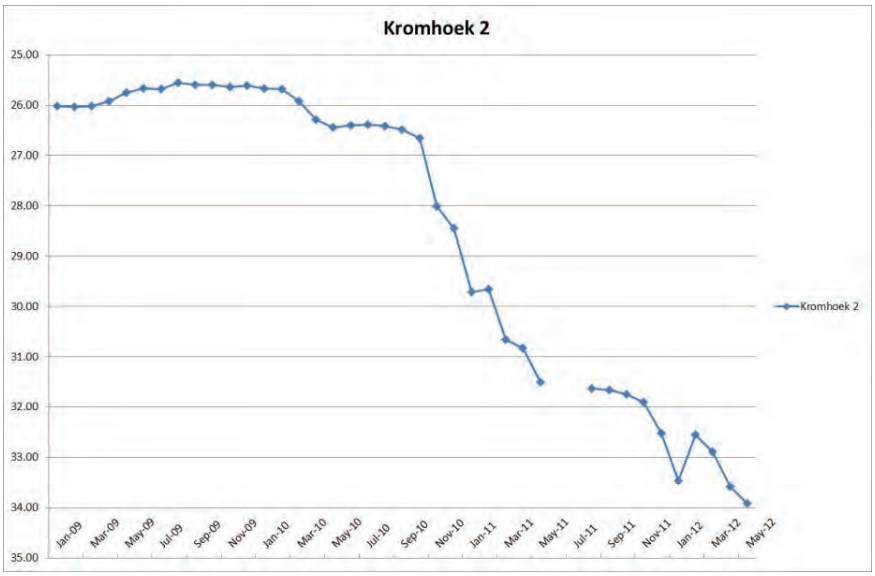

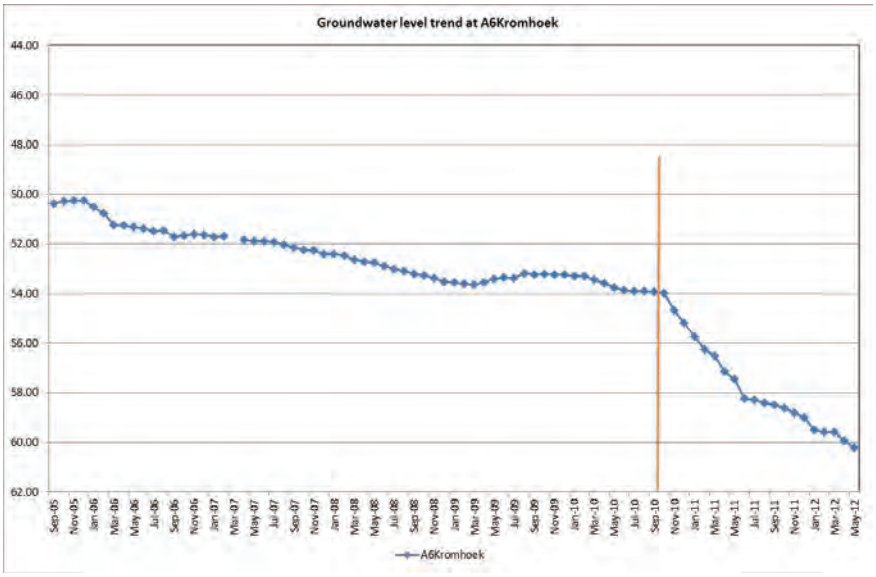

Figures 34a and b: Monitoring boreholes H26-0442 and H26-0604 on the farm Kromhoek indicating dramatic decline in ground water levels since abstraction in October 2010.

REFERENCES

Brandl, G. (2002). Summary of the preliminary report on the project: Construction of a geological-structural model for the Tshipise Fault Zone in the Alldays area, District Bochum, Northern Province. Unpub. Report. Department of Water Affairs and Forestry, Pretoria.

Fayazi, M., Orpen, W.R.G. (1989). Development of a water supply for Alldays from groundwater resources associated with the Taaibos fault. Techn. Rep. GH 3664, Department of Water Affairs and Forestry, Pretoria.

Du Toit, W.H., Whitehead, R.E., Maluleke, T. (2007) The Groundwater Potential of the Thipese Sandstone on the Farm Kromhoek 438 MS as a Source of Supply to the Town of Alldays; Technical report GH 4044, Directorate of Geohydrology, Department of Water Affairs and Forestry.

Gonfiantini, R., Froehlich, K., Araguás-Araguás, L., Rozanski, K. (1998). *Isotopes in Groundwater Hydrology in: Isotope tracers in catchment hydrology* (Kendall and McDonnell, Eds) 203-246.

Maloszewski, P., Zuber, A (1996). Lumped parameter models for interpretation of environmental tracer data. Manual on mathematical models in isotope hydrogeology. *Tecdoc-910.* IAEA, Vienna.

Mutheiwana, S.C. (2011). A multi-tracer study of the origins, systematics and hydrological linkages of high nitrate concentrations in ground water in Bochum District, Limpopo Province. MSc (Geosciences) Dissertation, University of the Witwatersrand, Johannesburg.

Van Wyk, E. (2001). Department of Water Affairs and Forestry, South Africa. Pvte. Communication

Van Wyk, E. (2004). Department of Water Affairs and Forestry, South Africa. Pvte. Communication. Verhagen, B.Th. Unpublished rainfall ^{3}H data

Verhagen, B.Th., Geyh, M.A., Froehlich, K., Wirth, K. (1991). Isotope hydrological methods for the quantitative evaluation of ground water resources in arid and semi-arid areas. - Development of a methodology. *Research Reports of the Federal Ministry for Economic Cooperation of the Federal Republic of Germany. Bonn.*

Verhagen, B.Th., Butler, M.J., Levin, M., van Wyk, E. (2002) Report to international meeting on IAEA project RAF/08/029: Isotopes in ground water resources assessment, Kampala, Uganda

Verhagen, B.Th., Butler, M.J., Van Wyk, E., Levin, M. (2004a). A multi-tracer study of the origins, systematics and hydrological linkages of high nitrate concentrations in ground water in Bochum District, Limpopo Province. Progress report to the WRC on project T5/1823

Verhagen, B.Th., Butler, M.J., van Wyk E. (2004b) Isotopes and chemistry suggest natural processes for high nitrate in Limpopo Province ground water. Extended abstracts, WISA 2004 Conference, Cape Town

Verster, H. (2012) Status Report on Groundwater Levels & Trends 1 May 2011 – 1 May 2012, Limpopo Region Directorate: Water Regulation and Use.

Lab	Sample	Farm	Sample	Latitude	Longitude	Water	Temp	E.C.	pH	Alk	TDS	E.C	pH	Na	Mg	Ca	F	Cl	NO3-N	SO4	TAL	Si	K	‰D	‰^{18}O	‰^{13}C	Tritium	Carbon-14		Radon	Depth	Casing	Strike	Yield	Geology
Number	Identification		Date			Level (m)	(°C)	(mS/m)		(meq/l)	(mg/l)	(mS/m)		(mg/l)	(mg/l)	(mg/l)	(mg/l)	(mg/l)	(mg/l)	(mg/l)	(mg/l)	(mg/l)	(mg/l)	(‰)	(‰)	(‰)	(T.U.)	(pMC)		(CPM)	(m)	(m)	(m)	(l/s)	
TT 1	TT 1	Brest	28-Oct-98	-22.77889	29.02222		26.4	253.0	8.4	10.3	1757	247.0	8.1	277.0	110.0	87.4	1.23	376.0	14.5	46.3	648.0	46.7	3.53	-26.0	-4.55	-9.74	1.0	±0.2	99.2	±2.1						
TT 2	TT 2	Greenfield	28-Oct-98	-22.78278	29.02250	10.0	24.8	104.0	8.1	7.6	671	83.4	8.2	48.9	61.1	38.0	0.86	32.9	14.5	0.8	346.0	42.4	2.40	-27.1	-4.31	-6.90	0.6	±0.2	102.1	±2.1						
TT 3	TT 3	Greenfield	28-Oct-98	-22.82722	29.05000	11.8	24.8	123.0	8.1	7.4	934	109.0	8.0	123.0	62.4	38.6	1.09	47.0	15.3	3.4	483.0	35.8	0.94	-25.1	-4.24	-9.74	0.6	±0.2	93.5	±2.0						
TT 4	TT 4	Taaiboschgroet	05-Nov-98	-22.85250	28.93528		25.0	148.0	8.4	8.3	938	119.0	8.3	152.0	47.7	40.7	0.52	118.0	11.7	39.8	398.0	29.5	2.21	-26.4	-4.98	-9.91	0.5	±0.2	89.0	±2.0						
TT 5	TT 5	Taaiboschgroet	05-Nov-98	-22.85333	28.93222		26.0	136.0	8.4	8.1	955	124.0	8.4	186.0	38.7	35.4	0.68	127.0	11.2	12.3	412.0	31.6	2.78	-30.5	-4.74	-10.16	0.4	±0.2	94.1	±2.0						
TT 6	TT 6	Rhone	05-Nov-98	-22.82917	28.96917		25.0	106.0	8.3	6.7	654	81.8	8.2	63.0	39.7	54.0	0.52	30.1	17.3	7.4	310.0	37.0	3.77	-33.7	-5.01	-10.47	0.0	±0.2	85.1	±2.0						
TT 7	TT 7	Louisiana	06-Nov-98	-22.87250	29.07861		27.0	140.0	8.3	9.4	1009	134.0	8.3	59.9	101.0	68.8	0.82	104.0	29.5	0.6	441.0	45.3	5.91	-24.5	-3.61	-8.19	0.3	±0.2	98.3	±2.1						
TT 8	TT 8	Taaiboschgroet	06-Nov-98	-22.85417	28.93389		26.0	155.0	8.2	8	929	121.0	8.3	173.0	39.8	38.2	0.67	117.0	10.0	13.1	410.0	32.2	2.97	-31.3	-5.00	-9.96	0.3	±0.2	98.4	±2.1						
TT 9	TT 9	Kromhoek	11-Nov-98	-22.91750	29.04750		27.0	116.0	7.9	6.7	699	89.9	7.8	33.7	52.3	70.5	0.43	43.5	28.4	10.9	296.0	48.2	1.45	-31.5	-4.51	-10.23	0.4	±0.2	99.9	±2.1						
TT 10	TT 10	Eldorado	13-Nov-98	-22.89833	28.83222		25.0	94.0	8.0	6.1	820	102.0	8.2	79.8	39.1	81.3	0.47	70.7	19.4	19.2	361.0	37.7	3.29	-37.0	-4.62	-9.15	2.0	±0.2	102.4	±2.1						
TT 11	TT 11	Rhode	13-Nov-98	-22.78500	28.93556		25.0		7.9	12.4	9770	1570.0	7.9	1659.0	1025.0	451.0	0.07	5124.0	0.8	1025.0	372.0	22.9	27.80	-37.7	-4.85	-10.31	0.8	±0.2	90.3	±2.0						
TT 12	TT 12	Connaught	13-Nov-98	-22.76833	29.17778		24.0	126.0	8.2	7.2	963	120.0	8.3	160.0	48.6	41.9	0.50	142.0	11.7	20.5	407.0	29.7	2.91	-35.8	-5.00	-10.70	0.1	±0.2	97.9	±2.1						
TT 13	TT 13	Johannesburg	17-Nov-98	-22.94667	28.96056		24.0	262.0	7.8	8.6	1475	234.0	7.8	141.0	150.0	127.0	0.31	602.0	22.1	55.9	246.0	29.1	2.03	-25.8	-2.96		1.7	±0.2								
TT 14	TT 14	Burgerrecht	17-Nov-98	-22.99000	28.95056		24.6	104.0	7.8	6.4	404	71.7	7.7	113.0	2.1	24.1	0.44	153.0	1.4	39.2	52.8	8.7	0.88	-35.4	-5.40		0.5	±0.2								
TT 16	TT 16	Burgerrecht	17-Nov-98	-23.00333	28.94861		25.3	114.0	7.9	6.8	788	109.0	7.7	67.0	44.9	82.3	0.26	83.4	41.1	12.1	258.0	41.6	1.25	-33.7	-5.21		1.3	±0.2								
TT 18	TT 18	The Glen	17-Nov-98	-23.00694	28.95556		26.5	242.0	8.3	7.7	1617	256.0	8.0	128.0	131.0	206.0	0.21	609.0	23.2	43.6	324.0	42.6	1.27	-33.2	-5.47		1.9	±0.2								
TT 26	TT 26	Glenfernis	17-Nov-98	-23.01333	28.99889		27.0		7.8	6.8	86	11.9	7.7	5.3	5.2	8.1	0.11	8.7	0.5	3.2	43.2	2.4	0.80	-28.9	-4.59										
TT 31	TT 31	Fontaine Du Champ	14-Jan-99	-22.89472	28.86500		26.2	114.0	7.8	7	798	102.0	7.9	176.0	11.4	43.3	0.24	108.0	4.9	28.1	335.0	14.0	1.34	-35.7	-4.76	-11.33	0.4	±0.2	63.4	±1.8						
TT 31A	TT 31A	Fontaine Du Champ	15-Jan-99	-22.89472	28.86500		27.1	104.0	8.0	6.4	792	103.0	8.0	177.0	11.4	43.5	0.24	107.0	3.9	25.2	335.0	14.3	1.24			-11.46			64.2	±1.8						
TT 32	TT 32	Johannesburg	09-Feb-99	-22.95722	28.96778		27.4	273.0	7.4	7.2	1868	267.0	7.3	151.3	136.4	186.9	0.52	292.3	127.7	56.5	390.3	37.4	2.85	-33.4	-4.08		4.3	±0.3								
TT 33	TT 33	Pax Intrantibus	10-Feb-99	-22.94111	28.92333		25.6	241.0	7.8	7.1	1527	219.0	7.8	96.4	117.6	168.6	0.41	217.4	105.1	104.7	290.5	38.4	2.61	-31.7	-4.16		5.6	±0.3								
TT 34	TT 34	Fonteine Du Champ	10-Feb-99	-22.90639	28.87472		24.2	167.0	8.1	6.9	1365	185.0	8.0	92.9	122.3	99.3	0.74	114.9	103.4	25.9	367.8	35.9	2.53	-29.5	-3.69		1.6	±0.2								
TT 35	TT 35	Eldorado	10-Feb-99	-22.90250	28.82250		25.7	72.0	7.7	6.5	333	44.6	7.6	52.2	11.5	21.3	0.46	24.0	10.7	26.4	122.2	24.9	0.73	-26.7	-4.17		2.0	±0.2								
TT 36	TT 36	Tooverfontein	11-Feb-99	-22.88750	28.77972						641	83.5	7.7	51.8	39.3	62.7	0.43	42.7	21.6	14.6	271.7	36.8	2.36	-30.9	-3.99		0.8	±0.2								
TT 37	TT 37	Kromhoek	11-Feb-99	-22.93333	29.02694		24.6	157.0	7.5	6.3	1123	152.0	7.8	39.0	99.9	116.5	0.53	90.6	65.2	15.0	386.5	34.8	1.39	-33.9	-4.69		0.2	±0.2								
TT 38	TT 38	Lovely	11-Feb-99	-22.97111	29.00000		26.3	221.0	7.4	7.5	1170	203.0	7.3	90.3	85.0	173.1	0.88	438.7	3.6	143.2	181.1	13.6	0.90	-35.9	-6.23		0.8	±0.2								
TT 39	H26-0142	Fontaine Du Champ	25-Aug-99	-22.87778	28.85444	31.0	25.4	169.0	6.2	9.1	1179	170.0	7.1	297.5	15.0	39.4	0.48	225.4	0.0	63.7	436.9	8.9	2.40	-30.5	-5.66	-14.45	0.5	±0.2	28.3	±1.5						
TT 40	H26-0144	Taaiboschgroet	24-Aug-99	-22.86333	28.90722	22.9	25.7	151.0	7.2	7.3	898	117.4	7.9	189.5	14.8	49.7	0.47	158.3	1.4	37.8	359.8	9.1	2.30	-29.3	-5.23	-10.80	0.4	±0.2	71.1	±1.9						
TT 41	H26-0151	Taaiboschgroet	24-Aug-99	-22.86583	28.90472	23.1	24.2	121.5	7.0	12.2	1029	113.6	7.8	127.7	52.6	67.6	0.45	33.7	6.0	8.2	583.5	29.5	0.60	-29.7	-5.25	-13.41	0.4	±0.2	95.6	±2.0						
TT 42	H26-0159	Fontaine Du Champ	25-Aug-99	-22.88111	28.85361	23.8	27.1	165.0	7.1	9.9	1035	122.6	7.8	148.9	33.5	82.6	0.48	70.3	20.6	20.4	481.4	30.4	1.30	-29.3	-5.13	-11.57	0.3	±0.2	103.1	±2.1						
TT 43	H26-0160	Fontaine Du Champ	25-Aug-99	-22.88194	28.86028	27.3	27.0	168.0	7.6	9.1	1011	145.0	7.9	208.0	23.0	58.3	0.37	189.0	3.3	30.4	398.6	15.1	1.10	-28.1	-5.26	-12.44	0.2	±0.2	66.6	±1.8						
TT 44	H26-0143	Fontaine Du Champ	01-Sep-99	-22.86944	28.86472	22.3				6.3	1068	170.0	8.0	260.3	20.0	52.9	0.19	281.4	2.5	70.6	303.7	11.3	1.50	-29.1	-4.84	-11.92	0.5	±0.2	63.1	±1.8						
TT 45	H26-0152	Fontaine Du Champ	31-Aug-99	-22.87889	28.87583	21.7	29.3	119.0	7.7	5.7	657	87.9	8.0	144.5	8.5	35.9	0.20	89.1	5.1	17.3	276.9	11.8	1.30	-29.8	-5.33	-15.23	0.9	±0.2	49.0	±1.7						
TT 46	H26-0156	Fontaine Du Champ	01-Sep-99	-22.88083	28.84917	22.8	21.0	122.0	7.1	6.5	704	91.0	8.2	178.8	6.7	23.6	0.22	92.1	3.0	18.9	302.3	14.7	0.90	-29.0	-4.83	-11.17	0.5	±0.2	53.6	±1.7						
TT 47	H26-0157	Fontaine Du Champ	31-Aug-99	-22.88083	28.84917	22.0	29.1	139.0	7.1	8.2	465	58.6	7.4	26.5	13.4	71.7	0.40	21.4	0.0	19.2	253.9	21.6	2.20	-28.0	-5.11	-18.42	2.9	±0.2	55.1	±1.7						
TT 48	H26-0158	Fontaine Du Champ	31-Aug-99	-22.87944	28.84056	18.4	27.4	163.0	6.7	9.1	975	117.5	7.6	128.7	35.8	86.5	1.06	53.1	24.2	20.3	444.0	39.3	0.90	-29.0	-4.41	-10.82	0.4	±0.2	88.5	±2.0						
TT 49	H26-0168	Fontaine Du Champ	01-Sep-99	-22.88083	28.87972	26.5	25.6	108.0	7.2	6.8	788	102.1	7.9	174.7	10.2	41.2	0.22	115.0	4.7	21.6	330.6	13.6	1.20	-28.9	-4.89	-11.42	0.7	±0.2	55.7	±1.7						
TT 50	H26-0169	Fontaine Du Champ	31-Aug-99	-22.88056	28.88528						654	87.4	8.1	140.4	7.6	40.9	0.22	86.6	5.0	16.6	277.6	13.2	1.18	-29.6	-4.80	-11.03	0.0	±0.2	54.5	±1.7						
TT 51	G35403	Presumption	15-Sep-99	-22.76970	29.12528	24.4	29.2	152.0	7.2	9.3	964	120.7	7.7	107.9	46.3	91.0	0.47	82.8	20.6	22.7	425.0	36.0	3.00	-30.7	-5.03	-13.26	0.9	±0.2	95.3	±2.0						
TT 52	G39019	Gansvley	14-Sep-99	-22.82500	29.05194	10.6	27.9	112.0	7.7	11.0	1023	122.9	8.1	115.1	69.6	54.3	0.90	73.6	15.9	6.2	517.8	36.0	0.88	-27.8	-4.04	-9.86	0.6	±0.2	96.7	±2.1						
TT 53	G39020	Gansvley	14-Sep-99	-22.84030	29.09056	39.2	27.8	106.0	8.5	0.8	418	78.4	9.0	120.6	1.0	25.8	0.31	180.5	0.1	61.4	22.2	12.7	0.59	-25.7	-3.64		0.3	±0.2	No CO2						
TT 54	G39086	Rhone	07-Sep-99	-22.83056	28.97389	12.1	25.3	111.0	7.8	6.5	711	91.6	7.7	84.7	42.8	48.4	0.42	82.4	11.5	10.2	320.3	28.5	0.88	-31.4	-5.02	-11.01	0.0	±0.2	78.3	±1.9						
TT 55	G39087	Rhone	08-Sep-99	-22.82861	28.97944	12.3	22.5	107.0	7.6	6.6	739	93.5	7.7	87.4	43.8	49.5	0.43	94.6	11.9	10.4	327.2	28.3	0.90	-32.2	-5.18	-10.84	0.8	±0.2	85.1	±2.0						
TT 56	G39093	Rhone	07-Sep-99	-22.82500	28.98611	11.9	28.1	118.0	7.9	6.7	688	89.1	8.0	82.6	36.7	53.8	0.38	63.4	10.7	9.7	322.0	27.9	0.90	-31.7	-5.31	-10.87	0.2	±0.2	87.9	±2.0						
TT 57	G39095	Rhone	07-Sep-99	-22.82750	28.98000						717	91.3	7.7	87.7	42.2	48.6	0.45	78.9	10.3	10.1	329.8	28.9	0.96	-32.4	-5.04	-10.97	0.1	±0.2	86.3	±2.0						
TT 58	G39098	Rhone	07-Sep-99	-22.82639	28.98000	12.3	27.3	115.0	8.0	6.9	695	89.2	7.6	80.4	40.0	50.9	0.38	72.5	10.2	11.4	322.3	28.1	0.91	-32.0	-5.10	-	0.8	±0.2	75.0	±1.9						

Lab	Sample	Farm	Sample	Latitude	Longitude	Water	Temp	E.C.	pH	Alk	TDS	E.C	pH	Na	Mg	Ca	F	Cl	NO3-N	SO4	TAL	Si	K	∂²H D	∂¹⁸O	∂¹³C	Tritium		Carbon-14		Radon	Depth	Casing	Strike	Yield	Geology
Number	Identification		Date			Level (m)	(°C)	(mS/m)		(meq/l)	(mg/l)	(mS/m)		(mg/l)	(mg/l)	(mg/l)	(mg/l)	(mg/l)	(mg/l)	(mg/l)	(mg/l)	(mg/l)	(mg/l)	(‰)	(‰)	(‰)	(T.U.)		(pMC)		(CPM)	(m)	(m)	(m)	(l/s)	
																										10.83									
TT 59	G39101	Ysselmonde	09-Sep-99	-22.83610	28.96083	13.3	27.3	97.0	7.6	6.7	813	114.8	7.7	88.3	54.3	67.7	0.37	148.0	12.1	13.4	316.8	28.5	1.00	-32.9	-5.33	-10.41	0.0	±0.2	78.0	±1.9						
TT 60	G39103	Ysselmonde	09-Sep-99	-22.83390	28.96639	13.5	24.0	94.0	7.6	7.2	785	106.6	7.6	89.1	51.0	61.0	0.38	106.0	11.4	14.3	337.8	28.6	1.04	-32.0	-4.99	-10.90	0.6	±0.2	78.0	±1.9						
TT 61	G39104	Greenfield	03-Sep-99	-22.82000	28.99500	9.0	24.7	114.0	7.8	6.6	680	88.2	7.9	88.4	37.4	45.3	0.47	59.5	9.6	9.0	325.5	28.6	0.80	-32.6	-4.86	-10.92	0.3	±0.2	80.8	±1.9						
TT 62	G39104-1	Greenfield	03-Sep-99	-22.82000	28.99444	9.3	23.8	111.0	8.4	7.2	689	88.2	7.7	88.2	39.3	44.0	0.47	66.1	9.5	9.4	326.9	28.4	0.87	-31.7	-4.96	-10.11	0.3	±0.2	81.5	±1.9						
TT 63	G39105	Greenfield	07-Sep-99	-22.81444	29.00806		24.4	117.0	7.7	6.8	723	94.8	7.9	96.7	39.7	49.5	0.39	70.4	12.4	9.0	329.2	28.4	0.74	-33.5	-4.84		0.0	±0.2	80.4	±1.9						
TT 64	G39106	Greenfield	07-Sep-99	-22.81470	29.00861		24.5	123.0	7.6	6.8	722	94.8	7.8	97.0	38.8	49.7	0.40	71.6	12.2	8.8	329.0	28.5	0.76	-32.5	-5.32	-10.32	0.2	±0.2	88.5	±2.0						
TT 65	G39125	Greenfield	02-Sep-99	-22.80310	29.03889	10.1	26.5	123.0	8.0	7.8	763	93.2	8.1	116.8	44.2	28.9	1.01	41.2	14.7	<4	380.4	36.6	0.86	-30.0	-4.48		0.1	±0.2	87.6	±2.0						
TT 66	G39126	Greenfield	02-Sep-99	-22.80330	29.03889	10.0	25.8	121.0	7.8	7.8	760	93.1	8.1	113.9	45.1	28.9	1.00	40.4	15.0	<4	379.6	36.4	0.93	-28.9	-4.52	-8.26	0.2	±0.2	90.6	±2.0						
TT 67	G39127	Greenfield	02-Sep-99	-22.80420	29.03889	10.2	25.6	116.0	8.1	7.7	724	90.0	7.9	79.4	56.3	32.7	0.82	37.2	14.1	<4	371.0	37.7	1.22	-28.7	-4.05	-8.50	0.1	±0.2	87.8	±2.0						
TT 68	G39137	Gansvley	14-Sep-99	-22.82940	29.05194	11.4	25.9	126.0	8.4	10.1	928	113.1	8.2	106.7	66.7	50.6	0.88	69.1	14.4	4.0	463.2	35.4	1.15	-30.6	-4.46		0.5	±0.2	94.8	±2.0						
TT 69	G39139	Gansvley	14-Sep-99	-22.82610	29.05194	8.1	25.7	120.0	7.6	10.8	1067	124.3	8.0	120.8	69.7	58.1	0.95	73.6	0.1	8.4	600.5	33.2	1.40	-29.1	-4.21	-10.09	0.7	±0.2	104.8	±2.1						
TT 70	PN1	Presumption	15-Sep-99	-22.82278	29.11250		29.4	83.0	10.2	0.7	358	68.0	9.7	108.2	<1	17.0	0.52	142.9	<0.04	53.8	28.2	16.6	0.40	-27.3	-4.05		0.1	±0.2	No CO2							
TT 71	PN2	Presumption	15-Sep-99	-22.76889	29.13556		27.0	101.0	7.8	6.4	667	84.8	8.0	80.5	27.6	59.3	0.47	47.4	15.2	8.3	307.5	40.3	1.58	-31.6	-5.16		0.5	±0.2	79.7	±1.9						
TT 72	YE1	Ysselmonde	08-Sep-99	-22.85778	28.98556	11.0	29.4	114.0	7.7	6.6	679	89.7	7.8	71.8	37.2	60.8	0.34	65.5	12.2	10.3	309.7	25.7	1.17	-30.0	-5.39	-11.38	0.4	±0.2	84.5	±2.0						
TT 73	YE2	Ysselmonde	08-Sep-99	-22.85139	28.95528	15.9	25.7	155.0	7.5	6.9	890	122.8	7.7	79.0	66.4	82.0	0.39	145.3	14.9	44.1	333.1	30.6	1.07	-31.6	-5.14		0.3	±0.2	84.7	±2.0						
TT 74	YE3	Ysselmonde	08-Sep-99	-22.85028	28.93806	13.7	27.3	159.0	7.5	8.4	982	138.0	7.8	165.6	49.8	48.6	0.41	143.5	10.8	16.3	416.7	28.0	1.20	-32.0	-5.08		0.2	±0.2	92.5	±2.0						
TT 75	YE4	Ysselmonde	08-Sep-99	-22.84000	28.94750	13.0	26.9	128.0	7.7	7.3	774	101.3	7.8	113.1	40.5	47.7	0.46	87.2	12.0	10.1	345.6	30.7	0.90	-30.3	-4.99	-10.17	0.1	±0.2	87.5	±2.0						
TT 76		Rhone	08-Sep-99	-22.83056	28.97444						705	93.5	7.8	87.9	40.9	50.8	0.43	73.7	11.4	10.1	319.6	28.2	0.90	-23.9	-4.03	-12.14	1.8	±0.2	111.2	±2.2						
TT 77	AugerA 0.5m	Blouberg N/R	14-Oct-00																					-38.4	-6.62										
TT 78	AugerA 0.75m	Blouberg N/R	14-Oct-00																					-38.1	-6.88										
TT 79	AugerA Seepage	Blouberg N/R	14-Oct-00																					-37.7	-6.61										
TT 80	AugerB 0.4m	Blouberg N/R	14-Oct-00																					Too small											
TT 81	AugerB 1.0m	Blouberg N/R	14-Oct-00																					Too small											
TT 82	AugerB 1.2m	Blouberg N/R	14-Oct-00																					Too small											
TT 83	AugerB 2.0m	Blouberg N/R	14-Oct-00																					-33.9	-6.09										
TT 84	AugerB 2.3m	Blouberg N/R	14-Oct-00																					-34.6	-6.25										
TT 85	AugerC 1.0m	Blouberg N/R	14-Oct-00																					Too small											
TT 86	G39104 10m	Greenfields	11-Oct-00	-22.82000	28.99500						726	98.3	7.8	92.2	41.9	51.3	0.45	103.7	11.5	16.4	301.7	28.7	0.93	-33.1	-5.17	-9.98	0.3	±0.2	88.8	±2.0						
TT 87	G39104 18m	Greenfields	11-Oct-00	-22.82000	28.99500						707	95.7	7.8	88.8	40.3	49.2	0.43	93.0	11.1	12.0	305.8	28.5	0.95	-31.4	-5.17	-10.14	0.8	±0.2	85.6	±2.0						
TT 88	G6 9m	Gansvlei	12-Oct-00	-22.82639	29.05194						1117	147.0	7.8	127.9	92.5	51.8	0.92	140.4	22.8	10.7	484.3	35.2	0.92	-27.3	-4.02	-9.43	0.4	±0.2	108.6	±2.1						
TT 89	G10 >11m	Rhone	13-Oct-00	-22.80917	29.05056						806	108.0	7.9	95.2	48.2	59.8	0.42	101.0	17.7	21.5	328.4	29.0	1.13	-34.2	-5.35	-10.35	0.8	±0.2	101.0	±2.1						
TT 90	G10 Tap	Rhone	13-Oct-00	-22.80917	29.05056						818	108.8	7.8	96.5	47.0	59.7	0.43	107.3	17.7	22.5	332.3	28.5	1.12	-34.8	-5.52		1.2	±0.2							
TT 91	G5 Fracture 26m	Rhone	13-Oct-00	-22.82833	28.98083						806	107.7	7.8	93.0	48.6	59.6	0.41	97.7	17.0	24.9	332.5	28.7	1.20	-33.2	-5.10		0.3	±0.2							
TT 92	G5 45m	Rhone	13-Oct-00	-22.82833	28.98083						808	107.3	7.7	91.0	50.1	59.8	0.41	96.8	16.8	24.9	335.5	28.5	1.14	-31.8	-5.06		1.3	±0.2							
TT 93	H26-0069	Eldorado	18-Oct-00	-22.89694	28.79972						560	73.5	8.1	72.9	20.8	49.2	0.26	59.4	7.0	4.1	262.3	34.2	2.42	-26.9	-4.42	-12.08	0.2	±0.2	44.5	±1.7						
TT 94	H26-0143 72m	Fontein du Champ	18-Oct-00	-22.87806	28.87111						793	125.9	8.4	231.7	10.2	10.6	0.16	270.8	0.1	<4	218.1	2.8	1.39	-29.5	-5.04	-12.15	0.0	±0.2	63.7	±1.8						
TT 95	H26-0152 67m	Fontein du Champ	18-Oct-00	-22.87861	28.87639						681	88.7	8.2	144.7	9.6	35.2	0.25	85.9	3.9	13.0	306.0	11.8	1.68	-30.8	-4.98	-10.90	0.4	±0.2	59.3	±1.8						
TT 96	H26-0196 <45m	Taaiboschgroet	16-Oct-00	-22.85333	28.93028						1035	151.0	8.1	212.7	36.2	43.7	0.68	179.1	3.9	25.8	424.5	29.2	1.54	-31.0	-4.87	-9.38	0.0	±0.2	91.1	±2.0						
TT 97	H26-0196 >45m	Taaiboschgroet	16-Oct-00	-22.85333	28.93028						1058	149.0	8.3	217.5	36.6	41.0	0.69	179.8	8.7	25.8	423.5	29.3	1.57	-32.3	-4.85		0.1	±0.2							
TT 98	H11-1052	Blouberg N/R	02-Feb-01	-22.98472	29.14722		27.4	90.1	6.4		420	56.5	8.2	36.1	20.6	47.7	0.15	33.2	14.7	<4	174.7	36.6	1.76	-35.4	-6.01	-15.31	0.0	±0.2	97.4	±2.1	20.7					
TT 99	H11-1066	Blouberg N/R	02-Feb-01	-22.99528	29.09472		27.6	25.1	5.6		77	10.3	7.4	8.0	4.7	4.4	0.15	<10	0.2	4.0	38.7	15.2	1.98	-36.8	-6.57	-17.79	0.0	±0.2	100.5	±2.1	567.1					
TT 100	H26-0003	Kromhoek	30-Jan-01	-22.92833	29.05306		29.8	132.2	6.5		603	76.6	8.1	33.5	44.7	61.8	0.37	26.4	30.6	15.0	233.4	39.7	1.30	-27.8	-4.08	-11.14	0.6	±0.2	113.4	±2.2	183.0					

Lab	Sample	Farm	Sample	Latitude	Longitude	Water	Temp	E.C.	pH	Alk	TDS	E.C	pH	Na	Mg	Ca	F	Cl	NO3-N	SO4	TAL	Si	K	²H/¹H D	¹⁸O	¹³C	Tritium		Carbon-14		Radon	Depth	Casing	Strike	Yield	Geology
Number	Identification		Date			Level (m)	(°C)	(mS/m)		(meq/l)	(mg/l)	(mS/m)		(mg/l)	(mg/l)	(mg/l)	(mg/l)	(mg/l)	(mg/l)	(mg/l)	(mg/l)	(mg/l)	(mg/l)	(‰)	(‰)	(‰)	(T.U.)		(pMC)		(CPM)	(m)	(m)	(m)	(l/s)	
TT 101	H26-0007	Kromhoek	30-Jan-01	-22.92889	29.04861		29.6	78.8	6.8		604	76.6	8.3	32.3	43.5	62.6	0.40	21.1	27.9	16.4	247.7	39.7	1.45	-25.3	-3.58	-9.71	1.0	±0.2	109.6	±2.2	118.5					
TT 102	H26-0121	Louisenthal	01-Feb-01	-22.95028	28.85500		30.3	126.6	6.7		595	75.2	8.3	42.3	41.1	57.4	0.25	47.7	8.7	5.2	296.0	39.7	2.22	-33.6	-4.90	-12.76	0.0	±0.2	83.6	±2.0	92.7					
TT 103	H26-0123	Louisenthal	01-Feb-01	-22.94083	28.80972		28.7	79.9	6.9		500	66.7	8.2	49.9	28.3	46.0	0.26	45.1	16.2	<4	208.5	39.7	2.25	-33.3	-5.02	-14.10	0.2	±0.2	83.0	±2.0	192.2					
TT 104	H26-0254	Genua	30-Jan-01	-22.99889	28.69972		31.4	132.7	6.5		627	81.9	8.1	46.1	35.9	73.9	0.21	44.0	38.5	16.3	195.7	39.7	1.37	-31.3	-4.81	-11.95	0.0	±0.2	102.2	±2.1	252.5					
TT 105	H11-1731	The Glen	20-Feb-01	-23.04944	28.94167	9.5	27.1	75.6	5.8		293	45.2	7.6	16.6	26.4	29.2	0.13	55.6	0.2	10.9	125.2	20.1	0.77	-30.2	-5.21	-16.12	2.5	±0.2	120.3	±2.2						
TT 106	H11-0744	Darling	21-Feb-01	-23.10111	28.80889	13.1	27.7	151.4	7.6		777	99.5	8.0	54.1	52.8	74.1	0.50	55.3	18.9	13.6	362.6	34.0	1.23	-25.7	-4.19	-9.44	2.4	±0.2	106.6	±2.1						
TT 107	H26-0041	Burgerregt	21-Feb-01	-22.98889	28.95111		28.8	200+	6.6		2019	299.0	7.8	135.4	147.8	210.4	0.23	326.6	184.6	65.6	256.5	38.7	2.76	-32.4	-4.77	-10.97	0.8	±0.2	112.1	±2.2						
TT 108	H11-0221	Glenfernis	22-Feb-01	-23.03361	28.98944	13.2	27.2	135.5	6.6		635	90.5	8.1	28.0	56.6	68.1	0.13	103.5	0.4	28.8	284.0	15.3	1.35	-26.2	-5.05	-15.62	2.1	±0.2	107.6	±2.1						
TT 109	H26-0051	Lovely	21-Feb-01	-22.97028	29.00056		28.1	26.7	9.4		191	32.3	9.5	62.3	<1	2.9	1.92	50.7	0.1	14.1	47.4	11.0	0.43	-33.1	-6.14	-15.46	0.5	±0.2	16.5	±1.4						
TT 110	H11-1149	Darling	20-Feb-01	-23.10111	28.80278	15.3	32.3	104.7	6.5		683	85.8	8.0	27.9	45.2	82.4	0.25	27.9	20.9	9.4	324.0	39.7	2.26	-29.6	-4.64	-11.00	0.4	±0.2	114.9	±2.2						
TT 111	Private BH	Darling	20-Feb-01	-23.08944	28.80750	20.3	29.8	200+	6.3		1350	184.0	8.0	101.6	112.3	114.8	0.76	161.8	55.1	71.3	444.0	32.5	1.97	-25.5	-4.13	-12.13	2.5	±0.3	108.4	±2.1						
TT 112	H11-1104	The Glen	20-Feb-01	-23.04750	28.93944	40.2	28.3	166.8	5.7		837	106.7	7.8	44.4	63.6	82.8	0.22	87.6	0.1	18.7	441.2	21.0	1.41	-34.2	-5.86	-16.31	1.5	±0.2	109.4	±2.2						
TT 113	H26-0407	Burgerregt	23-Feb-01	-22.97778	28.97306	16.0	29.6	192.5	7.6		935	140.0	8.2	158.2	14.3	105.6	0.40	221.3	4.5	90.2	265.5	20.8	0.88	-32.2	-5.54	-10.66	0.3	±0.2	115.3	±2.2						
TT 114	H26-0012	Kromhoek	23-Feb-01	-22.96167	29.03444	38.9	28.8	141.2	7.0		841	106.3	8.0	54.8	55.4	93.1	0.33	62.7	52.7	5.0	274.2	39.7	1.68	-35.2	-5.32	-9.15	0.0	±0.2	93.2	±2.0						
TT 115	G35403	Presumption	09-Mar-01	-22.77083	29.12556	20.9	28.5	182.0	7.2		1013	125.8	7.7	116.3	47.2	100.0	0.48	104.6	19.5	15.1	442.3	36.8	3.15	-32.6	-4.80	-12.90	0.3	±0.2	112.4	±2.2	1515.0					
TT 116	G39093	Rhone	07-Mar-01	-22.82611	28.98528	7.3	29.9	200+	7.4		935	148.0	8.0	120.7	68.9	82.4	0.53	182.3	4.0	21.7	360.0	33.1	1.37	-32.5	-4.97	-11.31	0.3	±0.2	97.8	±2.1	165.7					
TT 117	G39106	Greenfield	07-Mar-01	-22.81583	29.00806		26.9	169.7	7.9		876	128.2	7.9	104.9	55.6	65.6	0.37	175.1	13.7	20.0	322.0	28.5	1.00	-33.0	-5.10	-10.43	0.0	±0.2	92.4	±2.0	169.9					
TT 118	G39125	Greenfield	06-Mar-01	-22.80306	29.03611	8.5	26.6	99.9	8.0		729	93.0	8.2	113.7	44.6	29.0	1.05	47.3	4.0	6.5	384.1	38.4	0.93	-29.9	-4.22	-8.11	0.3	±0.2	98.7	±2.1	341.5					
TT 119	G39136	Gansvlei	07-Mar-01	-22.82944	29.05139	6.7	32.8	200+	6.9		1120	151.0	7.9	133.9	68.4	88.2	0.92	140.1	4.0	6.8	542.3	38.4	1.78	-28.8	-4.05	-10.81	0.3	±0.2	119.5	±2.2	71.0					
TT 120	H26-0113	Taaiboschgroet	06-Mar-01	-22.85139	28.93417		27.1	200+	7.2		1410	211.0	8.5	196.8	95.5	89.4	0.37	382.5	13.2	38.5	446.9	27.7	3.04	-33.6	-5.26	-9.24	0.5	±0.2	109.7	±2.2	264.5					
TT 121	H26-0152	Fonteine Du Champ	01-Mar-01	-22.87861	28.87639	15.1	28.7	111.3	7.5		660	89.2	8.1	134.6	10.6	36.4	0.21	89.9	6.0	20.4	278.9	12.1	1.56	-30.2	-4.92	-11.00	0.4	±0.2	61.8	±1.8	30.9					
TT 122	H26-0157	Fonteine Du Champ	01-Mar-01	-22.88139	28.84861	17.1	31.7	130.8	6.1		442	60.5	7.7	27.7	18.6	60.0	0.41	38.5	0.1	52.1	198.0	13.1	2.46	-33.0	-5.52	-17.24	1.9	±0.2	59.2	±1.8	9.7					
TT 123	H26-0158	Fonteine Du Champ	06-Mar-01	-22.87944	28.84083	14.0	30.1	191.5	6.5		1045	137.0	7.9	132.3	43.4	93.4	1.39	97.7	23.8	33.8	439.8	39.7	0.76	-33.8	-4.84	-10.87	0.3	±0.2	98.8	±2.1	94.2					
TT 124	H26-0308	Eldorado	27-Feb-01	-22.89722	28.83250		27.8	129.6	7.3		627	86.5	8.1	54.2	49.1	53.1	0.50	23.4	4.0	15.8	335.3	39.7	4.32	-26.6	-3.95	-9.56	1.5	±0.2	109.8	±2.2	48.4					
TT 125	11381	Pax Intrantibus	27-Feb-01	-22.95944	28.92472	7.5	28.9	170.5	7.1		879	111.1	8.1	78.5	30.7	119.4	0.25	92.0	8.9	14.1	412.9	33.6	1.27	-32.3	-4.59	-12.35	3.0	±0.2	112.9	±2.2	0.0					
TT 126		Ysselmonde	27-Feb-01	-22.84917	28.93722	6.7	25.2	200+	6.9		1864	288.0	7.6	242.4	135.3	140.0	0.32	615.2	9.8	92.5	484.8	28.8	3.44	-34.9	-5.20	-10.05	0.4	±0.2	107.4	±2.1	75.7					
TT 127	H26-0439	MP-01 51m	08-Nov-01	-22.88056	28.87472																					-12.66			54.7	±1.7		340	12	60	7	bas; sst; sil; tuf;sil; sst
TT 128	H26-0439	MP-01	08-Nov-01	-22.88056	28.87472																					-12.76			48.8	±1.7		340	12	60	7	bas; sst; sil; tuf;sil; sst
TT 129	H26-0441	TER-03 20m	19-Nov-01	-22.87222	28.98556						719	90.5	8.6	62.1	45.5	67.8	0.41	78.2	16.1	21.2	304.6	29.8	1.46			-10.45			94.5	±2.0	36.8	110	9	21	5	bas; dyke; bas
TT 130	H26-0441	TER-03 21m	19-Nov-01	-22.87222	28.98556						719	90.5	8.6	62.1	45.5	67.8	0.41	78.2	16.1	21.2	304.6	29.8	1.46			-10.16			93.7	±2.0		110	9	21	5	bas; dyke; bas
TT 131	H11-1745	SEM-04	21-Nov-01	-23.02361	28.87361						1080	180.0	8.1	145.8	80.5	85.6	0.30	437.7	5.3	32.8	218.0	12.5	7.71			No CO2			No CO2		40.2	165	9	140	0.2	gneiss
TT 132	H26-0442	KH-09	29-Nov-01	-22.94944	29.04111						222	30.7	8.9	61.5	<1	2.2	1.12	37.3	<0.04	26.1	75.8	23.2	0.56			-15.97			53.1	±1.7	10.0	160	6	84; 145	3.2; 9.5	bas; sst; bas
TT 133	H11-1746	SEM-06	23-Nov-01	-23.02333	28.87361						757	120.9	8.4	142.1	20.8	72.9	0.32	248.0	1.9	36.5	183.2	11.2	4.54								8.5	160	9	Dry		bas; gneiss
TT 134	H26-0444	ROS-11	04-Dec-01	-22.88056	29.07278						468	65.5	8.7	126.1	2.9	13.2	0.62	75.6	<0.04	58.7	154.4	8.2	2.35			-			41.5	±1.6	0.3	90	12	75	0.2	bas; sst; bas
TT 135	H26-0447	ROS-14	06-Dec-01	-22.88833	29.06861						561	68.2	8.6	153.7	2.0	1.1	0.42	51.1	0.5	33.1	254.5	6.5	1.12								1.2	200	119	127	1.6	bas; sst; bas; sst
TT 136	H26-0444	ROS-11	31-Jan-02	-22.88056	29.07278	11.5	31.4	31.3	9.5			31.3	9.5	65.0	<2	3.0	0.80	42.0	2.7	27.0		22.0	<1	-28.6	-3.99		0.6	±0.2				90	12	75	0.2	bas; sst; bas
TT 137	H11-1745	SEM-04	31-Jan-02	-23.02361	28.87361	55.0	28.6	162.8	7.1			162.8	7.1	135.0	74.0	157.0	0.30	386.0	4.7	36.0		28.0	4.30	-36.5	-5.21		0.3	±0.2				165	9	140	0.2	gneiss
TT	H26-0441	TER-03	01-Feb-02	-22.87222	28.98556	5.9	27.1	52.7	7.2			52.7	7.2	67.0	44.0	56.0	0.40	72.0	18.0	12.0		32.0	1.70	-32.5	-5.31		0.1	±0.2				110	9	21	5	bas; dyke; bas

Lab	Sample	Farm	Sample	Latitude	Longitude	Water	Temp	E.C.	pH	Alk	TDS	E.C	pH	Na	Mg	Ca	F	Cl	NO3-N	SO4	TAL	Si	K	δ^2D	δ^{18}O	δ^{13}C	Tritium		Carbon-14		Radon	Depth	Casing	Strike	Yield	Geology
Number	Identification		Date			Level (m)	(°C)	(mS/m)		(meq/l)	(mg/l)	(mS/m)		(mg/l)	(mg/l)	(mg/l)	(mg/l)	(mg/l)	(mg/l)	(mg/l)	(mg/l)	(mg/l)	(mg/l)	(‰)	(‰)	(‰)	(T.U.)		(pMC)		(CPM)	(m)	(m)	(m)	(l/s)	
138																																				
TT 139	H26-0442	KH-09	01-Feb-02	-22.94944	29.04111	48.4	30.1	63.1	7.8			63.1	7.8	46.0	46.0	61.0	0.50	41.0	18.0	11.0		40.0	2.50	-26.9	-3.65		0.0	±0.2					160	6	84; 145	3.2; 9.5	bas; sst; bas
TT 140	H26-0449	ROS-16	24-Jan-02	-22.86583	29.08167	7.5	26.5	79.3	7.4			79.3	7.4													-7.27			99.6	±2.1	0.0	150	12	18	3.6	soil; bas; sst; bas; sst;bas;sst
TT 141	H26-0449	ROS-16	31-Jan-02	-22.86583	29.08167	7.5	26.5	79.3	7.4		694	85.5	8.3	28.3	71.7	51.6	0.75	54.1	18.6	9.8	322.7	39.3	1.45	-29.4	-3.99	-8.12	0.4	±0.2	101.0	±2.1	139.1	150	12	18	3.6	soil; bas; sst; bas; sst;bas;sst
TT 142	H26-0445	ROS-12	31-Jan-02	-22.88028	29.07306	26.6	31.3	45.6	7.4		651	86.1	8.5	28.9	56.7	57.7	0.67	57.7	23.7	5.8	274.8	39.2	3.76	-28.0	-3.86	-7.93	0.4	±0.2	97.4	±2.1	63.7	83	12	75	2.25	bas
TT 143	H26-0439	MP-01	31-Jan-02	-22.88056	28.87472	36.8	31.7	22.3	7.9		214	31.9	7.9	27.4	10.3	19.5	0.29	29.9	2.9	<4	89.8	39.3	1.72	-32.5	-5.06	-14.17	0.2	±0.2	71.5	±1.9	24.1	340	12	60	7	bas; sst; sil; tuf;sil; sst
TT 144	H26-0456	UL-23	06-Feb-02	-22.87639	29.13611	39.2	26.4	54.1	8.3		434	52.5	8.3	19.2	19.2	61.2	0.24	29.7	4.9	11.1	222.1	39.3	1.22	-41.3	-6.07	-7.51	0.1	±0.2	100.2	±2.1	2.4	70	12	59	1.1	calcrete; bas; sst
TT 145	H26-0457	KH-24	08-Feb-02	-22.95000	29.04167	49.2			8.4		228	33.4	9.0	65.1	2.4	5.7	1.08	35.8	0.9	14.0	81.1	23.7	1.15	-32.4	-5.30	-12.94	0.0	±0.2	53.8	±1.8	3.3	237		118	40	bas; sst (white, clean)
TT 146	H11-1743	BB-06	10-Feb-02	-23.00028	29.04444	250			8.4		348	56.7	7.7	74.9	2.6	33.9	0.28	110.8	0.9	29.2	74.4	12.6	0.69	-36.7	-6.35	-12.26	0.0	±0.2	92.9	±2.1	6.8	250	5.5	Dry		qzte; bas
TT 147	H26-0458	DV-25	12-Feb-02	-22.88639	28.98361		29.0	92.0	8.2		793	102.5	8.4	84.1	46.0	73.7	0.39	128.9	13.5	21.0	309.7	26.1	1.51	-33.9	-5.34	-10.90	0.0	±0.2	95.8	±2.1	2.0	80		17-24	3.8	bas, v. weathered
TT 148	H26-0459	DV-26	13-Feb-02	-22.88639	28.98361		31.9	83.2	8.2		695	86.1	8.4	96.3	31.6	53.7	0.34	92.0	10.0	18.3	292.4	20.7	2.18	-32.8	-5.46	-10.73	0.1	±0.2	77.5	±1.9	5.1	167		167	40	bas; sst (white)
TT 149	H26-0460	GP-27	18-Feb-02	-22.94028	29.13500		29.1	55.3	8.4		468	59.2	8.4	89.7	11.3	20.9	0.44	35.3	9.6	11.8	208.2	24.3	1.25	-32.4	-5.49	-	0.0	±0.2	98.9	±2.1	11.2	190		15-19; 125	2.3; 6.3	weathered bas; sst (white)
TT 150	H26-0461	FF-28	28-Feb-02	-22.98194	29.18500	18.5	32.3	71.7	8.5		648	79.9	8.5	165.4	8.0	6.0	0.81	40.4	12.5	27.5	282.0	39.8	0.66	-36.3	-6.27	-12.35	0.0	±0.2	105.8	±2.1	0.0	43		23	0.2	bas
TT 151	H26-0466	FF-33	07-Mar-02				34.0	27.8	8.7		1561	303.0	8.2	484.6	7.3	98.2	0.23	878.2	0.1	53.4	27.6	10.1	4.21	-31.7	-5.90	No CO2	0.3	±0.2	No CO2		42.4	120				bas
TT 152	H26-0467	LJ-37	19-Mar-02	-22.83361	29.21944	27.9	20.9	50.2	7.5		813	99.4	8.4	63.9	52.0	75.7	0.49	80.8	10.2	18.3	389.1	39.0	1.69	-30.9	-4.62	-9.78	0.1	±0.2	75.1	±1.9	0.0	150		75; 95	1.2; 2.25	sand; sst (yell, wht, red, wht)
TT 153	H26-0469	LJ-39	20-Mar-02	-22.83194	29.22000	63.4	25.4	43.2	9.1		474	83.9	8.9	138.7	1.4	26.2	0.32	185.1	0.1	83.4	30.1	11.0	1.16	-29.1	-4.06	No CO2	0.0	±0.2	No CO2		0.0	120		79	1.36	bas
TT 154	H26-0447	ROS-14 (sst)	20-Mar-02	-22.88833	29.06861	22.8	39.4	39.4	7.6		519	66.8	8.3	87.2	15.2	32.4	0.65	36.7	7.4	11.0	246.0	19.7	2.53	-27.8	-4.00	-10.00	0.0	±0.2	91.8	±2.0	56.8	200	119	127	1.6	bas; sst; bas; sst
TT 155	H26-0457	KH-24 (sst)	24-Apr-02	-22.95000	29.04167	49.2	29.0	20.0	8.4		239	29.5	8.2	50.8	3.4	9.0	0.26	11.9	0.4	10.7	122.7	12.1	0.82	-32.6	-6.13	-15.03	0.0	±0.2	23.5	±1.5	21.4	237		118	40	bas; sst (white, clean)
TT 156	H26-0460	GP-27	25-Apr-02	-22.94028	29.13500			104.8	7.5		804	96.5	8.5	40.3	64.7	75.2	0.86	34.1	18.1	6.1	410.7	39.2	1.90	-32.0	-4.73	-9.01	0.6	±0.2	102.4	±2.1	72.8	190		15-19; 125	2.3; 6.3	weathered bas; sst (white)
TT 157	H26-0449	ROS-16	26-Apr-02	-22.86583	29.08167	7.5	25.8	98.8	7.6		707	91.0	8.0	29.0	69.9	55.4	0.78	54.9	19.2	4.9	332.5	39.2	1.48	-29.7	-4.11	-8.01	0.4	±0.2	99.4	±2.1	225.0	150	12	18	3.6	
TT 158	H26-0467	LJ-37	23-Sep-02	-22.83361	29.21944	28.05	20.9	50.2	7.5		786	95.6	7.9	64.1	50.8	67.1	0.45	71.2	8.6	12.0	394.0	37.3	1.39	-30.1	-4.59	-10.43	0.0	±0.2	84.3	±2.0	5.3	150		75; 95	1.2; 2.25	sand; sst (yell, wht, red, wht)
TT 159	H26-0439	MP-01	05-Oct-02	-22.88056	28.87472	36.8	31.7	22.3	7.9		234	35.3	7.8	24.9	9.2	20.6	0.27	35.3	2.7	5.3	102.5	38.0	1.38	-30.1	-4.76	-13.66	0.0	±0.2	69.2	±1.9	0.0	340	12	60	7	bas; sst; sil; tuf;sil; sst
TT 160	H26-0457	KH-24	12-Oct-02	-22.95000	29.04167	49.2	26.2	33.4	8.4		229	29.4	8.1	42.9	2.9	9.2	0.21	11.1	0.5	11.5	121.3	11.7	0.73	-31.5	-5.80	-15.26	0.0	±0.2	25.7	±1.5	0.0	237		118	40	bas; sst (white, clean)
TT 161	H26-0458	DV-25	19-Oct-02	-22.88639	28.98361				8.2		822	108.9	8.4	79.8	47.3	75.3	0.30	126.8	15.9	15.1	332.7	24.8	1.24	-31.3	-4.95	-10.75	0.0	±0.2	93.0	±2.0	5.9	80		17-24	3.8	bas, v. weathered
TT 162	H26-0467	Langjan	12-Mar-07	-22.83361	29.21944																			-31.0	-4.35	-10.08	0.0	±0.2	66.8	±1.8	22.4	150		75; 95	1.2; 2.25	sand; sst (yell, wht, red, wht)
TT 163	H26-0470	Gruisfontein	12-Mar-07	-22.84297	29.25428																			-29.5	-4.50	-8.96	0.1	±0.2	5.7	±1.3	64	120		Dry		sst; sst (yell, yell-red,red)
TT 164	H26-0505	Greenfields	12-Mar-07	-22.79558	28.99114																			-30.8	-4.45	-10.65	0.6	±0.2	55.3	±1.7	91.9	80	11	Dry		calcrete; sst; mudstn;sst
TT 165	H26-0510	Greenfields	12-Mar-07	-22.83889	29.00333																			-31.0	-4.74	-9.47	0.0	±0.2	58.3	±1.8	57.1	195	30			dol, bas; sst (wht-yell)
TT 166	H26-0439	Melpomene	13-Mar-07	-22.88056	28.87472						228	34.9	7.2	29.9	10.7	19.1	0.17	33.2	2.9	4.4	94.8	39.5	1.47	-31.3	-4.79	-11.67	0.4	±0.2	52.3	±1.7	35.7	340	12	60	7	bas; sst; sil; tuf;sil; sst
TT 167	H26-0484	Fonteine du Champ	13-Mar-07	-22.88528	28.78697																			-28.2	-4.17	-10.09	0.7	±0.2	87.9	±2.0	3.8	100	9	23		calcrete; bas; sst; mudstn
TT 168	H26-0488	Taaiboschgroet	13-Mar-07	-22.86250	28.92639																			-29.2	-4.25	-8.88	1.1	±0.2	101.0	±2.1	3.5	80	10.5	17	1.8	calcrete; bas
TT 169	H26-0487 (A)	Taaiboschgroet	13-Mar-07	-22.85889	28.92972																			-34.3	-5.63	-8.63	0.2	±0.2	0.0	±1.2	70.6	265	9	25	1.3	calcrete; bas; sst; bas;sst
TT 170	H26-0487 (B)	Taaiboschgroet	13-Mar-07	-22.85889	28.92972																			-35.5	-5.05	-9.12	0.0	±0.2	3.2	±1.2		265	9	25	1.3	calcrete; bas; sst; bas;sst
TT 171	H26-0516	De Vrede	14-Mar-07	-22.88722	28.98333																			-31.5	-4.78	-10.16	0.3	±0.2	89.2	±2.0	138.7					lineament
TT 172	H26-0443	Rosyth	14-Mar-07	-22.88022	29.07308																			-28.1	-3.79	-7.82	0.4	±0.2	92.3	±2.0		40	6	9	0.2	dolerite dyke
TT 173	H11-1743	Devon	14-Mar-07	-23.00028	29.04444						310	53.2	7.5	83.7	0.5	23.5	0.22	93.3	0.0	37.4	58.1	13.4	0.31	-36.6	-6.06	-13.82	0.0	±0.2	84.9	±2.0	3.9	250	5.5	Dry		qzte; bas
TT 174	H26-0457 (A)	Kromhoek	15-Mar-07	-22.95000	29.04167																			-32.2	-5.79	-11.70	0.0	±0.2	22.8	±1.5	1.3	237		118	40	bas; sst (white, clean)
TT 175	H26-0457 (B)	Kromhoek	15-Mar-07	-22.95000	29.04167																					-12.03	0.2	±0.2	21.8	±1.4		237		118	40	bas; sst (white, clean)

Lab	Sample	Farm	Sample	Latitude	Longitude	Water	Temp	E.C.	pH	Alk	TDS	E.C	pH	Na	Mg	Ca	F	Cl	NO3-N	SO4	TAL	Si	K	δ^2D	δ^{18}O	δ^{13}C	Tritium		Carbon-14		Radon	Depth	Casing	Strike	Yield	Geology
Number	Identification		Date			Level (m)	(°C)	(mS/m)		(meq/l)	(mg/l)	(mS/m)		(mg/l)	(mg/l)	(mg/l)	(mg/l)	(mg/l)	(mg/l)	(mg/l)	(mg/l)	(mg/l)	(mg/l)	(‰)	(‰)	(‰)	(T.U.)		(pMC)		(CPM)	(m)	(m)	(m)	(l/s)	
TT 176	H26-0606 (A)	De Vrede	15-Mar-07	-22.89413	29.04136						632	71.6	8.1	48.5	42.0	54.7	0.42	52.2	9.7	14.7	307.9	25.9	1.10	-29.4	-4.27	-9.49	0.6	±0.2	85.6	±2.0	10.6					bas; sst
TT 177	H26-0606 (B)	De Vrede	15-Mar-07	-22.89413	29.04136																					-9.71	0.0	±0.2	82.1	±1.9						bas; sst
TT 178	H26-0604	De Vrede	15-Mar-07	-22.89772	29.03794																			-26.1	-3.57	-7.92	0.3	±0.2	94.1	±2.0	2.7					bas; sst
TT 179	Lineament surface water	Terveen	19-May-10																					-2.7	-0.73		2.6	0.3								
TT 180	H26-0742 1st strike	Pax Intrantibus	21-May-10	-22.94749	28.91452							72.8												-29.1	-4.37	-9.70	0.0	0.2	43.3	1.6						
TT 181	H26-0744 1st and 2nd strike	Louisiana	02-Jul-10	-22.95083	28.85890																			-33.5	-4.47	-10.99	0.0	0.2	74.5	1.9						
TT 182	Lineament surface water	Terveen	01-Jul-10																					27.4	5.63											
TT 183	H26-0744 EOH 204m	Louisiana	14-Jul-10	-22.95083	28.85890							71.1												-32.1	-4.11	-10.74	0.2	0.2	56.3	1.8						
TT 184	H26-0121	Louisiana	14-Jul-10	-22.95028	28.85500																			-34.8	-4.52		0.2	0.2								
TT 185	H26-0744 177m	Louisiana	13-Jul-10	-22.95083	28.85890																			-31.1	-4.34		0.0	0.2								
TT 186	H26-0744 190m	Louisiana	13-Jul-10	-22.95083	28.85890																			-30.8	-4.06		0.0	0.2								
TN 01	H26-0445	Rosyth	06-Oct-03	-22.88028	29.07278		27.9	85.5	7.3	264.74	651	88.0	8.2	32.9	57.5	58.5	0.72	64.2	27.5	<6	253.2	1.5	3.56	-27.2	-3.72	-7.37	0.4	±0.2	95.2	±2.0	86.3	83	12	75	2.25	bas
TN 02	H26-0444	Rosyth	06-Oct-03	-22.88056	29.07278		28.1	90.2	7.22	62.952	219	38.9	9.2	69.8	<1	3.9	0.74	68.4	<0.11	20.6	44.1	18.8	0.55	-28.3	-3.85	No CO2	0.0	±0.2	No CO2		74.8	90	12	75	0.2	bas; sst; bas
TN 03	H26-0447	Rosyth	06-Oct-03	-22.88833	29.06861		30.2	64.0	8.97	265.96	504	62.1	8.8	127.1	3.6	7.4	0.62	34.0	5.0	15.3	238.8	12.3	2.39	-27.5	-3.93	-9.04	0.0	±0.2	74.8	±1.9	15.6	200	119	127	1.6	bas; sst; bas; sst
TN 04	H26-0449	Rosyth	06-Oct-03	-22.86583	29.08167		27.1	89.6	7.35	359.9	689	87.2	8.1	29.2	71.5	49.0	0.79	46.5	19.1	<6	330.6	2.6	1.46	-28.2	-3.83	-8.14	0.0	±0.2	96.0	±2.0	154.5	150	12	18	3.6	soil; bas; sst; bas; sst;bas;sst
TN 05	H26-0469	Langjan	07-Oct-03	-22.83194	29.21972		28.2	84.9	9.22	23.18	448	84.0	7.4	131.9	<1	27.0	0.35	185.2	<0.11	75.0	22.0	12.3	1.07	-28.5	-3.87	No CO2	0.0	±0.2	No CO2		50.9	120		79	1.36	bas
TN 06	H26-0467	Langjan	07-Oct-03	-22.83333	29.21944		27.5	99.6	6.93	422.12	771	94.8	8.2	66.6	49.9	71.0	0.48	62.6	8.5	8.4	387.3	2.0	1.56	-30.4	-4.40	-10.49	0.0	±0.2	66.0	±1.8	20.3	150		75; 95	1.2; 2.25	sand; sst (yell, wht, red, wht)
TN 07	H26-0510	Greenfields	07-Oct-03	-22.83889	29.00333		30.1	72.2	7.25		599	73.6	8.5	94.8	19.7	44.1	0.27	47.9	2.9	6.9	303.9	11.7	1.77	-29.9	-4.77	-10.20	0.2	±0.2	55.5	±1.7	35.2	195	30			dol, bas; sst (wht-yell)
TN 08	H26-0515	Pax Intrantibus	08-Oct-03	-22.94667	28.91472		28.1	79.7	7.22	119.56	537	82.5	8.1	101.0	13.8	47.7	0.43	123.9	12.4	23.5	139.9	22.5	0.97	-28.4	-4.06	-11.14	0.0	±0.2	112.8	±2.2	157.7	205	12	61; 165; 181	34	overburden; bas; sst (wht)
TN 09	H26-0491	Taaiboschgroet	08-Oct-03	-22.86167	28.91889		25.5	46.8	8.52	270.84	356	49.7	8.6	101.6	1.3	4.0	1.38	44.7	0.6	20.2	147.0	8.0	0.39	-31.7	-5.42	-10.35	0.2	±0.2	9.8	±1.3	103.9	200	10.5	25	0.93	bas; sst
TN 10	H26-0490	Taaiboschgroet	09-Oct-03	-22.86083	28.92194		25.4	104.2	7.51	261.08	716	104.2	8.1	172.0	1.3	50.8	0.43	164.6	15.9	33.2	182.3	18.0	0.64	-29.2	-4.43	-9.63	0.5	±0.2	89.5	±2.0	153.8	80	10.5	52	0.2	calcrete; bas; calcrete; bas
TN 11	H26-0489	Taaiboschgroet	13-Oct-03	-22.86361	28.92444		24.0	105.9	7.41	671	1263	173.0	8.1	215.6	55.9	75.6	0.60	197.8	35.8	33.1	429.1	29.7	2.67	-28.6	-4.14	-9.50	0.9	±0.2	106.5	±2.1	48.3	80	11	18	0.4	
TN 12	H26-0488	Taaiboschgroet	13-Oct-03	-22.86250	28.92639		24.2	121.4	7.44	688.08	1262	179.0	8.1	213.4	55.6	66.3	0.58	226.8	36.1	36.4	409.5	28.7	3.53	-28.7	-4.20	-9.07	0.5	±0.2	112.8	±2.2	99.1	80	10.5	17	1.8	calcrete; bas
TN 13	H26-0487	Taaiboschgroet	13-Oct-03	-22.85889	28.92972		27.8	47.1	8.75	880.84	417	53.0	8.5	120.9	<1	3.0	0.44	35.4	<0.11	28.0	187.1	6.9	0.65	-32.6	-5.56		0.1	±0.2	0.0	±1.2	137.1	265	9	25	1.3	calcrete; bas; sst; bas;sst
TN 14	TT 2	Greenfields	13-Oct-03	-22.78278	29.02250		27.3	119.4	7.52	753.96	1413	194.0	8.0	243.1	74.2	62.3	1.33	253.3	17.7	33.4	544.5	39.9	3.07	-28.6	-4.44	-9.70	0.6	±0.2	97.7	±2.1	2337.0					
TN 15	H26-0457	Kromhoek	14-Oct-03	-22.95083	29.04111		29.7	25.5	8.4	295.24	260	33.8	8.0	47.6	4.3	11.6	0.32	16.9	<0.11	<6	139.9	5.3	1.48	-29.5	-5.31	+2.73	0.3	±0.2	53.1	±1.7	6.8	237		118	40	bas; sst (white, clean)
TN 16	TT 37	Kromhoek	14-Oct-03	-22.93333	29.02694		27.6	103.7	7.27	866.2	1201	159.0	7.9	47.5	113.2	102.0	0.49	100.5	106.0	30.5	275.4	47.0	1.76	-26.1	-3.78	-10.60	0.5	±0.2	98.3	±2.1	245.7					
TN 17	TT 3	Greenfields	14-Oct-03	-22.82722	29.05000		32.1	88.1	7.5	707.6	1138	143.0	8.2	151.7	81.2	47.0	1.06	109.1	23.8	<6	523.5	36.6	1.07	-28.2	-3.90	-9.31	0.4	±0.2	99.9	±2.1	216.4					
TN 18	G39106	Greenfields	14-Oct-03	-22.81583	29.00806		31.9	82.8	7.81	485.56	836	112.5	8.3	106.6	51.6	62.9	0.48	145.2	16.6	11.6	314.4	30.2	1.01	-30.4	-4.75	-9.50	0.1	±0.2	82.9	±2.0	15.0					
TN 19	H26-0458	De Vrede	15-Oct-03	-22.88694	28.98333		25.8	75.5	7.26	446.52	869	115.3	8.0	86.6	48.5	83.8	0.31	130.9	18.3	18.0	343.2	24.6	1.70	-30.5	-4.96	-11.65	0.0	±0.2	90.0	±2.0	234.6	80		17-24	3.8	bas, v. weathered
TN 20	H26-0441	Terveen	15-Oct-03	-22.95000	29.04056		25.7	66.1	7.29	478.24	781	101.5	7.9	63.4	53.3	73.3	0.46	82.7	20.3	11.9	332.1	32.8	1.43	-29.7	-4.69	-10.57	0.1	±0.2	93.0	±2.0	205.8	110	9	21	5	bas; dyke; bas
TN 21	H26-0466	Fraaifontein	15-Oct-03				25.9	58.6	7.56	373.32	595	73.7	8.2	154.7	4.8	6.5	0.52	36.2	17.8	<6	253.5	2.1	0.41	-34.0	-5.67	-12.54	0.4	±0.2	96.9	±2.1	231.0	120				basalt
TN 22	H26-0461	Fraaifontein	15-Oct-03	-22.98194	29.18500		25.8	65.3	7.63	390.4	650	84.2	8.1	167.0	7.1	9.5	0.80	59.9	16.2	15.9	260.6	41.6	0.42	-34.0	-5.74	-12.93	0.0	±0.2	100.1	±2.1	292.8	43		23	0.2	basalt
TN 23	TT 18	The Glen	16-Oct-03	-23.00694	28.95556		27.1	219.0	6.68	505.08	1551	253.0	7.6	134.6	108.2	201.5	0.23	512.0	30.8	36.8	344.3	39.9	1.42	-33.5	-5.30	-12.88	0.2	±0.2	90.2	±2.0	88.8					
TN 24	H26-0041	Burgerrecht	16-Oct-03	-22.98889	28.95111		28.4	87.2	6.31	126.88	430	75.8	7.8	117.3	3.3	29.3	0.42	164.4	3.1	40.2	49.9	8.1	1.08	-30.8	-5.13	-10.99	0.0	±0.2	23.1	±1.5	105.0					
TN 25	TT 16	Burgerrecht	16-Oct-03	-23.00333	28.94861		29.4	120.1	6.98	422.12	795	112.5	8.0	80.7	39.8	89.1	0.26	153.7	22.0	7.4	266.1	39.9	1.34	-33.6	-5.20	-12.16	0.8	±0.2	95.2	±2.0	35.1					
TN 26	TT 12	Connaught	16-Oct-03	-22.76833	29.17778		30.5	112.6	7.24	529.48	853	109.3	8.1	87.8	42.7	84.0	0.41	92.5	26.9	<6	345.1	38.3	2.73	-30.9	-4.61	-10.18	0.1	±0.2	93.1	±2.0	55.2					

Lab	Sample	Farm	Sample	Latitude	Longitude	Water	Temp	E.C.	pH	Alk	TDS	E.C	pH	Na	Mg	Ca	F	Cl	NO3-N	SO4	TAL	Si	K	$\delta^{2}H$	$\delta^{18}O$	$\delta^{13}C$	Tritium		Carbon-14		Radon	Depth	Casing	Strike	Yield	Geology
Number	Identification		Date			Level (m)	(°C)	(mS/m)		(meq/l)	(mg/l)	(mS/m)		(mg/l)	(mg/l)	(mg/l)	(mg/l)	(mg/l)	(mg/l)	(mg/l)	(mg/l)	(mg/l)	(mg/l)	(‰)	(‰)	(‰)	(T.U.)		(pMC)		(CPM)	(m)	(m)	(m)	(l/s)	
TN 27	H26-0456	Ulster	20-Oct-03	-22.87611	29.13583		26.1	34.9	7.23	546.56	431	55.6	8.1	21.3	18.7	65.7	0.24	31.2	4.7	<6	220.6	1.9	1.14	-39.3	-5.96	-8.03	0.2	±0.2	93.4	±2.0	40.2	70	12	59	1.1	calcrete; bas; sst
TN 28	H26-0460	Ganspan	20-Oct-03	-22.94028	29.13472		22.2	52.2	7.84	353.8	799	96.1	8.1	40.0	61.9	77.6	0.83	48.1	20.0	<6	391.4	40.4	1.56	-30.0	-4.34	-8.44	0.0	±0.2	101.1	±2.1	76.2	43		23	0.2	bas
TN 29	H11-1745	Tuskow	25-Oct-03	-23.02361	28.87361		29.5	65.3	6.97	590.48	1151	174.0	8.1	125.9	79.1	69.6	0.38	268.8	5.3	34.5	446.5	29.2	4.99	-33.0	-4.94	-12.71	0.2	±0.2	74.4	±1.9	304.8	165	9	140	0.2	gneiss
TN 30	H26-0439	Melpomene	25-Oct-03	-22.95944	28.78333		28.5	23.5	7.05	175.68	217	31.7	7.9	26.1	8.5	19.2	<0.2	34.0	3.2	<6	90.8	4.4	1.53	-31.1	-4.83	-13.77	0.0	±0.2	71.8	±1.9	45.3	340	12	60	7	bas; sst; sil; tuf;sil; sst
TN 31	TT 34	Fonteine du Champ	26-Oct-03	-22.90639	28.87472		34.4	113.9	7.52	441.64	915	111.1	8.1	81.4	70.8	57.9	0.84	34.4	41.9	12.5	384.8	39.9	2.53	-26.5	-3.65	-8.24	0.2	±0.2	98.0	±2.1	51.3					
TN 32	H26-0308	Eldorado	26-Oct-03	-22.89722	28.83250		33.9	76.9	7.75		645	79.5	8.0	52.9	42.6	52.0	0.56	15.9	21.1	14.5	302.4	41.1	4.44	-28.7	-4.64	-8.25	1.9	±0.2	97.7	±2.1	153.8					
TN 33	H26-0121	Louisenthal	26-Oct-03	-22.95028	28.85500		33.6	47.0	7.58	448.96	609	78.5	7.8	40.5	43.6	56.9	0.29	48.2	11.7	<6	297.4	2.5	2.26	-31.5	-4.66	-12.10	0.3	±0.2	82.4	±2.0	100.3					
TN 34	H26-0254	Genua	27-Oct-03	-22.99889	28.69972		27.5	56.9	8.44	253.76	515	70.5	8.0	40.5	29.5	56.8	0.26	46.6	24.8	<6	186.4	1.9	1.19	-30.0	-4.47	-9.76	0.5	±0.2	97.6	±2.1	84.7					
TN 35	TT 32	Johannesburg	27-Oct-03	-22.95722	28.96778		28.0	123.7	7.75	563.64	1247	173.0	7.9	95.6	102.8	114.9	0.53	210.0	36.2	29.6	435.9	39.3	1.58	-29.6	-4.41	-10.98	0.7	±0.2	103.7	±2.1	33.8					
TN 36	TT 13	Johannesburg	27-Oct-03	-22.94667	28.96056		27.9	119.3	7.94	739.32	958	120.3	8.1	95.4	62.5	79.2	0.60	85.1	31.2	14.0	395.0	39.9	1.82	-27.1	-3.91	-10.07	1.6	±0.2	108.7	±2.1	49.5					
TN 37	H26-0003	Kromhoek	27-Oct-03	-22.92833	29.05306		26.5	81.6	7.97		628	82.0	8.1	32.8	45.1	62.6	0.41	39.7	33.4	11.4	234.8	42.0	1.38	-28.8	-4.41	-11.15	0.9	±0.2	103.4	±2.1	262.5					
TN 38	H26-0442	Kromhoek	27-Oct-03	-22.94917	29.04083		27.8	35.2	9.46		209	31.6	7.9	58.1	1.1	3.7	0.97	35.9	<0.11	11.8	79.2	23.6	0.71	-22.3	-3.64	-10.60	0.1	±0.2	-		87.9	160	6	84; 145	3.2; 9.5	bas; sst; bas
TN 39	H11-1149	My Darling	28-Oct-03	-23.10111	28.80278		26.8	41.0	6.91		731	87.6	8.0	32.5	47.6	87.7	0.36	30.3	14.2	<6	381.9	2.1	1.28	-27.4	-4.44	-11.67	0.9	±0.2	105.0	±2.1	249.9					
TN 40	11381	Pax Intrantibus	28-Oct-03	-22.95944	28.92472		27.0	67.1	7.18		723	91.2	8.0	103.6	25.7	67.9	0.24	108.6	16.7	13.3	269.2	33.7	1.15	-29.4	-4.39	-12.48	0.1	±0.2	108.0	±2.1	11.9					
TN 41	H26-0160	Fonteine du Champ	28-Oct-03	-22.88194	28.86028		27.4	75.6	7.4		887	127.0	8.1	186.0	27.1	22.8	0.36	177.6	<0.11	7.1	380.3	8.2	1.30	-28.4	-4.69	-13.33	0.1	±0.2	87.4	±2.0	23.9					
TN 42	G39136	Gansvley	29-Oct-03	-22.82944	29.05139		25.7	86.8	7.37		1148	143.0	8.4	150.6	75.6	51.2	1.14	109.0	25.2	<6	528.4	39.1	1.06	-27.9	-3.97	-8.95	0.1	±0.2	96.5	±2.1	70.5					
TN 43	PN 2	Presumption	29-Oct-03	-22.76889	29.13556		25.4	75.8	7.55		849	110.4	7.8	112.0	36.8	75.5	0.56	94.5	19.3	11.9	352.3	39.9	2.24	-30.8	-4.63	-11.30	0.7	±0.2	88.3	±2.0	227.6					
TN 44	TT 7	Louisiana	29-Oct-03	-22.87250	29.07861		26.6	68.9	7.78		857	105.0	8.1	52.4	74.6	55.9	0.88	52.1	32.1	3.0	385.8	40.0	5.87	-27.2	-3.91	-7.05	0.0	±0.2	96.7	±2.1	362.1					
TN 45	YE4	Ysselmonde	29-Oct-03	-22.84000	28.94750		27.7	31.6	7.68		1212	192.0	8.0	150.7	83.4	98.4	0.42	328.6	22.0	37.7	339.3	30.6	1.45	-30.2	-4.76	-8.82	0.7	±0.2	92.2	±2.0	89.5					
TN 46	TT 6	Rhone	29-Oct-03	-22.82917	28.96917		28.5	56.3	8.43		823	108.3	8.14	100.2	49.0	65.2	0.47	109.8	14.2	12.6	345.3	29.2	1.12	-30.7	-4.76	-9.43	0.5	±0.2	92.4	±2.0	84.5					

Annex 1. Data available in the study area

RAINFALL AND GROUNDWATER ISOTOPE ATLAS

AS Talma and E van Wyk

ABSTRACT

Environmental isotopes are becoming common tools in hydrological investigations and their use in the southern African region is increasing. The main application of the isotopes ^{18}O, ^{2}H (deuterium), ^{3}H (tritium), ^{14}C (radiocarbon), ^{13}C and ^{15}N has traditionally been in groundwater studies. The availability of quicker and cheaper isotope analysis techniques has opened the way for wider applications. Other disciplines in the hydrological sphere are therefore increasingly utilising isotopic techniques in their investigations.

Rainfall remains the basic input into ground and surface waters. While data of rainfall quantities are reasonably well known, information on its isotope composition is not. That sort of information is readily available from the IAEA GNIP website[1], but only for a few stations in our region (Cape Town, Pretoria, Windhoek and Harare). Isotope laboratories in the country have been collecting and analysing rainfall samples for the last four decades. These data are part of regular networks or ancillary to specific water related investigations. The results in laboratory files are not well-known to the community that can use the data profitably.

Isotope variations in rainfall are caused by a variety of climatically related factors that are generally understood, to the extent that they can be modelled on a world-wide scale. There is, however, a need to understand these effects on a local (southern African) scale. This has, up to now, only been done on a very limited scale. Compilation of data on a regional basis should improve an understanding of the processes leading to isotope variations in rainfall and therefore also moisture movement across the sub-continent.

The process of recharge of groundwater by rain is complex and poorly understood. The aridity of the sub-continent creates different conditions from the regions where most textbooks have been written. A much smaller proportion of rainfall ends up as groundwater and the selectivity of recharge events is important to understand. Stable isotope levels in rainfall are to some extent transferred to groundwater and the relation between the two water types reveals something of the recharge process. Following this reasoning it is evident that the isotope composition of groundwater becomes a characteristic of an area within a certain time slot. During periods with different climatic regimes the properties of the recharging groundwater will change consequently.

Various aspects of these effects have been studied on smaller scales in specific projects in the course of the last four decades when environmental isotope hydrology was established in South Africa. This project aims to consolidate this information and provide more general features of isotope concentrations in rainfall and groundwater.
The aims of this project as formulated at its inception are to:

- Assemble stable isotope and tritium data of rainfall across South Africa: published and unpublished.
- Add new data sets where available.
- Assess the major factors determining the isotope composition of rainfall in the region.
- Attempt to prepare an isotope atlas of South Africa.
- Find corresponding isotope data for groundwater.

The study area was defined as southern Africa south of the Kunene and Zambesi Rivers. Rainfall isotope data were obtained from the IAEA website and from South African isotope laboratories and were captured in a database after editing and quality control. This included unpublished CSIR results (CSIR-NET) which required considerable editing. A database in Excel format was set up following the structure of the GNIP data base. The new database contains ^{18}O, D (^{2}H) and tritium (^{3}H) analyses of 3738 samples from 36 stations across the region. Some stations have 40 years of data, others only 3 years. The data are mainly monthly cumulative rainfall samples (collected as per IAEA protocol), but also daily samples and some individual storms. Monthly and annual average values of all three isotopes were calculated and are listed separately in the database. In all cases cumulative averages were calculated in order to represent the closest approach to the total isotope input at a location.

[1] *The International Atomic Energy Agency (IAEA), in collaboration with the World Meteorological Organisation (WMO), established a world-wide sampling network to collect precipitation samples for isotope analysis, Global Network of Isotopes in Precipitation (GNIP). This has been in operation since the late 1950s. The data are downloadable and are widely used.*

DWA operates the National Groundwater Quality Monitoring Project (NGQMP) whereby 400 boreholes throughout the country are regularly sampled to be able to monitor water quality changes over time scales of years. Two sets of isotope analyses were obtained from these sampling six years apart.

ACHIEVEMENTS

- The activities of this project have provided a data base of isotopes (^{18}O, deuterium and tritium) in the form of all available data in a single spreadsheet. Separate sheets with monthly and annual average values have been produced. This provides a more detailed picture of the spatial and temporal distribution of isotope variations in rainfall.
- The project has made it possible for the CSIR-NET data to be published and prevent them from being lost.
- The characteristics of isotope patterning in rainfall have been established by assessing the effects of rainfall amounts, seasonality, altitude and continentality in a semi-quantitative way.
- Local Meteoric Water Lines[2] could be established for parts of the country. More specific ones can now be readily derived from the new data base.
- The long-term patterns of ^{18}O and deuterium rainfalls did not show any discernible climatic change effect over the period 1960-2000.
- The spatial distribution of the stable isotope composition of rainfall throughout the country could be established
- Temporal and spatial distributions of radio-active tritium in rainwater could be established across the region. These indicate the tritium rise to 1965 from nuclear weapon testing prior to that time, and the gradual decline of levels back to the original base level of the present time. The data can be used as input to groundwater flow models.
- An initial spatial distribution of the stable isotope composition of groundwater could be established. A start was made to evaluate the relation between the isotope composition of rainfall and groundwater, across the country. A case study by Dr E van Wyk to that effect has been included in the full report on CD.

INTRODUCTION

A wealth of environmental isotope and chemical data in rainwater and groundwater countrywide has been accumulated but data reduction and interpretation for much of this has not happened. In part this due to lack of capacity in the organisations involved, but also because the data were collected for limited objectives. The proposed study aims to analyse the existing data sets in terms of recharge, groundwater flow and mineralisation processes and to seek the various factors influencing these: climate (change), physiography, geology etc., The study area will be southern Africa which would include Botswana and Namibia provided enough data can be obtained.

AIMS OF THE PROJECT

The aims of this sub-project as formulated to the Water Research Commission are:

- Assemble rainfall stable isotope and tritium data across South Africa: published and unpublished.
- Add new data sets where available.
- Assess the major factors determining the isotope composition of rainfall in the region.
- Attempt to prepare isotope atlas of South Africa.
- Find corresponding isotope data for groundwater.

RAINFALL ISOTOPE DATA

Data sources

The data used in the rainfall isotope data compilation come from various sources:

- The IAEA established a Global Network of Isotope Precipitation (GNIP) sampling stations in 1960 in order to collect monthly cumulative rainfall samples for ^{18}O, D and tritium analysis (IAEA 2012a). Samples are collected by the national weather services in each country and, where possible, analysed by laboratories in the host countries. Relevant data for this project were downloaded from the agency website (IAEA 2006) and were supplemented by additional data obtained directly from IAEA and iThemba LABS (the present local laboratory).
- In addition the CSIR managed a similar sampling network (CSIR-NET) between 1979 and 1985 throughout South Africa and Namibia. No data have been published of this network.
- Additional monthly rainfall samples have been collected from various CSIR projects over the years (Vogel & van Urk 1975a, Vogel et al 1982, Meyer et al 2001).

[2] *Local Meteoric Water Lines are mathematical relations between the stable isotope ratios of hydrogen and oxygen. They are essential tools for isotope hydrologists to asses localised water types.*

- The University of Cape Town maintains regular sampling of rainfall on their campus (Harris et al., 2010).
- Daily rainfall data from the GRES2 project in Botswana (Beekman et al., 1998) were obtained from Dr Hans Beekman.

Additional rainfall isotope data have been generated by the South African Department of Water Affairs and reported by van Wyk (2010). These were collected with specially constructed cumulative samplers. The collection periods of these data varied from days to a few months. Interpretation of the DWA data has not been completed yet and publications are pending. Passing reference is made to these data in this chapter. Rainfall isotope samples have been obtained by the University of KwaZulu-Natal at Weatherley test site in the Eastern Cape between 2002 and 2010 (Lorentz et al 2008). These data are not included in this compilation.

RAINFALL ISOTOPE DATABASE

The scope of this project was defined as the southern African sub-continent south of the Kunene and Zambezi rivers. This includes South Africa, Namibia, Botswana, Lesotho and Zimbabwe. No data from Mozambique and Swaziland are available to the authors. Data from the GNIP stations on Marion and Gough islands have been included in the database.

A database in Excel format was set up following the structure of the IAEA GNIP data base (IAEA 2006). The database contains ^{18}O, D (^{2}H) and tritium (^{3}H) analyses of 3738 samples from 36 stations across the region (Table 1). These are mainly monthly cumulative rainfall samples (collected as per IAEA protocol), but also daily samples and some storms from Lobatse, Pretoria and Cape Town.

GNIP data were downloaded from the agency's website (IAEA 2006). CSIR-NET data were obtained from historical laboratory records. Considerable effort was required to eliminate duplication and to correctly identify sampling sites. Since much of the CSIR data had not been published earlier, it was necessary, in some cases, to go back to laboratory records as far back as 40 years ago to fill gaps and correct errors. For most samples the corresponding rainfall data was available. Where this was not the case, data from the compilation of Lynch (2003) using the Daily Rainfall Utility of Kunz (2012) were used.

Monthly and annual average values of all three isotopes were calculated and listed in the database. In all cases cumulative averages were calculated in order to represent the closest approach to the total isotope input at a location.

Table 1: Listing of rainfall data available for periods more than 2 years. Frequency of sampling(F) indicated as monthly (m), daily (d) and storm(s)

Station	F	SAWS ID	WMO ID	O	D	T	Data Source*	Period	Lat S	Lon E	Elev. m
Bloemfontein, airport	m	0261516		√	√	√	CSIR-NET	1970-80	29.10	26.30	1351
Cape Town, airport	m		6881600	√	√	√	IAEA-GNIP	1961-2007	33.97	18.60	44
Cape Town, UCT	mds			√	√	-	UCT	1995-2008	33.96	18.46	115
Central Kalahari, Botswana	d			√	√	-	GRES2	1994-95	24.06	25.26	1163
Charters Creek, KZN	m	0339732		√	√	-	CSIR	1970-73	28.20	32.42	23
Durban, old airport	m	0240808		√	√	√	CSIR-NET	1970-80	29.97	30.94	8
Estcourt, DWA	m	0268631		√	√	√	CSIR-NET	1970-80	29.05	29.85	1184
Gough Island	m	0000681	6890600	√	√	√	IAEA-GNIP	1960-2001	40.35	9.88W	54
Grootfontein, Namibia	m	1010186		√	-	√	CSIR-NET	1970-80	19.69	18.12	1405
Harare, Zimbabwe	m		6777400	√	√	√	CSIR-NET	1970-80	17.83	31.02	1471
Harare, Zimbabwe	m		6777400	√	√	√	IAEA-GNIP	1960-2003	17.83	31.02	1471
Lister point, KZN	m			√	√	-	CSIR	1970-73	27.97	32.38	9
Lobatse, Botswana	d			√	√	-	GRES2	1991-96	25.21	25.68	1207
Mafikeng, North West	m	0508232		√	-	-	CSIR-NET	1970-72	25.87	25.63	1277
Makatini Agric, KZN	m	0411323		√	√	-	CSIR	1989-92	27.38	32.18	73
Malwelwe, Botswana	d			√	√	-	GRES2	1993-95	24.08	25.03	1093
Manzengwenya, KZN	m	0412466		√	√	-	CSIR	1989-92	27.27	32.77	20
Marion Island	m	0000653	6899400	√	√	√	IAEA-GNIP	1961-2001	46.88	37.87	22
Mbazwana, KZN	m	0412180		√	√	-	CSIR	1989-92	27.50	32.60	80
Nelspruit, Agric	m	0555837		√	√	-	CSIR-NET	1970-80	25.45	30.97	660
Okavango	m			√	√	-	CSIR	1996-97			
Oxbow, Lesotho	m	0298193		√	-	-	CSIR-NET	1970-80	28.72	28.62	2591
Phelendaba, KZN	m	0412096		√	√	-	CSIR	1989-92	27.10	32.57	77
Polokwane, WB, Limpopo	m	0677802		√	-	-	CSIR-NET	1970-80	23.87	29.45	1230
Pretoria, Brooklyn	md			√	√	√	CSIR-NET	1967-72	25.77	28.22	1367
Pretoria, CSIR	md			√	√	-	CSIR-NET	1972-89	25.75	28.28	1377
Pretoria Forum	m		6826200	√	√	√	IAEA-GNIP	1958-2001	25.73	28.18	1330
Pretoria, Lynnwood Rd	m		6826201	√	√	√	IAEA-GNIP	1971-72	25.75	28.23	1369
Pretoria, Menlo Park	m			√	-	-	CSIR-NET	1996-2004	25.77	28.26	1431
Setshe, Botswana	d			√	√	-	GRES2	1995-96	23.98	25.25	1147

Station	F	SAWS ID	WMO ID	O	D	T	Data Source*	Period	Lat S	Lon E	Elev. m
Sihangwana (Tembe), KZN	m	0411723		√	√	-	CSIR	1989-92	27.05	32.42	69
Sodwana Bay, KZN	m	0376302		√	√	-	CSIR	1989-92	27.53	32.68	5
Stampriet (Rohrbeck), Namibia	m			√	-	-	CSIR	1982-86	24.22	18.41	1214
Taaiboschgroet (Greenfields), Limpopo	d			√	√	√	IAEA-RAF	1999-2005	22.85	28.90	812
Windhoek, CSIR	m			√	√	-	CSIR-NET	1970-72	22.53	17.08	1628
Windhoek, WB	m	0740154	6811000	√	√	√	CSIR-NET	1970-80	22.57	17.10	1728
Windhoek, WB	m	0740154	6811000	√	√	√	IAEA-GNIP	1961-2001	22.57	17.10	1728

**IAEA-GNIP data were analysed, at various times, by labs in Copenhagen, Vienna, Stockholm, Johannesburg and Pretoria.*

SAMPLING METHODS

The sampling method used for all of the monthly samples has remained the same over the years (IAEA 2012b). A standard rainfall gauge is used. This has a funnel to direct the rainfall into a (somewhat) closed off vessel. Every morning when the daily rainfall is recorded, the collecting vessel is emptied in a tightly closed bottle. At the end of a calendar month small quantity of water from the bottle is taken for analysis. The bottle is then emptied to collect the next month's sample. In this way a monthly cumulative sample is obtained.

In some project related sample collections, real cumulative sample collectors were used to save on manpower. The rainwater is then collected in a long tubular collector for periods of months. To prevent evaporation of the sample various techniques are used: ball valves, long flow tubes, oil coverings, etc. (Weaver and Talma 2005).

Analytical Laboratories

For the first decade of IAEA-GNIP the stable isotope analyses were done, on behalf of the IAEA, in the Copenhagen isotope laboratory (W. Dansgaard) and tritium at the University of Stockholm. Since 1968 analyses for GNIP in our region were done locally. Most of the GNIP samples were analysed in the Johannesburg laboratory (first as Nuclear Physics Research Unit, then the Schonland Institute, now iThemba LABS (NRF)). At times the Pretoria CSIR isotope laboratory (Natural Isotopes division (NPRL), Quaternary Dating Research Unit (Ematek, Environmentek, Natural Resources and the Environment)) undertook some of the isotope analyses of GNIP. Other samples were analysed in the IAEA laboratory in Vienna. CSIR-NET samples were analysed at CSIR. UCT rainfall samples were analysed by UCT. The GRES2 samples were analysed at the University of Groningen, Netherlands (CIO).

During the 45 years covered by these activities, analytical techniques changes dramatically. No attempt has been made to note the actual methods used or check on calibration of the methods.

Local Meteoric Water Lines

Fig. 1 shows the D-^{18}O plots of all the rainfall samples available. As a first cut the stations have been classified geographically as:

- Marine: Gough and Marion islands.
- Coastal: Cape Town and the stations from Kwazulu-Natal.
- Inland: All other stations within the borders of South Africa and Lesotho.
- Arid: Stations from Zimbabwe, Botswana and Namibia.

The deuterium and ^{18}O contents for all samples are well correlated (Fig. 1). Correlation coefficients (R^2) for the four groups vary between 0.72 and 0.93. The marine samples (Marion and Gough islands) are fairly close to the Global Meteoric Water Line ($\delta D = 8\delta^{18}O + 10$ ‰), which accords with the definition of GMWL (Dansgaard 1964).

The other samples are situated somewhat above the GMWL. The deviation from the GMWL is better tested by calculating the deuterium excess: the difference between the sample plot and the GMWL: $D_{xs} = \delta D - 8\delta^{18}O$.

The frequency distribution of D_{xs} for the four station categories shows a gradual shift from +10 for marine samples to higher D_{xs} inland and a wider distribution of the arid stations (Fig. 2). The marine samples are quite close to GMWL while the other samples are located at D_{xs} values of 5 to 25 ‰, with an average probably around 15 ‰. This shows the coastal and inland samples peaking around 14 to 16 ‰ while the arid zone samples show a much wider range. The latter indicate the influence of evaporation on the isotope values. Another way to look at this is to plot D_{xs} against ^{18}O (Fig. 3). This shows the evaporation enrichment in the fact that more lower D_{xs} values occur at higher ^{18}O.

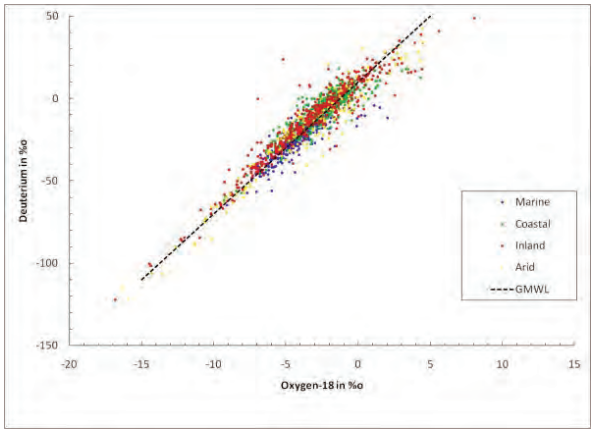

Figure 1: Deuterium ^{18}O plot of all the rainfall samples available. Sample stations have been classified according to locality.

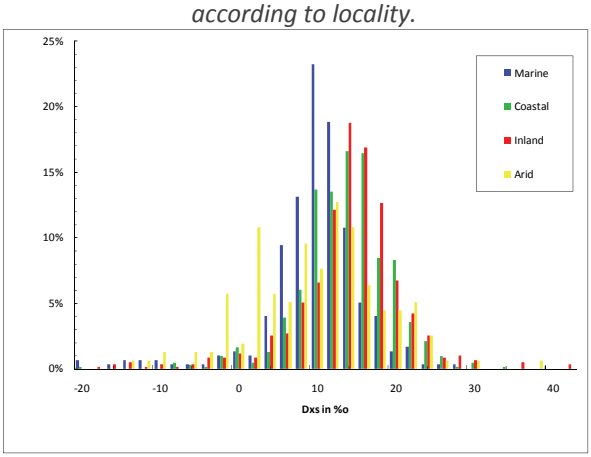

Figure 2: Frequency distribution of the values of Dxs obtained from all the rainfall samples. Classification of the sources was done as above

.

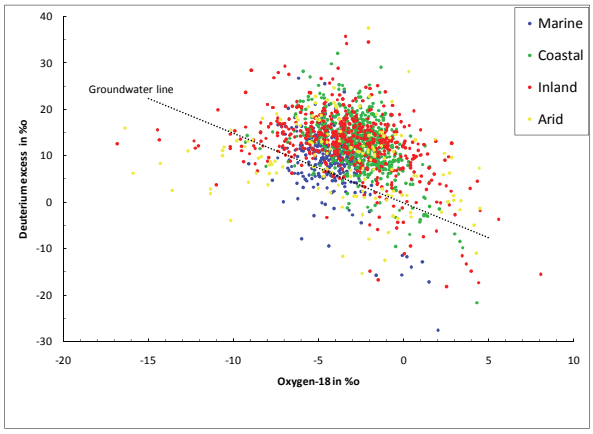

Figure 3: Plot of D_{xs} (deuterium excess) against ^{18}O of the rainfall samples. Sample classification was done as above. The dashed line shows the regression relation found for the sample plot of the groundwater samples.

RAINFALL STABLE ISOTOPE AVERAGES

The database assembled for, and presented with, this report contains all the samples for which isotope data are available. In addition various average values were calculated to provide trends and patterns.

Monthly averages

Samples collected in the standard way described above, reflect the monthly mean of daily precipitation weighted by the rainfall of that day. For a few stations, Brooklyn (Pretoria) and the GRES2 stations in Botswana, only daily rainfall values were available and monthly means were calculated for each month. These monthly means were only accepted, and listed, if they reflect more than 66% of the rainfall of that month.

Annual averages

Annual averages were similarly calculated. These are the weighted averages for each year. The year chosen was the hydrological year from October to September. The year was identified by the last year; i.e. the year '1991' in the yearly mean file represents the period from October 1990 to September 1991. In each case the calculated annual averages are reported together with their representativity. Representativity is expressed as the percentage of that year's rain that was included in the calculation. In some of the sources used, rainfall data was available for the months without samples. In other cases the rainfall for the missing months were found in the daily rainfall database of Lynch (2003) using the Daily Rainfall Utility of Kunz (2012). Since not all three isotopes were analysed on each sample, the representativity for the same year frequently differs for each isotope.

Long-term averages and trends

A long-term average of isotope values at a specific location is desirable. From a climatic point of view it should represent general features of the location. In many parts of the world the long-term mean of the stable isotope composition equals that of groundwater. The early work in southern Africa (Ehhalt et al 1963; Schiegl 1970; Vogel & van Urk 1975b) has shown that this is not the case here; certainly not in the inland areas. This will be discussed later.

For each site, long-term means have been calculated (Table 2). These numbers are the weighted averages for those years where the annual averages represent more than 66% of the year's rainfall. The quality of these averages is quite variable. ^{18}O has been measured much more and therefore is a more reliable average. Differences at nearby sites (as related elsewhere in this report) can be due to local variations and practices or to different sampling periods.

There is no discernible long-term trend in the ^{18}O record of the various Pretoria samples (Fig. 4). The least square correlation with time shows a slope of -0.007 ± 0.010 ‰ per year. That amounts to a total change of-0.34 ± 0.44 ‰ over the 45 year period of record. It is not clear why the period 1968 to 1980 shows a few very low $\delta^{18}O$ values (below -10 ‰) which are absent in any of the other years. In their compilation of stable isotope data of Cape Town (UCT) Harris et al. (2010) could not see a change in stable isotope content of rain for the period 1995 to 2008. Any climate change effect is therefore either not present or will have to be sought for from these data by more subtle means.

PLACE	SITE	SOURCE	DEUTERIUM		OXYGEN-18	
			δD ‰	years	$\delta^{18}O$ ‰	years
BLOEMFONTEIN	AIRPORT	CSIR-NET	-15	2	-4.1	7
CAPE TOWN	AIRPORT	GNIP	-14	17	-3.6	27
CAPE TOWN	UCT	UCT	-13	11	-3.3	12
CHARTERS CREEK, KZN		CSIR	-19	2	-4.0	2
DURBAN	AIRPORT (LBOTHA)	CSIR-NET	-8	3	-2.8	10
ESTCOURT	DWA	CSIR-NET	-13	3	-3.5	8
GOUGH ISLAND		GNIP	-22	15	-3.8	30
GROOTFONTEIN, NAMIBIA	WB	CSIR-NET			-7.2	10
HARARE	WB	GNIP	-30	30	-5.8	37
HARARE	WB	CSIR-NET	-32	6	-6.6	10
LISTER POINT, KZN		CSIR	-6	3	-2.4	3
LOBATSE, BOTSWANA	DGS	GRES	-13	4	-3.0	4
MAKATINI, KZN	AGRICULTURE	CSIR	-10	3	-2.5	3
MANZENGWENYA, KZN	FORESTRY	CSIR	-17	3	-3.4	3
MARION ISLAND		GNIP	-30	19	-4.6	33
MBAZWANE, KZN	FORESTRY	CSIR	-16	3	-3.5	3
NELSPRUIT	AGRIC RES	CSIR-NET			-3.2	6
OXBOW, LESOTHO		CSIR-NET			-5.3	37
PHELANDABA, KZN	IDC	CSIR	-16	3	-3.3	3
POLOKWANE		CSIR-NET			-3.9	9
PRETORIA	BROOKLYN	CSIR-NET	-23	4	-4.6	4
PRETORIA	CSIR	CSIR-NET	-3		-4.6	15
PRETORIA	FORUM	GNIP	-17	15	-3.6	24
PRETORIA	MENLO PARK	CSIR-NET	-16	9	-4.0	9
SIHANGWANA, KZN	TEMBE PARK HQ	CSIR	-12	3	-2.9	3
SODWANA BAY, KZN	PARK OFFICE	CSIR	-16	2	-3.4	2
STAMPRIET, NAMIBIA	ROHRBECK	CSIR			-0.8	2
WINDHOEK, NAMIBIA	WB	GNIP	-28	17	-5.4	28

Table 2: Long-term mean values of 18O and deuterium for all stations. The years over which the means have been calculated are shown.

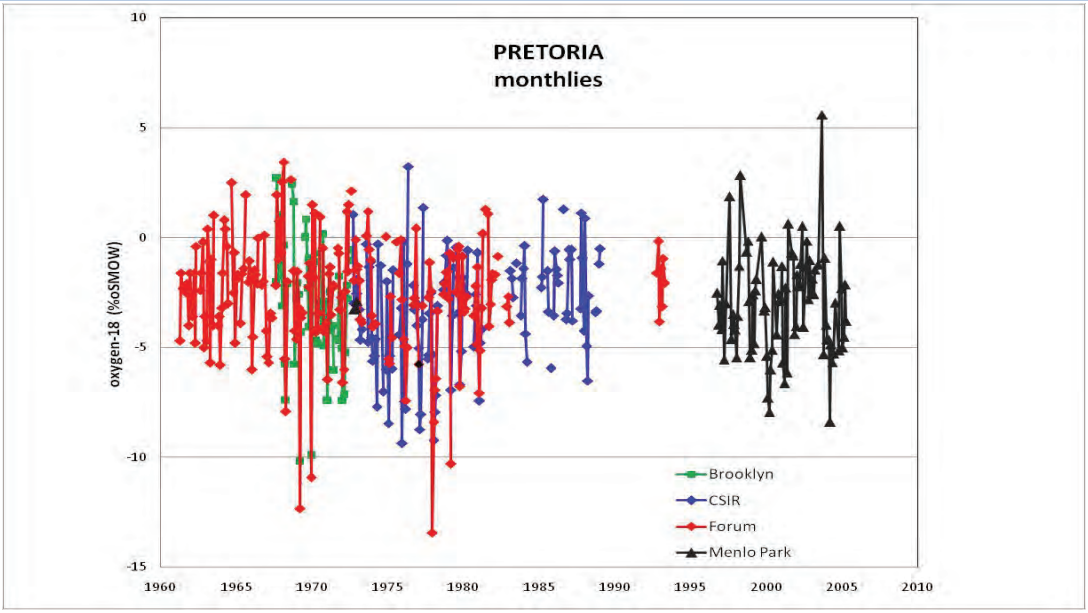

Figure 4: ^{18}Oxygen trend of monthly samples from four sites in Pretoria since 1958.

RAINFALL STABLE ISOTOPE EFFECTS

Isotope hydrology texts usually quote various factors that influence the isotope composition of rainfall at any specific location (e.g. Clark & Fritz 1997; Ingraham 1998; Gat 2001). The variations are all based on the rain-out concept: cloud masses lose their moisture through rain and the remaining cloud depletes in the heavy isotope. These concepts originate from temperate environments where the effects are frequently quite pronounced. The question is to what extent these various effects are visible in the rainfall isotope pattern in southern Africa. The effects will be demonstrated by ^{18}O since that is the isotope for which most data is available in the region.

Amount effect

The local amount effect of ^{18}O in rainfall is demonstrated by plots of δ^{18}O against monthly rainfall (monthly). Fig. 5 shows the amount effect for three GNIP stations; representative of the three Continental types defined above. In all three there is a trend towards higher ^{18}O values for the smaller monthly rainfalls. In arid Windhoek the δ^{18}O scatter is much higher than in Cape Town. Larger variations can occur from month to month and the data indicate that lower ^{18}O values are not always associated with high rainfall.

Partly this may be caused by the fact that these data sets use monthly samples. The clearest indication of an amount effect was shown in northern KZN (Fig. 6) where three extreme rainfall years (1990-1992) provided a very clear mean ^{18}O depletion during higher rainfall years in all six of the stations that were sampled (Meyer et al., 2001).

Seasonal effect

The seasonal ^{18}O effect in rain is demonstrated for the same three GNIP stations (Fig. 7). This shows the isotope values parallel to the amount effect: lower ^{18}O in the rainy season and high in the dry season. The pattern for Cape Town is different because it is the only locality in this data set in the winter rainfall area. The more arid the site, the larger the seasonal ^{18}O variation. Note that for some months not sufficient rainfall data are even available for a meaningful average.

Altitude effect

There are no clear data sets among the present compilation to demonstrate an altitude effect in a simple way. The stations are too widely spread and the localities with stations close to each other (Cape Town, Pretoria, and northern KZN) show very little relief. A major elevation difference happens in the case of Oxbow in Lesotho (Table 3) for which the only reference values could be Bloemfontein (240 km west) and Estcourt (130 km east). The elevation difference between Estcourt and Oxbow produces an 18O altitude effect of - 0.13‰/100m, which can be compared to the - 0.1 to -0.6 ‰/100m found elsewhere in the world (Vogel et al 1975, Gat 2001). Midgley & Scott (1994) reported 18O rainfall data from a single month's sampling over an altitude difference of 825m in the

Jonkershoek valley (near Cape Town). An altitude effect of -0.33‰/100m could be calculated. On the other hand, in the Agter-Witzenberg valley, 100 km north-east of Cape Town, Weaver et al. (1999) could not detect any 18O difference in rainfall over an altitude difference of 300m. This was attributed to the valley being in a rain-shadow (from the sea) and is also known to occur in some valleys in Switzerland (Siegenthaler & Oeschger 1980). Altitude effects are therefore very site-specific and must be used with caution.

Station	Elevation(m)	$\delta^{18}O$ (‰SMOW) long-term mean
Oxbow, Lesotho	2591	-5.3
Estcourt, KZN	1184	-3.5
Bloemfontein, FS	1351	-4.1

Table 3. Comparison of δ18O in rainfall with altitude

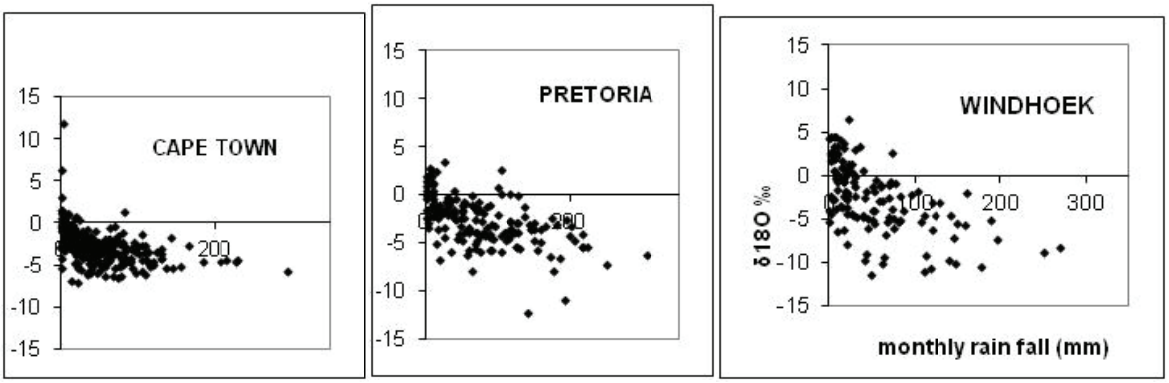

Figure 5: Plots of monthly $\delta^{18}O$ in rainfall against the monthly rainfall of three IAEA-GNIP stations. These stations represent the typical coastal, inland and arid classification used in other figures.

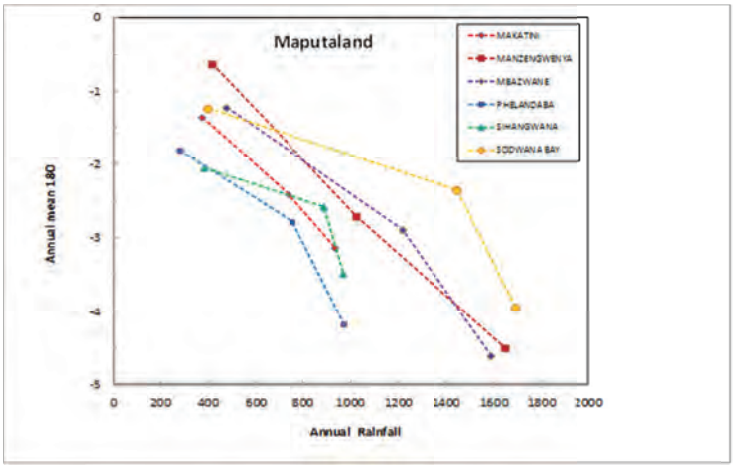

Figure 6: Relation between annual rainfall amount and annual 18O in rain for six stations over three years in northern KZN (Meyer et al., 2001).

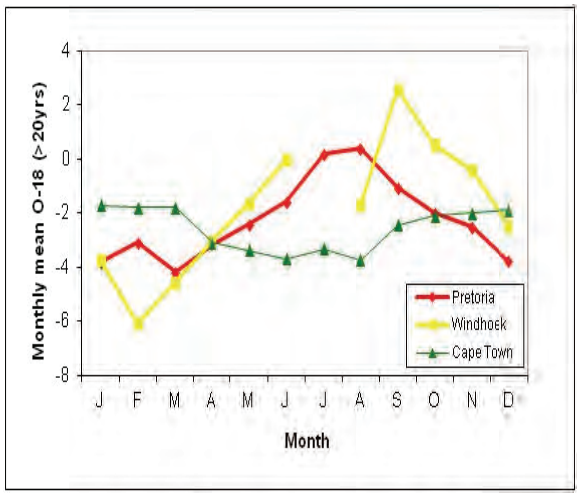

Figure 7: Seasonal plots of $\delta^{18}O$ in rainfall of three IAEA-GNIP stations. Each point represents the mean of the monthly $\delta^{18}O$ values available for that month. The stations represent the typical coastal, inland and arid classification used in other figures.

.

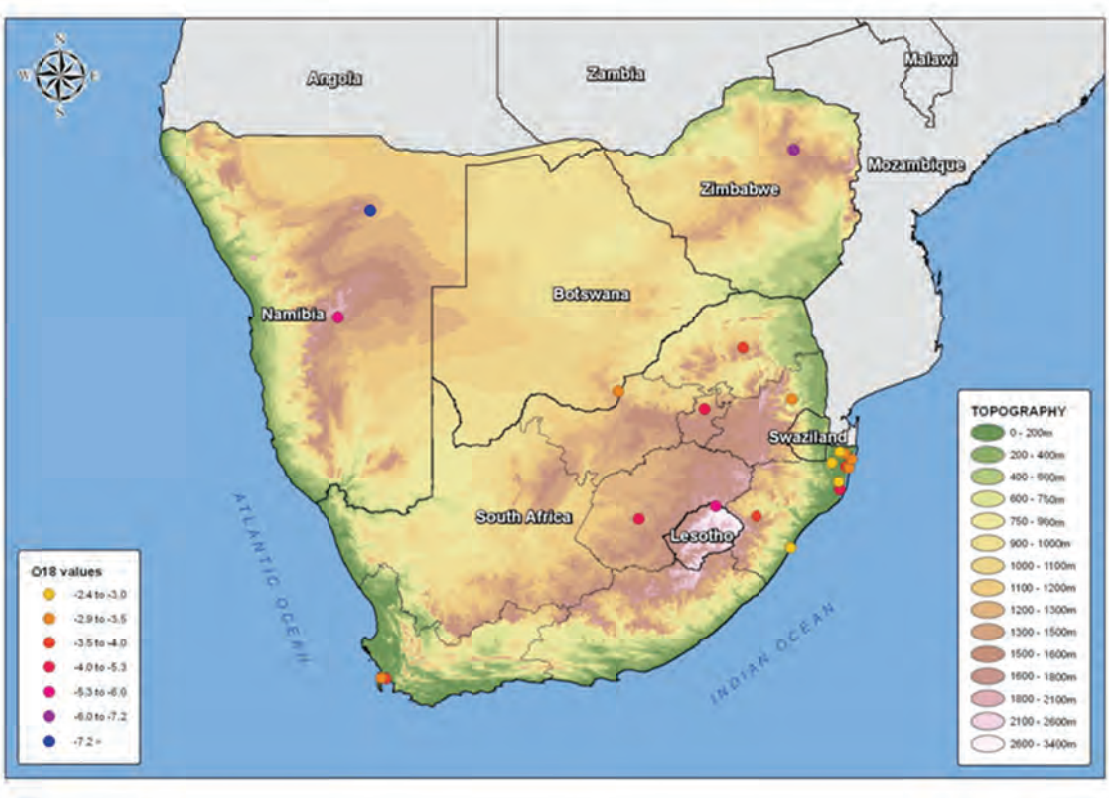

Figure 8: Distribution of mean rainfall 18O data across the sub-continent.

TRITIUM IN RAINFALL

This section lists the available tritium data from the sub-continent. The analysis of tritium in rainfall was the main driving force for the establishment of the IAEA GNIP programme in the late 1950s. There was fear that the world-wide spread of radioactivity from nuclear weapon tests could endanger human life over the long-term. Nowadays the tritium levels in the southern hemisphere have returned to the pre-bomb levels and it is the stable isotope compositions of water that have proved to be useful for understanding of the world's climate and hydrology. Tritium analysis has therefore become the Cinderella of GNIP.

Data availability

Table 1 lists the availability of tritium analyses as they have been captured in the project data base. The GNIP data base has been supplemented by further data from the CSIR-NET for a period of less than 10 years. The IAEA-RAF project at Taaiboschgroet, Limpopo, (see elsewhere in this report) has also generated tritium rainfall data.

Tritium time series

The main features of tritium levels in rainfall during the last 60 years in the southern hemisphere are the effects of nuclear weapon testing since 1954. These are a rise during the 1950s to maximum levels around 1965 and thereafter a decline to pre-bomb values of 2-3 TU (Fig. 9). The comparison of tritium values of with all the sites in the region shows some distinct features

- The coastal sites (Cape Town and Durban) have lower tritium (even below the NZ reference) but cross over after 1980
- The inland stations Windhoek, Grootfontein and Pretoria peaked the highest of all stations
- Pretoria started the bomb-peak rise two years before the other local sites
- The bomb peak of Harare followed close to that of the coastal sites, but flattened off with Taaiboschgroet to the present-day pre-bomb values of 2-3 TU
- This compilation of data can be used to derive tritium input curves for hydrological purposes.

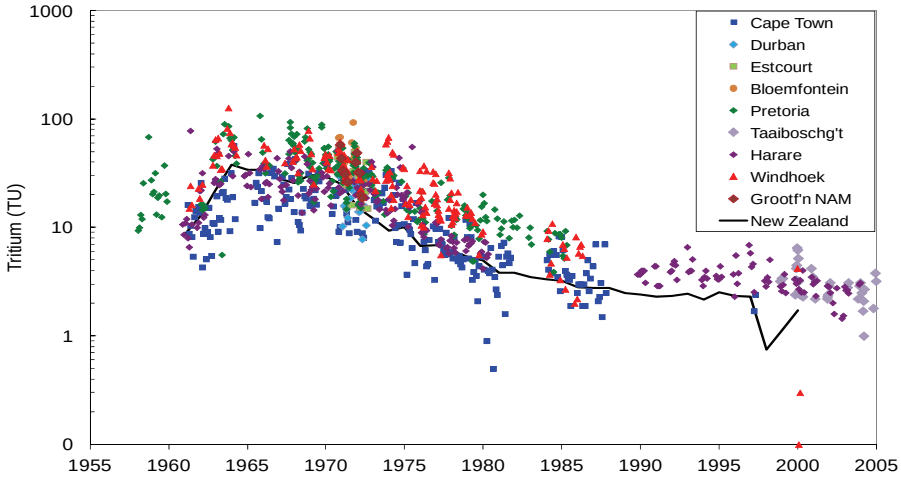

Figure 9: Time series of tritium analyses from the sub-continent since 1958. The comparison line is from Kaitoke, a marine site in New Zealand (IAEA 2011)

Representativeness of Data

Given the variability of rainfall in the area, the question arises as to how representative the data from a single site are to the local area or region. There certainly are various effects at work which can produce local isotope variations and workers in the more endowed countries are rapidly acquiring sufficient data to unravel these effects and produce generalized isotope distribution maps (Bowen & Revenaugh, 2003). For the purposes of this report, comparisons will be made between closely located sampling stations in Pretoria and Cape Town.

Pretoria sampling stations

Pretoria has five sites from which data have been obtained from time to time during the past five decades (Table 1).

- Lynnwood Road was the headquarters of the SA Weather Service until 1963. The building now houses the Communication Pathology department

of the University of Pretoria. SAWS records still refer to this station as "Pretoria WB".

- Forum building in Schubart Street in the Pretoria city centre was the next headquarters of the SA Weather Service and the location where samples for the IAEA network were collected.
- Brooklyn was an unofficial site at a residence (JC Vogel: 547 Sydney St).
- Menlo Park was another site at a residence (JC Vogel: 477 Kay Ave). The Menlo Park site was also used to collect samples for DWA and is referred to as 'Lynwood RF' by van Wyk (2010).
- CSIR was a rain gauge on top of building 4 on the CSIR campus in the East of Pretoria (old NPRL building).

Stable Isotope Comparison

The D - ^{18}O plot of all the Pretoria samples (Fig. 10) shows data superimposed on each other with no significant shifts between the various sampling sites (which are all within a 5 km radius from each other).
The low values all lie parallel but above the Global Meteoric Water Line, and have D_{xs} about +16‰. The higher values lie on an evaporation line with slope 6.68. This suggests evaporation effects that are not found in coastal areas.

The ^{18}O relation to monthly rainfall (Fig. 11) for the different sites in Pretoria is very similar to that found in other places all over the world. The lower ^{18}O content for greater monthly rainfalls seems to be a general effect with large scatter. Nevertheless, the five months with the highest rainfall do not show the lowest ^{18}O content.

The ^{18}O trend over 45 years (Figs. 4 and 12) shows large variations, basically determined by the amount effect. Overall the Forum ^{18}O data tend to be somewhat higher than those at CSIR. This is due to some samples within a year that have higher ^{18}O content.

Tritium comparison

Tritium comparisons have also been made. Fig. 13 shows a comparison between the data from three sites in the Pretoria area. The strong seasonality (high September values, decreasing within months) is quite evident. Comparisons of the data from the three sites are quite good and therefore any of them can be considered representative of the general area.

Fig. 14 shows the complete time series of rainfall tritium available for the Pretoria region. The data (of which the first decade originates from the Stockholm tritium laboratory) show the development of the bomb-tritium peak between 1955 and 1965 and its gradual recession in the following two decades.

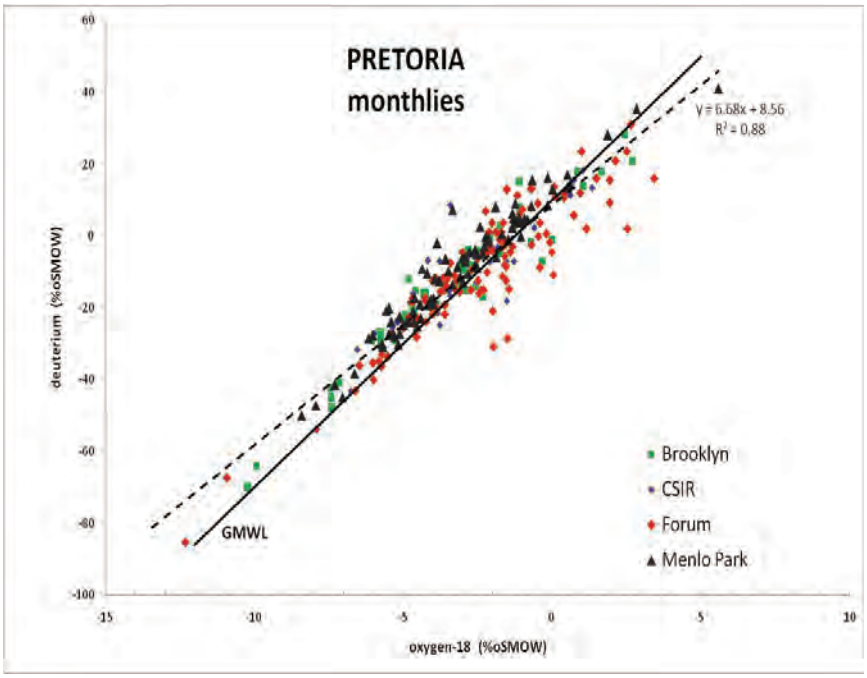

Figure 10: Deuterium-^{18}Oxygen plot of all the monthly rainfall data from four sites in Pretoria since 1958.

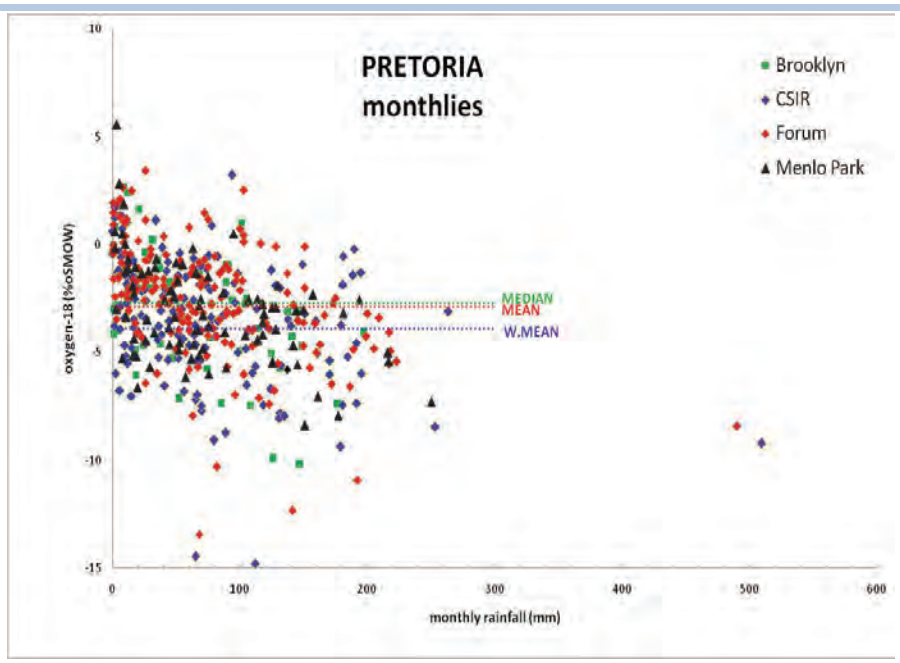

Figure 11: [18]Oxygen plot against monthly rainfall of all the data from four sites in Pretoria since 1958. Long-term mean, median and weighted (by precipitation) mean are indicated.

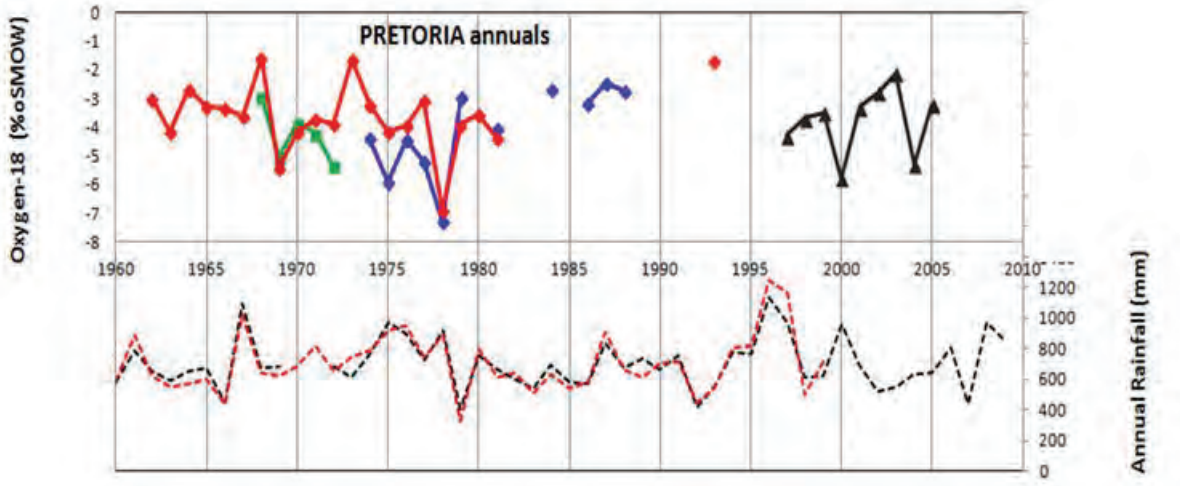

Figure 12: [18]Oxygen trend of annual mean values of data from four sites in Pretoria. The dashed line indicates total annual rainfalls of the same stations.

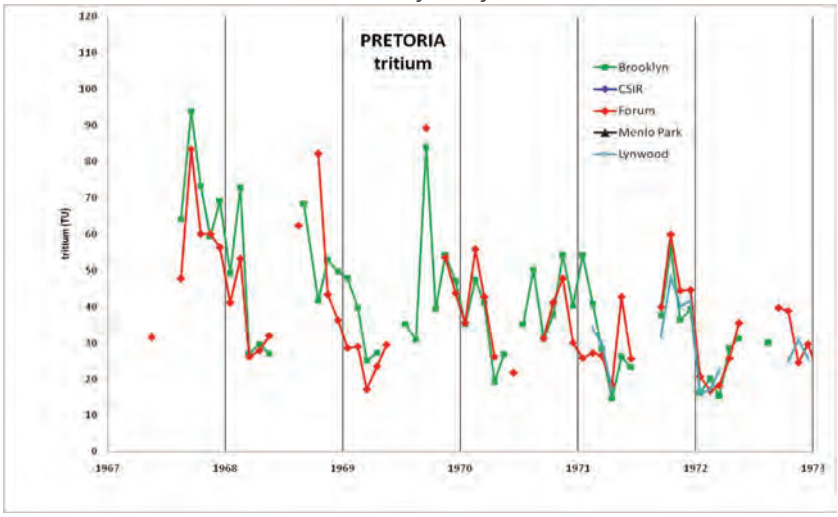

Figure 13: Rainfall tritium trends for 1965-1975 indicating the variations within three sites in Pretoria. The seasonal effect: high in September and falling off sharply afterwards, is quite evident.

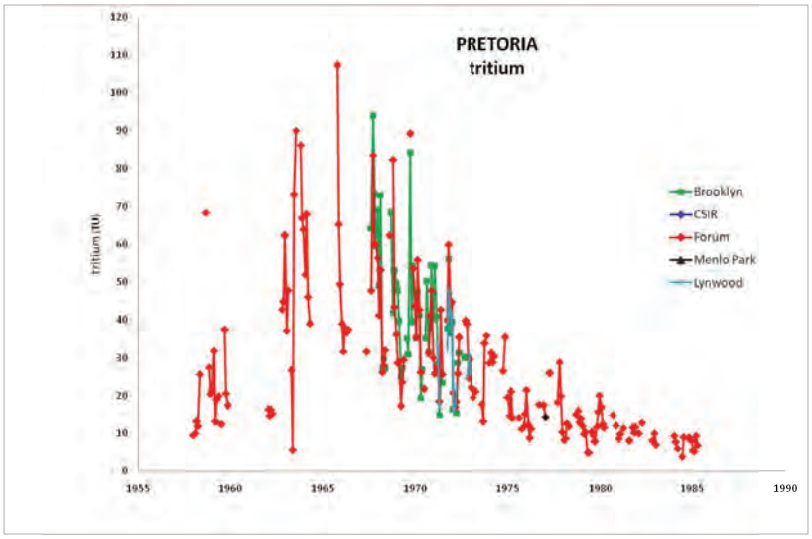

Figure 14: Rainfall tritium trend for three sites in Pretoria since 1960.

Cape Town Stable Isotope comparison

Cape Town airport has been sampled since the inception of the IAEA-GNIP programme in 1960. Since 1995 the Department of Geology at UCT have sampled rainfall for ^{18}O and D at the university campus in Rondebosch (Diamond and Harris, 1997; Harris et al., 2010). The overlap between these time series gives some indication of consistency between stations (Fig. 15). Overall, the variations, both monthly and annually indicate some correspondence and some differences. It must be stated that in the Cape Town case, even though the two stations are only 12 km apart, their situations are different. The airport is located on the Cape Flats and has a mean annual precipitation of 513mm (IAEA, 1992) while the university site against Table Mountain has MAP between 1000 and 1700mm (Harris et al., 2010).

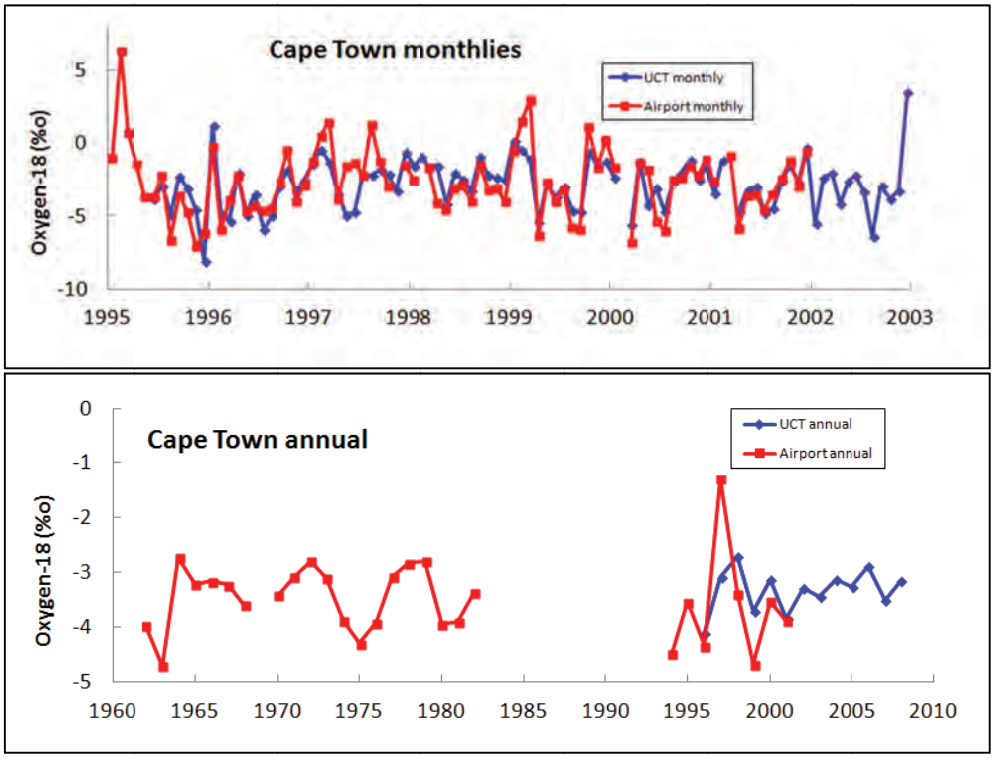

Figure 15: ^{18}O trend for two Cape Town sampling stations for comparison on monthly and annual National Groundwater Quality Monitoring Project data

GROUNDWATER

This programme, run by DWA since 1993, involves regular monitoring and chemical analyses of a set of 400 boreholes across the country (DWA 2010). During one of these runs (2006/7), analyses of ^{18}O and D were done at iThemba LABS, Johannesburg, on 281 samples from this sample set. This data set represents a sample distribution of groundwater ^{18}O and D content from all over the country and forms the basis of the groundwater atlas.

The spread of isotope concentrations ($\delta^{18}O$ and δD) is large: all but the highest are slightly above the Global Meteoric Water Line (GMWL) (Fig. 16). The very lowest $\delta^{18}O$ values (< -6‰ SMOW) are from the Northern Cape. Some of the highest ($\delta^{18}O$ > -1‰) are derived from irrigated areas where evaporation enrichment is likely to have occurred, which shows up as preferential ^{18}O enrichment of the sampled groundwater. 89% of the samples have D_{xs} > +10‰ (Fig. 17).

The data from the survey of 20067 have been plotted and kriged in order to obtain trends across the country. Fig. 18 shows the patterns obtained by Adam West from this data set. This is the first step in an exercise to map isotope variations across the sub-continent similar to his earlier work on South Africa tap water (West et al., 2011). The maps show:

- Low $\delta^{18}O$ and δD values along the Cape Folded belt indicative of the altitude of rainfall,
- Low $\delta^{18}O$ and δD values in the North Cape indicative of selective recharge to groundwater,
- High $\delta^{18}O$ and δD values along the west coast and northern KwaZulu-Natal where recharge is simply through sand with no selectivity,
- Lower of δD_{xs} in the inland corresponding to increasing evaporation rates

A second isotope sampling round by DWA has been completed (May-September 2012). The data will supplement the earlier 2006 survey and will give information of isotopic shifts that may have occurred in the course of six years.

Groundwater-rainfall relations

In the temperate climates it is common that the stable isotope composition of groundwater reflects the long-term mean composition of rainfall. In fact, soil profiles show how seasonal isotope variations smooth out vertically to produce the mean value of deeper groundwater (Clark & Fritz 1997). In more arid regions this is certainly not the case (Schiegl 1970; Vogel & van Urk 1975)
. Particularly in the interior of the country large differences between the stable isotope composition of rainfall (mean) and groundwater have been observed. The assemblage of rainfall data now available offers the opportunity to quantify this groundwater-rainfall interaction.

The explanation for the groundwater isotope shift lies in the evaporation of the small (generally isotopically higher) rainfall events (Obakeng, 2007). A generalised model based on monthly rainfall data can then be formulated that in every month only rainfall quantities in excess of a certain threshold value will recharge. The isotope composition of groundwater will then reflect the weighted mean value of all water contribution exceeding a threshold. This has been calculated for three very different rainfall stations (Fig. 19). In the case of Cape Town, no threshold is required to reach the commonly found average vale of $\delta^{18}O$= -3.5 ‰ found in the Cape Flats (Talma, unpublished measurements). In the case of Pretoria a threshold of 60mm and for Windhoek a threshold of 90mm is required to match the isotope composition of simulated recharge with local groundwater. To what extent these threshold numbers can be translated into recharge amounts (or the other way round) remains to be seen.

A much more detailed investigation of recharge processes using isotopes is presented in the case study by E van Wyk, attached to this chapter.

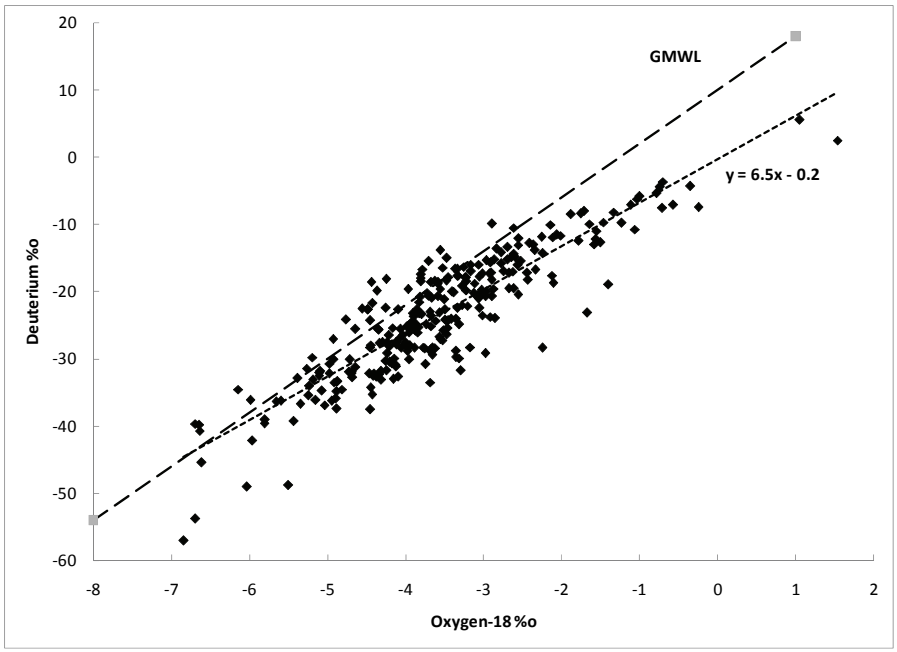

Figure 16: Deuterium-^{18}O plot of all groundwater samples from the DWA national groundwater pollution project collected from selected boreholes around South Africa. The Global Meteoric Water Line and the trend line though all the sample points are indicated.

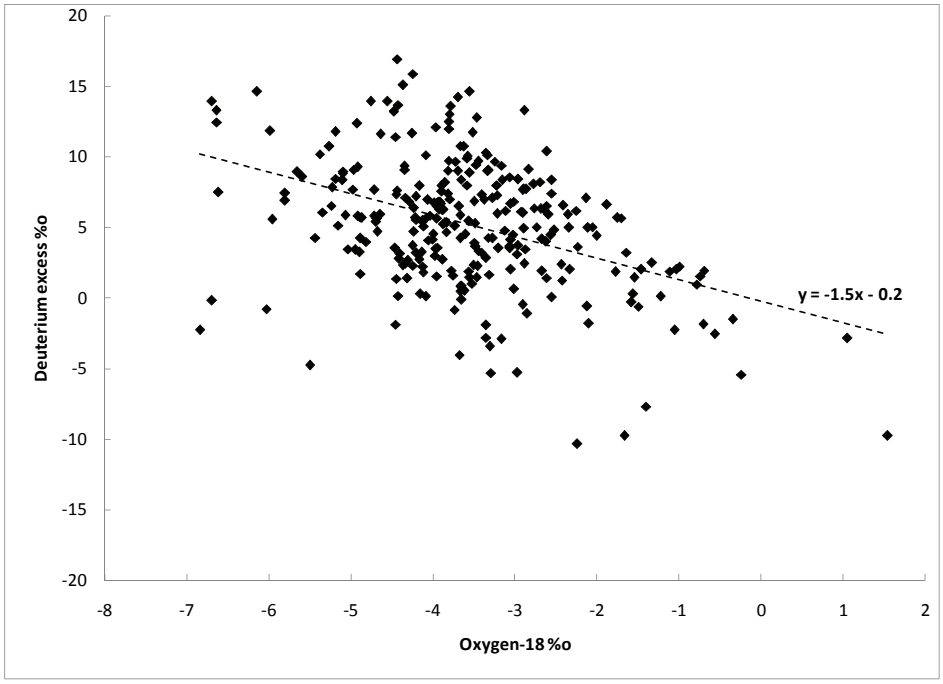

Figure 17: Plot of D_{xs} (deuterium excess) against ^{18}O of the groundwater samples from the DWA groundwater pollution programme. The RMS linear trend line through the points is shown.

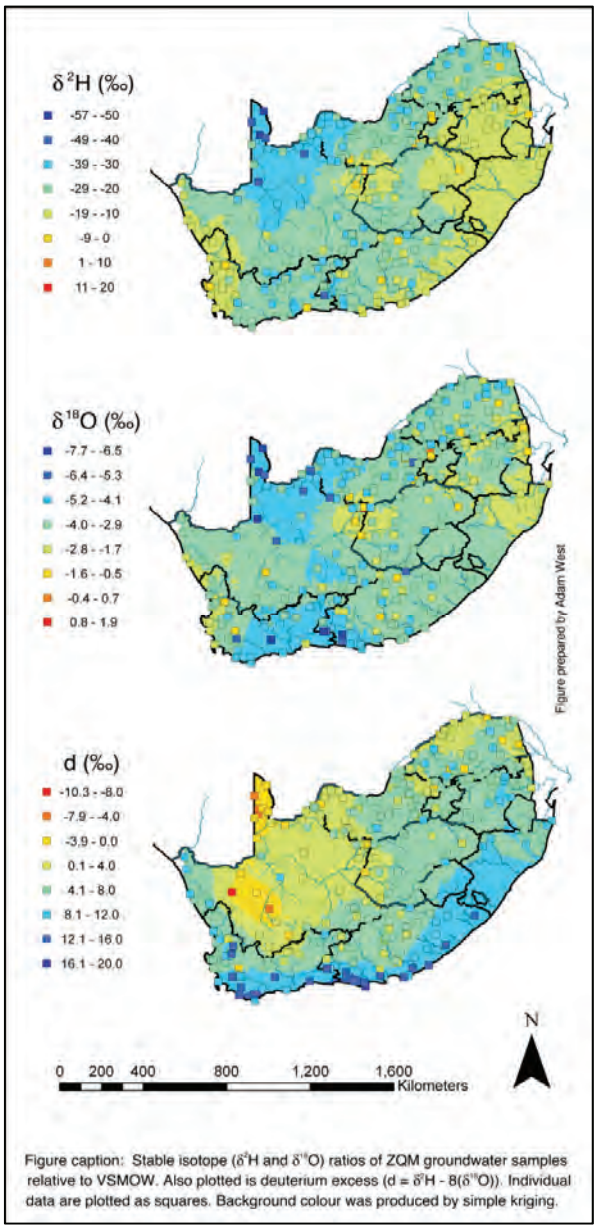

Figure 18: Kriging of stable isotope values from the DWA groundwater survey of 2006/7.

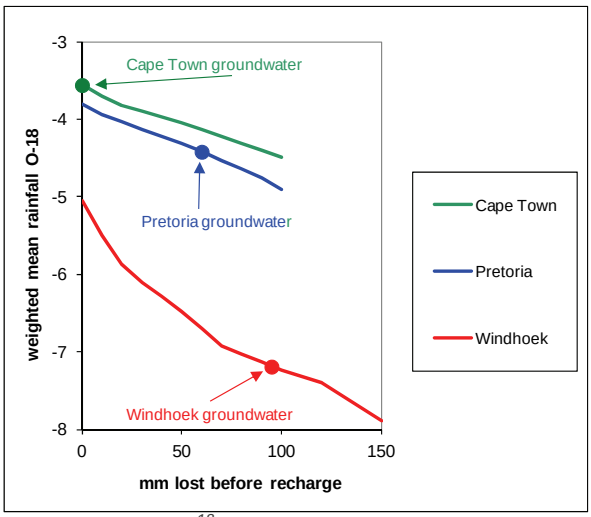

Figure 19: Calculations of weighted mean annual ^{18}O content based on monthly rainfall above various thresholds. The indicated groundwater values, suggest a likely cut-off for this model in each situation.

Recommendations for further work

The full rainfall data set, as it exists now, undoubtedly contains useful information that can still be unpacked. In the past there have been many groundwater projects throughout the region where isotopes were applied. These can contribute to a greater regional picture. Future work could include the following:

- Correlate the rainfall data with other meteorological/climatic parameters. This might lead up to its incorporation in meteorological models.
- Complete the evaluation of stable isotope data from the two isotopic sampling runs of the NGWQ programme.
- Evaluate existing tritium data obtained through the NGWQ programme.
- Expand the NGWQ groundwater data set with data from other projects countrywide to obtain a more detailed national coverage that will be suitable for more detailed mapping (Isoscapes)
- Modelling of the isotope relations between rainfall and groundwater.

CONCLUSIONS

This study has provided an opportunity to retrieve rainfall data that otherwise would likely be lost. The data sets are far from complete, but those are the consequences of working in an academic and commercial environment where priorities and funding have changed many times in the course of decades. The conclusions drawn from these data are by no means final. There is probably much more information hidden within these numbers. The availability of the data in digital form will hopefully stimulate further studies and if this were to happen, then the project will have justified itself.

ACKNOWLEDGEMENTS

This paper is a tribute to Dr John Vogel who passed away in 2012. He arranged the first sampling of rainfall for isotope analysis in southern Africa (Ehhalt et al., 1963) while he was still working in Germany. At the CSIR he set up the CSIR-NET in the late 1960s and actively supported it. During all this time he maintained rainfall measurement and sampling in his two residences and took an active interest in the DWA experiments in his garden.

CSIR-NET was established and maintained by D Bredenkamp, W Roether and H van Urk. Additional rainfall isotope data were obtained from M Butler (iThemba), C Harris (UCT), H Beekman (GRES), S Lorentz (UKZN), L Araguas-Araguas and S Terzer (IAEA). Adam West (UCT) kindly produced the kriged ^{18}O map for the groundwater network.

REFERENCES

Beekman, H.E., Selaolo, E.T., de Vries, J.J. (1998). Groundwater Recharge and Resources Assessment in the Botswana Kalahari. Executive summary GRES2. Department Geological Survey, Lobatse, Botswana. 48p.

Bowen G. J., Revenaugh J. (2003). Interpolating the isotopic composition of modern meteoric precipitation. *Water Resources Research* 39(10), 1299, doi:10.129/2003WR002086.**Clark, I.D., Fritz, P. (1997).** *Environmental Isotopes in Hydrogeology*, Boca Reton, NY: Lewis Publishers. Also athttp://www.science.uottawa.ca/~eih/.

Dansgaard, W. (1964) Stable isotopes in precipitation. Tellus 16, 436-468.

Department of Water Affairs, (2010). National Groundwater Quality Monitoring Project (NGwQMP). http://www.dwa.gov.za/Groundwater/NGQMP.aspx

Diamond, R.E., Harris, C. (1997). Oxygen and hydrogen isotope composition of Western Cape meteoric water. *S Afr J Sci 93(8), 371-374.*

Ehhalt, D.H., Knott, K., Nagel, J.F., Vogel, J.C. (1963). Deuterium and oxygen-18 in rain-water. *J Geophys Res* 68, 3775-3780.

Gat J. R., Mook W.G., Meijer H.A.J. (2001). Environmental Isotopes in the Hydrological Cycle, Volume 2: Atmospheric water. IHP-V, UNESCO, Paris, URL:http://www.naweb.iaea.org/napc/ih/IHS_resources3_publication_en.html

Harris, C., Burgers, C, Miller, J., Rawoot, F. (2010). O- and H-isotope record of Cape Town rainfall from 1996 to 2008, and its application to recharge studies of Table Mountain groundwater, South Africa. *South African Journal of Geology* 113, 33-56

IAEA (1992). Statistical Treatment of Data on Environmental Isotopes in Precipitation. Technical Reports Series. Vienna: International Atomic Energy Agency. 331p.

IAEA (2006). Isotope Hydrology Information System. The ISOHIS Database. http://www-naweb.iaea.org/napc/ih/IHS_resources_isohis.html

IAEA (2012a). Global Network of Isotopes in Precipitation: Description and mode of operation. http://www-naweb.iaea.org/napc/ih/IHS_resources_gnip.html

IAEA (2012b). GNIP Manual on sampling methods. http://www-naweb.iaea.org/napc/ih/documents/userupdate/sampling.pdf

Ingraham, N.L. (1998). Isotopic variation in precipitation. In: Kendall, C. & McDonnell, J.J. (editors), Isotope Tracers in Catchment Hydrology, Elsevier, Amsterdam. 87-118.

Kunz, R. (2012). Daily Rainfall Data extraction utiliy, version 1.4. Institute for Commercial Forestry Research, Pietermaritzburg.

Lorentz S, Bursey K, Idowu O, Pretorius, C., Ngeleka, K. (2008). *Definition and Upscaling of Key Hydrological Processes for Application in Models*. Report 1320/1/08. Water Research Commission, Pretoria.

Lynch, S. (2003). The development of a raster database of annual, monthly and daily rainfall for southern Africa. Report K5/1156. Water Research Commission, Pretoria.

Meyer, R., Talma, A.S., Duvenhage, A.W.A., Eglington, B.M., Taljaard, J., Botha, J.F., Verwey, J., van der Voort, I. (2001). Geohydrological investigation and evaluation of the Zululand Coastal Aquifer. Report 221/1/01. Water Research Commission, Pretoria, 51p.

Midgley, J.J., Scott, D.F. (1994). The use of stable isotopes of water (D and 18O) in hydrological studies in the Jonkershoek Valley. *Water SA* 20(2):151-154

Obakeng, O.T. (2007). Soil Moisture Dynamics and Evapotranspiration at the Fringes of the Botswana Kalahari. PhD thesis, Free Univ Amsterdam, 225p.

Schiegl, W.E. (1970). *Natural Deuterium in Biogenic Materials*. Univ of South Africa, Pretoria. Ph D thesis.

Siegenthaler, U., Oeschger, H. (1980). Correlation of ^{18}O in precipitation with temperature and altitude. Nature 285, 314.

Van Wyk, E. (2010). Estimation of episodic groundwater recharge in semi-arid fractured rock aquifers. PhD thesis. Univ Free State. 272p.

Verhagen, B.Th., Butler, M.J., Levin M. Van Wyk E. (2000). Environmental isotopes assist in groundwater sustainability assessment of the Taaibosch fault zone, Northern Province, South Africa. In: Groundwater, Past achievements and Future challenges, 673-678, Balkema, Rotterdam.

Vogel, J.C., van Urk, H. (1975a). Isotopic investigation of Lake St Lucia. Unpublished CSIR report.

Vogel, J.C., van Urk, H. (1975b). Isotopic composition of groundwater in semi-arid regions of Southern Africa. *J Hydrol* 25:23-36, 1975.

Vogel, J.C., Lerman, J.C., Mook, W.G. (1975). Natural isotopes in surface and groundwater from Argentina. *Hydrol Sci Bull* 20:203-221.

Vogel, J.C., Talma, A.S., Heaton, T.H.E. (1982). The age and isotopic composition of groundwater in the Stampriet artesian basin, SW Africa. CSIR Research Report. , 1982.

Weaver, J.M.C., Talma, A.S., Cave, L. (1999). *Geochemistry and Isotopes for Resource Evaluation in the Fractured Rock Aquifer of the Table Mountain Group*. Pretoria: Water Research Commission Report 481/1/99.

Weaver, J.M.C., Talma AS, (2005). Cumulative Rainfall Collectors - a tool for assessing groundwater recharge. Water SA 31(3), 283-290.

West, A, February, E, Bowen, G. (2011). Creating a map of stable isotopes in tap water across South Africa for hydrological, ecological and forensic applications. Consultancy report K8/892 to WRC, Pretoria.

CASE STUDY:

CORRELATIONS BETWEEN RAINWATER AND GROUNDWATER GEOCHEMISTRY SIGNATURES WITH REFERENCE TO EPISODIC RAINFALL EVENTS IN SEMI-ARID ENVIRONMENTS, SOUTH AFRICA

E. van Wyk

INTRODUCTION

The groundwater recharge cycle represents a significant component of the natural hydrological cycle (HC) driven by rainwater representing a dynamic effect of the groundwater HC as it is deposited in various quantities, each with a specific hydrochemical signature.

The multi-modal[3] generation of rainwater in the southern African is driven by summer and winter climate patterns. Although the atmospheric moisture is generated over oceanic regions, the origins and migration pathways of these airborne moisture masses are significantly different over the sub-continent. Rainwater carries a unique hydrochemical signal with it in frontal (winter season) and continental (summer season) weather systems, which after rainout, carries this signal to either surface water bodies and/or groundwater reservoirs. Seasonal and diurnal temperatures vary significantly, which drives extreme processes, viz. evaporation from surface water systems and transpiration by a most vegetation species occurring in various configurations of colonies.

The hydrogeological and climatic conditions in the Great Karoo Basin (e.g. Beaufort West area) represent a typical semi-arid hydro-environment. However, climatic patterns on the Nuweveld Mountains varies significantly from those on the southern Karoo planes, this phenomenon provides a unique opportunity to monitor differences in the recharge cycles and hydrochemical characteristics of rainwater and recharged groundwater (Van Wyk, 2010).

For regional background environmental stable isotopes (ESI) characterization, several additional monitoring sites in the semi-arid region of South Africa were included.

ESI's were applied in conjunction with the environmental geochemistry tracers (viz. chloride) to identify zones where direct groundwater infiltration mechanisms drive episodic recharge events. Special sampling techniques were used to sample individual rainfall events, bulk rainfall and groundwater profiles over a period of six (6) years from 2003. It includes the 2005-2006 summer rainfall season characterizing a significant rainfall depth, associated with a different hydrochemical signature.

A special rainfall (depth) and rainwater (hydrogeochemical signatures) monitoring programme was established to generate rainwater and groundwater from so-called hard rock terrains to study the interaction between rainfall and groundwater for a period of 5 (five) years; from the 2004-2005 HC to the 2009-2010 HC.

The monitoring network used for this study covered a significant portion of the semi-arid region of South Africa, and including the ESI data obtained from other hydrogeological studies, a summary of the Local Meteoric Water Lines for South Africa could be established. Table 1 presents the different Meteoric Water Line algorithms obtained from monitoring sites across South Africa from 2003-2009 (Van Wyk, 2010).

[3] Arctic maritime moisture in winter, Indian/South Atlantic maritime and continental evaporated moisture in summer.

Monitoring Terrain	Observation period	Co-variance (MWL)	Comments
GNIP (Global)	Since 1961	$\delta^2H = 8.0 \cdot \delta^{18}O + 10.0$	Craig (cited in Mazor 1997)
GNIP (Pretoria)		$\delta^2H = 6.5 \cdot \delta^{18}O + 6.37$	Mook (2000)
GNIP (Windhoek)		$\delta^2H = 6.6 \cdot \delta^{18}O + 7.04$	IAEA/WMO (2003)
Beaufort West	2003-2008	$\delta^2H = 5.4 \cdot \delta^{18}O + 2.6$	Western Cape, summer rainfall
Kalahari	2002-2009	$\delta^2H = 6.1 \cdot \delta^{18}O + 6.5$	Western Kalahari, summer rainfall
KwaZulu-Natal	2003-2006	$\delta^2H = 5.6 \cdot \delta^{18}O + 6.7$	Northern KZN, summer rainfall
Langebaan	2003-2006	$\delta^2H = 6.5 \cdot \delta^{18}O + 6.6$	Western Cape, winter rainfall
Sandveld	2003-2006	$\delta^2H = 5.8 \cdot \delta^{18}O + 5.2$	Western Cape, winter rainfall
Kuruman	2002-2008	$\delta^2H = 5.5 \cdot \delta^{18}O + 0.6$	Northern Cape, summer rainfall
Pretoria East	2003-2009	$\delta^2H = 6.0 \cdot \delta^{18}O + 5.0$	Gauteng, summer rainfall
Stella	2002-2009	$\delta^2H = 6.4 \cdot \delta^{18}O + 4.4$	Northern Cape, summer rainfall
Taaiboschgroet	2003-2006	$\delta^2H = 7.7 \cdot \delta^{18}O + 8.1$	Limpopo, summer rainfall

Table 1. Table of LMWL's (rainwater only) from this study and from published literature.

The deuterium excess for this study's monitoring terrains varies between 0.6 and 8.1 (average = 5.8). This phenomenon has been observed in southern African at different times and areas of rainfall isotope studies (Pers. comm., Butler 2010) and is probably an indication of relative humidity and temperatures; especially in the semi-arid environment of southern Africa.

Rainwater was collected over periods of 3 to 6 months in concealed acrylic vessels. The isotope results are in fact represented by differentiated rainwater samples from the so-called 'early' seasonal input (Oct_n to Dec_n) and 'peak' seasonal input (Jan_{n+1} to Apr_{n+1}) in the case of a 3-monthly interval.

The local meteoric water line for the Beaufort West area with a deuterium excess ('d excess) at +5 however indicates a slight rotation away from the global line. The specific data component responsible for this shift comes from rainfall collected from the Beaufort West Plain Area[4] during two prominent 'dry' seasons i.e. 2005 and 2007. The rainwater at Beaufort West however originates from summer rainfall conditions. Temperature (cloud forming), amount (dilution) and elevation (orographic) effects influence the local isotopic composition, hence leads to local shifts in the meteoric water line configuration (Dansgaard, 1964 and Kendall et al., 1998).

[4] A flat lying topographic area north-west of the town in front of the Nieuwveld Mountains of the Great Escarpment.

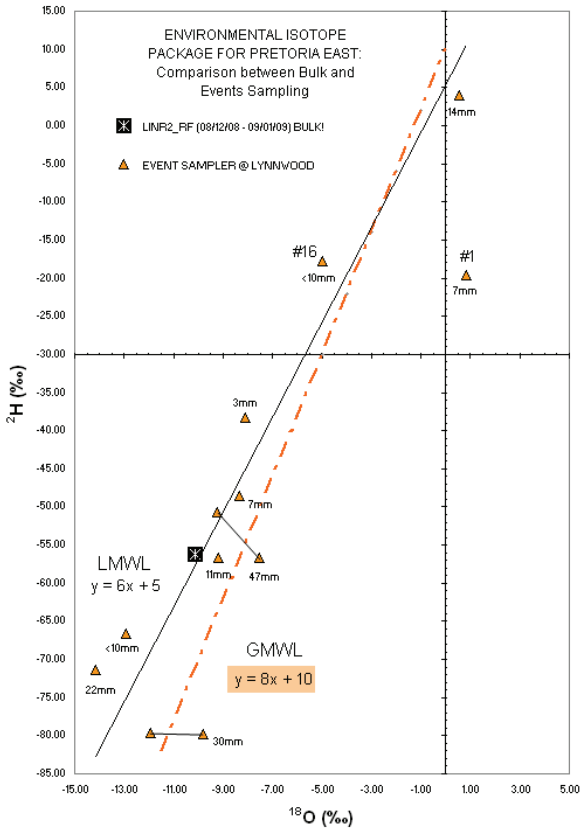

Figure 1: Isotopic composition of rainwaters from the Pretoria East Geosite illustrating the difference between bulk rainwater sampling (over a month) and individual rainfall sampling using the Rainfall Event Sampler.

Environmental Stable Isotopes (ESI's)

Rainwater collected during a specific rainfall season is an accumulation of several individual rainout events with obviously different isotopic signals. It has been observed through the rainfall sampling programme that heavy rainout events introduce a much lighter ESI addition to the local water signature, thus lighter values for both ^{2}H and ^{18}O which will 'shift' the isotopic composition towards the 'lighter' side on the meteoric water line which is referred to as the amount effect (Dansgaard, 1964). Analyses from special monitoring sites however confirm this signature and correlates high total rainfalls for example observed in 2006 and 2008 sampled (viz. monitoring sites at Kuruman, Pretoria-East and Stella); all monitoring sites recorded a 50 to 70% rainfall increase in 2006 and 2008 higher than the long-term averages. These rainfall events could be regarded as extraordinary in the sense that they were part of a fairly wet periods (3 to 7 days) including episodic rainfall events of 45 to 120mm. ESI-values for these high rainout events shifted the bulk rainwater sampled in the rainwater collector to –40(±4) ‰ δ^2H and -7(± 1) ‰ δ^{18}O respectively. The actual episodic rainout event input may at least represent 40% to 50% of the total water column in the collector tube.

What has been recorded as lighter isotopic signals in the above-mentioned cases can in fact be a mixture between even 'more' incoming negative isotope signals which can probably not be the result by the amount effect only, but long-term rainout events along the migration path of the moisture package.

A special rainfall event sampler has been constructed in an approach to sample individual rainout events. Unfortunately, due to logistical problems, only one of these units could be physically tested in Pretoria (Van Wyk, 2010).

The rainfall pattern over the test period was 142 mm of which three events were episodic rainfall events (Figure 1). The rainwater collected over the same period in the bulk rainwater sampler unit plots in the same region as the highest rainout event, viz. the one of 47 mm which occurred towards the later part of this sampling cycle. Two events, totalling 52mm (22mm + 30mm) report lighter isotopic values, which represent the most depleted isotopic signatures observed during the study period probably due to the specific sampling method used (viz. the rainfall event sampler).

The stable isotope data recorded with this method reveals a significant 'lighter' isotopic shift (-79.75 ‰ δ^2H, -14.16 ‰ δ^{18}O) from a series of 9 events. Similar rainfall ESI signatures are probably present at the other monitoring sites as well, but have been lost during the bulk sampling method originally used.

Conclusions

The isotopic composition of rainwater collected from eight (8) hard rock monitoring terrains in the semi-arid regions of South Africa, represents a set of relatively depleted ESI signatures which correlate with the ESI signatures observed from the local, shallow groundwater occurrences.

Normal ESI values for summer rainfall fluctuate between: -0.7 ‰ δ^2H / -0.3 ‰ δ^{18}O to -44 ‰ δ^2H / -7 ‰ δ^{18}O. These samples were obtained with the DWA bulk sampler unit which in fact is a collection of several rainout events collected over the three time intervals in the Hydrological Cycle, i.e. (i) the Oct_n to Dec_n or 'Early Rainfall' interval, (ii) the Jan_{n+1} to Apr_{n+1} or 'Peak Rainfall' interval, and (iii) May_{n+1} to Sep_{n+1} or 'Dry' interval.

An attempt to sample from individual rainfall events were achieved using a special rainfall event sampler installed in the Pretoria East urban area. Although several of the bulk rainwater samples reported slightly

lighter isotope signatures, these samples were in the region of -75±10 ‰ δ^2H / -10±2 ‰ $\delta^{18}O$.

GROUNDWATER SIGNATURES

The hydrological monitor programme implemented on this investigation was specifically focused on the rainwater-groundwater interaction. It involves hydrodynamics of direct recharge zones (so-called hard rock terrains), as well as the hydrochemical signature of the rainwater input, the runoff component and the recharged component by utilizing natural hydro-tracers.

The stable isotopes of hydrogen & oxygen have been used for (i) qualification of the multi-modal flow path through the unsaturated zone (i.e. matrix flow vs. macropore flow) and (ii) qualification of episodic recharge events (Nkotagu, 1996 and De Vries and Simmers, 2001).

The monitoring sites are all hard rock terrains; therefore the soil/regolith cover varied between 0.25 and 0.6m (Van Wyk, 2010). No soil/matrix water from the vadose zone could be collected due to the hard rock terrains. In addition, many down-the-hole video images from the DWA Bore Video Bank have been viewed for evidence of any moisture at the bottom of the rooting zone. Although these images are once-off recordings all year around, it could indicate that the matrix flow component of a recharge pulse in semiarid regions are significantly intercepted by plant transpiration which can be as high as 80% of surplus rainwater entering the rooting zone (Le Maitre et al., 2000).

Observations from several road/ravine cuttings and down-the-hole images show that in a majority of hard rock terrains, open joint/fractures occur in a complex geometry of vertical/horizontal/oblique joints (in sedimentary formations) and an ad hoc jointing/fracturing structure (in massive sedimentary/crystalline formations). Down-the-hole Image Logging, however reports that horizontal jointing occurs at a much lower interval/depth ratio than the vertical ones, although the aperture of the former one is more than 10-times larger.

Considering the short lag times (hours/days) between rainout events and water table responses, direct recharge at local scale by means of preferential flow regime (a macropore by-pass mechanism) instigated by an episodic rainout event, is probably the most effective process driving aquifer storage recharge events in semiarid regions.

WATER TABLE BEHAVIOUR DURING EPISODIC RECHARGE EVENTS

The direct recharge flow path through the vadose zone in hard rock terrains is governed by a preferential flow mechanism. The difference between matrix flow recharge and total recharge (fracture flow plus matrix flow) is at maximum in the case of fractured hard rock regions (Sukhija, et al., 2000). Direct recharged rainwater instigating a water table rebound in a local aquifer, is a combination of faster bypass flow (>60% by-pass flow mechanism) and slower diffuse drainage (<40% matrix flow based on the piston flow principle).

Time series hydrograph-hyetograph presentations indicate an effective short-term aquifer storage recharge (ASR) events producing a groundwater rebound of several meters as illustrated in Fig. 2. A special groundwater monitoring programme was initiated to sample pre-selected sections (0.25m intervals) of the water table rebound as it developed during the recharge event. No measurable enrichment due to evaporation was detected as the stable isotope signature did not indicate an evaporative signal (plots on the LMWL) (Van Wyk, 2010).

ESI Signals from a Water Table Mound (Rebound)

Once rainwater accumulates at ground surface and starts to infiltrate into the under drainage, a certain portion (volume) will be gradually diminished due to evapotranspiration. The isotopic signal of the infiltrated rainwater however can only be significantly altered by the evaporation component; hence plant transpiration has little impact on the isotopic composition (Sharma and Hughes, 1985).

It is expected that at hard rock terrains with an effective by-pass flow regime, the hydrochemical signal of the rebound water column could approach the hydrochemistry of the surplus rainwater (Nkotagu (1996); thus indicating minimal fractionation of the stable isotope signal due to superficial or rooting zone evaporation.

Rainwater that accumulates at ground surface as depression storage will be subjected to a direct atmospheric evaporation, thus enriched with respect to both ^2H and ^{18}O (Mazor, 1997). The resulting isotope values over time will plot on an Evaporation Line, below the local/global meteoric water line with a gradient lower than the Meteoric Water Lines.

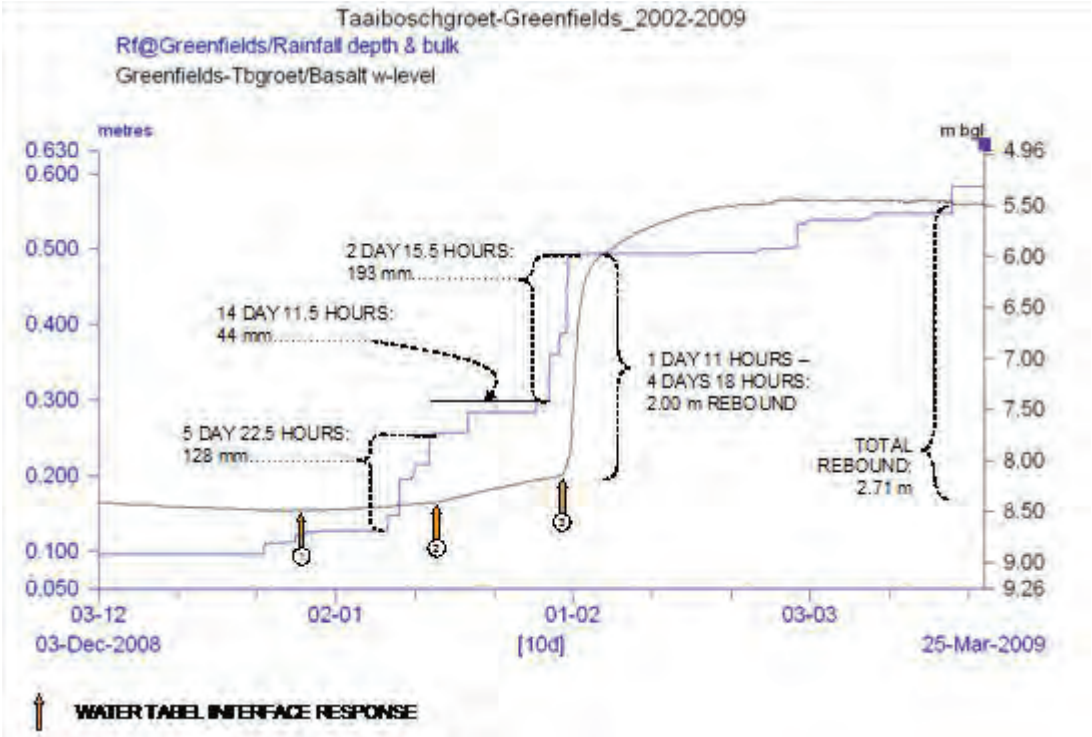

Figure 2: A rain-week scenario as it occurred from 29 - 31 Janaury 2009 (2 days and 15½ hours) in the Taaiboschgroet area, Limpopo Province with a total rainfall of 193 mm.

Isotope compositions in local groundwater at monitoring sites in the semi-arid region (Great Karoo, Kalahari and Northwest) indicate a more depleted signature than the local rainwater (see Harmon Craig Diagram in Fig. 3 below). The illustration represents the condition at the De Hoop Poort monitoring site at Beaufort West. The local groundwater isotopic composition falls at levels lower (-38±5.0 ‰ $\delta^{2}H$ and -6.5±2.5 ‰ $\delta^{18}O$) than the bulk rainwater compositions which simply mean that the recharged water responsible for this plot originates from a series of relatively depleted rainfall events, with individual isotopic compositions, even 'lighter' than the bulk sampled rainwater.

As discussed above, the actual bulk sample collected in the rainwater collector represents a mixture of individual rainouts over a period of 3 or 6 months. Natural variations in the rainwater isotope composition due to (i) the amount effect as a result of higher rainout events (Mazor, 1997), or (ii) a complete different isotope configuration in the atmospheric moisture, will therefore be suppressed by the heavier rainwater from the average rainfall events.

The physical infiltration process through the vadose zone is rather complex. Nkotagu (1997) has observed in a crystalline hard rock environment in Tanzania that (i) $\delta^{2}H$ and $\delta^{18}O$ values in shallow groundwater correlate with surface and rainwater isotopic composition, indicating that local rainwater recharges the shallow groundwater with little evaporation, possibly during flash floods, and (ii) isotopic values for groundwater are more depleted than the local rainwater and surface runoff thus indicating the local aquifers are recharged by rainwater originating from a higher altitude (the Altitude Effect), or that 'specific, local, heavy (depleted) rainfall events are responsible' (the Amount Effect).

The Altitude Effect has however been observed in the Beaufort West area from rainwaters sampled from the Nieuwveld Mountains on the farm Grazplaatz 113, sitting at 1729 meters above sea level and on the southern plains area (monitoring site G29870L – S32.16450°; E022.72585°, 1729 m amsl). The short lag time between the rainout events and the water table responses however does not confirm this mechanism; nor does a pressure migration affect due to the elevation difference between direct hard rock infiltration sites.

Depth related ESI variations

Groundwater samples from the water table interface have been sampled in order to observe whether layering of infiltrating rainwater based on the model of 'L-Shape Through-Flow Paths and Zones of Stagnation: (Mazor, 1997) may exist.

A series of 2 and 4m 'Column' samples from shallow cased bores (above water table fluctuation levels) were sampled on specific times before and after a particular recharge event. Samples were also obtained during ASR conditions, using an In Sito Stage Sampler (Van Wyk, 2010).

Isotopic compositions of the groundwater profile vary as shown in Fig. 4. This profile is from a shallow cased water bore in the De Hoop Poort area, District Beaufort West and shows a relatively depleted isotopic signal in the water column at approximately 1m below groundwater table (2.01m on June, 4th 2008). The isotopic value (i.e. -48.6 ‰ δ^2H, -9.9 ‰ δ^{18}O) at -1m bgl show a relationship with the bulk rainwater isotopic composition (-31.7 ‰ δ^2H, -5.37 ‰ δ^{18}O) collected between 01 October 2007 and 03 June 2008. During this rainfall period, two rainfall events (113mm over 13.2days and 62mm over 4 days) occurred that have generated an ASR event of 1.56 m.

The relevant Chloride Depth Profile responded in a similar way, although the chloride tracer concentration and migration is probably driven by a different mechanism due to the discrete flushing of the season's dry, atmospheric chloride into the unsaturated zone from the beginning of the rainfall period

In another case of variations, vertical isotopic composition with a discernible 'lighter' trend line, has been observed on the Stella Golf Course monitoring site close to a hard rock window of highly fractured Kraaipan rocks[5]. The physical water table recharge at this site was in the order of 17m during the period 09 February 2006 to 12 April 2006 after a six-day rain-week produced 246 mm starting on 6 February 2006. The vertical profiling of the hydrochemical in water bore G43982 done on 28 August 2008 is shown in Fig. 5.

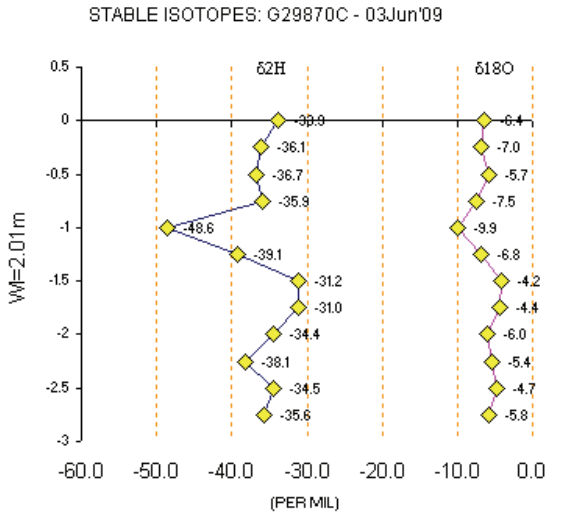

.

Figure 3. Isotopic composition of groundwater sampled using a 2 and 4m 'Column' and 19mm 'Skim' sampler in November 2008 in correlation with local rainwater sampled during the 2004-2008 period. Rainwaters containing the 'episodic' events in 2006 and 2008 are marked specifically

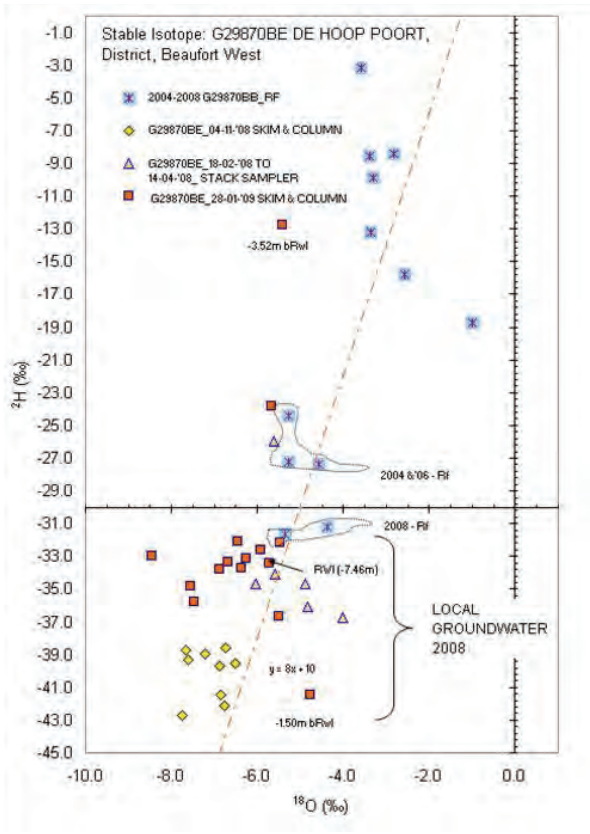

Figure 4: Isotopic composition in a 2.75m groundwater column in water bore G29870C in the De Hoop Poort area, District Beaufort West sampled at a 0.25m interval on 04 June 2008, some 73 days after water table declining has commenced following a water table rise of 1.56m over 66 days.

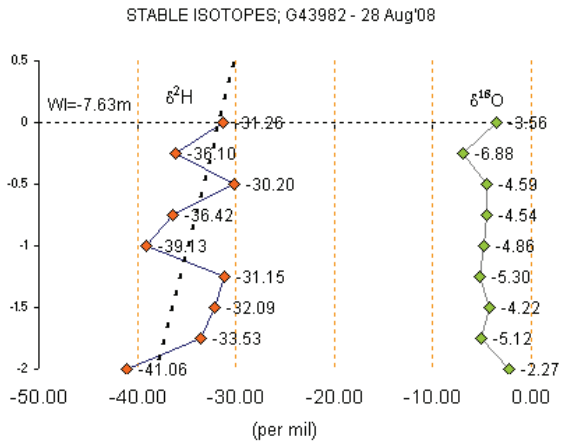

Figure 5: Vertical depth profile of isotope compositions on a 0.25m interval from water table (-7.63m bgl) in water bore G 43982, Stella Golf Course close to Kraaipan Group outcrop area (i.e. typical hard rock window area).

[5] Identification of this particular rock formation and it's occurrence in the local Ventersdorp Lava is still not solved. The area serves however as a major water supply zone for the town.

SUMMARY OF HYDROCHEMICAL FEATURES OF THE RECHARGE CYCLE

There is a measurable variation in the hydrochemical compositions of incoming rainwater, i.e. (i) origin of atmospheric moisture over oceans (ESI signature), (ii) addition of terrigeneous dust to the atmosphere (chloride mass balance – CMD), (iii) evaporation/fractionation during cloud/droplet formation along continental migration (ESI signature), (iv) physical effects (ESI signature influenced by temperature, altitude and continental effects) and (iv) the amount effect (ESI signature).

Specific rainout events, referenced as 'episodic events' form part of the annual rainfall pattern and occur during a sequence of rainout events over a period of 3 to 5 days; a period referred to as a rain-week. The rainfall character during these periods includes a distinctive lighter signal in both macro-chemistry and isotopic compositions.

Several cases exist at different spots in South Africa where the groundwater column contains water with a lighter isotopic composition than the bulk rainwater collected over months, quarterly and biannually. The observations at Stella-Naledi (Northwest Province) are a typical example (see Fig. 6 and explanation below).

The ESI composition of the recharging rainwater from the bulk rainwater input over the early and peak rainfall season plots around $^{18}\delta$=-3‰, $^{2}\delta$=-18‰ on the Harmon Craig diagram. Most groundwater's ESI signatures in this study are relative more negative on the LMWL, i.e. $^{18}\delta$=-6‰, $^{2}\delta$=-38‰. Observations from episodic rainfall events are relatively depleted ($^{18}\delta$=-10‰, $^{2}\delta$=-65‰ to $^{18}\delta$=-12‰, $^{2}\delta$=-78‰) which indicates that a considerable portion of this rainwater in fact moves directly to the saturated zone.

This confirms that a considerable large contribution of bypass flow is taking place in these fractured hard rock terrains. It was noted by researchers that where direct groundwater recharge is enhanced by bypass infiltration, the isotopic composition of the episodic rainwater input and the groundwater should not differ significantly (Nkotagu 1996).

De Vries and Simmers (2001), mentions that bypass flow, received during the early stages of the summer season on a dry and cracked ground surface and/or during extraordinary high rainfall events may contribute to 90% of a regions annual recharge. These extraordinary high contributions is probably taking place in extreme hard rock cases like the TMG ortho-sandstones, in total bare rock conditions (limited soil/regolith horizon).

The comparison between rainwater input in peak 2006 ($^{18}\delta$=-5.53‰, $^{2}\delta$ =-37.0‰), peak 2008 ($^{18}\delta$=-6.33‰, $^{2}\delta$=-29.59‰) and peak 2009 ($^{18}\delta$=-4.24‰, $^{2}\delta$=-31.29), and the groundwater around $^{18}\delta$=-6‰ and $^{2}\delta$=-37‰ is quite obvious and clearly signals the episodic rainfall input in 2006. The information illustrated in Figure 6 reports the following hydrogeochemical scenario: Spitkopreen is the ESI composition of the early and peak rainwater collected during years with minimum episodic rainfall events, i.e., 2002-2003, 2004-2005 and 2006-2007;

- HC's with episodic events, represents ESI composition of the early and peak rainwater collected during years with prominent episodic rainfall events, i.e. 2003-2004, 2005-2006 and 2007-2008.
- AKM-MON#1 represents the ESI composition sampled on 28 August 2008 from a 2 m column in the Mosita granite at Stella which represents a hard rock terrain with <0.25 m soil/regolith cover;
- G43991 represents the ESI composition sampled on 28 August 2008 from a 2 m column in the Kraaipan Group at Stella which represents a hard rock terrain with limited soil/regolith cover;
- G 44504 represents the ESI composition sampled on 28 August2008 from a 2 m column in the Mosita Granite Suite with thick soil/regolith cover. This site is situated close to several small depressions (pans). As indicated in Fig. 6.13, the ESI composition reports a strong evaporation signature (E.L.) in this groundwater which is to be expected from the accumulation of rainwater in these depressions. The grouping of the sample points is also much wider than those from samples in boreholes G43991 and AKM-MON#1. It was noted (Google image assessments) that some of these pans once flooded can store the local run-off for extended periods; and
- RES unit represents the ESI composition of the rainwater sampled using the RES unit. Although these samples were only collected between December 2008 and January 2009 and out-of-phase with those presented in Fig. 2, it still demonstrates the relatively depleted composition of individual cloud water samples.

Mook (2000) and Verhagen (2010) indicates that during prolonged rainfall events, i.e. the rain-week scenario, atmospheric conditions are remarkably different than during the normal isolated convection cell rainfall patterns normally encountered in the central South African region.

The relative humidity specifically plays a dominant role in the final hydrogeochemical composition of the rainwater, as the cloud water remains hydrogeochemically in equilibrium with the larger atmospheric mass with its unique hydrogeochemical character which probably is already considerably

depleted during several rainout events along its migration pathway from its origin, the Inter-Continental Transition Zone (ITCZ) and the equatorial ocean region.

To conclude, episodic rainfall events portray (i) the rain rate-depth configuration to effectively recharge and (ii) introducing a characteristic hydrogeochemical signature in the recharge-producing rainfall surplus and infiltrating rainwater.

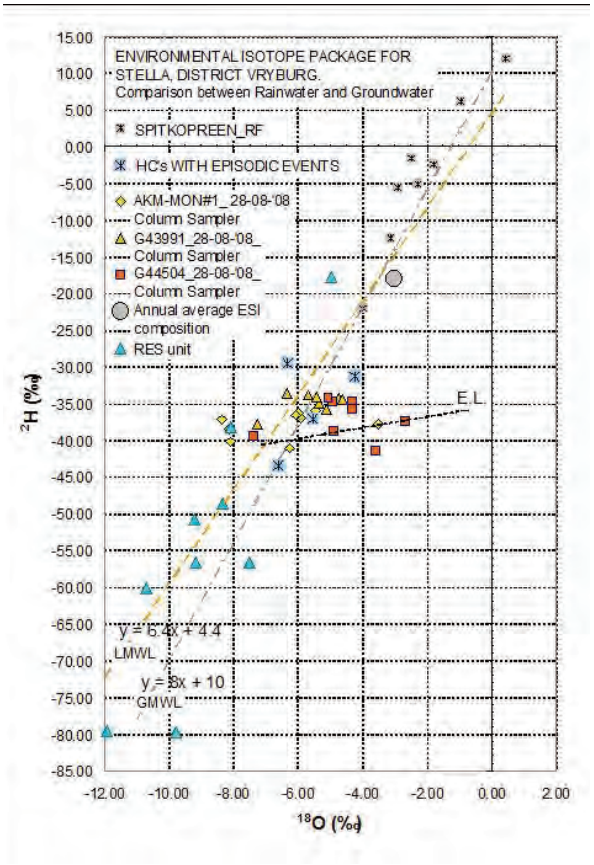

Figure 6: Comparison between the stable isotope composition of the 2002-2009 rainfall period and groundwater sampled form local boreholes where a water table mound of 2.84 m was recorded (E.L. indicates Evaporation Line).

CONCLUSION

A series of groundwater samples indicate that a significant component of recharge-producing surplus rainfall percolates vertically with minimum evaporation losses to the water table interface. This flow occur mainly by means of by-pass flow mechanisms (preferential flow via in situ macropores/joints) as indicted by a correlation between the isotopic composition of episodic rainfall events and the local groundwater isotopic signal. The stable isotope composition of most of the typical hard rock monitoring sites groundwater indicates a lighter isotopic characteristic (-38±5.0 ‰ δ^2H and -6.5±2.5 ‰ δ^{18}O) on the Local Meteoric Water Line.

A series of groundwater samples indicate that a significant component of recharge-producing surplus rainfall percolates vertically with minimum evaporation losses to the water table interface. This flow occur mainly by means of by-pass flow mechanisms (preferential flow via in situ macropores/joints) as indicted by a correlation between the isotopic composition of episodic rainfall events and the local groundwater isotopic signal. The stable isotope composition of most of the typical hard rock monitoring sites groundwater indicates a lighter isotopic characteristic (-38±5.0 ‰ δ^2H and -6.5±2.5 ‰ δ^{18}O) on the Local Meteoric Water Line.

The application of the traditional[6] stable isotope tracing through the unsaturated zone however was not possible due to the nature of the hard rock terrains. In addition, 'resident times' for recharged surplus rainwater residing in the unsaturated 'upper' fractured weather horizon is short lived. This water 'dries out'' over a few weeks as the result of the intense evapotranspiration in the semiarid regions. There should therefore not be a substantial difference between the rainwater and by pass flow recharge water if discrete sampling is possible.

The groundwater isotopic signature, however, indicates that the water residing in the upper fractured and weathered zone is measurable lighter than the average rainfall isotopic signature. Rainfall event sampling (RES), where individual rainstorms are sampled, reports an even lighter isotopic composition as observed through bulk sampling of rainwater. Isotope values from two experimental RES samplers are placed well below (-65 ‰ δ^2H, -12 ‰ δ^{18}O) the average groundwater isotope signature ((i.e. -38 ‰ δ^2H, -6 ‰ δ^{18}O).

REFERENCES

Butler, M. (2010). *Personal communication, iThemba Laboratories, University of the Witwatersrand, Johannesburg.*

Dansgaard, W. (1964). *Stable Isotopes in Precipitation. Tellus 16, pp 436-469.*

De Vries, J. J., I. Simmers. 2001*. Groundwater Recharge: An Overview of Processes and Challenges. Hydrolgogy Journal (2002). pp. 6-17.*

Gieske, A. (1992)*. Dynamics of Groundwater Recharge. A case study in Semi-Arid Eastern Botswana. 289 pp.*

Le Maitre, D.C., Scott, D.F. Colvin, C. (2000). *Information on interactions between groundwater and*

[6] *In-situ* soil moisture samples needs to be collected and analysed from ground zero to the water table interface. Soil samples are obtained by means of hollow stem drilling in stable unconsolidated formation. Results are not that consequent and recharge rates in one site area may vary by an order of magnitude (Gieske, 1996).

vegetation relevant to South African conditions : A review. Groundwater : Past Achievements and Future Challenges. Proceedings of the XXX IAH Congress on Groundwater. Cape Town, S.A. , 26 Nov.-1 Dec. 2000. pp 959-962.

***Mazor, E. (1997).** Chemical and Isotopic Groundwater Hydrology. The Applied Approach, 2nd Edition. 413 pp.*

***Mook, W.G. (2000).** Environmental Isotopes in the Hydrological Cycle. Principles and Applications. Technical Documents in Hydrology. No. 39, Vol I & IV.*

***Nkotagu, H 1997.** Application of environmental isotopes to groundwater recharge studies in semi-arid fractured crystalline basement area of Dodoma, Tanzania. Journal of African earth Sciences. Volume 22, No. 4, pp 443-457.*

***Sharma, M.L., and Hughes, M.W. (1985).** Groundwater Recharge Estimation using chloride, Deuterium and Oxygen-18 Profiles in the Deep Coastal sands of Western Australia. Journal of Hydrology Vol. 81 No1/2, 1985. pp 93-109.*

***Sukhija, B.S., Reddy, D.V., Nagabhushanam, P., Hussain, S. (2000).** Natural Groundwater Recharge Assessment: Role of Preferential Flow in semi-arid fractured aquifers. pp 331-336.*

***Verhagen, B. Th. 2010.** Personal communication, Professor Emeritus, School for Geosciences, University of the Witwatersrand, Johannesburg.*

***Van Wyk, E. (2010).** 'Estimation of Episodic Groundwater Recharge in Semi-Arid Fractured Hard Rock Aquifers', PhD Full, University of the Free State.*

KALAHARI GROUNDWATER ISOTOPE SYNTHESIS

AS Talma, B Th Verhagen, G Tredoux

ABSTRACT

The first studies using environmental isotopes in the Kalahari indicated that there are various localities where recharge occurs in spite of thick Kalahari sand layers. This went against the conventional wisdom at the time and established isotope hydrology as an investigative technique in the area. Since then many investigations have shown that groundwater in the region exhibits a wide range of recharge rates and groundwater residence times. This information has been acquired from through government-contracts as well as curiosity-driven projects across the Kalahari. The nature of these types of investigations is such that very little data has appeared in the formal scientific literature. Most of the data and the conclusions therefrom, have been reported in theses and in reports to the project funders (government departments and international organisations). The existence of such data is not always known and data extraction from the available sources is very laborious and prone to error.

The aim of this study is to collect reports from projects that utilised environmental isotopes and to extract the available isotope and the associated hydrochemical, geological and positional data. Interpretations that were based on such project data can then be reviewed when seen in larger context and common features established. Interpretations of such data in terms of recharge, groundwater flow and other hydrogeological aspects as a contribution to the understanding of the overall hydrogeology of the Kalahari can then be made. This will aid water resource decision makers and serve as a guide to the use of environmental isotopes in future groundwater resource investigations in similar hydrogeological situations.

Researchers from the CSIR isotope laboratory in Pretoria and the Environmental Isotope Laboratory (EIL) of the University of the Witwatersrand, Johannesburg, (now part of iThemba LABS Gauteng) have had major involvements in the Kalahari region since the late-1960s. These laboratories have also been the main producers of environmental isotope data in the region, in addition to some European laboratories. Most of the work was done in collaboration with hydrogeologists knowledgeably of the area. While the analytical data are often available to the laboratories, the background information usually resides with the collaborating institutions.

The Kalahari basin extends from Botswana into South Africa and Namibia, through Angola into DRC, Zambia and Zimbabwe. For the purpose of the present project, the study area was defined as that part of the Kalahari south of the Kunene and Zambezi rivers: that is Botswana, Namibia and South Africa.

This study is concerned with the use of the more common isotope ratios that have found wide application in the region and for which the local laboratories routinely cater. The stable isotopes in the water molecule, with their ratios $^{18}O/^{16}O$ and $^{2}H/^{1}H$ have been measured most generally[7]. Tritium (^{3}H) and radiocarbon (^{14}C) are the main indicators of groundwater residence (or age in some cases). The stable isotope ratio of carbon ($^{13}C/^{12}C$) is useful for the interpretation of carbonate solution in groundwater and its influence on ^{14}C levels in groundwater. Nitrogen isotopes, as $^{15}N/^{14}N$ in nitrate, have been used to identify groundwater nitrate sources.

The data that were obtained from the reports collected were translated to a standard format that can be generically listed. Provision had to be made for different usages in the three countries with respect to units (EC, NO_3 and alkalinity) and position (UTM and lat/long). Geology descriptions vary widely and have, for the time being, been maintained in the format that the original report authors have listed them. The main problem was the acquisition of positional data. Before GPS systems became general, location was not considered critical in these types of reports and in many cases only a cross on a map is available. Town, village and farm locations were used to locate borehole positions.

[7] Deuterium =2H

ACHIEVEMENTS

The database is structured as a flat Excel worksheet containing 2426 entries (= samples). It is estimated that this contains 70% of the potentially available samples. The data base fields are structured in such a way that they can be downloaded in an easily accessible data base system. The intention is that the data will be readily available to potential users through the distribution of the data on CD and storage in a public accessible data retrieval system (e.g. DWA and/or IAEA).

The elements of this data base have been set up in the course of this project. The data base has been populated with a fair number of samples, though not all of them have a full range of parameters entered. Positional data, in particular, is still lacking in many cases. These will require further follow-up.

A bibliography has been set up concurrent with the accumulation of reports. The bibliography lists all the sources of published information and reports containing isotope data from the Kalahari known to the authors and comprises 92 items at present.
Some general patterns that emerged from the data base with the presently available data:

- ^{18}O and deuterium roughly decreasing from east to west in accordance with prevailing rain gradients.
- Different local meteoric water lines for different areas. Some with evaporation signals, some not.
- Presence of high ^{14}C levels in many aquifers indicating local recharge

MOTIVATION AND AIMS OF THE PROJECT

Since the seminal paper in Nature on isotopic studies on Kalahari groundwater recharge (Verhagen et al., 1974), a number of groundwater investigations and surveys have shown that the region exhibits a wide range of recharge rates and groundwater residence times. This information has been acquired from both government-contract and curiosity-driven projects at a variety of sites across the Kalahari, mainly in Botswana as well as in Namibia and South Africa. Very little data is available in the formal scientific literature. Most of the data and the conclusions have been reported in theses and in reports to the project funders: government departments and international organisations. The existence of the data is not always known and extraction from the available sources very laborious and risky.

The aim of this study is to collect individual project reports and extract and compile available isotope and associated hydrochemical data. Interpretations based on this data can then be reviewed and common features sought for often very distinct project areas. An interpretation of this data in terms such as recharge, groundwater flow and other hydrogeological aspects as a contribution to the understanding of the overall hydrogeology of the Kalahari can then be made and will aid water resource decision makers at present and serve as a guide to the use of environmental isotopes in future groundwater resource investigations in similar hydrogeological situations.

METHODOLOGY

Area

The study area for this project has been defined as the Kalahari Thirstland. The SADC geological map produced by the Council for Geosciences in 1999 (Fig. 1) shows the Kalahari to extend from Botswana into South Africa (Northern Cape) Eastern Namibia, a major part of Angola and smaller portions of DRC, Zambia and Zimbabwe. For the purpose of the present project the study area was defined as the Kalahari south of the Kunene and Zambezi rivers: that is Botswana, Namibia and South Africa.

The sand cover in the area is of varying thickness, up to 400m near Oshakati (Namibia). In most of Botswana the thickness is in the order of 50-100m, with a few locations down to 150m and also some outcrops of pre-Kalahari rock above the sand. The geology underlying the Kalahari is quite complex (Fig. 2). The Karoo is the dominant aquifer, but basement rocks also provide good aquifers in places (e.g. Tsabong and Ghanzi).

The study area is arid with annual rainfalls less than 500mm and annual evaporation in excess of 3000mm (Thomas and Shaw, 1991). Groundwater recharge is therefore very episodic and difficult to measure (Beekman et al 1998; Obakeng 2007).

DATA AVAILABILITY

This study is concerned with the use of the more common isotope ratios that have found wide application in the region and for which the local laboratories routinely cater. The stable isotopes in the water molecule, with their ratios $^{18}O/^{16}O$ and deuterium ($=^{2}H$) $^{2}H/^{1}H$, have been measured most generally. Tritium (^{3}H) and radiocarbon (^{14}C) are the main indicators of groundwater residence (or age in some cases). The stable isotope ratio of carbon ($^{13}C/^{12}C$) is useful for the interpretation of carbonate solution in groundwater and its influence on ^{14}C. Nitrogen isotopes, as $^{15}N/^{14}N$ in nitrate, have been used to identify groundwater nitrate sources.

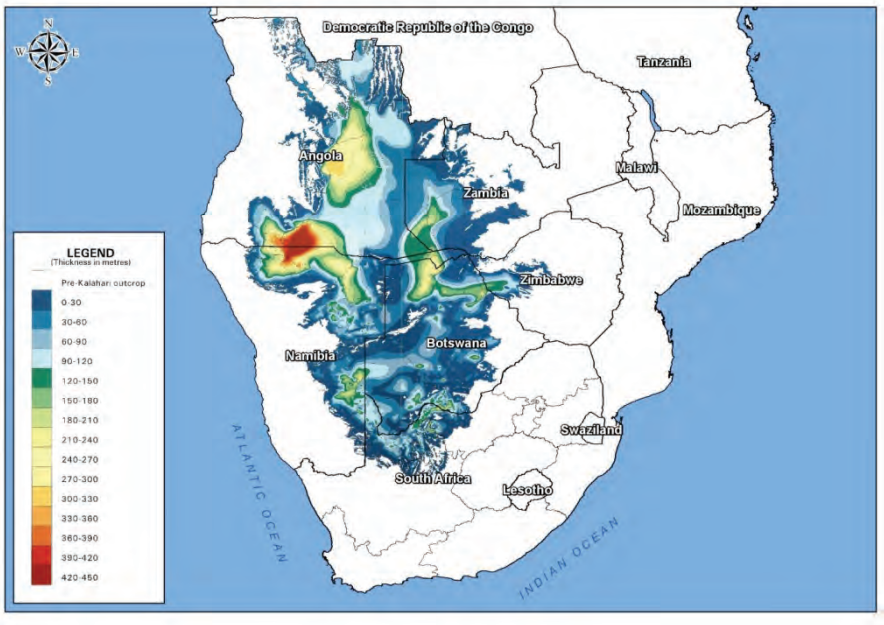

Figure 1: Location and thickness of the entire Kalahari basin

Figure 2: Map showing groundwater projects in the Kalahari that potentially include environmental isotope data. The letters indicate projects that were initially considered for inclusion.

Researchers from two environmental isotope laboratories in South Africa have had major involvement in the Kalahari region. The CSIR isotope laboratory in Pretoria has at various times been known as the Natural Isotopes division of NPRL, the Quaternary Dating Research Unit (QUADRU) and Natural Resources and the Environment (NRE).

The Environmental Isotope Laboratory (EIL) was part of the Nuclear Physics Research Unit, later the Schonland Research Institute of the University of the Witwatersrand, Johannesburg, and is now part of iThemba LABS Gauteng (NRF). These labs have been the main producers of environmental isotope data in the region. Most of the work was done in collaboration with hydrogeologists knowledgeably of the area. While the analytical data are often available, the background information usually resides with the collaborating institutions.

South African groundwater research in the Northern Cape Province was directed by the Department of Water Affairs (DWA/DWAF). The results were published in government reports or remained in files in the offices of the Department.

In Botswana most isotope data originate from regional projects undertaken by the Department of Geological Survey (DGS) and later the Department of Water Affairs (DWA). Botswana-based hydrogeological

consultants undertook regional surveys under contract to DGS or DWA. The results reside in reports to the sponsoring institutions and in theses that were undertaken with the same data. MSc and PhD theses were also undertaken independently by Botswana residents at universities in the UK, Germany and the Netherlands.

Before the independence of Namibia (1990) hydrogeological work, some with isotope components was done by CSIR and the (then) Geological Survey. Thereafter isotope data were generated by projects undertaken by organisations such as BGR, IAEA, JICA using isotope data generated by South African or overseas laboratories. Some of the data are available from reports.

Project list

The three authors of this report have been involved at various levels in investigations in the Kalahari since the 1970s. To a large extent the knowledge and background to this work is based on their experiences. Additional information has been obtained from many other interested and knowledgeable individuals.

The initial assessment of projects with suitable isotope data covered a large part of the study area (Fig. 2). Table 1 lists the projects or sites that are now considered as potentially yielding isotope data on the Kalahari. Some are small projects with a few dozen samples points; in others, a few hundred boreholes were sampled. Altogether they cover a substantial part of the Kalahari (Fig. 3).

Table 1: Listing of individual projects for which isotope data are known to exist at present

	Country	Year	Client	Isotope data	Full report
Bokspits TGLP	BW	2001	DWA	yes	
Botlhapatlou-Letlhakeng	BW	1991	DWA	yes	partial
Botlhapatlou-Letlhakeng	BW	1997	DGS	partial	partial
Botlhapatlou-Letlhakeng	BW	2009	DWA	yes	yes
Eastern Caprivi	NAM	2005	DWA	yes	yes
Eiseb Graben	NAM	2005	DWA	yes	yes
Ghanzi	BW	2005	CSIR	Yes	yes
Hunkhuwe-Lokolane	BW	2001	DGS	yes	partial
Jwaneng mine well fields	BW	ongoing	Wits	yes	yes
Kang-Phuduhudu	BW	2007	DWA	yes	full
Matsheng	BW	2008	DWA	yes	partial
Maun	BW	1997	DGS	yes	partial
Northern Cape, Gordonia	RSA		DWA		
Orapa mine well fields	BW	2001	Wits	yes	yes
Oshivelo artesian aquifer	NAM	2004	DWA	yes	yes
Palla Road	BW	1994	DWA	yes	yes
Serowe west wellfield	BW	1988	DGS	Yes	
Serowe/Orapa	BW	2005	BGR	yes	partial
Stampriet artesian basin	NAM	1982-2004	CSIR DWA IAEA JICA	yes	yes
Toteng-Sehitwe	BW	1993	DGS	yes	yes
Tsabong	BW	2002	DWA	yes	partial
Werda-Mabutsane-Sekoma	BW	2003	DGS	yes	partial

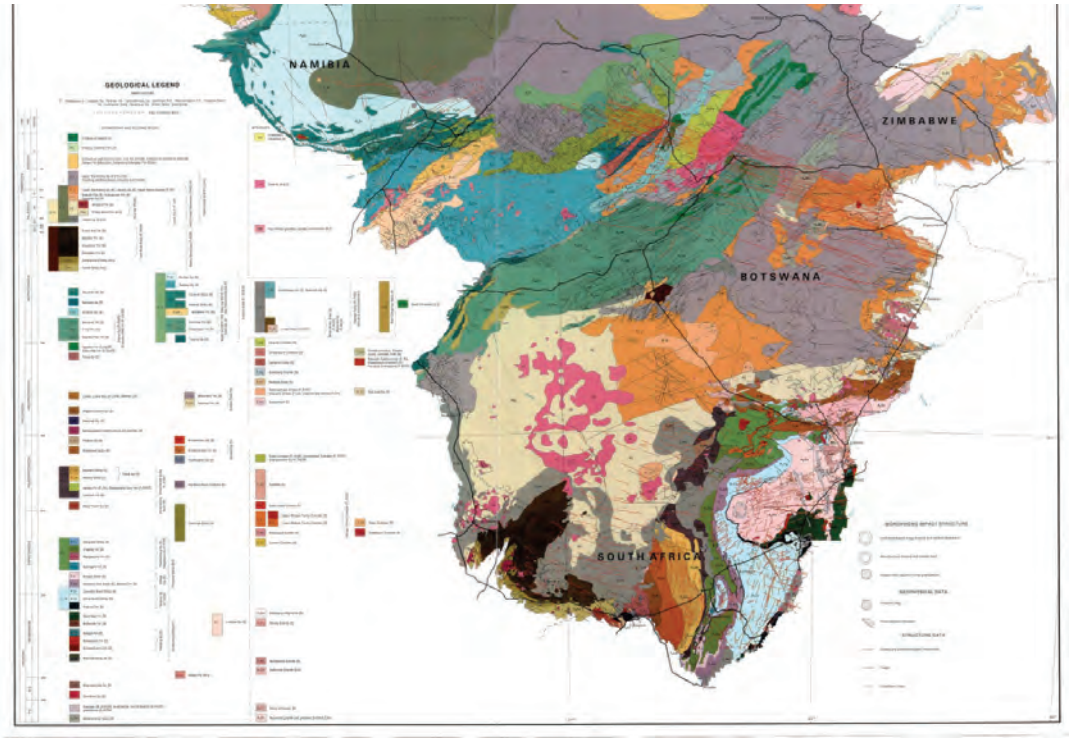

Figure 3: Sub-Kalahari geology of the study area.

Data collection

The South African Kalahari data were confined to projects commissioned by DWA. While the isotope data were available from the originating labs, the associated information on boreholes, geology and location could not all be located. In some cases recourse had to be sought to reading the geographic positions from copies of maps. This was the case in the attached case study on the Gordonia area.

For Namibia, permission was obtained from the Permanent Secretary for Agriculture, Water and Forestry for data to be released to the project. The data of the Stampriet artesian basin, originating from projects dating to the early 1970s, have been summarised by J Kirchner and G Tredoux. The information from the projects in Northern Namibia for which the Johannesburg lab provided data is sparse in the supplementary information.

The bulk of the isotope data used in this project originates from Botswana (Table 1). Permission was obtained from the Permanent Secretary for Minerals, Energy and Water Resources of Botswana for data to be released to the project. Reports of most of the government projects were found in the library of DGS in Lobatse. Electronic data was difficult to find at DWA and DGS due to staff changes. Some of the originating consultants were however able to supply most of the data in electronic format, which is an important time saver.

Data base

The data that were obtained were translated to a standard format (Table 2) that can be generically listed. Provision had to be made for different usages in the three countries with respect to units (EC, NO_3 and alkalinity) and position (UTM and lat/lon). Geology descriptions vary widely and have, for the time being, been maintained in the format that the original report authors have listed them. The isotopes listed are the ones that at one time or another were analysed in South Africa (Table 2). Exotic isotopes and dissolved gases (noble gases and CFCs) are not included. The main problem was the acquisition of positional data. Before GPS systems became general, location was not considered critical in these types of reports and in many cases only a cross on a map is available. Town, village and farm locations are then used to locate a borehole: hence the field in the database indicating the precision of location.

The database is presently structured as a flat Excel worksheet containing 2426 entries (= samples) It is estimated that this contains 70% of the potentially available samples. The data base is structured in such a way that it can be downloaded in an easily accessible system, for example the SA DWA groundwater archive (DWA 2012) or the IAEA ISOHIS (IAEA 2013) system. The intention is that the data will be readily available to potential users.

ISOTOPE DISTRIBUTIONS WITHIN THE KALAHARI AQUIFERS

The database is still incomplete especially so since many sample positions have not yet been entered. Nevertheless, the existing data available do allow some generalisations to be made already.

Fig. 4 shows the results of two studies in the Okavango Delta (Hutton & Dincer 1976, Tredoux & Talma 1997).
The surface water of the Okavango River shows steady isotope enrichment along the flow of the river.
This is strikingly reflected in the isotope composition of borehole water in and alongside the river bed. There is no isotopic sign of any direct rainfall recharge; all borehole waters show the signs of seepage from the Okavango River water. Similarly, aquifers along rivers in southern Botswana and the Northern Cape Province show low $\delta^{18}O$ indicative of recharge from the episodic river flows (see the Gordonia case study below).

Table 2: Data fields used in the Kalahari isotope data base

Serial_number	*Radiocarbon*
Who	*RadiocarbonSD*
Area	*Carbon13*
Country	*Nitrogen15*
Project	*pH_Field*
Place	*Temperature*
GpsLat	*pH_Lab*
GpsLon	*EC_mSm*
GpsPrecision	*EC_uScm*
UtmX	*TDS*
UtmY	*Ca*
SamDate	*Mg*
SamDetails	*Na*
LabReference	*K*
DataSource	*Cl*
SampleType	*SO4*
BhName	*HCO3*
Bh_ID	*CO3*
BhDepth	*F*
WaterLevel	*NO3_N*
BhType	*NO3*
YieldAsLitrePerSec	*NH4_N*
Aquifer	*NH4*
SamDepth	*TAL_mgCaCO3*
Oxygen18	*TAL_mEqL*
Deuterium	*Si*
Tritium	*Comments*
TritiumSD	

Deuterium-^{18}O plots for various projects throughout the Kalahari (Fig. 5) show a range of values on and just below the GMWL with a number of samples showing some extent of evaporation. There is a continental effect with the eastern group (Bothlapathlou, Serowe, Orapa) having higher δD and $\delta^{18}O$ than the western group (Oshivelo, Etosha and Otavi). A number of samples from most of these project areas are way below the GMWL and indicate some measure of evaporation enrichment.

A test for evaporation enrichment variations is to compare samples of different age within an aquifer. Using ^{14}C as the best proxy for age, its correlation with ^{18}O within individual areas is not evident (Fig. 6). The only area with some isotope change with time appears to be Bothlapathlou. Here detailed sampling along flow lines has shown older water to have lower ^{18}O and D content (Selaolo 1998, Kulongowski et al., 2004) consistent with the classical palaeowater types found worldwide (Edmunds 2005). Extensive previous work in the artesian basin of Stampriet has shown different stable isotope patterns in the confined aquifers in this basin (Vogel et al 1982, JICA 2002, Kirchner et al 2002). The high ^{14}C values in many parts of the Kalahari (Fig. 6) (confirmed by tritium data) indicate that recharge is occurring in many places, although the rates are uncertain.

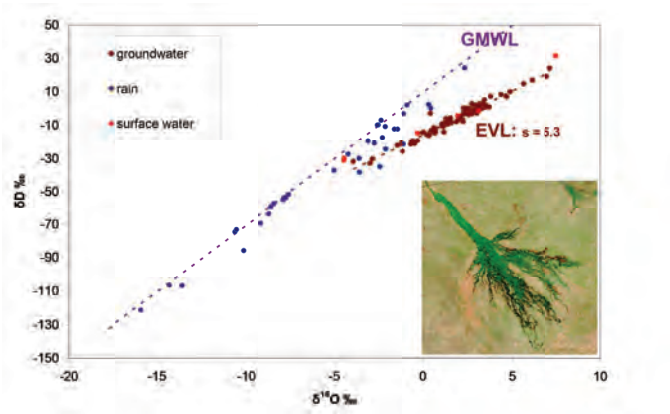

Figure 4: Stable isotope characterisation of infiltrated groundwater by the evaporated signal of Okavango surface water. Local rainfall is isotopically quite distinct.

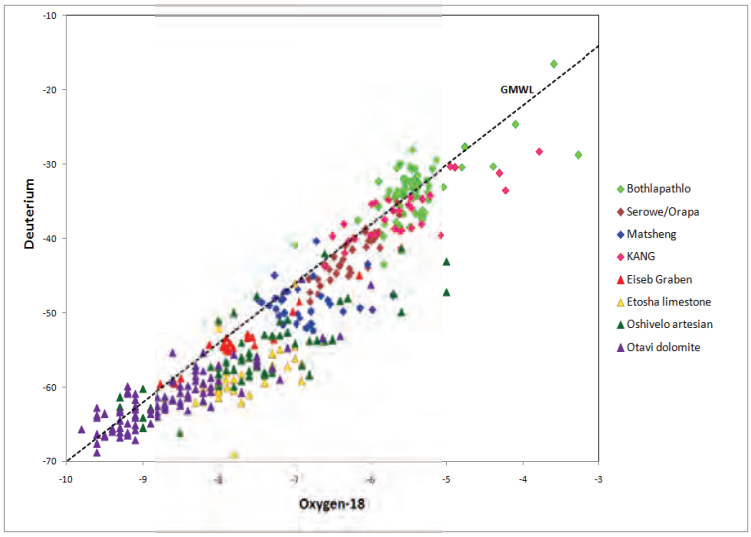

Figure 5: Deuterium-^{18}O plot for various projects throughout the Kalahari

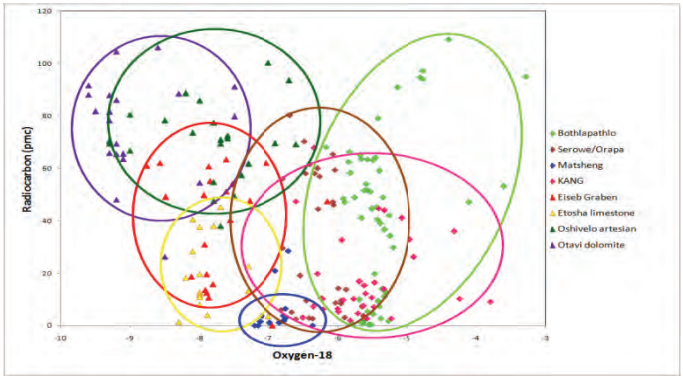

Figure 6: ^{14}C-^{18}O plots for various projects throughout the Kalahari

BIBLIOGRAPHY

A bibliography has been set up concurrent with the accumulation of data (Table 3). This lists all the sources of published information containing isotope data from the Kalahari known to the authors. In some cases only draft reports were available. The list now (March 2013) comprises 92 items.

Table 3: Bibliography of papers, reports and theses dealing with environmental isotopes in the Kalahari

2012	Stadler, S., Talma, A.S., Tredoux, G., Wrabel, J. 2012. Identification of sources and infiltration regimes of nitrate in the semi-arid Kalahari: Regional differences and implications for groundwater management. Water SA 38(2), 213-224
2010	Stadler, S., Osenbrück, K., Duijnisveld, W.H.M., Schwiede, M., and Böttcher, J., 2010b. Linking chloride mass balance infiltration rates with chlorofluorocarbon and SF6 groundwater dating in semi-arid settings: potential and limitations– Isotopes in Environmental and Health Studies 46 (3): 312 - 324.
2010	Stadler, S., Osenbrück, K., Suckow, A., Himmelsbach, T., Hötzl, H., 2010a. Groundwater flow regime, recharge and regional-scale solute transport in the semi-arid Kalahari of Botswana derived from isotope hydrology and hydrochemistry - Journal of Hydrology 388 (2010) 291–303.
2009	Osenbrück, K., Stadler, S., Sültenfuß, J., Suckow, A., Weise, S. M., 2009: Impact of recharge variations on water quality as indicated by excess air in groundwater of the Kalahari, Botswana. Geoch. Cosmoch. Acta 73, 911–922 .
2009	Talma, A.S., Tredoux, G. Engelbrecht, J.H.P., 2009. Behaviour of nitrogen in the unsaturated zone in southern Africa. In: Application of Isotopes to the Assessment of Pollutant Behaviour in the Unsaturated Zone for Groundwater Protection, TECDOC-1618, IAEA, Vienna
2008	DWA. Matsheng groundwater development project. Draft final report by Water Resources Consultants
2008	Stadler, S., Osenbrück, K., Knöller, K., Suckow, A., Sültenfuß D., J., Oster, H., Himmelsbach, T., Hötzl, H., 2008. Understanding the origin and fate of nitrate in groundwater of semi-arid environments. J. Arid Env. 72 (10), 1830-1842.
2007	DWA. 2007. Kang-Phuduhudu regional groundwater resources investigation and development project. Final report by Wellfields Consulting Services
2007	Schwiede, M. 2007. Nitrogen Dynamics and Nitrate Leaching from sandy Soils of the semi-arid Kalahari, Botswana. Ph.D. thesis, Univ Hannover.
2006	Cheney CS, Rutter HK, Farr JL and Phofuetsile P. 2006. Hydrological potential of the deep Ecca aquifer of the Kalahari, Botswana. Quarterly Journal of Engineering Geology and Hydrogeology, 39, 303-312.
2006	Sarma D, Simmonds ALE, Talma AS, Tredoux G and Moehadu OM (2006). Hydrochemical evolution and recharge of groundwater in the Olifantshoek Sequence Quartzite aquifer near Tsabong, Southwestern Botswana. Proc Conf of the Hydrological Association of Namibia, Windhoek, 23-25 March 2006.
2006	Verhagen, BT and Butler, MJ (2006). Long-term data series and the hydrological model of Jwaneng mine northern wellfield. In: Isotope assessment of Long term groundwater exploitation, TECDOC 1507. International Atomic Energy Agency, Vienna.
2006	Sarma D, Simmonds ALE, Talma AS, Tredoux G and Moehadu OM (2006). Hydrochemical evolution and recharge of groundwater in the Olifantshoek Sequence Quartzite aquifer near Tsabong, Southwestern Botswana. Proc Conf of the Hydrological Association of Namibia, Windhoek, 23-25 March 2006.
2006	Verhagen, B.T.and Butler, M.J. (2006). Long-term isotope data series and the hydrological model of Jwaneng mine northern well field. In: Isotopic assessment of long term groundwater exploitation, IAEA-TECDOC 1507, 97-125, International Atomic Energy Agency, Vienna..
2006	Stadler, S. Investigation of Natural processes leading to Nitrate enrichment in Aquifers of Semi-Arid environments. PhD thesis. University of Karlsruhe. 238p.
2005	Stadler, S. 2005. Investigation of natural processes leading to nitrate enrichment in aquifers of semi-arid regions. Ph.D. Thesis., Dept Appl. Geol., Univ. Karlsruhe. Available as: Schriftenreihe angewandte Geologie Karlsruhe (2006) 71. 238p.
2005	Tredoux, G., Engelbrecht, J.F.P., Talma, A.S., 2005. Nitrate in groundwater in arid and semi-arid parts of southern Africa. In: Environmental Geology in Semi-Arid Environments, Vogel, H., Chilume, C., (eds), 121-133, Dept. Geol. Surv., Lobatse. 289p
2005	Talma, A.S., Tredoux, G., 2005. Isotopic source identification of nitrate in the groundwater of semi-arid southern Africa. In: Environmental Geology in Semi-Arid Environments, Vogel, H., Chilume, C., 92-102, Dept. Geol. Surv., Lobatse. 289p.
2004	DWA/BGR 2004. Groundwater investigations in the Eiseb graben. Main hydrogeological report. Report of Technical Cooperation Project No. 2001.2475.0, Volume IV.GW.3.1. Windhoek, Namibia.
2004	Kulongoski JT, Hilton DR and Selaolo ET, 2004. Climate variability in the Botswana Kalahari from the late Pleistocene to the present day. Geophysical Research Letters 31, L10204.
2003	Rahube, 2003. Recharge and Groundwater resources evaluation of the Lokalane-Ncojane Basin (Botswana) using numerical modelling. MSc thesis
2003	Wellfields Consulting Services. 2003. Werda-Mabutsane-Sekoma TGLP groundwater Survey (Project 10/2/18/2000-2001). Report to DGS, Lobatsi
2003	Geoflux. 2003. Bokspits TGLP area groundwater potential survey. Report to DGS, Lobatsi
2003	Xu Y and Beekman HE (eds) 2003. Groundwater recharge estimation in southern Africa. UNESCO IHP series 64, UNESCO, Paris, 207p.
2002	JICA, 2002: The Groundwater Potential Evaluation and Management Plan in the Southeast Kalahari (Stampriet) Artesian Basin in the Republic of Namibia, Final Report submitted to the Department of Water Affairs, Namibia.

2002	Kirchner, J., Tredoux, G., Wierenga, A., and Christelis, G., 2002: Applying environmental isotopes to a Hydrogeological model of the Stampriet Artesian Basin. IAEA regional model project RAF/8/029. Department of Water Affairs, Windhoek.
2002	Department of Water Affairs 2002. Tsabong Groundwater Resources Investigation. Final report produced by Resource Services, Gaborone.
2002	Palla-Road Groundwater Resources Investigation. Phase 1. CBT 10/3/26/91-92. Final Report. Appendix 10. Environmental Impact Assessment.
2002	De Vries, J.J., Simmers, I., 2002. Groundwater recharge: an overview of processes and challenges. Hydrogeol. J. 10, 5-17.
2001	Chilume, C.J., 2001: Hydrogeological Assessment of the South-western Karoo basin. A case study from Lokalane, Botswana.
2001	Resources Services, 2001: Tsabong Groundwater Investigation Assessment and Development. Final Report. Department of Water Affairs. Gaborone. Botswana.
2001	Wellfield Consulting Services (WCS), 2001: Hunhukwe/Lokalane Groundwater Survey Project (TB 10/2/1/98-99), Wellfield Consulting Services, Final Report submitted to the Department of Geological Survey, Lobatse, Botswana.
2001	Department of Water Affairs (2001a) Final Report, Tsabong groundwater investigation, assessment, and development project (TB10/3/24/98-99). Resources Services, Gaborone, Botswana.
2000	Schaffner B, Chen YY, Kelepile T, Kinzelbach W, Carlsson L and Mannathoko I, (2000). Scientific support for sustainable groundwater management: A modelling study in Botswana using environmental tracers. In: Sililo, O. (ed), Groundwater: Past Achievements and Future Challenges, 291-296, Balkema, Rotterdam, 2000 1144p.
1999	Beekman HE, Selaolo ET and de Vries JJ (1999). Groundwater recharge and resources assessment in the Botswana Kalahari. GRES II project: executive summary, Dept of geological Survey, Lobatse; University of Botswana, Gaborone: Free University Amsterdam, Netherlands.
1999	Wrabel J 1999. Estimation of groundwater recharge in semi-arid Namibia using the Chloride-Mass-Balance-Approach (in German). PhD thesis, Univ Wurzburg. Published in Hydrogeologie und Umwelt, Vol 16, 1-155.
1999	Verhagen, B.Th., Bredenkamp, D.B., Janse van Rensburg, H. and Farr, J. (1999). Recharge quantification with radiocarbon: independent corroboration in three Karoo aquifer studies in Botswana. International Symposium on Isotope Techniques in Water Resources Development and Management. IAEA-SM-361. IAEA, Vienna
1998	Tredoux, G., Masie, M. & Talma, A.S. 1998. Characterisation of the Shashe river aquifer system by means of hydrochemistry and stable isotopes. "Groundwater in Arid Climates". Conference at the University of Botswana, Gaborone, 23-25 June 1998.
1998	Selaolo, E.T., (1998) Tracer studies and groundwater recharge assessment in the eastern fringe of the Botswana Kalahari. Published PhD thesis Free University Amsterdam, the Netherlands.
1998	Stute, M and Talma, AS (1998). Glacial temperatures and moisture transport regimes reconstructed from noble gases and ^{18}O in Stampriet aquifer, Namibia. In: Isotope Techniques in the Study of Environmental Change: Proceedings of Symposium SM-349, 14-18 April 1997. 307-318. IAEA, Vienna, 932pp.
1997	Beekman HE and Selaolo ET (1997). Groundwater recharge and resources assessment in the Botswana Kalahari – Hydrochemical, isotope and noble gases tracer study in the Letlhakeng-Botlhapatlou area. GRES II project: technical report, Dept of geological Survey, Lobatse; University of Botswana, Gaborone: Free University Amsterdam, Netherlands.
1997	Beekman HE, Selaolo ET, van Elswijk, R, Lenderink N and Obakeng, OTO (1997). Groundwater recharge and resources assessment in the Botswana Kalahari – Chloride and isotope profiling studies in the Letlhakeng-Botlhapatlou area and the Central Kalahari. GRES II project: technical report, Dept of geological Survey, Lobatse; University of Botswana, Gaborone: Free University Amsterdam, Netherlands.
1997	Nijsten GJ and Beekman HE (1997). Groundwater recharge and resources assessment in the Botswana Kalahari – Groundwater flow study in the Letlhakeng-Botlhapatlou area. GRES II project: technical report, Dept of geological Survey, Lobatse; University of Botswana, Gaborone: Free University Amsterdam, Netherlands.
1997	Tredoux, G and Talma, AS (1997). Maun Groundwater Development Project: Hydrochemistry and Environmental Isotopes. Report to Eastend Investments, Botswana. CSIR contract report ENV/S-C97092.
1996	Beekman, H.E., Gieske, A. and Selaolo, E.T. (1996) GRES – groundwater recharge studies in Botswana (1987-1996). Botswana Journal of Earth Sciences, V 3, pp. 1-17.
1996	Morosini, M., 1996b: Chemical-Isotopic Character, Origin and Evolution of Groundwater in Western Ghanzi District, Botswana. Hydrogeochemical Report for the TGLP Ghanzi/Makunda Groundwater Survey. Department of Geological Survey.
1996	Verhagen, B. Th., Marobela, C., Sawula, G. and Kgarebe, B. (1996) Geohydrological and mineralization studies with environmental isotopes in a large Kalahari ranching development. Isotopes in Water Resources Development. IAEA-SM-336.91-105. IAEA, Vienna.
1996	Morosini, M., 1996. Chemical-isotopic character, origin and evolution of groundwater in western Ghanzi District, Botswana. Dept. Geol. Surv., Lobatse, Botswana. 56p, figures and tables.
1995	Bredenkamp, D.B., Botha, L.J., van Tonder, G.J., and van Rensburg, H.J. (1995). Manual on Quantitative Estimation of Groundwater Recharge and Aquifer Storativity. Pretoria: Water Research Commission. TT 73/95.
1995	Gieske, A. Hydrodynamics of 14C analysis in unconfined aquifers. In: Groundwater '95, Midrand: Ground Water Division of the Geol Soc of S Afr, 1995,
1995	Verhagen, B.T., Levin, M., Farr, J., and Gumiremhete, R. Groundwater recharge in the Kalahari: unravelling the evidence from Jwaneng mine to Palla Road, Botswana. Ground Water '95. In: Conf. on Ground water Recharge and Rural Water Supply, Midrand, South Africa, 1995.

1995	Verhagen, B.T., Marobela, C., Sawula, G., and Kgarebe, B. Geohydrological and mineralisation studies with environmental isotopes in a large Kalahari ranching development. In: Isotopes in Water Resources Management. Procs Symposium, Vienna: IAEA, 1995, p. 91-106.
1995	Verhagen, B.Th., 1995. Semiarid zone groundwater mineralization processes as revealed by environmental isotope studies. In: Application of Tracers in Arid Zone Hydrology, Adar, E., Leibundgut, C., 245-266. IAHS Publ. 232
1994	DWA., 1994: Palla-Road Groundwater Resources Investigation. Phase 1. CBT 10/3/26/91-92. Final Report. Appendix 10. Environmental Impact Assessment.
1994	Molebatsi, T. (1994) Occurrence and origin of saline groundwaters of the Tsabong Region, south-west Botswana. Thesis submitted in partial fulfilment of M.Sc. Degree, University College London.
1994	Van Rensburg HJJ and Bush RA, (1994). Jwaneng northern wellfield - modelling of groundwater flow with optimized management recommendations on wellfield utilization. Anglo American Corporation, Report CED/029/04
1994	Carney, J.N., Aldiss, D.T. and Lock, N.P. (1994) The geology of Botswana. Bulletin 37. Geological Survey of Botswana.
1994	Molebatsi, T. (1994) Occurrence and origin of saline groundwaters of the Tsabong Region, south-west Botswana. Thesis submitted in partial fulfilment of M.Sc. Degree, University College London.
1994	Geoflux (1994) Groundwater potential survey. Toteng/Sehitwa TGLP area. TB 10/2/90-91. Final report to Geological Survey Dept. Vol.1 232 pp. Gaborone
1994	BRGM, 1994. Mmamabula Groundwater resources investigation: Phase II Khurutse area. Report to DGS, tender TB 10/2/3/90-91, 1994
1992	Gieske, A. (1992). Dynamics of Groundwater Recharge: A Case Study in Semi-Arid Eastern Botswana. Free University, Amsterdam.
1991	BRGM (1991). Evaluation of groundwater resources (GS10): Letlhakeng-Botlhapatlou groundwater project, main report. BRGM, Orleans, France.
1991	SMEC,WLPU,SGAB (1991) Botswana national water master plan study. Final report to DWA, (LCCN 95980213). Gaborone.
1991	Verhagen, B.T. (1991) Detailed geohydrology with environmental isotopes – A case study at Serowe, Botswana. Isotope Techniques in Water Resources Development 1991; IAEA-SM-319. 345-362. IAEA, Vienna.
1990	Verhagen, B.T. Isotope hydrology of the Kalahari: Recharge or no recharge? Palaeoecology of Africa 21:143-158, 1990.
1989	Verhagen, B.T. and Brook, M.C. (1989) The isotope hydrology of the northern well field, Jwaneng diamond mine, Botswana. In: Proc Symp: Ground Water and Mining, Randburg: p. 161-169.
1988	Phofuetsile Thesis UCL 1988. Hydrochemistry of the Groundwater in the Kalahari-south western Botswana.
1988	Swedish Geological Survey (1988). Serowe: Groundwater resources evaluation project. Final Report CTB No 10/2/7/84-85 to BGS, Botswana. SGAB International, Stockholm, 286pp.
1987	Verhagen, B.T. 1987. Environmental isotopes suggest a recharge model for the well field supplying Jwaneng Mine, Botswana. In: Isotopes Techniques in the Water Resources Development, Vienna: IAEA.
1985	Levin, M, Talma, AS and Vogel, JC (1985). Geohydrological investigation of an uranium anomaly near Vanzylsrus in the northern Cape Province. Trans. geol. Soc. S. Afr. 88, 529-540.
1985	Verhagen, B.T. 1985 Isotope hydrology of ground waters of the Kalahari, Gordonia. Trans geol Soc S Afr 88(3):517-522, 1985.
1985	Verhagen, B.T. (1985) Rain recharge to Kalahari ground waters as revealed in a wellfield. In: Groundwater 1985, Programme and extended abstracts of a symposium, Johannesburg: Geological Society of South Africa, p. 114-116
1984	De Vries, J.J., 1984: Holocene depletion and active recharge of the Kalahari groundwaters: a review and an indicative model. J. Hydrol. 70, 221-232.
1984	Heaton, T.H.E., 1984. Sources of the nitrate in phreatic groundwater in the Western Kalahari. J. Hydrol. 67, 249-259.
1983	Verhagen, B.T. (1983) Environmental isotope study of a groundwater supply project in the Kalahari of Gordonia. In: Isotope Hydrology, IAEA, Vienna. 415-432.
1983	Heaton, T.H.E., Talma, A.S., Vogel, J.C., 1983. Origin and history of nitrate in confined groundwater in the Western Kalahari. J. Hydrol 62, 243 -262.
1982	Mazor, E. 1982 Rain recharge in the Kalahari - a note on some approaches. J Hydrol 55:137-144, 1982.
1982	Vogel, JC, Talma, AS and Heaton, THE (1982). The age and isotopic composition of groundwater in the Stampriet artesian basin, SW Africa. CSIR Research Report.
1982	Foster, S.S.D., Bath, A.H., Farr, J., and Lewis, W.J. The likelihood of active groundwater recharge in the Botswana Kalahari. J Hydrol 55:113-136, 1982.
1982	Verhagen, B.T. (1982) The isotope hydrology of ground waters of the Kalahari, Gordonia. In: Ground Water '82. Abstract. Johannesburg: Geol. Soc. S.Afr. Ground Water Div., 117-122.
1982	Huyser, D.J., 1982. The Chemical Quality of the Underground Waters of South-West Africa/Namibia (in Afrikaans). Vol 1-3, Dept. Wat. Aff., Pretoria/Windhoek.
1981	Vogel, JC, Talma, AS and Heaton, THE (1981). Gaseous nitrogen as evidence for denitrification in groundwater. J. Hydrol. 50, 191-200.
1980	Mazor, E., Bielsky, M., Verhagen, B.T., Sellschop, J.P.F., Hutton, L., and Jones, M.T., 1980. Chemical composition of groundwaters in the vast Kalahari Flatland. J Hydrol 48:147-165, 1980.
1979	Dziembowski ZM, Verhagen BT, Salgado HR, Smith PE, Erasmus CJH & McGeorge IB (1979). Ground water studies in the Gamogara catchment. Report to the Water Research Commission. Nuclear Physics Research Unit, Johannesburg.

1979	*Verhagen, B.Th., Smith, P.E., McGeorge, I. and Dziembowski, Z.M. (1979) Tritium profiles in Kalahari sands as a measure of rain recharge. Isotope Hydrology 1978 Vol.II. IAEA-SM-228. 733-751. IAEA, Vienna.*
1977	*Mazor, E., Verhagen, B.T., Sellschop, J.P.F., Jones, M.T., Robins, N.E., Hutton, L., and Jennings, C.M.H. (1977). Northern Kalahari groundwaters: Hydrologic, isotopic and chemical studies at Orapa, Botswana. J Hydrol 34:203-234.*
1976	*Hutton, L.G. & Dincer, T. (1976): Chemistry and stable isotope composition of Okavango Delta waters. Investigation of the Okavango Delta as a Primary Water Resource for Botswana. UNDP/FAO, AG:DP/BOT/71/506, Technical Note 23.*
1975	*Vogel, J.C. and van Urk, H. Isotopic composition of groundwater in semi-arid regions of Southern Africa. J Hydrol 25:23-36, 1975.*
1974	*Jennings CMH, 1974. The hydrogeology of Botswana. PhD thesis University of Natal, Pietermaritzburg*
1974	*Verhagen, B.T., Mazor, E., and Sellschop, J.P.F. Radiocarbon and tritium evidence for direct recharge to groundwater in the northern Kalahari. Nature 249:643-644, 1974.*
1974	*Vogel, JC, Thilo L and Van Dijken M 1974. Determination of groundwater recharge with tritium. Journal of Hydrology 23 , 131-140.*
1969	*Vogel, J.C. and Bredenkamp, D.B. A study of the subterranean water in the Southern Kalahari with the aid of Carbon-14 dating and isotope analysis. Pretoria: NPRL, CSIR. , 1969.*

RECOMMENDATIONS FOR FURTHER WORK

It has not been possible, within the time frame of the present project, to complete the data base. There are project data sets that have not yet been made available to the authors. There are sites that are incomplete: especially with the all-important positional data. These gaps need to be filled.

Once there is more data available, will it be possible to evaluate sub-regions for communality of properties. A start of this process is made with the three case studies presented on the CD version. These evaluations can then be extended.

CONCLUSIONS

The elements of a data base have been set up in the course of this project. The data base has been populated with a fair number of samples, though not all of them have a full range of parameters entered. Positional data, in particular, is still lacking in many cases. These will require further follow-up. A start has been made in drawing together written material, either published or not in readily accessible form, to act as basis for an envisioned regional hydrogeological concept of the Kalahari.

Acknowledgements

A work of this nature is heavily dependent on collaboration of other individuals. We thanks the following for their help in providing and procuring data used during this project; J Kirchner (Windhoek), Z Dziembowski and E van Wyk (Pretoria), T Bakaya, R Gumiremhete, J Farr (Gaborone), M Butler (Johannesburg). We thank S Adams, G Christelis and I Mannathoko for their assistance in obtaining official approval from the authorities. We appreciate the help of E Bertram, E van Wyk (DWA) and S Terzel (IAEA) with data base issues.

REFERENCES

Beekman, H.E., Selaolo, E.T. (1997). Groundwater recharge and resources assessment in the Botswana Kalahari – Hydrochemical, isotope and noble gases tracer study in the Letlhakeng-Botlhapatlou area. GRES II project: technical report, Dept of Geological Survey, Lobatse; University of Botswana, Gaborone: Free University Amsterdam, Netherlands.

DWA (2013). The National Groundwater Archive. Department of Water Affairs, Pretoria. URL: http://www.dwa.gov.za/groundwater/nga.aspx

Edmunds, W.M. (2005). Groundwater as an archive of climatic and environmental change. In : Aggarwal PK, Gat JR & Froehlich K (eds), Isotopes in the Water Cycle: past, present and future of a developing science, 341-352. Springer, Dordrecht, 381p.

Hutton, L.G., Dincer, T. (1976). Chemistry and stable isotope composition of Okavango Delta waters. Investigation of the Okavango Delta as a Primary Water Resource for Botswana. UNDP/FAO, AG:DP/BOT/71/506, Technical Note 23.

IAEA (2012). Isotope Hydrology Information System, International Atomic Energy Agency, Vienna. URL: http://www-naweb.iaea.org/napc/ih/IHS_resources_isohis.html

JICA, (2002) The Groundwater Potential Evaluation and Management Plan in the Southeast Kalahari (Stampriet) Artesian Basin in the Republic of Namibia, Final Report submitted to the Department of Water Affairs, Namibia.

Kirchner, J., Tredoux, G., Wierenga, A., Christelis, G. (2002). Applying environmental isotopes to a Hydrogeological model of the Stampriet Artesian Basin. IAEA regional model project RAF/8/029. Department of Water Affairs, Windhoek.

Kulongoski, J.T., Hilton, D.R., Selaolo, E.T. (2004). Climate variability in the Botswana Kalahari from the late Pleistocene to the present day. Geophysical Research Letters 31, L10204.

Obakeng, O.T. (2007). Soil moisture dynamics and evapotranspiration at the fringe of the Botswana

Kalahari. PhD thesis, Free University Amsterdam. 225pp.

Selaolo, E.T. (1998). Tracer studies and groundwater recharge assessment in the eastern fringe of the Botswana Kalahari. PhD thesis, Free University Amsterdam, the Netherlands.

Thomas, D.S.G., Shaw, P.A. (1991). The Kalahari Environment. Cambridge University Press, Cambridge. 284p.

Tredoux, G., Talma, A.S. (1997). Maun Groundwater Development Project: Hydrochemistry and Environmental Isotopes. Report to Eastend Investments, Botswana. CSIR contract report ENV/S-C97092.

Verhagen, B.T., Mazor, E., Sellschop, J.P.F. (1974). Radiocarbon and tritium evidence for direct recharge to groundwater in the northern Kalahari. *Nature* 249:643-644.

Vogel, JC, Talma, A.S. Heaton, T.H.E. (1982). The age and isotopic composition of groundwater in the Stampriet artesian basin, SW Africa. Research Report, CSIR, Pretoria.

CASE STUDY

ENVIRONMENTAL ISOTOPE CONTRIBUTION TO A MULTI-DISCIPLINARY GROUNDWATER RESOURCE ASSESSMENT IN EASTERN BOTSWANA

B. Th. Verhagen

A comprehensive groundwater assessment was conducted in the south-eastern Kalahari of Botswana at Palla Road in the early 1990s by Wellfield Consulting Services, Gaborone in cooperation with the International Institute for Aerospace Surveys and Earth Sciences, Enschede, Netherlands (WCS 1995).

This project had some unique features in that a variety of approaches to the estimation of rain recharge to an already established groundwater resource was being considered with the aim of expanding the extraction capacity both as an emergency and later a standby supply to the national water grid of Botswana. A further feature was that this was undertaken in a typical Kalahari environment, albeit at the edge of what is regarded as the main Kalahari basin of that country.

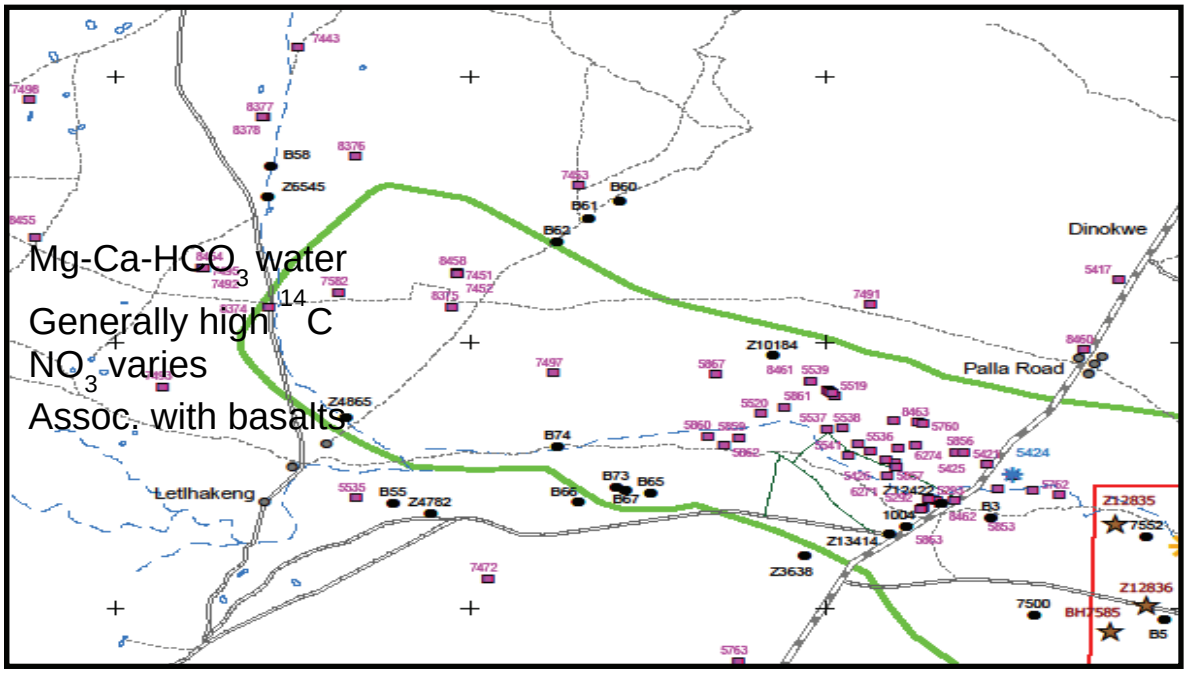

Figure 1: Map of the Palla Road project area showing Ntane sandstone observation and other borehole positions

The primary objective of the project was quantitatively to evaluate the groundwater resources of the Ntane Sandstone aquifer in the Palla Road region, eastern Botswana, to assess the ability of these resources to make a significant contribution to the North South Carrier Water Transfer Scheme. Pre-existing information, which was largely concentrated in the existing Palla Road Wellfield area, indicated that the Ntane Sandstone aquifer underlying the 1650 km^2 of the Palla Road Project Area (23.0-23.7S; 26.1-26.9E; Fig. 1) has considerable resource potential. A conceptual hydrogeological model indicated a Ntane (Stormberg) sandstone aquifer largely covered by varying thicknesses of Stormberg basalt. The entire area is covered by Kalahari deposits up to 40m deep.

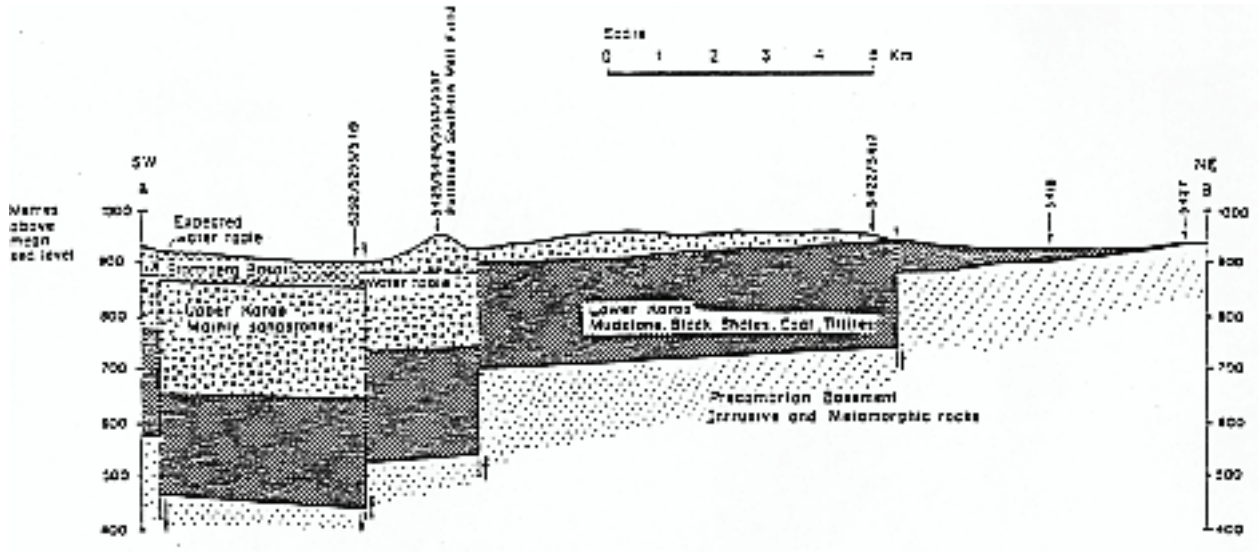

Figure 2: Schematic model NE-SW section through the Palla Road study area showing considerably block-faulted Karoo geology

Five major arcuate northwest/southeast trending structures constitute a horst-graben environment in these upper Karoo strata. A NE-SW model geological section is shown in Fig. 2. These structures also strongly influence the piezometry of the project area, with an elongate piezometric low aligned parallel to the structures (Fig. 3). The area is generally featureless with some Karoo outcrops with a general topographical gradient directed NW-SE. The same applies to the regional piezometry. A total of 43 exploratory boreholes were drilled, a small number specially constructed in order to gather data on the deeper Ecca aquifers.

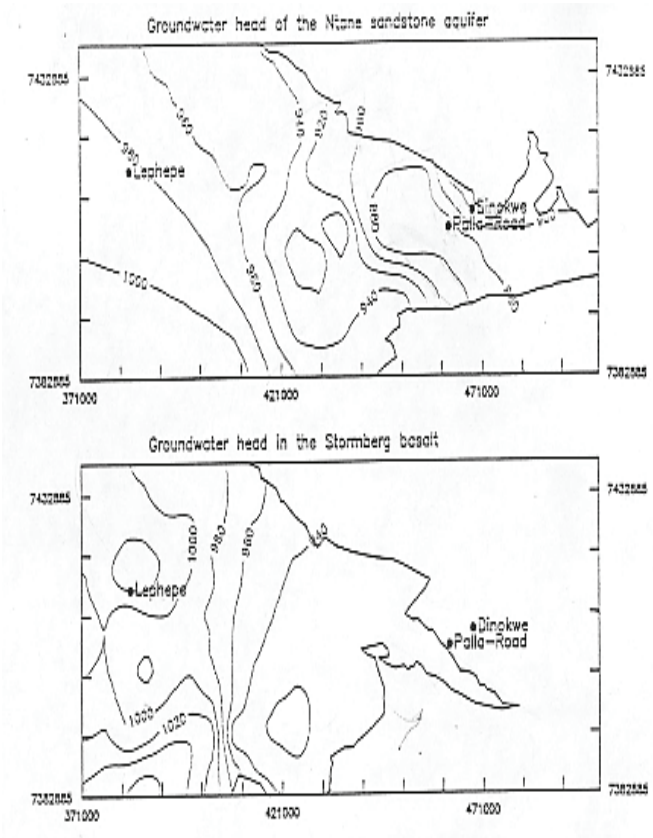

Figure 3: Piezometric heads in the Ntane sandstone and overlying basalt respectively. Faulting re-directs groundwater flow towards the SE

Water quality in the basalt and sandstone aquifers is generally good, except for often high salinities encountered in the underlying Ecca or the bottom of the Ntane sandstone profile.

A number of studies were conducted to quantify the volume and distribution of recharge to the main Ntane Sandstone aquifer system. These included the investigation of the chloride mass balance of the groundwater system, analysis and interpretation of the environmental isotope composition of the groundwater body and an evaluation of the areal recharge potential by means of a detailed GIS study calibrated by chloride measurements on shallow auger holes. An additional activity included a numerical model of the Ntane Sandstone aquifer assembled and calibrated, involving the integrated evaluation of all data. The numerical model allowed the quantification of the groundwater resources, and an evaluation of their behaviour under abstraction conditions.

The groundwater resources of the Ntane Sandstone aquifer in the Palla Road region were found to be eminently capable of satisfying the immediate demands of the North South Carrier system during the 1997-1999 period of potential shortfall. Thereafter, it was recommended that the groundwater resources be regarded as a strategic resource, and should be allowed to recover by natural replenishment for future emergency use.

Environmental isotope study

The primary aim of the isotope hydrology component of this study was to obtain an independent assessment of recharge. In the event, in spite of a rather sparse coverage of the area with data points, isotope data was able to provide information on various other aspects of the hydrogeology of the area.

Principles of recharge assessment

At the time execution of the project, thermonuclear tritium levels in rain water were still dropping significantly, which made the use of some cumulative mixing model relevant in groundwater residence time assessment. The exponential mixing model (Zuber 1994) using historical atmospheric ^{14}C and rainfall ^{3}H data can be used to calculate ^{14}C - ^{3}H pairs for different mean resident times of a phreatic groundwater body receiving diffuse recharge. Plotting such pairs for range of residence times, observed values can be used to assess appropriate mean residence times T.

Groundwater recharge values R in the project area have been calculated using the equation:

$$R = \frac{H.n}{T}$$

The three parameters utilised are the

- depth of penetration of the saturated zone (H)
- mean total porosity of the aquifer the units penetrated (n)
- mean residence time of the column of water extracted from the borehole (T).

The equation is based on the concept of the rate of turnover of a representative water column in the aquifer as being equal to the recharge rate. The calculation has only been carried out for those boreholes for which the requisite information is available.

1. Radiocarbon values from which mean residence times can be calculated, using the exponential mixing model
2. The height of water column. The radiocarbon values available are often for certain horizons only, with the result that the values likely to pertain to the relevant water column can only be estimated, based on these point values.
3. Matrix porosities of 2-5% and fracture porosities of 13-14% have been previously estimated (SGAB, 1988) for the Ntane Sandstone at Serowe. A mean porosity of about 5%, based on the Serowe study, has also been used in an earlier investigation of the Palla Road area (SMEC et al. 1991). It was stated that this latter value was obtained from long-term pumping tests, and can thus be assumed to be an `effective porosity'.

It can reasonably be assumed that only the "transmissive" fracture porosity, and a portion of the matrix porosity, will respond to hydraulic changes on the time-scale of a pumping test, thus implying that the derived porosity value will be an underestimate of the true porosity. However, the relevant porosity value required for the ^{14}C tracer-based calculation of residence time should lie closer to the total, or matrix plus fracture, porosity. The tracer will diffuse into all interconnected water-filled pores, as does the dissolved solid load in the case of transient tracer inputs, and of radioactive isotopes, the degree to which the total porosity is occupied will depend on the balance between the diffusive time constant and the characteristic input transient time of the tracer.

Using a porosity of 5% for the Ntane Sandstone aquifer should therefore produce a conservative value in the isotope calculation of recharge.
Discussion of Isotope Data

Isotope data and other available on the Palla Road project have been entered into the comprehensive Kalahari data base.

Frequency distribution of ^{14}C values

A frequency histogram of all radiocarbon measurements performed in this project is illustrated in Fig. 4. Of the cases where there is reliable information on boreholes (30 in all), the majority of the values (23) apply to the Ntane Sandstone. The remaining data apply to basalt or basalt plus Ntane Sandstone. A few cases with <40 pMC are for the Ecca, all associated with high salinity. The histogram can, therefore, not be meaningfully subdivided into lithological units. Its most striking feature is the pronounced maximum around 80 pMC, with a considerable proportion (about 30%) of the measurements >80 pMC and some 50% of the measurements >75 pMC.

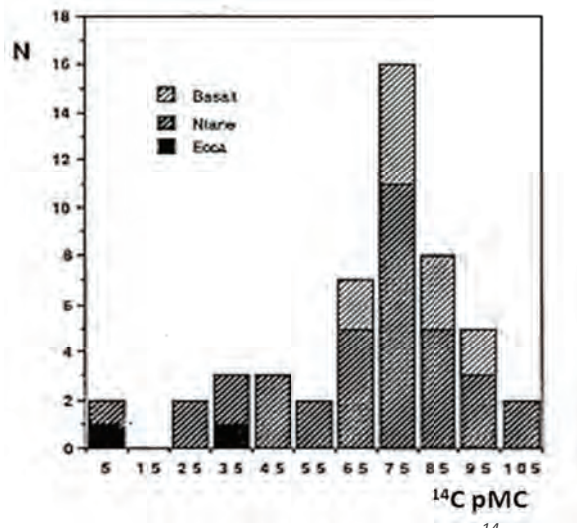

Figure 4: Frequency histogram of ^{14}C values displayed according to the lithological horizons in which they were sampled

The remainder of the data forms an almost continuous distribution down to low radiocarbon concentrations. Although the data set is somewhat sparse for such a large project area (some 1500 km^2), and some of the sub-sets are geographically concentrated, a general qualitative interpretation of the radiocarbon data is of a dynamic (relatively shallow) hydrology, overlying a more static, deeper-seated system.

Very deep groundwater of very high mineralisation has low values of ^{14}C. The in situ ^{14}C values of the deep groundwater are likely to be even lower, or vanishing, as the samples taken would have unavoidably been mixtures with shallower water. In addition, it should be noted that several radiocarbon samples were of inadequate size as a result of the low associated alkalinity.

The frequency histogram of ^{14}C values (Fig. 4) also indicates a lithological association. Basalt samples fall exclusively in the range 65 pMC to 95 pMC, indicating that the basalt, on average, contains more recent water. Groundwater in the basalt is, therefore, generally mobile. Lower values of ^{14}C, for more stagnant water, are contained exclusively in the Ntane Sandstone and the Ecca. Values >100 pMC are for samples from hand dug wells tapping shallow (perched) groundwater.

Geographic distribution of ^{14}C values

The geographic distribution of ^{14}C (and ^{3}H) values is shown in (Fig. 5).

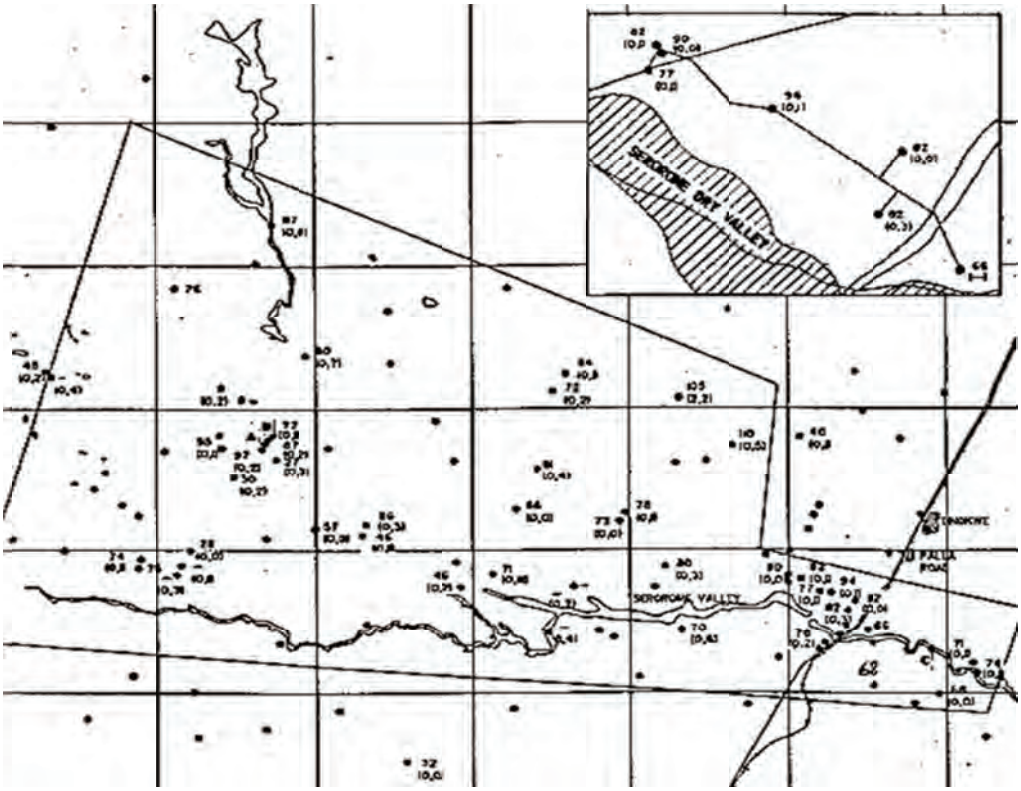

Figure 5: Geographic distribution of ^{14}C and ^{3}H values in groundwater. No clear regional trends are observable. Inset: Values for the pre-existing Palla Road wellfield boreholes.

The ^{14}C data shows no clear evidence of geographic trends although values >80 pMC are found in the west, generally associated with the palaeo drainage; in the relatively shallow groundwater of the Modubane area; and in the Palla Road Wellfield. It should be cautioned, however, that these groups are probably partially artificial, in that they are associated with particular target areas of the study. They do, nevertheless, emphasise the widespread presence of actively recharged groundwater over the entire area.

Radiocarbon depth profiles.

Three depth profiles of ^{14}C have been obtained, for boreholes 7436, 7439 and 7552. Samples were taken at different depth during the drilling of the borehole. Values have been entered on the lithological logs of the three boreholes in Fig. 6. An unexpected feature is that in each case there is a measurable increase in ^{14}C values between the first strike and next deepest sample. At first glance this might appear as a contradiction: in the presence of recharge the upper layer should be the youngest.

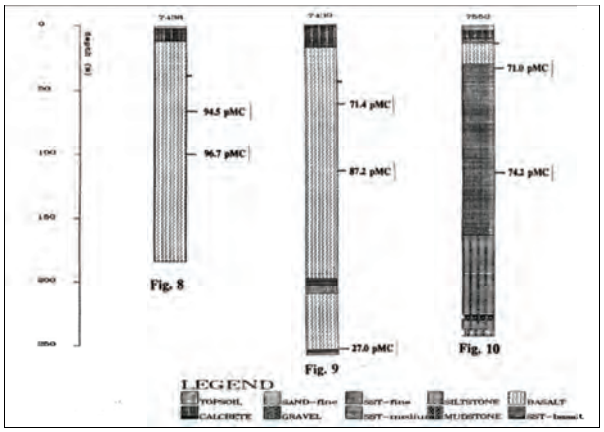

Figure 6: ^{14}C values of samples taken during drilling of three observation boreholes in basalt, Ntane sandstone and at the Ntane/Ecca contact

However, a possible explanation of this phenomenon is thought to lie in the nature of the water strikes, and the varying transmissive properties of the different water strikes were in fractures. Much higher yielding fractures may be found deeper in the hole. The lower intersection of apparently `younger' water may thus simply be a reflection of the mobility of the groundwater at different depths, with much greater throughflow and hence younger water. In the case of BH 7439, drilled in basalt, there was a dramatic increase in ^{14}C over 30 metres. The final value of 27 pMC, at its ultimate depth of 256 metres at the Ntane Sandstone contact, is probably a mixture over the entire column: the in situ value in the aquifer at that depth probably being much lower.

The adjacent borehole BH 7436, was likewise drilled into a downthrown block of basalt, yet gave significantly higher and increasing ^{14}C values, at depths 25 metres and 60 metres below the final piezometric level. These higher values probably reflect the enhanced transmissivity of the basalt as a result of fracturing associated with a nearby fault. Both boreholes BH 7439 and BH 7436 suggest that relatively recent water penetrates to considerable depths within the basalt sequence. It may thus be inferred that such recharge will be balanced by significant lateral flow in the basalt.

The low ^{14}C value of 30 pMC for first strike water in BH 7438, indicating a mean residence time of several thousands of years, is not necessarily in contradiction to these conclusions. The strike occurred at the basalt/Ntane Sandstone contact, indicating that the groundwater at this location is largely confined by the basalt. This further emphasises the heterogeneity of the system which, away from major faults, appears to be less transmissive, more closely confined, and having a more restricted throughflow.

Radiocarbon Evidence of Regional Movement

The environmental isotope data set does not allow for any conclusions regarding regional movement. The conditions under which samples were taken vary from borehole to borehole (either pumped samples, or water strike samples taken during drilling), and there are numerous and abrupt changes of lithology. The data base is also too limited to provide an adequate areal coverage from which trends could become apparent. On the other hand, ^{14}C values greater than 80 pMC are encountered at numerous locations (Fig. 5). When generalised over the entire Project Area, this would imply that areal recharge occurs on a broad scale, which in turn implies that areal trends in groundwater age will not be discernible.

Tritium data

The bulk of the tritium values observed in the area of study lie at the limit of detection (0.2 ± 0.2 TU). In order to assess this data, it is assumed that values of < 0.3 TU are indistinguishable from 0. This places a lower limit of a century on the mean residence time of most of the groundwater in the area.

Radiocarbon values are plotted against tritium in Fig. 7. Also shown are plots of the exponential mixing model values, which may be expected for initial (recharge) values of 80%, 90% and 100% of atmospheric levels respectively. Only in a minority of cases are significant ^{3}H values (> 0.4 TU) observed; and in only two cases of shallow groundwater, Lethakeng and Patadikibidu wells, are values >1 TU encountered. Tritium values therefore constrain the interpretation of the ^{14}C data.

There is, however, an intrinsic difficulty in establishing a "recent" groundwater value, in other words the percentage of the ^{14}C value in atmospheric CO_2, reflected in the TDIC of infiltrating water when it reaches the saturated zone. The overall conclusion from the ^{14}C -^{3}H relationship in Fig. 7 is that the initial concentration of ^{14}C is probably > 90% of atmospheric. Wells such as Modubane and Patadikibidu provide an opportunity to observe the processes of development of the isotopic composition of groundwater at the water table. At Modubane well ground water is shallow, has ^{14}C > 100 pMC and yet contains little tritium. This may be evidence of ^{14}C transport through the vadose zone other areas.

Through a process of iterative integration of variable input values, the exponential model calculates pairs of tritium and radiocarbon values for different mean residence times. There are, however, other factors which may cause pairs of ^{14}C-^{3}H values to deviate from the idealisation of the model. Tritium labels the water molecule itself, and not, as in the case of ^{14}C, a dissolved constituent. In locations where the infiltrating rain water reaches the water table with an alkalinity lower than elsewhere in the saturated zone, the ^{3}H value in groundwater will be in excess of what is predicted by the exponential model on the basis of the accompanying ^{14}C.

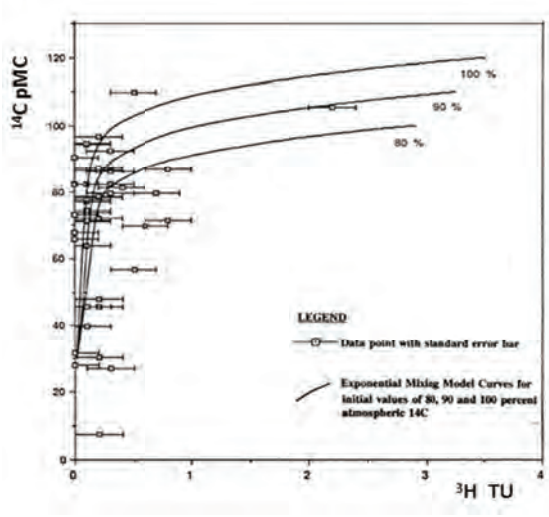

Figure 7: ^{14}C values plotted against ^{3}H for all samples. Also shown are exponential model plots based on known inputs for three dilutions of recharge $_{14}C$. Note the low ^{3}H values for ^{14}C > 90 pMC

The reverse may also hold. Mixing of components of differing isotopic and chemical composition also occurs in boreholes. As most ^{3}H values lie close to the detection limit, individual measurements may lie just outside the expected statistical limits. These various factors contribute to the scatter of tritium values, seen in Fig. 7.

The exponential mixing model furthermore assumes a steady recharge input, which would produce the locus of ^{14}C -^{3}H pairs for different mean residence times as is shown in the plot of Figure.7. Some of the ^{3}H values are "too low" when compared with the corresponding ^{14}C values > 90pMC, whilst others are 'too high" for lower ^{14}C values. This is interpreted as indicating that significant recharge to the deeper ground water in the area is episodic, i.e. at intervals comparable to the decay time of mean natural tritium values in rain to the detectable limit, i.e. of the order of 50-100 years. Only the shallow groundwater, such as that tapped by hand-dug wells, will record the more ongoing, but lesser recharge events.

Stable Isotope Data

Oxygen-18 frequency distribution

The frequency distribution of $\delta^{18}O$ values in the Project Area is shown in Fig. 8. The distribution can be seen as bi-modal, the major maximum lying at about -5.4 ‰, with a lesser maximum at about -4.8 ‰. It is striking that for this extensive area the range of values is relatively narrow.

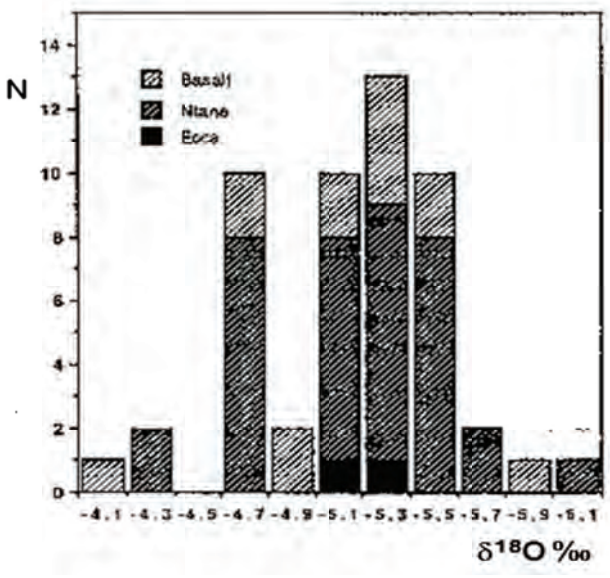

Figure 8: Frequency distribution of $\delta^{18}O$ values for samples with lithological associations.

Lithological associations of the samples are shown in Fig.8 but are not reflected in the histogram. The basalt values are spread over the entire range of $\delta^{18}O$ values, which leads to the conclusion that the $\delta^{18}O$ values are controlled more by physiographic differences and variable rainfall selectivity, than by lithology. The two samples allocated to the Ecca group together, which might suggest that the characteristics of the Ecca groundwater reflect more restricted recharge regime.

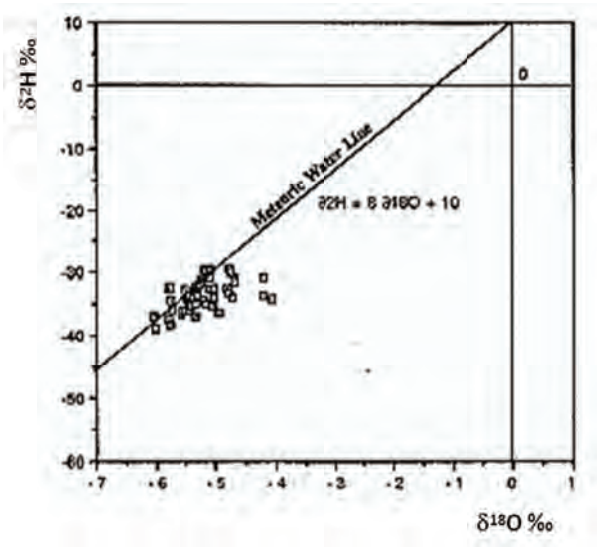

Figure 9: δ^2H - $\delta^{18}O$ diagram for all Palla Road groundwater samples. Note tight clustering and limited evaporation enrichment

Deuterium (δ^2H) measurements are plotted against $\delta^{18}O$ in Fig. 9. Many of the points cluster rather tightly around the (global) meteoric water line (MWL) to within the estimated standard deviation on individual measurements (± 1 ‰ for δ^2H ± 0.1 ‰ for $\delta^{18}O$). However, some of the data points to fall to the right of the MWL. This is compatible with a limited degree of kinetic (surface) evaporation prior to infiltration, a phenomenon observed elsewhere in the Kalahari (e.g. Verhagen, 1984).

The Palla Road stable isotope data has also been plotted in Fig.10, together with similar data for recent projects at Toteng/Sehitwa TGLP (Geoflux, 1993); Trans-Kalahari Road (WCS, 1993); Mmamabula (BRGM, 1993) and the range of values for Serowe (SGAB, 1988). This diagram emphasises the regional dependence of the stable isotope data in the Kalahari. The Mmamabula data shows considerable overlap with the adjacent Palla data range although with a greater trend towards evaporative values.

There is a partial overlap with the few Trans-Kalahari Road data points. The same applies to the data field for Serowe, an area with similar hydrogeology on the eastern edge of the Kalahari basin. However, the latter two data sets extend to more negative values than at Palla Road as the project areas extended further westwards into the Kalahari basin. This is clearly the case at Toteng/Sehitwa, data extending to much more negative values, probably a function of climate and rainfall selectivity (Verhagen, 1984).

It also shows a strong evaporation trend characterised by the bounding $\delta^2H = 5.5\ \delta^{18}O$ - 6‰ trend line, which is similar to evaporation trends elsewhere in the Kalahari. As opposed to Palla Road, the area is characterised by numerous surface evaporation features.

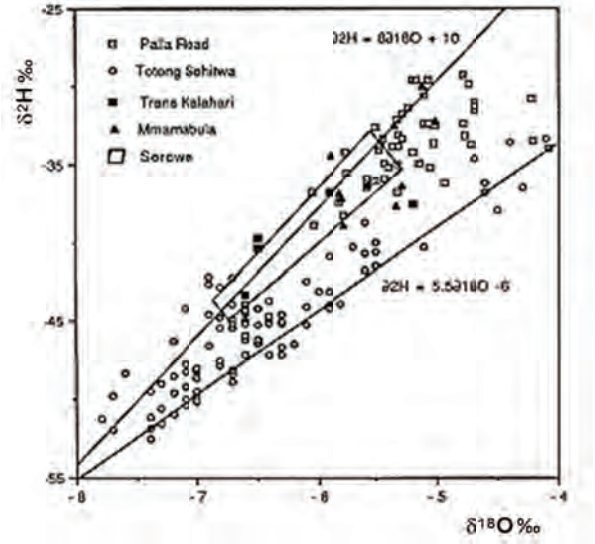

Figure 10: Comparison of δ^2H - $\delta^{18}O$ values for Palla Road and various other Kalahari areas

This comparison between the various regions emphasises the influence of local geographic and physiographic conditions on the stable isotope composition of Kalahari groundwater. The Palla Road data does, however, form a relatively tight cluster which reflects the relative physiographic uniformity and absence of surface evaporative features such as pans small variations in rainfall selectivity over this fairly extensive area.

No rainfall samples for isotope analysis had been taken during this project, although some results are available for the adjacent Mmamabula area. Such results have shown a correlation of stable isotope values with rainfall, and appear to confirm the rainfall selectivity of the recharge process, with the more intense rainfall events contributing preferentially to recharge. However, such short time series of rainfall observations should be taken as a general and qualitative guide to interpretation only.

^{14}C and ^{3}H evidence for the Project Area tends to indicate that periodic major recharge events are significant in establishing the hydrological conditions observed in the area, and these may be 50 - 100 year events. The weighted mean stable isotope compositions of such events would be expected to lie somewhere within the range of the presently observed groundwater values.

Recharge assessment with environmental isotopes

Recharge values calculated from ^{14}C and ^{3}H data are summarised in Table 1.

With few exceptions, the calculated values appear to be reasonable, although highly variable. As was to be expected, the highest recharge values are observed in the Palla Road Wellfield, although 21.7 mm/a for BH 5944 appears excessive. It is possible that this spurious the value might be the result of recent water being drawn in during exploitation. The mean value for the set of 24 values, spread over the Project Area, is 3.5 mm/a when the result for BH 5944 is included, and 2.7mm/a when this value is excluded. Part of this input should be assumed to be dissipated by the same evapotranspirative loss mechanisms as appear to be operating in the rest of the Kalahari, i.e. by vapour transport through the unsaturated zone and transpiration by phreatophytes (Verhagen, 1990). The balance should result in regional drainage. Hydrogeological observations, supported in a few instances by isotope data, have shown that groundwater flow occurs mainly along fracture zones, and that drainage is channelled to, and probably leaves the area, in the southeast. However, largely as a result of the geographic spread of the points sampled, the overall hydraulic continuity suggested by the piezometric contours is not unequivocally reflected by the environmental isotope data.

Conclusions from Environmental Isotope Data

- There is widespread evidence of significant areal recharge over the entire Project Area. Recharge rates ranging from 0.2 to 21.7 mm/year have been estimated at 24 boreholes. The highest rates are observed in the Palla Road Wellfield. The mean value over the entire study area is 2.7- 3.5 mm/annum.
- The proportionately low 3H values accompanying ^{14}C > 80 pMC at many sampling points suggests that significant rain recharge in the Project Area is episodic. Recharge events of significance may have a recurrence period of the order of 50 years or longer.
- Depth profiles obtained during drilling at three sites, show that modern recharge water can penetrate deep into both the Ntane Sandstone and the basalt aquifers. This is taken as evidence of significant lateral water transport along extensive fracture systems.
- Isotopic data does not show clear contrasts between the two main aquifers: the basalt and the Ntane Sandstone. This suggests regional hydraulic continuity, in which surface and structural controls appear to be the more important influences than the specific aquifers themselves.
- Carbon-13 and carbon-14 data corroborate piezometric evidence that indicates that the (then existing) Palla Road Wellfield does not lie in the central groundwater drainage zone of the Project Area, which itself appears to be closely related to the principal fracture zones trending WNW-ESE.

Table 1: Recharge rates calculated from isotope data

Bh No.	Aquifer			Calculated recharge mm/a
	Ntane	Ntane+basalt	basalt	
5719	*			1.1
7352	*			1.2
5944	*			21.7
5520	*			1.5
2404			*	5.1
1004		*		1.1
Z4579		*		0.4
Z669	*			1
1711	*			0.7
944	*			0.6
7435	*			0.9
7436			*	6.2
7439			*	2.5
7443	*			3
7451	*			4.2
7388	*			3.5
7453	*			5.9
7492		*		0.2
7493	*			1.8
7527		*		1
7528		*		0.5
7494		*		0.3
7497		*		6.1
7552	*			4.9

- Isotopic data suggest that the Palla Road Wellfield groundwater is recharged mainly through nonvadose processes, such as occasional flooding of the Serorome River bed, or overland sheet flow from the north during exceptional rainfall events.
- The ^{14}C value for BH 5719, at the eastern limit of the Palla Road wellfield and at the lowest end topographically and piezometrically, shows that groundwater movement is retarded in this direction and that drainage is directed southwards.

- The regional hydraulic continuity indicated by the piezometric contours is not unequivocally reflected in the isotope data. This would support the concept that the most significant regional drainage occurs mainly through fracture zones associated with major faults.

Summary Conclusions from Chloride Mass Balance

- Although the Ntane Sandstone and basalt aquifers are subjected to localised salinisation by leakage from the underlying Ecca as a result of structural disturbances, careful selection of data points which have not been affected in this manner has allowed the Chloride Mass Balance technique to be used to assess recharge.
- Applying recently determined data on total chloride deposition in rainfall to the Palla Road Project Area has indicated that recharge to the Ntane Sandstone and basalt aquifers is in the range of 4 mm/annum to 8 mm/annum.

Summary Conclusions from GIS Recharge Evaluation

- The application of GIS techniques, in order to integrate a considerable number of varied parameters which influence the potential for recharge from rainfall, has enabled an aerial picture of recharge potential to be produced
- The GIS technique essentially provides a qualitative assessment of recharge potential. A simple and somewhat experimental, soil chloride sampling programme from 24 auger holes spread over the project area has enabled the GIS results to be quantified, such that the areal distribution of recharge volumes has been determined.
- Results from the shallow profile soil chloride sampling, although having certain anomalous values and being too few to be statistically representative, generally indicate a recharge value for the greater part of the area of between 2 mm/annum and 5 mm/annum.
- The use of GIS in assessing the dimensions and nature of the components of the regional catchment has enabled the inflow, or external inputs, to the Project Area (and, more specifically, to the groundwater model area) to be determined.
- The GIS recharge investigation has been very complimentary to the success of the groundwater modelling exercise and, in particular, the results derived from the GIS work have enabled a realistic quantitative recharge matrix to be applied to the model.
- Recharge volumes influencing the area of the groundwater model have been estimated from areal recharge and from regional catchment contributions.

Overall conclusions concerning the Ntane sandstone aquifer

The Ntane Sandstone aquifer undoubtedly has the greatest groundwater potential of all the geological units in the Palla Road area and contains groundwater resources of sufficient magnitude to warrant development, A number of general conclusions concerning the Ntane Sandstone, drawn from the closely related recharge studies, are presented below:

- The Ntane Sandstone aquifer is almost certainly in hydraulic continuity with fracture aquifers in the lower part of the Stormberg basalt, most especially in the west of the area. Lack of trends in areal distribution of environmental isotope indicates that much of the regional groundwater flow in the Ntane Sandstone is preferentially along fracture zones. Deep circulation of recent groundwater, controlled by fracturing, is evident.
- The Ntane Sandstone groundwater is locally confined, but can be regarded as regionally unconfined, since recharge from precipitation is indicated by environmental isotopes and hydrochemistry (Mazor et.al 1977).
- Where the Ntane Sandstone is covered by basalt, groundwater is usually older, with higher alkalinity but low mineralisation. Where basalt cover is absent, Ntane Sandstone water is recent and is characterised by low mineralisation, especially alkalinity, indicating local recharge through the sand cover.
- Adjacent to some of the principal structures there are clear indications of localised leakage of highly mineralised Ecca groundwater into the Ntane Sandstone aquifer.
- -Isotopic indications are that recharge `events' in the Ntane Sandstone are most probably episodic, both in terms of recent recharge (of the order of several decades) and major recharge inputs (pluvial periods)
- -Various techniques of recharge estimation that have been applied. These indicate that a large proportion of the project area underlain by the Ntane Sandstone (and basalt) provides a surface (surficial deposits + vegetation) which is conducive to good recharge potential, and that areal recharge for this zone for modelling purposes may be assumed to lie in the range of 2 to 5 mm/annum.

REFERENCES

BRGM (1993) *Mmamabula Groundwater Resources Investigation Phase II - Khurutshe Area. Appendix 4: Recharge Study. Dept. Geological Survey, Botswana.*

Fontes, J C, Garnier, J M (1979) *Determination of the initial 14C activity of the total dissolved carbon. Water Resources Research. 15, 399-413*

Geoflux (1993) *Toteng/Sehitwa TGLP groundwater resources Investigation. Dept. Geological Survey, Botswana.*

Mazor, E, Verhagen B Th, Sellschop, J P F, Jones, M T, Robins, N E, Hutton, L and Jennings, C M H (1977) *Northern Kalahari groundwaters: hydrologic, isotopic and chemical studies at Orapa, Botswana. Jnl of Hydrology 34, 203*

SGAB (1988) *Serowe Groundwater Resources Evaluation Project. Final Report. CTB No. 10/2/7/84-85. Dept. of Geological Survey, Botswana.*

Verhagen, B. Th. (1984) *Environmental isotope study of a groundwater supply project in the Kalahari of Gordonia. Isotope Hydrology 1983. IAEA Vienna. pp. 415- 432.*

Verhagen, B. Th. (1990) *Isotope hydrology of the Kalahari: Recharge or no recharge? Palaeoecology of Africa V.21.(A.A. Balkema/Rotterdam/Brookfield). pp. 143-158*

Verhagen, B. Th., Geyh, M. A,, Froehlich, K, Wirth, K. (1991) *Isotope hydrological methods for the quantitative evaluation of ground water resources in arid and semi-arid areas. Fed. Ministry for Econ. Coop., FRG. ISBN 3-8039-0352-1.*

Verhagen, B. Th.(1992) *Detailed geohydrology with environmental isotopes: A case study at Serowe, Botswana. Isotope Techniques in Water Resources Development 1991. IAEA, Vienna. pp. 345-362.*

WCS (1993) *Trans-Kalahari Road Groundwater Potential Study, Report to Dept. Water Affairs, Botswana.*

WCS (1995) *Palla Road groundwater investigations Phase I – Final report. International Institute for Aerospace Surveys and Earth Sciences; Wellfield Consulting Services,*

Zuber, A (1994) *"On calibration and validation of mathematical models for the interpretation of environmental tracer data in aquifers". Mathematical Models and Their Applications to Isotope Studies in Groundwater Hydrology. IAEA-TECDOC-777, Vienna. 11*

CASE STUDY

ISOTOPE AND CHEMICAL FEASIBILITY OF GROUNDWATER IN GORDONIA AS A SOURCE FOR A LOCAL RETICULATED SUPPLY

B. Th. Verhagen

INTRODUCTION

The district of Gordonia of the Northern Cape Province of South Africa forms the southern-most section of the Kalahari thirstland. It was predominantly a sheep-raising farming area and relied almost exclusively on ground water, drilled for by individual farmers. Boreholes generally have poor yields: many are dry. Apart from certain areas, water quality ranges from poor to impotable and rest levels may be deeper than 100 metres. An intensive investigation was conducted in 1980-83 to establish the feasibility of a central water supply to the individual farms, based on certain areas where good quality ground water was known to exist. This investigation involved borehole surveys, geophysical measurements, exploratory and supply borehole drilling and hydrochemical observations. An environmental isotope study (Verhagen, 1983) was conducted in parallel to this investigation in order to assist in the interpretation of the other data and to elucidate the relationship between the different water bodies, groundwater movement and the development of the varied hydrochemistry.

DESCRIPTION AND GEOLOGY

The area is typical Kalahari with a cover of aeolian sand which forms parallel dunes fixed by vegetation (Fig.1). Surface water features are the beds of the ephemeral Kuruman, Molopo and Nossob Rivers, some minor drainage lines and pans, ranging from a few tens of metres to several kilometres in diameter. These may contain some surface water after heavy downpours. Mean annual precipitation is 200 mm, of which 60% falls between January and April. During 1974-77 the Kuruman River flowed along its entire length following exceptional rains of 3 x the annual mean from its distant dolomitic catchment.

Karoo shales and tillites and the earlier Nama sedimentary sequence were deposited in a basin of lower Karoo and earlier rocks. The Kalahari cover consists of gravel, sandy clay and sandstone, clay and crete, both calcareous and silicious. This cover can reach a thickness of 100 m or more over palaeo-drainages in the Kalahari floor, but thins considerably to the west and south-west, where the Karoo becomes locally exposed. The surface elevation drops from about 1000 mamsl in the east to about 800 m in the south-west.

HYDROGEOLOGY

Groundwater is generally unconfined to semi-confined. Piezometric levels range in depth from a few tens of metres to 160 metres and lie mainly within the pre-Kalahari rocks and occasionally in the lower sections of the Kalahari formation. Yields from successful farm boreholes range from less than 0.1 Ls^{-1} in argillaceous sections to 1.3 Ls^{-1}. Some production boreholes drilled for the central supply produced up to 7 Ls^{-1} from semi-consolidated sands in the river bed.

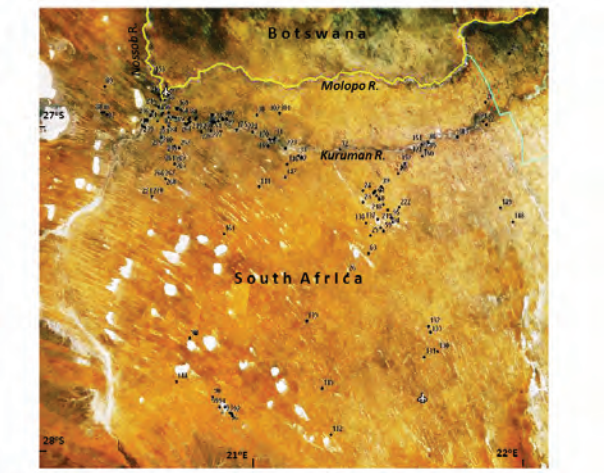

Figure 1: Image of study area, showing ephemeral rivers, fixed dunes, pans and numbered sampling points.

Groundwater quality is good (less than 1000 mgL^{-1} TDS) in the aquifers below the Kuruman River, in the rock exposure areas to the east and in deep Kalahari deposits. Towards the west and south-west quality deteriorates to TDS more than 60 000 mgL^{-1}. Smit (1977), following earlier studies by Martin (1961), assumed that infiltrating rainfall is quantitatively lost by evapotranspiration and assumed that effective recharge would occur only along the river course during infrequent floods. This approach, applied to the present study area by Levin (1980) assumed that effective recharge would occur only along the river courses during infrequent floods. Gradual salination would then occur during regional-underflow.

Certain aspects of the hydrochemistry and of the regional drainage of Gordonia, however, appeared to be in conflict with this philosophy. Examining sand moisture profiles and conditions in underlying aquifers, Verhagen et al. (1979) indicated that a tributary of the Kuruman River appeared to have minimal influence on its surrounding groundwater.

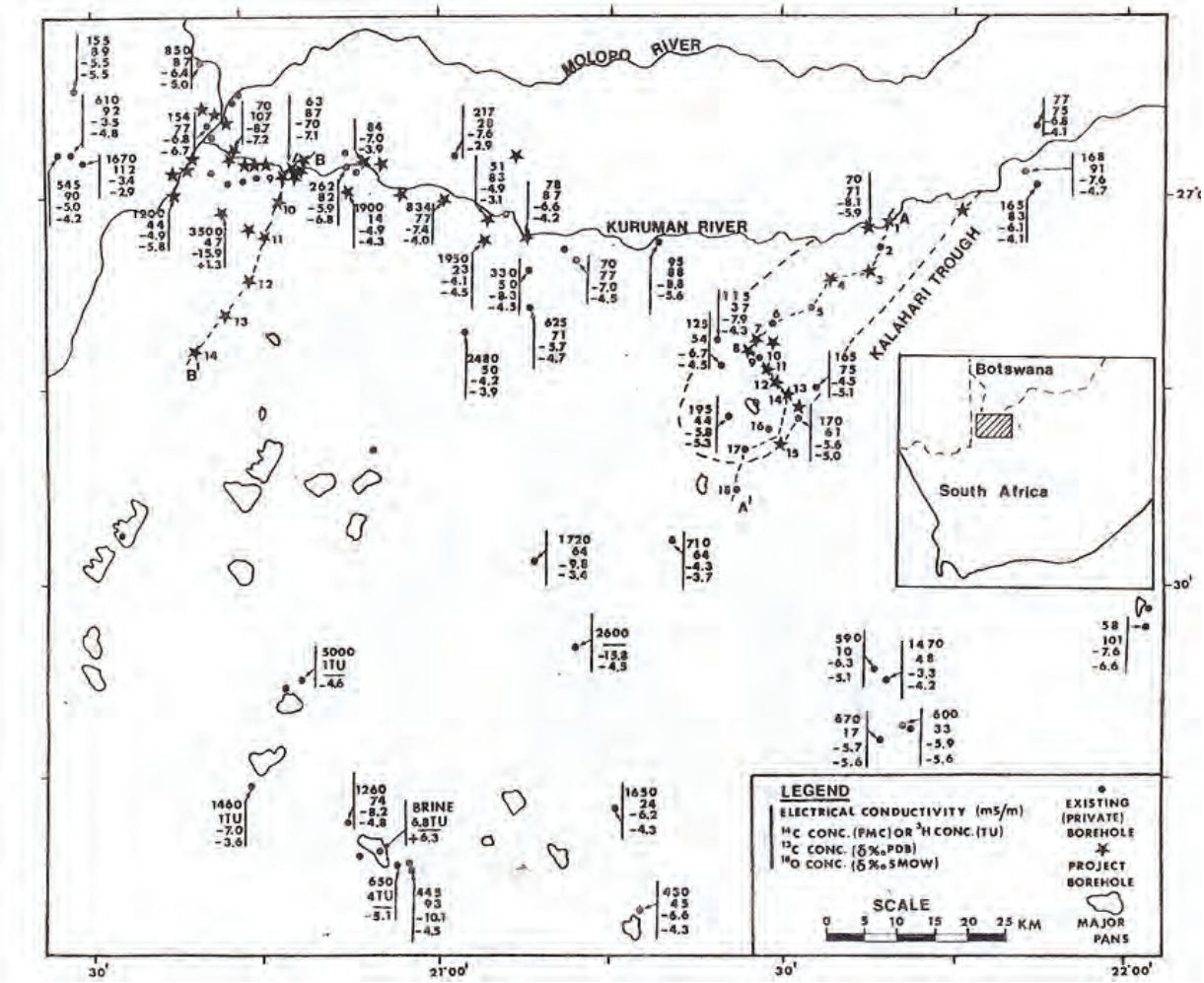

Figure 2: Map of the study area showing borehole positions sampled during both project phases with EC, pMC, TU, $\delta^{13}C$ and $\delta^{18}O$ listed for each point and the two section line A-A' and B-B'

PHASE I OF STUDY

The Phase I isotope study was undertaken on existing farm boreholes. The results of this survey are summarised below. The measurements were conducted more than 30 years ago with higher environmental values of tritium and radiocarbon due to nuclear fallout.

Borehole surveys and early geophysical investigations, located a trough of deep Kalahari sediments (up to 120 m) filling a palaeo-valley stretching south-westwards away from the Kuruman River bed (Fig. 2). Over some 30 km the ground water in this trough remains at TDS < 1000 mg L^{-1}, but this rises abruptly at the south-western end, and the sides of the trough. The rest levels lie for the greater part within the Kalahari. This fresh water body was considered as a possible source

for sustained exploitation for the central supply scheme.

This trough or palaeo-valley had been identified by Vogel and Bredenkamp (1969) as transporting water recharged during flooding of the Kuruman River south-westwards to an area where their study found anomalous values of both ^{14}C and ^{2}H.

Another source considered was the aquifer under the river bed itself. The majority of farms along the river have relatively shallow (~50m) boreholes providing good quality ground water taken to be derived from periodic river flow. Following the regional underflow philosophy it was assumed that the fresh water in the Kalahari trough was in its turn derived from this source.

In the immediate vicinity of the river radiocarbon concentrations are >80pmc, tritium concentrations up to 4 TU, with $\delta\ ^{13}C < -8‰$ and $\delta\ ^{18}O < -5.6‰$. The groundwater is mainly fresh (TDS~500mg/L) with Ca-Mg-HCO_3 dominance, compatible with infiltration from surface flow in the river or local rain recharge.

Ground water in the trough area, excepting those close to the river, gave radiocarbon concentrations in the range 35-75 pmc, with low (~ 0.5TU) tritium concentrations and $\delta^{13}C$ in the range -4.5‰ to -10‰, There are no geographical trends observable in this data, such as a systematic decline in ^{14}C values away from the river bed.

Observations on some other boreholes, notably in the extreme north-west of the study area (See Fig. 1) indicated that salinities up to 30 000 mg/L could be found in some apparently very recent (high ^{14}C) groundwater. This suggested that salinity was not necessarily coupled to long residence times or distance of underflow. The above results were obtained from existing farm boreholes, on which generally scant information was available.

PHASE II OF STUDY

Observation boreholes were sunk along two profiles south-westwards from the Kuruman River in the east and west of the study area (Fig.2). Samples for isotopic and chemical analysis were obtained from these boreholes, if and when conditions allowed.

Isotopic data from this phase show that $\delta\ ^{13}C$ values rise southwards from the river but at some distance become more uniform. This might be taken as evidence for dissolution/ exchange reactions reaching equilibrium during underflow. However, local influences are observed, such as low values of -10‰ which are associated with average to high radiocarbon concentrations.

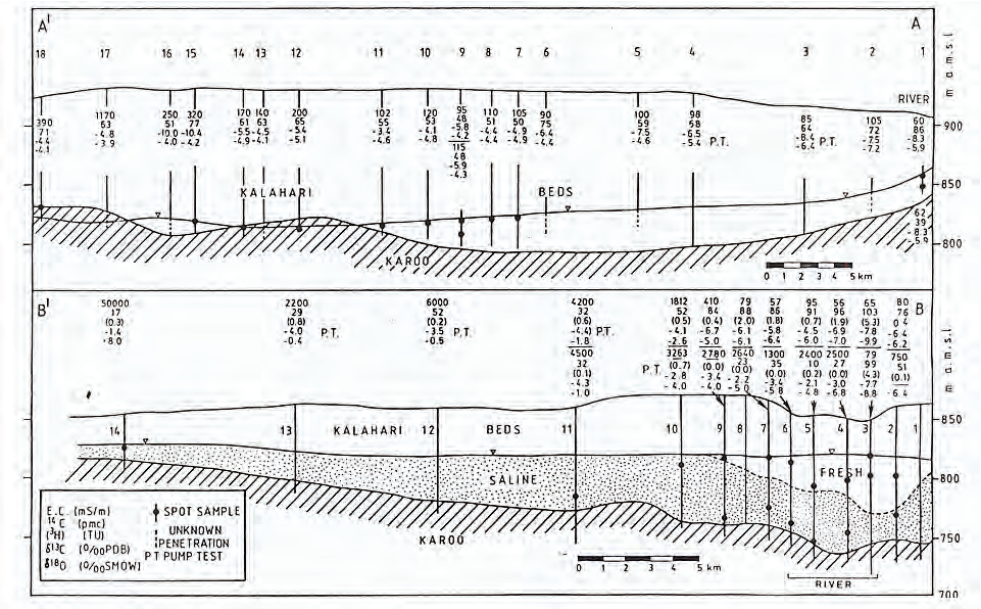

Figure 3: Sections A-A' and B-B' along which project boreholes were sunk as well as some existing farm boreholes. As in Fig. 2, measured parameters are shown with each sampling point

The $\delta^{18}O$ values <-5.6‰ similarly rise southwards from the river. Further south they however then become more uniform. In fact, they fall within a narrow range of values for the rest of the trough samples, off the profile, with some greater scatter in large tracts of the rest of the study area, excluding the saline waters in the western profile B-B' Three types of samples were taken: first strike water; at various depths during drilling; at various times during pump tests.

DISCUSSION OF DATA

1. Profile A-A'

Profile A-A' was chosen to incorporate a maximum number of sampling points along the Kalahari trough. It is shown in section in Fig.3. Piezometric heights at individual boreholes for some distance follow the regional dip of about 0.8‰. Borehole 1, closest to the river was very low yielding as a result of the (locally) considerable clay content of the aquifer. The high piezometric level may have been an exaggerated mound, slowly descending since recharge during 1974-77. (cf profile B-B').

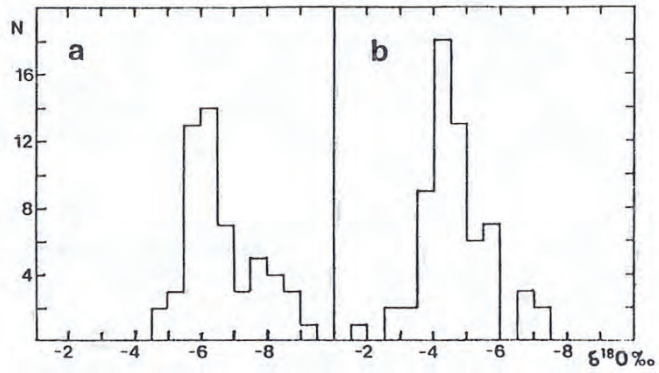

Figure 4: Histograms of $\delta^{18}O$ values of groundwater a) in or close to the river bed and b) in the area around the Kalahari trough .

A histogram (Fig.4a) of groundwater $\delta^{18}O$ values in, or close to the river bed, with a maximum at about -6.5‰, and away from the river in the area of the trough (Fig.4b), with a maximum at about -4.5‰ with considerable difference in position of the maxima strongly suggests different recharge mechanisms for the two groups of groundwater.

The position of each borehole on or close to the profile line down the trough has been projected onto the section A-A', showing water quality and isotopic data.

The first strike ^{14}C value for borehole 1, at the river is 86 pMC. The value 10 metres down is considerably lower, confirming poor vertical displacement. Away from the river, ^{14}C concentrations at boreholes 2, 3 and 4, are also lower, but represent more or less mean values for the saturated zone. At greater distances the ^{14}C values become quite heterogeneous, and do not parallel at all the increase in salinity observed towards the south-west of the profile.

Except possibly in its immediate vicinity (3-5 km) there is no geographical trend away from the river, confirming the trend seen in the ^{14}C data of Phase I. On the other hand, first strike water gave ^{14}C values of up to 77 pmc where surrounding production wells produce considerably lower values. There is a priori evidence of ^{14}C and therefore age stratification within the saturated zone in some localities.

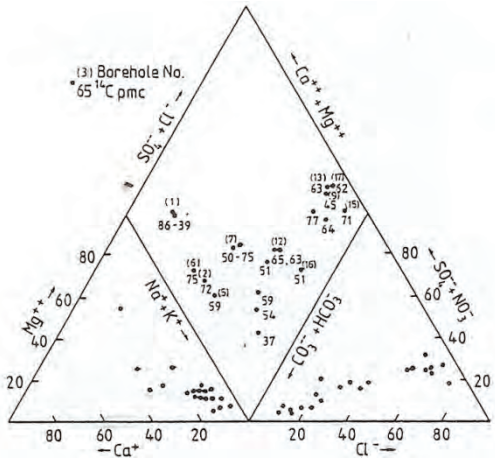

Figure 5: Trilinear diagram of major ion composition of Kalahari trough waters, with ^{14}C concentration and number for boreholes on section A-A'.

The chemical composition of groundwater along the trough is fairly heterogeneous. A trilinear diagram of major ion composition ratios in the trough area (Fig. 5) shows a scatter of points from Ca-Mg-HCO_3 dominance near the river to $NaHCO_3$ and NaCl dominance at greater distance.

2. Profile B-B'

The western profile of boreholes was drilled across the river bed in an area of planned exploitation and continued south-south-west- wards into usually saline and alkaline groundwater. The piezometric surface (Fig.3, B-B') shows practically no gradient. A minor

mound of a few metres was still observable below the river bed, some 5 years after the last flooding.

Drilling showed the limited extent of the fresh water body within the river bed aquifer and an abrupt transition from fresh to saline water. A very fine clay layer observed in the drilling material appears to have been responsible for sharply separating the fresh and saline water.

The conductivities and isotope levels observed in spot samples and during pump tests are shown for profile B-B' (Fig. 3). For the holes 10-14, away from the river bed, very high salinities, up to near saturated values go hand in hand with enriched values of $\delta^{18}O$ and relatively low ^{14}C concentrations ranging from 17 to 52 pMC. $\delta^{13}C$ values fall in roughly the same range as those for section A-A', but trend to more positive values in the extremely saline waters. Groundwater in the area had alkalinities up to 300 $meqL^{-1}$ (Fig. 8) and pH values up to 10. The chemical composition for borehole 11 (Fig. 6) is typical for the area.

The in situ values of $\delta^{18}O$ in the saline water under the river are therefore considerably lighter than in the saline waters further south along the section up to near-saturation, are observed with enriched values of $\delta^{18}O$ relatively low C. The conductivities and isotope levels observed in spot samples and during pump tests are given in Fig.3, B-B'.

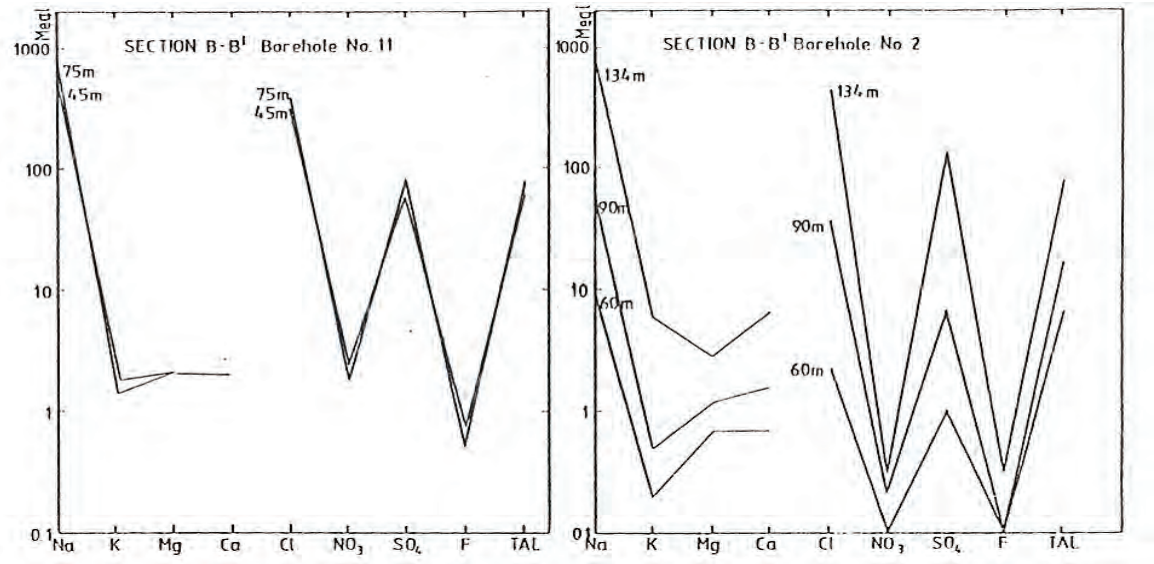

Figure 6: Schoeller diagrams of the chemistry of water samples from southern saline section along profile B-B' at two different depths and a similar data set for three samples at different depths from the river bed

In the river bed the fresh water generally had high ^{14}C (84 -102 pMC) with tritium 0.5-5.5TU. The deeper saline water shows chemical characteristics, similar to those further south in the section, with low values of ^{14}C. Values of $\delta^{18}O$ are more negative (-4.0‰ to -6.8‰) than for the extremely saline cases (-2.6‰ to +8.0‰). Mean tritium values in the upper fresh water is 1.6TU compared to 0.1TU for the underlying saline water, implying that the latter would have been diluted by at most 20%.

The piezometric height of the fresh water lens was somewhat higher than for the saline horizon. Fig. 6 shows the chemical composition at three different depths in borehole 2. As the samples were taken whilst drilling, there could have been no contamination due to sampling of the shallower sample by deeper saline water. The pattern suggests intrusion of the fresher waters by saline water probably before the flood, with a slight preponderance of alkalinity in the fresh end-member.

DISCUSSION OF THE ISOTOPE AND HYDROCHEMICAL DATA

1. The Oxygen-18 - Deuterium diagram

The oxygen-18 data are plotted against deuterium measurements for the whole study area in Fig.7. The majority of points fall on or around the global meteoric water line (Dansgaard 1964).

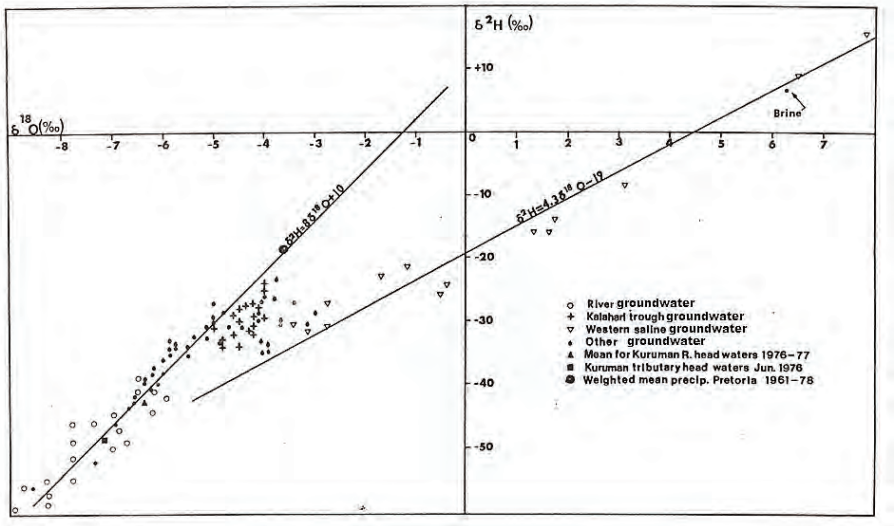

Figure 7: δ^2H-$8\delta^{18}O$ diagram for samples taken from the Kalahari trough; from outside the trough; the river bed and highly saline samples. The Global Meteoric Water Line and a kinetic enrichment regression through the saline sample points are shown

Rainfall isotope records for Pretoria http://www-naweb.iaea.org/napc/ih/IHS_resources_gnip.html some 700 km to the east are used for comparison. The Pretoria weighted mean places this groundwater data in perspective. Thus, all the groundwater occurrences fall in the "lighter" sector of the diagram, with the exception of the saline water in the west and south west. The latter lie on an evaporation line and have undergone kinetic isotope enrichment before entering the sub-surface. All 'normal' groundwater appears to have experienced a degree of rainfall selection, i.e. recharging preferentially during heavier rainfalls. This effect is observed in the Kalahari generally (Mazor et al., 1974; 1977).

Most depleted is river water as taken to be reflected in those samples obtained from the aquifer below or close to the river. The highly infrequent flooding of the Kuruman River has been seen to occur, as it did in 1974-77, during exceptional weather, with rain falling during prolonged, overcast, cool and moist conditions. Although the points shown are associated mainly with recently recharged water, any such recharge which occurred in the past should have carried a similar range of $\delta^{18}O/\delta^2H$ values. Mean values for Kuruman River head waters and for the major tributary in samples taken during 1976-77 are given for comparison. It is striking that after 300 km of flood flow under low gradients, the infiltrated water shows no clear sign of evaporation.

As can also be seen in the histograms of Fig.4 and in Fig.7 the Kalahari trough and associated groundwater forms a much tighter group. The values lie closer to the mean precipitation value and somewhat off the MW line, suggesting a slight degree of surface evaporation, compatible with rapid infiltration into dunes and some surface delay in the numerous small pans and pan-like areas that are found everywhere in the "streets" or inter-dune valleys. The uniformity of the stable isotope signal over such an extended area is probably controlled by its uniform physiography as echoed by uniformity in $\delta^{18}O$ found in Namibia (Vogel and van Urk, 1975).

The stable isotope values for the highly saline groundwater in section B-B' give an insight into its origins. The degree of evaporation seen in some cases is even more extreme than that which is associated (Fig. 7) with the saturated NaCl brines in the floors of major pans. The water must have been exposed at the surface for some considerable time, either as accumulated rain before infiltration into the floors of minor pans which abound in the area, or possibly by the occasional rise of the relatively shallow water tables during past extreme precipitation/flooding events to above surface level.

2. High alkalinities and radiocarbon concentrations.

As is shown by Verhagen et al. (1979) and the above discussion, regional flow models do not appear to be valid in the Kalahari under present climatic conditions.

Numerous local closed- basin conditions and local salinity develop.

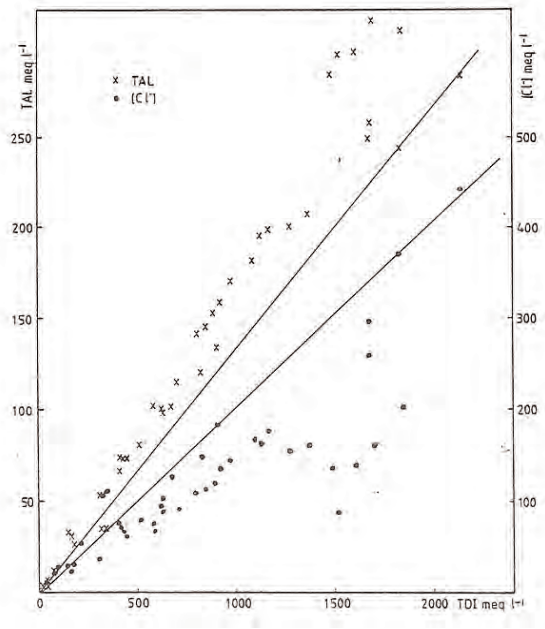

Figure 8. Chemical development of western saline waters, showing growth of Cl^- and total alkalinity with total dissolved ions.

The growth of alkalinity and Cl in the extreme case of the western saline groundwater is shown in Fig. 8 (cf. Fig. 7). Bounding lines for Cl and alkalinity concentrations have been added as a visual guide. The most probable genesis is from an original evaporitic environment, from which Ca and Mg had largely precipitated. Any further development would have found Na as the major cation, resulting in the roughly parallel development of Cl and alkalinity, known as the common ion effect (Drever 1982). Deviations from the trend lines show competing tendencies in the two anion concentrations.

The quasi-parallel trend in Cl^- and total alkalinity is already evident in relatively low (~10 $meqL^{-1}$) concentrations. As the dominant cation in most, even fresh, groundwater in the study area is sodium, it is possible that groundwater often displays a dissolved inorganic carbon (DIC) concentration higher than the value in the infiltrating recharge water. The DIC in the infiltrating recharge water is thus diluted by the higher concentrations already present in the groundwater.

Anomalously low radiocarbon concentrations are observed in the western saline groundwater, even where it is fairly shallow under water-table conditions. Great caution should therefore be exercised in interpreting ^{14}C concentrations in terms of water ages in this type of environment, especially where alkalinities are high.

CONCLUSIONS

Hydrochemical and isotope data suggest strongly that in both the eastern and western profiles studied, the demonstrable influence of the river spreads laterally to the extent of at most a few kilometres.

In the western profile (B-B'), active recharge is observed in the riverbed, interpreted to be driven mainly by flooding. The fresh water lens is laterally and vertically restricted, possibly by a semi-pervious clay layer. The chemical characteristics and isotope values provide a strong contrast with the surrounding and underlying saline water. The latter has a clear evaporation signal, which can be related to the density of pans in the area and the relatively shallow water table. Although the ^{14}C levels are low, just measurable tritium and the high sodium-alkalinity suggest that they do not represent high water ages.

In the Kalahari trough (profile A-A'), water with isotope characteristics different from aquifers underlying the river is found. There is no large-scale aging trend with distance in the ^{14}C data, whilst individual values of 75-77 pMC suggest components of recent recharge. Due to unavoidable mixing during sampling, and the delay in recognizing saturated conditions during drilling, even higher ^{14}C concentrations might be present at the top of the saturated zone. The $\delta^{18}O$ values are highly uniform and different from those in the river bed. They are somewhat lighter than the probable mean present-day precipitation, as observed by Vogel and Bredenkamp (1969).

This rules out the possibility that the groundwater in the trough, as well as in most of the remaining study area away from rivers, are remnants of earlier "pluvial" climatic periods. These should have carried isotope signals at least as depleted as those found in the aquifers below the river, which in all probability mostly infiltrated during the exceptionally wet period and floods of 1974-77. These results should sound a cautionary note on palaeoclimatic interpretations of stable isotope concentrations in groundwater in such semi-arid environments. The existence of numerous pans in the west may indicate the earlier existence of an evaporitic basin in the region of confluence of the

three rivers. Extensive and thick calcareous deposits are being incised by the rivers; saturated NaCl brines are found in major pans. These evaporitic conditions seem to be confined to the west. Wetter periods could however have leached the Kalahari deposits of the trough in the east and temporarily set in motion regional drainage. Aerosol deposition and enrichment in the unsaturated zone, gradually salinizes the water at present. Lower transmissivities make such leaching much less effective, such as in the bedrock aquifers.

Groundwater in neither of the two target areas studied appeared to be promising for a centralised fresh water supply which should be sustained for indefinite periods. In the west, the lens of fresh water is obviously of limited extent and would require careful management in order to maintain its quality. Sustainable groundwater extraction from the trough in the east would have had to rely mainly on local, diffuse vertical recharge, as is the case in most parts of the Kalahari. Any contribution from infiltrating flood water in the river would be minor.

ACKNOWLEDGEMENTS

The then Head of the Division of Geohydrology, Department of Environmental Affairs Mr J R Vegter, who initiated the Gordonia study; staff who provided logistical and sampling support and for numerous discussions. Staff of the Geophysics Division of the Council for Scientific and Industrial Research enabled exchange of ideas and encouragement. Chemical analyses were performed by the chemical laboratories of the Dept. of Environmental Affairs and isotope measurements by the Environmental Isotope Laboratory of the then Nuclear Physics Research Unit.

REFERENCES

Dansgaard, W. (1964) Stable isotopes in precipitation. Tellus 16, 436-468.

De Beer, J.H., Duvenhage, A.W.A., Meyer, R., Huyssen, R.M.J. (1981). *Report Kon/GS/80/1. C.S.I.R. Pretoria.*

Drever, J.I. (1982).*The Geochemistry of natural waters. Prentice-Hall*

Levin, M. Report PEL-272 (1980). *Atomic Energy Board, Pretoria. ISBN 086960 709x*

Mazor, E., Verhagen, B.Th., Robins, N.E., Sellschop, J.P.F., Hutton, L.G. (1974) *Isotope Techniques in Groundwater Hydrology 1974. 1, 203.I.A.E.A., Vienna.*

Mazor, E., Verhagen, B.Th., Robins, N.E., Sellschop, J.P.F., Hutton, L.G., Jennings, C.M.H. (1977). *Northern Kalahari groundwaters: hydrologic, isotopic and chemical studies at ORAP, Botswana. J. Hydrology 34, 203-234.*

Smit, P.J. (1977) *Die geohidrologie in die opvanggebied van die Molopo rivier in the noordelike Kalahari. Thesis Univ of the Orange Free State, Bloemfontein.*

Verhagen, B.Th., Smith, P.E., McGeorge, I., Dziembowski, Z. (1979). Isotope Hydrology 1978. *2, 733. IAEA, Vienna.*

Verhagen, B.Th. (1983). *Isotope Hydrology , IAEA, Vienna, 415-432.*

Vogel, J.C., Van Urk, H. (1975) *Isotopic composition of groundwater in semi-arid region of Southern Africa. J Hydrology(1-2):* **25, 23.**

SURFACE WATER AND GROUNDWATER INTERACTION IN THE UPPER CROCODILE RIVER BASIN

Tamiru Abiye

The degree of interaction between surface water and groundwater depends on aquifer characteristics and water availability. Mixing of different quality water, most of the time, could have negative effect on aquatic environment and groundwater dependent ecosystem. Interactions could be controlled by geological setting and hydrogeological parameters. However, manmade interaction takes place in mining areas as a result of disruption of hydrogeological and hydrological systems. In such areas discharge of mineralized groundwater potentially alters the quality of fresh surface water. Similarly, acid mine decant which is generated from mining areas from the leaching of slimes dumps. On the other hand, acid decanting from abandoned shafts impacts the quality of surrounding streams and through seepage, affects the quality of groundwater.

The upper Crocodile River basin is well-known for its large-scale urbanization and industrial activities with substantial water demand for various sectors where the main water supply for the area is derived from treated surface water, while the vast rural communities rely on groundwater for domestic and agricultural use, which is abstracted from weathered crystalline rocks and dolomitic aquifers. Moreover, groundwater plays a strategic role in supplying water for large irrigation activities in the area.

The basin encompasses the Cradle of Human Kind World Heritage site (CHKWHS) which hosts hominid and other animal fossils located within the Pretoria group quartzite and Malmami dolomites. The CHKWHS is being extensively threatened by acid mine decant derived from gold mines through progressive dissolution of the carbonate aquifer and heavy metal precipitation. Furthermore, ground and airborne geophysical surveys have also identified subsurface acid mine drainage pathways into the CHKWHS. In the abandoned mines, rebound of water table through natural and inter-basin recharge generates continuous discharge of acidic water loaded with heavy metal. With growing water supply demand, the groundwater resource assumes increasing importance and needs an appropriate protection both from users and decision makers. The continuous discharge of acidic water into the environment puts tremendous pressure on the available fresh water resources both due to pollution load that threatens dolomitic groundwater besides raising the level of acidic water levels in the karstic aquifer.

Stream discharge measurement, hydrogeochemical and environmental isotope based study was undertaken in the upper Crocodile River basin to conceptualize surface water and groundwater interaction. Both hydrogeochemical and environmental isotope data have been integrated to identify the impact of acid mine decant and classification of different water groups in the area. The impact of the acid decant on the groundwater quality has been clearly noted with high total iron (≈1200 mg/L) and SO_4 (≈5000 mg/L). The continuous discharge of acidic water throughout a year indicates the presence of regional groundwater circulation that maintains the base flow and recharges springs.

Environmental isotopes data reveals the presence of dominantly shallow groundwater circulation within the fractured crystalline rocks while deep circulation exists within the dolomitic aquifers. Regional groundwater circulation is characterized by compartmentalized aquifer system with distinct hydrogeochemical and environmental isotope signature.

The amount of acid mine decant that seeps into dolomitic aquifer from Rietspruit close to the Sterkfontein cave, varies between 24 and 56 M m^3 per year which needs to be managed through appropriate treatment intervention.

Classification of the groundwater type was also carried out to augment the result of the statistical method on the basis of concentration data of major cations and anions for borehole water samples. Hydrogeochemical data are plotted on a piper diagram in such a way that the geochemical grouping of the various classes of water is accomplished. The detailed hydrogeochemical characteristics of the groundwater are interpreted as follows: Classification of the groundwater type was also carried out to augment the result of the statistical method on the basis of concentration data of major cations and anions for borehole water samples. Hydrogeochemical data are plotted on a piper diagram in such a way that the geochemical grouping of the various classes of water is accomplished. The detailed hydrogeochemical characteristics of the groundwater are : a high Na, Ca, Mg, HCO_3 and SO_4 concentrations that circulates within the dolomitic aquifer that are partially affected by acid mine impact; the second hydrogeochemical group which is characterised by high Ca, Mg and HCO_3 and low Na and SO_4 concentration that circulates within a perstine groundwater condition in the dolomitic aquifer; the third hydrogeochemical group which is low in Na, Ca, Mg, SO_4, HCO_3 (Max ≈ 150 mg/L) concentration, and Si content indicateing groundwater circulating within the shallow fractured/weathered crysralline rocks such as granite gneiss; and the last group is characterised by low Na, Ca, Mg, SO_4 (very low) and , high Si (max ≈ 29 mg/L) concentration which is circulating within the quartzite and alluvial aquifers and are impacted by acid mine decant.

ABSTRACT

A combined hydrogeochemical and environmental isotope study has been undertaken in the upper Crocodile River basin besides discharge monitoring survey along Rietspruit, the main tributaries to Crocodile River in order to conceptualize surface water and groundwater interaction process and to explore the classification of groundwater in relation to the geological setting. Special emphasis was given to the groundwater quality that has been impacted by the century long gold mining, agricultural and urban activities. The geology of the study area is characterized by Precambrian crystalline rocks (metamorphosed granitic plutons) and the Witwatersrand Supergroup rocks as wells as dolomites of the Transvaal Supergroup. In the meta-sedimentary rocks of the area, the surface water and groundwater interaction is highly visible within the carbonate rocks (dolomites) that are characterized by wide spread karstic structures, developed along weak tectonic zones. Multivariate statistical analysis revealed the presence of four distinct hydrogeochemical clusters that are related to different host rocks with a trace of acid mine decant. The environmental isotope data reveal that the dolomitic springs contain old (low ^{3}H) groundwater with depleted stable isotopes indicating high altitude recharge with deep circulation.

INTRODUCTION

Surface water and groundwater interaction studies are vital to implement effective management of water resources (Winter, 1999; Sophocelous, 2002). It is a known fact that well-managed water resources are vital for sustainable socio-economic development. Water resource quality degradation due to a variety of human impacts, water resource quantity depletion (streams, lakes and the groundwater), wetland drainage and pollution, and the respective impact on biota can be managed through integrated investigation of groundwater-surface water interaction (Winter, 1999). The effects of the regional physiographic framework along with climate and geology play a significant role in groundwater-surface water interaction (Winter, 1999). It is an imperative to understand the hydrogeological environment (topography, geology and climate) in order to investigate groundwater-surface water interactions (Sphocleous, 2002). Several studies can be cited in an attempt to investigate groundwater-surface water interaction with the help of analytical/semi-analytical models (Darama, 2001; Butler et al., 2001; Chen and Yin, 2003; Bakker and Anderson, 2003; Butler et al, 2007).

In the Upper Crocodile River basin (Fig. 1), the majority of groundwater discharge occurs through fractures or as a baseflow to streams or as springs and overflow from mine shafts. Surface water and groundwater interaction is also important in the context of water quality management where contaminated groundwater through Acid Mine Drainage (AMD) threatens the surface water system and in turn affects groundwater in the dolomites. Understanding the interaction between surface water and groundwater can be important for water resources management and pollution control. The degree of interaction depends on a number of factors including topography, underlying geology, subsurface hydraulic properties, temporal variation in precipitation, and local groundwater flow patterns (Oxtobee and Novakowski, 2002; Saleh, 2011; Anibas et al., 2011).

Since fractured crystalline rocks constitute the principal aquifer system in the area, streams flow directly on the bedrock due to thin soil cover and consequently the nature of the exchange between the surface water and local aquifer is extremely complex along a flow path. Several streams in the area disappear into sinkholes and some lose water while crossing the hidden or soil-filled sinkholes. The century old gold mining activity in the area has threatened the environment both chemically and physically. The most critical problem that has come to the reality after mine closure is the rapid rise in groundwater table over the last three decades by generating acid mine decant directly into surface water and seepage into shallow groundwater through fractures In the upper Crocodile River basin, the most noticeable interaction takes place in the form of:

1. Streams recharge into fractured and kart aquifers besides alluvials
2. Groundwater discharge in the form of baseflow into streams
3. Acid mine decant into streams and shallow fractured and weathered aquifers.

Since the area is characterized by arid/semi-arid environment, where rainfall is seasonal and highly variable, groundwater discharge as a baseflow is a major component of the water in streams. The stream discharges increase significantly during rainy months due to low infiltration capacity of rocks. Groundwater and surface waters transport and spread contaminants from spatially limited industrial areas or mining areas to extensive downstream regions (Tornqvist et al., 2011). Therefore, mining, industrial and agricultural activities generate most contaminants in the West Rand area, which is the main source region. The contamination of either surface water or groundwater

could affect the ecology supported by these water bodies. Thus, depletion of water quality through mine waste leakages and seepages into groundwater pose health and ecological problems to people, livestock and environment as a whole.

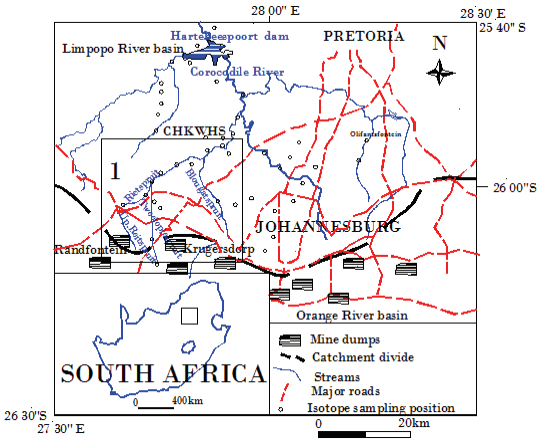

Figure 1: Location map of the upper Crocodile River basin, Gauteng (inset map for Fig. 7)

The main challenging issue in the area is the presence of AMD from the Harmony Gold mine which crosses the Krugersdorp game reserve and CHKWHS and ends up in the Hartbeespoort dam through numerous tributaries of Crocodile River. The available surface water and ground water of the area is intensively utilized by local communities for various purposes.

Surface water and groundwater interaction in the area is mostly controlled by factors such as differences in head between the streams and groundwater, the availability of hidden karst structures, lithological heterogeneity and the availability of AMD. It was also noted that treated sewage disposal from the settlement (e.g. Krugersdorp municipality) is deteriorating the quality of water resources in the basin.
The continuous leaching of slime dams in the area increases toxic chemical load into the surrounding water resources. Consequently, acidity of infiltrating water poses a risk on dolomites through dissolution processes.

The focus for this project was driven by the fact that the Crocodile River has experienced very complex human impact caused by more than a century of mining and associated large scale groundwater withdrawal. The mine water decant and anthropogenic waste disposal into the Crocodile river and its tributaries which feed the Hartbeespoort dam which is intensively used for agricultural activity. Acid mine decant, which pollutes streams in the area, needs to be investigated to a reasonable detail if one strives to make a sound understanding of impact on surface water and fresh groundwater resource areas. Numerous spring points with very low pH (close to 2.8) as a result of acid mine discharge through dikes and tectonic structures were observed inside Krugersdorp game reserve.

OBJECTIVES

The main objective of this project was to investigate surface water and groundwater interaction dynamics with special emphasis on Crocodile River basin in reference to acid mine decant and groundwater quality change by means of environmental isotopes. In order to substantiate the isotope results, stream discharge measurement and hydrogeochemical survey have been implemented. The result of the research will ultimately help to understand the local and intermediate groundwater flow system and the manner in which around water interacts with surface water, which will assist in the water quality control.

METHODOLOGY

A literature review and field surveys were carried out in order to conceptualize the hydrogeology of the area and simplified geological map for the area has been compiled. From the literatures it was noted that the groundwater of the area is under strong influence of mining activities.

A water quality monitoring program was developed especially in the West Rand area in order to understand the degree of surface and ground water interaction. During the field investigations, digital Crison and Orion instruments were used to capture pH, EC, TDS and Eh values of water. The field measurements were undertaken at different seasons for over five years. These measurements were useful in identifying seasonal variations in treated sewage effluents flow in Blougatspruit through rapid EC and pH variations, spatial change in AMD dilution in Rietspruit.

All accessible water points were sampled for $\delta^{18}O$, $\delta^{2}H$ and ^{3}H determination from July 2008 to April 2012, while few points were sampled at different seasons. These samples were analysed at iThemba Labs, Gauteng. Environmental isotopes are widely used to gain an insight into the groundwater flow dynamics, mixing and recharge conditions. Locally isotopes have been successfully used to study recharge condition in other sedimentary basins in South Africa (Sami, 1992; Adams et al., 2001) to characterize recharge mechanism and geochemical processes in semi-arid and arid environments.

Stream flow measurement along Rietspruit (West Rand) and its major tributaries (Blougatspruit,

Tweelopiespruit) that are likely to contain acid mine decant from Randfontein gold mine areas, has been carried out using a Global Water flow meter 25/08/2011 and 25/02/2012. All streams in the area traverse the CHKWHs and join the Crocodile River which flows towards Hartbeespoort dam.

Selected groundwater quality data from the National groundwater database of the Department of Water Affairs (DWA) have been used for hydrogeochemical interpretation using multivariate statistical techniques: Hierarchical Cluster Analysis based on the Ward's Minimum Variance cluster method and Factor Analysis based on principal component.

STREAM NETWORK

Streams in the study area are quick to respond to rain event and within an hour of the beginning of a rain event, significant increase in the stream flow occur which is attributed to low degree of infiltration because of impermeable nature of crystalline rocks. Dendritic type of drainage pattern is characteristic features of the area. The existence of perennial streams in the area indicates the presence of high discharge source while flowing over impermeable rocks outcrop in the form of disconnected stream. On the other hand, streams that flow over dolomitic aquifer have continuous interaction with groundwater. The continuous release of acid mine water play paramount role in regulating the discharge of streams even during the dry season.

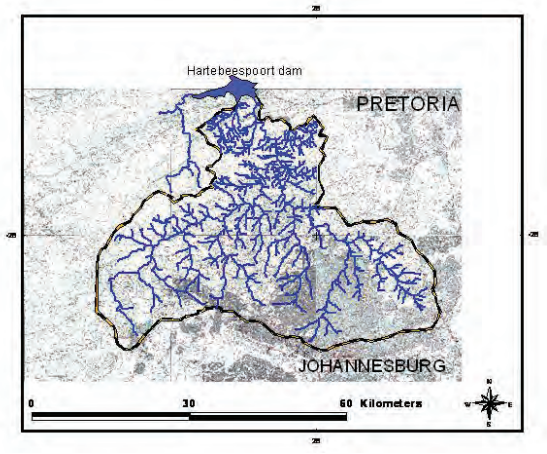

Figure 2: Stream network in the study area.

Crocodile River drains into the Hartbeespoort dam with main tributaries such as Bloubankspruit, Rietspruit, Tweelopiespruit and Blougatspruit with numerous small tributaries in the area (Fig. 2).

GEOLOGICAL FRAMEWORK

The Upper Crocodile River basin is composed of basement crystalline rocks of Archean age. They are broadly classified as granitic rocks, meta-sedimentary and meta-volcanics (Fig. 3). The Johannesburg dome consists of Archean greenstones remnants (c. 3.34 Ga, Poujol and Anhaeusser, 2001) and intruded by tonalite, granodiorite, granite and migmatites, unconformably overlain by meta-sedimentary rocks of < 3000 Ma (Barton et al., 1989; Armstrong et al., 1991; Barton et al., 1999). The Johannesburg dome is unconformably overlain by the sedimentary successions of the Witwatersrand Supergroup and is one of the few mid-Archaean granite-greenstone inliers exposed in the central part of the Kaapvaal Craton (Poujol and Anhaeusser, 2001). The tonalites are the oldest rock types, migmatites are intermediate in age and granodiorite and granite are the youngest (Barton et al., 1999).
The oldest granitic rocks comprise a suite of tonalitic and trondjemitic gneisses and migmatites that occupy most of the northern half of the dome. Exposure of similar rocks also occurs on the southern edge of the dome and unconformably underlies the Witwatersrand Supergroup (Meyers et al., 1990; Barton et al., 1999). The Witwatersrand basin is an arcuate structural basin lying within the Kaapvaal Craton. The Witwatersrand Supergroup is divided into the Lower West Rand Group and the upper Central Rand Group. The former conformably overlies volcanics of the Dominion Group and non-conformably overlaps Archean basement rocks of the Kaapvaal Craton. The south-central portion consists mainly of a variety of homogeneous, medium grained granodioritic rocks. Locally, all rocks contain a gneissic fabric and is less developed in the granodiorite and the tonalitic and trondjemitic group includes dioritic, tonalitic and trondhjemitic gneisis and migmatites (Poujol et al., 2001). The Witwatersrand Supergroup unconformably overlies basement granitoids and greenstones, as well as sedimentary and volcanic rocks of the Dominion Group.

It is made of thick terrigenous sequence comprising arenaceous and argillaceous sedimentary rocks. The deposition took place between 3074 and 2714 Ma (Robb and Meyer, 1995).

The part of Witwatersrand basin that lies close to Johannesburg dome is grouped under west rand, central rand and east rand groups. The west rand group consists primarily of quartzites and shales. The central rand group consists of different proportion of quartzites and shales where the sequence consists mainly of quartzites and conglomerates (McCarthy, 2006). The Early Proterozoic Transvaal sequence comprises of relatively undeformed, unmetamorphosed volcanic rocks, quartzites, shales,

dolomites iron formations, conglomerates and diamictites (Eriksson and Clendenin, 1990). The Transvaal Sequence is made of relatively undeformed, unmetamorphosed volcanic rocks, quartzites, shales, dolomites, iron formations, conglomerates and diamicites (Eriksson and Clendenin, 1990).

HYDROGEOLOGICAL SETTING

The upper Crocodile River basin has a semi-arid climate with mean annual rainfall ranging from 600 to 700 mm/year (DWAF, 1992; Barnard, 2000). However, the estimated annual rainfall from 24 years of data obtained from South African Meteorological Service for central Johannesburg station (Fig. 3) is 711.63 mm. The majority of rainfall occurs between October and March, mostly as a frontal type characterized by frequent thunderstorms, while winter months (June to August) are characterized by cold dry weather; these months are non-productive from groundwater recharge perspective. The pan evaporation reported by Hobbs (2011) for the West Rand area is in the rage of 2200 mm/yr.

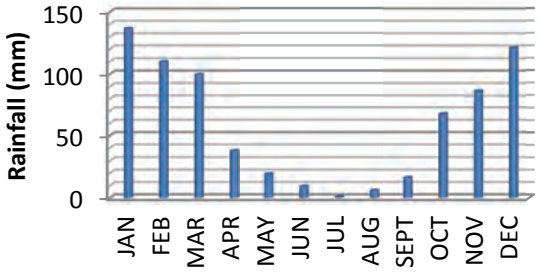

Figure 3: Monthly rainfall for Johannesburg station (Lat. S -26.1500 Long E 28.2300)

The study area is underlain by crystalline basement rocks of granitic gneisses, the meta-sedimentary rocks of Witwatersrand Supergroup as wells as dolomites of the Transvaal Supergroup (Barnard, 2000). The general hydrogeological aspect of the region has been well described in the Johannesburg hydrogeological map and associated explanatory note (Barnard, 1999 and 2000).

The hydrogeology of the area is characterized by secondary aquifers especially within the weathered and fractured crystalline rocks (granite, granitic gneiss, tonalite, quartzite); karst aquifers in the dolomite and intergranular aquifers in alluvial deposits along river valleys. In general, the heterogeneous hydrogeological setting of the area is as a result of rock deformation, secondary structure development and weathering processes.

Most of the fractured and weathered granitic rocks that outcrop in the study area have generally low and variable groundwater productivity (borehole yield varies between 0.01 l/sec and 0.98 l/sec)., while the groundwater yield in the dolomitic aquifers ranges from 15 l/sec to 124 l/sec which was estimated from DWA groundwater database (Abiye et al., 2011). It has been reported that dolomites are well known productive aquifers in different parts of South Africa (Bredenkamp et al., 1986; Buttrick et al., 1993; Bredenkamp and Xu, 2003; Holland and Wittüser, 2009). These aquifers are intersected by impervious and semi-pervious syenite and dolerite dykes, which divide them into separate groundwater compartments (Coetzee et al., 2009; Holland and Wittüser, 2009; Abiye et al., 2011). Due to the soluble nature of dolomitic formations they potentially provide good recharge sites which eventually generate high yielding springs that are associated with dykes and tectonic depressions. During the field surveys it was observed that the presence of dykes associated with local perched aquifers, which are frequently represented by low yielding springs and wetlands. High yielding have also been observed in association with karst structures in the dolomites such as the Ngosi spring in the CHKWHS (Malapa area) with an approximate discharge rate of more than 100 l/s. Alluvial deposits which are found along the stream valleys may yield as much as 16 l/sec (Barnard, 2000).

The extensive gold mining operation to a depth of hundreds of meters in the Witwatersrand Supergroup and play paramount role in connecting different groundwater basins both at shallow and deep horizons as well as inter-basin groundwater transfer. Evidence of the hydrogeological connectivity within the study area is the presence of continuous discharge of acid mine decant from the Randfontein area into the CHKWHs, where a measured discharge of about 1 m^3/s is recorded in front of Krugersdorp game reserve compound. The widespread presence of acid mine decant in the area has an impact on the Malmani dolomites that are regarded as productive aquifers and host hominid fossils. Field investigations show that networks of dissolution cavities have developed along tectonic lines in the dolomitic areas along which sinkholes exist. In the Malapa area, for example, disappearance of springs through sinkholes is a common feature aligned along a linear fracture line. The consequence of acid mine drainage on dolomitic rocks has a far reaching impact through the expansion of dissolution cavities that may threaten valuable archaeological evidence of the origin and evolution of humanity besides water quality deterioration. The impact of acid mine decant on the groundwater quality has already been clearly noted with high total iron (≈1200 mg/l) and SO_4 (≈5000 mg/l) (Abiye, 2011). The continuous discharge of acidic water throughout a year indicates the presence of regional groundwater circulation that maintains the base flow and recharges springs. According to Hobbs and Cobbing (2007), the rate of acid mine decant in the area ranges between 18,000 m^3/day and 36,000 m^3/day.

From hydrogeological point of view, the rocks that outcrop in the study area fall under hardrock category with low groundwater productivity except dolomites that contain dissolution cavities and consequently produce huge quantity of groundwater.

According to the Johannesburg hydrogeological map of 1: 500 000 scale, and explanatory note (Barnard, 2000); four aquifer types have been identified in the area.

- An intergranular aquifer in the alluvial covered zones,
- Fractured aquifer in the Witwatersrand Supergroup associated with fractures, fissures and joints
- The karstic aquifer in the dolomites
- The intergranular and fractured aquifer in the crystalline rocks

However, from repeated and detailed field surveys it was noted that groundwater occurrence in the area can be categorized into three groups: near surface occurrence within the weathering profile; occurrence within fractures, dykes and shear zones; and occurrence within dissolution cavities in the dolomites. The main characteristic features of groundwater occurrence in the highly productive dolomitic aquifer are pockets of conduits which are compartmentalized primarily by structural discontinuities such as strike slip faults. However, locally dikes and quartz veins generate perched system. The presence of recharging meteoric water through dykes and faults and the influx of thermal water along fractures within the deep gold mines in the Witwatersrand basin have been documented by Duane et al. (1997). Therefore, occasionally these dykes and faults also play important role in regulating recharges in the area

The semicircular deformation of the Witwatersrand and Transvaal Supergroup rocks around Archean granitic pluton could play substantial role in delaying groundwater circulation in the area However, the randomly oriented left lateral strike slip faults with minor occurrence of right lateral strike slip faults could act as a conduit for groundwater flow. The area is intensively deformed, fractured and dissected by dikes. Since dikes constitute an important structural set up of the crystalline rocks, they act as conduits for groundwater circulation besides compartmentalizing role in some instances. Owing to the fact that the area is made of deformed crystalline rocks, the main hydrostructures are represented primarily by fractures and weathered zones. The fractured quartzites that form the water divide between the northern Limpopo River basin and the southern Orange River basin are intensively fractured, which provide suitable media for vertical recharge. Granitic gneisses and quartzites, instead, are characterized by massive structures with wide fracture network while shales contain very tight fractures along inclined beds to the south. Dissolution structures are peculiar features of dolomites which are identified as productive aquifers in South Africa.

The alluvials which are found along stream valleys are highly productive in areas such as the lower Crocodile River valley (down-stream of Hartbeespoort dam). Such aquifers produce as much as 16 l/s (Barnard, 2000). In the dolomitic aquifer, the occurrence of cavities varies from place to place which is based on the intercalation found in dolomites. Such variability depend the type of dolomite (dolomite containing chert layers and those without chert), the availability of acidic infiltrating water, the amount of groundwater moving through the system and the degree of saturation with respect to calcite and dolomite. In large part of the area, dolomitic rocks have notorious reputation due to the occurrence of sinkholes due to the formation of dissolution cavities. The presence of acid mine drainage which is generated from the slime damps and abandoned gold mines have a potential to dissolve carbonate rocks such as dolomites. The occurrence of a series of dissolution cavities along preferential groundwater flow direction is a characteristic feature in the dolomites. Appearance and disappearance of springs is also a common feature in the area, which is controlled by availability of the karst structures.

SURFACE WATER AND GROUNDWATER INTERACTION PROCESS

In fluvial systems, the mixing of river water and groundwater is localized along the river banks and also beneath the river flow. Groundwater flow is generally parallel to the higher hydraulic conductivity fluvial plain. Exchange of chemical constituents between surface water and groundwater could occur at a stream channel scale where the infiltrating water diffuses to a wider area through fractures and dissolution structures. Local, shallow surface water circulation into the underlying sediments creates areas of groundwater recharge and discharge within zones generally characterized as gaining or losing stream sections (Woessner, 2000). Many facets of the interaction of ground water and surface water takes place in the area where karst structures act as a main sink point.

Through seepage, dissolved uranium and other heavy metals migrate from tailings deposits of gold mines via groundwater into adjacent fluvial systems. The extent of associated stream contamination is determined, inter alia, by the retardation of dissolved contaminants along the pathway and the rate in which polluted groundwater enters the stream channel (Winde and van der Walt, 2004). In the study area both chemicals and isotopes are being exchanged between surface water and groundwater (Fig. 4).

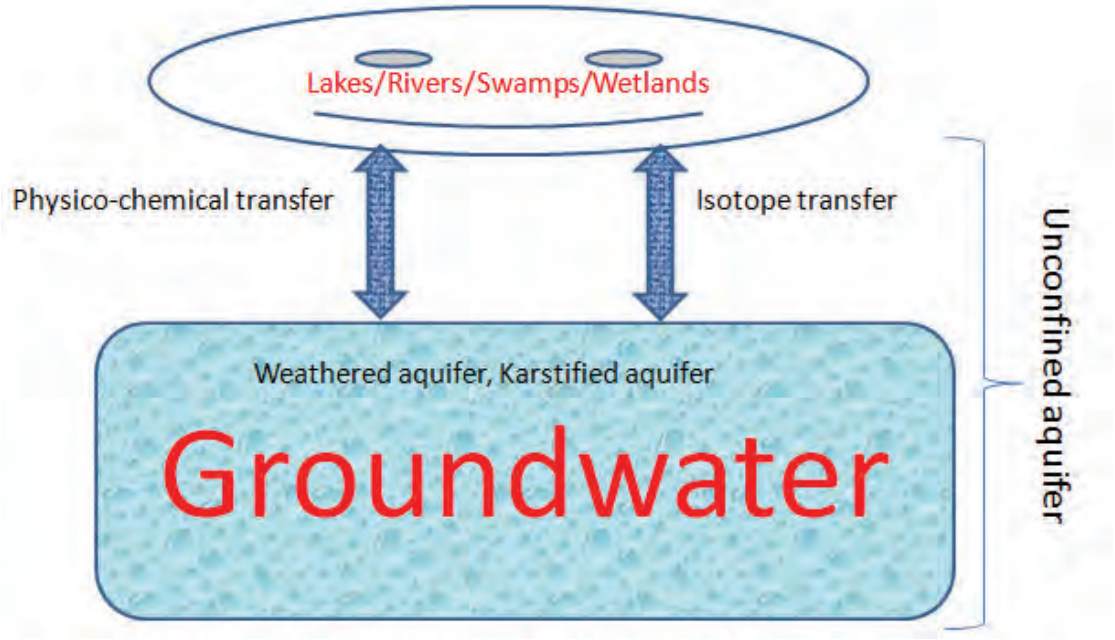

Figure 4: Conceptual interaction model in the study area

It has been repeatedly observed that no sensible water resource management can be designed without holistically looking at the multi-faced surface water and groundwater interaction (Sophocleaous, 2002). In semi-arid area, one of the most important surface water and groundwater connections is through groundwater recharge (Newman et al., 2006) which is the main process observed in the study area, in the form of acid mine decant. Control area outside the mine impact zone has been assessed to validate the result. In the area, the majority of groundwater discharge occurs through fractures, as a base flow into streams, as springs and overflow from mine shafts. Surface water and groundwater interaction is an important process in riparian zones, with relevance to water budgets, biogeochemical, and ecological processes (Sophocleous, 2002). This interaction is also important in the context of water quality management in the case when the resource is subjected to human and environmental consumption where the resource is exposed to waste disposal and acid mine decant. Understanding the interaction between groundwater and surface water can be important for water resources management, and in the determination of migration pathways for contaminants. The degree of interaction can depend on a number of factors including topography, underlying geology, subsurface hydraulic properties, temporal variation in precipitation, and local groundwater flow patterns (Oxtobee and Novakowski, 2002).

Since the meta-sedimentary and plutonic rocks constitute the principal aquifer in the area as a result of secondary structures streams flow directly on the bedrock and the nature of the exchange between the surface water and local aquifer is extremely complex. In some cases there is fast exchange due to karstification of dolomites. Several streams in the area disappear into sinkholes and some loses water when it crosses the hidden karst structures. Since the catchment is characterized by arid/semi-arid environment, where rainfall is seasonal and highly variable, groundwater discharge is a major component of the water in the streams in the form of baseflow during a dry season. The volume of water increases significantly during rainy months due to low infiltration capacity of rocks.

Investigation of the interaction between surface water and groundwater is critical in order to determine the effects of water quality for management practices. The interaction process as a result of exchange of fluxes is often characterized by a high temporal and spatial variability. Commonly the type of interaction is described by the direction of the exchange fluxes distinguishing between influent (flowing in) fluxes and effluent (flowing out) fluxes (Krause et al., 2007). Such fluxes are important to focus on due to the danger posed on water quality in the area.

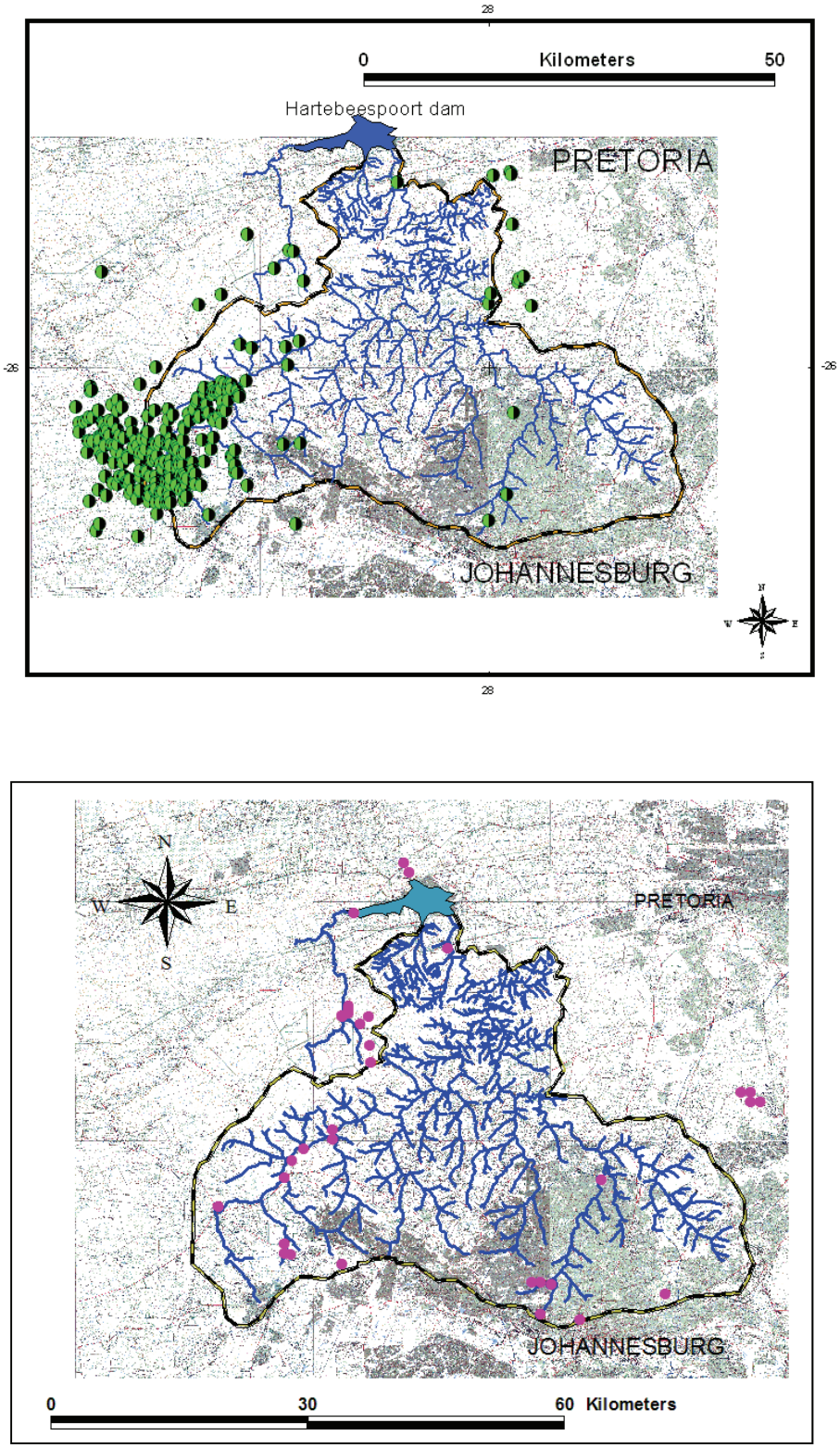

Figure 5: Boreholes (top) and environmental isotopes (bottom) sampling points.

Metal contaminated acidic groundwater discharges into surface water bodies traverses through open mines, fractures and dissolution cavities. The interaction process in the area is primarily determined by acid mine decant that manifests itself through direct discharge on surface and through springs. However, alkaline groundwater in dolomites has a potential to neutralize the acid (buffers) as a consequence of dissolution which could potentially affects the CHKWHS. In order to thoroughly characterize the interaction process, boreholes presented in Fig. 5 and environmental isotopes data point in Fig. 6 have been analysed and interpreted.

APPLICATION OF ENVIRONMENTAL ISOTOPES

The stable isotopes of ^{2}H and ^{18}O occur naturally in precipitation and provide a seasonal meteoric signal in temperate, continental systems that are often attenuated in shallow groundwater (Clark and Fritz, 1997). Seasonal stable isotope variations in precipitation have been used to study the movement and the source of subsurface water in various settings of the upper Crocodile River basin.

There is a frequent lose stream water to ground water as they traverse the highly permeable alluvials and karst structure. Stable and radioactive isotopes have been effectively used in the study of groundwater and surface water interaction studies (Alpers and Whittemore, 1990; Ojiambo, et al., 2001; Oxtobee and Novakowski, 2002; Leybourne et al., 2006). Environmental tracers have advantages over artificial tracers because they are present in recharge water from natural or anthropogenic sources and thus do not require injection (Long et al., 2008). Tritium (^{3}H) is important environmental tracer that is useful to understand the circulation rate of groundwater.

The stable isotope ^{18}O is useful for determining source water areas when different source waters have unique isotopic signatures.

River water levels and topography are certainly the main causes of the exchange between groundwater and river water through the riverbank. Stable isotopes, such as ^{18}O, are useful tools that allow water movement to be traced. The study of water mixing assists an understanding of the availability of water in riparian soils. River water levels and topographical details are certainly the main causes of the inflow of groundwater through the river bank (Lambs, 2000; Lambs et al., 2002). It is generally considered that groundwater is characterized by stable flow, even temperature and a stable chemical composition that reflects the underlying aquifer geology.

The attenuation of precipitation signals by the underlying catchment has been used to evaluate the mean residence time for stream baseflow using sinusoidal relationships and other models that describe flow path distributions (Maloszewski et al., 1983; Pearce et al., 1986; DeWalle et al., 1997). These models assume that the isotopic attenuation reflects the mean residence time of transport from recharge through the entire flow system and that the recharge is uniformly distributed in time.

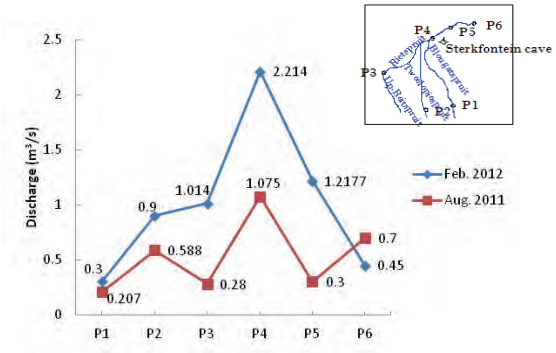

Figure 6: Discharge variation along Rietspruit and its tributaries in the CHKWHS

RESULTS AND DISCUSSIONS

Stream hydrograph

Fig. 6 presents the flow rate along the Rietspruit and tributaries as measured on 25/08/2011 and 25/02/2012. The main-stem of the Rietspruit shows variable discharge. The increase between P3 and P4 is related to base flow contribution and the presence of additional small tributaries. The measured loss is in the range of 0.78 m^3/s in the month of 25/08/2011 (24.5 million m^3/yr) and 1.764 m^3/s in the month of 25/02/2012 (55.6 million m^3/yr). P2 that contains AMD drains the Krugersdorp Game Reserve and contributes to higher discharge values at P4 as a result of springs in the game reserve in combination of major upstream tributaries (P1 and P3).

HYDROGEOCHEMICAL CONSIDERATION

Detailed interpretation of physico-chemical and chemical parameters of water could potentially reveal the degree of surface water and groundwater interaction through dilution or precipitation process. Two specific areas were targeted for detailed hydrogeochemical analysis in the West Rand: Sterkfontein and Malapa.

The field measured parameters show considerable variation (Table 1) as a result of the presence of different quality water and frequent interaction along a

flow path. High EC/TDS water is derived from AMD with very low pH which joins the surface water resources of the area. As the water flows downstream, pH tend to increase with reduction in EC/TDS values as a result of dilution with dolomitic water or precipitation along a flow path

The plot of Fig. 7 shows changes in field measured parameters as a result of interaction of different water groups and hydrogeochemical processes. pH shows increasing trend due to buffering reaction while other parameters show decreasing trend as the acidic water flows downstream.

The diamond plot on Fig. 8 clearly shows the presence of mixed water and acidic end member while carbonate water is represented in the anion triangle.

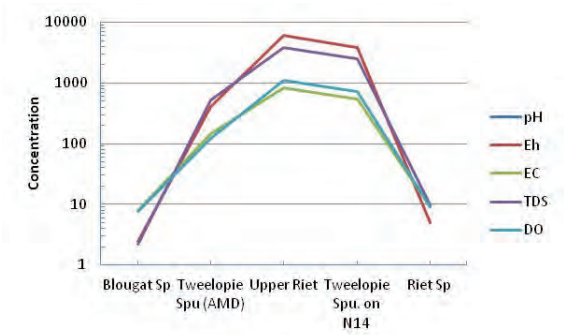

Figure 7: Variation of field measured parameters (Table 3) along a Rietspruit.

A plot on Fig 9a portrays that Ca and Mg show linear mixing line that suggests similar source for Ca and Mg (dolomitic aquifer), mixed water and shallow circulating water. Fig 9b shows change in chemical constituent downstream as a result of mixing or precipitation process

The hydrogeochemical results from the Malapa area (Table 4) show that pH progressively increases as water flows downstream where alkalinity is influenced by degassing of the water as it interacts with the atmosphere. High TDS values are mainly related to Ca and HCO_3 ions, which are predominantly a function of carbonate dissolution. It was noted that the calcium concentration decreases with decreasing altitude in the Malapa area which could be due to calcite precipitation forming tufa deposit. All springs can be classified as Ca, Mg-HCO_3 water. From the springs settings it is possible to observe that the spring sources are structurally controlled by faults, joints and dykes.

Plate 1. AMD in West Rand Dilution of AMD takes place by the waters derived from quartzites and dolomites which buffers the pH and precipitate most of the chemical constituents in the form of oxides along the flow path (Plate 1) which shows ferric iron hydroxide (reddish in colour) precipitate along the route abandon by the Rietspruit. This process potentially attenuates heavy metal load through deposition on the stream bed. The chemical analysis for the Malapa area (Table 3) shows uniform composition with slight increase in pH

Table 1: Field measured parameters (mean values)

Parameters	Blougat Sp	Tweelopie Spu (AMD)	Upper Riet	Tweelopie Spu. on N14	Riet Sp
pH	7.28	2.40	7.87	2.22	7.71
Eh (mv)	120	404	146	520	120
T(°C)	21.9	22.9	23.7	23.8	24.4
EC (µS/cm)	412	6050	840	3840	1104
TDS (mg/L)	2640	3860	534	2460	711
DO (mg/L)	9.27	4.9	9.11	9.71	9.15

Table 2: Chemical data from streams and AMD in the West Rand area (CHKWHS)

Parameter	Blougat Sp.	Tweelopie Sp.	Upper Riet Sp.	Riet Sp. 1 (above Sterkfontein Cave)	Riet Sp. 2 (below Sterkfontein. Cave)	Rainbow farm
pH	7.75	3.00	3.55	6.79	7.80	7.83
EC (µS/cm)	210	2120	987	*833*	152.6	151.5
Ca (mg/l)	32	626	197	146	10.1	7.7
Mg (mg/l)	13.5	172	55	48	11.7	3.8
Na (mg/l)	16.4	99	64	57	7.2	8.6
K (mg/l)	3.4	9.6	6.6	5.6	1.5	1.8
Cl (mg/l)	24	104	56	49	14.7	10.3
SO_4 (mg/l)	60	4096	1243	880	15.0	7.5
TH ($CaCO_3$) mg/l	135	2271	718	562	73	35
HCO_3 mg/l	99	20	20	37	82	34
NO_3 mg/l	13.4	0.9	8.8	17.1	6.6	5.2

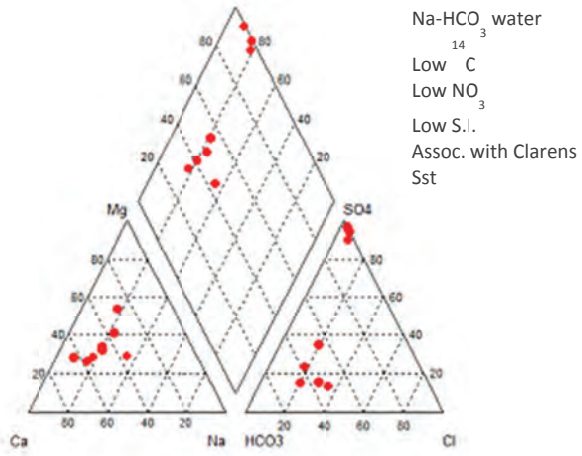

Figure 8: Piper plot for the West Rand samples.

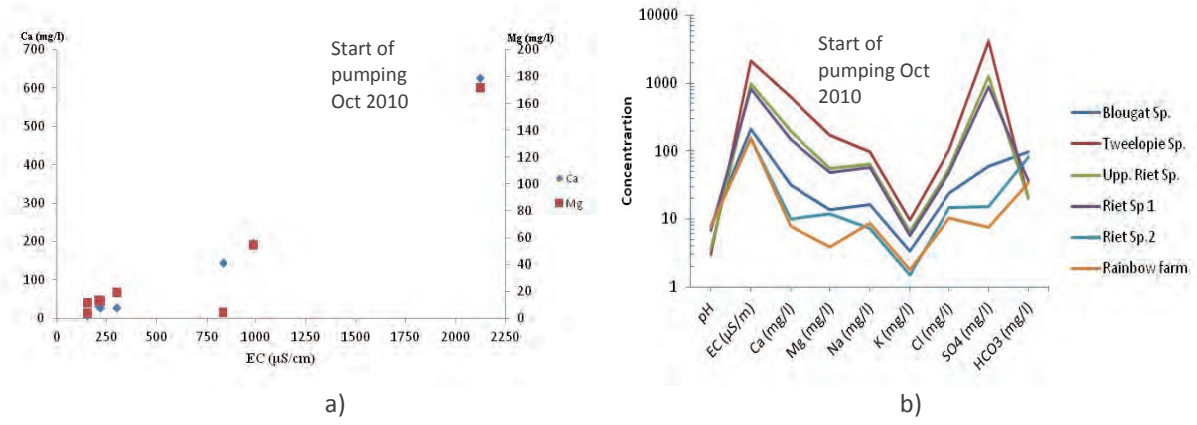

a) b)

Figure 9: Ca and Mg control over EC (a) and a semi log plot for chemical constituent in the Sterkfontein area (table 2)

Table 3: Major ion composition of background samples (Malapa area)

Parameters	Thari e Ntso spring (1)	Thari e Ntso sp 100m below (2)	Ngosi sp (3)	Bokamoso sp (4)	On the Tuffa (5)	mixed sps (6)
pH	8.1	8.3	8.2	8.3	8.4	8.5
EC (mS/m)	35.3	32.4	37.7	34.7	34.8	28.6
Ca (mg/l)	38	32	41	38	34	31
Mg (mg/l)	23	24	26	24	24	20
Na (mg/l)	1.6	1.5	1.5	1.5	1.3	1.8
K (mg/l)	0.5	0.2	0.4	0.3	0.3	0.4
Tot. Alka (mg/l)	184	172	199	189	187	154
HCO_3 (mg/l)	224	207	243	226	221	219
CO_3 (mg/l	Nil	1	Nil	2	4	5
Cl (mg/l)	2.4	2.4	1.4	1	1.4	2
SO_4 (mg/l)	2.9	2.4	2.1	0.6	1.9	1
NO_3 (mg/l)	3.3	2.2	1.9	1.7	2.1	2

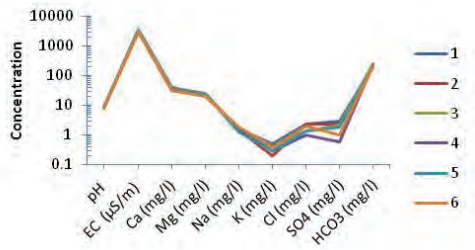

Figure 10: A semi-log plot for chemical constituents in the Malapa area which are not affected by surface water.

Fig 10 depicts uniform chemical pattern as a result of source of water from similar source, in this case dolomitic aquifer, and absence of dilution or interaction with different water source. The groundwater chemistry data obtained from DWA National groundwater database (Fig. 11) reveals the presence of both mixing of water resources in the area as the concentration ranges from HCO_3 to SO_4. Further, the data distribution is related to the chemical control as a result of reverse ion exchange with simple mixing and dissolution of carbonate rocks. Due to complexity in the aquifer setting and mining activities, the nature of interaction is heterogeneous. However, high SO_4 and HCO_3 content reveals potential end members with mixed water in lies in between. The end members are represented by AMD and dolomitic groundwater respectively.

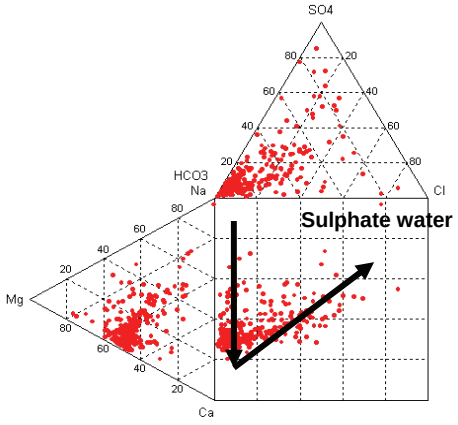

Figure 11: Durov diagram shows reverse ion exchange and carbonate dilution.

SPATIAL VARIABILITY OF CHEMICAL CONSTITUENTS

Characterization of spatial distribution of ions shades light on the affinity of chemical constituent to a certain geological formation or groundwater mineralization processes. In order to understand the hydrogeochemical complexities in the Upper Crocodile River basin, detailed spatial maps have been prepared (Fig 12).The spatial plots demonstrate complex chemical distribution in the lower left corner which is identified as Krugersdorp area including CHKWHS. Some chemical constituents show uniform pattern which could imply the control of similar geochemical process and lithological setting with the direction of groundwater flow from south to north.

.

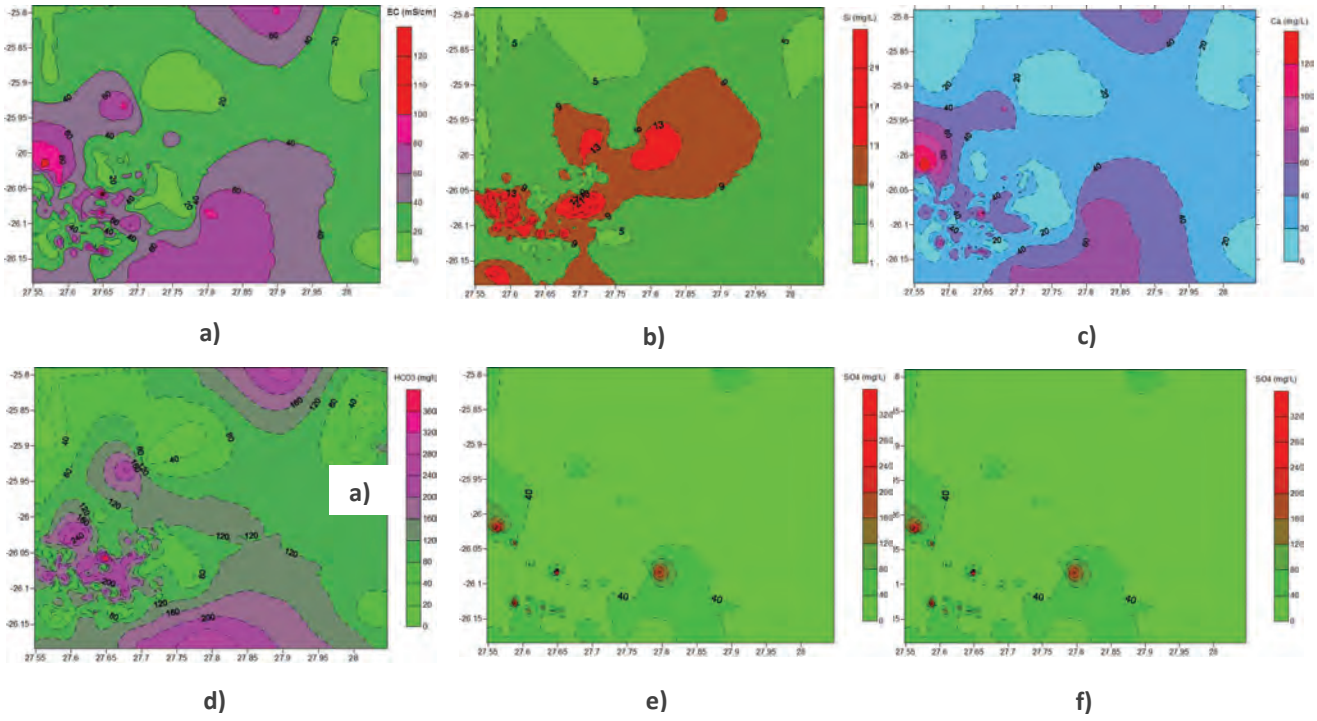

Figure 12: Spatial variation of chemical constituents in the project area

STATISTICAL ANALYSIS

Principal Component Analysis

Principal Component Analysis (PCA) a statistical tool used to descriminate common catagories out of a data cluster to draw reasonable conclusion. PCA was used to identify chemistry of dominant groundwater types thereby identifying common geochemical categories and grouping of water quality types besides the interrelations to the aquifer. For the PCA eight dominant ions were considered; namely Ca, Mg, Na, K, Cl, SO_4, HCO_3 and Si. It is evident from the data that four principal components (PCAs) account for 89.86% of the total variablity in the data set (Table 4).

The loadings are the correlations between the original variable and the individual components. The values indicate roughly the relative contribution/importance of each ions in each principal component. The result shows that Ca, Mg, Na and SO4 have maximum loading on PC1, which could be considred as a principal chemical cosntituent of the aquifer in the area except SO4, which is derived from AMD, while HCO3 has highest loading on PC2 and PC3. The clustering of most of the data points to the origin shows significantly dissimilar information. Fig 14a shows loading of PC2 on PC1 with HCO3, K and Cl. Possible occurrence could be shallow groundwater with a source from a shale dominated recharge zone, which is the main lithology on the northeren slope of the watershed. Fig 13b shows loading of PC3 on PC1 with HCO3, Mg and Ca. Possible source is likely to be dolomitic rocks. Fig 13d shows loading of PC4 on PC1 with Cl, Na and Mg. For such type of source rock is deducted to be an aquifer of acidic crystalline rock such as granite and gneiss. However, Cl can be generated from marine precipitarion, urban pollution etc.

Table 4: PCA distribution in four component

Eigenvectors				
	PC1	PC2	PC3	PC4
Na	0.372665	0.484661	0.012693	0.224661
K	0.218158	0.387749	0.452492	-0.31314
Ca	0.447612	-0.37114	-0.11681	0.068698
Mg	0.471797	-0.29192	-0.04209	-0.09529
HCO_3	0.341808	-0.38735	0.409976	-0.36072
SO_4	0.340796	-0.03258	-0.51891	0.317685
Cl	0.396605	0.450692	0.039485	0.069234
Si	-0.01756	-0.19382	0.58375	0.775779
Eigenvalue	3.744856	1.371638	1.171647	0.900693
Proportion	46.81%	17.15%	14.65%	11.26%
Cumulative	46.81%	63.96%	78.60%	89.86%

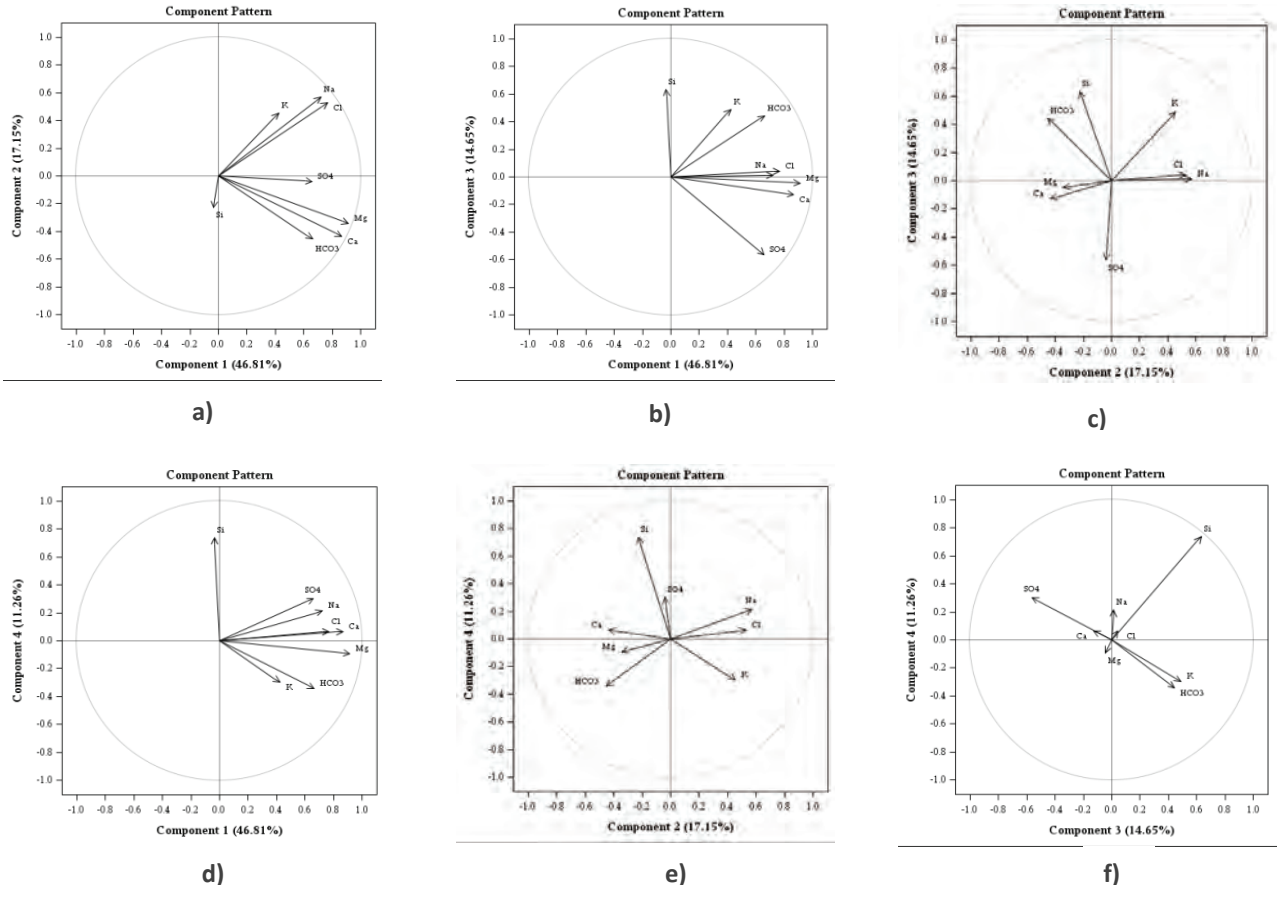

Figure 13: Loading plots of component 1 to 4. Plot f exclusively shows silica leaching.

HIERARCHICAL CLUSTER ANALYSIS

HCA was performed on the hydrogeochemical parameters for selected DWA boreholes within the study area which considers similarity in hydrogeochemical concentration and regroups the samples. Fig. 14 shows four clusters of specific hydrogeochemical groupings presumably due to similar geochemical processes within the aquifer or similar sources. The cumulative variance of the four clusters is 99.32% with the maximum and minimum semi-partial R^2 of 0.3705 and 0.0607, respectively, indicating more acceptable hydrogeochemical clusters in the area. The identified clusters clearly show the hydrogeochemical footprints in the area due to lithological control and AMD impact.

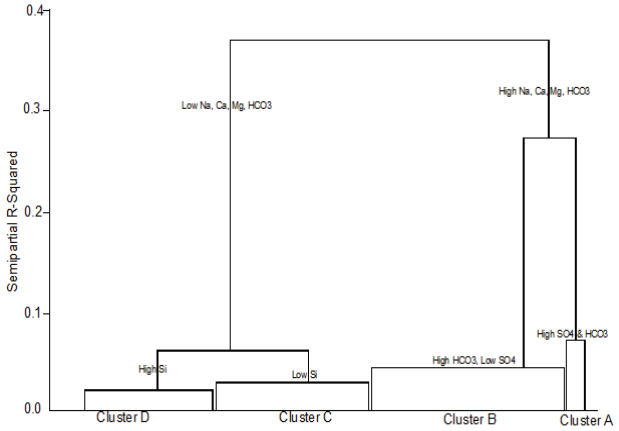

Figure 14: Four hydrogeochemical clusters in the area

Classification of the groundwater type was also carried out to augment the result of the statistical method on the basis of concentration data of major cations and anions for borehole water samples. Hydrogeochemical data are plotted on a piper diagram (Fig 14) in such a way that the geochemical grouping of the various classes of water is accomplished. The detailed hydrogeochemical characteristics of the groundwater are interpreted as follows:

- Cluster A has high Na, Ca, Mg, HCO_3 and SO_4 concentrations which could be attributed water resident within dolomitic aquifer. The high sulphate content could be derived from acid mine decant. This group is identified as sodium bicarbonate-sulphate and calcium bicarbonate type water.
- Cluster B has high Ca, Mg and HCO_3 with low Na and SO_4 concentration and it is attibuted to the relatively uncontaminated groundwater within the parts of the dolomitic aquife (could be deep circulation system). This group is identified as calcium –magnesium bicarbonate type water.
- Cluster C has low Na, Ca, Mg, SO_4, HCO_3 (Max ≈ 150 mg/L) concentration and low Si concentration. This cluster indicates groundwater belonging to fractured/weathered crystalline rocks such as granitic gneiss with predominantly shallow circulation. This group is identified as sodium bicarbonate type water
- Cluster D has low Na, Ca, Mg, SO_4 (very low) and high Si (max ≈ 29 mg/L) concentrations. This cluster could belong to quartzite and alluvial aquifers. This group is identified as Sodium sulphate type water

HCA has identified different hydrogeochemical groupings within the groundwater of the study area with variable chemistry which reveals an indication of the impact of acid mine decant on groundwater quality. In order to substantiate the results of the cluster plot, piper diagram (Fig. 15) has been prepared with all clusters represented in all identified facies.

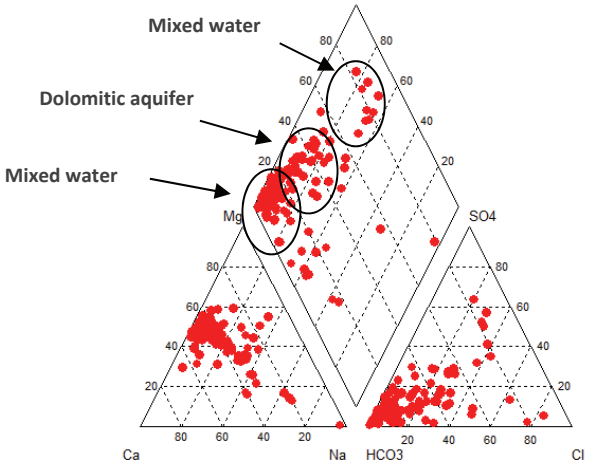

Figure 15: Hydrogeochemical facies in relation to cluster classification

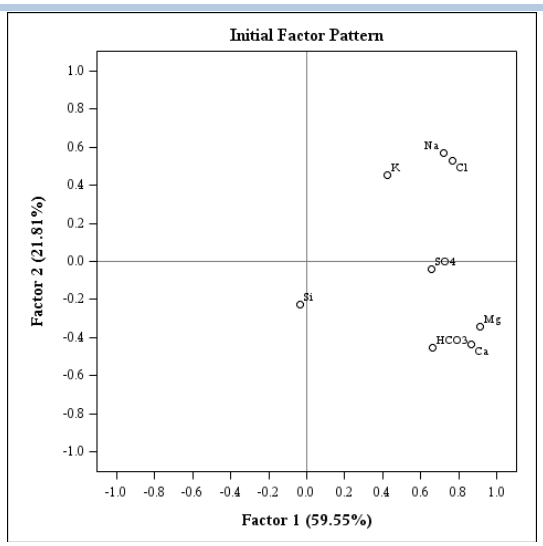

a)

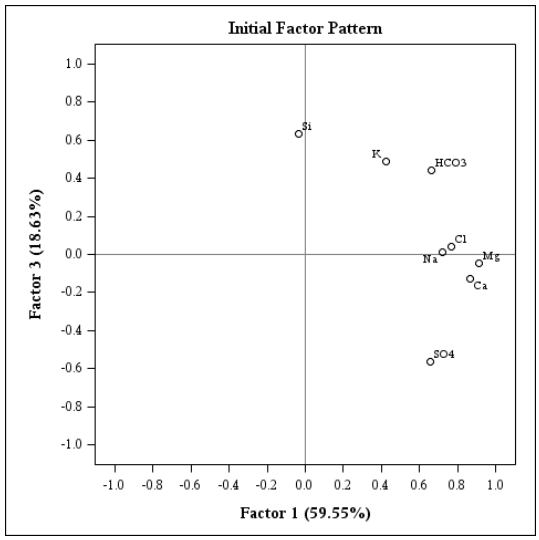

b)

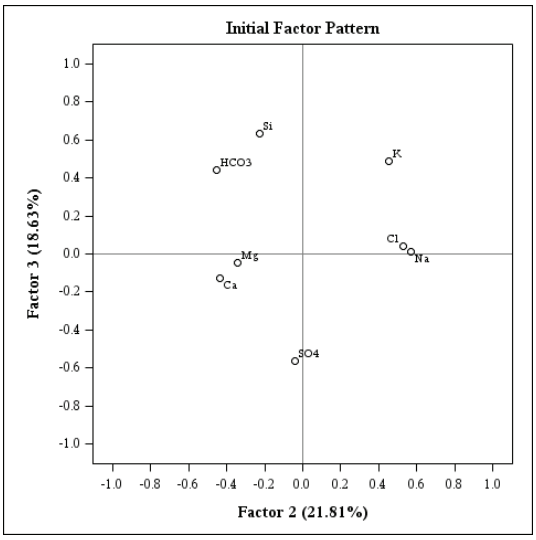

c)

Figure 16: Three factors plot that constitute unimpacted groundwater in the area

FACTOR ANALYSIS

Factor analysis is another tool implemented to identify common hydrogeochemical variables as a factor based on the principal components. It has been performed through correlation matrix without rotation where the communalities of variables define the variance. Three factors have been identified that are higher than 80% except for K, SO_4 and Si (Fig. 16). Since the natural abundance of K is low in the area, the remaining ions: SO_4 and Si are associated with the impact of acid mine decant, which were not reported as an important factor by factor analysis. Therefore, factor analysis did not pick up the hydrogeochemical changes due to acid mine drainage impact. Hence, the three factors (Figs. 16a, b, c) reveal the background natural geochemical composition in the area.

The results show that the control of Factor 1 over Factor 2 is represented by Na, K and Cl ions (Fig. 16a) while influence of Factor 1 over Factor 3 is marked by Na, K, HCO_3, and Cl ions and partially by Si (Fig. 16b). The dominant Factor among all is Factor 1 with high Ca, Mg, HCO_3 and SO_4 ions which represents groundwater from dolomitic aquifer with partial impact from acid mine decant.

Individual factors are characterized by:
Factor 1: Ca, Mg, HCO_3, SO_4
Factor 2: Na, K, Cl
Factor 3: Na, K, Cl, HCO_3, Si

Based on the presence of SO4 and Si ions, factor 1 and 3 shows the influence of acid mine impact on fresh water resource of the area.

ENVIRONMENTAL ISOTOPE INTERPRETATION

Isotopes of $\delta^{18}O$, $\delta^{2}H$ and ^{3}H are widely used to gain an insight into the groundwater flow dynamics, mixing and recharge conditions. Locally isotopes have been successfully used to study recharge condition in other sedimentary basins in South Africa (Sami, 1992; Adams et al., 2001) to characterize recharge mechanism and geochemical processes in semi-arid and arid environments. Most of the data for the study area plot below the Local Meteoric Water Line (LMWL) and indicate recharge that took place after evaporation process. Clark and Fritz (1997) indicated that for local investigations as in the case of the study area, it is important to compare surface and ground water data with the LMWL. Few stream samples plot above the LMWL as a result of impact by the rainwater. Of

course, summer season is hot and rainy and is main source of recharge to the aquifers of the area.

The stable isotope plot also portrays mixing trend where the end members are deep circulating water in dolomites (depleted with $\delta^{18}O$ and $\delta^{2}H$) and stream (relatively enriched) where shallow boreholes lie in between and could be a mixing product. The mean values for $\delta^{18}O$, $\delta^{2}H$ and ^{3}H for the rain samples is -4.11(‰), -17.26 (‰) and 5.32±0.4 T.U. respectively. The rain water isotope plot above the LMWL which, according to Clark and Fritz (1997), could be due to low humidity in the vapour. The plot on Fig. 17 further shows that AMD has intimate relation with shallow groundwater which is a clear evidence for its source from shallow aquifers.

The data obtained from the study area (Table 7) have been plotted below the LMWL where dolomitic springs are depleted with respect to $\delta^{18}O$ and $\delta^{2}H$. They represent deep circulating karst springs in the Malapa area. Streams with relatively enriched stable isotopes shows frequent interaction with meteoric water and have relation with shallow circulating groundwater. The data plotted between the highly depleted springs and stream samples are from groundwater that contains mixed water.

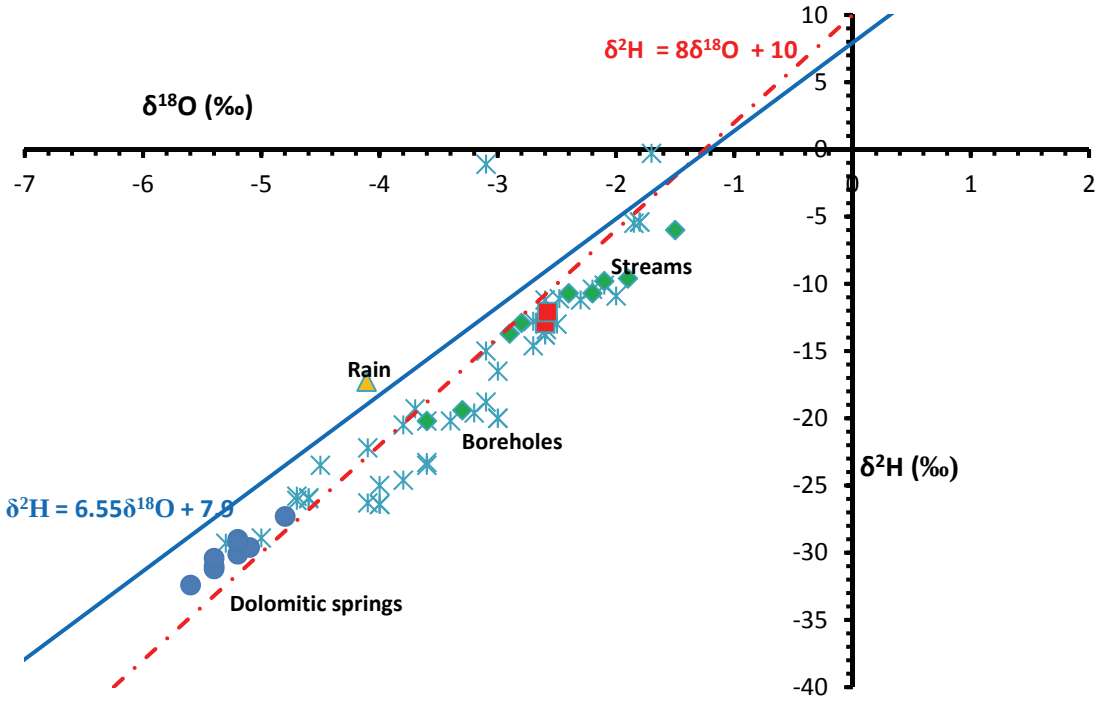

Figure 17: Stable isotope plot for the water samples taken in the upper Crocodile River Basin.

From the tritium results (Table 5) it is noted that dolomitic springs are older than 6 decades and are depleted with respect to $\delta^{18}O$ and $\delta^{2}H$ which suggests the presence of deep circulating groundwater within the karst structure where the flow mechanism is dominantly diffusive type. The shallow circulating groundwater is subjected to recent recharge with relatively enriched $\delta^{18}O$ and $\delta^{2}H$. The rain water plots above the LMWL could be related to the condensation effect which is controlled by regional air circulation from the South Atlantic and Indian Ocean air masses. One of highly productive springs in the Sterkfontein area within the CHKWHS, is known as Ngosi spring, which emerges as a group of springs from karstified dolomite. For this particular spring, the measured $\delta^{18}O$, δD and ^{3}H values are -5.42‰, -31.0‰, 0.6±0.2 TU, respectively. The data show that this spring is categorized as old water with more than five decades in circulation which indicates low permeability of dolomitic aquifer. The groundwater samples with nil tritium have been underground for a long time (>50 years) and are not derived from the present day rainfall. The groundwater samples with zero (near zero) tritium have been in circulation for a long time (>50 years) and are not derived from the present day rainfall. The low value of ^{3}H for the acid mine decant at Randfontein which is 1.8±0.3 TU shows that discharge of relatively old water which is in circulation for over 2 decades. The stable isotope values show evaporation effect due to the fact that the samples were collected before AMD joins the Krugersdorp game reserve and it was exposed for evaporation. As the AMD progresses downward, the tritium value increases due to mixing with shallow circulation recent water.

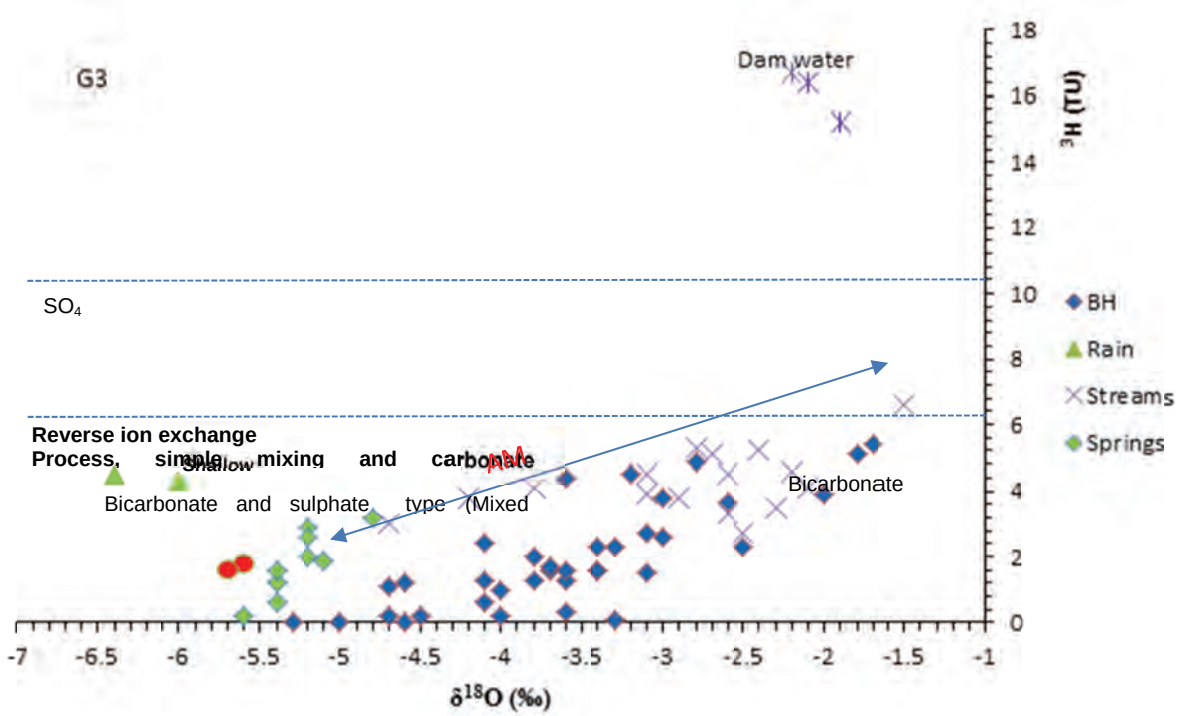

Figure 18: Sample grouping based on $\delta^{18}O$ and ^{3}H relation

Table 5: Environmental isotope results from upper Crocodile River basin (2009-2012)

Description	Lat (S)	Long (E)	pH	TDS (mg/L)	EC (µS/cm)	Eh (mv)	$\delta^{18}O$ (‰)	δD (‰)	^{3}H (T.U.)
Westdene Dam Inlet Aug. 2008	-26.18	27.99	7.44	171.9	269	-32.6	-3.11	-15.0	3.9±0.3
Emmarentia Dam Outlet Aug. 2008	-26.15	28.00	7.20	106	167	-15	-2.72	-12.8	5.1±0.4
Conrad Drive Bridge Aug. 2008	-26.04	28.05	7.99	149.1	233	-40.5	-2.44	-10.7	5.2±0.4
Broederstroom Crocodile River Aug. 2008	-25.80	27.89	8.21	181.4	284	-52	-1.51	-6.0	6.6±0.4
Hartbeespoort Dam West Arm Aug. 2008	-25.76	27.79	9.60	146.4	229	-125.1	-1.89	-9.6	15.2±0.7
Hartbeespoort Left Bank Canal Aug. 2008	-25.72	27.85	9.37	148.9	232	-111.5	-2.13	-10.1	16.4±0.7
Crocodile River Near Brits Aug. 2008	-25.71	27.85	8.84	158.1	247	-87.7	-2.24	-10.4	16.7±0.7
Kaal River Aug. 2008	-25.92	27.81	18.70	328	210	-39.9	-3.14	-1.1	4.5±0.4
Thari e Ntso spring (Malapa) Apr 2009	-25.90	27.81	7.51	116.2	181.4	-15.7	-5.17	-29.0	2.9±0.3
Malopo Spring (Malapa) Apr 2009	-25.87	27.81	8.47	120.7	188.9	-64.5	-4.75	-27.3	3.2±0.3
Ngosi Spring 1 (Malapa) Apr 2009	-25.87	27.78	7.65	140.2	220	-22.2	-5.42	-31.0	0.6±0.2
Ngosi Spring 1 (Malapa) Apr 2009	-25.88	27.80	7.77	145.5	228	-29.5	-5.40	-31.2	1.2±0.2
Malapa Culvert (Malapa) Apr 2009	-25.87	27.79	8.53	110.6	172.6	-73.2	-5.39	-30.4	1.6±0.3
Mixed sp (Malapa) Apr 2009	-25.86	27.79	8.59	87.4	136.5	-75.2	-5.23	-30.1	2.0±0.3
Malapa st1 (Malapa) Apr 2009	-25.87	27.79	8.52	77.8	121.4	-76.5	-5.11	-29.6	1.9±0.3
Malapa st2 (Malapa) Apr 2009	-25.86	27.79	8.38	108.1	168.9	-63.1	-5.17	-29.2	2.6±0.3
Bokamosa spring (Malapa) Apr 2009	-25.87	27.78	7.66	110	172.3	-31	-5.64	-32.4	0.2±0.2
Blougat spr 1 (WR) July 2010	-26.08	27.74	7.52	118.8	185.3	-0.1	-2.89	-13.7	3.8±0.3
AMD Randfontein mine (WR) July 2010	-26.11	27.72	3.55	1502	2350	198.1	-2.49	-13.0	1.8±0.3
Ds. Bloubankspruit (WR) July 2010	-25.99	27.77	7.53	216	337	-18.2	-2.22	-10.7	4.6±0.4
Reit st (WR) July 2010	-26.03	27.72	7.57	217	339	-21.9	-2.09	-9.8	4.1±0.4
Ups. Bloubankspruit (WR) July 2010	-26.00	27.76	7.82	225	352	-35.3	-2.49	-13.0	2.7±0.3
Reitspruit (WR) July 2010	-26.03	27.72	7.90	194.3	303	-38.1	-2.61	-12.9	3.3±0.3
Strekfon str July 2010	-26.00	27.77	7.82	229	358	-25.4	-2.31	-11.2	3.5±0.3
Montegomeryspruit July 2010	-26.15	27.99	8.12	135.8	212	-48.9	-2.80	-12.9	5.3±0.4
Emmarentia St at Victory park July 2010	-26.14	28.01	8.24	112.6	176	-39.8	-2.63	-11.2	4.5±0.4
Rain JHB 12/2010	-26.19	28.03	6.00	72	120	12	-6.37	-31.6	4.5±0.4
Tweelopie Sp (AMD) May 2011	-26.11	27.72	3.00	1502	2350	200	-5.65	-20.4	1.6±0.3

Description	Lat (S)	Long (E)	pH	TDS (mg/L)	EC (µS/cm)	Eh (mv)	$\delta^{18}O$ (‰)	δD (‰)	^{3}H (T.U.)
Riet Sp May 2011	-26.03	27.72	4.60	1200	1750	89	-3.77	-20.5	4.1±0.4
Rain JHB 01/ 2011	-26.19	28.03	6.00	69	120	2.5	-5.98	-30.8	4.3±0.4
Rain JHB 31/12/2011	-26.19	28.03	6.16	170	110	156	-3.81	-10.2	4.5±0.4
Blougat S. Apr 2012	-26.05	27.44	7.21	4120	2640	120	-2.48	-11.1	4.2±0.4
Tweelope S. Apr 2012	-26.11	27.72	2.78	6050	3860	404	-2.59	-13.4	2.5±0.3
Upper Riet S. Apr 2012	-26.23	27.78	7.04	840	534	146	-1.85	-5.5	2.5±0.3
Riet S. Apr 2012	-26.23	27.78	7.11	1104	711	120	-2.58	-12.1	2.9±0.3
Wits camp. Apr 2012	-26.19	28.03	6.42	173.6	259	159	-2.70	-14.6	3.2±0.4
Rain JHB 11/1/2012	-26.19	28.03	6.69	30	19	200.4	-0.23	3.5	8.0±0.5

At least three groups of water can be identified based on $\delta^{18}O$ and ^{3}H distribution (Fig.18). Group 1 (G1) represents both shallow and deep circulating groundwater in weathered aquifer and dolomites respectively where the tritium value is lower than the current rain value in the area. G2 represents shallow or water in streams except couple of samples with depleted $\delta^{18}O$ due to deep water mixing. G3 represent samples collected from Hartbeespoort dam with very high tritium content.

The environmental isotope signal for the acid mine decant shows an average value of -5.6‰ for $\delta^{18}O$, -22.0‰ for $\delta^{2}H$, and 1.8 T.U. for ^{3}H, which could be interpreted as water discharged from deep circulating groundwater from wider hydrogeological basin due to its location on the water divide. Its depleted oxygen isotope and high redox potential values (right quadrant of Fig. 19) provides an important evidence for its content in oxidizing minerals. Due to its positive Eh as a result of high concentration of iron, most of the samples which are impacted by acid mine water plot on the upper quadrant of Fig. 20 while deep circulating dolomitic water plot in the lower portion of the graph (reducing environment).

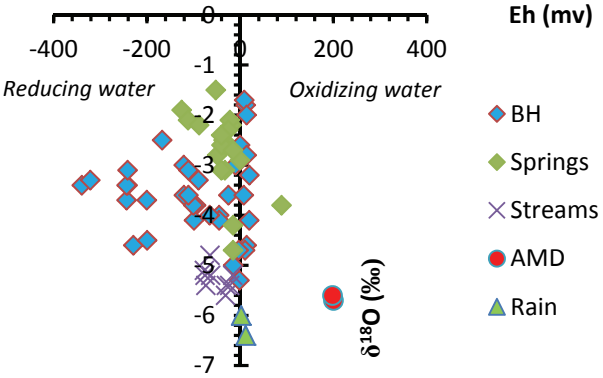

Figure 19: $\delta^{18}O$ vs. Eh plot

It is highly likely that the value from the acid mine decant samples could not be reasonably interpreted in relation to recharge from the local rainfall that has a Tritium value of 4.5 T.U. (typical local rain value). Generally, the composite data evidently illustrates the presence of different aquifer systems (shallow weathered, fractured and deep karstified) in the area with variable recharge and circulation dynamics. It is also evident that perennial streams and shallow boreholes are enriched with respect to heavy isotope due to evaporation effect while deep circulating karstic springs contain depleted water due to recharge from high altitude and more wider catchment (Fig. 19 left quadrant and Fig. 20 lower quadrant). The isotope signature of the springs which represents relatively old water with roughly with more than five decades in circulation (low ^{3}H) which again is related to high altitude recharge and/or recharge from wetter climate (old and depleted stable isotope signal) indicating the presence of deep circulation groundwater in the dolomitic aquifer.

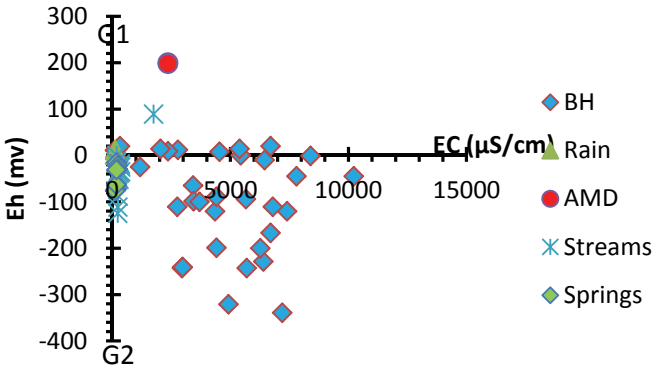

Figure 20: EC vs Eh plot showing oxidizing and reducing water distribution

Deuterium excess (*d-excess*=$\delta^{2}H-8\delta^{18}O$) interpretation was undertaken in order to characterize the likely source of precipitation of the area which gives rise to the recharge to the deep aquifer. The $\delta^{18}O$ value was plotted against *d-excess* (Fig. 21) and the distribution has a range of variation from 2‰ to 24‰, which shows the influence of both local and regional moisture circulation in the area except for samples with high *d-excess* that most likely indicate local moisture source at very low humidity of vapour. Globally *d-excess* averages about 10‰, but varies due to variations in humidity, wind speed and sea surface temperature during evaporation, accordingly, the low d-excess values reflect high humidity during formation of vapour mass (Clark and Fritz, 1997).

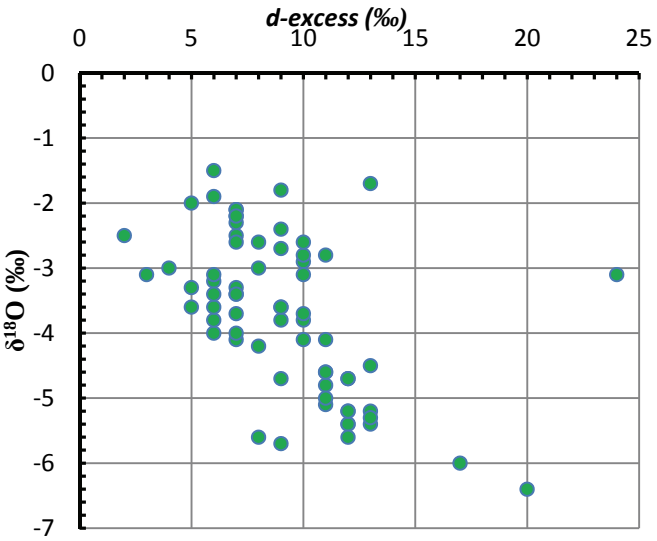

Figure 21: Plot of d-excess versus $\delta^{18}O$ for water samples within the study area.

Temporal variation in environmental isotope has been studied through monitoring of environmental isotope (Table 6).

Table 6: Seasonal isotope monitoring results. S (summer) and W (winter).

			Summer samples				Winter samples			Changes		
Summer	Lat (S)	Log (E)	$\delta^{18}O$ (‰)	δD (‰)	^{3}H (T.U.)	Winter	$\delta^{18}O$ (‰)	δD (‰)	^{3}H (T.U.)	Ratio	$\delta^{18}O$ (‰)	$\delta^{2}H$ (‰)
S1	-26.1784	28.0908	-4.71	-28.8	3±0.3	W1	-3.1	-14.2	3.1±0.4	Str1-S/str1-W	1.52	2.03
S2	-26.1584	28.0909	-4.24	-25.3	3.8±0.3	W2	-2.72	-12.8	5.1±0.4	Str2-S/str2-W	1.56	1.98
S3	-26.0200	27.721	-3.65	-20.4	3.6±0.3	W3	-2.61	-12.9	3.3±0.3	Str3-S/str3-W	1.38	1.58
S4	-26.6789	27.7821	-3.77	-20.5	4.1±0.4	W4	-2.09	-9.8	4.1±0.4	Str4-S/str4-W	1.8	2.09

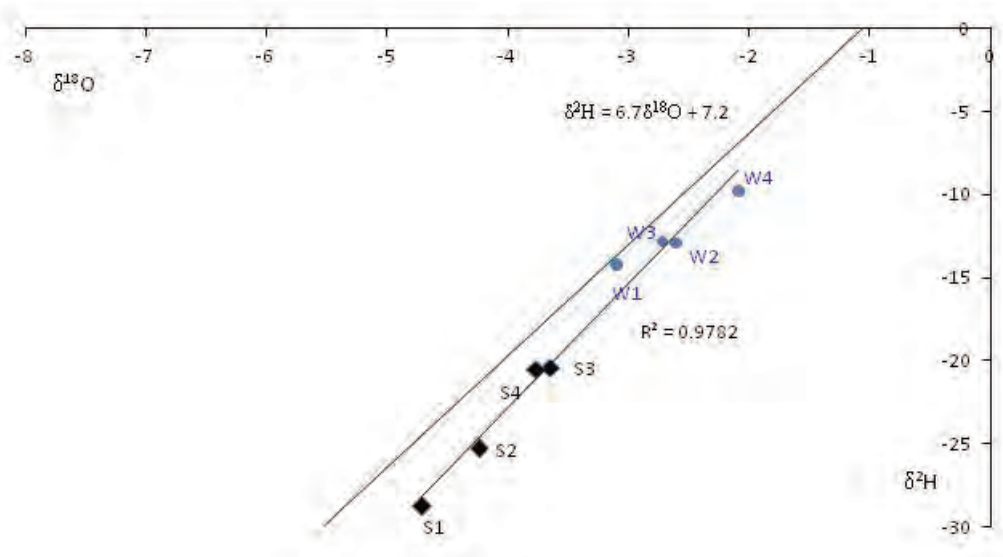

Figure 22: Monitoring plot for stable isotope as in Table 5.

Seasonal stable isotope monitoring data (Table 2) and plot (Fig. 22) show that winter samples (June-Aug, cold and dry) are enriched with respect to $\delta^{18}O$ and $\delta^{2}H$ while summer samples (Dec-Feb, hot and rainy) are relatively depleted. This may be attributed to different seasonal evaporative rates. The shift in Isotopic ratio between summer and winter samples can be attributed to dilution from summer rainfall. High dilution factors (S4/W4) correspond to samples collected from relatively permeable weathered crystalline aquifers.

CONCLUSIONS

Hydrogeochemical and environmental isotope based study was undertaken in the upper Crocodile River Basin to conceptualize groundwater and surface water interaction and its provenance besides exploring groundwater flow patterns within the basement rocks. Environmental isotopes data reveal the presence of dominantly shallow groundwater circulation within the fractured crystalline rocks and deep circulation within the dolomitic aquifers. Regional groundwater circulation is characterized by compartmentalized aquifer system with distinct hydrogeochemical and environmental isotope signals.

Surface water and groundwater interaction in the Crocodile River basin is mostly controlled by factors such as differences in head between the streams and groundwater, the local geomorphology the availability of hidden karst structures, and the groundwater flow geometry.

Both hydrogeochemical and environmental isotope data have been integrated to identify the impact of acid mine decant in the area. The impact of the decant on the groundwater quality has already been clearly noted with high tot. Fe (≈1200 mg/L) and SO_4 (≈5000 mg/L). The continuous discharge of acidic water throughout a year indicates the presence of regional groundwater circulation that maintains the base flow and recharges springs.

The amount of acid mine decant that seeps into dolomitic aquifer as measured close to the Sterkfontein cave varies between 24 $m^3$and 56 M m^3 per year which needs to be managed through appropriate treatment intervention. Four distinct hydrogeochemical groupings were identified in the groundwater. These are:

- high Na, Ca, Mg, HCO_3 and SO_4 groundwater that circulates within the dolomitic aquifer and is partially affected by acid mine impact
- high Ca, Mg and HCO_3 and low Na and SO_4 groundwater in dolomitic aquifer
- low Na, Ca, Mg, SO_4, HCO_3 (max ≈ 150 mg/L) groundwater circulating within the shallow fractured/weathered crystalline rocks
- low Na, Ca, Mg, SO_4 (very low) and, high Si (max ≈ 29 mg/L) groundwater which is circulating within the quartzite and alluvial aquifers and is impacted by acid mine decant.

The $\delta^{18}O$ and $\delta^{2}H$ of rivers reflect how the relative amount of precipitation and groundwater vary with time, and how the isotopic compositions of the sources themselves change over time. Seasonal variations will be larger in streams where recent precipitation is the main source of flow, and smaller in streams where groundwater in the form of baseflow is the dominant source. Due to complex mining activities and geological setting of the basin, the isotopic compositions of streams and shallow groundwater are increasingly affected by subsequent alterations of the water quality by selective recharge and runoff, mixing with older groundwater in the dolomitic aquifer and newer rain water, and by evaporation.

REFERENCES

Abiye, T.A, Mengistu H., Demlie, M.B. (2011) Groundwater resource in the crystalline rocks of the Johannesburg area, South Africa. *Journal of Water Resources and Protection* 3(4): 199-122. doi:10.4236/jwarp.2011.34026

Alpers C.N., Whittemore D.O. (1990) Hydrogeochemistry and stable isotopes of ground and surface waters from two adjacent closed basins, Atacama Desert, northern Chile. *Applied Geochemistry.* Vol, 5, pp. 719-734.

Anibas, C., Buis, K., Verhoeven, R., Meire, P., Batelaan, O. (2011) A simple thermal method for seasonal spatial patterns of groundwater-surface water interaction. *Journal of Hydrology,397:93-104.*

Bakker, M., Anderson, E.I. (2003) Steady Flow to a well near a stream with a Leaky Bed. *Ground Water 41(6): 833 – 840.*

Barnard, H.C. (2000) An explanation of the 1:500,000 general hydrogeological map. Department of water affairs and forestry, Pretoria, Johannesburg, RSA.

Butler, J.J. Jr., Zlotnik, V.A., Tsou, M.S. (2001) Drawdown and stream depletion produced by pumping in the vicinity of a partially penetrating stream. Ground Water 39(5): 651 – 659.

Chen, X., Yin, Y. (2003) Semi analytical Solutions for Stream Depletion in Partially Penetrating Streams. Ground Water 42(1): 92 – 96.

Clark, I.D., Fritz, P. (1997) Environmental isotopes in hydrogeology. Lewis Publishers, Boca Raton, FL p. 328.

Darama, Y. (2001) An Analytical Solution for Stream Depletion by Cyclic Pumping of Wells Near Streams with Semi pervious Beds. *Ground Water 39(1): 79 – 86.*

DeWalle, D.R., Edwards, P.J., Swistock, B.R., Aravena, R., Drimmie, R.J. (1997). Seasonal isotope hydrology of three Appalachian forest catchments. *Hydrological Processes 11, 1895–1906.*

Duane, M.J, Pigozzi, G., Harris, C. (1997) Geochemistry of some deep gold mine waters from the western portion of the Witwatersrand basin, South Africa. *J. Afri. Earth Sciences. 24(1/2):105-123.*

Eriksson, P.G., Clendenin, C.W. (1990) A review of the Transvaal Sequence, South Africa. *J. Afri. Earth Sciences 10(1/2): 101-116.*

Eriksson, P.G., Altermann, W., Hartzer, F.J. (2006) The Transvaal Supergroup and its precursors. In" The Geology of South Africa". Johnson, M.R Anhaeusser C.R, and Thoms, R.J eds.p 237-260.

Fleckenstein, J.H., Krause, S., Hannah, D.M., Boano, F. (2010). Groundwater-surface water interactions: New methods and models to improve understanding processes and dynamics. *Advances in Water Resources, 33:1291-1295.*

Gascoyne, M. (2004) Hydrogeochemistry, groundwater ages and sources of salts in a granitic batholiths on the Canadian Shield, Southern Manitoba. *Appl. Geochemistry 19: 519-560.*

Krause, S., Bronstert, A., Zehe, E. (2007) Groundwater–surface water interactions in a North German lowland floodplain – Implications for the river discharge dynamics and riparian water balance. *Journal of Hydrology (2007) 347, 404– 417*

Lambs, L. (2000) Correlation of conductivity and stable isotope ^{18}O for the assessment of water origin in river system. *Chem. Geol. 164:161–170.*

Lambs, L., Loudes, J.P., Berthelot, M. (2002). The use of the stable oxygen isotope (O^{18}) to follow the water distribution and absorption in riparian woodlands. *Nukleotika 47, S71–S74.*

Lambs, L. (2004). Interactions between groundwater and surface water at river banks and the confluence of rivers. *Journal of Hydrology, 288: 316-326.* Liang, X., Xie, Z. 2003. Important factors in land-atmosphere interactions: surface runoff generations and interactions between surface and groundwater. *Global and Planetary Change, 38:101-114.*

Leybourne, M.I., Clark, I.D., Goodfellow, W.D. (2006) Stable isotope geochemistry of ground and surface waters associated with undisturbed massive sulfide deposits; constraints on origin of waters and water–rock reactions. *Chemical Geology 231 (2006) 300–325*

Long, A.L., Sawyer, J.F., Putnam, L.D. (2008) Environmental tracers as indicators of karst conduits in groundwater in South Dakota, USA. *Hydrogeology Journal 16: 263–280*

Maloszewski, P., Rauert, W., Stichler, W., Herrmann, A. (1983) Application of flow models in an alpine catchment area using tritium and deuterium data. *Journal of Hydrology 66, 319–330*

McCarthy, T.S. (2006) The Witwatersrand Supergroup. In" The Geology of South Africa". Johnson, M.R Anhaeusser C.R, and Thoms, R.J eds. P155-186.

Mendoza, J.A., Ulriksen, P., Picado, F., Dahlin, T. (2008) Aquifer interactions with a polluted mountain river of Nicaragua. *Hydrol. Process.* 22, 2264–2273

Meyers, R.E, McCarthy, T.S, Stanistreet, I.G. (1990) A tectono-sedimentary reconstruction of the development and evolution of the Witwatersrand Basin, with particular emphasis on the Central rand Group*, S. Afri. J. Geol. 93:180-201.*

Newman, B.D., Vivoni E.R., Groffman A.R. (2006) Surface water–groundwater interactions in semiarid drainages of the American southwest. *Hydrol. Process.* 20, 3371–3394

Ojiambo B.S., Poreda R.J., Lyons W.B. (2001) Groundwater/surface water interactions in Lake Naivasha, Kenya, using $\delta^{18}O$, δD, and $^{3}H/^{3}He$ Age dating. Groundwater 39 (4):526-533.

Oxtobee, J.P.A., Novakowski K. (2002) A field investigation of groundwater/surface water interaction in a fractured bedrock environment. *Journal of Hydrology 269 (2002) 169–193*

Palakodeti, R.C., LeBoeuf E.J., Clarke J.H. (2009) Tool for assessment of process importance at the groundwater/surface water interface. *Journal of Environmental Management 91 (2009) 87–101*

Pearce, A.J., Stewart, M.K., Sklash, M.G. (1986) Storm runoff generation in humid headwater catchments: 1. Where does the water come from? *Water Resources Research 22, 1263–1272.*

Poujol, M., Anhaeusser, C.R. (2001) The Johannesburg Dome, South Africa: new single zircon U-Pb isotopic evidence for early Arcahean granite-greenstone development within the central Kaapvaal Craton. *Precambrian Research 108: 139-157.*

Robb, L.J., Meyer, F.M. (1995) The Witwatersrand Basin, south Africa: Geological framework and mineralization processes*. Ore Geology Reviews 10: 67-94*

Saleh, F., Flipo, N., Habets, F., Ducharne, A., Oudin, L., Viennot, P., Ledoux, E. (2011). Modeling the impact of in-stream water level fluctuations on stream-aquifer interactions at the regional scale. *Journal of Hydrology, 400:.490-500.*

Sophocleous, M. (2002) Interactions between groundwater and surface water: the state of the science. *Hydrogeology Journal 10: 52 – 67.*

Tornqvist, R., Jarsjo, J., Karimov, B. (2011). Health risks from large-scale water pollution: Trends in Central Asia. *Environmental International, 37:435-442.*

Winde F, van der Walt I.J. (2004). The significance of groundwater–stream interactions and fluctuating stream chemistry on waterborne uranium contamination of streams—a case study from a gold mining site in South Africa. *Journal of Hydrology 287 (2004) 178–196*

Winde, F., van der Walt, I.J. (2004). The significance of groundwater–stream interactions and fluctuating stream chemistry on waterborne uranium contamination of streams—a case study from a gold mining site in South Africa. *Journal of Hydrology, 287:178–196.*

Winter, T.C. (1999) Relation of streams, lakes, and wetlands to groundwater flow systems. *Hydrogeology Journal 7: 28-45.*

Woessner, W.W. (2000) Stream and fluvial plain ground water interactions: rescaling hydrogeologic thought. *Ground Water 38, 423–429.*

Zlotnik, V.A., Huang, H., Butler, J.J. Jr. (1999) Evaluation of stream depletion considering finite stream width, shallow penetration, and properties of streambed sediments. In: Proceedings of Water 99, Joint Congress, Brisbane, Australia: 221 – 226 (also available at: www.kgs.ukans.edu/StreamAq).

PROGRAM DEBUGGING AND APPLICATION THROUGH CASE STUDIES

Yongxin Xu and Liang Xiao

INTRODUCTION

The deliverables reported in this report includes (1) a box-model in CD and the Guidelines of the software. The Guidelines is described in such a manner that the results of application of this software in some dolomite aquifers in the country are compared with the previous ones obtained from other methods.

SOFTWARE AND GUIDELINES

Environmental tracers, which are introduced into groundwater systems either naturally or artificially, can be used for interpretation of key parameters leading to estimation of groundwater recharge. Tracers selected for the application can be Tritium, C14, and others (CFC and SF6). The advantage and disadvantage are discussed by Kinzelbach et al (2002). In general, the interpreting approaches can be grouped under headings of zero dimension model or box model and distributed model or dimensional model. The software to be developed places an emphasis on the former. Based on flow dynamics, three basic tracer methods further considered in this project include (1) Piston flow model, (2) exponential flow model and (3) dispersion model. Additional one method can be further considered is called Ribs model.

METHODS

The box model is based on concept of a transfer function that produces transformed output from an input time series. Although the transfer functions are discussed in many literatures, it is still challenging to develop user friendly software for their application in real world.

According to Beyerle (2002), for a given tracer input function, a box model calculates the convoluted theoretical output depending on: (1) the transfer function (either for a piston flow, an exponential or a dispersion model, see Fig. 1a-c); and 36 and (2) the parameters of this particular transfer function (mean residence time t, dispersion parameter d). By comparing observed and calculated concentrations, one can identify these parameters. The mathematical bases of box models, as well as a spread sheet for working with them, are provided in a separate Excel workbook. Please note that the choice of the box model should respect the general aquifer situation, as characterised by the Fig. 1.

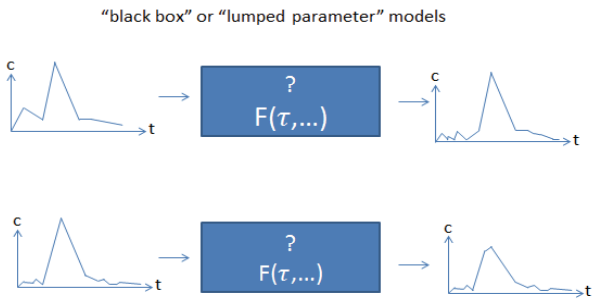

Figure 9: Schematic principle of box models

1. Piston model

a) In the piston flow model the flow lines are assumed to have the same transit time, and the hydrodynamic dispersion and diffusion are negligible (Fig. 2). Therefore, the tracer moves from the recharge area as if it was

in a can. The response function is given by Dirac delta function. The output concentration at a given time is equal to the input concentration at the time Tau (See parameters below) earlier.

b) Tau is the transit time of the tracer, user can adjust its value to get the best simulation.

c) The parameter Start No signifies the number that your simulation starts from. It is required to be less than the total number of your data rows.

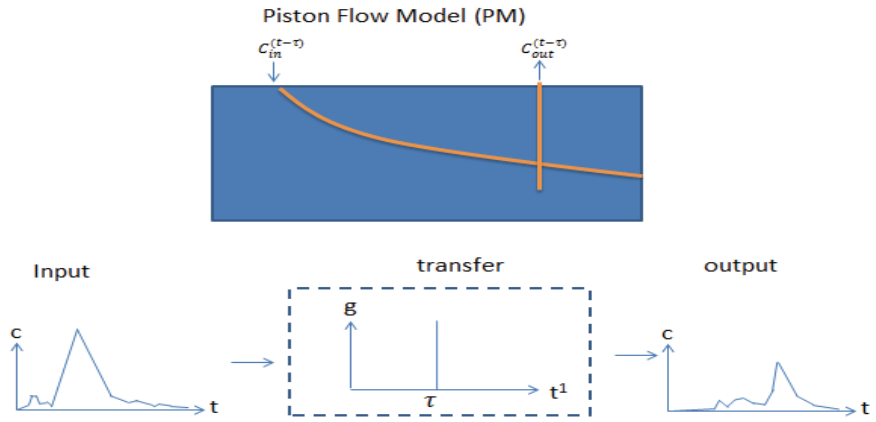

Figure 2: Piston flow model and corresponding transfer function (the out concentration is additionally influenced by radioactive decay)

2. Exponential model

a) In the exponential model, the flow lines are assumed to have the exponential distribution of transit times, i.e., the shortest line has the theoretical transit time equal to zero, and the longest line has the transit time equal to infinity (Fig. 3). It is assumed that there is no exchange of tracer between the flow lines.

b) The parameter Tau signifies the average transit time (age) of tracer, which unambiguously defines the whole transit time distribution. User can adjust its value to get the best simulation.

c) The parameter Start No signifies the number that your simulation starts from. It is required to be less than the total number of your data rows.

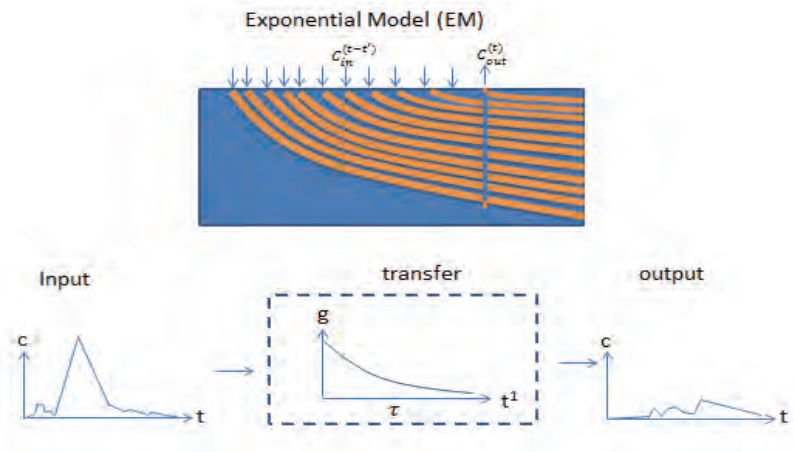

Figure 10: Exponential model and corresponding transfer function (the out concentration is additionally influenced by radioactive decay)

3. Dispersion model

a) In the dispersion model, the flow lines are assumed to have the exponential distribution of transit times (Fig. 4). However tracer exchanges between the flow lines, which is different from exponential model.

b) The parameter Tau signifies the average transit time (age) of tracer, which unambiguously defines the whole transit time distribution. User can adjust its value to get the best simulation.

c) The parameter Start No signifies the number that your simulation starts from. It is required to be less than the total number of your data rows.

d) The parameter Lamda is the decay coefficient. Lamda= Ln(2)/(half life).

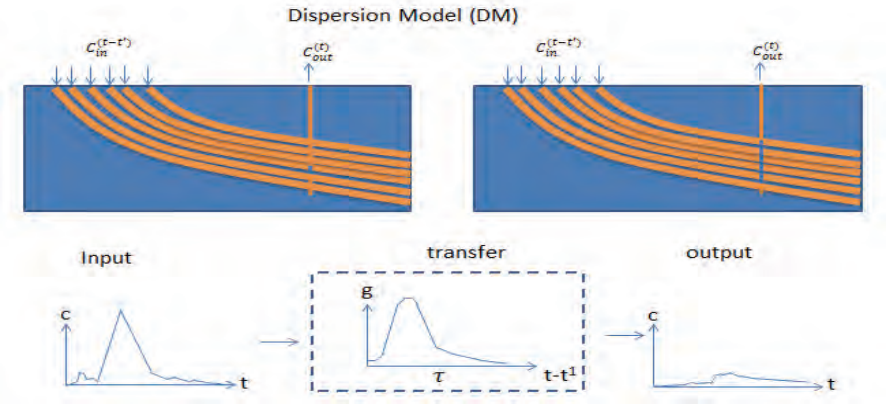

Figure 4: Dispersion model and corresponding transfer function (the out concentration is additionally influenced by radioactive decay)

4. Combination of exponential and dispersion model

a) In the exponential-piston flow model, the aquifer is assumed to consist of two parts in line, one with the exponential distribution of transit times, and another with the distribution approximated by the piston flow.

b) The parameter Tau signifies the average transit time (age) of tracer, which unambiguously defines the whole transit time distribution. User can adjust its value to get the best simulation.

c) The parameter Start No signifies the number that your simulation starts from. It is required to be less than the total number of your data rows.

d) The parameter f is the ratio of the total volume to the volume with the exponential distribution of transit times.

e) The parameter Lamda is the decay coefficient. Lamda= Ln(2)/(half life).

PROGRAM DEBUGGING AND APPLICATION THROUGH CASE STUDIES

The debug and calibration of the model has been carried out through case studies. To this effect, the UWC team made contacts with Mr Siep Talma, Prof Chris Harris and Dr Dave Bredenkamp. As results of discussions, a few cases are selected from Dr Bredenkamp's work. The UWC team had a meeting with Dr Bredenkamp in Pretoria on 9 April 2012. A case study that was used for simulations of spring age in dolomite aquifer in South Africa is attached in Annex A. A possible application of the program was discussed with Dr Orlando Mauricio Quiroz Londono and Dr Sebastian Grondona from the National University of Mar Del Plata, Argentina on 22 Oct 2012.

GUIDELINES

The developed software was applied in the known cases in some dolomite aquifers. It is necessary to have a guidebook to facilitate the smooth application of the software for intended purposes. The Guidelines is attached in Annex A.

SUMMARY

The models are reviewed and implemented on a spreadsheet Excel Book. For user-friendly purpose, many functions and visualizations are made available through use of VBA available within the Excel Book. In total four models are made available for practical applications, including (1) piston model, (2) Exponential model, (3) dispersion model and (4) combination of exponential and dispersion model. It is recommended that the Guidelines should always be consulted for a practical simulation.

A user-friendly VBA based software called Box-model in spreadsheets was developed (Annex A and on the accompanying CD). A guide manual is produced to assist a user for application of the software. It is recommended that the software should be tested and verified using data collected during this project.

REFERENCES

Kinzelbach W., Aeschbach W., Alberich C., Goni I.B., Beyerle U., Brunner P., Chiang W.-H., Rueedi J., Zoellmann K. (2002) A Survey of Methods for Groundwater Recharge in Arid and Semi-arid regions. Early Warning and Assessment Report Series, UNEP/DEWA/RS.02-2. United Nations Environment Programme, Nairobi, Kenya. ISBN 92-80702131-3.

Beyerle, U. (2002). Groundwater Dating using Environmental Tracers and Black Box Models in Kinzelbach et al (eds): A Survey of Methods for Groundwater Recharge in Arid and Semi-arid regions. Early Warning and Assessment Report Series, UNEP/DEWA/RS.02-2. United Nations Environment Programme, Nairobi, Kenya. ISBN 92-80702131-3.

ANNEX A:

CALIBRATION OF TRACER BOX MODEL: A CASE STUDY OF SPRINGS IN DOLOMITE AQUIFER, SOUTH AFRICA

Liang Xiao and Yongxin Xu

The box models, sometimes called lumped parameters models, are frequently used to predict the average age of groundwater. These models include piston flow model, exponential model, dispersion model and exponential-piston flow model. In this case study, mean resident time of springs from dolomite aquifer, South Africa, is simulated based on the use of above mentioned box models. C^{14} is applied as the environmental tracer for groundwater dating

.

1. Simulation Process

Background data from atmosphere and modified observation data of C^{14} from each spring are used as input data for black box models. A case from Molopo Spring is used for interpretation of simulation process of each black box model.

1.1 Piston Flow Model

In the piston flow model the flow lines are assumed to have the same transit time, and the hydrodynamic dispersion and diffusion are negligible. Therefore, the tracer moves from the recharge area as if it was in a can. The response function is given by Dirac delta function. The output concentration at a given time is equal to the input concentration at the time Tau (See parameters below) earlier. The calculated result of piston flow model is as showed in Frg.1. The average resident time of groundwater is 59months, which corresponds to 0.17 years.

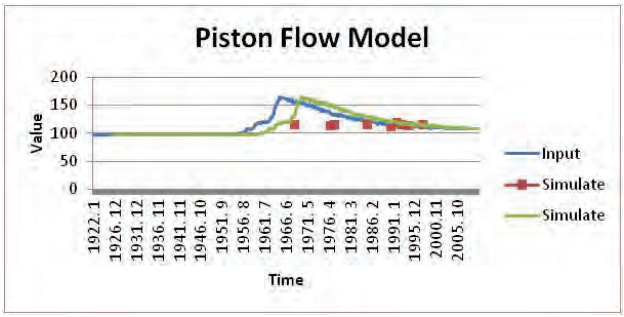

Fig.1 calculated result of Piston Flow Model

1.2 Exponential Model

In the exponential model, the flow lines are assumed to have the exponential distribution of transit times, i.e., the shortest line has the theoretical transit time equal to zero, and the longest line has the transit time equal to infinity. It is assumed that there is no exchange of tracer between the flow lines. The parameter Start No is assigned to be 19. The parameter Lamba is the decay coefficient of C^{14}, which is equal to be 0.00012. As showed in Frg.2, the average resident time of groundwater is 267 month, which is the same with 22.25 years.

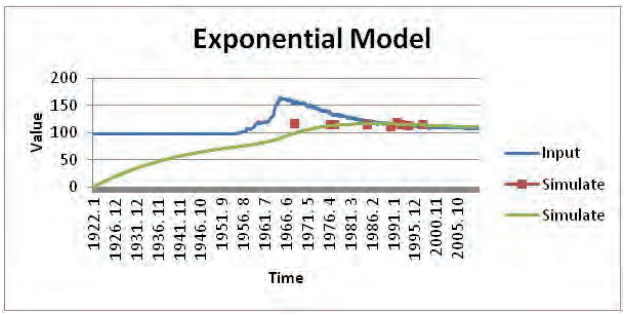

Fig.2 Calculated Result of Exponential Model

1.3 Dispersion Model

In the dispersion model, the flow lines are assumed to have the exponential distribution of transit times. However tracer exchanges between the flows lines, which is different from exponential model. There are three parameters in dispersion model, including Start No, decay coefficient and Delta. Start No is assumed to be 19. The decay coefficient of C14 is 0.00012. The

parameter Delta stands for the Dispersion Parameter, which is used to be 0.5. Referring to Fig. 3, the average resident time of groundwater is 273 month, which is equivalent to 22.75 years.

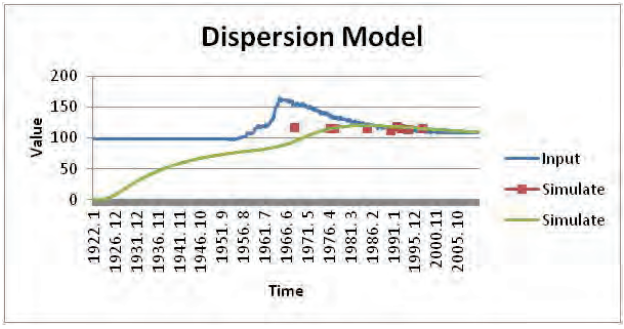

Fig.3 Calculated Result of Dispersion Model

1.4 Exponential-Piston Flow Model

In the exponential-piston flow model, the aquifer is assumed to consist of two parts in line, one with the exponential distribution of transit times, and another with the distribution approximated by the piston flow. There are four parameters in exponential-piston flow model, including Start No, decay coefficient, parameter f and Delta. Start No is assumed to be 19. The decay coefficient of C14 is 0.00012. The parameter f is the ratio of the total volume to the volume with the exponential distribution of transit times, which is 0.3 in this case study. Referring to Fig. 4, the average resident time of groundwater is 255 month, which is amount to 21.25 years.

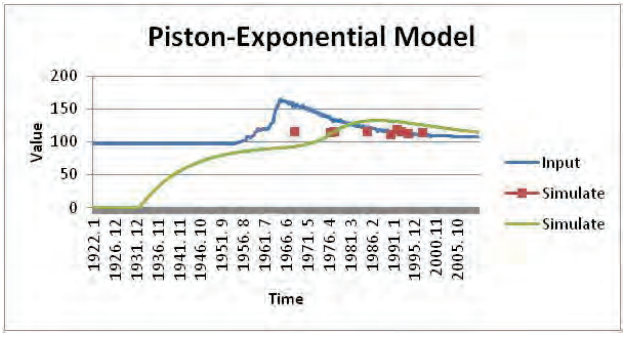

Fig.4 Calculated Result of Exponential-Piston Model

2. Simulation results

Mean resident time of other springs draining water from dolomite aquifers, South Africa, in the last 40 years are also simulated based on the process mentioned above. The results are listed as follows.

Table 1 Mean resident time of springs from Black Box Model

Area	Research sites	Corrected parameter (Cobs/P)*	Turnover (years) from Bredenkamp	Resident time from Black Box Model							
				Piston		Exponential		Dispersion		Exponential-piston	
				years	Difference	years	Difference	years	Difference	years	Difference
Grootfontein Zeerust	Buffelshoek	0.77	16.20	3.33	-12.87	18.75	2.55	20.67	4.47	21.25	5.05
	Olievendraai	0.86	8.60	13.00	4.40	14.83	6.23	14.50	5.90	15.25	6.65
	Molopo	0.71	21.90	4.92	-16.98	22.25	0.35	22.75	0.85	21.25	-0.65
	Vergenoeg	0.77	10.60	12.92	2.32	19.33	8.73	19.83	9.23	20.08	9.48
	Doornfontein	0.82	9.10	14.58	5.48	17.83	8.73	18.67	9.57	18.92	9.82
	Paardevlei	0.79	10.00	10.83	0.83	14.92	4.92	15.58	5.58	16.42	6.42
	Stinkhoutb	0.77	10.10	3.50	-6.60	4.17	-5.93	13.25	3.15	32.83	22.73
Pretoria	Grootftn	0.72	12.70	12.50	-0.20	19.92	7.22	19.00	6.30	16.92	4.22
West Rand	Turffontein	0.73	17.30	14.17	-3.13	18.50	1.20	16.83	-0.47	15.67	-1.63
Kuruman	Kur A	0.60	22.40	1.00	-21.40	23.92	1.52	16.58	-5.82	11.92	-10.48
	Manyed B	0.82	7.43	10.33	2.90	12.75	5.32	13.08	5.65	10.00	2.57
Marico Schoonspr	Schoonspr	0.78	12.20	14.17	1.97	21.08	8.88	21.75	9.55	23.75	11.55
	Maloneys	0.47	16.10	25.25	9.15	16.92	0.82	17.42	1.32	22.92	6.82

**Personal Communication with Dr David Bredenkamp (2012)*

Practically, it is indicated that different box model fit into different hydrogeological conditions. The unsuitable box model will lead to wrong simulation results of groundwater age. The applicable conditions of each box model are presented in the software guideline. In this case study, the piston flow model is not suitable for the age simulation of springs in dolomite aquifer, South Africa.

USE OF ISOTOPES IN CATCHMENT HYDROLOGY, VEGETATION UPTAKE AND NON-POINT SOURCE POLLUTION ANALYSES

Simon Lorentz,
Carl Freese, Craig Orchard, Vincent Chaplot, Seraphine Grellier, Jennifer Pickles and Julius Kollongei

INTRODUCTION

The use of isotopes in surface water hydrology has been a rapidly growing method for identifying the sources, pathways and response times of components of discharge making up stream water flow. Isotopes have been used initially to aid in hydrograph separation, but detailed definition and quantification of flow pathways has increasingly added value to water quality, evapotranspiration, surface water-groundwater interaction and low flow studies. Despite the use of isotopes to define and often quantify specific hydrological processes, the spatial and temporal variations in isotope behaviour in the various compartments in the hydrological system as well as the degree of variation of these behaviours, often confound the application of isotopes in hydrological process understanding at different scales (Kendall and McDonnell, 2003).

In South Africa, the temporal variability of the rainfall isotope behaviour has thwarted past efforts to derive meaningful deductions on surface water hydrological processes. However, with the introduction of methods for cheap and rapid analysis of stable isotopes of water (^{2}H and ^{18}O), temporal and spatial variations can be observed and useful hydrological process behaviours deduced.

This report summarizes the use of stable isotopes of water in three tracts of research, namely, Catchment hydrology; Local processes of tree water uptake and soil water evaporation and Non-point source pollution.

CATCHMENT HYDROLOGY

Stable isotopes of water ($\delta^{18}O$ and $\delta^{2}H$) have been used in small research catchments, Weatherley (Umzimvubu basin) and Potshini (Thukela Basin) to evaluate details of the hydrological cycle. In the Weatherley catchment, the focus has been on estimating hillslope response mechanisms, flowpathways and travel times. The response of the whole research catchment is then examined in terms of contributing flow regimes. In the Potshini research catchment, responses at increasing scales are examined through the use of isotopes, reflecting the different dominant contributing fluxes at different scales

WEATHERLEY

Introduction

The Weatherley research catchment, located in Molteno and Clarens formations, has been instrumented for observing meteorological variables and overland flow, soil water, near surface and deep groundwater and stream water responses since 1995 (Figure 1). The subsurface soils have been characterised, while temporal and spatial distribution of water in the subsurface have been observed through geophysics surveys. Details of the hydrometric studies are presented in the Water Research Commission report K5/1320 (Lorentz et al., 2008). Specific analyses of rainfall, small catchment and hillslope water isotope responses are presented here.

Site description

A research catchment of some 1.5km^{2}, Weatherley, was established in 1995 in a grassland zone, prior to the introduction of trees in 2002, near the town of Maclear in the northern Eastern Cape province. The catchment was instrumented with two met stations, soil moisture and tension sensors, groundwater level sensors, surface runoff plots and two stream gauging weirs, dividing the catchment into upper and lower subcatchments (Fig.1).

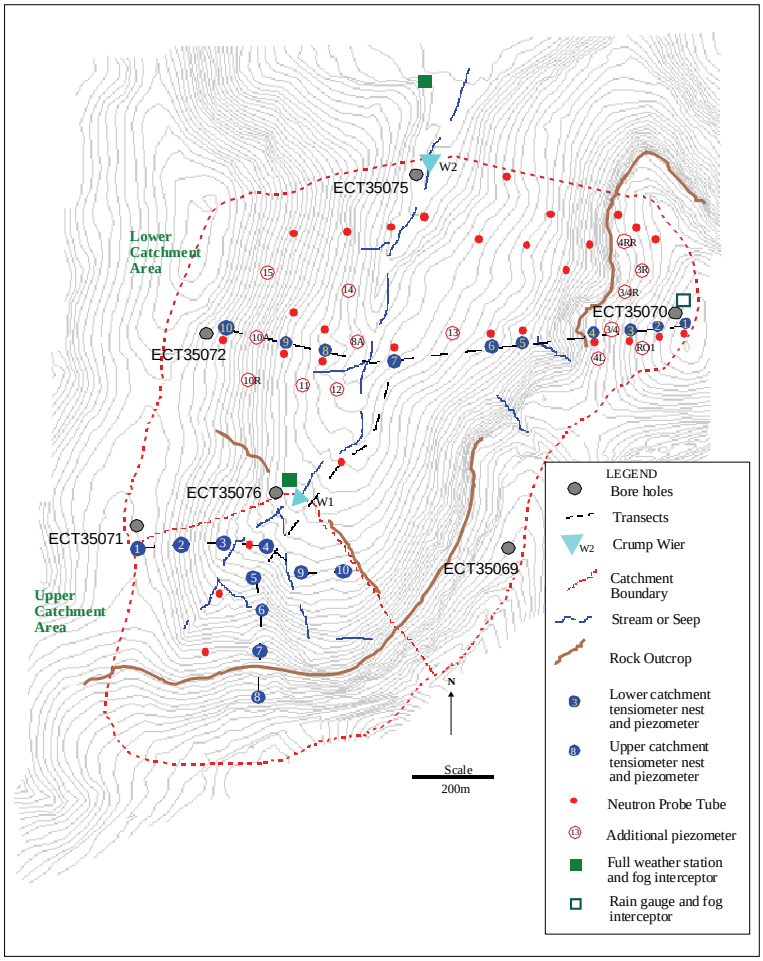

Figure 1: The Weatherley research catchment, showing weirs, boreholes, soil water sensor and piezometer stations, weather station and additional rain gauge.

Methodology

Isotope samples were collected in a multi-sample rainfall collector, by hand from piezometers inserted in the soil profile to the soil/saprolite interface throughout the catchment; from five boreholes established in the molten/clarens mudstone and sandstone layers; from specific seepage faces at the toe of hillslopes and automatically from the downstream weir (W2 in Figure 1). These samples were taken on a monthly basis as well as during two period of intensive measurement (December 2002 - January 2003 and November 2009 - March 2010).

The rainfall sampler comprised a closed system of cascading flow into sequential sample bottles. The stream sampler comprised an ISCO water sampler which
was set up to draw samples from the stream in response to increasing discharge. During low flows, the sampler was set to sample at a specified volume of streamflow.

Hence, infrequent sampling occurred during low flows while multiple samples were collected during a rainfall event.

The samples were returned to the University of KwaZulu-Natal and analysed using a Los Gatos Research (LGR) Liquid Water Isotope Analyzer by laser absorption. Each measurement was conducted 6 times to provide a high value precision. Results are presented in δ notation *i.e.* parts-per-million deviations from Vienna Standard Mean Ocean Water (V-SMOW) as $\delta^{2}H$ and $\delta^{18}O$.

Infiltration mixing algorithms and hillslope response convolution algorithms were developed to estimate the response dynamics of four typical hillslopes. End member mixing analyses were used to quantify contributions to streamflow from specific sources. The algorithms used for these analyses are presented with the results.

Results and discussion

Rainfall

Rainfall samples were collected and analysed for $\delta^{18}O$ and $\delta^{2}H$ during the wet seasons of 2002-2003; 2008-2009 and 2009-2012 (Fig. 2), using a sequential sampler, which samples at approximately 6mm increments. The range of rainfall isotope values is large, with $\delta^{18}O$ varying between -6 and +4 $^{o}/_{oo}$.

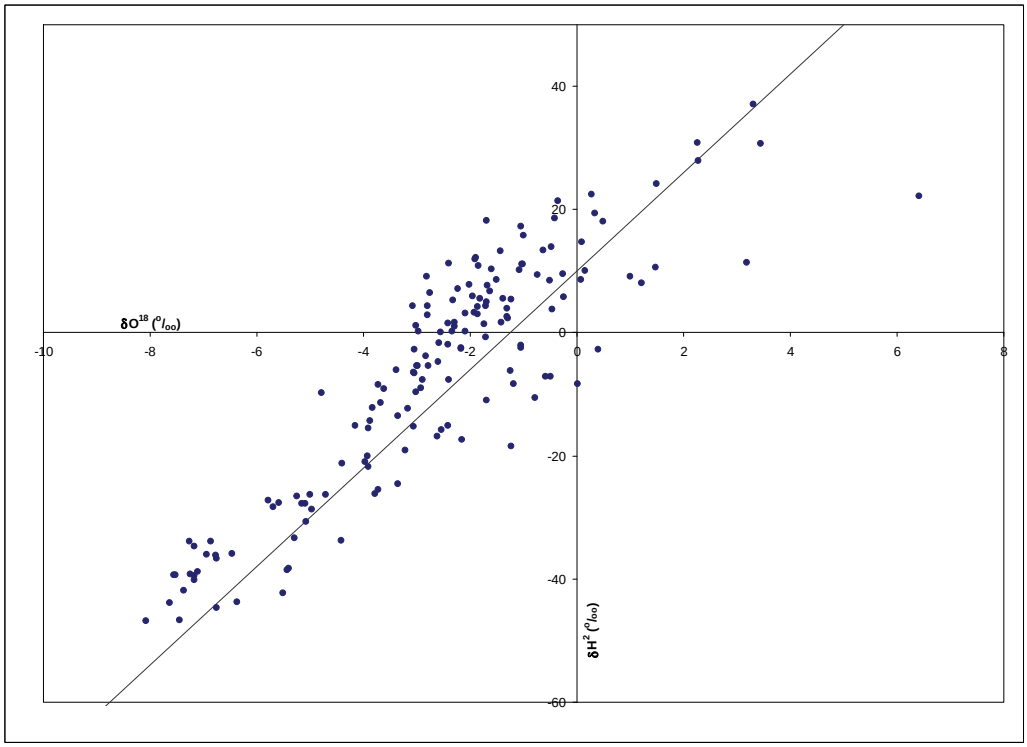

Figure 2: $\delta^{18}O$ and $\delta^{2}H$ distribution of rainfall samples at Weatherley during 2002 and 2009-2012 sampling campaigns.

Progressive depletion of ^{18}O was observed in the rainfall series of December 2002-January 2003 (Fig. 3), while rapid depletion occurred on an event basis in the 2008-2009 and 2009-2010 wet seasons.

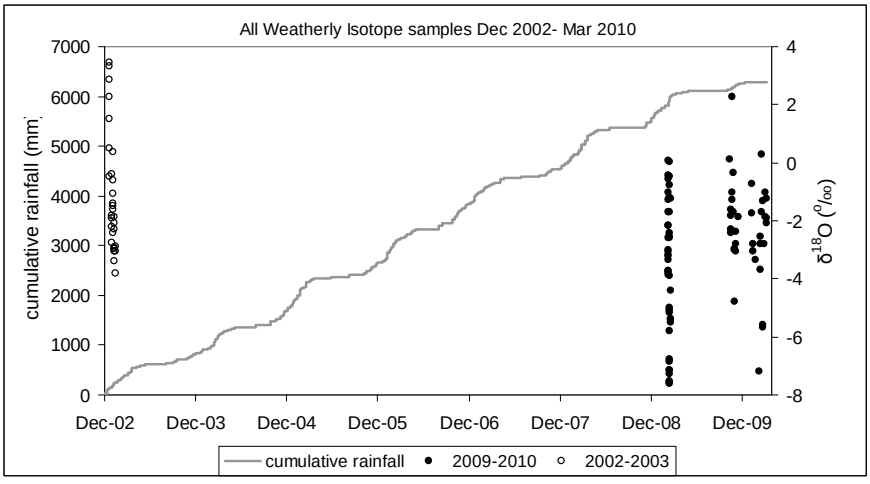

Figure 3: Range of rainfall $\delta^{18}O$ and $\delta^{2}H$ values during 2002 and 2009 events.

Although there is a wide range of isotope delta values in the rainfall, two distinguishing patterns seem to describe the type of rainfall occurring at the site as shown in Fig. 4 (Lorentz *et al*., 2008). An attempt at determining what sort of weather systems may contribute to these isotope signatures was made by obtaining descriptions of the rainfall from the S.A. weather services The steeper isotope rainfall pattern (parallel to the GMWL) appears to originate from rainfall

drawn in from the Indian ocean off the east coast, whereas the flatter pattern is developed from frontal rainfall events, where enrichment may occur during its decent.

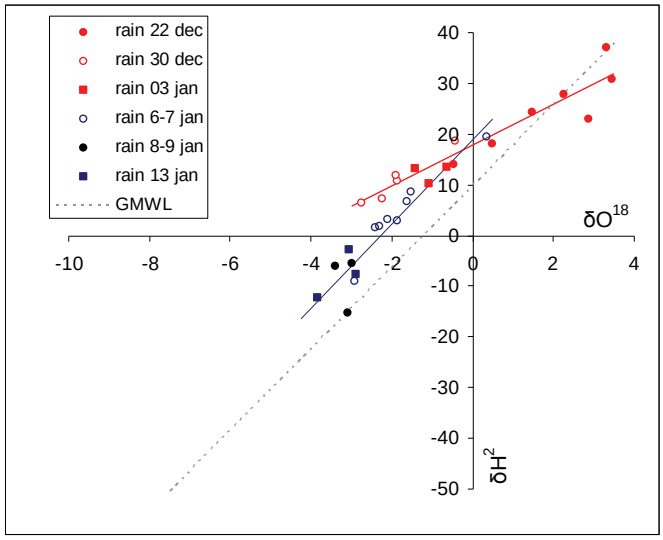

Figure 4: Intra-event rainfall $\delta^{18}O$ vs. $\delta^{2}H$ slopes for events in December 2002 and January 2003.

Although the isotope ratio for a series of rainfall events varies significantly, both within and between the events, the streamflow response is significantly dampened (Figure 5). Clearly mixing in the soils and groundwater plays a dominant role in delivery of water to the stream channel. These contributions are studied in the following section.

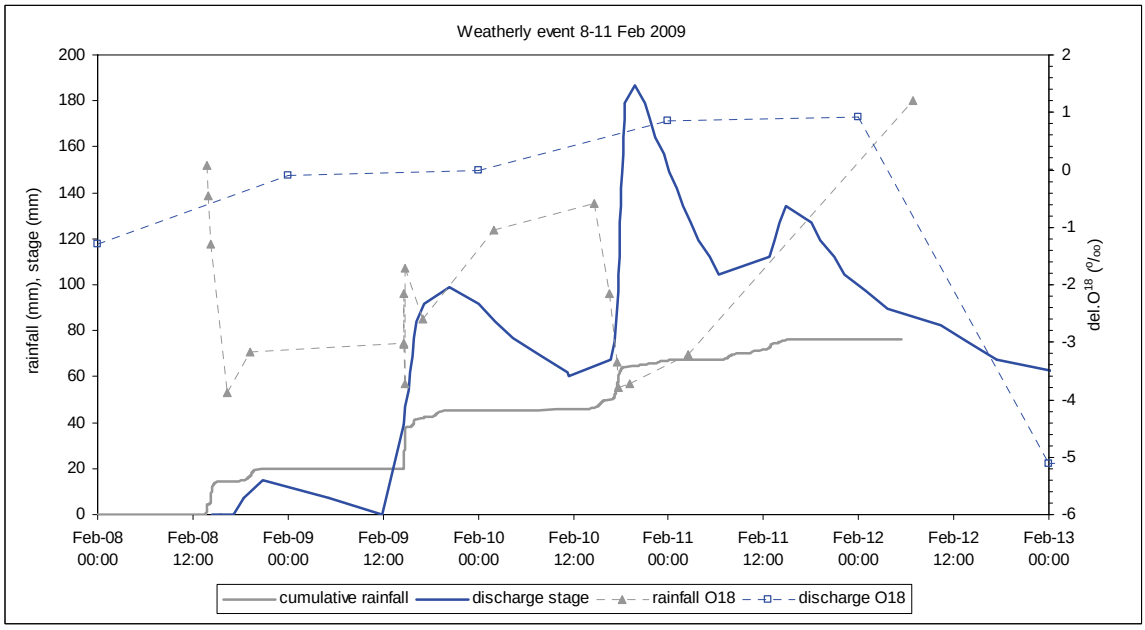

Figure 5: Rainfall and runoff $\delta^{18}O$ values during February 2009.

Four typical hillslope response types were identified in the Weatherley catchment through hydropedology surveys. The isotope response these hillslopes were simulated using a two step algorithm. The first step required estimating the isotope ratio values of the infiltrated rainfall at the soil/saprolite interface. The mixed hillslope response at the toe or discharge point of the hillslope was then estimated using a convolution response model with the infiltrated water as the excitation time series.

The infiltrated water ^{18}O isotope ratios, δ_{in}, were estimated using an infiltration rate constant, α for a series of rainfall events, P, as illustrated in Equation 1 of Fig. 6. A constant groundwater isotope ratio δ_{GW}, was assumed. An initial δ_{GW} value was taken as the observed groundwater values for each hillslope during the analysis period. Small adjustments to this value were made to improve the correlation between observed and simulated $\delta(t)$ time series at the hillslope discharge point.

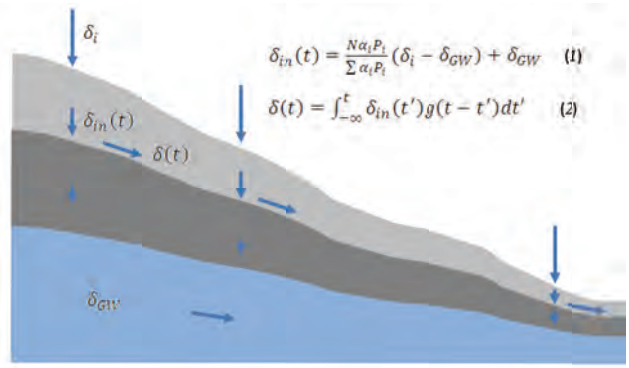

Figure 6: Schematic model for isotope simulation at the Weatherley hillslopes comprising an infiltrated signal prediction (1) and lateral flow mixing convolution integral (2).

An advection, dispersion response function, $g(t)$ was used in the convolution integral. This is given as:

$$g(t) = \left(\frac{4\pi Dt}{\tau}\right)^{-1/2} t^{-1} e^{\left[-1\left(1-\frac{t}{\tau}\right)^2 \tau(4Dt)\right]} \quad (3)$$

where D is the dispersion coefficient and τ is the response time in days.

The results of the application of this algorithm are shown for the hillslope section in the lower catchment, stations 1 to 4, (Fig. 1) for a series of events in February 2009 in Fig. 7. The rainfall series between 26 January and 22 February 2009 was used to develop the excitation signal (infiltrated water) for the convolution, applied between 1 February and 8 March 2009. The behaviour of the observed isotopes is faithfully reproduced, particularly the drop in $\delta^{18}O$ from 0 to -5 in mid-February (Fig. 7).

The analysis was repeated for the period October 2009 to April 2010 (Fig. 8). Here the simulated response is not as convincing, but the drop in $\delta^{18}O$ of the observed seepage from the toe of the hillslope section (LC04seepage) in early March 2010, is adequately simulated.

Results of similar analyses on hillslope segments in the lower catchment along observation stations 12 down to 8 and in the upper catchment along two hillslopes, one contributing to upper catchment station 1 and the other to upper catchment station 3 /4 are presented in Appendix A.

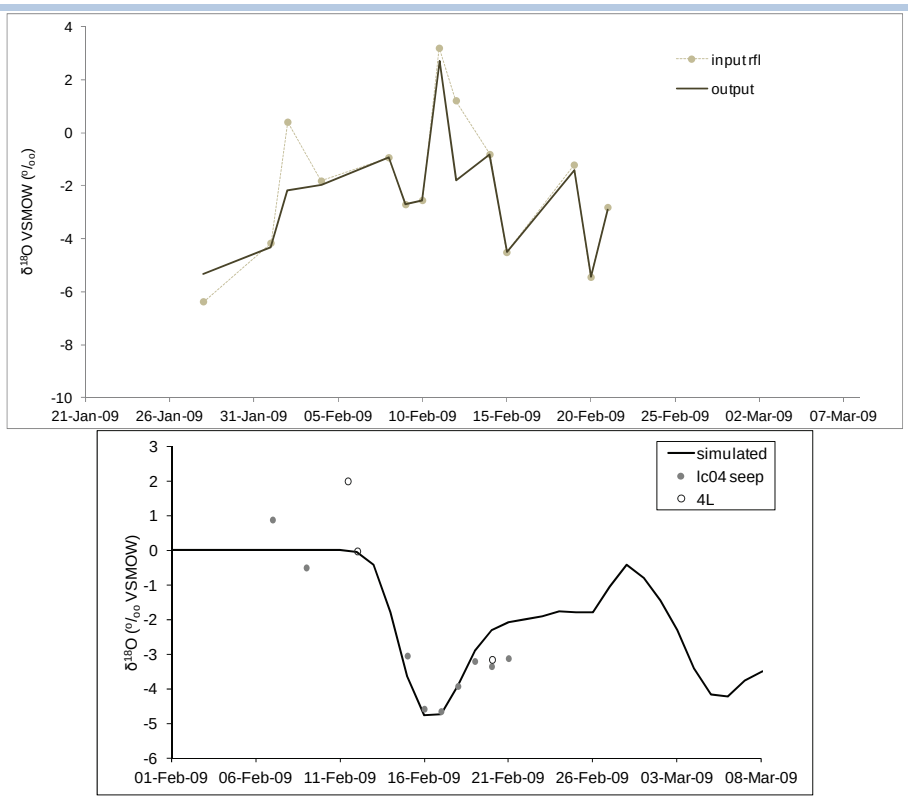

Figure 7: Results of infiltrated water time series $\delta_{in}(t)$ (above) and simulated $\delta(t)$ at the base of the Lower Catchment 1-4 hillslope, $\delta^{18}O$ during February 2009 (below).

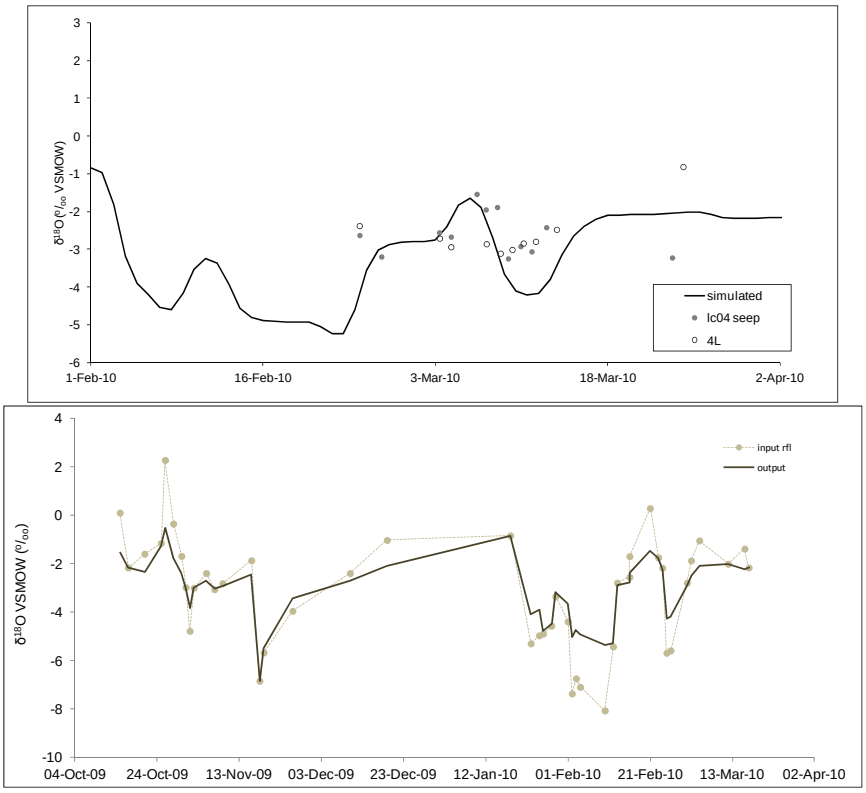

Figure 8: Results of infiltrated water time series $\delta_{in}(t)$ (above) and simulated $\delta(t)$ at the base of the Lower Catchment 1-4 hillslope, $\delta^{18}O$ during March 2010.

Although the correlation coefficients for these analyses are low (Table 1), it is evident that the hillslopes in the lower catchment respond differently to those in the upper catchment. Dispersion coefficients in the lower catchment hillslopes range from 0.0015 to 0.003 while response times range between 12 and 18 days, while in the upper catchment, the dispersion coefficients range between 0.09 and 0.3 and the response time range between 9 and 10. It is clear from the observed responses that the upper catchment hillslopes are well mixed, while the lower hillslopes reflect a pulse-like response.

Table 1: Summary of hillslope response analyses in the Weatherley research catchment.

Hillslope	Date	D	τ (days)	R^2
LC 4	February 2009	0.002	18	0.81
LC 4	March 2010	0.003	12	0.24
LC 8	February 2009	0.0015	12	-
LC 8	March 2010	0.002	12	0.27
UC 1	February 2009	0.30	10	-
UC 1	March 2010	0.30	10	0.19
UC 3/4	February 2009	0.09	9	-
UC 3/4	March 2010	0.09	9	0.41

Note: - = too few observations for regression analysis

Catchment scale

A convolution integral response model (2) was applied on a catchment-wide basis using the same advection-dispersion equation (3) with the event volume averaged rainfall $\delta^{18}O$ values as the excitation time series. The simulated results were matched to the observed $\delta^{18}O$ time series as shown in Fig. 9. The simulated response is systematically higher than the observed, reflecting the omission a groundwater component in the simulation. The dispersion coefficient was 0.003 and the response time was 22 days. The mixing on a catchment-wide scale thus indicates a dominance of the lower catchment hillslopes, while the response time is higher than any of those simulated in the hillslopes, again, possibly reflecting the slower response of the groundwater component or the retardation in the riparian wetland zones.

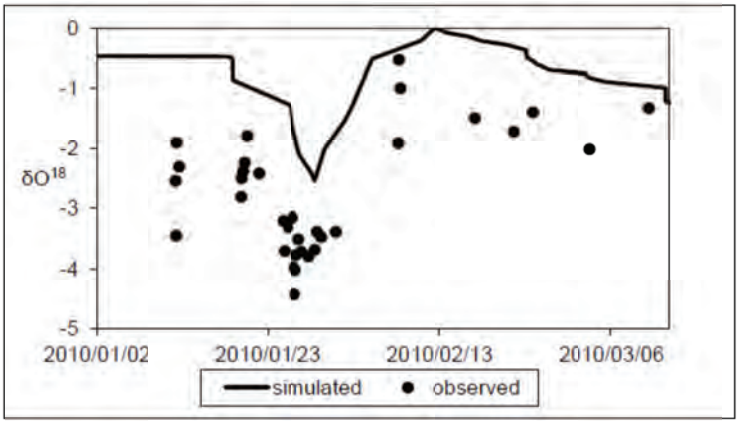

Figure 9: Application of a convolution analysis to the rainfall runoff response at the Weatherley catchment using the $\delta^{18}O$ isotope (January 2010), R^2 = 0.34.

The general importance of hillslope water and groundwater in mountainous catchments is commensurate with findings in many other catchments around the world (Buttle, 1994). Observed silica, electrical conductivity (EC), chloride and stable isotopes of water where observed in the hillslopes, groundwater and runoff in the Weatherley catchment during February 2004 by Wenninger *et al*. (2008) (Fig. 10).

A three-component hydrograph separation by end-member mixing analysis, using silica and EC, confirmed the high contribution of pre-event components (hillslope stored water) and yielded additional information about a shallow subsurface water component, where water is delivered rapidly in preferential flow pathways close to the soil surface (Fig. 11). The mean value of this shallow hillslope component is about 16% of the total runoff generated, but during some events (i.e. 2b, 3b and 4a-4c) when a perched water table was developed within the soil layer, the component

increased to 26% of total event discharge. This important role of the shallow subsurface component in the runoff generation process could be also qualitatively confirmed by the regime of the isotopic signals even though it was not possible to use them for a quantitative hydrograph separation.

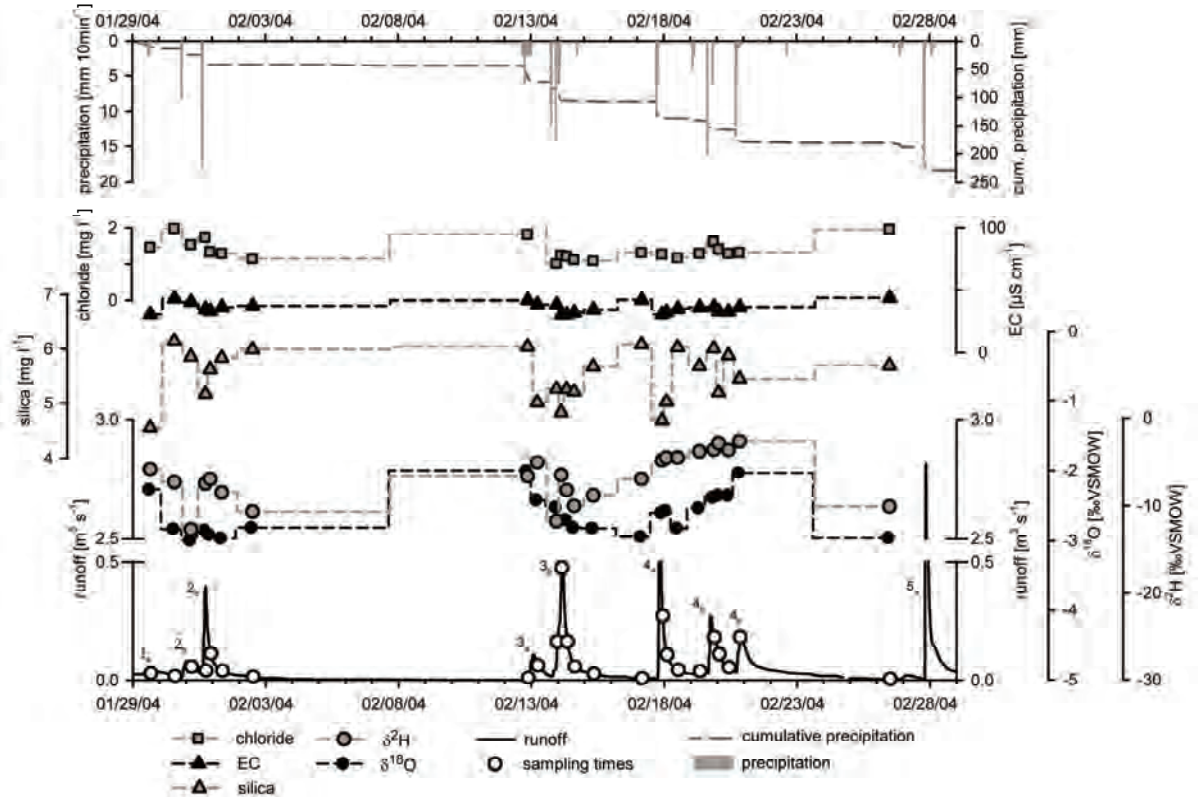

Figure 10: Rainfall, runoff and tracer (Silica, Chloride, EC, $\delta^{18}O$ and $\delta^{2}H$) responses at the lower weir of the Weatherley research catchment, February 2004 (after Wenninger et al., 2008).

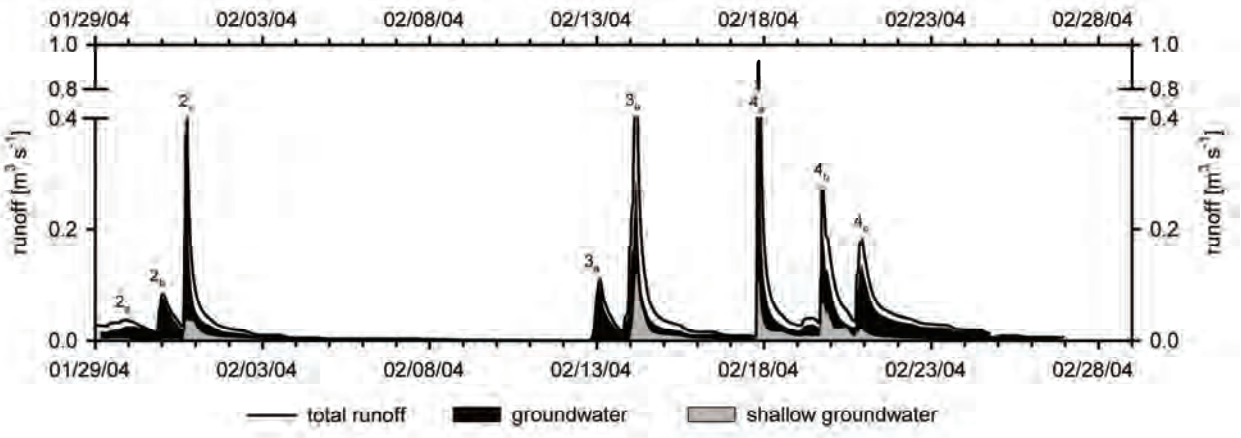

Figure 11: Results of the three-component (event water, hillslope groundwater and near surface water (shallow groundwater)) separation using dissolved silica and EC as tracers for events 2a-4c from 29 January 2004 – 29 February 2004.

The isotope values for samples collected during a typical series of events between the 2nd and 8th of January, 2003 are shown in Fig. 12. A two component, end-member analysis was performed by estimating the average end members for the hillslope water and rainfall or event water contributions to streamflow. The end members (EM) were estimated by calculating volume averaged values for the rainfall and the streamflow samples and averaging the values of the hillslope source. This simple end member analysis indicates that the streamflow average lies closer to the hillslope groundwater end member than it does to the rainfall end member (EM). A linear interpolation between the end members reveals that the hillslope source contributes 60% of the total surface flow, while event water (rainfall) contributes 40%. Hence the contribution of overland flow and near surface rapid response runoff would comprise 40% and the remainder would emanate from the hillslope groundwater, whether from the soil/bedrock interface or from the fractured rock aquifer.

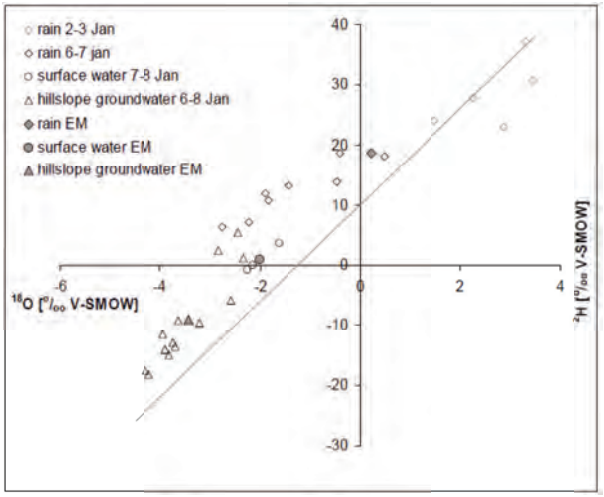

Figure 12: Relationship between $\delta^{18}O$ and $\delta^{2}H$ for rainfall, runoff and hillslope groundwater during January 2003 (After Lorentz et al., 2008).

Isotope samples collected during the dry season (August 2004) showed the stream discharge biased towards the isotope concentrations of seepage samples which were collected from rock outcrops, where they had been subject to evaporation and this exhibited the enriched concentrations (Fig. 13). A line drawn between these sample values and the hillslope groundwater sample values, intersects the streamflow sample values. This indicates that a mixture of near surface water, seeping from outcrops in the upper hillslopes, and hillslope groundwater in the seepage zones and wetlands contributes to the low flow discharges.

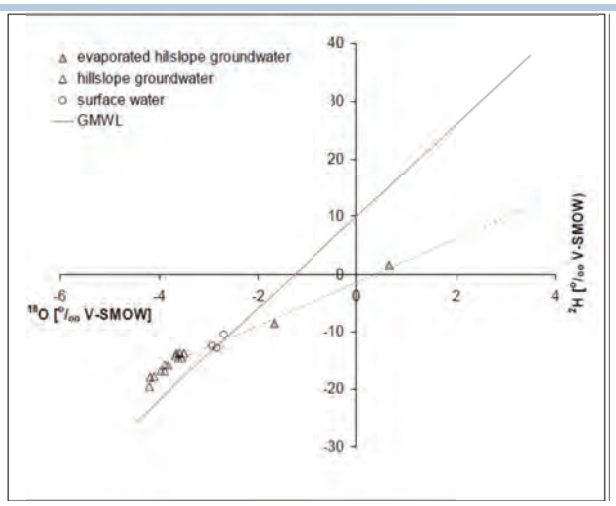

Figure 13: Relationship between $\delta^{18}O$ and $\delta^{2}H$ for rainfall, runoff and hillslope groundwater during August 2004 (After Lorentz et al., 2008).

Conclusion

While stable isotope values of rainfall vary significantly within and between events, high frequency sampling of rainfall and various components of the hydrological response, during and between events, has yielded sufficient data to allow for the evaluation of different hillslope dynamics and component contributions to streamflow in the Weatherley research catchment.

THUKELA

(Craig Orchard, Vincent Chaplot and Simon Lorentz)

A research catchment, Potshini, was established in the headwaters of the Thukela basin to evaluate the impacts of water use in small scale agriculture. Together with hydrometry, geophysics and soil surveys and sampling for nutrients, carbon and sediments, isotopes have been used to estimate the relative contribution of event and pre-event water at increasing scales. The work is fully reported in the Water Research Commission report K5/1808.

Introduction

The Potshini Catchment is located within the KwaZulu-Natal province, South Africa (Figure 14). The area that this study is concerned with is a 1000 ha catchment (longitude: 29.36°; latitude: 28.82°) located in the upper Thukela Basin (30,000km²) near the town of Bergville. Details of the catchment, hydrometric observations and surveys are reported in Water Research Commission report K5/1904.

Site description

The climate in the area is sub-tropical, humid and with a strongly seasonal summer rainfall pattern (October–March) (Schulze, 1997). The nearest government-maintained weather station located 10 km to the east of the study site in the town of Bergville, had a mean annual precipitation of 684 mm per annum over the past 30 years, with a potential evaporation of 1600 mm per annum and a mean annual temperature of 13°C (Schulze, 1997), with frosts that are common in winter.

At the Potshini study site, the altitude ranges from 1080 to 1455 masl. The relief is relatively gentle with a mean slope gradient of about 15.7 %, but with steep slopes of 50-70 % found in the upper part of the catchment, whereas in the vicinity of the catchment outlet and on the plateau, the topography is relatively flat all the way to the 1000 hectare catchment outlet.

Soils are formed from the Karoo Supergroup and Beaufort Group parent materials. The geology exhibits a horizontal, alternating succession of fine-grained sandstone, shale, siltstone and mudstone (King, 2002). A main dyke of Karoo Dolerite is intruded in these horizontal layers in the upper portion of the micro-catchment, giving specific weathering features of rounded boulders. Soils developed from sandstones and dolerites are Acrisols (ISSS Working Group, 1998) and Inanda soil form (Soil Classification Working Group, 1991). Within hillslopes, deep Acrisols (~2 m) characterize the footslope and Gleysols the bottomland. Bottomlands (Bo) exhibit features of waterlogging, such as a surface dark grey A horizon, enriched in organic matter. At the footslope (F) position, the soils are well-drained (Figure 14). The midslope (M) position exhibits a similar soil profile, but much shallower. The soils at the terrace (T) and the shoulder (SD) have developed from dolerites. Finally, the soils found at the other shoulder location (SS) are derived from sandstones and are yellow in colour.

Methodology

Water samples were extracted from accumulative rainfall collector; from piezometers (shallow groundwater) and boreholes on the hillslopes; from small (1x1m) overland flow runoff plots; automatically via an ISCO sampler from an H-flume constructed in the main drainage channel in an upper catchment of 23 ha; automatically at a lower H-flume draining 100 ha and by the stream at a point draining 1000 ha, by intermittent grab sampling (Figure 14). The samples were returned to the University of KwaZulu-Natal in Pietermaritzburg for analysis using the Research (LGR) Liquid Water Isotope Analyzer by laser absorption. The samples were also analysed for chemical species, Na, Si, Mg, Ca, Fe, Al, N-NH_3, N-NO_3^-.

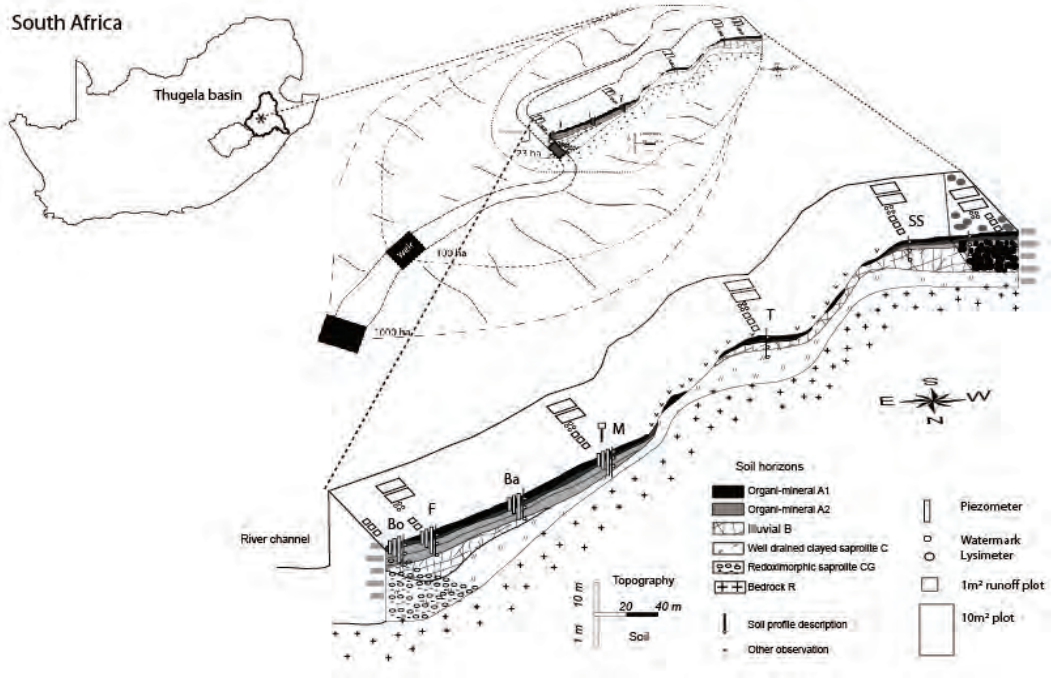

Figure 14: Schematic of the Potshini research catchment and hillslope monitoring

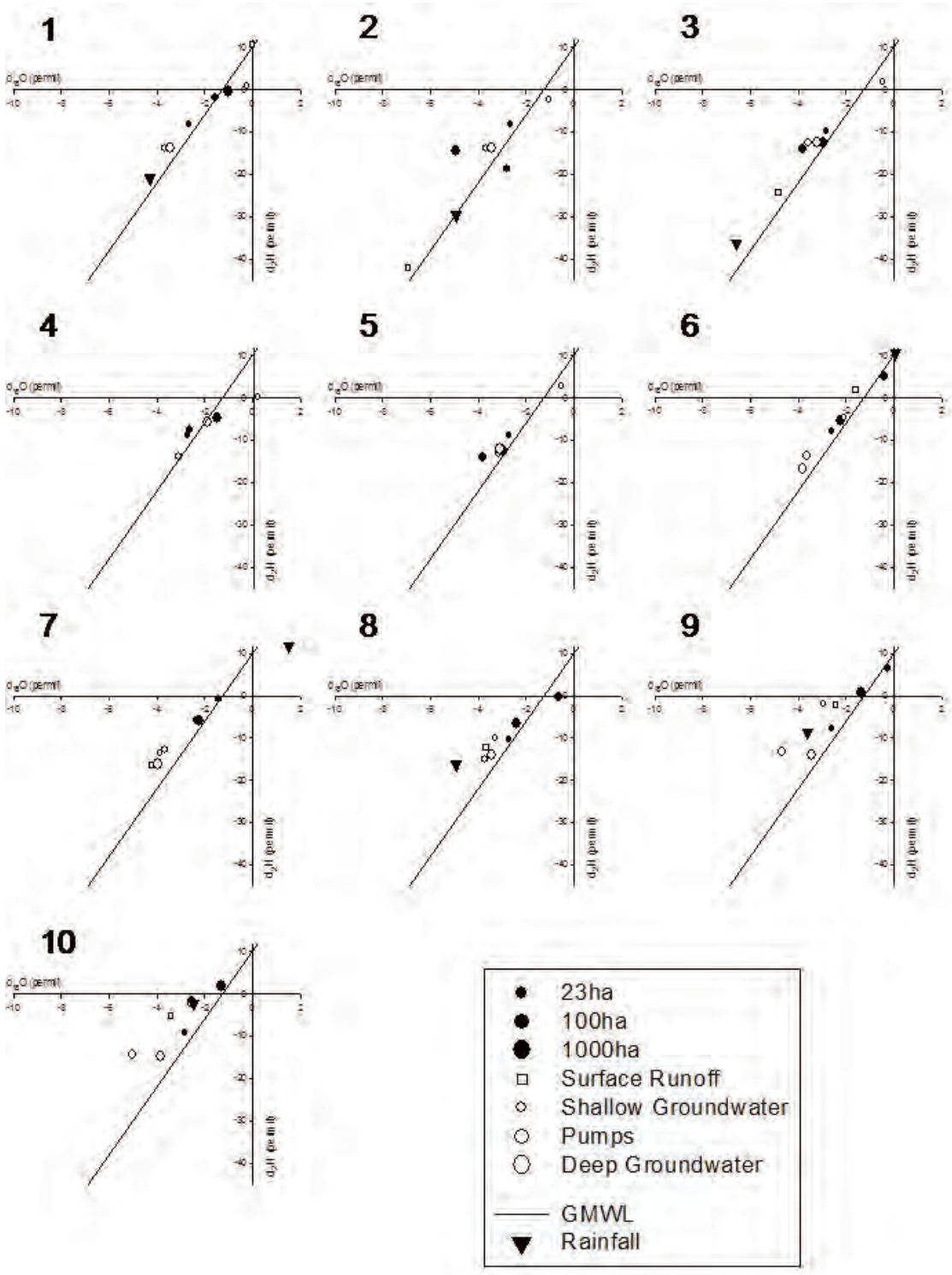

Figure 15: $\delta^{18}O$ and $\delta^{2}H$ relationships for sampling at different scales for 10 events during February and March 2011.

Results and discussion

Isotope values for ten events reveal a large variation in rainfall isotope values, with the $\delta^{18}O$ ratio ranging from -7 to +1.5 $^{o}/_{oo}$ for the ten events (Fig. 15). In general, the local scale observations follow the rainfall signal, but even at 1x1 m^2 runoff plot scale (small squares in Fig. 15), there seems to be some mixing. At the 100 ha scale the $\delta^{18}O$ ratios remain with a band ranging between -4 and -1 $^{o}/_{oo}$.

The use of water isotopes in conjunction with chemical elements allowed for end for member mixing analysis for the period from 22 February to 1 April 2011 and for all 3 monitored catchments to be performed.

The mean contribution of the three selected water sources (Overland Flow, Soil Water, Groundwater) is presented in Table 2. This gives an indication and insight of the spatial variations of the runoff generated at the different scales.

Table 2: The mean contribution of the 3 main water sources for the 3 catchment scales

	23ha	100ha	1000ha
	----------%----------		
Overland Flow	22	22	8
Soil Water	15	28	37
Groundwater	63	50	55

The results presented are an initial attempt at performing general estimates of the sources contributing to runoff at the three monitored catchment outlets.

Groundwater was estimated to contribute the most to the total runoff at all the three nested catchments. The mean groundwater contribution was 63% at 23ha, 50% at 100ha and 55% at 1000ha. The mean soil water contribution to catchment runoff increased from 15% at 23ha to 28% at 100ha and to 37% at 1000ha. Overland flow, or event water contribution was almost stable at 22% at 23ha and 22% at 100ha but highly decreased to 8% at the 1000ha catchment outlet.

From these results there was a general trend for soil water contributions to increase with the increase in catchment size.

The evolution over time of the contribution of the three water compartments at the 23 ha micro-catchment and 100 ha catchment outlet is displayed in Figs. 16 and 17 respectively. On 22 February 2011 the antecedent cumulative precipitation was 22.8 mm and 31.2 mm for the previous 3 and 7 days, respectively, which can be considered as a rainy period. A dry spell occurred between the 3rd to the 15th of March, followed by a wet period. The calculation of the mixing of sources at the 1000ha catchment outlet, again, showed that the largest contribution to catchment runoff was that of groundwater during both events as well as the period of low flow. This approach allows for an insight into the temporal variations of the sources of runoff at the catchment outlets in conjunction with the spatial variations of catchment runoff at different scales.

Overland flow (OF) or event water, at 60 % was the highest contributor to runoff at the 23 ha micro-catchment during the initial rainfall event. It increased to 97% on 2 March 2011. Over time the OF contributions decreased, which coincided with increased contributions from soil water. OF contribution was 0% during the dry spell of the first half of March and towards the end of the period. Soil water, that initially contributed nothing to the micro-catchment runoff, increased over time with a peak at 51% on 27 March 2011. A reason for the low initial contribution of soil water is that the water from the first rains is stored in the soil profile rather than moving through it. Once the soil moisture deficit is satisfied, soil water contributions increased. However, soil water started contributing on 2 March 2011, after which soil moisture consistently contributed water to micro-catchment runoff. Groundwater contributions at the micro-catchment outlet were with 100% the highest during periods of low flow when there was no rainfall. Groundwater still contributed to micro-catchment flow during events but the contribution was low (lowest event contribution being 2.5%).

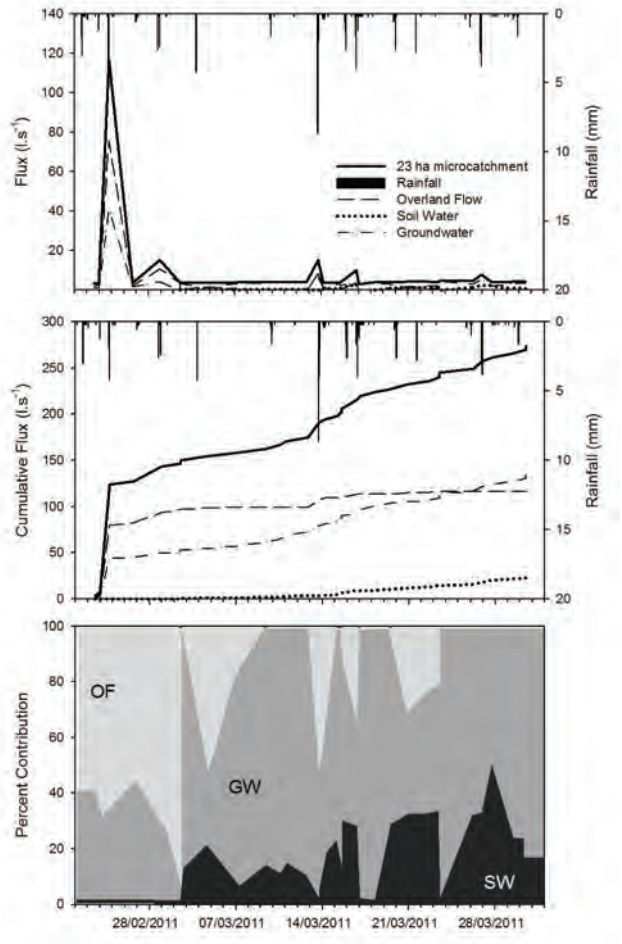

Figure 16: Mixing and contributions of the sources contributing to catchment runoff at the 23ha micro-catchment

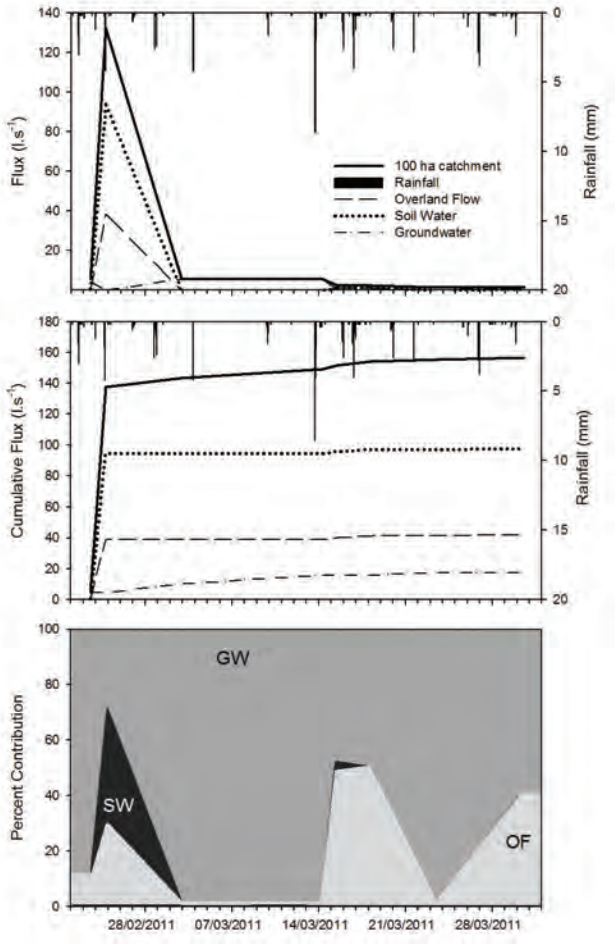

Figure 17: Mixing and contributions of the sources contributing to catchment runoff at the 100ha catchment

The mixing of the sources contributing to catchment runoff at the 100ha catchment is shown in Fig. 17. Soil water had the greatest contribution (40%) to catchment runoff at the initial storm, followed by OF (30%) and groundwater (30%). Groundwater contribution was 100% during periods of low flow. For the 2 out of the 3 distinct events of the period for the 100ha catchment outlet, soil water and overland flow contributed similar amounts of water to the catchment runoff (50% contributions from each of soil water and overland flow). The event which occurred on 24 February 2011 had a 71% contribution from soil water and 21% from overland flow.

Conclusion

This approach allows for an insight into the temporal variations of the sources of runoff at the catchment outlets at different scales.

Groundwater contributions at the micro-catchment (23 ha) outlet were the highest (100%) during periods of low flow when there was no rainfall. Groundwater still contributed to micro-catchment flow during events but the contribution was low (lowest event contribution being 2.5%).

At the 100 ha scale, it was found that soil water and overland flow only contributed to catchment runoff during events.

Stable isotopes of water have been used extensively to determine local scale hydrological processes (Kendall and McDonnell, 2003). In this section we demonstrate two applications. The first is the use of $\delta^{18}O$ and $\delta^{2}H$ to estimate the location of root water uptake by invading *Acacia sieberiana* in an eroded site in the KwaZulu-Natal Drakensberg foothills. The second is the use of $\delta^{18}O$ and $\delta^{2}H$ to evaluate the evaporation processes from porous media of two different textures.

VEGETATION UPTAKE

(Seraphine Grellier)

Introduction

The site occurs over the northern catchment divide of the Potchini research catchment in the Drakensberg foothills (Figure 18). Encroachment by *Acacia sieberiana* var. *woodii* and associated gulley formation is observed in the valley. The water uptake of the trees was of interest in order to assess the reasons for encroachment and the consequences to land management.

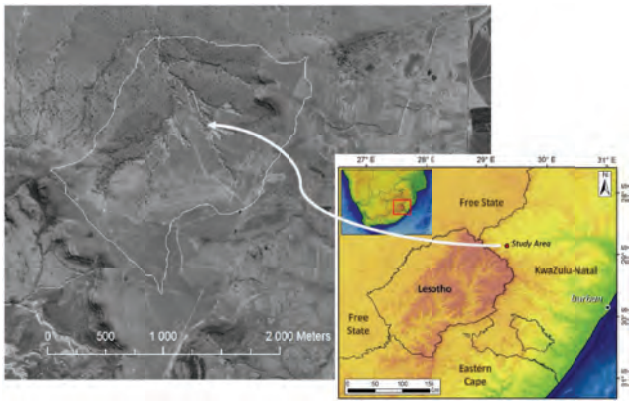

Figure 18: Location of the grazing area over the ridge north of the Potshini research catchment (Grellier 2011).

Site description

The natural vegetation is classified as Northern KwaZulu-Natal moist grassland biome (Mucina and Rutherford, 2006).

The geology of the site is characterized by fine-grained sandstones, shales, siltstone and mudstones of the Beaufort and Ecca Groups of the Karoo Supergroup that alternate in horizontal successions (King, 2002). Unconsolidated colluvial deposits from the Pleistocene fill the valleys. These soils are very prone to linear erosion in gullies, locally called "dongas" (Botha, 1994, Rienks et al. 2000). Dykes of dolerite from the Jurassic, from 1 - 8 m wide intrude the parent rock (Mucina and Rutherford 2006). The general soil type of the bottom of the watershed is luvisol (World Reference Base 1998) with two well-delimited main horizons. Horizon A is coherent, with brown colour (10YR 4/1 to 10YR 4/3) and 20% clay, with many fine and medium roots. The Bt Horizon (up to 50% clay) is dark brown, very coherent and hard with a coarse blocky structure.

Figure 19: Gulley erosion in the grazing area where encroachment of Acacia sieberiana occurs.

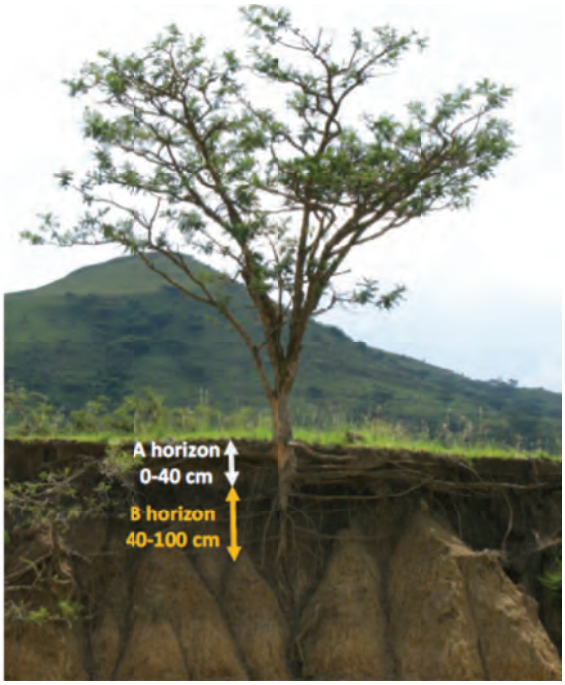

Figure 20: Assumed uptake zones from A and B horizons of the Acacia sieberiana, showing root distribution of a tree on the edge of the gulley.

Methodology

The depth of water uptake of *Acacia sieberiana* of different size classes in this sub-humid mountainous grassland of KwaZulu-Natal (South Africa) was examined. Water potential measurements of acacia leaves at predawn and midday were done to assess the water stress of acacias during the year. Soil samples, up to 2 m depth, and stems of acacias were analyzed for water isotopes ($\delta^{18}O$) along a catena in dry and wet seasons. Samples were collected from specific positions on the catena and from large and small individual trees, both under and outside the canopy.

Results and discussion

Typical water content and isotope profiles are shown for the upper, middle and lower positions on the transect in Fig. 21. $\delta^{18}O$ values, as is typical, exhibit increasing depletion with depth.

Two water uptake zones were defined. The first was the A-horizon and the second, the B and deeper horizons. From these two source zones, a mixing model was applied to determine the dominant source supplying the stem as sampled at the same time. The results are presented in Table 3.

Table 3: Two sources mixing-model applied on depth of water uptake by Acacia sieberiana in a duplex soil. Source A= A horizon (0-40cm); source B= B horizon + deeper horizons (>40cm). Three zones in the catena (Upper, Middle, Lower) and three sizes of Acacia (Tall, Medium, Small) are presented for each sampling period (Sept. 2009 and Feb. 2010) (Grellier 2011).

			September 2009		February 2010	
Zone	Size	Source	fraction of uptake	confidence interval	fraction of uptake	confidence interval
Upper	Tall	A	0,13 ± 0,12	0<fA<0,36	0,27 ± 0,14	0<fA<0,72
		B	0,86 ± 0,12	0,63<fB<1	0,72 ± 0,14	0,27<fB<1
	Med	A			0,32 ± 0,07	0,17<fA<0,48
		B	-4,74<Horizon B values (-4,73)		0,67 ± 0,07	0,51<fB<0,83
	Small	A	0,28 ± 0,27	0<fA<1		
		B	0,72 ± 0,27	0<fB<1	-4,65<Horizon B values (-4,3)	
Middle	Tall	A				
		B	-5,14<Horizon B values (-4,44)		-5,10<Horizon B values (-4,68)	
	Med	A				
		B	-5,05<Horizon B values (-4,44)		-4,88<Horizon B values (-4,68)	
	Small	A	-2,75>Horizon A values (-3,55)		0,08 ± 0,14	0<fA<41
		B			0,92 ± 0,14	58<fB<1
Lower	Tall	A				
		B	-4,59<Horizon B values (-4,01)		-4,73<Horizon B values (-4,3)	
	Med	A				
		B	-4,95<Horizon B values (-4,01)		-5,32<Horizon B values (-4,3)	
	Small	A	-2,12>Horizon A values (-3,82)		0,58 ± 0,91	0<fA<1
		B			0,41 ± 0,91	0<fB<1

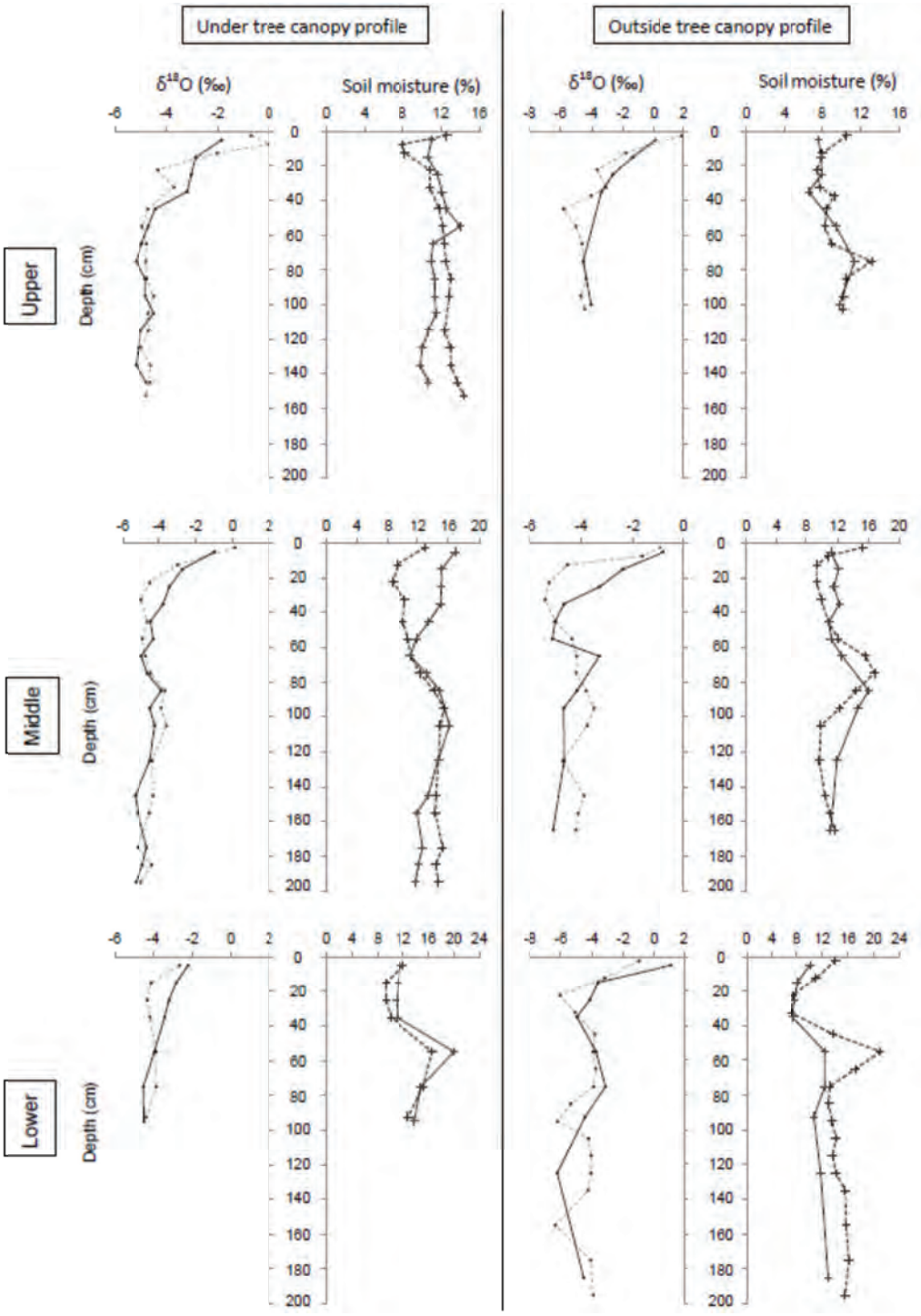

Figure 21: Soil water content and $\delta^{18}O$ distribution in profiles sampled under acacia canopy and outside the canopy at the three zones in the catena (upper, middle, lower) in September 2009 (dotted lines) and in February 2010 (solid lines).

Note: When $\delta^{18}O$ (‰) values of acacia stem was higher than the average $\delta^{18}O$ (‰) values of the A horizon or lower than average $\delta^{18}O$ (‰) values of the B horizon, the model was not valid (grey cells) as water uptake depth was considered predominantly from A horizon or B horizon.

In September, when grass is dormant, small acacias favour uptake from the A horizon, while in February, when competition with grass is strong, small acacias eventually switched to using water from deeper layers. The upper zone of the catena produced slightly different results as small acacias favor deeper layers even in September. Nonetheless, on closer scrutiny of the small acacia data for this zone (-4.09 ‰) and the corresponding soil water $\delta^{18}O$ profiles, it is deduced that small acacias may take up water at the interface between the A and B horizons (40 cm) in September but clearly favour deeper layers in February (probably around 80 cm depth where soil moisture increased). This indicates that roots of 0.2-1 m height acacias may be as deep as 80 cm.

Medium-sized acacias have the same behaviour as tall acacias. In the lower and middle zones of the transect they exclusively transpired water from deeper layers, sometimes even deeper than the maximum depth sampled, because $\delta^{18}O$ values were lower than the $\delta^{18}O$ values observed in the B horizon. However in the upper zone of the transect, the medium and tall trees had an opposite behaviour to small acacias. They took up water mostly in deep layers in September, but in February, they switched partially to shallower layers.

Conclusion

^{18}O isotopes were successfully used to evaluate the soil water uptake by transpiration of acacia trees of different growth stages and in different positions on a catena.

SOIL WATER EVAPORATION

Introduction

The process of evaporation of soil water includes the movement of water by capillary forces as well as diffusion of the soil water vapour. Most numerical models consider only the capillary fluxes in estimating evaporation from soil in response to an atmospheric demand. However, in certain porous media, vapour fluxes could be significant. In this study we compare the isotope ratios of capillary and vapour fluxes from a fine slimes material and a coarse sandy material to illustrate the differences in the soil water evaporation loss process.

Site description

A very fine slimes and a sand sample were collected from mining site in northern KwaZulu-Natal. These were returned to the University of KwaZulu-Natal for testing at the Agricultural Faculty grounds in Pietermaritzburg.

Methodology

Two columns (300 mm dia. 1.5m high) were instrumented for capillary suction and volumetric water content monitoring using 6 mm diameter cermic cup tensiometers, automated with pressure transducers and 100 mm long Time Domain Reflectometer probes, driven by a Campbell Scientific TDR100 wave generator, respectively (Fig. 22). The columns were saturated from the base and evaporation was induced by exposure to outside radiation, temperature, humidity and wind. Rain was prevented from falling into the columns by a transparent canopy and the columns were positioned in a lysimeter pit so that their top surfaces were at ground level. Periodic water samples were extracted from the column in the unsaturated and saturated zones. In addition, vapour samples were extracted from the surface using a cold trap. All samples were analysed for $\delta^{18}O$ and $\delta^{2}H$.

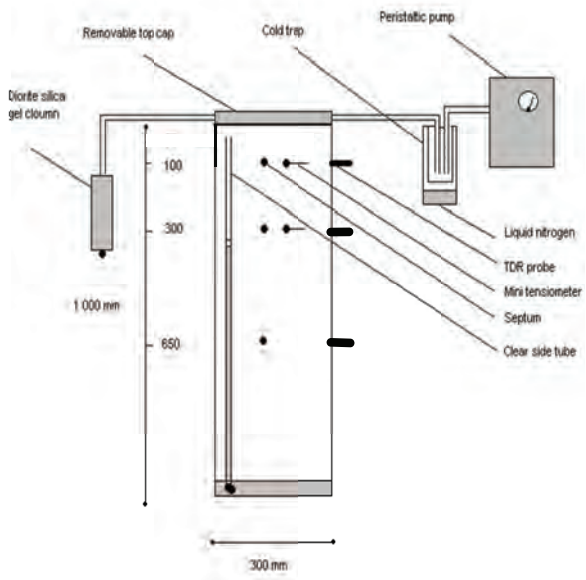

Figure 22: Schematic layout of the columns and instrumentation, showing the vapour sampling cap and cold trap.

The water retention and hydraulic conductivity of the two materials are shown in Figure 23. Porosities are similar, but the slimes material has a significantly higher water holding capacity than the sand material. The hydraulic conductivity of the sand material (2 mm/h) is higher than the slimes (0.08 mm/h).

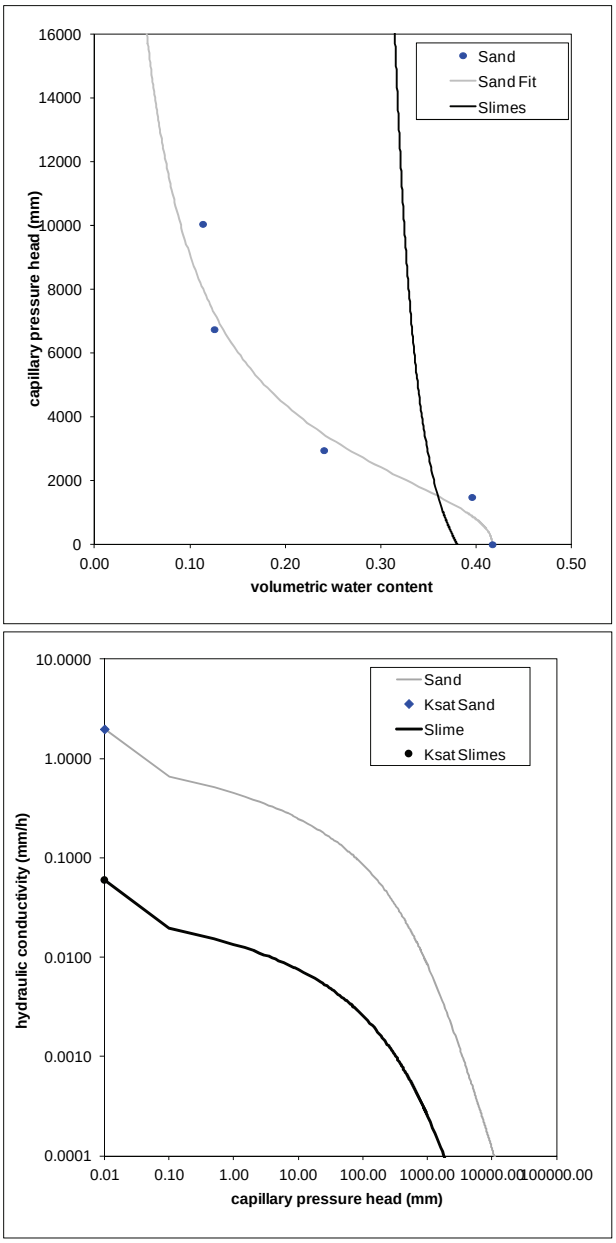

Figure 23: Water retention (top) and hydraulic conductivity (bottom) characteristics for the slimes and sand samples.

Results and discussion

After one week of drying through surface evaporation the slimes material surface began to crack (Fig. 24). The sand material shrank slightly, but no significant cracking was observed. The near-surface (100 mm below surface) of the slimes and sand materials dried out at similar rates during the two weeks of the trial. Water contents at 100 mm below surface (Top sensor) in the slimes reduced from 0.56 to 0.33, while in the sand water contents reduced from 0.57 to 0.35 (Fig. 25). Slight reductions in water content at 300 mm below surface (Middle sensor) were observed in the slimes material (0.58 to 0.54), while no significant reduction in water content was observed in the sand material at that depth.

Figure 24: Columns showing the top of the slimes material (top) and sand material (bottom) after one week of evaporation.

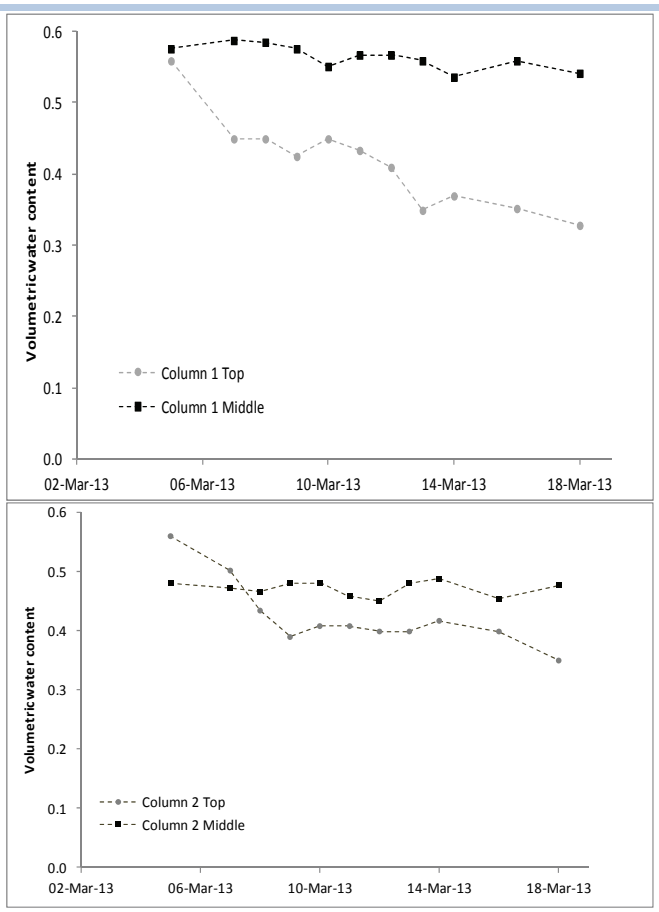

Figure 25: Drying history of volumetric water content in the top and middle sensing points for the slimes (above) and sand (below) over the first 12 days.

Various attempts have been made to estimate evaporation from soil surfaces (Barnes and Turner, 2003; Braud *et al*., 2009; Sutanto *et al*., 2012). Difficulty is encountered in estimating the kinetic fractionation factor, even with extremely well controlled experimental setups (Braud *et al*., 2009). Nevertheless, isotopes should provide insight into the processes occurring in different material.

The $\delta^{18}O$ and $\delta^{2}H$ relationships are shown for the slimes and sand in Fig. 26. It is evident that the soil pore water is progressively enriched with proximity to the surface in the sand material, while the slimes samples are all grouped around the original saturation liquid, although sampling from the upper (100 mm) position in the slimes material was not possible after the first week of evaporation. A sample extracted from the middle position (300 mm) in the slimes was significantly evaporated ($\delta^{18}O$ +15 $^{o}/_{oo}$) after one week (12 March), whereas that in the sand at the same position was still at the initial value (Fig. 27). The vapour samples were all depleted ($\delta^{18}O$ -11 $^{o}/_{oo}$), well below the initial water ($\delta^{18}O$ -2 $^{o}/_{oo}$).

These data indicate that the upwards advection of water in response to the drying at the surface, is higher in the sand than in the slimes material, where interstitial water is evidently lost through vapour flow in the slimes, with slow upwards migration.

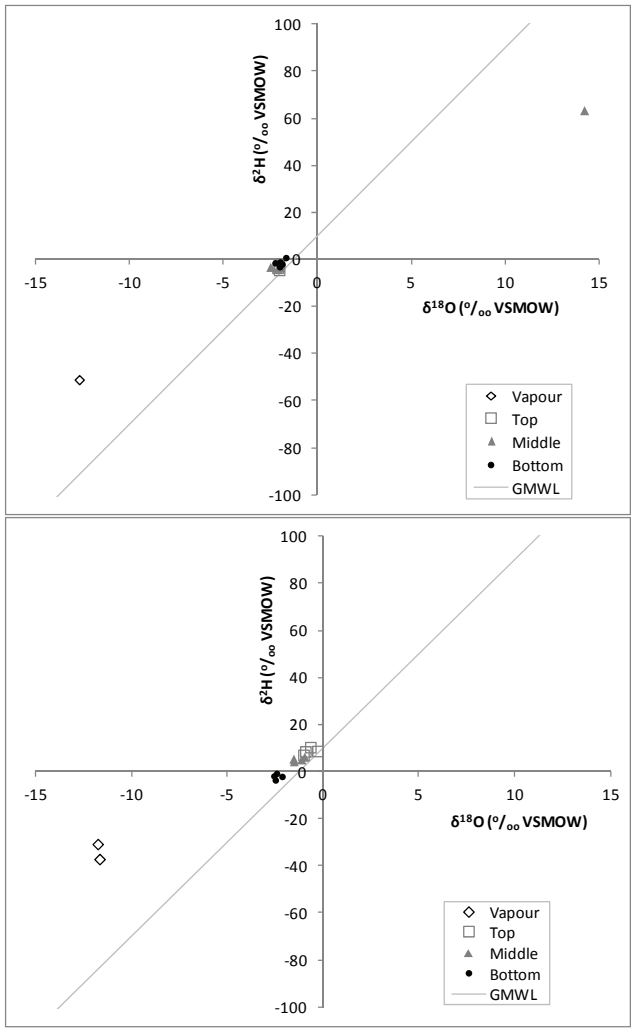

Figure 26: $\delta^{18}O$ and $\delta^{2}H$ relationship for vapour and soil water from top, middle and bottom sampling points for the slimes (above) and sand (below).

The depleted isotope values in the vapour extracted from the surface are similar to those observed by Braud *et al*. (2009). Their study showed initial vapour values that were significantly depleted, but became more enriched as the evaporation process proceeded, levelling out at the values of the initial wetting liquid and then becoming depleted again through back diffusion close to the surface.

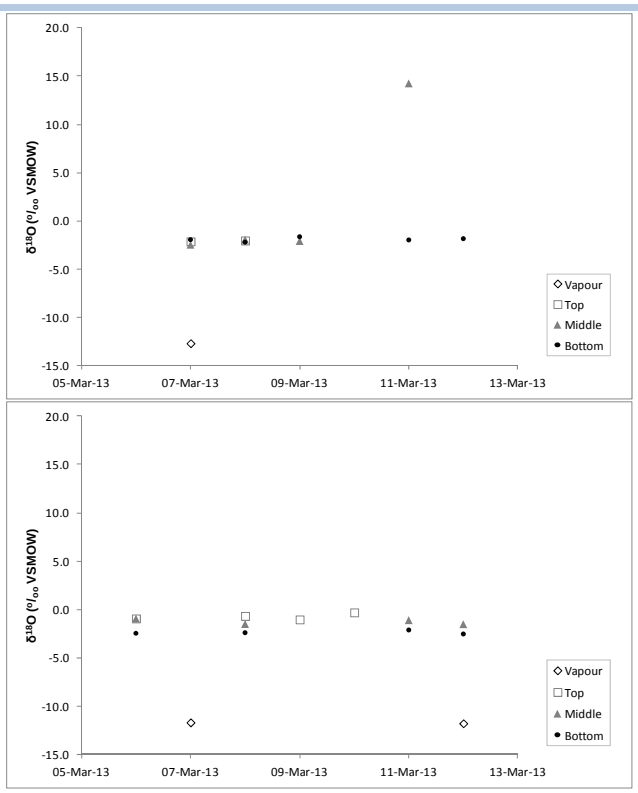

Figure 27: Time series of $\delta^{18}O$ of vapour and soil water from top, middle and bottom sampling points for the slimes (above) and sand (below).

Conclusion

Differences in the hydraulic characteristics of two materials (slimes and sand) have resulted in different soil water evaporation processes. These results are evident in $\delta^{18}O$ and $\delta^{2}H$ isotope variation in the profiles of the materials. The sand appears to supply water to the surface through advection, whereas the slimes losses water through vaporisation below the surface of the profile.

NON-POINT SOURCE POLLUTION

Wartburg Nutrients

(Julius Kollongei and Simon Lorentz)

Introduction

Evaluation and subsequent remediation of Non-Point Source (NPS) pollution from agricultural land use, requires an understanding and quantification of the connectivity of the contributing land forms as well as the stream network. In this project, (WRC K5/1808, Definition of Process Zones and Connectivity in Catchment Scale NPS Processes), isotopes were used to estimate the proportion of catchment contributing to the stream network so that nutrient and sediment loading could be assigned to the appropriate source areas. The study occurred in the Mkabela catchment near Wartburg in the KwaZulu-Natal midlands.

Site description

Drainage of the site is from north to south. The predominant land use is sugar cane, but some vegetable cropping, pasture and forestry exist in the catchment.

The soil survey conducted on the Mkabela catchment indicated that there are a nine soil types including the Avalon (Av), Cartref (Cf), Clovelly (Cv), Glencoe (Gc), Hutton (Hu), Katspruit (Ka), Longlands (Lo), Westleigh (We) (Fig. 28), (Le Roux, *et al.*, 2006). The soil types Westleigh, Avalon and Longlands are the only ones that can be related to the ERT survey area; they are described in Table 4.

Table 4: Brief description of the soil types found in the study area (le Roux et al., 2006)

Soil Type	General Characteristics
Avalon (Av)	The Avalon soil type surveyed to 120 cm depth and consists primarily of soft plinthic B horizons which is a sandy yellow-brown apedal B horizon underlain by hard plinthic horizons.
Cartref (Cf)	Shallow, sandy soils with very little water holding capacity found on steep, short, convex hillslopes.
Clovelly (Cv)	Associated with, and similar to, Longlands soil type.
Glencoe (Gc)	Similar to Avalon soil type, but dominated by hard plinthic subhorizon; found on steeper slopes of higher relief. Parent material is thought to be the Natal Group Sandstone (NGS).
Hutton (Hu)	Found near crest and midslopes of high relief, steep hillslopes. Moderately drained, underlain by NGS.
Katspruit (Ka)	Clayey, strongly gleyed soils found on low-relief (10-15 m) terrain, particular valley bottoms.
Longlands (Lo)	The Longlands soil type was surveyed up to 120 cm depth and consists of soils that are sandier than the Avalon soils with similar profile of soft plinthic B horizons well developed underlain by hard plinthic horizons.
Westleigh (We)	The Westleigh soil type was surveyed up to 110 cm depth and consist a poorly drained hydrosequence dominated by clayey soils with prominent mottling and deep, clayed subsoils.

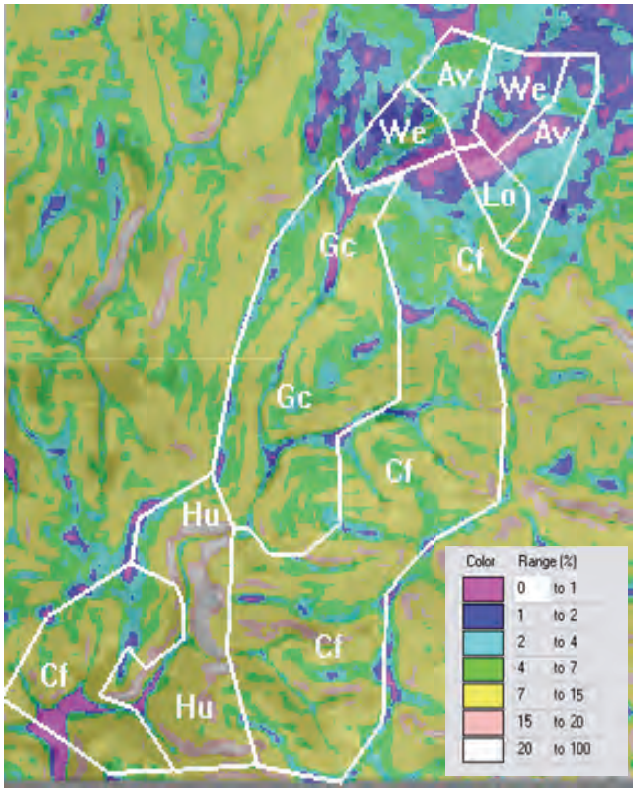

Figure 28: Six dominant soil sequence zones (hillslope types) found in the Mkabela catchment. Colours represent the slope range, (after le Roux et al., 2006).

According to le Roux, *et al.* (2006), the Westleigh and Longland soil types are underlain by the Natal Group sandstone while the Avalon soil type is underlain by sedimentary rocks of the Dwyka Group and sandstone of the Natal Group.

A geological map (Fig. 29) indicates the presence of the Natal sandstone. The Dwyka group is also found at the north of the catchment.

Methodology

Water quality and stable isotopes of water, ^{18}O and ^{2}H, have been determined for samples collected from the catchment headwaters to the outlet, some 12km downstream. Samples were collected from overland flow Runoff Plots, from the Flumes in the water ways of the sugar cane and at the grab sample sites named, Road Crossing, Dam in, Dam 1 Out, Dam 2 Out, Bridge 1 and Bridge 2 as shown in Figure 30.

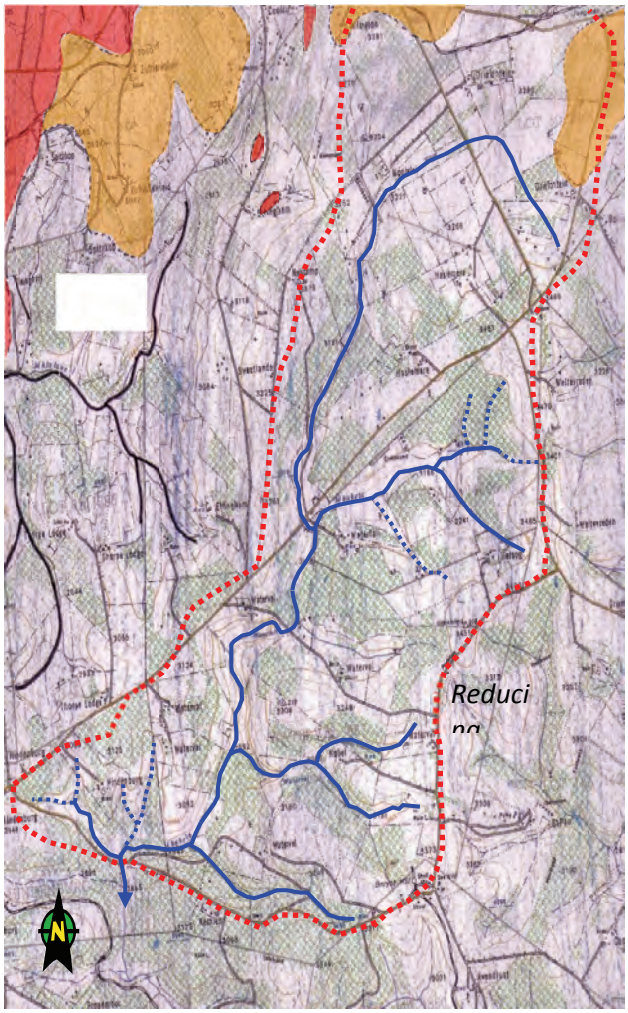

Figure 29: Geology of the Makabela catchment as derived from Council for Geosciences survey.

Results and discussion

The isotope data have been plotted in three ways:

- As a time series for each station from January 2009 to January 2011,
- For specific events, showing the responses to rainfall and runoff,
- As snap-shot profiles from the headwaters to the catchment outlet for specific wet and dry periods (10 January, 28 February and 15 December 2009, 7 June 2010 and 11 January 2011).

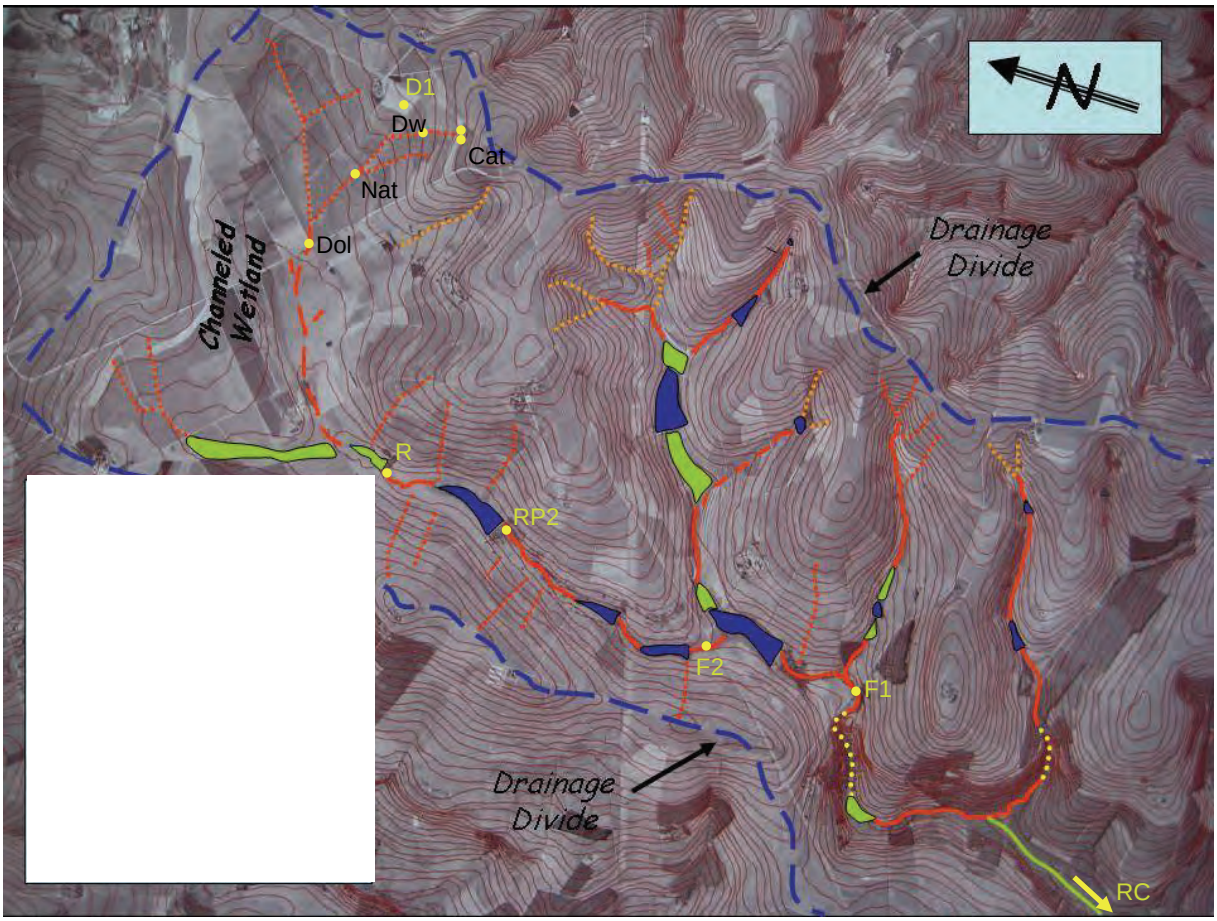

Figure 30: The Mkabela catchment showing the sampling stations.

The time series of ^{2}H and ^{18}O isotope results for 2009 are presented in Fig. 31 to 33 for individual monitoring stations, starting at the outlet of the catchment, Bridge 2, (Fig. 31) and ending at the runoff plots in the headwaters, (Fig. 33). Distinct behaviours are identified from these results:

- In the downstream stations (Bridge 2, Bridge 1 and Dam Out), the isotope ratios become lighter during the dry period between April and October, except during rainfall events (Fig. 31);
- All isotope ^{2}H and ^{18}O comparisons (right, Fig. 31), reveal an evaporated source of water with regression slopes lower than the Global Meteoric Water Line (GMWL). This reflects the retardation impact of the many farm dames between the Flumes (Figure 32, middle and bottom, right) and the catchment outlet, Bridge 2 (Fig. 31, top right);
- Comparison of the evaporation signal from the Dam Out station to the catchment outlet, Bridge 2, shows a decreasing influence of evaporation (Fig. 31, right) in the downstream direction as the contribution from adjacent land sources increases relative to upstream reservoir discharges (this is analysed further in the following sections);
- The isotope signals during the dry period do not reach the values determined for the groundwater borehole values (Approximately ^{2}H -14$^{o}/_{oo}$ and ^{18}O -3.5 $^{o}/_{oo}$) (Figure 33 bottom) indicating that reservoir storage and local hillslope contributions both contribute to the low flows.

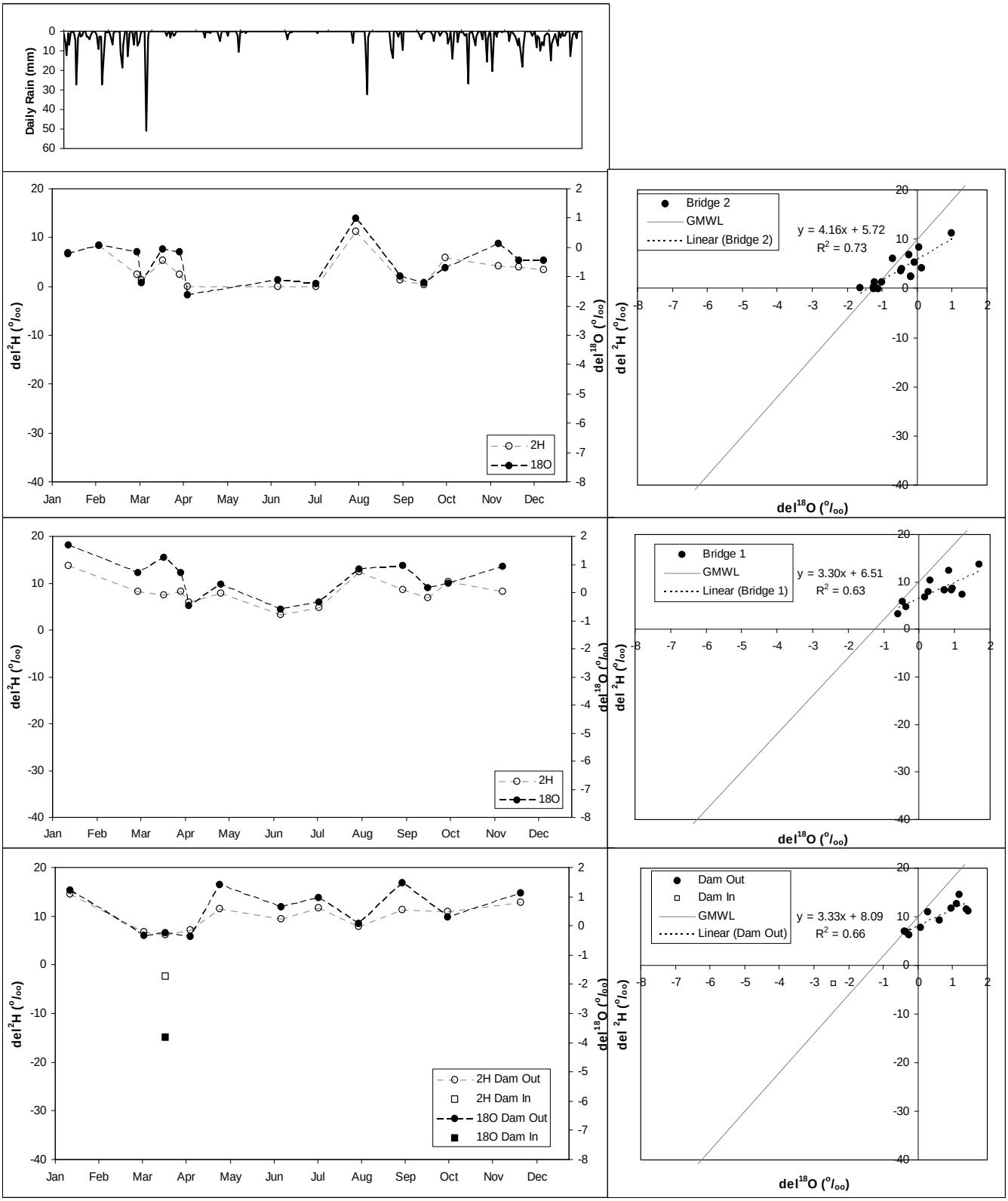

Figure 31: Rainfall and isotope responses for 2009 at the monitoring stations: Bridge 1, Bridge 2, Dam Out and Dam In.

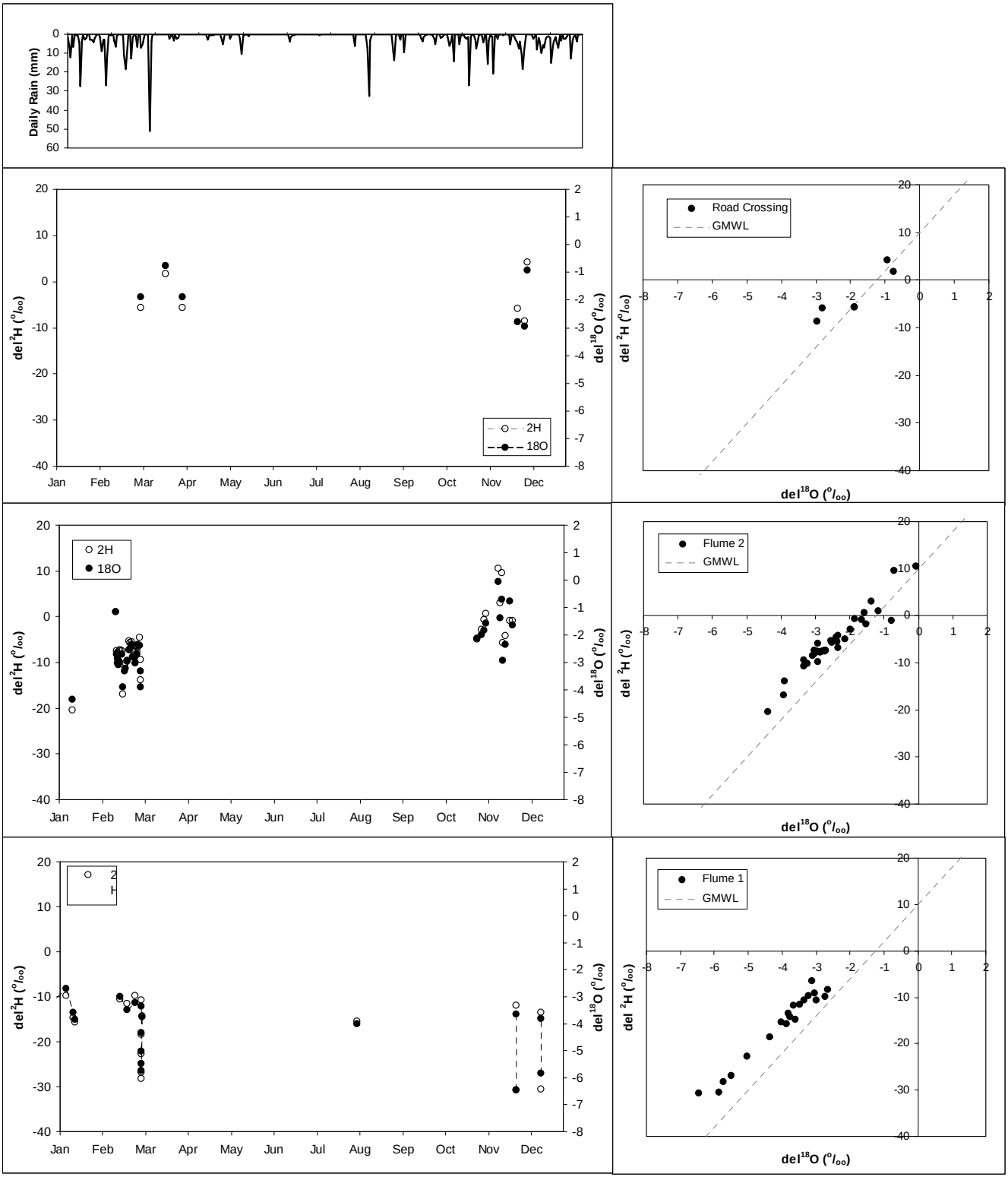

Figure 32: Rainfall and isotope responses for 2009 at the monitoring stations: Road Crossing, Flume 2 and Flume 1.

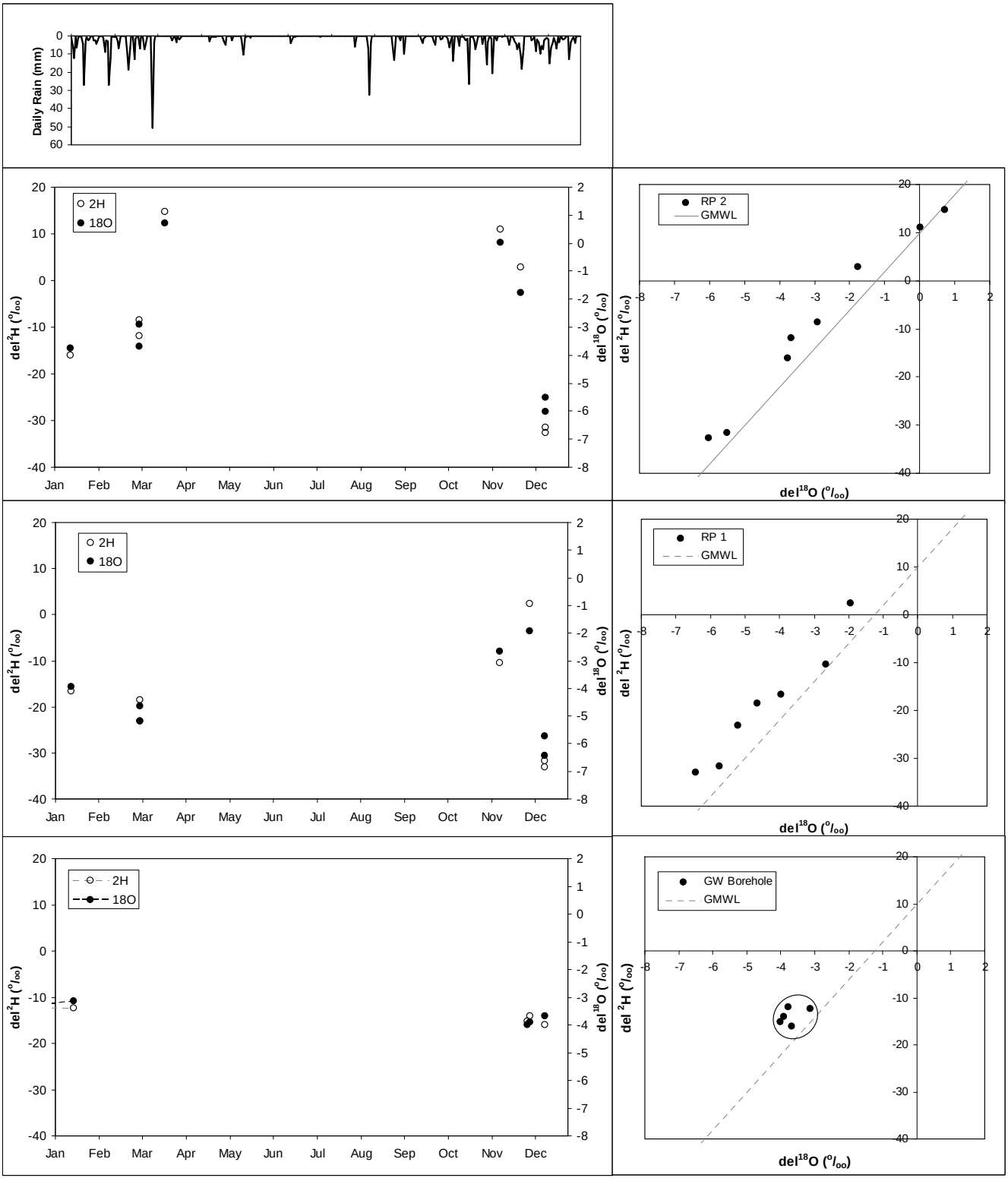

Figure 33: Rainfall and isotope responses for 2009 at the monitoring stations: Runoff Plot 2, Runoff Plot 1 and Groundwater Borehole, BH.

- The isotope comparisons for Flume 2 and Flume 1 (Fig. 32, right) show little evidence of evaporation and generally reflect the rainfall patterns represented by the runoff plot samples (Fig. 33, right). This indicates a significant contribution from event rainfall to the two flumes. Nevertheless, large changes in isotope ratios occur during events (this is analysed in following sections);

- The groundwater borehole signal remains constant during dry and wet conditions for the two years of monitoring.

Similar observations can be made for the time series of 2010. A unique sampling sequence during a rainfall event of 35mm on 10 November 2010 shows that the isotope values vary widely within an event and reflect relative contributions of event and pre-event water, even at the large scale sampling stations. These contributions are evaluated in the following section.

Isotope Event Results

The isotope ratios for selected precipitation events have been analysed for rainfall and runoff at the headwater flume stations. These include events on 10 January 2009, (27mm), 28 February 2009, (51mm), 27 January 2010 (43mm) and 10 November 2010. In addition, samples were collected periodically throughout the catchment during the event of 10 November 2010. Details of these four events are presented in Appendix B.

The 28 February 2009 results show a distinct drop in isotope ratio during the event (Fig. 34). The runoff at Flume 1 has an increasing contribution from the event water, indicated by the progressive change in the isotope ratios, from the initial value close to the groundwater signal, towards the isotope ratio of the event water. (The event water isotope signal is reflected by that for the runoff plots collected on 2 March 2009, although this sample will be an average of the rainfall contributing to overland flow during the event). The contribution from event water (rainfall) peaks about 2 hours after the peak of the discharge event, at which time most of the discharge is contributed by event water. Following this peak, the runoff contributions are increasingly dominated by the subsurface water (Fig. 34). The discharge isotope signal has returned to values representative of the groundwater within 24 hours of the cessation of the rainfall.

During less intense events, such as the one on 27 January 2010, the isotope ratios do not decrease significantly, although the sample representation is small. Thus, there appears to be a threshold of event magnitude and intensity which controls the connectivity of overland flow and subsurface event water discharge to the lower slopes in the sugar cane fields.

Three isotope samples were collected from the flumes during the event of 10 November 2010 (Figure B4.6). The resultant isotope values have been used, together with end member values for the groundwater and average rain water, to render the fractional contribution of the subsurface or pre-event water to the total discharge at Flume 2. This pre-event contribution comprises 19% of the total discharge at the peak of the event and typically returns to 100% of the contribution within 24 hours of the cessation of rain (Figure B4.6).

Also sampled during this event was the network of stations downstream of the flumes. The Road Crossing and Dam-In stations both show significant response to the event water (Fig. B4.6), but, with discharge from the first dam consisting only of the over flow, no evidence of event water is discernible (Fig. B4.7, left). The rainfall event has thus only displaced resident water from the dam. At the outlet of the second dam, however, event contributions are evident again (Dam 2 Out Figure B4.7). This indicates effective retention of event water in the upper wetland and first dam, but discernible contributions from event water through the following two, smaller impoundments. It is interesting to note, however, that the NO_3-N and P concentrations in the outlet from the large upper dam (Dam 1) increase dramatically during the event, (Fig. B4.3), indicative of possible disturbance of the impounded water in Dam 1, yielding a peak in nutrient load from the reservoir, despite the absence of event water. This rise in NO_3-N and P concentrations is not present in the outflow from the second two impoundments, where the discharge is diluted by event water.

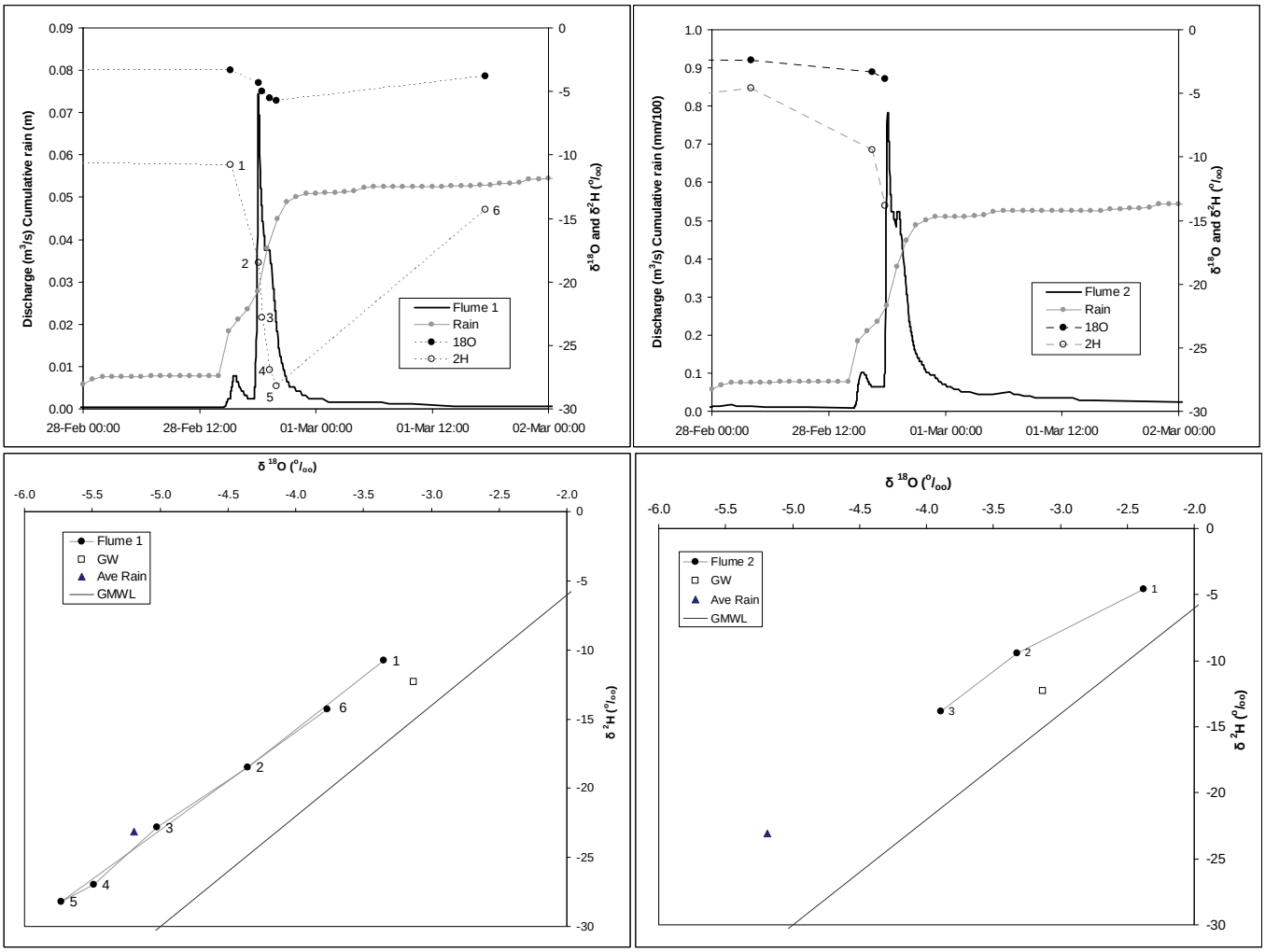

Figure 34: Rainfall, discharge and isotope responses at Flume 1 (left) and Flume 2 (right) for the event of 28 February 2009.

Isotope Transects

In order to get an indication of the sources of water, sediments and nutrients from the headwaters to the catchment outlet, sampling events were conducted in which the complete stream network was sampled within a 2 hour period. Selected events have been analysed for 10 January, 28 February, 15 December 2009, 7 June 2010 and 11 January 2011. The 11 January 2011 sampling campaign comprised comprehensive sampling throughout the catchment with negligible precipitation in the preceding four days.

The stable isotope signals at the two flumes differ slightly on 7 January 2011 (Fig. 35), reflecting different mixes of water. The recorded isotope delta values at Flume 1 are similar to that in the groundwater as reflected in the borehole sample, BH. This is not surprising as there is a spring upslope of the first flume. The isotope delta values at Flume 2 reflect a mixture of groundwater and possibly hillslope water from preceding rain (a total of 20mm precipitation occurred during the preceding 7 days). The isotope values at the Road Crossing and the Dam In sampling stations are similar to those at Flume 2. However, further downstream, samples at the Dam 1 Out and Dam 2 Out stations reflect the evaporation from the reservoirs which occur between the Dam In and Dam Out stations. These isotope values are highly enriched and are similar for Dam 1 and Dam 2 outlets.

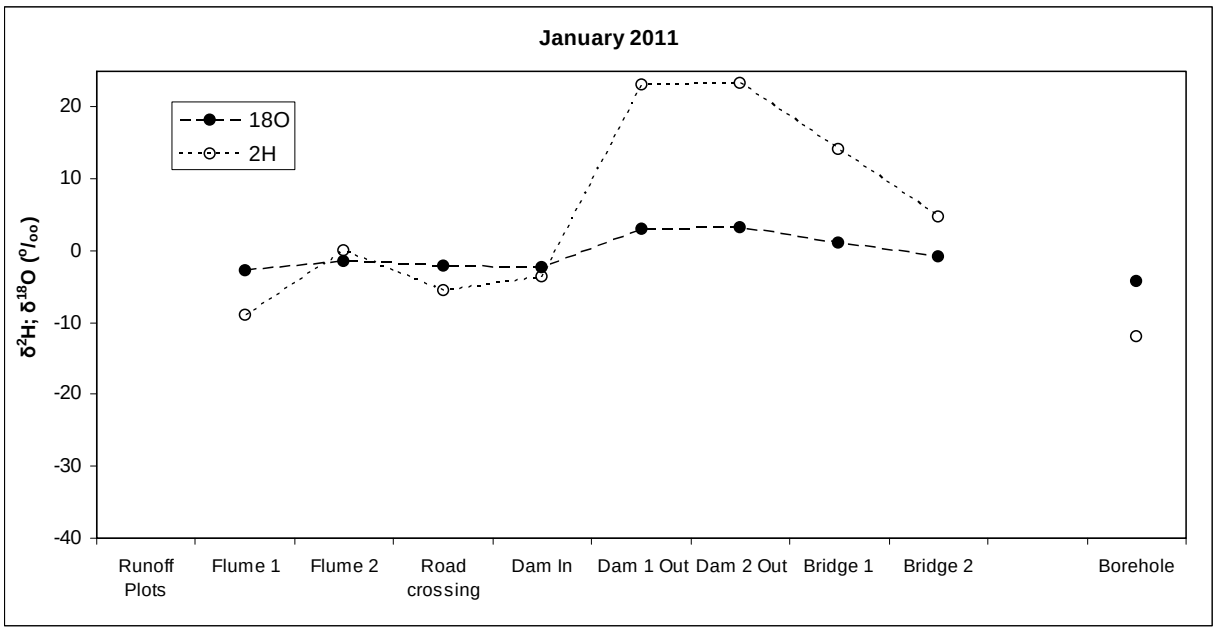

Figure 35: Isotope transect results from the headwater Flumes to the outlet at Bridge 2 for the event of 7 January 201

Downstream of the reservoir outlets, the isotope values at the Bridge 1 and Bridge 2 stations reflect a mixture of upstream inflow from the impounded tributaries as well as contributions from the land units between the reservoirs and the Bridge sampling stations. The isotope ratios, (Fig. 36), can be used to estimate the proportion of the discharge, at each of the Bridge stations, emanating from local land units, downstream of the reservoirs.

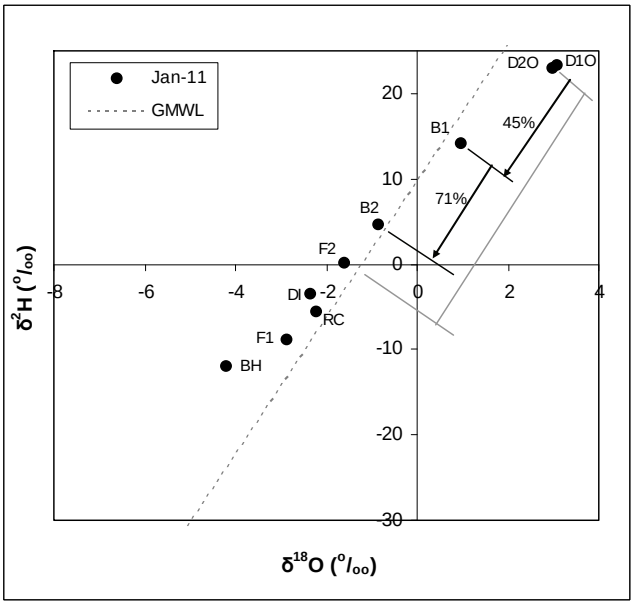

Figure 36: Isotope $\delta^2H/\delta^{18}O$ ratios for the transect results for the event of 7 January 2011.

First, it is assumed that the eastern, impounded tributary, upstream of Bridge 1 (Figure 47), will yield a similar evaporated isotope signal as that in the discharge from the Dam Out stations (D1O and D2O in

Fig. 36). Next, the isotope values of the contributing land units between the reservoir outlets and the Bridge stations (Fig. 37) are assumed to be similar to the Flume 2 values.

Using the $\delta^{18}O$ values a simple mass balance mixing model can be developed with the end members as the combined discharge from the impounded tributaries (Q_{DO} Fig. 37); the contribution to stream flow of the land unit between the impoundments and the Bridge stations (Q_{LUi}) and the Bridge station discharge (Q_{B1} and Q_{B2}). For the discharge at the first bridge station, this takes the form of:

$$Q_{B1}.\delta_{B1} = Q_{DO}.\delta_{DO} + Q_{LU1}\,\delta_{LU1}$$

Where:

δ_{B1} = $\delta^{18}O$ value at the Bridge 1 station,

δ_{DO} = $\delta^{18}O$ value for discharge from both impounded tributaries and

δ_{LU1} = $\delta^{18}O$ value for discharge from the sub-catchment (3.6km^2) between the most downstream reservoir and the Bridge 1 station.

Figure 37. Water flux (Q) and isotope delta (δ) values for land segments downstream of the farm dams.

Recognizing that $Q_{B1} = Q_{DO} + Q_{LU1}$, the ratio of discharge from the contributing sub-catchment to the total discharge at the Bridge station, can be expressed as a function of the isotope ratios as in:

$$\frac{Q_{LU1}}{Q_{B1}} = \frac{\delta_{B1} - \delta_{DO}}{\delta_{LU1} - \delta_{DO}}$$

For the sampling event of 11 January 2011, this ratio is 45%, which implies that just less than half the discharge at Bridge 1 is generated from the 3.6km^2 sub-catchment between the most downstream reservoir and the Bridge 1 station. Similar estimates can be performed for the Bridge 2 station. These show that for the 11 January 2011 sampling event, the contribution from the 13km^2 sub-catchment between the Bridge 1 and Bridge 2 stations, comprises 71% of the total discharge at Bridge 2 (Fig. 37). Analysis of the remaining selected sampling events yields the contributions listed in Fig. 38.

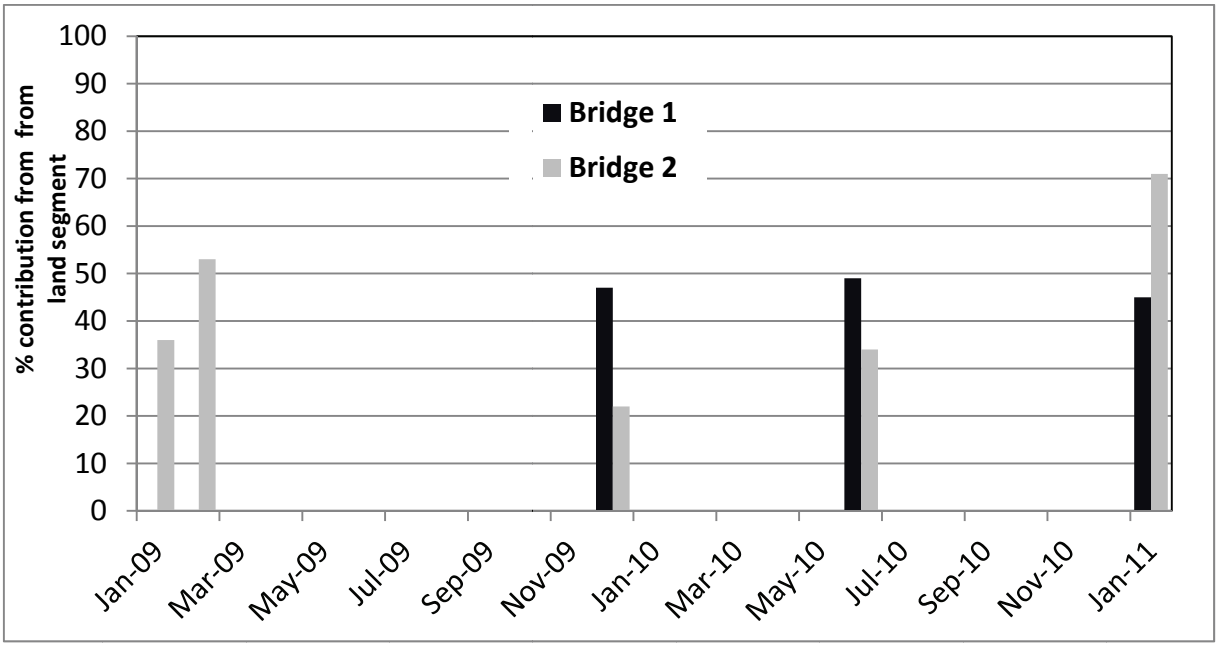

Figure 38. Discharge percent contribution of land segments between reservoir outlet and sampling points (Bridge 1 and Bridge 2).

The isotope values consistently show decreased evaporated signals at the Bridge 1 and Bridge 2 stations, reflecting the significant contribution from non-impounded sources between the dams and the downstream reaches. This progressive return of the isotope signal to the MWL indicates complete connection between the contributing hillslopes and stream in the landscape between the Dam Out and Bridge stations. This connectivity continues through the base flow period, as reflected by the analyses for June 2010 where 49% of the discharge at Bridge 1 and 34% of that at Bridge 2 are contributed by the relatively small connected sub-catchments immediately upstream of the Bridge stations (Fig. 38).

Conclusion

^{18}O and ^{2}H isotopes of water are effective in assessing the contributions of different sources of water influential in transporting nutrients and sediments in catchments.

Wartburg Sediments

Sediment sources and sinks have also been identified in the Makabela catchment through the application of geochemistry and isotopes of metals. Details are published in Lorentz *et al*., 2011 and Miller *et al*., 2012.

CONCLUSIONS

Stable isotopes of water have been used in a variety of studies at the University of KwaZulu-Natal. The use of isotopes, together with hydropedology and geophysics surveys and catchment hydrometry have been used to define processes at hillslope and small research catchment scale using end-member mixing algorithms as well as unit response function convolution integration. The use has been extended to the catchment scale of 1000 ha using end member mixing analysis. At the local scale, stable isotopes of water have been used to define sources of tree water uptake. Evaporation processes from columns of two porous media of different texture have also been defined using ^{18}O and ^{2}H isotopes. The use of these isotopes to define water connectivity in the landscape and streams has enhanced our ability to interpret the movement of nutrients and sediments in agricultural catchments.

ACKNOWLEDGMENTS

The assistance of Cobus Pretorius (Chief Technician, Hydrology) Siphiwe Mfeka (Field and Lab assistant), Pauline Ferry, Gonca Okay and Sibonelo Mabaso is gratefully acknowledged in producing this report.

REFERENCES

Barnes, CJ and Turner, JV. 2003. Isotopic exchange in soil water. In Kendall C and McDonnell J.(*eds*) Isotope tracers in catchment hydrology. Elsevier pp839

Braud. I., Biron, P., Bariac, T., Richard, P., Canale, L., Gaudet, JP. And Vauclin, M. 2009. Isotopic composition of bare soil evaporation water vapour Part I: RUBIC IV experimental setup and results. *J. Hydrol*. 369(1):1-16.

Botha GA, Wintle AG, Vogel JC. 1994. Episodic late Quaternary palaeogully erosion in northern KwaZulu-Natal, South Africa. *Catena* 23: 327-340.

Freese, C., Lorentz, S., le Roux, P., van Tol, J. and Vermeulen, D. 2009. The Use of Hillslope Response Characterisation in Modelling Selected South African Catchments. *14th SANCIAHS SYMPOSIUM: Pietermaritzburg, 21-23 September 2009*

Grellier, S. 2011. Hillslope encroachment by *Acacia sieberiana* in a deep-gullied grassland of KwaZulu-Natal (South Africa). PhD Dissertation submitted to Université Pierre & Marie Curie, Paris 6 in June 2011.

Kendall C and McDonnell J. 2003. Isotope tracers in catchment hydrology. Elsevier pp839

King GM. 2002. *An explanation of the 1:500 000 general hydrogeological map*. Department of Water Affairs and Forestry: Pretoria, South Africa.

Lorentz S.A., Goba P. and Pretorius J. 2001. Experiments and Measurements of Soil Hydraulic Characteristics. Report to the Water Research Commission on the Project *Experimentation and Laboratory Measurement for Hydrological Process Research.* Water Research Commission Report 744/0/01, Pretoria, South Africa.

Lorentz, S., Bursey, K., Idowu, O., Pretorius, J. and Ngaleka, K. 2008. Definition and upscaling of key hydrological processes for application in models. WRC Report 1320/1/08. Water Research Commission, Pretoria, South Africa.

Lorentz S, Miller J, Lechler P, Mackin G, Lord M, Kollongei J, Pretorius J, Ngeleka K, Zondi N and le Roux J. 2011. Definition of Process Zones and Connectivity in Catchment Scale NPS Processes. Water Research Commission Report, K5/1808/1/11. Pretoria, South Africa.

McGuire, KJ., DeWalle, DR. and Gburek, WJ. 2002. Evaluation of mean residence time in subsurface waters using oxygen-18 fluctuations during drought conditions in the mid-Appalations. *J. Hydrol.* 261(1):132-149.

Miller, JR., Mackin, G., Lechler, P., Lord, M. and Lorentz, S. 2012. Influence of basin connectivity on sediment source, transport, and storage within the Mkabela Basin, South Africa. *Hydrol. Earth Syst. Sci.*, 10151–10204, 2012

Mucina L, Rutherford MC. 2006. *The vegetation of South Africa, Lesotho and Swaziland*. Strelitzia 19, South African National Biodiversity Institute: Pretoria, South Africa

Sutanto, SJ., Wenninger, J., Coenders-Gerrits, AMJ and Uhlenbrook, S. 2012. Partitioning of evaporation into transpiration, soil evaporation and interception: a comparison between isotope measurements and a HYDRUS-1D model. *Hydrol. Earth Syst. Sci.* 16:2605-2616.

Talma S., Lorentz S. and Woodborne S. 2006. South African contribution to the Rivers CRP. IAEA Cooperative Research Programme: *Design criteria for a network to monitor isotope compositions of runoff in large rivers (F3.20.03).* Project R12286.

Isotope Inter-Lab Assessments

Samples circulated to South African labs by Siep Talma were analysed using the UKZN Los Gatos machine. Results were accurate (Table 5).

The laser analyser was used to measure isotope values for samples sent by IAEA as part of an international laboratory comparison. Regrettably the standards requested from the IAEA did not arrive in time and the results of the unknown samples were not submitted. Nevertheless, the results of the IAEA blind sample analyses were good, despite the use of in-house standards which had been calibrated two years previously.

Table 5 Results of the South African Isotope Laboratory Comparison

		SAF-1	SAF-2	SAF-3
		differences from average		
CSIR	$\delta^{18}O$	-0.65	-0.29	0.08
IAEA	$\delta^{18}O$	-0.01	0.00	0.08
iThemba	$\delta^{18}O$	-0.03	-0.05	-0.01
UCT	$\delta^{18}O$	0.33	0.24	-0.06
UKZN	$\delta^{18}O$	0.37	0.11	-0.09
Average		*-0.45*	*-3.31*	*-9.48*
CSIR	$\delta^{2}H$	-2.91	-0.70	-0.10
IAEA	$\delta^{2}H$	0.06	-0.81	-0.67
iThemba	$\delta^{2}H$	0.09	0.30	-0.80
UCT	$\delta^{2}H$	-0.74	-0.83	2.43
UKZN	$\delta^{2}H$	3.50	2.03	-0.85
Average		*-4.79*	*-31.30*	*-77.50*

APPENDIX A

HILLSLOPE RESPONSE ANALYSIS FOR THE WEATHERLEY CATCHMENT

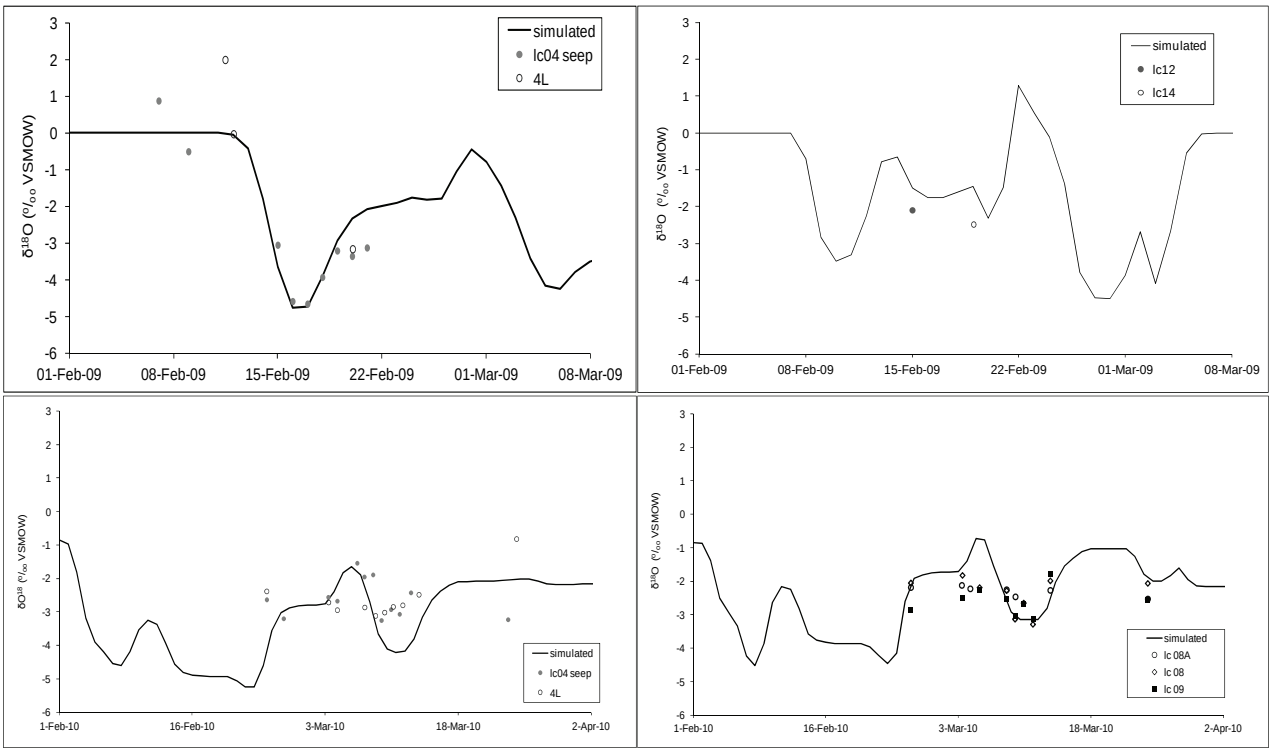

Figure A.1 Weatherley Lower Catchment (LC) isotope responses for hillslopes LC01-04 (above) and LC08-12 (below) for February 2009 (left) and March 2010 (right).

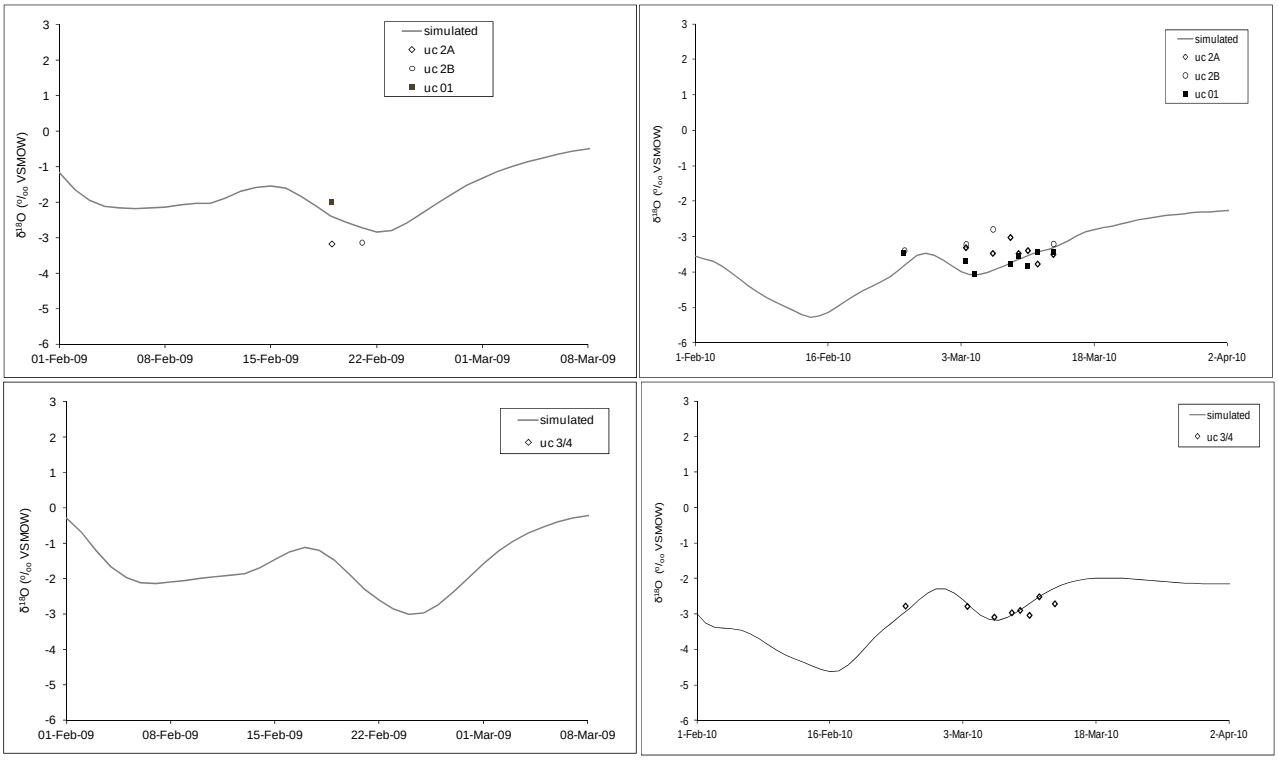

Figure A.2 Weatherley Upper Catchment (UC) isotope responses for hillslopes UC01-02 (above) and UC3/4 (below) for February 2009 (left) and March 2010 (right).

APPENDIX B

RAINFALL – RUNOFF EVENT ISOTOPE RESPONSES, WARTBURG CATCHMENT

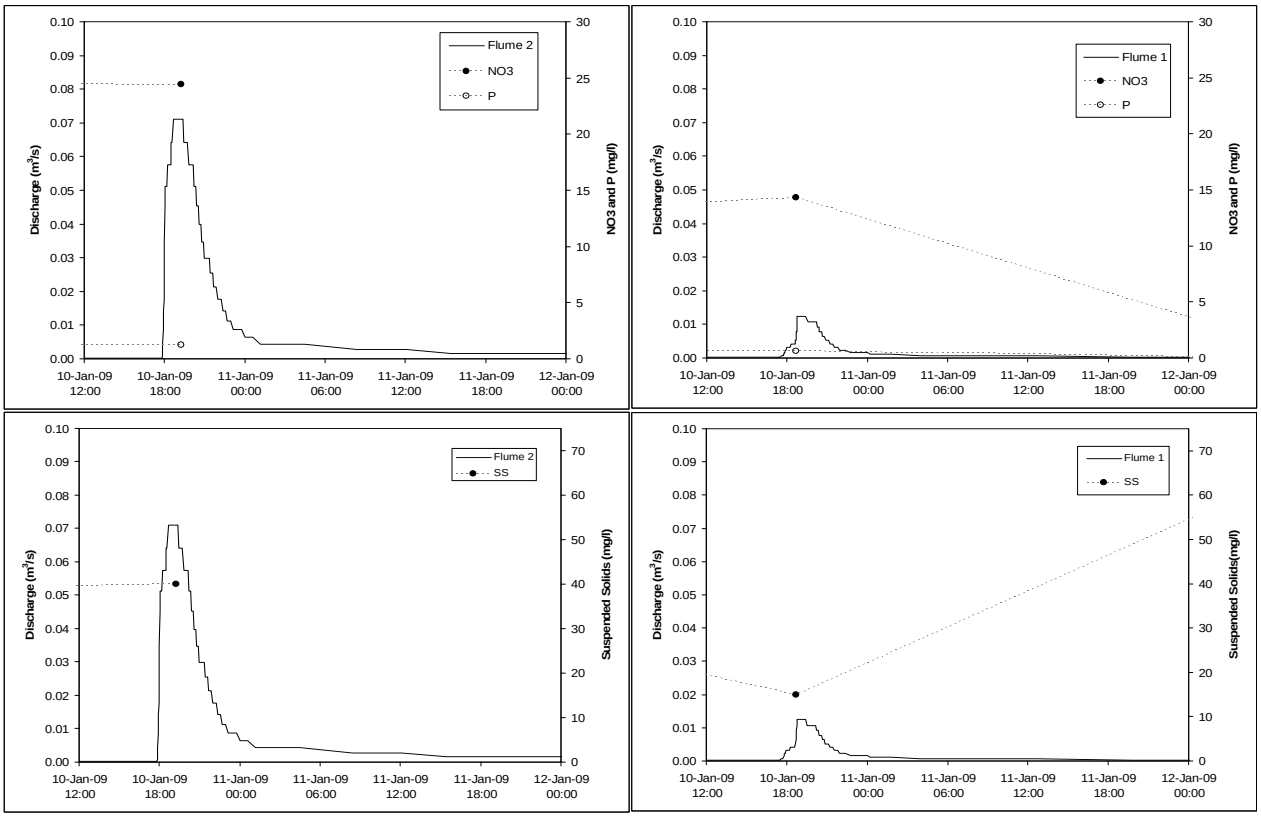

Figure B1.1. Rainfall, runoff Nitrate and P (above) and Suspended Solids (below) responses for Flume 1 (left) and Flume 2 (right) for event of 10 January 2009.

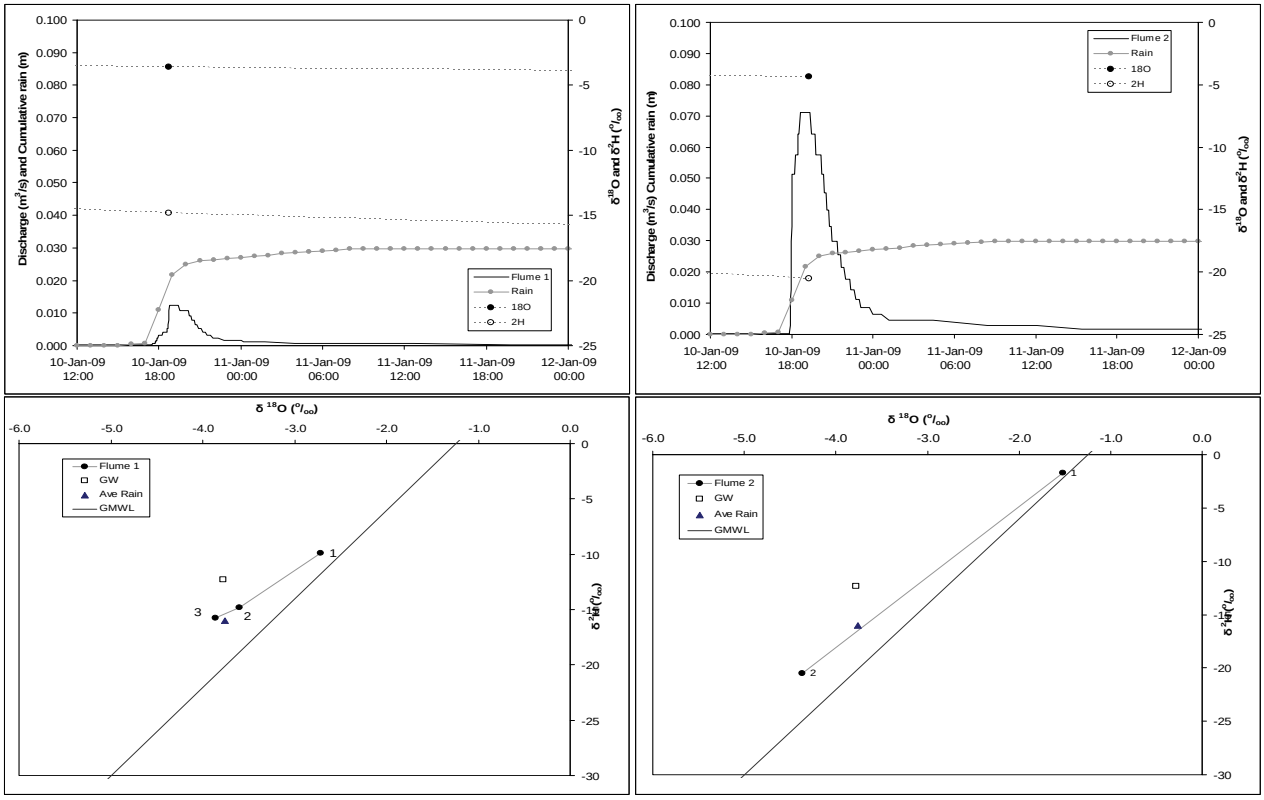

Figure B1.2. Rainfall, runoff and Isotope responses for Flume 1 (left) and Flume 2 (right) for event of 10 January 2009.

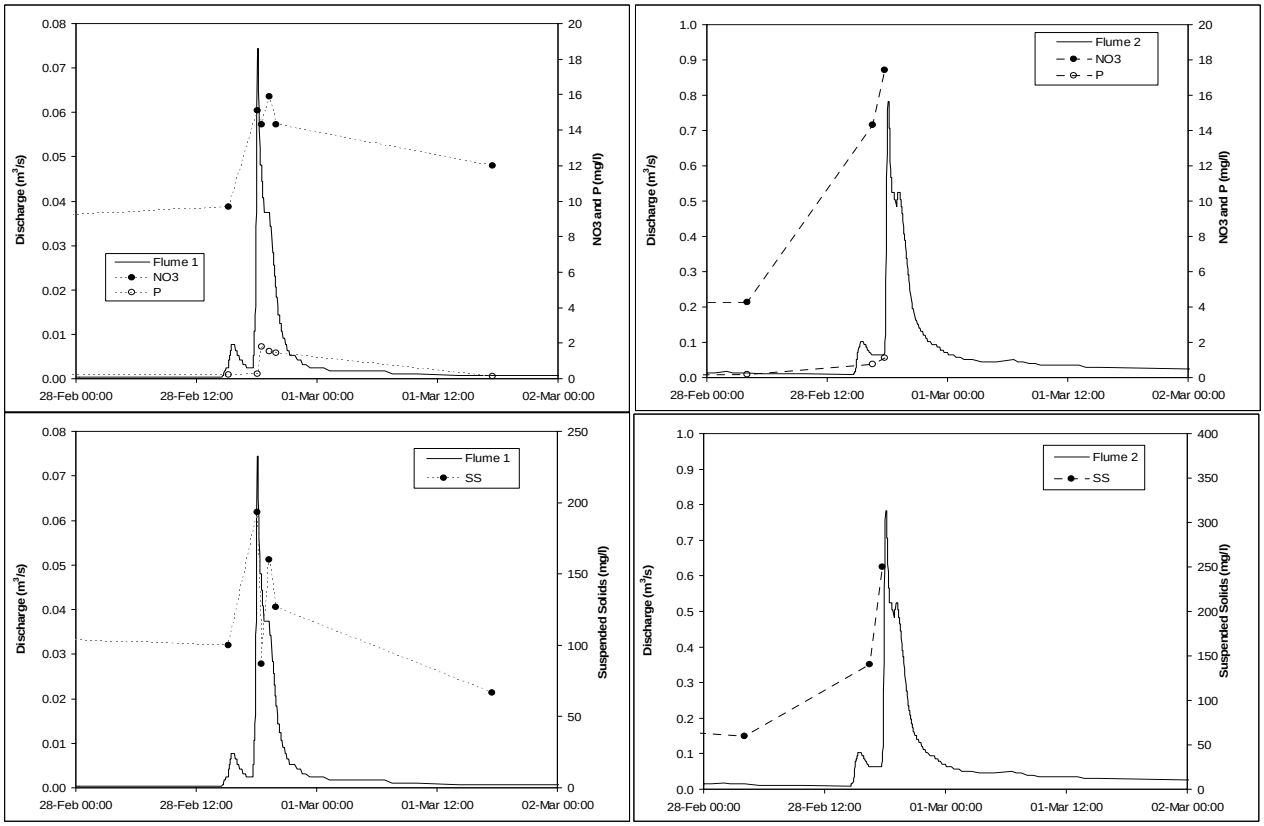

Figure B2.1. Rainfall, runoff Nitrate and P (above) and Suspended Solids (below) responses for Flume 1 (left) and Flume 2 (right) for event of 28 February 2009.

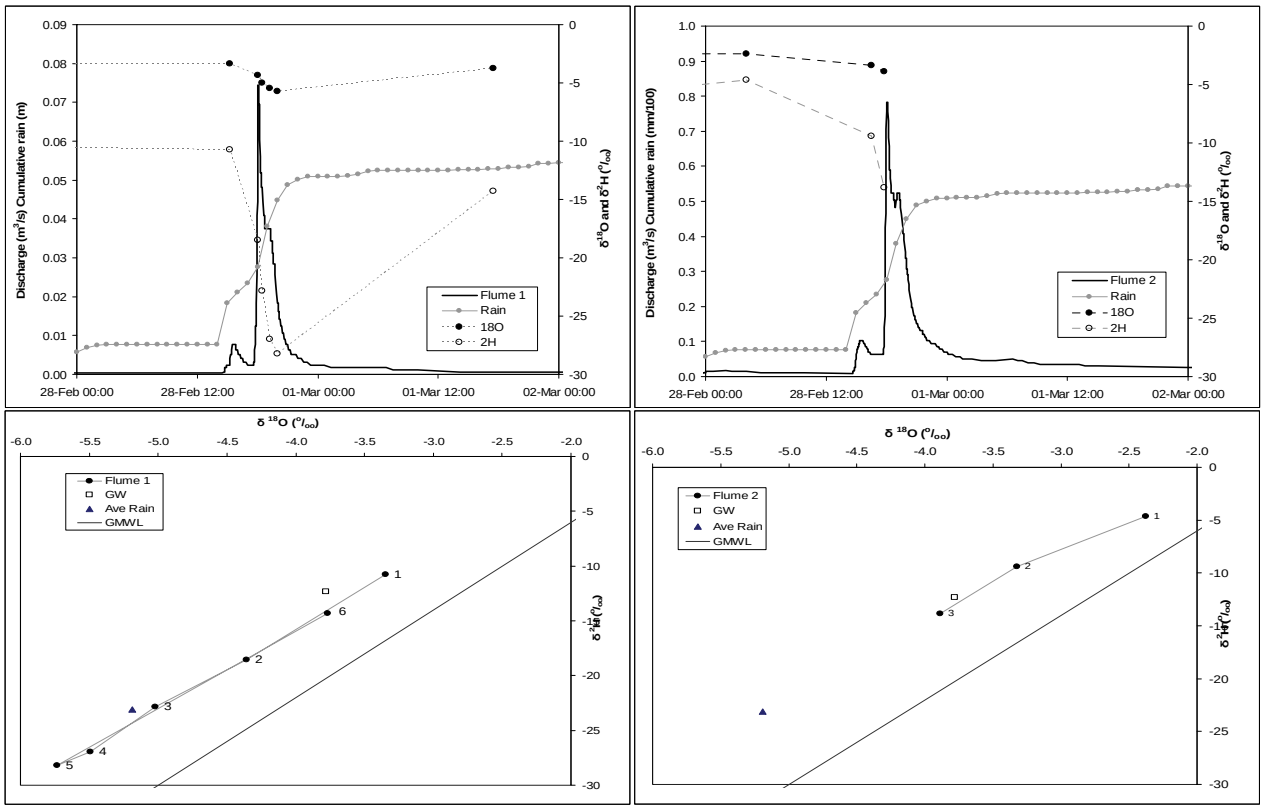

Figure B2.2. Rainfall, runoff and Isotope responses for Flume 1 (left) and Flume 2 (right) for event of 28 February 2009

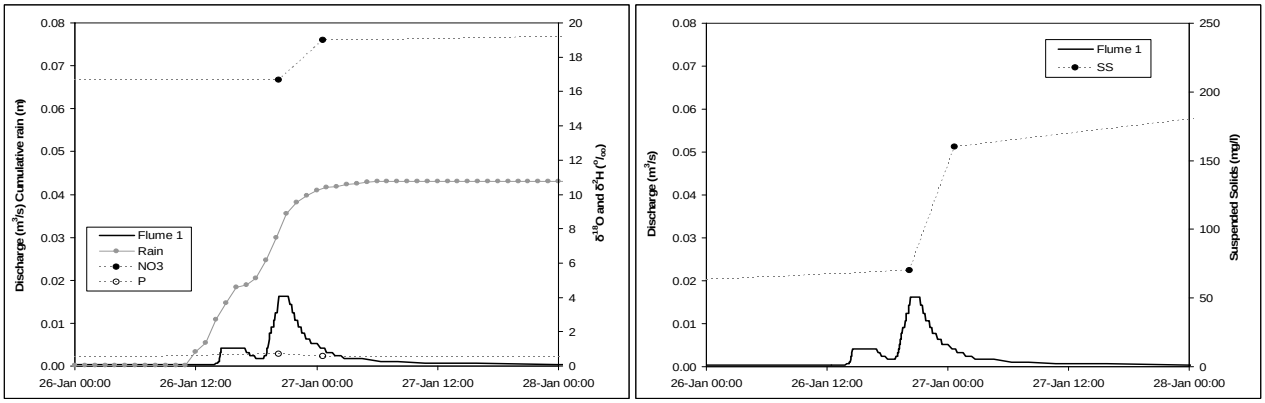

Figure B3.1. Rainfall, runoff Nitrate and P (left) and Suspended Solids (right) responses for Flume 1 for event of 27 January 2010

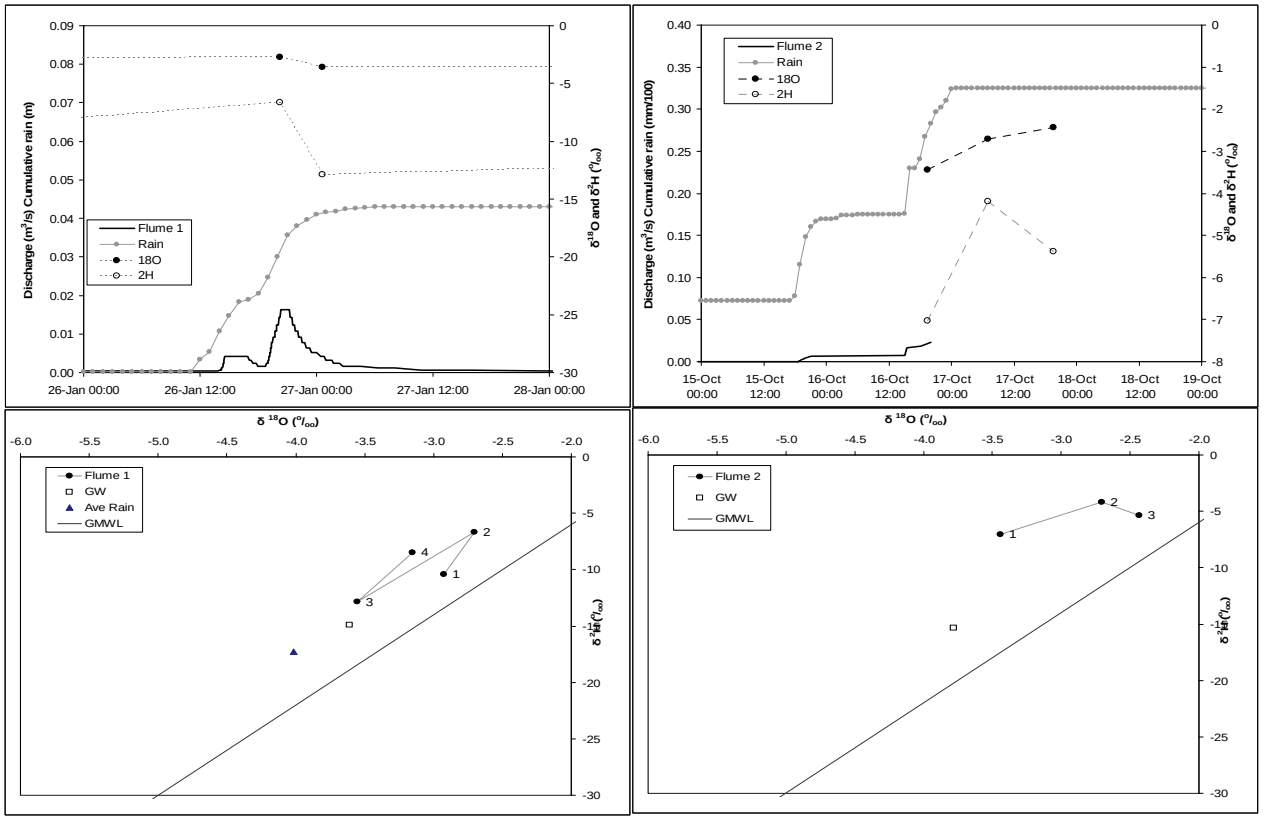

Figure B3.2. Rainfall, runoff and Isotope responses for Flume 1 (left) and Flume 2 (right) for event of 28 February 2009.

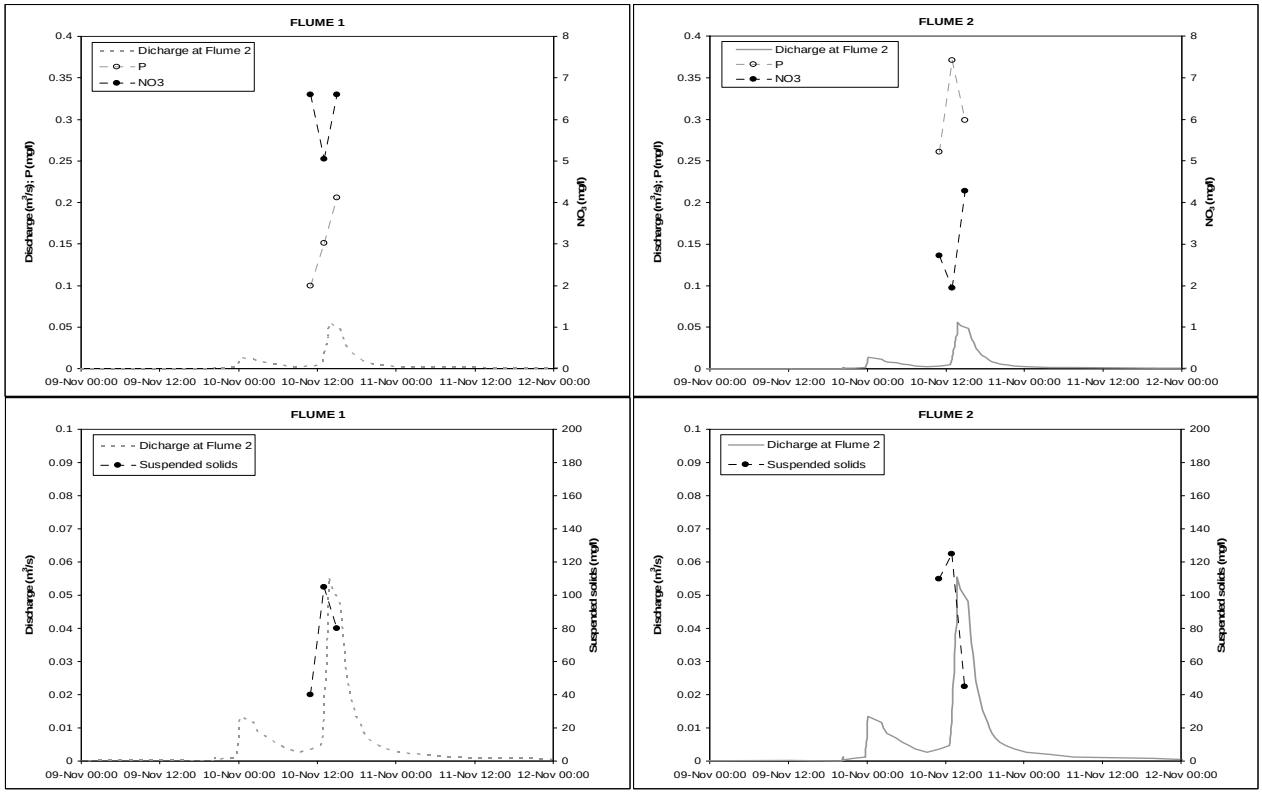

Figure B4.1. Rainfall, runoff Nitrate and P (above) and Suspended Solids (below) responses for Flume 1 (left) and Flume 2 (right) for event of 10 November 2010

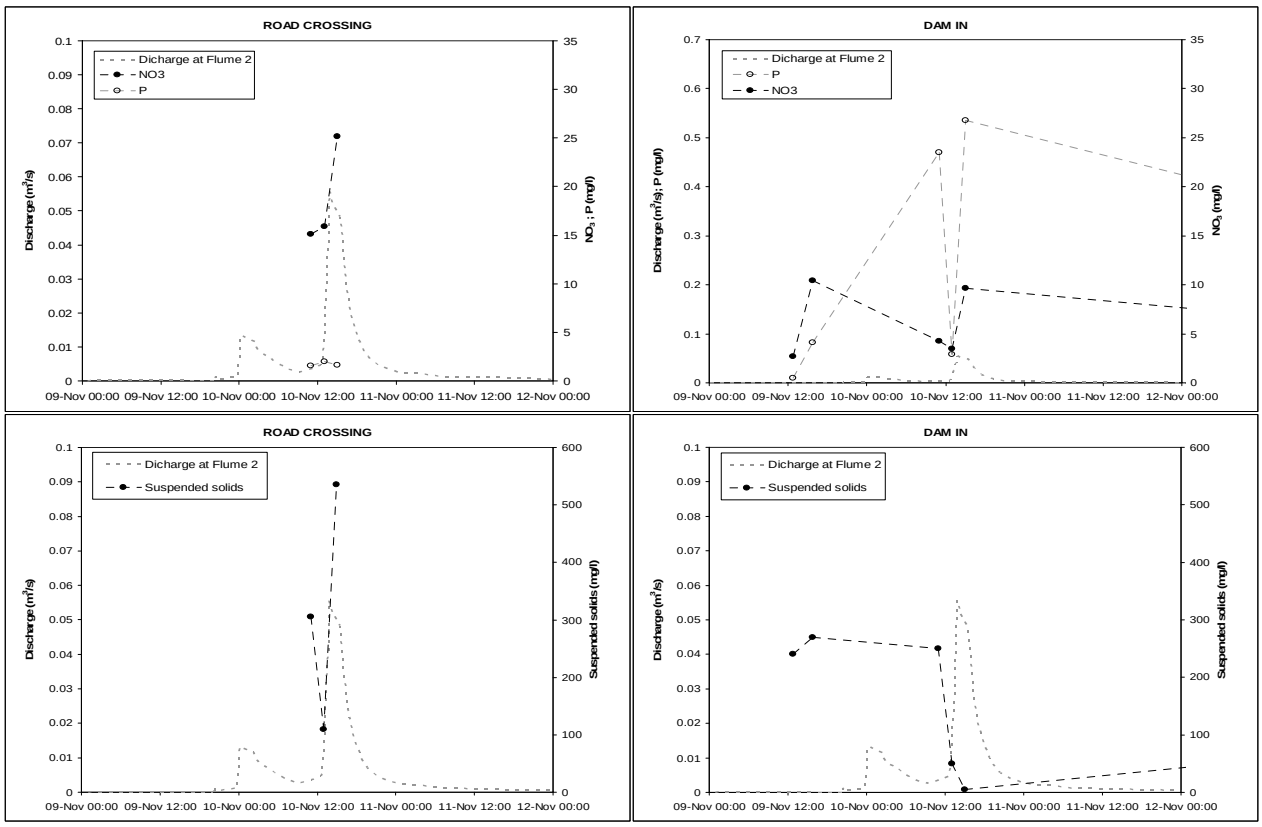

Figure B4.1. Rainfall, runoff Nitrate and P (above) and Suspended Solids (below) responses for Flume 1 (left) and Flume 2 (right) for event of 10 November 2010

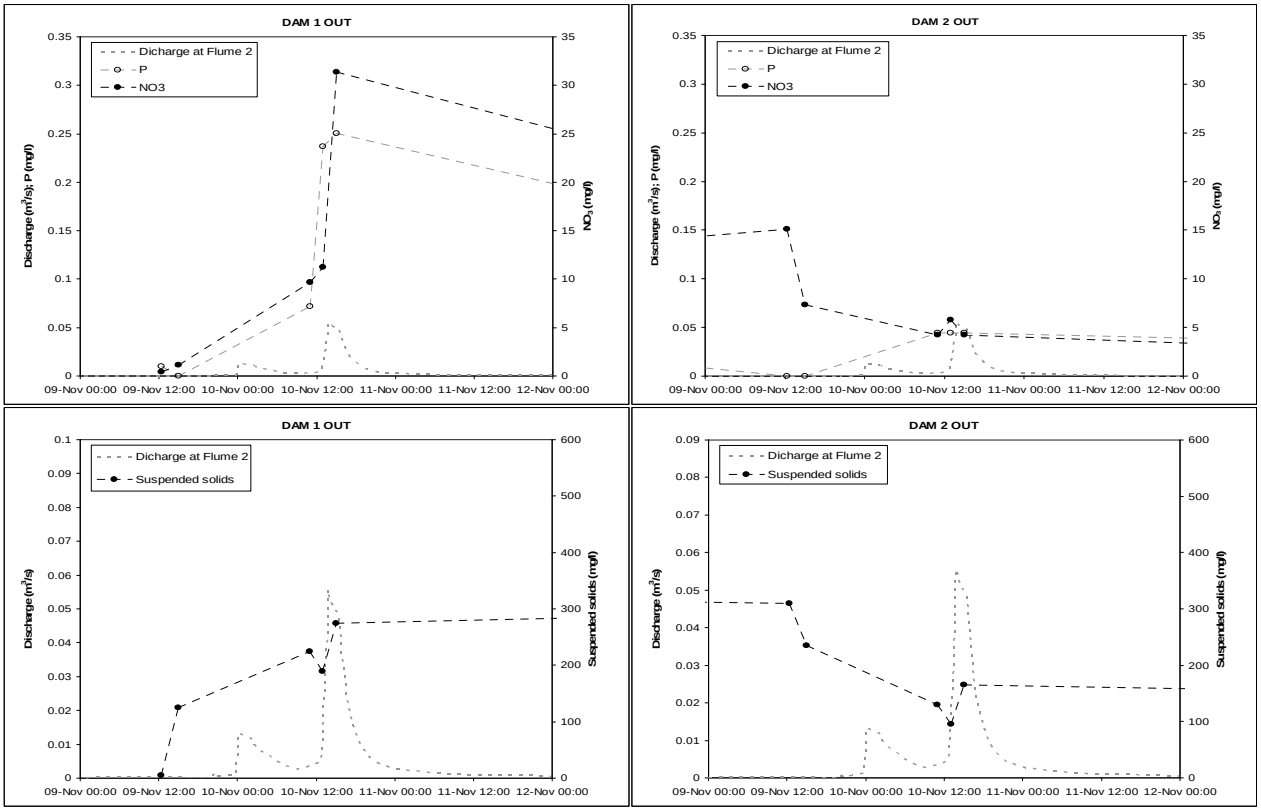

Figure B4.2. Rainfall, runoff Nitrate and P (above) and Suspended Solids (below) responses for Road crossing (left) and Dam In (right) for event of 10 November 2010.

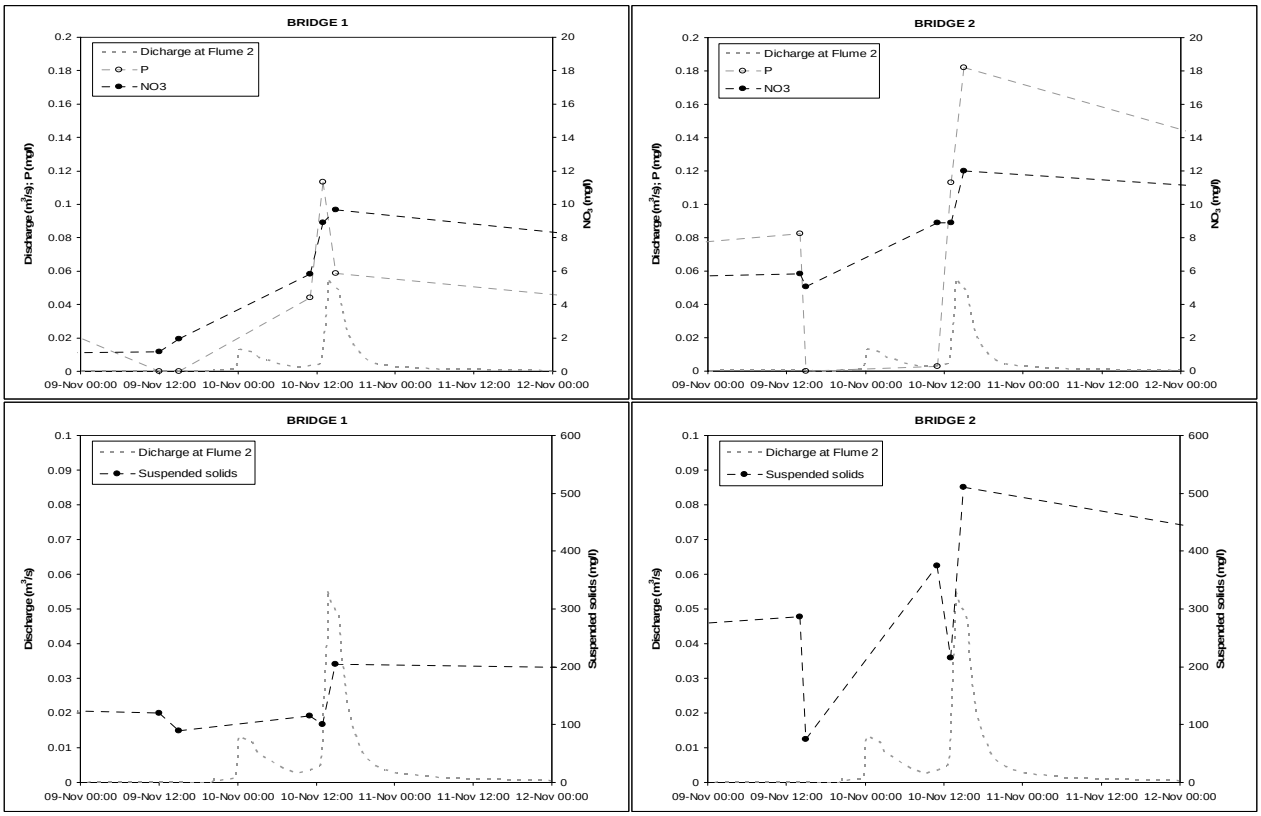

Figure B4.3. Rainfall, runoff Nitrate and P (above) and Suspended Solids (below) responses for Dam 1 Out (left) and Dam 2 Out (right) for event of 10 November 2010.

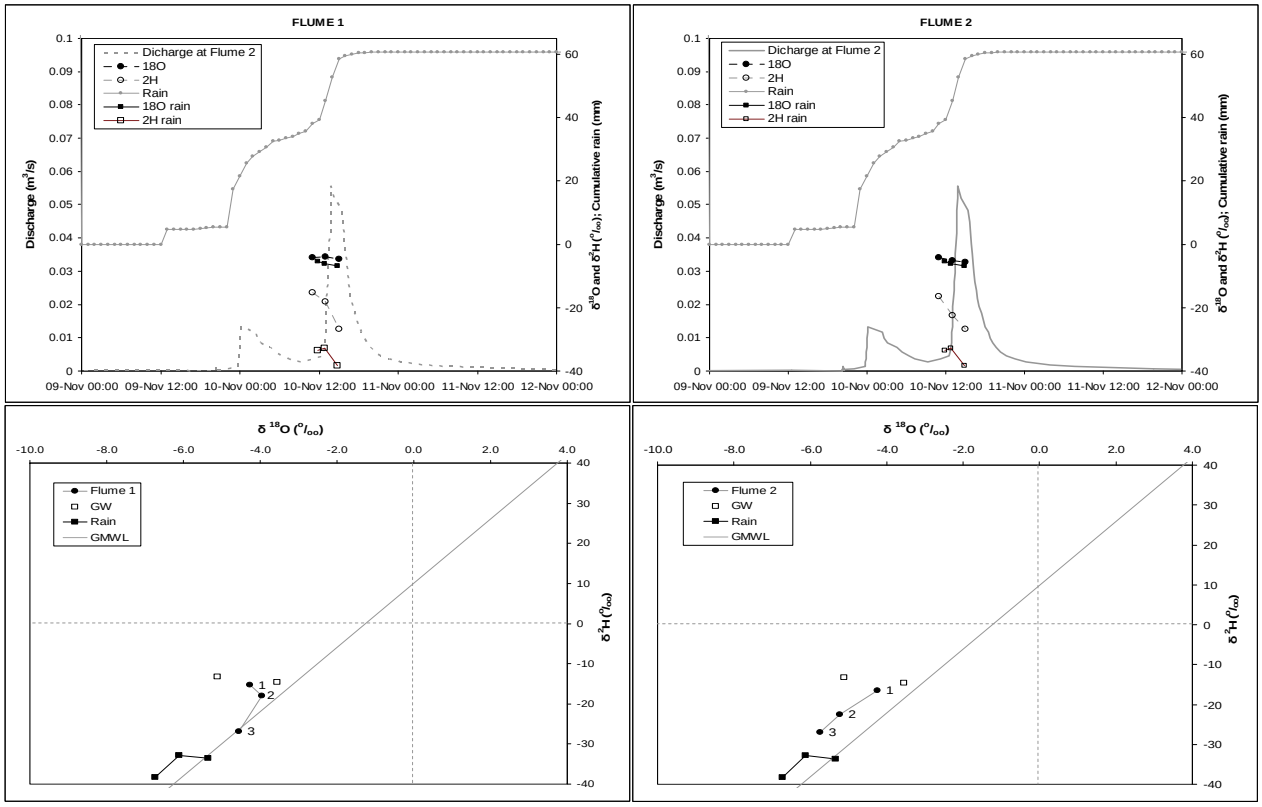

Figure B4.4. Rainfall, runoff Nitrate and P (above) and Suspended Solids (below) responses for Bridge 1 (left) and Bridge 2 (right)for event of 10 November 2010.

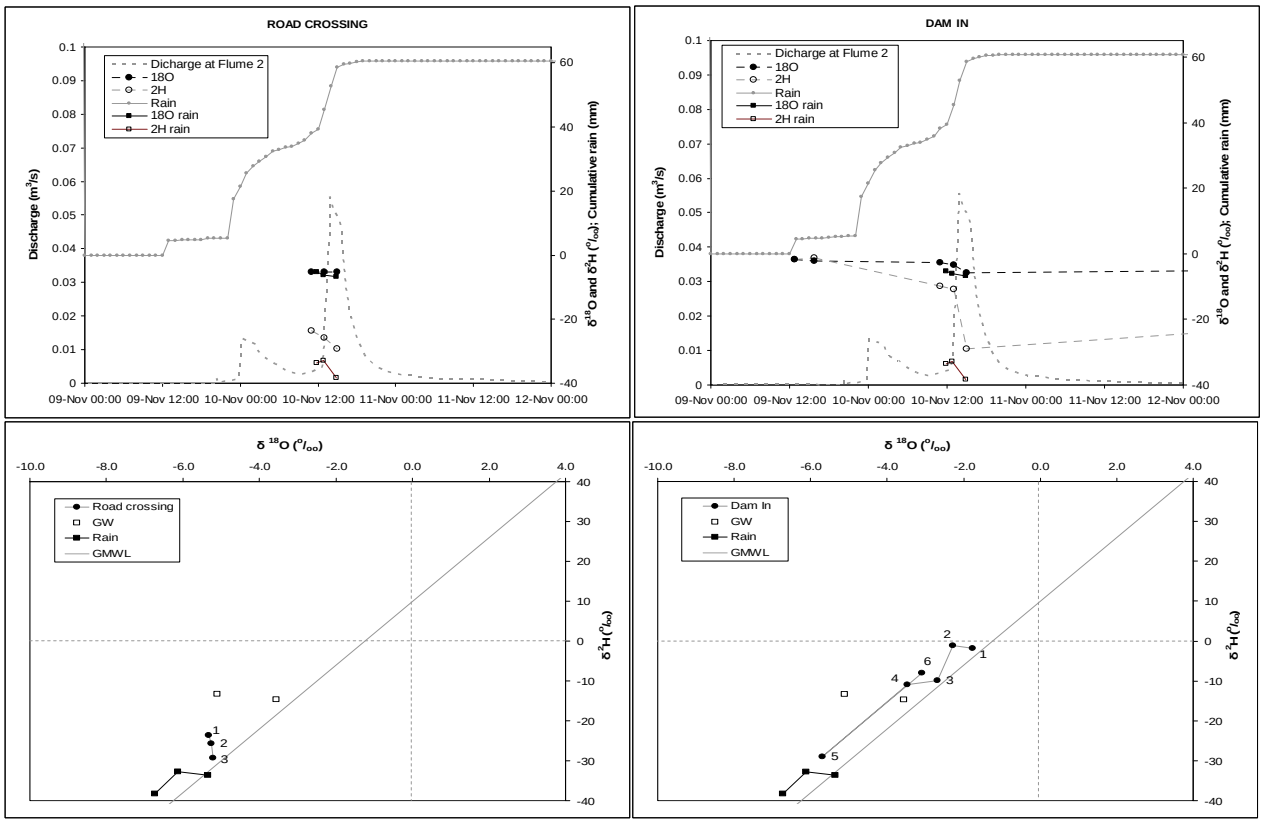

Figure B4.5. Rainfall, runoff and Isotope responses for Flume 1 (left) and Flume 2 (right) for event of 10 November 2010.

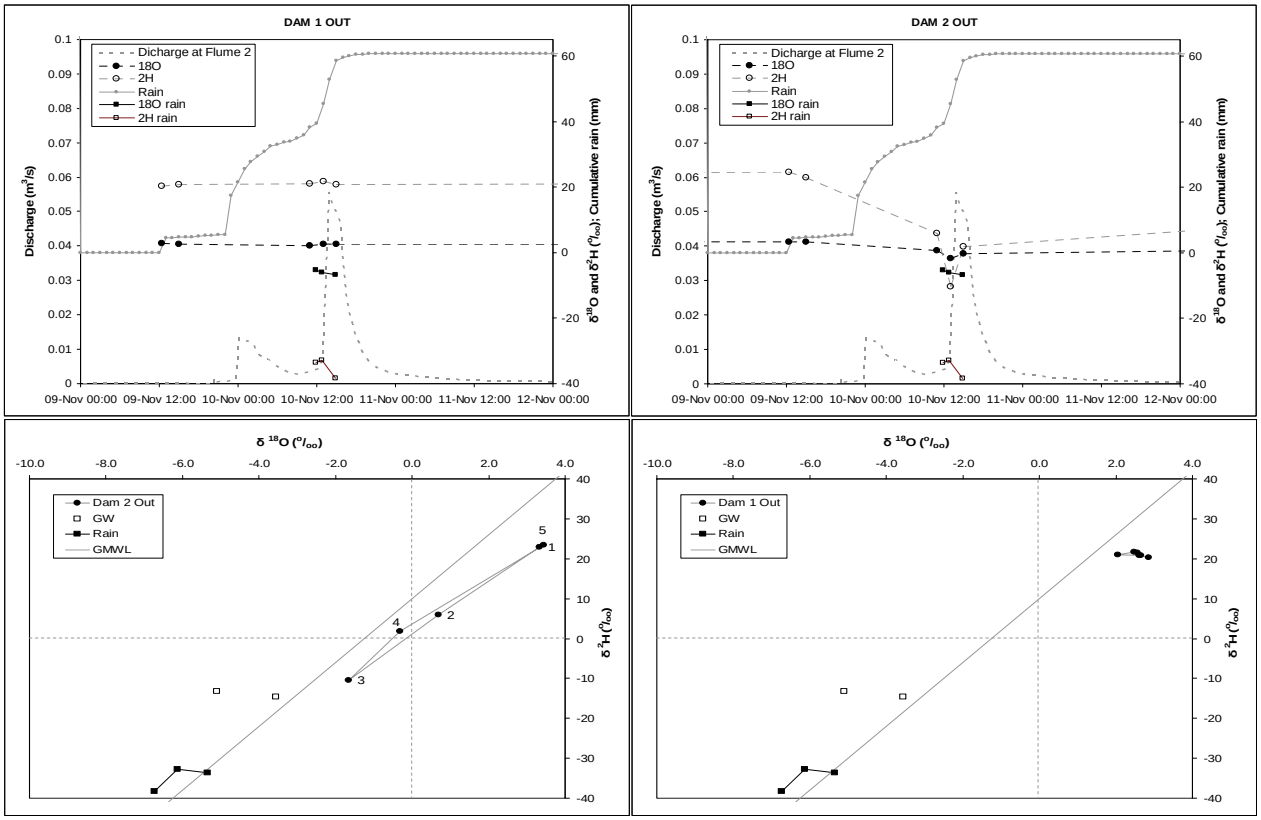

Figure B4.6. Rainfall, runoff and Isotope responses for Road crossing (left) and Dam In (right) for event of 10 November 2010.

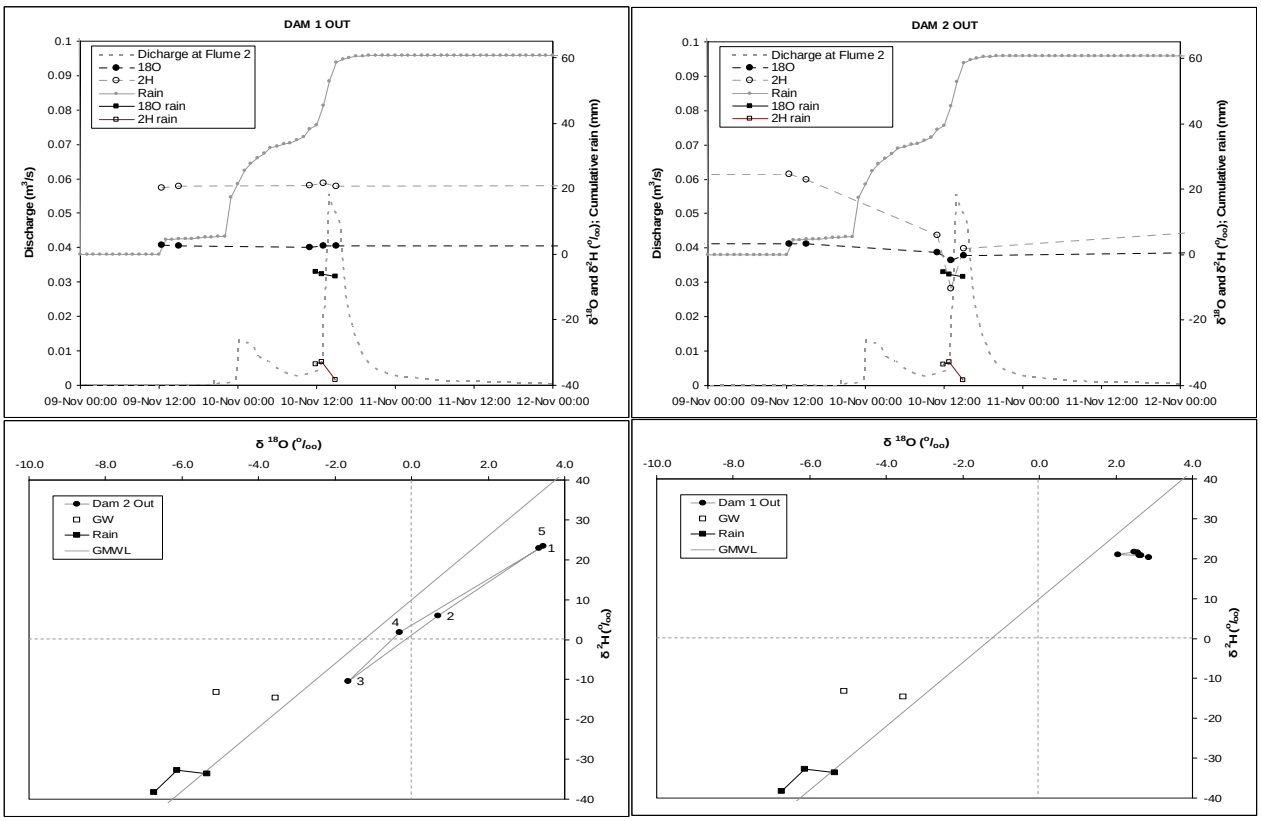

Figure B4.7. Rainfall, runoff and Isotope responses for Dam 1 Out (left) and Dam 2 Out (right) for event of 10 November 2010.

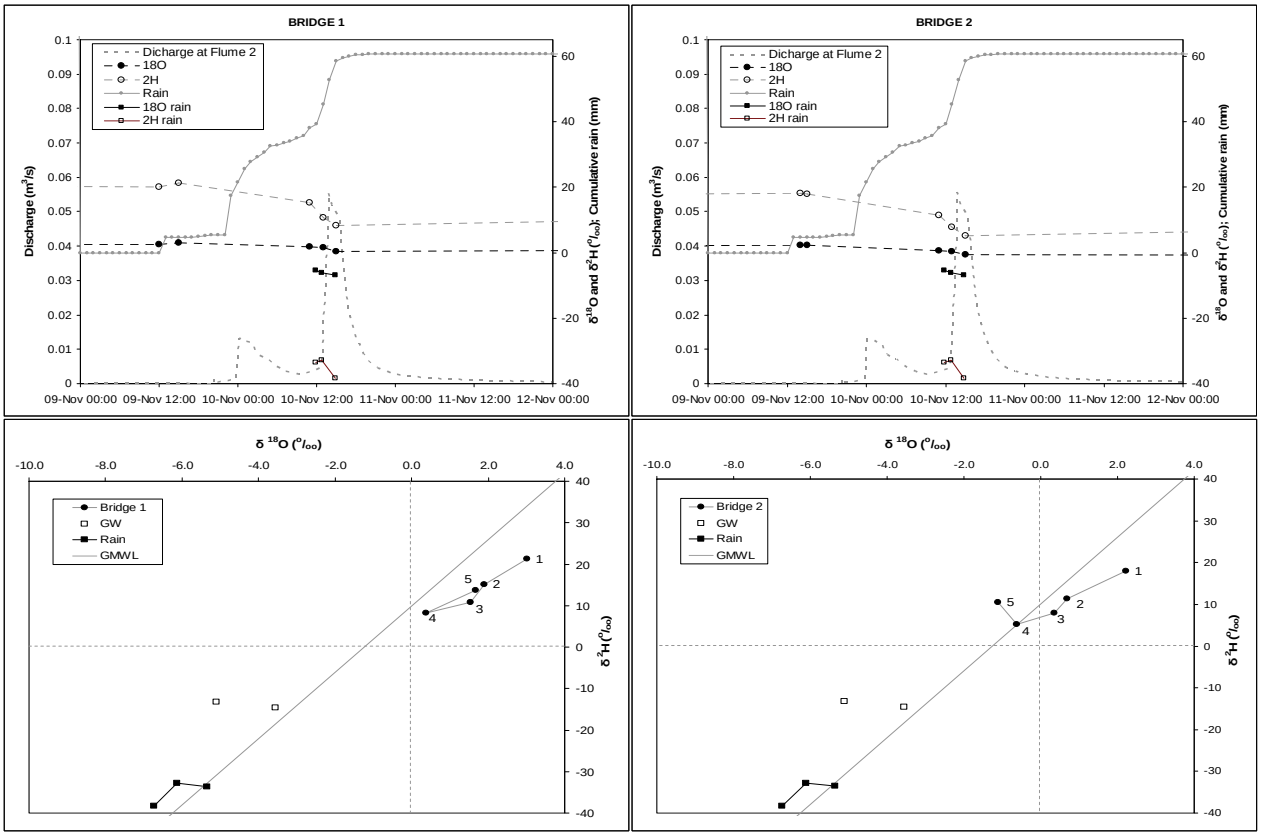

Figure B4.8. Rainfall, runoff and Isotope responses for Bridge 1 (left) and Bridge 2 (right) for event of 10 November 2010.